Title
Boundaries and Defects in Quantum Field Theory and Gravity

ISBN
9798184140889

Author
Kim, Seolhwa

Publication Date
2026-07-23

Peer reviewed|Thesis/dissertation

UNIVERSITY OF CALIFORNIA
Los Angeles

Boundaries and Defects in Quantum Field Theories and Gravity

A dissertation submitted in partial satisfaction
of the requirements for the degree
Doctor of Philosophy in Physics

by

Seolhwa Kim

2026

ABSTRACT OF THE DISSERTATION

Boundaries and Defects
in Quantum Field Theories and Gravity

by

Seolhwa Kim
Doctor of Philosophy in Physics
University of California, Los Angeles, 2026
Professor Per J. Kraus, Chair

Boundaries and defects host localized interactions of the dynamic degrees of freedom and provide the certain conditions on the field at the location of them. In guage theories and gravity, the dynamics of the large gauge degrees of freedom is localized on the boundary and are best described within the covariant phase space formalism using the symplectic form and boundary action. When the gravitational effects are strong, these large gauge degrees of freedom dress the on-shell matter action, which can be described using Hamiltonian formulation by integrating out these edge modes. We present the two efficient methods of computing the symplectic form associated with the boundary degrees of freedom. We then consider the near-extremal charged black holes in 4d, where the gravitational effects are enhanced at low temperature and study the Hawking radiation at near-horizon AdS_2 using the Hamiltonian formulation, with emphasis on comparing this to the JT gravity. Extending this perspective to study of defects, we develop a Lagrangian based method for computing the higher structure of non-invertible defects and compute the associators of the duality and triality defects in the 4d Maxwell theory. We then consider a family of codimension-1 non-conformal defects in the free non-compact boson theory and relate the two descriptions—localized interaction and discontinuous relations and study its scaling behavior and effects in spectrum.

The dissertation of Seolhwa Kim is approved.

Michael Gutperle

Thomas T. Dumitrescu

Eric D'Hoker

Per J. Kraus, Committee Chair

University of California, Los Angeles

2026

To my grandmother,

who talked with me before I can remember

and helped me find my first words,

and to my parents

TABLE OF CONTENTS

LIST OF FIGURES

LIST OF TABLES

ACKNOWLEDGMENTS

I am deeply grateful to my advisor, Professor Per Kraus, for six years of guidance and mentorship. His remarkable work ethic, his careful approach to difficult problems, and his ability to answer my often ill-defined questions pedagogically and from first principles have profoundly shaped the way I think about physics. I am especially grateful to him for introducing me to the joy of computation.

I would also like to express my sincere appreciation to my committee members, Professors Eric D'Hoker, Thomas Dumitrescu, and Michael Gutperle, for teaching me physics and for helping to create an inspiring intellectual environment for theoretical physics at UCLA.

It has been a privilege to work with my collaborators Orr, Richard, Ruben, Suzanne, and Zhengdi. I am grateful for the experience of figuring things out together and for the enthusiasm and companionship that made our projects much more enjoyable. I am also indebted to Kostis, Luigi, and Theo for teaching me about generalized symmetries and for always being willing to discuss related questions.

My time at UCLA was greatly enriched by the TEP graduate students. I am especially grateful to Richard for countless conversations about physics and everything beyond it, and to Anna, Christina, and Stephen for making our group feel warm and welcoming.

I have also been fortunate to meet many wonderful postdocs and friends from different places. I am grateful to Adar, Aryan, Bruno, David, Diego, Dima, Edgar, Enrico, Gabi, Giulia, Gurleen, Kassi, Kristian, Luke, Matteo, Michael, Joe, Joel, Jonah, Paul, Peter, Pratik Manwani, Pratik Sathe, Reed, Roger, Roman, Saeedeh, Yifan, Yillin, and Yoojung for their friendship, companionship, and the many memories we shared. In particular, my Korean friends—Hanbit, Jinho, Seulchan, and Wanki—provided friendship, encouragement, and motivation without which completing this Ph.D. would not have been possible.

Finally, I owe my deepest gratitude to my parents and to Tavit for their unwavering love and support throughout this journey.

Co-author contributions Chapter 2 of this thesis is based on [2], which was the result of collaboration with Richard Myers and Per Kraus. Chapter 3 is based on [6], a result of collaboration with Suzanne Bintanja and Per Kraus. Chapter 4 is based on [5], a result of collaboration with Orr Sela and Zhengdi Sun. Finally, chapter 5 is based on [4], a result of collaboration with Per Kraus and Zhengdi Sun.

VITA

2016	B.S. Physics and Electrical Engineering, Pohang University of Science and Technology
2018	M.S. Physics, Korea Advanced Institute of Science and Technology
2020–2026	Teaching Assistant, Department of Physics and Astronomy, University of California, Los Angeles
2021–2026	Graduate Student Researcher, Department of Physics and Astronomy, University of California, Los Angeles

PUBLICATIONS

[1] S. Kim and E. D. Stewart, *Constraining Affleck-Dine Leptogenesis after Thermal Inflation*, JCAP 09 (2020) 045, arXiv:1904.13158 [hep-ph]

[1] S. Kim and E. D. Stewart, *Constraining Affleck-Dine Leptogenesis after Thermal Inflation*, JCAP 09 (2020) 045, arXiv:1904.13158 [hep-ph]

[2] S. Kim, P. Kraus, and R. M. Myers, *Systematics of boundary actions in gauge theory and gravity*, JHEP 04 (2023) 121, arXiv:2301.02964 [hep-th]

[3] S. Kim, P. Kraus, R. Monten, and R. M. Myers, *S-matrix path integral approach to symmetries and soft theorems*, JHEP 10 (2023) 036, arXiv:2307.12368 [hep-th]

[4] S. Kim, P. Kraus, and Z. Sun, *Codimension one defects in free scalar field theory*, JHEP 06 (2025) 065, arXiv:2502.19547 [hep-th]

[5] S. Kim, O. Sela, and Z. Sun, *Higher structure of non-invertible symmetries from Lagrangian descriptions*, arXiv:2509.20540 [hep-th]

[6] S. Bintanja, S. Kim, and P. Kraus, *Enhanced correlations in hawking radiation from near-extremal collapse*, arXiv:2607.12989 [hep-th]. https://arxiv.org/abs/2607.12989

CHAPTER 1

Introduction

In gauge theories and gravity, asymptotic or actual boundary plays an important role by setting a stage for the various dynamic degrees of freedom. A part of pure gauge or gravity degrees of freedom that are associated with the large gauge transformations do not propagate in the bulk and instead their dynamics are localized on the boundary. This can be seen from the fact that their contribution to the symplectic form is localized on the boundary. As such, their dynamics is described by the boundary action, which can be computed by solving the Gauss's law constraints and plugging the solutions back to the action. Or alternatively, one can work in the covariant phase space formalism and compute the symplectic form Ω by solving $i_V\Omega = -\delta Q_V$ for the asymptotic symmetry generated by the vector V and associated charge Q_V, which can then be used in computing the boundary action. These procedures generally involve solving the differential equations, which can be complicated.

Restricting to gauge orbits around a single solution, one can circumvent this complexity using some simplified methods that do not involve solving a differential equation. These methods are the main subject of chapter 2, where we derive two such methods, check against known results for 3d Chern-Simons theory and AdS_3 gravity with various boundary conditions, and compute the symplectic form for the new situations such as low spin gravity and Einstein-Maxwell theory in AdS_5 which has the near horizon $\mathrm{AdS}_3 \times \mathbb{R}^2$.

On the other hand, the dynamics of the matters in the gravitational theories is often described using the minimal coupling to the fixed background. However, there are some special circumstances where the quantum gravitational effects should be incorporated to describe the dynamics of matter. One example is the Hawking radiation in the large, near extremal charged black holes, where this happens at the near horizon AdS_2 region and dominates any fluctuations associated with the small curvature of the bulk. In the near horizon region, the boundary gravitons associated with the asymptotic symmetry dress the matter's on-shell action localized on the boundary and their action can be computed using the aforementioned covariant space formalism. Alternatively, the enhanced Hawking radiation can be studied within the Hamiltonian formulation by Arnott-Deser-Misner (ADM), in which the boundary gravitons associated with asymptotic symmetry are integrated out or gauge fixed to provide the effective action for the matter fields. This formulation is essential in studying the observables in Unruh vacuum suitable for the evaporating near-extremal black holes, which has a single boundary as explained in chapter 3.

For thermal correlation functions, the two methods should agree at least classically, which we verify by computing and manipulating the ADM Hamiltonian for the 4d near-extremal black holes in chapter 3. However, the two formulations don't necessarily predict the same loop contributions because their effective dynamic degrees of freedoms are different, resulting in different regularization schemes. Nonetheless, we later show that the two descriptions predict the same value for some 1-loop correlation functions.

Similarly to the boundary, defects host localized interactions which have far reaching effects in low energy behavior of the system, and provide the generally discontinuous relation of the fields across them similar to the boundary conditions. When the energy and momentum flux are continuous across the defect, it doesn't cost any energy to deform the defect and it is called topological. Topological defects generate the symmetries in the generalized sense including non-invertible symmetries that mix the local operators with the twist operators.

These topological defects are mainly described by the fusion rules between two defects. However, this is not all, and the topological relations (morphisms) involving three or more defects require extra specifications known as higher structure, such as the associativity rules of three defects, and analogous notions for four or more defects. Generally, these are given by the TQFTs at the interface between two different configurations of the defects. These are RG invariant data of the theory that sometimes constrain the dynamics of the system through Ward identity. These data can be computed using the Lagrangian or localized interaction description of the defect by collapsing the network of two configurations that the target morphism connects, using the boundary conditions that are consistent with the localized interaction given in the defect Lagrangian. We describe this in detail in chapter 4, where we demonstrate its operation by applying to the $\mathbb{Z}_N$ Tambara-Yamagami symmetry category of 2d compact boson, associated with the T-duality and the $\mathbb{Z}_N$ subgroup of the shift and winding symmetries for the verification of the method and to the non-invertible duality and triality defects associated with the $\mathbb{Z}_N$ electric 1-form symmetry in the 4d Maxwell theory to derive new results.

Albeit less studied, generic defects are not conformal. They behave nontrivially under scaling and can change correlators, spectrum, and entropy. A challenge in studying non-conformal defect is the lack of analytic control. But a defect added as a perturbation to a free theory is expected to be tractable. With that expectation, we consider free non-compact scalar theory in 2d in chapter 5 by first presenting two descriptions—localized interaction and discontinuous matching conditions—of the non-conformal defects and providing a map between them. We then use either description appropriate for the situation to study the scaling behavior of the defect through its anomalous dimension and operator product expansion and the new spectrum or excitations by studying the defect Hilbert space, defect entropy, excitation energy introduced by the instantaneous space-filling defect and the density of states at high temperature. Although the defect hosts only quadratic interactions, lots of this study couldn't be done analytically when the defect has marginal or irrelevant couplings. We could still study the relevant defect analytically and found the existence of pathology in the spectrum for some defects and bizarre x^x type of behavior in various quantities.

Each chapter begins with its own introduction that explains the motivation and existing literatures in more detail. Chapters 2, 3, 4 and 5 are based on [2], [6], [5] and [4], respectively.

CHAPTER 2

Systematics of Boundary Actions in Gauge Theory and Gravity

2.1 Introduction and Summary

In gauge theories and gravity, physical degrees of freedom of the pure gauge or gravity consist of the propagating gauge fields or gravitons plus the large gauge transformations or diffeomorphisms around fixed solutions. The dynamics of the latter is localized on the boundary (asymptotic or actual) in a sense that their contribution to symplectic form and such are localized on the boundary. Famous examples include Wess-Zumino-Witten (WZW) action for the 3d Chern-Simons theory, the Alekseev-Shatashvili action for the 3d gravity with negative cosmological contant and JT gravity for the AdS_2 gravity.

As such, their dynamics, e.g. correlation functions, are described by boundary action, which can be obtained from the symplectic form in the asymptotic symmetry basis. The way one gets the symplectic form or boundary action is nontrivial; it involves solving the equation $i_V\Omega = -\delta Q_V$ where V is the phase space vector associated with the asymptotic symmetry and Q_V is the associated Noether charge. Alternatively one can solve the constraint equation known as Gauss's law constraint and plug the solutions back to the action.

However, none of these processes are always simple as solving the equation is not always guaranteed. We provided an alternative way of computing the symplectic form associated with the boundary degrees of freedoms, the ones associated with the asymptotic symmetry and their mixing with boundary part of matters. We found that the former process based on the covariant phase space formalism can be simplified restricted to the gauge orbit around a single solution, using two different methods.

First method is specialized for the case when the momentum is conserved. Inthat case, we provide a general solution to $i_{V_\xi}\Omega = -\delta P$, where $\xi = 1$ corresponds to translation symmetry and P is the associated Noether charge. The solution of phase space 1-form symplectic potential is given by

$$\Theta = \int \mathrm{d}x \left[\kappa_{\Phi\Phi}\Phi'\delta\Phi + \kappa_{\Phi\Psi}\Phi'\delta\Psi + \kappa_{\Psi\Psi}\Psi'\delta\Psi + P'_{\Phi}\delta\Phi + P'_{\Psi}\delta\Psi\right] \tag{2.1.1}$$

where Φ, Ψ are the boundary degrees of freedom with distinct transformation under V_ξ. We provide the proof of uniqueness of this solution in the main text along with its application to AdS_3 gravity with standard Dirichlet boundary condition on the metric and the warped AdS_3 which has gravitational Chern-Simons term for the unique boundary condition, which agree with known Alekseev-Shatashvili action.

Our second method is based on the phase spac 1-form valued field W that we call transfer field, contracting with which leaves a phase space differential forms invariant, i.e. $i_W Z = pZ_p$ for a phase space p-form Z. Hence the phase space variation can be identified with Lie derivative with respect to it, $\delta\phi = i_W\delta\phi$. Using this, $i_W\Omega = 2\Omega = +\delta Q_W$, where the sign is flipped in last equality reflecting the fact that W is a phase space 1-form valued vector. By skipping the step of solving $i_W\Omega = \delta Q_W$, this method simplifies the computation of the symplectic form, and we demonstrate this on 5d Chern-Simons theory and aforementioned gravitational theoreis.

After checking its consistency with the known result, we use these methods to compute the boundary action and symplectic form of low spin gravity and 5d Einstein-Maxwell theory with negative cosmological constant, which admits an asymptotically AdS_5 solution that has a near horizon $\mathrm{AdS}_3 \times \mathbb{R}^2$ geometry.

2.2 Review of Boundary Actions

In this section we discuss general aspects of boundary modes, their origin in terms of large gauge transformations, and the construction of an action that describes them.

2.2.1 $U(1)$ CS theory on $M = D \times \mathbb{R}$

To get oriented, we first quickly review the simple and classic example of Chern-Simons theory on a spatial disk and the corresponding boundary gauge modes, following the original Lagrangian approach [7]. This approach is based on solving the Gauss law constraint and substituting back into the action, yielding a total derivative. While this method works well here, it is not so easy to adapt to other examples such as gravity in the metric description. For this reason we go on to develop more flexible methods based on a covariant phase space analysis.

The action for for Abelian CS theory on a spatial disk cross time is

$$\begin{aligned} S &= k \int_M A \wedge \mathrm{d}A + S_{bndy} \\ &= -k \int_M \mathrm{d}^3x (A_r \partial_t A_\phi - A_\phi \partial_t A_r + 2A_t F_{\phi r}) + S'_{bndy} \ , \end{aligned} \tag{2.2.1}$$

where we integrated by parts and absorbed the boundary term into S'_{bndy}. We choose boundary conditions $\delta(A_t - A_\phi)|_{\partial M} = 0$.

Specializing to the case $(A_t - A_\phi)|_{\partial M} = 0$, a good variational principle is achieved by taking

$$S_{bndy} = 0, \qquad S'_{bdy} = -k \int_{\partial M} \mathrm{d}t \mathrm{d}\phi A_\phi^2 \ . \tag{2.2.2}$$

A_t is a Lagrange multiplier enforcing the constraint $F_{\phi r} = 0$, which is solved by writing

$$A_\phi = \partial_\phi \alpha \ , \quad A_r = \partial_r \alpha \ , \tag{2.2.3}$$

with $\alpha(r,t,\phi+2\pi)=\alpha(r,t,\phi)$. Plugging this back into the action, the bulk terms become a total derivative, and we arrive at the chiral boson action

$$S = k\int_{\partial M} \mathrm{d}t\mathrm{d}\phi(\partial_\phi\alpha\partial_t\alpha - \partial_\phi\alpha\partial_\phi\alpha) \ . \tag{2.2.4}$$

The basic equal time Poisson-Dirac bracket is

$$\{\alpha(\phi), \partial_\phi\alpha(\phi')\} = \frac{1}{2k}\delta(\phi-\phi') \ . \tag{2.2.5}$$

The Hamiltonian and charges generating infinitesimal gauge transformations by λ are

$$H_t = k\int_0^{2\pi}(\partial_\phi\alpha)^2\mathrm{d}\phi, \qquad H[\lambda] = 2k\int_0^{2\pi}\lambda\partial_\phi\alpha\mathrm{d}\phi \ . \tag{2.2.6}$$

The theory describes a $U(1)$ current $J = k\partial_\phi\alpha$ whose Fourier modes obey a $U(1)$ current algebra. The current-current-correlator is

$$G_{JJ}(w) = \langle J(w)J(0)\rangle = -\frac{k}{4\pi\sin^2\left(\frac{w}{2}\right)} \ , \quad w = \phi+t, \quad \overline{w} = \phi - t \ . \tag{2.2.7}$$

2.2.1.1 Physical relevance of boundary modes

Inasmuch as the preceding analysis shows that boundary modes can carry nonzero energy and momentum, they are established as being nontrivial physical states. Nonetheless, their "pure gauge" character leads one to wonder, at least upon first hearing, whether they might be ignorable in some sense, for example by decoupling from the rest of the physical system in which they are embedded. However, it is not hard to show that the boundary modes do have measurable consequences on other observables.

To expose these effects we can think of coupling the theory in the disk region to some external system comprised of charged matter that couples to the CS gauge field at the boundary of the disk. In the simplest incarnation we can take the system to live on the boundary of the disk, and to be completely explicit we consider a charged scalar field example,

$$S = k\int_M A\wedge \mathrm{d}A + \int_{\partial M}\mathrm{d}^2x(D^\mu\Phi)^*D_\mu\Phi \ . \tag{2.2.8}$$

The covariant derivative is taken to correspond to a gauging of the scalar shift symmetry, $D_\mu\Phi = \partial_\mu\Phi - iqA_\mu$. This is convenient, since the associated current, $J^\Phi_\mu = i(\partial_\mu\Phi - \partial_\mu\Phi^*)$ decomposes into dimension $(1,0)$ and $(0,1)$ operators, which is not the case for the current associated to phase rotations of the scalar.[1] Repeating the previous steps we arrive at the action

$$S = \int \mathrm{d}^2x \left[-2k\partial_\phi\alpha\partial_{\overline{w}}\alpha + 4\partial_w\Phi^*\partial_{\overline{w}}\Phi + 2iq\partial_\phi\alpha(\partial_{\overline{w}}\Phi - \partial_{\overline{w}}\Phi^*)\right] \tag{2.2.9}$$

with $\partial_w = \frac{1}{2}(\partial_\phi + \partial_t), \partial_{\overline{w}} = \frac{1}{2}(\partial_\phi - \partial_t)$. The coupling of α to Φ has no effect on the energy spectrum of the theory, as follows from the fact that the coupling can be removed by a redefinition of Φ. There is a nontrivial effect on scalar correlators, in particular on the two-point function of the current $J^\Phi_{\overline{w}}$. This effect reflects the fluctuating phase acquired by a charged particle on traveling between the two operator insertion points on the boundary. Treating q as a perturbation, we can readily sum up contributing diagrams by performing Wick contractions, resulting in

$$\begin{aligned} G^{(q)}_{J^\Phi J^\Phi}(p) &= \langle J^\Phi_{\overline{w}}(p) J^\Phi_{\overline{w}}(-p)\rangle_q \\ &= \sum_{m=0}^{\infty} (-4q^2)^m [G_{J^\Phi J^\Phi}(p)]^{m+1}[G_{\alpha\alpha}(p)]^m \\ &= \frac{G_{J^\Phi J^\Phi}(p)}{1 + 4q^2 G_{J^\Phi J^\Phi}(p) G_{\alpha\alpha}(p)} \ , \end{aligned} \tag{2.2.10}$$

where the $q = 0$ correlators are

$$\begin{aligned} G_{J^\Phi J^\Phi}(p) &= \langle J^\Phi_{\overline{w}}(p) J^\Phi_{\overline{w}}(-p)\rangle \sim \frac{p_{\overline{w}}}{p_w} \\ G_{\alpha\alpha}(p) &= \langle \partial_\phi\alpha(p)\partial_\phi\alpha(-p)\rangle \sim \frac{p_\phi}{kp_{\overline{w}}} \ . \end{aligned} \tag{2.2.11}$$

At $q = 0$ the correlator behaves as $p_{\overline{w}}/p_w$ corresponding to $1/\sin^2(\frac{\overline{w}}{2})$ in position space. As $q\to\infty$ the correlator tends to zero, with leading behavior $\frac{k}{q^2}\frac{p_{\overline{w}}}{p_\phi}$; being polynomial in p_t, this vanishes for unequal times.

[1] The non-invariance of this current under large gauge transformations is not a concern since such transformations are to be viewed as global symmetries.

The point to be emphasized here is that the boundary modes leave a detectable imprint on the scalar correlators, and so are clearly "real."

2.2.2 Review of covariant phase space formalism

We begin with a brief review of the covariant phase space formalism, which will also serve to establish notation for the remainder of this chapter. Along the way, we make comments about precisely where boundary conditions enter the formalism, as these will be useful to keep in mind later. For a more detailed review, see for example [8–11].

2.2.2.1 Action and covariant phase space

We consider a theory defined on a $D = d + 1$ dimensional spacetime M which admits a foliation by codimension-1 slices which we will generally denote by Σ. The, potentially asymptotic, boundary structure of M can then be decomposed into $\partial M = \Sigma_+ \cup \Gamma \cup \Sigma_-$ where $\Sigma_\pm$ are the slices in the asymptotically far future and past and Γ is formed by unioning the boundaries of all the slices. On this spacetime we consider a theory with fields ϕ whose dynamics are described by an action

$$S[\phi] = \int_M L + \int_{\partial M} \ell \tag{2.2.12}$$

where L is the D-form Lagrangian and ℓ is some allowed d-form boundary contribution[2], which we assume to be local functionals of the fields.

Throughout we will use δ to denote the exterior variational derivative, which we refer to as the variation. Particular infinitesimal transformations of the fields will be thought of as vector fields V on field space. The action of a vector V on a field ϕ will then be denoted by

[2]Though we use the same symbol ℓ for the boundary contribution over all of ∂M, there need be no relation between ℓ on Γ and ℓ on $\Sigma_\pm$. Shifts in this ℓ on either always produce shifts in the canonical 1-form by something δ exact and so do not change the symplectic structure.

the contraction[3] $i_V \delta\phi$. By integrating by parts, the variation of the Lagrangian may always be written

$$\delta L = E \wedge \delta\phi + \mathrm{d}\theta \tag{2.2.13}$$

for some θ. Setting $E = 0$ will be our equations of motion. We note that θ is always ambiguous up to addition of a d-closed form which we will return to shortly[4].

Using this identity, the variation of the action is given by

$$\delta S = \int_M E \wedge \delta\phi + \int_{\Sigma_+ - \Sigma_-} (\theta + \delta\ell) + \int_\Gamma (\theta + \delta\ell). \tag{2.2.14}$$

In order to have a good variational principle we require that the on-shell variation have no support on Γ which then requires

$$(\theta + \delta\ell)|_\Gamma = \mathrm{d}B \tag{2.2.15}$$

for some B. Of course, this B can always be absorbed into a redefinition of θ. However, we note that for a generic theory, the LHS above will not automatically take the form of a total derivative. Instead, there will be terms which only vanish upon the imposition of boundary conditions. This means that the B here generally depends on the boundary conditions we choose for our theory, and the existence of B may impose conditions on what we choose for

[3] Though here we prefer the contraction on variation notation to denote infinitesimal transformation, the reader may find it helpful to recall that the following are equivalent: $i_V \delta F[\phi] = \mathcal{L}_V F[\phi] = V(F[\phi])$ where $\mathcal{L}_V$ denotes the Lie derivative on field space and $V(F[\phi])$ is the action of the vector field V on the function F on field space.

[4] In the literature, e.g. [9], it is often mentioned that θ is also ambiguous up to addition of a δ-closed form. While this is true, any such shift in θ is equivalent to shifting ℓ. So we take the perspective that θ has no δ ambiguity, but ℓ remains to be chosen.

ℓ[5]. As a simple example, starting from the action (B.4.20) we find

$$\theta = -kA \wedge \delta A, \qquad B = 0 \tag{2.2.16}$$

with chiral boundary conditions.

It will be useful later to keep explicit which objects depend on the boundary conditions and which do not. So while it is possible to absorb B into a redefinition of θ, we will refrain from doing so in order to avoid reference to boundary conditions when writing θ.

It's also useful to observe that having a good variational principle is equivalent to slice independence of the symplectic form. The potential for the symplectic form is always found by extracting what remains of the action's variation from the initial and final time slices; we write $\mathcal{A}$ to denote this. Here we have

$$\delta S = \int_{\Sigma_+ - \Sigma_-} \mathcal{A} = \int_{\Sigma_+ - \Sigma_-} (\theta + \delta\ell - \mathrm{d}B) \tag{2.2.17}$$

after the imposition of (2.2.15). This means we should choose our symplectic form to be[6]

$$\Omega = \int_\Sigma \omega = \int_\Sigma \delta\mathcal{A} = \int_\Sigma \delta(\theta - \mathrm{d}B). \tag{2.2.18}$$

Though the ultimate argument for using this object as our symplectic form will be that it produces the desired Poisson brackets, we can see an immediate benefit by taking a second variation of (2.2.17), which implies that this Ω is independent of the slice we choose.

It is, however, useful to observe that we can show more directly that the slice independence of Ω is precisely equivalent to the demand (2.2.15), and hence the demand for a good variational principle. To see this we take a second variation of (2.2.13) to find

$$-\delta(E \wedge \delta\phi) = \mathrm{d}\delta\theta = \mathrm{d}\omega \tag{2.2.19}$$

---

[5]A standard example of this would be the need to include the Gibbons-Hawking-York term in the Einstein-Hilbert action with Dirichlet boundary conditions, though in that case we may choose $B = 0$ depending on our gauge fixing, see e.g. [11] for details.

[6]Throughout this work we ignore the complications that come from the possibility of non-trivial phase space topology, including the possibility of a symplectic form with non-trivial De Rahm cohomology.

so the symplectic current is closed on-shell. Hence $\Omega(\Sigma)$ is independent of the slice Σ if and only if the pullback of ω to Γ vanishes. This demand can be rewritten as $\omega|_\Gamma = \delta(\theta|_\Gamma - \mathrm{d}B) = \delta[(\theta + \delta\ell)|_\Gamma - \mathrm{d}B]$ so the condition (2.2.15), obtained from demanding a good variational principle, is equivalent[7] to the slice independence of the symplectic form.

As a final comment about this definition for the symplectic form, we should discuss the distinction between the phase space and prephase space. We will generally take prephase space to consist of all configurations of the fields which obey the boundary conditions and the equations of motion. On this space the quantity (2.2.18) will generally be degenerate and hence cannot be a proper symplectic form[8]. For this reason, it's often referred to as the presymplectic form.

To form the actual phase space, we need to perform a symplectic quotient and mod out the null directions of the symplectic form. This is a matter of viewing the prephase space as a bundle whose fibers are the null directions and whose base space is our true phase space. The mathematical details were laid out in [12], but in practice the result is that Ω is a non-degenerate 2-form on the base space and so working on the true phase space is a matter is ignoring those variables whose variation lies along the pure gauge directions[9].

[7]Strictly speaking, the slice independence of the symplectic form only implies (2.2.15) up to a δ-closed form, but locally on phase space such a form can be written as exact and absorbed into a redefinition of ℓ.

[8]This is closely related to the lack of deterministic evolution on prephase space; specifying the fields and some number of their derivatives on a Cauchy slice may not uniquely determine the same data on a later time slice. The most common way to exhibit this non-uniqueness is by specifying a configuration and applying to it a gauge transformation which differs from the identity only at times later than the first slice. We would thus have two solutions to the equations of motion whose data agree on one slice but disagree on another.

[9]If we are being strict, this is the statement that, at least locally, a section of the bundle is diffeomorphic to the base space.

2.2.2.2 Symmetries and charges

With the covariant phase space framework now in place, it will be important for us to review how symmetries enter the picture. A vector field V on phase space is typically defined to be a symmetry if its action on the Lagrangian is a total derivative:

$$i_V \delta L = \mathrm{d}k_V \tag{2.2.20}$$

for some k_V. Contracting V onto (2.2.13) it now follows that

$$\mathrm{d}J_V \equiv \mathrm{d}(i_V\theta - k_V) = E \wedge i_V \delta\phi. \tag{2.2.21}$$

So $J_V = i_V\theta - k_V$ is the conserved Noether current associated to V.

Though any vector field V satisfying (2.2.20) admits a conserved Noether current, constructing the Noether charge is not always as a simple as integrating the current over a time slice. There may be non-trivial boundary contributions to the true Noether charge H_V in order for it to satisfy

$$i_V\Omega = -\delta H_V. \tag{2.2.22}$$

For general symmetries, one must directly evaluate the contraction on the symplectic form, but for gauge symmetries we may find the charges by another, sometimes more efficient, method. This was pointed out in [13] for the special case of diffeomorphism charges in diffeomorphism invariant theories, but with the Theorem 1 of Appendix A.2 it's simple to generalize this calculation to any gauge transformation, as we review now[10].

We suppose V_λ generates a gauge transformation with gauge parameter λ, defined such that $V_0 = 0$ so $\lambda = 0$ is the identity transformation. Taking an additional variation of

[10] Some additional simplifications that can help in computations are possible in the special case of diffeomorphisms even when the theory is not diffeomorphism invariant, as when gravitational Chern-Simons terms are included in the action. This still makes use of Theorem 1 and was pointed out in [14]. We review it in Appendix A.3.

(2.2.21) it follows that, on-shell,

$$\mathrm{d}(\mathcal{L}_{V_\lambda}\theta - \delta k_\lambda) = 0 \tag{2.2.23}$$

where we have abbreviated $k_{V_\lambda} = k_\lambda$. Thus we have a form closed for all free functions λ and Theorem 1 tells us that there must exist a phase space 1-form Π_λ, constructed locally from the fields and λ, such that

$$\mathcal{L}_{V_\lambda}\theta - \delta k_\lambda = \mathrm{d}\Pi_\lambda. \tag{2.2.24}$$

With this, it now follows from (2.2.18) that

$$\delta J_\lambda = -i_{V_\lambda}\omega + \mathrm{d}(\Pi_\lambda - i_{V_\lambda}\delta B). \tag{2.2.25}$$

Thus if there exists a function C_λ such that

$$\Pi_\lambda - i_{V_\lambda}\delta B = \delta C_\lambda, \tag{2.2.26}$$

(2.2.25) implies

$$i_{V_\lambda}\Omega = -\delta \int_\Sigma (J_\lambda - \mathrm{d}C_\lambda). \tag{2.2.27}$$

We note that the existence of C_λ is not guaranteed and will typically depend on the boundary conditions chosen for the theory[11]. The expression (2.2.27) now identifies the correct boundary Noether charge as being the integral of J_λ with some additional boundary contributions.

Since J_λ is closed for all λ, and is linear in λ, we can go further and compute a local functional, referred to as the Noether-Wald charge, Q_λ such that $J_\lambda = \mathrm{d}Q_\lambda$. With this the Noether charge may be written

$$H[\lambda] = \int_{\partial\Sigma} (Q_\lambda - C_\lambda) \tag{2.2.28}$$

[11] The insufficiency of (2.2.20) alone to ensure the existence of a charge satisfying (2.2.22) is pointed out many placed in the literature. In e.g. [9, 10], integrability conditions are required as we see here and in [11] an auxiliary condition, there eq. (4.16), is required.

which has support only on the boundary of our Cauchy slice. Furthermore, we note that the only place the boundary conditions enter into this expression is through C_λ, as J_λ and Q_λ depend only on the Lagrangian of the theory.

Since the charges (2.2.28) have support only on the boundary, it follows immediately that any gauge transform whose parameters λ have compact support away from any boundaries must produce vanishing Noether charge. The vector fields generating these transformations are thus identified from (2.2.27) as null directions of the presymplectic form which need to be modded out in the symplectic quotient. The non-zero Noether charges generate the large gauge transformations of the theory and are evidently localized to the boundaries of the spacetime. In the case these boundaries are asymptotic, the large gauge transformations are said to be asymptotic symmetries.

2.2.3 Where boundary actions come from

Using the machinery of the covariant phase space we can understand the, rather weak, sufficient conditions for producing boundary modes and gain some insight into the conditions under which the action for the theory is supported exclusively on the boundary. To transform this question into one which is easier to work with we first recall the phase space action. Writing the symplectic form for the theory as $\Omega = \delta\Theta$, the phase space action is given by[12]

$$S[\gamma] = \int_\gamma \Theta - \int_\gamma H_t \mathrm{d}t \tag{2.2.29}$$

where γ is some path through phase space parametrized by t. To orient ourselves it's useful to recall that for point particles $\Theta = p\delta x$ so

$$S = \int p\delta x - \int H_t \mathrm{d}t = \int (p\dot{x} - H_t)\mathrm{d}t \tag{2.2.30}$$

[12]Of course, Θ is not unique. Different Θ correspond to holding different data fixed in the initial and final configurations. For a point particle, $\Theta = p\delta x$ is the correct potential for varying with the initial and final position of the particle held fixed.

where the dot denotes the derivative along the path.

If time translation is a local symmetry, as it is in a diffeomorphism invariant theory, then by Theorem 1 the Hamiltonian generating time translation H_t is supported on the boundary. While this gives a boundary contribution to the action, we would still be left asking about when we receive boundary contributions from Θ and about what happens when time translation is not a local symmetry. We can obtain a better characterization of boundary contributions to the action which will help answer both of these questions by first introducing some notation.

Consider a generic theory with fields ϕ and some gauge group. We denote the action of a gauge group element with gauge parameters[13] α on ϕ by $T_\alpha[\phi]$. For example, if ϕ is a complex scalar field of charge q, $T_\alpha[\phi] = e^{iq\alpha}\phi$. If ϕ is a $U(1)$ connection we would have $T_\alpha[\phi] = \phi + d\alpha$.

Now, we are always free to consider the field redefinition to gauge orbit variables where we pick a class of gauge-fixed configurations $\overline{\phi}$ so a general configuration is in the gauge orbit of some $\overline{\phi}$: $\phi = T_\alpha[\overline{\phi}]$. This separates the prephase space into gauge directions, parametrized by the α, and non-gauge directions, parametrized by the gauge inequivalent $\overline{\phi}$.

In these variables if we write[14] $H_t = \int_\Sigma J_t$, $J_t[\overline{\phi}, \alpha]$ is a local function of α. Since J_t is closed for all functions α, Theorem 1 tells us that we can construct a local potential $Q_t[\overline{\phi}, \alpha]$ such that

$$J_t[\overline{\phi}, \alpha] = J_t[\overline{\phi}, 0] + \mathrm{d}Q_t[\overline{\phi}, \alpha]. \tag{2.2.31}$$

That is to say the current separates into a component we would find if we had immediately fixed the gauge, and a boundary contribution which contains all the effects of the gauge

[13]For later convenience we assume that $\alpha = 0$ is the identity transformation and that these α are free functions on spacetime as might be obtained by exponentiating a Lie algebra about the identity.

[14]In this section only we assume for convenience that J_t has been defined to include all necessary boundary contributions already so H_t is the full Noether charge satisfying (2.2.22).

modes α, though it's notably also free to depend upon boundary excitations in the gauge fixed $\overline{\phi}$ directions. We note that $J_t[\overline{\phi}, 0] = 0$ when time translation is a gauge symmetry.

A similar argument works on the symplectic form. There are only three types of components that can appear in the symplectic form when we go to gauge orbit variables. This fixes the generic form of the symplectic form to be

$$\omega = \omega_{\overline{\phi}\overline{\phi}}[\overline{\phi}, \alpha]\delta\overline{\phi} \wedge \delta\overline{\phi} + \omega_{\overline{\phi}\alpha}[\overline{\phi}, \alpha]\delta\overline{\phi} \wedge \delta\alpha + \omega_{\alpha\alpha}[\overline{\phi}, \alpha]\delta\alpha \wedge \delta\alpha \tag{2.2.32}$$

where the coefficients should generally be understood to contract on any indices we have suppressed in $\delta\overline{\phi}$ and $\delta\alpha$, and may also contain derivatives that operate on the field variations.

Since the $\delta\alpha$ are completely free function in the bulk and $\mathrm{d}\omega = 0$ on-shell by (2.2.19), we may again apply theorem 1 but now using $\delta\alpha$ instead of α as our free functions. We thus conclude[15]

$$\omega = \omega_{\overline{\phi}\overline{\phi}}[\overline{\phi}, \alpha]\delta\overline{\phi} \wedge \delta\overline{\phi} + \mathrm{d}\tilde{\omega}_b[\overline{\phi}, \alpha] \tag{2.2.33}$$

where we have put a tilde on $\tilde{\omega}_b$ because it will not be the complete contribution to the boundary symplectic form. Importantly, $\tilde{\omega}_b$ is a local functional of the fields.

We can go further by invoking theorem 1, this time on the α dependence of $\omega_{\overline{\phi}\overline{\phi}}[\overline{\phi}, \alpha]\delta\overline{\phi} \wedge \delta\overline{\phi}$. The result is evaluating $\omega_{\overline{\phi}\overline{\phi}}$ at $\alpha = 0$ and an additional, locally constructed contribution to the boundary symplectic form:

$$\omega = \omega_{\overline{\phi}\overline{\phi}}[\overline{\phi}, 0]\delta\overline{\phi} \wedge \delta\overline{\phi} + \mathrm{d}\omega_b[\overline{\phi}, \alpha]. \tag{2.2.34}$$

Like with H, the symplectic form separates into a bulk component that we would have found by gauge fixing from the very beginning and a boundary term which encapsulates the entire effect of the gauge symmetry.

[15] Less formally, one can understand that there ultimately cannot be any $\delta\alpha$ components appearing in the bulk or Ω would have non-zero contractions on small gauge transformations.

We can choose both of these terms to be δ closed on phase space separately[16]. It then follows that we can find separate potentials and the symplectic potential current $\mathcal{A}$ breaks up into two terms,

$$\mathcal{A}[\overline{\phi}, \alpha] = \mathcal{A}_M[\overline{\phi}] + \mathrm{d}\mathcal{A}_{\partial M}[\overline{\phi}, \alpha]. \tag{2.2.35}$$

Our arguments about the Hamiltonian and symplectic form together imply that the action must also break up into two terms, one supported on the bulk obtained from gauge fixing, and one supported only on the boundary[17]:

$$S = \int \mathrm{d}t \int_{\Sigma} \Big(i_V \mathcal{A}_M[\overline{\phi}] - J_t[\overline{\phi}, 0] \Big) + \int \mathrm{d}t \int_{\partial\Sigma} \Big(i_V \mathcal{A}_{\partial M}[\overline{\phi}, \alpha] - Q_t[\overline{\phi}, \alpha] \Big) \tag{2.2.36}$$

where V generates the path the action is evaluated on. So all gauge theories will reduce to a bulk component which is gauge fixed, and a boundary term which contains all the dynamics of the boundary gauge modes. Importantly, this boundary action may contain interactions not only among the boundary fields α, but also with the boundary values of the bulk gauge fixed fields $\overline{\phi}$.

2.2.4 Discussion

The result (2.2.36) establishes boundary contributions to the action as a generic feature of gauge theory independent of whether we are able to solve constraints and directly reduce the action to the boundary as in 3d CS theory. But the nature of this boundary action varies

[16]To see this, suppose to the contrary that the variation of the bulk term in (2.2.34) is not δ closed but varies to something spacetime exact, $\delta(\omega_{\overline{\phi}\overline{\phi}}[\overline{\phi}, 0]\delta\overline{\phi} \wedge \delta\overline{\phi}) = \mathrm{d}\omega_M$, which then cancels against part of $\mathrm{d}\delta\omega_b$. This ω_M cannot contain any dependence on α or $\delta\alpha$, so if a cancellation occurs it's sufficient to consider $\alpha = \delta\alpha = 0$. But our use of theorem 1 implies $\omega_b = 0$ in this case, so no cancellation can occur, requiring $\mathrm{d}\omega_M = 0$, and the terms in (2.2.34) are separately closed.

[17]One should be careful to take the orientation of $\partial\Sigma$ in these integrals to be the one induced by writing $(M) = \tau \wedge n \wedge (\partial\Sigma)$ where τ is the normal form to the slices Σ and n is the (outward) normal form to Γ. This is a convention consistent with Stokes theorem, see [11] for more details.

from case to case, the main controlling factor being the structure of the asymptotic symmetry group. For example, Einstein gravity in $\mathrm{AdS}_{D>3}$ with standard asymptotically AdS boundary conditions has a finite dimensional asymptotic symmetry given by the $\mathrm{SO}(D-1,2)$ isometry group of the global AdS vacuum. Thus instead of a boundary field theory we have a boundary quantum mechanics, with one quantum mechanical degree of freedom corresponding to each generator.

To illustrate this we consider the even simpler case of pure Maxwell theory in asymptotically flat space. The phase space variables are $(\vec{A}, \vec{E})$ subject to the Gauss law constraint $\vec{\nabla} \cdot \vec{E} = 0$, and we impose that these vanish at spatial infinity. The symplectic form is $\Omega \sim \int_\Sigma \delta\vec{E} \cdot \wedge \delta\vec{A}$. This symplectic form together with the boundary conditions require that the gauge parameters $\alpha(\vec{x})$ become spatially constant at infinity. Writing $\vec{A} = \vec{\bar{A}} + \vec{\nabla}\alpha$, we have

$$\Omega \sim \int_{\partial\Sigma} \vec{n} \cdot \delta\vec{E} \wedge \delta\alpha \sim \delta Q \wedge \delta\alpha \tag{2.2.37}$$

where Q is the total electric charge. As the Hamiltonian has no dependence on α, the boundary action is simply $S_\alpha = \int dt Q\dot{\alpha}$, whose equation of motion is simply charge conservation. This boundary contribution is actually familiar in another guise. In particular, consider the Euclidean theory with periodic imaginary time, $t \cong t + \beta$. Since Q is constant on-shell we have $S_\alpha = Q \int dt\dot{\alpha} \equiv \beta\mu Q$, which identifies the boundary mode α as being proportional to the chemical potential.

Turning now to the case of an infinite dimensional asymptotic symmetry group, here we do expect to get a boundary field theory. This boundary field theory may either be a free theory, as in $U(1)$ CS theory, or interacting, as in non-Abelian CS theory or 3D gravity. In general, it's clear that the existence of interactions is closely tied to the bulk theory having a non-Abelian asymptotic symmetry group.

We may also ask more practically how to compute (2.2.36). In principle, once we go to gauge orbit variables all stages of the calculation here are algorithmic as reviewed in

Appendix A.2. But to use the gauge orbit variables we would first need to classify the gauge-inequivalent solutions. Since we are working in a canonical formulation it would be sufficient to find all gauge-inequivalent initial data, but that would still mean solving the constraints of the theory explicitly.

Instead, one could could imagine taking $\overline{\phi}$ to be some perhaps incomplete class of initial data solving the constraints and consider the dynamics of this subspace of the full phase space. For example by considering a special subspace such as a moduli space of black hole solutions.

The logical extreme of these ideas would be to take $\overline{\phi}$ to be a single solution, so we are looking at the gauge orbits about a background configuration. In this case $\delta\overline{\phi} = 0$ and $A_M = 0$ so the entire symplectic form lives on the boundary. This simplification allows more efficient computational methods than the gauge orbit variable strategy described above. Three such methods are described in the next section.

2.3 Computing Gauge Orbit Actions

As discussed in Section 2.2.4, we may have reason to consider only certain sectors of a theory. The particular case of interest here is where we consider a single gauge fixed configuration $\overline{\phi}$ and orbits around it. This means $\delta\overline{\phi} = 0$ and $\mathcal{A}_M = 0$. The remainder of the bulk term in the action (2.2.36) then integrates to some constant and we are left with only the boundary contribution to the action and more efficient methods of calculation are available to us. This section is concerned with describing three such methods.

The first is less generically applicable, but very efficient when it applies as it directly computes $\mathcal{A}_{\partial M}$ instead of the boundary symplectic form ω_b. The other two methods are concerned with computing ω_b and are based on the existence of a particular 1-form valued vector field on phase space.

It's important to note that as $\delta\overline{\phi} = 0$ suggests, these methods treat $\overline{\phi}$ as a background field so any components $\mathcal{A}_{\partial M}$ might have had in the $\delta\overline{\phi}$ directions will not be captured by these computations.

2.3.1 The momentum method

For all the 3D gravity examples considered in this work there exists a very efficient method for deducing the boundary action [15]. We describe it here in general terms.

Supposing that expressions for boundary charges H_ξ are known, to write down the boundary action we require knowledge of the boundary symplectic potential Θ, defined via $\Omega = \delta\Theta$. A direct approach to obtaining it is to first extract Ω via the relation $i_{V_\xi}\Omega = -\delta H_\xi$, and then compute Θ by solving $\delta\Theta = \Omega$. We now discuss how, under suitable assumptions, we can write down the solution for Θ directly, bypassing the laborious procedure just mentioned. This method was used in the case of cutoff AdS_3 gravity [15].

We consider a boundary with a single spatial dimension with coordinate x, which may live either on the circle or line. The boundary field theory variables are written as (Φ, Ψ), where Ψ could stand for a collection of fields. On the circle or line, these fields are taken to obey periodic boundary conditions or vanish at infinity respectively. Under phase space vector fields V_ξ, which we can think of as reparametrizations of x, the fields transform as

$$\begin{aligned}\delta_\xi\Phi &= i_{V_\xi}\delta\Phi = \xi + \Phi'\xi \\ \delta_\xi\Psi &= i_{V_\xi}\delta\Psi = \Psi'\xi\end{aligned} \tag{2.3.1}$$

where $' = \partial_x$. The inhomogeneous term in $\delta_\xi\Phi$ corresponds to Φ being the field associated with x-reparametrizations. Now suppose that the charge corresponding to constant ξ (we take $\xi = 1$ and denote this charge by P) is constrained to take the form

$$P = \int \mathrm{d}x \left[\kappa_{\Phi\Phi}\Phi'^2 + \kappa_{\Phi\Psi}\Phi'\Psi' + \kappa_{\Psi\Psi}\Psi'^2 + P_\Phi'\Phi' + P_\Psi'\Psi'\right] \tag{2.3.2}$$

where the κ's are constant and the functions (P_Φ, P_Ψ) are local functions of $(\Phi', \Phi'', \ldots; \Psi', \Psi'', \ldots)$, i.e. do not depend on undifferentiated fields. The basic result is that up to a δ-exact term, the unique Θ which solves

$$i_{V_\xi}\Omega = -\delta P \ , \quad \xi = 1 \tag{2.3.3}$$

is given by

$$\Theta = \int \mathrm{d}x \left[\kappa_{\Phi\Phi}\Phi'\delta\Phi + \kappa_{\Phi\Psi}\Phi'\delta\Psi + \kappa_{\Psi\Psi}\Psi'\delta\Psi + P'_\Phi\delta\Phi + P'_\Psi\delta\Psi\right] \ . \tag{2.3.4}$$

To prove this, we first note that it is straightforward to verify that (2.3.3) is satisfied, so only the question of uniqueness remains. To analyze uniqueness we consider a correction to the symplectic form,

$$\Delta\Omega = \int \mathrm{d}x \left[\delta X'_\Phi \wedge \delta\Phi + \delta X'_\Psi \wedge \delta\Psi\right] \ , \tag{2.3.5}$$

where the functions (X_Φ, X_Ψ) are constrained to obey the same general properties of (P_Φ, P_Ψ). We compute

$$\begin{aligned} i_{V_\xi}\Delta\Omega &= \delta \int \mathrm{d}x \left[X'_\Phi\Phi' + X'_\Psi\Psi'\right] \\ &= -\delta \int \mathrm{d}x \left[X''_\Phi\Phi + X''_\Psi\Psi\right] \end{aligned} \tag{2.3.6}$$

We need this to vanish in order not to spoil (2.3.3). Vanishing of the integrand in the second line of (2.3.6) requires $X''_\Phi = X''_\Psi = 0$, since the two terms cannot cancel each other under the assumed form of (X_Φ, X_Ψ). However, this implies that (X'_Φ, X'_Ψ) are constants, which implies that $\delta X'_\Phi = \delta X'_\Psi = 0$, so that $\Delta\Omega = 0$. The remaining possibility is that the integrand in (2.3.6) is a total derivative. This requires $X'_\Phi = \frac{\delta F}{\delta \Phi}$ and $X'_\Psi = \frac{\delta F}{\delta\Psi}$ for some F. However, this leads to $\Delta\Omega = \int \mathrm{d}x\delta^2 F = 0$, so we again get no contribution.

The upshot is that just from consideration of P we are led to a unique result for Ω and an explicit result for its potential Θ. It follows, assuming that our underlying theory is consistent, that this Ω will solve $i_{V_\xi}\Omega = -\delta H_\xi$ for all large gauge transformations V_ξ, as can of course be checked in specific examples.

We conclude this section with comments on the assumed structure (2.3.2), which follows from a particular gauge invariance. To make the discussion concrete we consider the boundary theory in the context of pure gravity in AdS_3. Setting $\kappa = 0$ corresponds to the orbit built on a pure AdS_3 background. This background is invariant under isometries that act as translations, boosts, and dilatations on the boundary coordinates. Taking the functions (Φ, Ψ) to be general linear functions of x corresponds to acting on the background by one of these isometries; since this does nothing to the background such functions are pure gauge, and so all charges must vanish for such functions. This implies that only derivatives of such functions can appear in P, and that each term must contain at least one second derivative. This leads to (2.3.2), possibly after integrating by parts. The same comments apply to $\Delta\Omega$. Turning on κ, which corresponds to a nonzero mass AdS_3 background, breaks some of the isometries, allowing the quadratic terms like $\kappa_{\Phi\Phi}\Phi'^2$ to appear. In fact, a more general expression like $\kappa_{\Phi\Phi}\Phi'^n$ for some $n > 2$ might also be anticipated, but only the $n = 2$ case will arise in our examples. This is important, since the logic leading to (2.3.4) no longer holds for the $n > 2$ case. In fact, given the simple form of the κ dependent part of that charges will arise, it's easy to write down the corresponding contribution to the boundary action by inspection.

2.3.2 The transfer field

Consider a variation of our fields in the gauge orbit variables $\phi = T_\alpha[\overline{\phi}]$, as in Section 2.2.3. Since we are taking $\overline{\phi}$ to be fixed, the variation can only change α. But since ϕ is constructed by applying a gauge group element to the configuration $\overline{\phi}$, this variation must be equivalent to the action of some Lie algebra element on ϕ.

The situation is essentially identical to the story which comes up when studying spontaneous symmetry breaking, in particular the broken part of the symmetry group's non-linear action on Nambu-Goldstone bosons when studying spontaneous symmetry breaking, see for example [16, 17]. The idea is that $\delta\alpha$ defines a Lie algebra element at the origin of the gauge group while $\overline{\phi}$ has been transported to g. So to perform the variation of ϕ we need to transport $\delta\alpha$ to the tangent space at g. Schematically, we can think of this as inserting the identity in the action on $\overline{\phi}$ to write

$$\delta\phi = (\delta T_g)[\overline{\phi}] = (\delta T_g T_g^{-1})[\phi] \tag{2.3.7}$$

so the variation of ϕ is equivalent to the action of this Lie algebra element valued as a 1-form on phase space.

Since Lie algebra elements are the generators of group transformations, there must exist some W which implements the action of this Lie algebra element. Because the algebra element is valued as a 1-form on phase space, W must be a $(1,1)$ tensor on phase space, which we think of as a 1-form valued vector field and refer to as the transfer field. This gives W the very special defining property

$$\delta\phi = i_W \delta\phi. \tag{2.3.8}$$

While the property (2.3.8) is ultimately the formal property we will exploit to compute the boundary symplectic form, we will also need to explicitly compute the transfer field. So it will be useful to see how the rather abstract discussion above can be realized in some simple examples.

The simplest example is of a $U(1)$ connection $A = \overline{A} + \mathrm{d}\alpha$. Here we have explicitly

$$\delta A = \mathrm{d}\delta\alpha = i_{V_{\delta\alpha}} \delta A \tag{2.3.9}$$

so $W = V_{\delta\alpha}$ implements the gauge transformation with gauge parameter $\delta\alpha$, as might be expected for an Abelian group where translating $\delta\alpha$ is trivial.

The next simplest case is where A is a connection for some non-Abelian group. Now the gauge orbit is $A = g^{-1}\overline{A}g + g^{-1}\mathrm{d}g$. Here $g = g(\alpha)$ is defined by the exponential map. For simplicity we could take $g = \exp(\alpha)$ with α valued in the Lie algebra. We may now write

$$\delta A = [A, g^{-1}\delta g] + \mathrm{d}(g^{-1}\delta g) = i_{V_{g^{-1}\delta g}} \delta A \tag{2.3.10}$$

so $W = V_{g^{-1}\delta g}$ generates a gauge transformation with 1-form valued gauge parameter $g^{-1}\delta g$. We also note that this examples gives a concrete realization of the schematic manipulation (2.3.7).

As a final example of W for this section, we consider diffeomorphisms. Take the diffeomorphism to be $y^\alpha = f^\alpha(x)$ and consider for simplicity the diffeomorphism orbit of a scalar field $\phi(x) = \overline{\phi}(f(x))$. Taking the variation of this scalar field,

$$\begin{aligned}
\delta\phi &= \delta f^\alpha(x) \frac{\partial\overline{\phi}(y)}{\partial y^\alpha}\Big|_{y=f(x)} \\
&= \delta f^\alpha(x) \frac{\partial x^\mu}{\partial y^\alpha}\Big|_{y=f(x)} \frac{\partial\overline{\phi}(f(x))}{\partial x^\mu} \\
&= \mathcal{L}_\xi \phi
\end{aligned} \tag{2.3.11}$$

so the variation is equivalent to the action of the Lie derivative with respect to the 1-form valued (spacetime) vector field[18]

$$\xi^\mu = \frac{\partial(f^{-1})^\mu}{\partial y^\alpha}\Big|_{f(x)} \delta f^\alpha(x). \tag{2.3.12}$$

Hence $W = V_\xi$. This fact was also noted in [11] where it was used to circumvent some technical difficulties in JT gravity.

With these examples in mind, there is one additional property of W which will be important going forward. Denote by w the Lie algebra element whose action W generates. In our examples we have $w = \delta\alpha$ for the $U(1)$ gauge group, $w = g^{-1}\delta g$ for the non-Abelian gauge group, and for diffeomorphisms we have (2.3.12).

Importantly, this w is some functional of $\delta\alpha$. Equally as important, this functional need not be invertible as can be seen in the non-Abelian example[19]. This will be important going forward because to apply Theorem 1 we need free functions. In our setup $\delta\alpha$ are free, but w may or may not be, depending on the details of the gauge group. For example, the relation between δf and ξ in (2.3.12) remains invertible despite diffeomorphisms being non-Abelian.

[18] In practical calculations, it is much simpler to move the Jacobian factor to the left and compute the variation of f by a diffeomorphism, then defining ξ by inverting the Jacobian. This is the approach taken in the examples of Sections 2.3.5.2 and 2.3.5.3.

[19] Invertibility fails for the same reason $A = g^{-1}\mathrm{d}g$ is not invertible for $\mathrm{d}\alpha$: if A is not flat no such $\mathrm{d}\alpha$ exists.

While the relation between w and $\delta\alpha$ is not invertible, it is injective, and hence is invertible on the image of all $\delta\alpha$. This means δw may always be expressed in terms of only w again. We can see this in our examples. The $U(1)$ case is uninteresting because $\delta w = 0$, but in the non-Abelian case we find

$$\delta w = \delta(g^{-1}\delta g) = -(g^{-1}\delta g) \wedge (g^{-1}\delta g) = -w \wedge w, \tag{2.3.13}$$

so the general invertibility of $w(\delta\alpha)$ is unimportant to this rewriting of δw, as claimed.

The example of diffeomorphisms is slightly more complicated, but nonetheless can be worked out to find

$$\delta\xi^\mu = \xi^\nu \wedge \nabla_\nu \xi^\mu, \tag{2.3.14}$$

assuming we are working with a torsionless connection so the affine part of the covariant derivative does not contribute to this expression.

2.3.3 The transfer field method

Now that we have an understanding of the transfer field W, we can give a technique for computing the boundary symplectic form. From the definition (2.2.18), it would clearly be sufficient to show that the bulk $\delta\theta$ term is a total derivative. We may use the transfer field to write

$$\theta = i_W \theta \tag{2.3.15}$$

since in every term of θ, the 1-form factor can be replaced as in (2.3.8).

Since W generates the action of the Lie algebra element w, it follows that

$$\theta = i_W \theta = J_w + k_w \tag{2.3.16}$$

where J_w is the Noether current (2.2.21) associated to the gauge transformation generated by w and k_w is defined by (2.2.20).

But as discussed in Section 2.2.2, $J_w = \mathrm{d}Q_w$ and hence

$$\omega = \delta\theta - \mathrm{d}\delta B = \delta k_w + \mathrm{d}\delta(Q_w - B). \tag{2.3.17}$$

So to find ω_b it is sufficient to find a potential for δk_w by solving $\delta k_w = \mathrm{d}\tilde{k}_w$.

Since by (2.2.19) we have $\mathrm{d}\omega = 0$ on-shell, we must also have $\mathrm{d}\delta k_w = 0$[20]. Now δk_w depends on the free functions[21] $\delta\alpha$ so we may apply theorem 1 to conclude the existence of a locally constructed $\tilde{k}_w$.

It should be commented that while $\delta\alpha$, and the fact that $\delta\alpha = 0$ corresponds to the identity, ensures the existence of $\tilde{k}_w$, it would be more computationally efficient to use w as the free function whenever possible. This can be done when the relation between w and $\delta\alpha$ is invertible, as discussed in the previous section. The invertibility in the case of diffeomorphisms will be leveraged in Section 2.3.5.2.

Hence we have found

$$\omega_b = \tilde{k}_w + \delta(Q_w - B) \tag{2.3.18}$$

which has the advantage of cleanly separating the boundary condition dependence of ω_b into the δB term since $\tilde{k}_w$ and Q_w depend only on the Lagrangian.

This technique is straightforward to apply to $U(1)$ CS theory on $D \times \mathbb{R}$ with chiral boundary conditions. We recall for this theory (2.2.16), note $k_\lambda = k\lambda \mathrm{d}A$, and consider a solution $\overline{A}$ to the equations of motion, so $\mathrm{d}\overline{A} = 0$. The gauge orbit around this solution is then $A = \overline{A} + \mathrm{d}\alpha$. As discussed in the previous section we have $w = \delta\alpha$.

[20] We could also argue more directly that $\delta \mathrm{d}k_w = \delta i_W \delta L = \delta^2 L = 0$ since $i_W \delta L = \delta L$ by (2.3.8).

[21] In general, the imposition of boundary conditions will restrict what functions α we allow ourselves to consider near the boundary. However, the only place the boundary conditions enter in these arguments is through B, and in particular the closure of δk_w requires no reference to boundary conditions. So we should imagine performing these manipulations before imposing any boundary conditions which would then restrict the allowed $\delta\alpha$.

Since $k_\lambda = 0$ on-shell in this theory, we have $\tilde{k}_w = 0$. Then following (2.3.18), the boundary symplectic form must be

$$\omega_b = \delta Q_w = k \delta A \wedge \delta\alpha \tag{2.3.19}$$

where we have used $B = 0$. This integrates to

$$\Omega = k \int_0^{2\pi} \mathrm{d}\phi \, \partial_\phi \delta\alpha \wedge \delta\alpha \tag{2.3.20}$$

and produces the usual Kac-Moody algebra (3.3.24) expected for $U(1)$ CS theory on the disk. Using the Hamiltonian (3.3.15) and the phase space action (2.2.36) we reproduce the expected boundary action (3.3.50).

2.3.4 Computing Ω from the Noether charges

In the previous section we were able to leverage the transfer field to write (2.3.15). It's simple to see that this generalizes to any 1-form on the gauge orbit, not just θ. With some additional though we can go beyond 1-forms and obtain a similar result for any p-form on the orbit.

To see how this works, consider $i_W(\delta\phi^a \wedge \delta\phi^b)$ where we have restored the indices a and b labeling our fields. Computing the contraction we find

$$\begin{aligned} i_W(\delta\phi^a \wedge \delta\phi^b) &= (i_W \delta\phi^a) \wedge \delta\phi^b + \delta\phi^a \wedge (i_W \delta\phi^b) \\ &= 2\delta\phi^a \wedge \delta\phi^b \end{aligned} \tag{2.3.21}$$

where in the second line we have used the defining relation (2.3.8) for W. It's important to keep track of the sign on the second term because W is 1-form valued and must be commuted past the first factor.

With this sign understood, the generalization to a form of any degree is immediate: we simply march through the factors in the wedge product to perform the contraction and then use the definition of W to rewrite the contraction back in terms of the original form. Hence, for any p-form Z on phase space we have the generalized identity

$$i_W Z = pZ. \tag{2.3.22}$$

We can leverage this to very efficiently compute the boundary symplectic form ω_b on the gauge orbit directly from the Noether charges. The key is to observe that the contraction on an arbitrary 2-form may be rewritten into the form

$$i_W(\delta\phi^a \wedge \delta\phi^b) = -\left[\delta\phi^b \wedge (i_W\delta\phi^a) - \delta\phi^a \wedge (i_W\delta\phi^b)\right]. \tag{2.3.23}$$

That is, if we make sure to commute the contracted part to the right of the expression, we obtain the negative of the expression we would have found if W was not valued as a 1-form.

It follows that if we compute $i_W\Omega$ and make sure to commute all the contractions to the right, we must obtain

$$i_W\Omega = +(\delta H[\tilde{w}])|_{\tilde{w}=w} \tag{2.3.24}$$

since we have already argued that W generates the action of a Lie algebra element. Note that on the right hand side we compute the variation of H before evaluating at the gauge parameter w. This is because w enters through the contraction on the right and so clearly cannot have a variation applied to it.

Combining this with our general observation (2.3.22) it follows that the symplectic form on the gauge orbit is given by

$$\Omega = \frac{1}{2}(\delta H[\tilde{w}])|_{\tilde{w}=w} \tag{2.3.25}$$

where the expression on the right should be understood as placing all factors of w to the right of any variations, and the variation taken treating $\tilde{w}$ as an arbitrary, but not 1-form valued, Lie algebra element. One must be cautious not to interpret (2.3.25) as meaning $\Theta = \frac{1}{2}H[w]$. The order in which the variation and the evaluation at $\tilde{w} = w$ occur are important for this result, as will be seen our examples in Section 2.3.5.

We may again revisit our $U(1)$ CS example to demonstrate this approach. Indeed, looking at (2.3.19) we can already see the basic structure of (2.3.25) since $B = 0$ with our chiral boundary conditions. But going through the details to make sure the coefficients come out correct, particularly since (2.3.19) uses the Noether current and not the complete Noether charge, we start with the charges (3.3.15). Then (2.3.25) tells us to vary the charge, treating $\tilde{w}$ as any large gauge parameter in the theory, which generally may mean it's state-independent or some state-dependent function of some other parameters determining the large gauge transformations. Here there are no such complications as $\tilde{w}$ is state-independent and we find

$$\frac{1}{2}\delta H[\tilde{w}] = k\int_0^{2\pi} \tilde{w}\delta A_\phi \mathrm{d}\phi. \tag{2.3.26}$$

The final step in computing (2.3.25) is to evaluate this charge at $\tilde{w} = w \equiv \delta\alpha$. But when we do so, we must make sure that we first move all $\tilde{w}$ factors to the right of δA_ϕ. Doing so,

$$\Omega = k\int_0^{2\pi} \mathrm{d}\phi \delta A_\phi \wedge \delta\alpha = k\int_0^{2\pi} \mathrm{d}\phi \partial_\phi \delta\alpha \wedge \delta\alpha \tag{2.3.27}$$

which again matches the expected Kac-Moody expression (3.3.50).

2.3.5 Examples

Here we apply our methods to three examples. First we consider $U(1)$ CS theory in $D = 5$. This theory, with our chosen boundary conditions, is only marginally more complex than the example of $U(1)$ CS theory in $D = 3$ that we have been considering. It is also simple enough that we are able to implement the manipulations in Section 2.2.3 to find (2.2.34) with non-gauge directions included.

In Sections 2.3.5.2 and 2.3.5.3 we consider Einstein-Hilbert gravity in $D = 3$ with two different sets of boundary conditions. First we consider standard asymptotically AdS_3 boundary conditions and then the boundary conditions described in [18]. The latter are designed to produce a theory similar to what we will see in topologically massive gravity, considered in Section 2.4.

Finally, we mention that the example of $SU(2)$ CS theory in $D = 3$ is considered in Appendix A.4. There we also show that the results of our methods match the standard results expected from the CS/WZW correspondence.

2.3.5.1 U(1) CS in $D = 5$

As a first example which isn't quite as trivial as $U(1)$ CS in $D = 3$ we consider $U(1)$ CS in $D = 5$. Since we work near the boundary the details of the bulk geometry are irrelevant. We fix the boundary geometry, though the details of this geometry will not be paramount to most of our manipulations, to be $\mathbb{R} \times S^1 \times S^2$. On the boundary we choose coordinates x^i, $i = 1, 2, 3, 4$ with x^1 the coordinate on the $\mathbb{R}$, which we think of as time, x^2 the angular coordinate on S^1, and x^3, x^4 some coordinates on the S^2. To make contact with the $D = 3$ CS theory, it will sometimes be useful to write $t \equiv x^1$ and $\phi \equiv x^2$.

For this example we choose our boundary conditions to fix A_3 and A_4 to be arbitrary functions of x^3 and x^4 on the boundary while we fix $A_1 = A_2$ to be an arbitrary function of x^1 and x^2. This will allow us to draw parallels to $U(1)$ CS in $D = 3$ on the cylinder in the final result. It is useful to note that with these boundary conditions the only non-zero boundary components of F are F_{12}, which depends dynamically on A_1 (and hence A_2), and F_{34} which is a fixed function of only x^3 and x^4.

The Lagrangian for this theory is

$$L = A \wedge F \wedge F \tag{2.3.28}$$

which varies to produce

$$\delta L = 3F \wedge F \wedge \delta A - 2\mathrm{d}(F \wedge A \wedge \delta A). \tag{2.3.29}$$

Thus the equations of motion, $F \wedge F = 0$, do not imply that all solutions are flat connections. Considering the condition (2.2.15), we see that our chosen boundary conditions allow us to choose $\ell = B = 0$.

Since $B=0$, the full symplectic current for the theory is given by

$$\omega = -2\delta(F\wedge A)\wedge\delta A. \tag{2.3.30}$$

Now, this theory is sufficiently simple that we are able to explicitly carry out the gauge-orbit described in Section 2.2.3. We suppose $\overline{A}$ is some solution to the equations of motion and we consider the gauge orbits around this configuration, $A=\overline{A}+\mathrm{d}\alpha$. It's straightforward to find

$$\omega = -2\delta(\overline{F}\wedge\overline{A})\wedge\delta\overline{A} - 2\mathrm{d}[\delta(\alpha\overline{F})\wedge\mathrm{d}\delta\alpha + \delta(\alpha\overline{F})\wedge\delta\overline{A} - \delta(\overline{F}\wedge\overline{A})\wedge\delta\alpha] \tag{2.3.31}$$

so we realize the expected split into the gauge-fixed part and the boundary part depending on the large gauge transformations parametrizing the orbit. Here we can also see that the boundary component of the symplectic form supports components which mix variations in the gauge-fixed configuration with variations along the orbit. Indeed, there is even a component which involves no variations of α.

But here we are interested only in the components along the orbit directions, so we take $\delta\overline{A}=0$ to find

$$\omega_b = -2\overline{F}\delta\alpha\wedge\mathrm{d}\delta\alpha. \tag{2.3.32}$$

Integrating this over the boundary and using our boundary conditions the full symplectic form on the orbit is given by

$$\begin{aligned}\Omega &= -2\int_{\partial\Sigma}\overline{F}_{34}\delta\alpha\wedge\partial_2\delta\alpha\mathrm{d}x^2\wedge\mathrm{d}x^3\wedge\mathrm{d}x^4\\ &= 2\left(\int_{S^2}\overline{F}\right)\int_0^{2\pi}\partial_\phi\delta\alpha\wedge\delta\alpha\mathrm{d}\phi.\end{aligned} \tag{2.3.33}$$

Because we have chosen our boundary conditions to factor the S^2 from the $\mathbb{R}\times S^1$, we obtain the same Kac-Moody symplectic form as would be expected from the $U(1)$ CS theory on the cylinder, but now with an effective level set by our boundary conditions via the magnetic flux through the S^2.

Using that the Hamiltonian generating time evolution is

$$
\begin{aligned}
H_t &= 2\int_{\partial\Sigma} \overline{F}_{34} A_2^2 \mathrm{d}x^2 \wedge \mathrm{d}x^3 \wedge \mathrm{d}x^4 \\
&= 2\left(\int_{S^2} \overline{F}\right) \int_0^{2\pi} (\overline{A}_\phi + \partial_\phi \alpha)^2 \mathrm{d}\phi.
\end{aligned} \tag{2.3.34}
$$

Constructing the phase space action via (2.2.36) we thus find

$$
S = 2\left(\int_{S^2} \overline{F}\right) \int \left[\partial_\phi \alpha \left(\partial_t \alpha - \partial_\phi \alpha - 2\overline{A}_\phi\right) - \overline{A}_\phi^2\right] \mathrm{d}t\mathrm{d}\phi. \tag{2.3.35}
$$

Since we have restricted ourselves to the gauge orbit, α is our only dynamical variable in this action and, in particular, this means the final $\overline{A}_\phi^2$ term can be dropped as an additive constant to the action. In this example it's possible to observe explicitly from (2.3.31) that, had we not restricted to the gauge orbit of some fixed $\overline{A}$, the $\overline{A}_\phi$ terms here would represent an explicit coupling between the bulk, $\overline{A}$, and boundary, α, degrees of freedom.

This result can, of course, also be obtained by the techniques introduced in the previous sections. Taking first the approach of Section 2.3.3 we note that

$$
i_{V_\lambda} \delta L = \mathrm{d}\lambda \wedge F \wedge F = \mathrm{d}(\lambda F \wedge F) \tag{2.3.36}
$$

so k_λ vanishes on-shell and will make no contribution. For the other ingredient, we calculate

$$
J_\lambda = i_{V_\lambda}\theta - k_\lambda = 2\mathrm{d}(\lambda A \wedge F). \tag{2.3.37}
$$

Thus, since $B = 0$ with our chosen boundary conditions, we find from (2.3.19)

$$
\omega_b = 2\delta(A \wedge F) \wedge \delta\alpha = 2\mathrm{d}\delta\alpha \wedge \overline{F} \wedge \delta\alpha \tag{2.3.38}
$$

since $w = \delta\alpha$ for the $U(1)$ orbit, matching (2.3.32). From this point, imposing the boundary conditions to find the true symplectic form (2.3.33), and hence the action (2.3.35), is unchanged.

If we instead took the route of Section 2.3.4 we would need to compute the full Noether charges

$$
H[\lambda] = 4\left(\int_{S^2} \overline{F}\right) \int_{S^1} \lambda A \tag{2.3.39}
$$

which requires that we use the boundary conditions to obtain. For example, that we fix A_3 and A_4 completely on the boundary tells us that $\lambda = \lambda(x^1, x^2)$. The formulation (2.3.25) now tells us to write

$$\Omega = 2\left(\int_{S^2} \overline{F}\right) \int \delta A \wedge \delta\alpha. \tag{2.3.40}$$

Writing this explicitly in coordinates and with $\delta A = \delta \mathrm{d}\alpha$ this clearly reproduces (2.3.33) and the rest of the boundary action story follows.

2.3.5.2 Asymptotically AdS$_3$ Einstein-Hilbert gravity

As a second example, we can derive the Alekseev-Shatashvili symplectic form [19] for asymptotically AdS$_3$ Einstein-Hilbert gravity. All three approaches can be worked out in this example. We start by recalling some facts this theory.

The action and canonical 1-form for this theory are given by

$$L = \frac{1}{16\pi G}\sqrt{-g}(R+2)\mathrm{d}^3x, \qquad \theta = \frac{1}{16\pi G}\sqrt{-g}(\nabla^\nu \delta g_{\lambda\nu} - g^{\mu\nu}\nabla_\lambda \delta g_{\mu\nu})(\mathrm{d}^2x)^\lambda. \tag{2.3.41}$$

Where expressions are more conventionally expressed in terms of the Brown-Henneaux central charge we write $c = 3/2G$. We will also need later that

$$k_\xi = i_\xi L = -\frac{1}{4\pi G}\sqrt{-g}\xi^\mu(\mathrm{d}^2x)_\mu \tag{2.3.42}$$

where we have used the equations of motion to simplify things.

In Fefferman-Graham coordinates the asymptotically AdS$_3$ solutions to the equations of motion are given by the Bañados metrics [20]

$$\mathrm{d}s^2 = \frac{\mathrm{d}\rho^2}{4\rho^2} + \frac{1}{\rho}(\mathrm{d}w + \rho\overline{L}(\overline{w})\mathrm{d}\overline{w})(\mathrm{d}\overline{w} + \rho L(w)\mathrm{d}w) \tag{2.3.43}$$

where $w = \phi + t$ and $\overline{w} = \phi - t$ are convenient coordinates on the boundary and $\rho > 0$ is the radial coordinate such that the boundary is located at $\rho = 0$. Note that $\overline{w}$ is not the complex conjugate of w as we are working in Lorentzian signature. The boundary stress tensor associated to these metrics is given by

$$T_{ww} = -\frac{1}{4G}L, \quad T_{\overline{w}\overline{w}} = -\frac{1}{4G}\overline{L}, \quad T_{w\overline{w}} = 0. \tag{2.3.44}$$

The asymptotic vector fields which preserve the boundary conditions are

$$\xi^w = \epsilon(w) - \frac{1}{2}\partial_{\overline{w}}^2\overline{\epsilon}(\overline{w})\rho + \mathcal{O}(\rho^2) \tag{2.3.45}$$

$$\xi^{\overline{w}} = \overline{\epsilon}(\overline{w}) - \frac{1}{2}\partial_w^2\epsilon(w)\rho + \mathcal{O}(\rho^2) \tag{2.3.46}$$

$$\xi^\rho = \left(\partial_w\epsilon(w) + \partial_{\overline{w}}\overline{\epsilon}(\overline{w})\right)\rho + \mathcal{O}(\rho^0), \tag{2.3.47}$$

where $\epsilon(w)$ and $\overline{\epsilon}(\overline{w})$ are free functions labeling the vector field. While these vector fields do not change the conformal metric on the boundary, they do change the components subleading in ρ, and hence the stress tensor by

$$i_{V_\xi}\delta T_{ww} = 2T_{ww}\epsilon' + T'_{ww}\epsilon + \frac{c}{12}\epsilon''' \tag{2.3.48}$$

$$i_{V_\xi}\delta T_{\overline{w}\overline{w}} = 2T_{\overline{w}\overline{w}}\overline{\epsilon}' + T'_{\overline{w}\overline{w}}\overline{\epsilon} + \frac{c}{12}\overline{\epsilon}'''. \tag{2.3.49}$$

The charges associated with the diffeomorphisms are then easily constructed by

$$H[\xi] = -\frac{1}{2\pi}\int_0^{2\pi}(T_{ww}\epsilon - T_{\overline{w}\overline{w}}\overline{\epsilon})\mathrm{d}\phi. \tag{2.3.50}$$

Going to the gauge orbit means integrating up the variations (2.3.48) under an infinitesimal diffeomorphism to a finite one. If the finite diffeomorphism on the boundary is given by

$$w' = f(w), \quad \overline{w}' = \overline{f}(\overline{w}) \tag{2.3.51}$$

then we have

$$T_{ww} = \frac{c}{12}\left(\frac{\kappa}{2}f'^2 + \{f, w\}\right), \quad T_{\overline{w}\overline{w}} = \frac{c}{12}\left(\frac{\overline{\kappa}}{2}\overline{f}'^2 + \{\overline{f}, \overline{w}\}\right) \tag{2.3.52}$$

where the Schwarzian derivative is

$$\{f, w\} = \frac{f'''}{f'} - \frac{3}{2}\frac{f''^2}{f'^2}. \tag{2.3.53}$$

In this orbit, the diffeomorphism $f(w) = w$ and $\overline{f}(\overline{w}) = \overline{w}$ evidently produces constant $T_{ww}, T_{\overline{w}\overline{w}}$. The κ and $\overline{\kappa}$ parametrize what this constant value is, and thereby parametrize the diffeomorphism inequivalent metrics (2.3.43). The case $\kappa = \overline{\kappa} = 1$ produces global AdS.

At $\rho = 0$, (2.3.45) defines a diffeomorphism on the boundary which acts on the f and $\overline{f}$ as

$$i_{V_\xi}\delta f = f'\epsilon, \qquad i_{V_\xi}\delta\overline{f} = \overline{f}'\overline{\epsilon}. \tag{2.3.54}$$

This can be obtained by composing two diffeomorphisms and we may also verify that this transformation rule is compatible with (2.3.48) and (2.3.52) together. Since we have the momentum written down now as

$$P = H[\partial_\phi] = -\frac{c}{24\pi}\int_0^{2\pi} \mathrm{d}\phi \left[\left(\frac{\kappa}{2}f' - \frac{1}{2}\left(\frac{1}{f'}\right)''\right)f' - \left(\frac{\overline{\kappa}}{2}\overline{f}' - \frac{1}{2}\left(\frac{1}{\overline{f}'}\right)''\right)\overline{f}'\right] \tag{2.3.55}$$

where we have used that $\{f, w\} = -\frac{1}{2}\left(\frac{1}{f'}\right)'' f'$ up to addition of total derivatives, we may observe that it takes the form (2.3.2) required for the momentum method.

It therefore follows that the canonical 1-form is given by

$$\Theta = -\frac{c}{24\pi}\int_0^{2\pi} \mathrm{d}\phi \left[\left(\frac{\kappa}{2}f' - \frac{1}{2}\left(\frac{1}{f'}\right)''\right)\delta f - \left(\frac{\overline{\kappa}}{2}\overline{f}' - \frac{1}{2}\left(\frac{1}{\overline{f}'}\right)''\right)\delta\overline{f}\right]. \tag{2.3.56}$$

The variational of this potential can indeed be massaged into the more standard form

$$\Omega = -\frac{c}{48\pi}\int_0^{2\pi}\left[\left(\frac{\delta f' \wedge \delta f''}{f'^2} - \kappa\delta f \wedge \delta f'\right) - \left(\frac{\delta\overline{f}' \wedge \delta\overline{f}''}{\overline{f}'^2} - \overline{\kappa}\delta\overline{f} \wedge \delta\overline{f}'\right)\right]\mathrm{d}\phi. \tag{2.3.57}$$

of the Alekseev-Shatashvili symplectic form.

Using the canonical 1-form (2.3.56) in (2.2.29) together with the Hamiltonian $H[\partial_t]$ produces the Alekseev-Shatashvili action

$$S = -\frac{c}{24\pi}\int \mathrm{d}^2x \left[\kappa f'\partial_{\overline{w}} f - \left(\frac{1}{f'}\right)''\partial_{\overline{w}} f - \overline{\kappa}\overline{f}'\partial_w\overline{f} - \left(\frac{1}{\overline{f}'}\right)''\partial_w\overline{f}\right]. \tag{2.3.58}$$

We may also obtain these results by the technique in Section 2.3.4. Since we already know the charges, the only ingredient still needed in (2.3.25) is the 1-form valued gauge parameter w. Since we are working with diffeomorphisms this means we need to work out (2.3.12). In this case things are simplified somewhat because we evidently only require the vector field ξ evaluated at $\rho = 0$ since the subleading components of (2.3.45) are not needed to compute the charge H.

Now, (2.3.54) gives the variations of f and $\overline{f}$ under an arbitrary asymptotic diffeomorphism, the 1-form valued vector field with parameters ϵ_δ and $\overline{\epsilon}_\delta$ must satisfy

$$\begin{pmatrix} \delta f \\ \delta \overline{f} \end{pmatrix} = \begin{pmatrix} f' & 0 \\ 0 & \overline{f}' \end{pmatrix} \begin{pmatrix} \epsilon_\delta \\ \overline{\epsilon}_\delta \end{pmatrix}. \tag{2.3.59}$$

This is evidently (2.3.12) evaluated on the boundary and with the Jacobian factor moved to the other side of the equality.

It now follows that (2.3.25) gives

$$\begin{aligned} \Omega &= -\frac{1}{4\pi} \int_0^{2\pi} (\delta T_{ww} \wedge \epsilon_\delta - \delta T_{\overline{w}\overline{w}} \wedge \overline{\epsilon}_\delta) \mathrm{d}\phi \\ &= -\frac{c}{48\pi} \int_0^{2\pi} \left[\delta \left(\frac{\kappa}{2} f'^2 + \{f, w\} \right) \wedge \frac{\delta f}{f'} - \delta \left(\frac{\overline{\kappa}}{2} \overline{f}'^2 + \{\overline{f}, \overline{w}\} \right) \wedge \frac{\delta \overline{f}}{\overline{f}'} \right] \mathrm{d}\phi. \end{aligned} \tag{2.3.60}$$

Integrating by parts this expression can can be shown to equal (2.3.57).

We can also obtain this result by computing (2.3.18). For this computation we will need the potential Q_ξ for the Noether current J_ξ and the potential $\tilde{k}_\xi$ for δk_ξ. Much of this discussion is independent of the choice $\Lambda = -1$ and $D = 3$, so we will leave these undetermined until they are actually needed to simplify our expressions. The Noether-Wald charge is well known as the so-called Komar term [21, 10],

$$Q_\xi = -\frac{1}{16\pi G} \sqrt{-g} \nabla^\mu \xi^\nu (\mathrm{d}^{D-2} x)_{\mu\nu}. \tag{2.3.61}$$

The computation of $\tilde{k}_\xi$ is straightforward from (2.3.42) if we use (2.3.14). With this we find

$$16\pi G\delta k_\xi = -\frac{4\Lambda}{D-2}\left[\delta\xi^\mu\sqrt{-g} + \frac{1}{2}\sqrt{-g}g^{\alpha\beta}\delta g_{\alpha\beta}\wedge\xi^\mu\right](\mathrm{d}^{D-1}x)_\mu$$
$$= \frac{4\Lambda}{D-2}\sqrt{-g}\nabla_\lambda(\xi^\lambda\wedge\xi^\mu)(\mathrm{d}^{D-1}x)_\mu. \tag{2.3.62}$$

From this we identify

$$\tilde{k}_\xi = -\frac{1}{16\pi G}\frac{2\Lambda}{D-2}\sqrt{-g}\xi^\mu\wedge\xi^\nu(\mathrm{d}^{D-2}x)_{\mu\nu}. \tag{2.3.63}$$

The boundary symplectic form is therefore given by (2.3.18) to find

$$\omega_b = \delta Q_\xi + \tilde{k}_\xi$$
$$= -\frac{1}{16\pi G}\sqrt{-g}\left[\nabla_\lambda\xi^\lambda\wedge\nabla^\mu\xi^\nu + \delta(\nabla^\mu\xi^\nu) + \frac{2\Lambda}{D-2}\xi^\mu\wedge\xi^\nu\right](\mathrm{d}^{D-2}x)_{\mu\nu}. \tag{2.3.64}$$

Computing

$$\delta(\nabla^\mu\xi^\nu)(\mathrm{d}^{D-2}x)_{\mu\nu} = -\left[\nabla^\lambda\xi^\mu\wedge\nabla_\lambda\xi^\nu - \frac{1}{2}R_{\alpha\beta}{}^{\mu\nu}\xi^\alpha\wedge\xi^\beta\right](\mathrm{d}^{D-2}x)_{\mu\nu} \tag{2.3.65}$$

the boundary symplectic form becomes

$$\omega_b = -\frac{1}{16\pi G}\sqrt{-g}\left[\nabla_\lambda\xi^\lambda\wedge\nabla^\mu\xi^\nu - \nabla^\lambda\xi^\mu\wedge\nabla_\lambda\xi^\nu - \frac{1}{2}R_{\alpha\beta}{}^{\mu\nu}\xi^\alpha\wedge\xi^\beta + \frac{2\Lambda}{D-2}\xi^\mu\wedge\xi^\nu\right](\mathrm{d}^{D-2}x)_{\mu\nu}. \tag{2.3.66}$$

If we now specialize to $D = 3$ where

$$R_{\alpha\beta}{}^{\mu\nu} = \delta^\mu_\alpha R^\nu_\beta - \delta^\nu_\alpha R^\mu_\beta - \delta^\mu_\beta R^\nu_\alpha + \delta^\nu_\beta R^\mu_\alpha - \frac{1}{2}R(\delta^\mu_\alpha\delta^\nu_\beta - \delta^\nu_\alpha\delta^\mu_\beta) \tag{2.3.67}$$

and use the equations of motion to write

$$R_{\mu\nu} = 2\Lambda g_{\mu\nu}, \qquad R = 6\Lambda, \tag{2.3.68}$$

(2.3.66) can be simplified to

$$\omega_b = -\frac{c}{24\pi}\sqrt{-g}\Big[\nabla_\lambda\xi^\lambda\wedge\nabla^\mu\xi^\nu - \nabla^\lambda\xi^\mu\wedge\nabla_\lambda\xi^\nu + \Lambda\xi^\mu\wedge\xi^\nu\Big](\mathrm{d}^1x)_{\mu\nu}. \tag{2.3.69}$$

It's straightforward to evaluate (2.3.69) on the metric (2.3.43) on the computer. We restrict the vector field ξ to take the form (2.3.45), where now ϵ and $\overline{\epsilon}$ should be understood as the 1-form valued ϵ_δ and $\overline{\epsilon}_\delta$ we used earlier and introduced in (2.3.59). Doing so we find the $\phi = \frac{1}{2}(w + \overline{w})$ component of (2.3.69) to be

$$\begin{aligned}\omega_b|_{\partial\Sigma} &= \frac{c}{24\pi}\frac{1}{\rho}\partial_\phi(\overline{\epsilon}\wedge\epsilon)\mathrm{d}\phi \\ &+ \frac{c}{48\pi}\left[4L\epsilon'\wedge\epsilon - 4\overline{L}\overline{\epsilon}'\wedge\overline{\epsilon} + \overline{\epsilon}'\wedge\epsilon'' + \overline{\epsilon}''\wedge\epsilon' - \epsilon'''\wedge\epsilon + \overline{\epsilon}'''\wedge\overline{\epsilon}\right]\mathrm{d}\phi + \mathcal{O}(\rho).\end{aligned} \tag{2.3.70}$$

Since we will integrate this over the circle to form the symplectic form we are free to drop total derivatives. In particular this means the divergent term above may be dropped. Furthermore, in the $\mathcal{O}(\rho^0)$ term the two terms which mix ϵ and $\overline{\epsilon}$ combine to a total derivative. So the symplectic form factorizes into a holomorphic and antiholomorphic term as expected,

$$\Omega = \frac{c}{48\pi}\int_0^{2\pi}\left[(4L\epsilon' - \epsilon''')\wedge\epsilon - (4\overline{L}\overline{\epsilon}' - \overline{\epsilon}''')\wedge\overline{\epsilon}\right]\mathrm{d}\phi. \tag{2.3.71}$$

But recalling (2.3.44) and (2.3.48) we have

$$\delta L\wedge\epsilon = \frac{1}{2}(4L\epsilon' - \epsilon''')\wedge\epsilon \tag{2.3.72}$$

and similarly for $\overline{L}$. Of course, we identify the RHS here as being precisely the factor which appears in (2.3.71). Making the replacement we recover the first line of (2.3.60).

2.3.5.3 New AdS boundary conditions

Here we again consider the Einstein-Hilbert Lagrangian (2.3.41) in $D = 3$, but this time we consider the modified boundary conditions described in [18]. Many of the details in the calculations here are similar to those which appear in topologically massive gravity, to be discussed in Section 2.4, so the manipulations here will be useful as a warmup in addition to a demonstration of the techniques in Section 2.3. We write an arbitrary Fefferman-Graham gauge metric as

$$\mathrm{d}s^2 = \frac{\mathrm{d}\rho^2}{4\rho^2} + \frac{1}{\rho}\left(g^{(0)}_{ab} + \rho g^{(1)}_{ab} + \mathcal{O}(\rho^2)\right)\mathrm{d}x^a\mathrm{d}x^b \tag{2.3.73}$$

where again $\rho > 0$ is the radial coordinate with asymptotic boundary at ρ and $x^a = (t, \phi)$ are the coordinate on the boundary with $\phi \sim \phi + 2\pi$. As before we will use the coordinates $w = t + \phi$ and $\overline{w} = -t + \phi$ for convenience[22].

The boundary conditions considered in [18] can be phrased as fixing the components

$$g^{(0)}_{\overline{w}\overline{w}} = 0, \quad \partial_{\overline{w}} g^{(0)}_{ww} = 0, \quad g^{(0)}_{w\overline{w}} = \frac{1}{2}, \quad g^{(1)}_{\overline{w}\overline{w}} = 4G\Delta \tag{2.3.74}$$

with Δ a fixed constant. Importantly, one can check that, while it is slightly modified from the Gibbons-Hawking-York boundary term, there indeed exists a choice of ℓ such that $B = 0$ in (2.2.15).

The Einstein equations can be solved exactly for metrics obeying these boundary conditions. The analog of the Bañados metrics for this case are

$$\begin{aligned} \mathrm{d}s^2 =& \frac{\mathrm{d}\rho^2}{4\rho^2} + \frac{1}{\rho}\mathrm{d}w(\mathrm{d}\overline{w} + \partial_w P \mathrm{d}w) + 4G[L\mathrm{d}w^2 + \Delta(\mathrm{d}\overline{w} + \partial_w P\mathrm{d}w)^2] \\ &+ (4G)^2 \Delta \rho L \mathrm{d}w(\mathrm{d}\overline{w} + \partial_w P \mathrm{d}w) \end{aligned} \tag{2.3.75}$$

where $P = P(w)$ and $L = L(w)$ are free functions parametrizing the solutions.

Furthermore, the asymptotic vector fields which preserve these boundary conditions are given by

$$\begin{aligned} \xi^\rho &= \rho\epsilon' \\ \xi^w &= \epsilon + \mathcal{O}(\rho^2) \\ \xi^{\overline{w}} &= \sigma - \frac{1}{2}\rho\epsilon'' + \mathcal{O}(\rho^2) \end{aligned} \tag{2.3.76}$$

where $\epsilon(w)$ and $\sigma(w)$ are free functions parametrizing the diffeomorphism.

These diffeomorphisms act on the parameters P and L by

$$\begin{aligned} i_{V_\xi}\delta P &= \sigma + P'\epsilon, \\ i_{V_\xi}\delta L &= 2L\epsilon' + \epsilon L' - \frac{1}{8G}\epsilon'''. \end{aligned} \tag{2.3.77}$$

[22] These coordinates relate to the coordinates (r, t^+, t^-) which appear in [18] by $\rho = 1/r^2$ and $t^+ = w$, $t^- = -\overline{w}$. Later we will meet a pair of functions (P, L) which were $(\overline{P}, \overline{L})$ in [18].

The charges associated to these diffeomorphisms can be computed to be

$$H[\epsilon,\sigma] = \int_0^{2\pi} \frac{\mathrm{d}\phi}{2\pi} \left[\left(\Delta P'^2 - L\right)\epsilon + \Delta(1+2P')\sigma\right]. \tag{2.3.78}$$

From (2.3.77) it's clear that the ϵ part of the transformation acts just like (2.3.48) on L while the σ part of the transformations acts to shift P. This means we can integrate up (2.3.77) to find

$$P = g(w), \qquad L = -\frac{1}{8G}\{f,w\}. \tag{2.3.79}$$

This can be done explicitly by applying the finite diffeomorphism

$$\begin{aligned}
\rho' &= f'\rho + G\Delta\frac{f''^2}{f'}\rho^3 + \mathcal{O}(\rho^4),\\
w' &= f + 2G\Delta f''\rho^2 + \mathcal{O}(\rho^3),\\
\overline{w}' &= \overline{w} + g - \frac{1}{2}\frac{f''}{f'}\rho + \mathcal{O}(\rho^3),
\end{aligned} \tag{2.3.80}$$

where $f(w)$ and $g(w)$ are free functions, to the background metric, which we choose to be an extremal BTZ black hole,

$$\mathrm{d}s^2 = \frac{\mathrm{d}\rho'^2}{4\rho'^2} + \frac{1}{\rho'}\mathrm{d}w'\mathrm{d}\overline{w}' + 4G\Delta\mathrm{d}\overline{w}^2. \tag{2.3.81}$$

Diffeomorphisms act on the orbit parameters by

$$i_{V_\xi}\delta f = f'\epsilon, \qquad i_{V_\xi}\delta g = \sigma + g'\epsilon, \tag{2.3.82}$$

which can be found by composing diffeomorphisms or deducing the transformation rule from (2.3.77) and (2.3.79). Using (2.3.79) we may also write the momentum as

$$\begin{aligned}
P = H[1,1] &= \Delta + \int_0^{2\pi}\frac{\mathrm{d}\phi}{2\pi}\left[\Delta(2+g')g' + \frac{1}{8G}\{f,w\}\right]\\
&= \Delta + \int_0^{2\pi}\frac{\mathrm{d}\phi}{2\pi}\left[\Delta g'g' - \frac{1}{2}\frac{1}{8G}\left(\frac{1}{f'}\right)''f'\right]
\end{aligned} \tag{2.3.83}$$

where in the second line we have used that $\{f, w\} = -\frac{1}{2}\left(\frac{1}{f'}\right)'' f'$ up to the addition of total derivatives. As was the case in (2.3.55), this momentum is of the form (2.3.2) for the momentum method. The canonical 1-form is given by

$$\Theta = \int_0^{2\pi} \frac{\mathrm{d}\phi}{2\pi} \left[\Delta g' \delta g - \frac{1}{16G} \left(\frac{1}{f'}\right)'' \delta f\right]. \tag{2.3.84}$$

From this and the Hamiltonian $H_t = H[1, -1]$ we obtain the phase space action

$$S = \int \frac{\mathrm{d}t\mathrm{d}\phi}{2\pi} \left[\Delta g'(\dot{g} - g') - \frac{1}{16G} \left(\frac{1}{f'}\right)'' (\dot{f} - f')\right]. \tag{2.3.85}$$

To instead apply our other techniques, (2.3.82) supplies the analog of (2.3.59), now taking the form

$$\begin{pmatrix} \delta f \\ \delta g \end{pmatrix} = \begin{pmatrix} f' & 0 \\ g' & 1 \end{pmatrix} \begin{pmatrix} \epsilon_\delta \\ \sigma_\delta \end{pmatrix}. \tag{2.3.86}$$

With all of these expressions for this theory we are well positioned to compute the boundary symplectic form via the methods in Sections 2.3.3 and 2.3.4. To make things even easier, we may note that (2.3.69) applies for any theory governed by the Einstein-Hilbert Lagrangian, independent of the boundary conditions we impose, so long as $B = 0$, which happens to be the case for this theory.

Performing the evaluation we find that again the divergent $1/\rho$ term is a total derivative as it was for asymptotically Dirichlet boundary conditions while the finite term can be massaged to yield

$$\Omega = \int_0^{2\pi} \frac{\mathrm{d}\phi}{4\pi} \left[\delta(L - \Delta P'^2) \wedge \epsilon_\delta - 2\Delta \delta P' \wedge \sigma_\delta\right], \tag{2.3.87}$$

which one may check has canonical 1-form (2.3.84). Furthermore, comparing this expression to the the charges (2.3.78) it's immediately clear that the prescription (2.3.25) reproduces (2.3.87) as well. Thus both the techniques of Sections 2.3.3 and 2.3.4 lead to the same phase space action (2.3.85).

2.3.6 Comparison of techniques

We have presented several techniques for computing actions governing boundary modes. It is useful to discuss the computational advantages offered by each approach.

When applicable, the momentum method is the most efficient approach. As presented, it applies to $D = 3$ diffeomorphism orbits built on bulk solutions that are translationally invariant in the boundary directions. The needed inputs are simply expressions for the boundary Hamiltonian and momentum charges written in terms of the orbit variables. The prescription involves using integration by parts to write the momentum in a canonical form, after which the canonical 1-form Θ can be read off. Together with the expression for the Hamiltonian, the boundary action follows. A great advantage here is that one gets Θ directly, bypassing the need to solve $\delta\Theta = \Omega$. Also noteworthy is that it can be applied order by order in perturbation theory, for example by expanding in powers of the boundary fluctuations. This method proved very effective in [15].

The other methods we discussed are less efficient but have a wider range of applicability. Using the transfer vector to invert $i_V\Omega = -\delta H_V$ requires that we we have computed all of the Noether charges, rather than just the momentum. Of course this has the advantage that it is applicable in any dimension and with any type of gauge orbit. Additionally, while the computation of the Noether charges will generally be sensitive to the boundary conditions of the theory, once the charges are computed the actual computation (2.3.25) is immediate. As seen in the examples (2.3.60) and (2.3.87), the resulting form for Ω may not make solving $\delta\Theta = \Omega$ immediate.

The transfer field method is likely the most computationally involved of the three approaches, but has the unique advantage of offering a clean separation between contributions depending on the Lagrangian of the theory and the boundary conditions imposed. In the case one wishes to study a Lagrangian under a variety of boundary conditions, this method could become more efficient than the others which would require that we recompute the Noether charges with each set of boundary conditions. For example, once (2.3.69) was known for $D = 3$ Einstein-Hilbert theory, there was essentially no additional computation required to apply it in the example in Section 2.3.5.3 beyond working out the new class of asymptotic vector fields.

As a final point here, we note that while computing the Noether charges generally involves solving a condition (2.2.26) to obtain the charges, each step in the transfer field method can in principle be completed algorithmically. This opens the possibility that, given θ and k_w for the theory, the computation of both Q_w and $\tilde{k}_w$ can be automated on the computer, leaving only the computation of B to obtain an expression for (2.3.18).

2.4 Application to Topologically Massive Gravity

Topologically massive gravity [22] is described by the Einstein-Hilbert action supplemented with a gravitational CS term,

$$S_{TMG} = \frac{1}{16\pi G} S_{EH} - \frac{l}{96\pi G\nu} S_{CS} \tag{2.4.1}$$

with[23]

$$\begin{aligned} S_{EH} &= \int \mathrm{d}^3x\sqrt{g}\left(R + \frac{2}{l^2}\right) + S_{bndy} \\ S_{CS} &= \int \mathrm{Tr}\left(\Gamma \wedge \mathrm{d}\Gamma + \frac{2}{3}\Gamma\wedge\Gamma\wedge\Gamma\right) \ . \end{aligned} \tag{2.4.2}$$

Here the connection 1-form is ${\Gamma^\alpha}_\beta = \Gamma^\alpha_{\beta\mu}\mathrm{d}x^\mu$, where $\Gamma^\alpha_{\beta\mu}$ are the usual Christoffel symbols built out of the metric. We take $\nu > 1$ and henceforth set $l = 1$. Our interest in applying our general techniques to this theory is to illustrate various issues that are not present in simpler examples, in particular the the non-diffeomorphism invariance of the action and the existence of solutions with relatively exotic "warped" asymptotics. We find that these pose no obstacle to implementing our general procedure to find the boundary action.

[23] It is straightforward to check that the boundary action may be chosen such that $B = 0$ in (2.2.15).

We will be particularly interested in solutions [23] that are the warped analog of the more familiar Bañados geometries [20],

$$ds^2 = L^2\left[\frac{dr^2}{r^2} + u^2\left(dt + \hat{K}d\phi + (r + r^{-1}\hat{\mathcal{L}})d\phi\right)^2 - (r - r^{-1}\hat{\mathcal{L}})^2 d\phi^2\right], \quad \phi \cong \phi + 2\pi \tag{2.4.3}$$

where

$$L^2 = \frac{1}{\nu^2+3}, \quad u^2 = \frac{4\nu^2}{\nu^2+3}. \tag{2.4.4}$$

(2.4.3) is a solution to S_{TMG} for any functions $\hat{K} = \hat{K}(\phi)$ and $\hat{\mathcal{L}} = \hat{\mathcal{L}}(\phi)$. Setting $\hat{K} = \hat{\mathcal{L}} = 0$ gives the analog of Poincaré AdS$_3$; constant values of $(\hat{K}, \hat{\mathcal{L}})$ can be obtained by quotienting the vacuum solution (analogous to how one obtains BTZ); $(\hat{K}, \hat{\mathcal{L}})$ with nontrivial dependence on ϕ (analogous to the Bañados geometries) are obtained by applying asymptotic symmetry transformations to the solutions with constant values.

The solutions (2.4.3) live in a phase space defined by boundary conditions that are preserved by the asymptotic coordinate transformations $x^\mu \to x^\mu + \chi^\mu$ which have the large r behavior

$$\begin{aligned}
\chi^\phi &= \xi^\phi + \frac{1}{2r^2}\partial_\phi^2\xi^\phi + \dots \\
\chi^t &= \xi^t - \frac{1}{r}\partial_\phi^2\xi^\phi + \dots \\
\chi^r &= -r\partial_\phi\xi^\phi + \dots
\end{aligned} \tag{2.4.5}$$

Here $\xi^{t,\phi} = \xi^{t,\phi}(\phi)$ are arbitrary periodic functions of ϕ. Under an infinitesimal diffeomorphism of the form (2.4.5) we have

$$\begin{aligned}
\delta\hat{\mathcal{L}} &= -\frac{1}{2}\partial_\phi^3\xi^\phi + 2\hat{\mathcal{L}}\partial_\phi\xi^\phi + \partial_\phi\hat{\mathcal{L}}\xi^\phi \\
\delta\hat{K} &= \partial_\phi\xi^t + \partial_\phi(\hat{K}\xi^\phi)
\end{aligned} \tag{2.4.6}$$

Associated to any boundary preserving vector field $\xi = \xi^\mu\partial_\mu$ is a charge $H[\xi]$. For example, the charges associated with rigid time and angular translations, i.e energy and angular momentum, are

$$
\begin{aligned}
M &= \frac{1}{uL} H[\partial_t] = \frac{1}{12\pi G}\int_0^{2\pi} \hat{K}\mathrm{d}\phi \\
J &= H[\partial_\phi] = -\frac{1}{6\pi G} uL \int_0^{2\pi}\left[\left(1+\frac{1}{u^2}\right)\hat{\mathcal{L}} - \frac{1}{4}\hat{K}^2\right]\mathrm{d}\phi
\end{aligned} \tag{2.4.7}
$$

as will be derived below.[24]

To derive the charges we can consider S_{EH} and S_{CS} independently of each other. That is, the action $S = C_1 S_{EH} + C_2 S_{CS}$ yields charges $Q' = C_1 Q'_{EH} + C_2 Q'_{CS}$, so we can extract Q'_{EH} and Q'_{CS} by setting one of $C_{1,2} = 0$. This is allowed because the procedure to obtain Q is linear, and the current J_{EH} is conserved in the S_{EH} theory, and likewise for J_{CS}.

2.4.1 Einstein-Hilbert contribution

As in (2.3.61) we have

$$
Q^{EH}_\chi = -\varepsilon^{\alpha\beta}{}_\phi \nabla_\alpha \chi_\beta \mathrm{d}\phi, \tag{2.4.8}
$$

where ε is defined in Appendix A.1. Evaluating this on (2.4.3) gives

$$
\begin{aligned}
Q^{EH}_\chi = \Big\{ & Lu(u^2-1)r^2\xi^\phi + 2Lu(u^2-1)\hat{K}r\xi^\phi + Lu^3 r\xi^t \\
&+ Lu\Big[u^2(2\hat{\mathcal{L}} + \hat{K}^2) - 6\hat{\mathcal{L}}\Big]\xi^\phi + Lu^3\hat{K}\xi^t + O(r^{-1})\Big\}\mathrm{d}\phi
\end{aligned} \tag{2.4.9}
$$

The term proportional to r^2 is constant on the phase space and so will be omitted in what follows. The same goes for the last term on the first line. On the other hand, there is a linearly diverging term in the first line which is not constant on phase space; this term will cancel a similar term in the CS contribution, yielding a finite result as $r \to \infty$.

Following the comments in Appendix A.3,

$$
C^{EH}_\chi = i_\chi \theta^{EH} = -u^3 L\hat{K}\xi^t \mathrm{d}\phi + O(r^{-1}) \tag{2.4.10}
$$

where θ^{EH} is given by (2.3.41).

[24] Original references for the derivation of the charges and asymptotic symmetry algebras include [24–28].

2.4.2 CS contribution

The Lagrangian 3-form $L_{CS} = \mathrm{Tr}(\Gamma \wedge \mathrm{d}\Gamma + \frac{2}{3}\Gamma^3)$ has variation

$$\delta L_{CS} = E^{\gamma\rho}\delta g_{\gamma\rho}\sqrt{-g}\mathrm{d}^3x + \mathrm{d}\theta^{CS} \tag{2.4.11}$$

with

$$\begin{aligned} E^{\gamma\rho} &= -\nabla_\beta R^{\beta\rho}{}_{\mu\nu}\varepsilon^{\gamma\mu\nu} = -2C^{\gamma\rho} \\ \theta^{CS} &= \mathrm{Tr}(\delta\Gamma \wedge \Gamma) - 2\delta g_{\kappa\rho}R^\rho{}_\delta \mathrm{d}x^\kappa \wedge \mathrm{d}x^\delta\ , \end{aligned} \tag{2.4.12}$$

where $C^{\gamma\rho}$ is the Cotton tensor and the Ricci tensor $R_{\mu\nu}$ is formed from the Riemann tensor $R = \mathrm{d}\Gamma + \Gamma^2$ as $R_{\mu\nu} = R^\alpha{}_{\mu\alpha\nu}$. We also recall that in $D = 3$ the Riemann tensor can be expressed in terms of the Ricci tensor; in terms of the Riemann two-form this amounts to the identity

$$R^\alpha{}_\beta = \left[\delta^\alpha_\gamma R_{\delta\beta} - g_{\beta\gamma}R^\alpha{}_\delta - \frac{1}{2}R\delta^\alpha_\gamma g_{\delta\beta}\right]\mathrm{d}x^\gamma \wedge \mathrm{d}x^\delta \tag{2.4.13}$$

Following the discussion in Appendix A.3 to compute the charges, the Noether current corresponding to the bulk vector field χ is

$$J^{CS}_\xi = i_{V_\chi}\theta^{CS} - i_\chi L_{CS} - Y_\chi\ . \tag{2.4.14}$$

where Y_χ defined via

$$\begin{aligned} \mathrm{d}Y_\chi &= \delta_\chi L_{CS} - \mathcal{L}_\chi L_{CS} \\ &= \mathrm{Tr}(\mathrm{d}v \wedge \mathrm{d}\Gamma) \end{aligned} \tag{2.4.15}$$

with $v^\alpha{}_\beta = \partial_\beta\chi^\alpha$. We take

$$Y_\xi = -\,\mathrm{Tr}(\mathrm{d}v \wedge \Gamma)\ . \tag{2.4.16}$$

We also have

$$\begin{aligned} i_{V_\chi}\theta^{CS} &= \nabla_\beta\nabla_\gamma\chi^\alpha dx^\beta \wedge \Gamma^\gamma{}_\alpha + \mathrm{Tr}(i_\chi R \wedge \Gamma) - 2(\nabla_\kappa\chi_\rho + \nabla_\rho\chi_\kappa)R^\rho_\delta \mathrm{d}x^\kappa \wedge \mathrm{d}x^\delta \\ i_\chi L_{CS} &= \mathrm{Tr}(i_\chi\Gamma\mathrm{d}\Gamma - \Gamma \wedge i_\chi R) \end{aligned} \tag{2.4.17}$$

Using these relations along with (2.4.13), some algebra leads to

$$J_\chi^{CS} = dQ_\chi^{CS} \tag{2.4.18}$$

with

$$Q_\chi^{CS} = \partial_\gamma \chi^\alpha \Gamma^\gamma{}_\alpha + \nabla_\gamma \chi^\alpha \Gamma^\gamma{}_\alpha + \chi^a\big[-4R_{a\delta} + Rg_{a\delta}\big]\mathrm{d}x^\delta \ . \tag{2.4.19}$$

The full charge is

$$H_\chi^{CS} = \int_{\partial\Sigma} \left[Q_\chi^{CS} - C_\chi^{CS}\right] \tag{2.4.20}$$

where C_χ^{CS} is obtained by solving $\delta C_\chi^{CS} = i_\chi\theta$, which can be written explicitly as

$$\delta C_\chi^{CS} = (\delta\Gamma^\alpha_{\kappa\beta}\Gamma^\beta_{\delta\alpha} - \delta\Gamma^\alpha_{\delta\beta}\Gamma^\beta_{\kappa\alpha})\chi^\kappa \mathrm{d}x^\delta - 2(\delta g_{\kappa\rho}R^\rho{}_\delta - \delta g_{\delta\rho}R^\rho{}_\kappa)\chi^\kappa \mathrm{d}x^\delta \tag{2.4.21}$$

To proceed further we need to specify the asymptotic form of the solutions of interest. Taking the solutions to be of the form (2.4.3) it is straightforward to compute

$$\begin{aligned}
Q_\chi^{CS} &= \Big\{Lu(u^2-1)r^2\xi^\phi + 2u(u^2-1)L\hat{K}r\xi^\phi + u(u^2-1)Lr\xi^t \\
&\quad + L\Big[u\left(u^2 - \frac{2}{3}\right)\hat{K}^2 + \left(2u^3 - \frac{10}{3}u + \frac{8}{3u}\right)\hat{\mathcal{L}}\Big]\xi^\phi + Lu\left(u^2 - \frac{2}{3}\right)\hat{K}\xi^t + O(r^{-1})\Big\}\mathrm{d}\phi \\
C_\chi^{CS} &= \Big\{-u\left(u^2 - \frac{2}{3}\right)L\hat{K}\xi^t + O(r^{-1})\Big\}\mathrm{d}\phi
\end{aligned} \tag{2.4.22}$$

Again, we can ignore terms that are constant on phase space. In writing these expressions we have also restored the $1/6\nu$ appearing in (2.4.1).

2.4.3 Total charge

The total charge is

$$H_\chi = \frac{1}{16\pi G}\int_{\partial\Sigma} \left[(Q_\chi^{EH} - C_\chi^{EH}) - (Q_\chi^{CS} - C_\chi^{CS})\right] \ . \tag{2.4.23}$$

Noting the cancellation between (non-constant) diverging term, we arrive at a finite result in the large r limit,

$$H_\chi = \frac{1}{16\pi G}\int_{\partial\Sigma}\left[\frac{4}{3}uL\hat{K}\xi^t - \frac{8}{3}uL\left((1+\frac{1}{u^2})\hat{\mathcal{L}} - \frac{1}{4}\hat{K}^2\right)\xi^\phi\right]\mathrm{d}\phi \ . \tag{2.4.24}$$

2.4.4 Lower spin gravity formulation

While Einstein gravity in three dimensions can be recast as a CS theory (with gauge group $SL(2,\mathbb{R})\times SL(2,\mathbb{R})$), this no longer holds in the presence of a gravitational CS term because the theory is no longer topological. However, the subsector of the theory described by the solutions (2.4.3) can be described by a CS theory, namely one with gauge group $SL(2,\mathbb{R})\times U(1)$, so-called "lower spin gravity" [29, 30]. The choice of gauge group is dictated by the isometry group of the warped vacuum solution. In particular, there is a fairly simple relation such that the charges and symplectic form of the two theories are mapped to each other. Since the equations of CS theory are much easier to deal with than those of TMG, this provides a simpler route to isolating the boundary degrees of freedom. The simplification arises essentially because the bulk degrees of freedom have been omitted.

The action is

$$S=\frac{k}{4\pi}\int \mathrm{Tr}\left(A\wedge \mathrm{d}A+\frac{2}{3}A\wedge A\wedge A\right)+\frac{\overline{k}}{8\pi}\int \overline{A}\wedge \mathrm{d}\overline{A} \tag{2.4.25}$$

Here A is an $SL(2,\mathbb{R})$ connection and $\overline{A}$ is a $U(1)$ connection. The $SL(2,\mathbb{R})$ generators obey $[L_m,L_n]=(m-n)L_{m+n}$ and we use the two-dimensional representation, for which $\mathrm{Tr}\,L_1L_{-1}=-1$.

$$\begin{aligned} a &= (L_1-\hat{\mathcal{L}}L_{-1})\mathrm{d}\phi+(\omega_1L_0+\omega_2L_{-1})\mathrm{d}t \\ \overline{a} &= K\mathrm{d}\phi+\mathrm{d}t\ . \end{aligned} \tag{2.4.26}$$

Here, as is standard, the boundary connections $(a,\overline{a})$ are related to bulk connections $(A,\overline{A})$ by a gauge transformation that encodes the radial dependence,

$$A=b^{-1}ab+b^{-1}\mathrm{d}b\ ,\quad \overline{A}=b\overline{a}b^{-1}+b\mathrm{d}b^{-1}\ , \tag{2.4.27}$$

where $b=e^{-\frac{1}{2}L_0\ln r}$. Gauge transformations act as

$$\delta a=\mathrm{d}\epsilon+[a,\epsilon]\ ,\quad \delta\overline{a}=\mathrm{d}\overline{\epsilon} \tag{2.4.28}$$

with $\epsilon = \epsilon_1 L_1 + \epsilon_0 L_0 + \epsilon_{-1} L_{-1}$. The form of (2.4.26) is preserved by taking $\epsilon_0 = -\partial_\phi \epsilon_1$ and $\epsilon_{-1} = \frac{1}{2}\partial_\phi^2 \epsilon_1 - \hat{\mathcal{L}}\epsilon_1$, To connect to the metric description we trade $(\epsilon_1, \bar{\epsilon})$ for (ξ^ϕ, ξ^t) according to

$$\epsilon_1 = \xi^\phi \ , \quad \bar{\epsilon} = \xi^t + \hat{K}\xi^\phi \ , \tag{2.4.29}$$

with

$$\hat{K} = \frac{4\pi}{\bar{k}} K \ . \tag{2.4.30}$$

The gauge transformations then act as

$$\begin{aligned} \delta\hat{\mathcal{L}} &= -\frac{1}{2}\partial_\phi^3 \xi^\phi + 2\hat{\mathcal{L}}\partial_\phi \xi^\phi + \partial_\phi \hat{\mathcal{L}}\xi^\phi \\ \delta\hat{K} &= \partial_\phi \xi^t + \partial_\phi(\hat{K}\xi^\phi) \end{aligned} \tag{2.4.31}$$

reproducing (2.4.6).

We can now apply relations reviewed in Appendix A.4 for CS theory. Letting V denote the phase space vector field implementing an infinitesimal gauge transformation with parameters $(\epsilon, \bar{\epsilon})$ we have $i_V \Omega = -\delta H[\epsilon, \bar{\epsilon}]$ with

$$\begin{aligned} H[\epsilon, \bar{\epsilon}] &= \frac{k}{2\pi}\int_{\partial\Sigma} \mathrm{Tr}(\epsilon a) + \frac{\bar{k}}{4\pi}\int_{\partial\Sigma} \overline{\epsilon a} \\ &= \int_0^{2\pi} \mathrm{d}\phi \left[\left(\frac{k}{2\pi}\hat{\mathcal{L}} + \frac{\bar{k}}{8\pi}\hat{K}^2 \right) \xi^\phi + \frac{\bar{k}}{4\pi}\hat{K}\xi^t \right] \\ &= \int_0^{2\pi} \mathrm{d}\phi (\mathcal{L}\xi^\phi + K\xi^t) \ , \end{aligned} \tag{2.4.32}$$

where we have defined $\mathcal{L}$ according to

$$\hat{\mathcal{L}} = \frac{2\pi}{k}(\mathcal{L} - \frac{2\pi}{\bar{k}}K^2) \ . \tag{2.4.33}$$

The second line of (2.4.32) agrees with (2.4.24) under the identification

$$k = \frac{uL}{3G}\left(1 + \frac{1}{u^2}\right) \ , \quad \bar{k} = -\frac{uL}{3G} \ . \tag{2.4.34}$$

We conclude that there is a simple relation between the canonical structure of lower spin gravity and the class of solutions (2.4.3) to TMG.

One can also build the metrics (2.4.3) out of the $SL(2,\mathbb{R})\times U(1)$ connection, in analogy with the corresponding relation in ordinary 3D gravity. See [29] for details. Gauge transformations in the CS theory will map to diffs in the metric formulation, as follows from the fact that we have already mapped the transformations on the phase space variables $(\hat{\mathcal{L}},\hat{K})$.

2.4.5 Boundary action for warped AdS$_3$

To compute the boundary action our first task is to obtain expressions for the charges evaluated on a given orbit. The finite diff functions are written as (Φ, T) with

$$\Phi = \phi + \xi^\phi \ , \quad T = t + \xi^t \ . \tag{2.4.35}$$

The infinitesimal transformations are given in (2.4.31). The first expression is familiar and exponentiates via the Schwarzian derivative and the second expression is easily handled to yield

$$\begin{aligned}\hat{\mathcal{L}}(\phi) &= (\partial_\phi\Phi)^2\hat{\mathcal{L}}_0 - \frac{1}{2}\{\Phi(\phi),\phi\}\\ \hat{K}(\phi) &= \partial_\phi\Phi\hat{K}_0 + \partial_\phi T(\Phi)\end{aligned} \tag{2.4.36}$$

where the constant values $(\hat{\mathcal{L}}_0,\hat{K}_0)$ serve as parameters labelling the orbit under consideration. Translating to unhatted variables, as appear in the charge expression $Q=\int \mathrm{d}\phi(\mathcal{L}\xi^\phi + K\xi^t)$ we have

$$\begin{aligned}\mathcal{L}(\phi) &= (\partial_\phi\Phi)^2\mathcal{L}_0 - \frac{k}{4\pi}\{\Phi,\phi\} + \partial_\phi\Phi\partial_\phi T K_0 + \frac{\overline{k}}{8\pi}(\partial_\phi T)^2\\ K(\phi) &= \partial_\phi\Phi K_0 + \frac{\overline{k}}{4\pi}\partial_\phi T \ .\end{aligned} \tag{2.4.37}$$

To extract the boundary symplectic potential Θ we use the momentum method. The momentum, i.e. generator of ϕ translations, is

$$P = H[\xi=\partial_\phi] = \int_0^{2\pi}\mathcal{L}(\phi)\mathrm{d}\phi \ . \tag{2.4.38}$$

To apply the momentum method we are instructed to write P in the form

$$P = \int (P_\Phi \Phi' + P_T T')\mathrm{d}\phi \tag{2.4.39}$$

which is achieved by taking[25]

$$\begin{aligned} P_\Phi &= \mathcal{L}_0 \Phi' + \frac{k}{8\pi}\left(\frac{1}{\Phi'}\right)'' \\ P_T &= K_0 \Phi' + \frac{\bar{k}}{8\pi} T' \ . \end{aligned} \tag{2.4.40}$$

The symplectic potential is then

$$\Theta = \int \mathrm{d}\phi \left[\left(\mathcal{L}_0 \Phi' + \frac{k}{8\pi}\left(\frac{1}{\Phi'}\right)'' \right) \delta\Phi + \left(K_0 \Phi' + \frac{\bar{k}}{8\pi} T' \right) \delta T \right] \ . \tag{2.4.41}$$

The Hamiltonian corresponding to time translations is

$$H = Q[\xi = \partial_t] = \int K \mathrm{d}\phi = 2\pi K_0 \ , \tag{2.4.42}$$

so the kinetic term in the action is obtained by making the replacements $(\delta\Phi, \delta T) \to (\dot{\Phi}, \dot{T})$. The fact that this H is a constant on phase space reflects the fact the solutions in this theory are time independent. More interesting dynamics are obtained by choosing a Hamiltonian that generates translations along the vector field $\partial_t + \Omega\partial_\phi$. This is appropriate for computing a partition function of the form $\mathrm{Tr}\, e^{-\beta(H+\Omega P)}$. Such partition functions are the appropriate ones to consider for two reasons [31]. First, unitary representations of the warped current algebra have H unbounded from below while P is positive definite, so $\Omega > 0$ is required for convergence. Second, the black hole solutions (2.4.3) (with constant $(\hat{\mathcal{L}}, \hat{K})$) have horizon Killing vector field (defined to be the vector field that vanishes at the bifurcation surface)

$$\begin{aligned} \xi_H &= \partial_t + \Omega \partial_\phi \\ &= \partial_t + \frac{1}{2\sqrt{\hat{\mathcal{L}}} + \hat{K}} \partial_\phi \end{aligned} \tag{2.4.43}$$

[25] We should note that $\mathcal{L}(\phi)$ has several terms which contain only first derivatives; as discussed in section (2.3.1), since they are purely quadratic their contribution to Ω is easily found by directly solving $i_V \Omega = -\delta Q_V$ for such terms.

Ω must be positive for a smooth horizon, as can be seen from the expression for the surface gravity

$$\kappa = \frac{\sqrt{\hat{\mathcal{L}}}}{\sqrt{\hat{\mathcal{L}}} + \hat{K}/2} \ . \tag{2.4.44}$$

As in all of our examples, the boundary action captures all of the information regarding the warped spacetimes that is dictated by symmetry. For instance, it can be used to compute correlators of the currents, as well one loop corrections to the partition function coming from the boundary modes.

2.5 Emergent Boundary Modes

As developed so far, boundary field theories arise due to the imposition of boundary conditions that are preserved by some infinite dimensional group of transformations that act nontrivially at the boundary. However, situations can arise in which the boundary in question is not a sharp boundary in the sense of terminating the space on which the theory lives, but rather an interface that connects the original region to an "outer region". The question is whether or not the boundary modes survive; that is, are they effectively transported to the outer region?

This situation arises naturally in the AdS/CFT context. For example, one might have an AdS_3 solution which appears as the near horizon limit of some non-asymptotically AdS_3 solution M. Is the asymptotic symmetry group of the AdS_3 region visible at the boundary of the larger spacetime M? From the dual CFT point of view, the AdS_3 region encodes physics in the deep IR, so one is asking about how to these IR degrees of freedom are realized in terms of the UV description.

We will flesh out how this works in a particular example. Five-dimensional Einstein-Maxwell theory (with $\Lambda < 0$) admits an asymptotically AdS_5 solution that has a near horizon $\mathrm{AdS}_3 \times \mathbb{R}^2$ factor which we compactify to T^2 [32]. The T^2 is supported by a nonzero Maxwell field strength. We show how the boundary graviton phase space is visible at the AdS_5 boundary. Including also a CS term $A\wedge F\wedge F$, the AdS_3 region supports boundary photons, and we again show how these appear in the full description. These results are consistent with the low energy correlators computed in [33], which are sensitive to the emergent boundary modes. For related work see [34, 35].

2.5.1 Background solution

We first briefly summarize the relevant features of the solution; more details may be found in [32]. The action is

$$S = -\frac{1}{16\pi G_5}\int \mathrm{d}^5x\sqrt{g}\left(R + F^{MN}F_{MN} - 12\right) + \frac{k}{12\pi G_5}\int A\wedge F\wedge F \tag{2.5.1}$$

We consider a solution of the form

$$\begin{aligned} \mathrm{d}s^2 &= \frac{\mathrm{d}r^2}{L(r)^2} + 2L(r)\mathrm{d}x^+\mathrm{d}x^- + e^{2V(r)}\mathrm{d}x^i\mathrm{d}x^i\ , \quad i=1,2 \\ F &= b\mathrm{d}x^1\wedge\mathrm{d}x^2 \end{aligned} \tag{2.5.2}$$

The function L can be found in terms of V, but numerics are required to find V. We will only need the asymptotics. As $r\to\infty$ we have AdS_5 asymptotics,

$$L(r) = 2r + \dots\ , \quad e^{2V(r)} = c_V r + \dots \tag{2.5.3}$$

for some constant c_V.

As $r\to 0$ we have $\mathrm{AdS}_3\times T^2$ asymptotics,

$$L(r) = 2br + \dots\ , \quad e^{2V(r)} = 1 + \dots \tag{2.5.4}$$

Fluctuations of the metric and gauge field with polarizations and spacetime dependence restricted to the AdS_3 directions are governed by an effective 3d Einstein-CS theory, so if we place a boundary in this region we will find the usual 2d boundary photons and gravitons. On the other hand, the asymptotic symmetry group at the AdS_5 boundary is finite dimensional, which leads to the aforementioned question of how the near horizon boundary modes are visible in terms of observables computed at the AdS_5 boundary.

2.5.2 Boundary photons

2.5.2.1 Linearized solutions

We considered a linearized gauge field perturbation of the form

$$\delta A = a_+(r, x^+)\mathrm{d}x^+ \ . \tag{2.5.5}$$

It obeys

$$Le^{2V}\frac{\partial a_+}{\partial r} + -2kba_+ = 0 \tag{2.5.6}$$

The solution which is smooth at the origin (assuming $k > 0$) is

$$a_+(r, x^+) = \epsilon(x^+)e^{-2kb\int_r^\infty \frac{\mathrm{d}r'}{L(r')e^{2V(r')}}} \tag{2.5.7}$$

This has asymptotics:

$$\begin{aligned} r\to 0: &\qquad a_+(r, x^+) = \epsilon(x^+)r^k + \dots \\ r\to\infty: &\qquad a_+(r, x^+) = \epsilon(x^+)\left(1 - \frac{kb}{c_V r} + \dots\right) \ . \end{aligned} \tag{2.5.8}$$

The $1/r$ falloff term implies a nonzero boundary current $J_+ \sim \epsilon(x^+)$. This solution is not quite what we want however, since normalizable solutions, corresponding to vanishing source in the dual CFT, should vanish in the large r limit. We can remedy this by performing a gauge transformation. We first of all write

$$\epsilon(x^+) = -\partial_+\lambda(x^+) \tag{2.5.9}$$

and then perform a gauge transformation with parameter $\Lambda(r, x^+) = f(r)\lambda(x^+)$ where

$$\lim_{r\to 0} f(r) = 0 \ , \quad \lim_{r\to\infty} f(r) = 1 \ . \tag{2.5.10}$$

After the gauge transformation we have

$$
\begin{aligned}
a_+ + \partial_+\Lambda &= \partial_+\lambda(x^+)\left(f(r) - e^{-2kb\int_r^\infty \frac{dr'}{L(r')e^{2V(r')}}}\right) \\
a_r + \partial_r\Lambda &= \lambda(x^+)\partial_r f(r) \\
a_- + \partial_-\Lambda &= 0
\end{aligned}
\tag{2.5.11}
$$

such that all components vanish at both small and large r, as desired. It is apparent that these modes are not pure gauge, as they carry a nonzero field strength.

2.5.2.2 Symplectic form

We now wish to compute the symplectic form restricted to the space of these linearized solutions. In particular, we compute the full $D = 4 + 1$ symplectic form for these non-pure gauge solutions. We will see that the result agrees with what we would get by considering pure gauge modes living in the near horizon AdS_3, with a boundary imposed in that region.

Since all polarizations and spacetime dependence of the fluctuations is confined to three dimensions it is convenient to dimensionally reduce the action (2.5.1). Keeping the gauge field terms, after integrating over the T^2 the action can be written as

$$S = \frac{bV_2}{4\pi G_5}\int_{M_3} L \tag{2.5.12}$$

where V_2 is the coordinate volume of T^2 and

$$L = \frac{1}{2}\Phi F \wedge \star F + kA \wedge F \tag{2.5.13}$$

where $\Phi = b^{-1}e^{2V}$. We will consider $S = \int L$ and tack on the $\frac{bV_2}{4\pi G_5}$ prefactor at the end. Proceeding as usual, we vary the action with respect to the gauge field and write the result as in (2.2.13), $\delta L = E_A \delta A + \mathrm{d}\theta$ yielding the field equation

$$\mathrm{d}[\Phi \star \mathrm{d}A + 2kA] = 0 \tag{2.5.14}$$

and the symplectic form $\Omega = \int_\Sigma \omega$ with

$$\omega = \delta\theta = -\Phi\delta A \wedge \star \mathrm{d}\delta A - k\delta A \wedge \delta A \tag{2.5.15}$$

The fluctuation (2.5.11) takes the form $A = a + \mathrm{d}\Lambda$ where a obeys

$$\Phi \star \mathrm{d}a + 2ka = 0 \ . \tag{2.5.16}$$

Using this we have

$$\Omega = k \int_\Sigma \left(\delta a \wedge \delta a - \mathrm{d}\delta\Lambda \wedge \mathrm{d}\delta\Lambda\right) \ . \tag{2.5.17}$$

In the case of interest $a = a_+ \mathrm{d}x^+$ and so the first term vanishes, while the second terms is an exact form. Restoring the prefactor, we then obtain the symplectic form

$$\Omega = -\frac{kbV_2}{4\pi G_5} \int_{\partial\Sigma} \delta\Lambda \wedge \mathrm{d}\delta\Lambda \ . \tag{2.5.18}$$

This symplectic form lives on the AdS_5 boundary. However, and this is the main point, the form of the result is precisely the same as would have been obtained by just considering the pure CS action $\frac{kb}{4\pi G_5}\int A \wedge F$ defined on the near horizon AdS_3 region. It is furthermore easy to verify that the boundary currents take the same form as well. This shows very explicitly how the near horizon boundary photon degrees of freedom are effectively transported to the AdS_5 boundary. The mechanism for this is not entirely trivial; in particular, note that the fluctuation modes we used in this analysis are not pure gauge in the near horizon region, yet the symplectic form defined on them agrees with that of pure gauge modes in AdS_3.

2.5.3 Boundary gravitons

2.5.3.1 Linearized solutions

We now consider a fluctuation around the metric in (2.5.2) by considering

$$\mathrm{d}s^2 = \frac{\mathrm{d}r^2}{L^2} + 2L\mathrm{d}x^+\mathrm{d}x^- + M(\mathrm{d}x^+)^2 + e^{2V}\mathrm{d}x^i\mathrm{d}x^i \tag{2.5.19}$$

where we will work to linear order in $M = M(r, x^+)$. For $r \ll 1$ background metric contains the AdS$_3$ factor $\mathrm{d}s_3^2 = \frac{\mathrm{d}r^2}{4b^2r^2} + 4br\mathrm{d}x^+\mathrm{d}x^-$. In this near horizon region, a boundary graviton is obtained by applying a diff $x^\mu \rightarrow x^\mu + \xi^\mu$ with

$$\xi = \epsilon(x^+)\partial_+ - \partial_+\epsilon(x^+) r \partial_r - \frac{1}{8b^3 r}\partial_+^2\epsilon(x^+)\partial_- \ . \tag{2.5.20}$$

This yields a fluctuation of the form

$$M = -\frac{1}{2b^2}\partial_+^3\epsilon(x^+) \ . \tag{2.5.21}$$

The fluctuation (2.5.21) is not a solution of the linearized Einstein equations outside the near horizon region. Our task is to extend (2.5.21) to a solution in the full spacetime that respects the AdS$_5$ asymptotics. As shown in [33] such a solution is obtained by multiplying (2.5.21) by $-2bL^c(r)$, where

$$L^c(r) = L(r)\int_\infty^r \frac{\mathrm{d}r'}{L(r')^2 e^{2V(r')}} \ . \tag{2.5.22}$$

The asymptotics of this function are

$$\begin{aligned} r\rightarrow 0 \qquad & L_0^c(r) \sim -\frac{1}{2b} \\ r\rightarrow \infty \qquad & L_0^c(r) \sim -\frac{1}{4c_V r} \ . \end{aligned} \tag{2.5.23}$$

So the desired fluctuation mode is

$$M = b^{-1}L^c(r)\partial_+^3\epsilon(x^+) \ . \tag{2.5.24}$$

This non-pure gauge solution carries a nonzero AdS$_5$ boundary stress tensor ($c = 3/2G_3$ is the near horizon Brown-Henneaux central charge),

$$T_{++} = -\frac{c_V c}{96\pi}\partial_+^3\epsilon(x^+) \tag{2.5.25}$$

which is the same form as the contribution to the AdS$_3$ boundary stress tensor coming from the pure gauge mode (2.5.21).

2.5.3.2 Symplectic form

The fluctuation modes found above are not yet in a form suitable for computing the symplectic form. Indeed, contracting two such perturbations with the general gravitational symplectic form will give zero; this follows from symmetry considerations, as each perturbation carries two lower + indices and there are no available upper + indices to soak these up. The issue is that the perturbation is singular at $r = 0$ due to the breakdown of coordinates there. We can fix this by performing a compensating diff that zeroes out the perturbation as $r \to 0$ but acts trivially at large r. Let $f(r)$ interpolate smoothly between -1 and 0 in going from small to large r. We then act with a diff of the form (2.5.20) except with $\epsilon(x^+)$ replaced by $f(r)\epsilon(x^+)$. We write the combined perturbation as

$$\phi + \phi_f \ . \tag{2.5.26}$$

By construction, it vanishes as $r \to 0$ and is equivalent to our original perturbation at large r. The symplectic form contracted against two such perturbations is[26]

$$\Omega(\phi_1 + \phi_{1f}, \phi_2 + \phi_{2f}) \ . \tag{2.5.27}$$

Now, $\Omega(\phi_1, \phi_2) = 0$ as already noted. Also $\Omega(\phi_{1f}, \phi_2 + \phi_{2f}) = 0$. This follows since ϕ_{1f} is a pure diff mode, and Ω contracted against a pure diff mode localizes to the boundary of Σ, but $\phi_2 + \phi_{2f}$ vanishes as $r \to 0$ and ϕ_{1f} vanishes as $r \to \infty$, so both boundary terms are zero.

All that survives is therefore $\Omega(\phi_1, \phi_{2f})$. This again localizes to the boundary, but now we get a nonzero boundary term at small r, Since $\phi_1 = -\phi_{1f}$ at small r, this boundary term is precisely the same expression as appears in the symplectic form of pure diff modes in AdS_3.[27] So we once again find that the perturbations defined on the full spacetime carry

[26] Here we are using the notation $\Omega(\phi_1, \phi_2) = i_{V_2} i_{V_1} \Omega$, where V_i denotes the phase space vector field corresponding to the linearized perturbation ϕ_i.

[27] This relative minus sign is cancelled by the minus sign that occurs when we switch from taking the boundary to be inner versus outer.

the same symplectic form as the pure gauge near horizon modes.

CHAPTER 3

Hamiltonian Formulation for Near-Extremal Charged Black Holes in 4d

3.1 Introduction and summary

Black holes provide an interesting set up where gravity, quantum mechanics and thermodynamics meet. Thermodynamic description of the black holes are based on the Bekenstein-Hawking entropy [36], which is an area of the horizon and Hawking temperature [37], which is the surface gravity at the horizon which fit nicely into the first law of thermodynamics with obvious notation.

$$\delta M = T_H \delta S + \Omega \delta J + \Phi \delta Q \tag{3.1.1}$$

Black hole thermodynamics, however, can break down when the black hole has an electric charge. The charged black holes have two horizons $r_\pm$, seperated by the difference between the mass and charge. The geometry is described by Reissener-Nordstrom metric.

$$\begin{gathered} \mathrm{d}s^2 = -f(r)\mathrm{d}t^2 + \frac{\mathrm{d}r^2}{f(r)} + r^2 \mathrm{d}\Omega_2^2, \qquad f(r) = \frac{(r-r_+)(r-r_-)}{r^2}, \\ r_\pm = GM \pm \sqrt{G^2M^2 - GQ^2} \end{gathered} \tag{3.1.2}$$

When this seperation is small, i.e. $M \approx \sqrt{G}Q$ or $r_+ \approx r_-$, the black hole is called near-extremal. Near extremal black holes have provided an important setup for analytic study of black holes such as black hole mergers and black hole microstate counting. Interestingly, thermodynamic description seems to fail for those near-extremal black holes.

Even without a symmetry to protect it, the near-extremal black holes have large entropy

$S = \frac{\pi r_+^2}{4G}$ at low temperature $T_H = \frac{r_+ - r_-}{4\pi r_+^2}$, and hence it appears to be in the thermodynamic regime. However, the excitation energy away from the extremality at low temperature below a certain mass gap, $T < M_{gap}$, is not enough for radiating one Hawking quantum, as can be seen by using the definition of thermodynamic quantities.

$$\delta E = M - Q = \frac{T^2}{M_{gap}}, \quad M_{gap}^{-1} \equiv \frac{l^2 r_0^3}{G(l^2 + 6r_0^2)} \tag{3.1.3}$$

Therefore, to describe the radiation as well as the physics near the horizon, one has to incorporate the quantum gravitational effects.

Indeed, the near-extremal black holes do radiate quantum mechanically. To see this, one can take the near horizon limit by rescaling the coordinates, which has the $AdS_2 \times S^2$ geometry. It has a long throat while the rest of the bulk has the small curvature and thus the quantum effect near the horizon is dominant. Banerjee and Saha [38] computed the 1-loop determinant of the Euclidean path integral at the near horizon region of the 4d black hole, and found that the excitation above the extremality gets a quantum correction

$$\delta E' = \partial_\beta \log Z \sim \frac{3}{2} T > T \tag{3.1.4}$$

which is large enough for radiating a Hawking quantum.

This was possible because the quantum gravitational effects are boosted at low temperature through the effective rescaling of the coupling from $G \to \frac{\beta G}{2\pi}$. These quantum gravity effects have been described by Jackiw-Teitelboim (JT) gravity [39, 40].

JT gravity is an effective description of the near horizon AdS_2 region of the Euclidean black hole in the s-wave sector. The gravity part of the JT action is the Schwarzian derivative of the boundary graviton, which is a pseudo Nambu-Goldstone boson associated with the broken reparameterization symmetry of the boundary time, and the on-shell action for scalar fields is given by the bi-local action dressed with the boundary graviton.

Using this action, one can compute the gravity observables such as 1-loop correction to the excitation energy and the boundary quantum mechanics observables. Through the analytic continuation to the Lorentzian time, they correspond to the thermal correlation functions in the thermal state where the ingoing and outgoing modes have the same structure of the correlation function.

However, the evaporating black holes obtained by collapse of a star are described in the Unruh vacuum, where the outgoing radiation has thermal correlation function at late time while the ingoing correlation in the past is not thermal. To describe this state, inherently Lorentzian description is needed.

One can attempt to analytically continue the Schwarzian action. This is problematic when the boundary is single sided because it has the solutions of equations of motion that have instability or wrong sign kinetic term, which are not removed by fixing the $SL(2,\mathbb{R})$ gauge symmetry.[1]

One way forward is using the Hamiltonian or Arnowitt-Deser-Misner (ADM) formulation, based on the geometry as the foliation of the metric along the boundary time. The non-dynamical gravitational degrees of freedom are integrated out by imposing the associated constraints and the resulting Hamiltonian for the dynamic degrees of freedom (the scalar field) is localized on the boundary. However, evaluated on the solution to the constraints, the ADM Hamiltonian appears to be a non-local action in the bulk, which has quartic scalar interaction at the leading order in G. This seems to be highly contrasting to the JT gravity at first sight.

However, using the energy momentum conservation and highly nontrivial total derivative formula, one can turn bulk integral into a boundary integral of a non-local interaction. One then can integrate *in* boundary gravitons to match the action with the JT gravity plus scalar bilocal action.

[1]This is because the gauge charges evaluated on them on one boundary do not vanish. However, for the two-sided boundary, the difference of the charges on the left and right boundaries, $Q_L - Q_R$, can be made to vanish and remove the instability.

This identification, which is highly nontrivial, guarantees the agreement in tree-level correlation functions, which we illustrate by explicit computations of tree-level 4-point functions of the two boundary scalars. On the other hand, the loop corrections to the correlation functions are not guaranteed to match because the two theoreis have different dynamic degrees of freedom which generally adopt different types of regularization schemes (counter terms) for the UV divergences. However, our explicit computations using the Hamiltonian formulation and JT gravity show these agree, albeit not straightforwardly.

In principle, our ADM Hamiltonian can be used in computing other bulk observables both real-time (using Schwinger-Keldysh contour and interaction picture) and Euclidean time (using mode expansion of propagators, i.e. working in the momentum space). We leave that for the future work.

The rest of this chapter proceeds as follows. In section 3.2, we explain the breakdown of thermodynamics in the near-extremal black holes and the compute the quantum correction to the partition function. In section 3.3, we review the well-established JT gravity as the low temperature effective description for the near extremal black hole and compute the tree-level 4-point functions of two boundary scalars and 1-loop 2-point functions. In section 3.4, we compute the ADM Hamiltonian as a bulk integral and illustrate how we identify it with the JT action defined on the boundary by integrating in the boundary gravitons. Lastly in section 3.5, we compute the tree-level 4-point and 1-loop 2-point functions using the ADM Hamiltonian in the Euclidean time and find the agreement with the JT computations. We also sketch the computation of real time 4-point function using the interaction picture and Schwinger-Keldysh contour.

3.2 Motivation for the ADM formulation of the 4d near-extremal charged black holes

3.2.1 Breakdown of thermodynamics

The semi-classical thermodynamics of the black holes [36, 37, 41] is based on the Hawking temperature, T, the mass of the black hole M and the Bekenstein-Hawking entropy given by the area law $S = \frac{A}{8\pi G_N}$. For the near-extremal Reissener-Nodrdstrom black holes in 4d, the excitation above the extremality is given by

$$\delta E = M - Q = \frac{T^2}{M_{gap}}, \quad M_{gap}^{-1} \equiv \frac{l^2 r_0^3}{G(l^2 + 6r_0^2)}, \tag{3.2.1}$$

where r_0 is the horizon radius of the extremal black holes. Imagine adding some matter and consider the backreaction. When $T < M_{gap}$, the black hole cannot radiate Hawking quanta with energy T to relax to extremal black hole due to this energy gap, and semi-classical thermodynamic description breaks down.

Another way to see this is using the heat capacity. In the presence of backreaction by matters, the semi-classical description is valid if the change in temperature through absorption/emission of a Hawking quantum is much less than the current temperature of the black hole [42] .

$$\langle \Delta T \rangle = \left| T \frac{\partial T}{\partial M} \right| = \frac{T}{C} \ll T \quad \text{or} \quad C \gg 1 \tag{3.2.2}$$

where $C = \left(\frac{\partial M}{\partial T}\right)_{Q,J}$ is the heat capacity.[2] When this bound is not satisfied, it is ambiguous to use which temperature for the thermodynamic description—before absorption/emission

[2]Using the equilibrium relation $\delta E - T\delta S = 0$ in the grand canonical ensemble, this condition can be recast as the lower bound on the change in entropy given by C_Q.

$$T\frac{\partial S}{\partial T} \gg 1 \quad \text{or} \quad \langle \Delta S \rangle = T\frac{\partial S}{\partial M} \gg C \tag{3.2.3}$$

or after or somewhere in the middle. Practically, this means that the black hole does not radiate or absorb a Hawking quantum semi-classically.

Additionally, the continuum thermodynamic description is valid within a certain energy window around the macroscopic mean energy. This is evident by writing the partition function as the functional integral.

$$Z(\beta) = \int \mathrm{d}E \; e^{-S(E)+\beta E} \tag{3.2.4}$$

The continuum thermodynamics description corresponds to the saddle point approximation (SPA) of this integral. The saddle point $E = E_*$ is at

$$\left.\frac{\partial S}{\partial E}\right|_{E_*} = \beta \tag{3.2.5}$$

Expanding the exponent around the saddle point,

$$\begin{aligned} -S(E) + \beta E &= -S(E_*) + \beta E_* - \frac{1}{2} S''(E_*)(E - E_*)^2 + \cdots \\ &= -S(E_*) + \beta E_* + \frac{CT^2}{2}(E - E_*)^2 + \cdots \end{aligned} \tag{3.2.6}$$

where we used

$$\begin{gathered} \tilde{\beta}(E) \equiv \frac{\partial S}{\partial E}, \quad \tilde{\beta}(E_*) = \beta \\ \left.\frac{\partial^2 S}{\partial E^2}\right|_{E_*} = -\left.\frac{1}{\tilde{T}^2}\frac{\partial \tilde{T}}{\partial E}\right|_{E_*} = -\left.\frac{1}{C\tilde{T}^2}\right|_{E_*} = -\frac{1}{CT^2} \end{gathered} \tag{3.2.7}$$

the SPA is valid when the perturbation around the saddle point is small, e.g.

$$\Delta E = |E - E_*| \ll T\sqrt{C} \tag{3.2.8}$$

When $C \lesssim 1$, thermal fluctuations $\Delta E \sim T$ can push a state out of this window.

For both cases Eqs. (B.4.20) and (3.4.41), the continuum thermodynamics becomes invalid when $C \lesssim 1$. For the finite systems, the heat capacity decreases ($C \to 0$) as the temperature is lowered due to the third law of thermodynamics. On the other hand, since the heat capacity is an extensive quantity, it scales with the number of degrees of freedom

N, which increases in thermodynamic limit, $N \to \infty$ and hence the heat capacity remains to be $\mathcal{O}(1)$, allowing the continuum thermodynamic descriptions.

Extremal black holes are exception to this rule. Despite enormous entropy $S = \frac{A}{4G_N}$ even at small temperatures, the extremal black holes have a very small heat capacity, $C_Q \sim 0$. (And $T \sim 0$.) For example, for the 4d Reissener-Nordstrom black holes,

$$\mathrm{d}s^2 = -f(r)\mathrm{d}t^2 + \frac{\mathrm{d}r^2}{f(r)} + r^2\mathrm{d}\Omega^2 \tag{3.2.9}$$

where

$$\begin{aligned} f(r) &= 1 - \frac{2GM}{r} + \frac{GQ^2}{r^2} \equiv \frac{(r-r_+)(r-r_-)}{r^2} \\ r_\pm &= GM \pm \sqrt{G^2M^2 - GQ^2} \end{aligned} \tag{3.2.10}$$

the Hawking temperature, Bekenstein-Hawking entropy and the heat capacity are given by

$$T_H = \frac{f'(r_+)}{4\pi} = \frac{r_+ - r_-}{4\pi r_+^2}, \qquad S = 4\pi r_+^2, \qquad C_Q = \left(\frac{\partial T_H}{\partial M}\right)_Q = -\frac{2\pi r_+^2 (r_+ - r_-)}{r_+ - 3r_-} \tag{3.2.11}$$

From this, we see that the heat capacity decreases $C_Q \to 0$ in the extremal limit $r_+ - r_- \to 0$.

Thus, despite the large entropy, thermodynamic description is invalidated once the back-reaction is incorporated for the extremal black holes, and one must consider potentially very different quantum gravitational effects.

3.2.2 Quantum gravitational effects from the near horizon JT gravity

The near-extremal Reissener-Nordstrom black holes have a very long throat near the horizon, and hence the quantum fluctuations at this region dominate. To see this nearly AdS_2 region near the horizon, we parameterize the extremality using ϵ

$$r_\pm = r_0 \pm \epsilon \tag{3.2.12}$$

and take the near-horizon limit

$$t = \frac{r_0^2}{\lambda}\tau, \quad r = r_0 + \lambda\rho \tag{3.2.13}$$

in the metric, where $\epsilon = \lambda\rho_h$, to obtain

$$\mathrm{d}s^2 = r_0^2\left[-(\rho^2-\rho_h^2)\mathrm{d}\tau^2 + \frac{\mathrm{d}\rho^2}{\rho^2-\rho_h^2} + \mathrm{d}\Omega_2^2\right] + 2\lambda r_0\rho\left[(\rho^2-\rho_h^2)\mathrm{d}\tau^2 + \frac{\mathrm{d}\rho^2}{\rho^2-\rho_h^2} + \mathrm{d}\Omega_2^2\right] + \mathcal{O}(\lambda^2) \tag{3.2.14}$$

The resulting near-horizon geometry is $\mathrm{AdS}_2 \times S^2$ to the leading order in λ, however, considering the correction from the deviation from the extremality, the geometry is not asymptotically AdS_2. Nonetheless, the geometry has a very long throat near the horizon $\rho \simeq \rho_h$, and hence the quantum fluctuations at the near horizon region dominate the path integral.

Using the 1-loop determinant of the Euclidean path integral at the near horizon region, the authors of [38] showed that the near-extremal black holes indeed can radiate quantum mechanically and there is no M_{gap} in the spectrum of the near-extremal black holes unlike some supersymmetric black holes. Indeed, the quantum gravitational effects get boosted at low temperature at the near horizon region of the Euclidean black holes. We explain these in the following subsection.

3.2.2.1 1-loop Euclidean path integral

Banerjee and Saha [38] computed the Euclidean path integral at the near-horizon region of the near-extremal black hole in 4d, without resorting to the effective Schwarzian description and showed that the quantum effects at the near horizon region lift the excitation away from the extremality of the near-extremal black hole to above the energy of a Hawking quantum T, i.e. quantum effects resolve the issue with the semi-classical/thermodynamic description by removing the M_{gap} and allow the radiation. The leading low T behavior of their Euclidean path integral computed in 4d agrees that of the effective Schwarzian theory computed by [43]. We sketch Banerjee and Saha's computation of the Euclidean path integral in the following.

Consider an Euclidean near-extremal 4d Reissener-Nordstrom black hole, in the specific $U(1)$ gauge field background

$$A_t = iQ\left(\frac{1}{r_+} - \frac{1}{r}\right), \quad F_{rt} = \frac{iQ}{r^2} \tag{3.2.15}$$

Treating the near-extremal solution as the perturbations around the extremal geometry,

$$g_{\mu\nu}^{NX} = g_{\mu\nu}^{X} + h_{\mu\nu}, \quad A_{\mu}^{NX} = A_{\mu}^{X} + a_{\mu} \tag{3.2.16}$$

and integrating out these fluctuations, the authors get the 1-loop determinant of the quadratic kinetic operator in their action. The actions of the fluctuations are

$$\begin{aligned} S_{\text{diffeo}} &= -\frac{1}{2}\int d^4x\sqrt{\tilde{g}}\left(\tilde{\nabla}_A h^{AC} - \frac{1}{2}\tilde{\nabla}^C h\right)\left(\tilde{\nabla}^B h_{BC} - \frac{1}{2}\tilde{\nabla}_C h\right), \\ S_{\text{gauge}} &= -\frac{1}{2}\int d^4x\sqrt{\tilde{g}}\left(\tilde{\nabla}_A a^A\right)^2 \end{aligned} \tag{3.2.17}$$

Writing the quadratic kinetic operator as

$$S^{(2)} \equiv \int d^4x\sqrt{\tilde{g}}\Psi\tilde{\Delta}\Psi \tag{3.2.18}$$

the Euclidean path integral to 1-loop order is given by the determinant of the kinetic operator.

$$Z = \int \mathcal{D}\Psi \mathrm{e}^{-S^{(2)}} = \frac{1}{\sqrt{\det(\tilde{\Delta})}} \tag{3.2.19}$$

To compute the eigenvalues of the kinetic operator, we solve the eigenvalue problem to the first order in T. Namely, we decompose the kinetic operator, eigenfunctions and their eigenvalues into the extremal and near-extremal linear in T parts

$$\tilde{\Delta} = \Delta^0 + T\Delta^{(c)}, \quad f_n = f_n^0 + Tf_n^{(c)} + \mathcal{O}(T^2), \quad \tilde{\Lambda}_n = \Lambda_n^0 + T\Lambda_n^{(c)} + \mathcal{O}(T^2) \tag{3.2.20}$$

where Δ^0, Λ_n^0 are those of the extremal geometry ($T = 0$ contribution). Then we solve the first order perturbation

$$\left(\Delta^0 + T\Delta^{(c)}\right)\left(f_n^0(x) + Tf_n^{(c)}(x)\right) = \left(\Lambda_n^0 + T\Lambda_n^{(c)}\right)\left(f_n^0(x) + Tf_n^{(c)}(x)\right) \tag{3.2.21}$$

Using $\Delta^0 f_n^0(x) = \Lambda_n^0 f_n^0(x)$, this reduces to

$$\Delta^{(c)} f_n^0 + \Delta^0 f_n^{(c)} = \Lambda_n^{(c)} f_n^0 + \Lambda_n^0 f_n^{(c)} \tag{3.2.22}$$

and

$$\log Z = -\frac{1}{2}\sum_n \log\tilde{\Lambda}_n \tag{3.2.23}$$

Only zero modes of extremal geometry contributes The extremal kinetic operator Δ^0 has both continuous and discrete, normalizable non-zero modes and discretely degenerate, normalizable zero modes. Some of the zero modes are shared by $\tilde{\Delta}$ and Δ^0 with zero eigenvalues (i.e. simultaneous zero modes), whose nontrivial measure contributes to $\log Z \sim \log(a + bT^2)$ where $a \neq 0$. Each of these eigenfunctions contributes to $\log Z$ by

$$
\begin{aligned}
\text{Non-zero modes :} \quad & \log\left(\Lambda_n^0 + T\Lambda_n^{(c)}\right) \sim \log \Lambda_n^0 + \frac{T\Lambda_n^{(c)}}{\Lambda_n^0} + \mathcal{O}(T^2) \\
\text{Simultaneous zero modes :} \quad & \log\left(a + bT^2\right) \sim \log a + \mathcal{O}(T^2) \\
\text{Exclusive zero modes :} \quad & \log\left(T\Lambda_n^{(c)}\right) \sim \log T + \mathcal{O}(T^2)
\end{aligned}
\tag{3.2.24}
$$

We recall that thermodynamics broke down when the mean energy $\langle E \rangle = \log Z$ of the black hole away from the extremality M_0 is less than the energy of a Hawking quantum, $\sim T$ below $T \lesssim M_{gap}$. To remedy the issue, the quantum effects should be stronger than terms in $\log Z$ analytic in T. Hence, the relevant contributions come from the zero modes of the extremal kinetic operator, that are not zero modes of the total kinetic operator $\tilde{\Delta}$.

The zero modes of extremal part of the kinetic operator are made of the normalizable vector modes v^μ and discrete, normalizable tensor modes $w_{\mu\nu}$. Isolating the parts from the (degenerate) zero modes of the extremal part of kinetic operator in the mode expansion of the metric and $U(1)$ gauge fields fluctuations

$$
\begin{aligned}
a_\mu &= E_1 v_\mu + E_2 \varepsilon_{\mu\nu} v^\nu \\
h_{\mu i} &= \frac{1}{\sqrt{\kappa}} \left(E_3 \partial_i v_\mu + \tilde{E}_3 \varepsilon_{\mu\nu} \partial_i v^\nu + E_4 \varepsilon_{ij} \partial^j v_\mu + \tilde{E}_4 \varepsilon_{ij} \varepsilon_{\mu\nu} \partial^j v^\nu \right) \\
h_{\mu\nu} &= \frac{r_0}{\sqrt{2}} \left(\nabla_\mu \hat{\xi}_\nu + \nabla_\nu \hat{\xi}_\mu - g_{\mu\nu} \nabla^\rho \hat{\xi}_\rho \right) + E_6 w_{\mu\nu}; \quad \hat{\xi}_\mu = E_5 v_\mu + \tilde{E}_5 \varepsilon_{\mu\nu} v^\nu
\end{aligned}
\tag{3.2.25}
$$

For the tensor modes $w_{\mu\nu}$, the eigenvalues to $\mathcal{O}(T)$ are

$$
\Lambda\left[w_{\mu\nu}^n\right] = \frac{n\pi T}{2r_0} \tag{3.2.26}
$$

Using this, the 1-loop determinant is

$$\begin{aligned}\log Z_{\text{tensor}} &= -2 \cdot \frac{1}{2} \sum_{n\geq 2} \log \Lambda \left[w^n_{\mu\nu} \right] \\ &= -\sum_{n\geq 2} \log \left(\frac{n\pi T}{2r_0} \right) \\ &= \log \left(\prod_{n\geq 2} \frac{2r_0}{n\pi T} \right) .\end{aligned} \tag{3.2.27}$$

Using the Zeta-function regularization, we get the $\frac{3}{2}\log T$ contribution:

$$\prod_{n\geq 2} \frac{\alpha}{nT} = \frac{1}{\sqrt{2\pi}} \frac{T^{3/2}}{\alpha^{3/2}} \tag{3.2.28}$$

i.e.

$$\log Z_{\text{tensor}} \sim \frac{3}{2} \log T \tag{3.2.29}$$

There are two types of vector modes—one with S^2 eigenvalue $l = 0$ and $l = 1$. The $l = 0$ vector modes remains to be the zero modes of the linearlized near-extremal kinetic operator, which contributes to $\mathcal{O}(T^2)$ to the $\log Z$, i.e. they do not have $\log T$ contribution.

On the other hand, the normalizable vector modes with $l = 1$ are no longer zero modes of the near-extremal kinetic operator. Long story short, their 1-loop determinant is

$$\log Z_{l=1 \text{ vector}} = 3 \log \left(\frac{\pi^{3/2}}{\sqrt{2\pi}} \frac{T^{3/2}}{(4r_0)^{3/2}} \right) + 3 \log \left(\frac{4r_0}{\pi T} \right) \tag{3.2.30}$$

at low T, it behaves as

$$\log Z_{l=1 \text{ vector}} \sim \frac{3}{2} \log T \tag{3.2.31}$$

Combining the normalizable tensor modes $w_{\mu\nu}$ and the $l = 1$ vector modes v_μ, the 1-loop determinant from the zero-mode of the extremal kinetic operator is

$$\log Z = \log \left(\frac{\pi^{3/2}}{\sqrt{2\pi}} \frac{T^{3/2}}{(2r_0)^{3/2}} \right) + 3 \log \left(\frac{\pi^{3/2}}{\sqrt{2\pi}} \frac{T^{3/2}}{(4r_0)^{3/2}} \right) + 3 \log \left(\frac{4r_0}{\pi T} \right) \tag{3.2.32}$$

which, at low T, goes as

$$\log Z \sim 3 \log T \tag{3.2.33}$$

This low T behavior of Euclidean path integral is the same as that of the effective Schwarzian description of the JT gravity, computed by [43], although the near-extremal black hole's near horizon region is not exactly asymptotically AdS_2 unlike the JT gravity.

As it dominates the energy of a single Hawking quantum $\sim T$, we conclude that the near extremal black holes can radiate the Hawking quanta at all temperature, ane there is no M_{gap} in the spectrum of the near-extremal black hole unlike the supersymmetric black holes, which cannot be arbitrarily close to extremality [44–46].

In addition to this, Turiaci and Illiesiu (2020) [43] found that there is no ground state degeneracy.

3.2.2.2 Boosted quantum gravitational effect at low *T*

As we will explain in detain in Section 3.3, the 4d near extremal RN black holes restricted to the s-wave sector are described by the low energy effective description known as the Jackiew-Teitelboim (JT) gravity [47–49].

$$I = -\frac{\phi_0}{16\pi G}\left[\int \sqrt{g}R + 2\int_{bdy} K\right] - \frac{1}{16\pi G}\left[\int d^2x\phi\sqrt{g}(R+2) + 2\int_{bdy}\phi_b K\right] + S_M[g,\chi] + \cdots \tag{3.2.34}$$

where ϕ is a fluctuation around the dilaton, which controls the volume of S^2 and χ is a scalar field. The first square braket is topological Euler characteristic. Integrating out the dilaton fluctuation ϕ in the bulk term of the second integral forces the geometry locally AdS_2. The third term is the Gibbons-Hawking-York (GHY) term for the well-defined variational principle given the Dirichlet boundary conditions. Finally, the backreaction from the matter causes the dilaton to diverge on the boundary. To regulate this, we introduce the cut-off boundary and impose the Dirichlet boundary conditions.

$$g|_{\mathrm{bdy}} = \frac{1}{\epsilon^2}, \quad \phi_b = \phi|_{\mathrm{bdy}} = \frac{\phi_r(u)}{\epsilon} \tag{3.2.35}$$

The Dirichlet boundary condition on metric manifests that the trajectory of the cut-off surface is parameterized by a curve $t(u)$

$$\frac{1}{\epsilon^2} = g_{uu} = \frac{t'^2 + z'^2}{z^2} \longrightarrow z = \epsilon t' + \mathcal{O}\big(\epsilon^3\big) \tag{3.2.36}$$

The extrinsic curvature contains the Schwarzian derivative of the boundary curve $t(u)$

$$K = 1 + \epsilon^2 \mathrm{Sch}(t(u), u) + \mathcal{O}(\epsilon^4), \quad \mathrm{Sch}(t(u), u) \equiv \frac{t' t'''}{t'^2} - \frac{3t''^2}{2t'^2} \tag{3.2.37}$$

and hence the GHY term gives rise to the famous Schwarzian action for the boundary curve $t(u)$.

$$I_{\mathrm{Sch}} = -\frac{1}{8\pi G_N} \int \mathrm{d}u \; \phi_r(u) \mathrm{Sch}(t(u), u), \quad \phi_b(u) = \frac{\phi_r(u)}{\epsilon^2} \tag{3.2.38}$$

The Schwarzian action is invariant under the $SL(2, \mathbb{R})$ transformation

$$t(u) \mapsto \frac{at(u) + b}{ct(u) + d}, \quad ad - bc = 1 \tag{3.2.39}$$

The solution of this action is $t(u) = \tan \frac{\pi u}{\beta}$ up to the $SL(2, \mathbb{R})$ transformation. The fluctuation around this solution

$$t(u) = \tan \frac{\tau(u)}{2}, \quad \tau(u) = \frac{2\pi}{\beta} u + \epsilon \left(\frac{2\pi u}{\beta} \right) \tag{3.2.40}$$

is described by the action

$$\begin{aligned} I &= -C \int_0^\beta \mathrm{d}u \, \mathrm{Sch}(t, u), \quad C \equiv \frac{\bar{\phi}_r}{8\pi G} \\ &= -C \int_0^\beta \mathrm{d}u \left[\mathrm{Sch}(\tau, u) + \tau'^2 \, \mathrm{Sch}(t, \tau) \right] \\ &= -C \int_0^\beta \mathrm{d}u \left[\mathrm{Sch}(\tau, u) + \frac{1}{2} \tau'^2 \right] \\ &= -\frac{2\pi^2 C}{\beta} - \frac{4\pi^2 C}{\beta^2} \int_0^\beta \left[\epsilon' \left(\frac{2\pi u}{\beta} \right) + \epsilon''' \left(\frac{2\pi u}{\beta} \right) \right] \mathrm{d}u \\ &\quad - \frac{4\pi^2 C}{\beta^2} \int_0^\beta \frac{1}{2} \left[-3\epsilon'' \left(\frac{2\pi u}{\beta} \right)^2 + \epsilon' \left(\frac{2\pi u}{\beta} \right)^2 - 2\epsilon^{(3)} \left(\frac{2\pi u}{\beta} \right) \epsilon' \left(\frac{2\pi u}{\beta} \right) \right] + \mathcal{O}(\epsilon^3) \end{aligned} \tag{3.2.41}$$

The constant piece contributes to the entropy of the black holes. Removing the total derivatives (second integral) and amending the integral range to $u' \equiv \frac{2\pi u}{\beta} \in [0, 2\pi]$, we are left with the action

$$I_{\text{Sch}} = \frac{\pi \bar{\phi}_r}{4G\beta} \int_0^{2\pi} \mathrm{d}u' \left(\epsilon''^2 - \epsilon'^2 \right) + \mathcal{O}(\epsilon^3) \tag{3.2.42}$$

From this we see that the effective gratiational coupling is boosted at low temperature (that appears in the propagators of the boundary graviton, $\epsilon(u')$.

$$G \to \frac{\beta}{2\pi} G \tag{3.2.43}$$

3.2.3 Motivation for the real-time and ADM formulations

Wick rotation of Euclidean observables corresponds to correlation in thermal state, where ingoing and outgoing Hawking radiation are the same. On the other hand, the radiation from charged black holes obtained by a collapsing star are described by Unruh vacuum that we explain in the next subsection. This requires a dedicated Lorentzian description.

The effective Schwarzian description relies on the $SL(2, \mathbb{R})$ symmetry corresponding to the zero modes of Schwarzian. However, the Lorentzian boundary (geodesic completion) is more complicated and $SL(2, \mathbb{R})$ sym is not obvious. One way forward is using the Hamiltonian (ADM) formulation, that we turn to in the next next section 3.4.

3.3 JT gravity and bilocal matter action

3.3.1 Universal s-wave sector of 4d near-extremal charged black holes

Continuing the discussion of the Euclidean near extremal black holes, the Einstein-Hilbert and Maxwell action

$$S_{\text{Einstein-Maxwell}} \sim \frac{1}{l_P^2} \int d^4x \sqrt{g} \left(R_g - \frac{l_P^2}{4} F_{\mu\nu} F^{\mu\nu} \right) \tag{3.3.1}$$

where $l_P = 16\pi^2 G_N$, restricted to the s-wave and magnetic monopole subsector,

$$ds^2 = h_{ij}dx^i dx^j + \Phi^2 d\Omega^2, \quad F = Q\sin\theta d\phi \wedge d\theta, \quad \Phi^2 = \phi_0 + \phi \tag{3.3.2}$$

where Φ^2 is the dilaton that controls the volume of the S^2, reduces to

$$S_{\text{Einstein-Maxwell}} \sim \frac{4\pi}{l_P^2}\int \mathrm{d}t\mathrm{d}r\sqrt{h}\left[\Phi^2 R_h + 2(\partial\Phi)^2 + 2 - \frac{1}{2}\Phi^{-2}Q^2 l_P^2\right] \tag{3.3.3}$$

which is a special instance of the bigger family of dilaton actions.

$$I = \frac{1}{16\pi G_N}\int d^2x\sqrt{-h}\left[\Phi^2 R_h + \lambda(\partial\Phi)^2 - U\left(\Phi^2/d^2\right)\right] \tag{3.3.4}$$

The constant dilaton mode ϕ_0 is a Lagrange multiplier that forces the equation of motion

$$\frac{2}{\ell_{\text{AdS}}^2} + \frac{1}{d^2}U'\left(\phi_0/d^2\right) = 0, \tag{3.3.5}$$

Substituting this into the action, we are left with

$$\begin{aligned} I = \frac{1}{16\pi G_N}\Bigg[\int d^2x\sqrt{h}\left(\phi_0 R_h - U\left(\phi_0/d^2\right)\right) + \int d^2x\sqrt{h}\phi\left(R_h + \frac{2}{\ell_{\text{AdS}}^2}\right) \\ + \int d^2\sqrt{h}\frac{\lambda}{4}\frac{(\partial\phi)^2}{\phi_0+\phi}\Bigg] + \mathcal{O}\left(\frac{l_{AdS}^2\delta E^2}{Q^2}\right) \end{aligned} \tag{3.3.6}$$

The first integral is constant and a part of the (topological) Euler characteristic. The last integral is of $O\left(\frac{l_{AdS}^2\delta E^2}{Q^2}\right)$, which can be subleading in the near extremal limit. The second integral is so called Jackiew-Teitelboim (JT) gravity, which describes the low energy effective theory of the near extremal charged black hole in the s-wave sector. In the rest of the section, we work with this low energy effective action.

$$I_{grav;bulk} = S_0 - \frac{1}{16\pi G_N}\int_M d^2x\sqrt{h}\phi\left(R_h + 2\right) + \mathcal{O}\left(\frac{l_{AdS}^2\delta E^2}{Q^2}\right) \tag{3.3.7}$$

3.3.2 Cut-off boundary to regulate backreaction of matter

Adding a matter to the dilaton gravity results in instability in dilaton on the boundary, $\Phi^2|_{bdry} = \infty$. To see this, we divide the action into

$$S = I_{grav} + S_{\text{matter}} \tag{3.3.8}$$

and on the conformal gauge,

$$\mathrm{d}s^2 = -e^{2\omega(u^+,u^-)}\mathrm{d}u^+\mathrm{d}u^- \tag{3.3.9}$$

the equation of motion from varying h^{++} is

$$-e^{2\omega}\partial_+\left(e^{-2\omega}\partial_+\Phi^2\right) = T_{++}^{\text{matter}} \tag{3.3.10}$$

Using this, the T_{++} integrated along the null direction can be related to the values of Dilaton on the boundary.

$$\int_0^\pi du^+ e^{-2\omega}T_{++}^{\text{matter}} = \left[e^{-2\omega}\partial_+\Phi^2\right]\Big|_{u^+\to 0} - \left[e^{-2\omega}\partial_+\Phi^2\right]\Big|_{u^+\to\pi} \tag{3.3.11}$$

We assume the AdS_2 extending to the boundary. This is used to replace the conformal gauge with the global AdS_2 metric, which, on the boundary, behaves as

$$\begin{aligned} e^{2\omega} \sim \frac{1}{\sin^2(u^+)} &\sim \frac{1}{(u^+)^2} \quad \text{for } u^+\to 0 \\ &\sim \frac{1}{(u^+-\pi)^2} \quad \text{for } u^+\to\pi \end{aligned} \tag{3.3.12}$$

Since $T_{++}^{matter} > 0$, the dilaton diverges at the boundary.[3]

To regulate this, one introduces the cut-off, $r = r_c = \frac{1}{\epsilon}$ or $z = \epsilon$.[4] On the cut-off boundary, we impose the Dirichlet boundary conditions on the metric and dilaton.

$$g|_{\text{bdy}} = \frac{1}{\epsilon^2}, \quad \phi_b = \phi|_{\text{bdy}} = \frac{\phi_r(u)}{\epsilon} \tag{3.3.15}$$

---

[3] And now Sarosi associates this singularity to the irrelevant deformation, which sources the non-normalizable modes of matter solution. Their logic is that the irrelevant deformation deforms the UV CFT away from the IR CFT, which corresponds to having non-AdS geometry on the boundary (UV) and instead the boundary smoothly connects to the asymptotically flat spacetime.

[4] As a side remark, one can translate this to the boundary CFT language by using the holographic RG flow.

$$\begin{aligned} \text{Boundary at } z=0 \quad (r>r_c) \quad &\leftrightarrow \quad \text{UV} \\ \text{Interior } z\gg 0 \quad (r<r_c) \quad &\leftrightarrow \quad \text{IR} \end{aligned} \tag{3.3.13}$$

The interior starts out as an empty AdS_2 dual to IR CFT_1 near the horizon and smoothly connects to asymptotically flat space, dual to a different QFT_1 in UV, through an irrelevant deformation.

$$S_{CFT_{IR}} \to S_{QFT_{UV}} = S_{CFT_{IR}} + \int J\mathcal{O}\,\mathrm{d}u, \quad \Delta_{\mathcal{O}} > d = 1 \tag{3.3.14}$$

The boundary condition on the metric manifests that the cutoff surface $(t(u), z(u))$ is parameterized by the curve $t(u)$

$$\frac{1}{\epsilon^2} = g_{uu} = \frac{t'^2 + z'^2}{z^2} \longrightarrow z = \epsilon t' + \mathcal{O}\big(\epsilon^3\big) \tag{3.3.16}$$

The reparameterization (conformal sym. in 1d) $u \mapsto f(u)$ *changes* the cut-off surface to a new curve, $t'(u) = t \circ f(u)$ due to the boundary condition and is a symmetry (of the bulk gravitational action) that is spontaneously broken to $SL(2, \mathbb{R})$.

$$t(u) \mapsto \frac{at(u) + b}{ct(u) + d}, \quad ad - bc = 1 \tag{3.3.17}$$

For the well-defined variational principle given the Dirichlet boundary conditions, we can add the Gibbons-Hawking-York (GHY) boundary terms to the Euclidean action. In total, the action is

$$S_{\text{Einstein-Maxwell}} \sim S_0 - \frac{1}{16\pi G_N}\left[\int_M d^2x\sqrt{h}\phi\,(R_h + 2) + 2\int_{\partial M} \phi_b K\right] \tag{3.3.18}$$

The extrinsic curvature has the Schwarzian derivative of $t(u)$

$$K = 1 + \epsilon^2 \mathrm{Sch}(t(u), u) + \mathcal{O}(\epsilon^4) \tag{3.3.19}$$

The constant piece is combined with the curvature term to form the Euler characteristic (topological number). The Schwarzian piece

$$I_{\text{Sch}} = -\frac{1}{8\pi G_N}\int \mathrm{d}u\ \phi_r(u)\mathrm{Sch}(t(u), u), \quad \phi_b(u) = \frac{\phi_r(u)}{\epsilon^2} \tag{3.3.20}$$

is the action of the boundary curve $t(u)$[5] It is invariant under the $SL(2, \mathbb{R})$ reparameterization (which forms the zero modes of the Schwarzian).

where J is a source and $\mathcal{O}$ is an irrelevant operator deformation. We work only within the cut-off, in the near-horizon AdS region. The irrelevant source introduces a non-normalizable modes to the matter solution and also is responsible for the blow-up of dilaton on the boundary.

[5]Since this is the boundary action, the reparameterization (conformal) symmetry is not explicitly broken *yet*. This is explicitly broken by the boundary condition of dilaton as will be explained in the main text.

3.3.3 Solutions and symmetries of JT gravity

Indeed, the reparameterisation (1d conformal) symmetry explicitly broken in JT gravity, which allows the finite energy density. To see this, recall the Einstein-Maxwell action restricted to s-wave sector of the near-extremal black hole.

$$I = -\frac{\phi_0}{16\pi G}\left[\int \sqrt{g}R + 2\int_{bdy} K\right] - \frac{1}{16\pi G}\left[\int d^2x\phi\sqrt{g}(R+2) + 2\int_{bdy}\phi_b K\right] + I_M[g,\chi] + \cdots \tag{3.3.21}$$

The variation of the gravitational part is

$$\begin{aligned}\delta S = \int d^2x\sqrt{-g}\Bigg[&\left(\frac{1}{2}(R+2)\Phi g^{\mu\nu} - R^{\mu\nu}\Phi + \nabla^\mu\nabla^\nu\Phi - g^{\mu\nu}\nabla^2\Phi\right)\delta g_{\mu\nu} \\ &-\Phi_0\left(R^{\mu\nu} - \frac{1}{2}Rg^{\mu\nu}\right)\delta g_{\mu\nu} + (R+2)\delta\Phi\Bigg] \\ &+\int_{\partial M} dx\sqrt{|\gamma|}\left[2(K-1)\delta\Phi + \left(r^\nu\nabla_\nu\Phi - \Phi\right)\gamma^{\alpha\beta}\delta\gamma_{\alpha\beta}\right]\end{aligned} \tag{3.3.22}$$

Before discussing the boundary conditions, we note that the Dilaton term *explicitly* breaks the bulk diffeomorphism invariance down to a $U(1)$ gen by $\xi^\mu = \epsilon^{\mu\nu}\partial_\nu\phi$ as can be seen by $\delta_\xi\phi = \xi^\mu\partial_\mu\phi$.

The dilaton's boundary condition (3.3.15) should allow the equation of motion for the dilaton to have a solution. One of the equations of motion is obtained by varying action with respect to the metric

$$\frac{\delta S}{\delta g^{\mu\nu}} = T^\phi_{\mu\nu} \equiv \frac{1}{8\pi G}\left(\nabla_\mu\nabla_\nu\phi - g_{\mu\nu}\nabla^2\phi + g_{\mu\nu}\phi\right) = 0 \tag{3.3.23}$$

The solution to this equation is parameterized by three free parameters A, B, C

$$\phi(t,z) = \frac{A + Bt + C(t^2+z^2)}{z} \tag{3.3.24}$$

The DBC that allows this solution is

$$\phi|_{bdry} = \frac{\phi_r(u)}{\epsilon} \tag{3.3.25}$$

This provides a relation between the coefficients A, B, C and the boundary curve $\tilde{t}(u)$ given by

$$\frac{A + B\tilde{t}(u) + C\tilde{t}^2(u)}{\tilde{t}'(u)} = \phi_r(u) \tag{3.3.26}$$

One can find all solutions in the following way. First, we can fix the A, B, C to certain values A_0, B_0, C_0 and find the solution $\tilde{t}_0(u)$. Then we can do a $SL(2,\mathbb{R})$ on $\tilde{t}$ on the LHS and take the new coefficients of the new coordinate, A', B', C'. All A, B, C are reachable from any arbitrary A_0, B_0, C_0 via $SL(2,\mathbb{R})$ transformation in this way. Since the differential equation has the unique solution, this means that we found all solutions. This also means that some $\tilde{t}(u)$ cannot be reached from a solution $\tilde{t}_0(u)$ via $SL(2,\mathbb{R})$, and hence they are not consistent with the boundary conditions. Thus, the reparameterization symmetry is explicitly broken down to $SL(2,\mathbb{R})$.

Then again, the choice of the cut-off surface $\langle t(u)\rangle$ spontaneously breaks this already explicitly broken reparameterization symmetry. Since they are already explicitly broken, the excitations $\tilde{t}(u)$ around these (further) spontaneously broken generators are *pseudo* Nambu-Goldstone bosons (NGB) instead of Goldstone bosons.

Since we broke the conformal symmetry down to $SL(2,\mathbb{R})$, the NGBs can have a (derivative) action. This is the Schwarzian action given by

$$I = -\frac{1}{8\pi G}\int du\phi_r(u)\,\mathrm{Sch}(t,u) \tag{3.3.27}$$

The symmetries and their breaking are summarized in Table 3.1.

Indeed, this effective action reproduces the same equation of motion for the dilaton. To see this, let's write the full Lagrangian apart from the overall coefficient.

$$\mathcal{L} = \phi_r\left[\frac{t'''}{t'} - \frac{3}{2}\left(\frac{t''}{t'}\right)^2\right] \tag{3.3.28}$$

	EH gravity	JT gravity
Symmetries	Full diffeomorphism symmetry Full reparameterization symmetry, spontaneously broken to $SL(2,\mathbb{R})$	Diffeomorphisms: only the $U(1)$ generated by $\xi^\mu = \epsilon^{\mu\nu}\partial_\nu\phi$ • Explicitly broken to $SL(2,\mathbb{R})$ • Spontaneously broken to $SL(2,\mathbb{R})$ by the choice of cutoff
Boundary graviton $\tilde{t}(u)$	Goldstone boson of reparameterization symmetry	Pseudo-Goldstone boson

Table 3.1: Symmetries of Einstein–Hilbert and JT gravity and their breaking.

The variation of Lagrangian is

$$\begin{aligned}
\delta\mathcal{L} &= \frac{\delta\mathcal{L}}{\delta t'}\delta t' + \frac{\delta\mathcal{L}}{\delta t''}\delta t'' + \frac{\delta\mathcal{L}}{\delta t'''}\delta t''' \\
&= \frac{\mathrm{d}}{\mathrm{d}u}\left[\frac{\delta\mathcal{L}}{\delta t'''}\delta t'' + \frac{\delta\mathcal{L}}{\delta t''} - \frac{\mathrm{d}}{\mathrm{d}u}\frac{\delta\mathcal{L}}{\delta t'''}\right] + \left[\frac{\delta\mathcal{L}}{\delta t'} - \frac{\mathrm{d}}{\mathrm{d}u}\frac{\delta\mathcal{L}}{\delta t''} + \frac{\mathrm{d}^2}{\mathrm{d}u^2}\frac{\delta\mathcal{L}}{\delta t'''}\right]\delta t' \\
&= \frac{\mathrm{d}}{\mathrm{d}u}\left[\cdots\right] - \frac{\mathrm{d}}{\mathrm{d}u}\left[\frac{\delta\mathcal{L}}{\delta t'} - \frac{\mathrm{d}}{\mathrm{d}u}\frac{\delta\mathcal{L}}{\delta t''} + \frac{\mathrm{d}^2}{\mathrm{d}u^2}\frac{\delta\mathcal{L}}{\delta t'''}\right]\delta t \\
&= 0
\end{aligned} \tag{3.3.29}$$

From this, the equation of motion is

$$\frac{\mathrm{d}}{\mathrm{d}u}\left[\frac{\delta\mathcal{L}}{\delta t'} - \frac{\mathrm{d}}{\mathrm{d}u}\frac{\delta\mathcal{L}}{\delta t''} + \frac{\mathrm{d}^2}{\mathrm{d}u^2}\frac{\delta\mathcal{L}}{\delta t'''}\right] = 0 \tag{3.3.30}$$

Each term is given by

$$\begin{aligned}
&\frac{\delta\mathcal{L}}{\delta t'} = \phi_r\left(-\frac{t'''}{t'^2} + \frac{3t''^2}{t'^3}\right) \\
&\frac{\delta\mathcal{L}}{\delta t''} = \phi_r\left(\frac{-3t''}{t'^2}\right), \quad \frac{\mathrm{d}}{\mathrm{d}u}\frac{\delta\mathcal{L}}{\delta t''} = \left(-\frac{3\phi_r t''}{t'^2}\right)' \\
&\frac{\delta\mathcal{L}}{\delta t'''} = \frac{\phi_r}{t'}, \quad \frac{\mathrm{d}^2}{\mathrm{d}u^2}\frac{\delta\mathcal{L}}{\delta t'''} = \left(\frac{\phi_r}{t'}\right)''
\end{aligned} \tag{3.3.31}$$

Hence, the equation of motion is

$$\left[\left(\frac{\phi_r}{t'}\right)'' + \left(\frac{3\phi_r t''}{t'^2}\right)' + \phi_r\left(-\frac{t'''}{t'^2} + \frac{3t''^2}{t'^3}\right)\right]' = 0 \tag{3.3.32}$$

This can be more concisely written as

$$\left[\frac{1}{t'}\left(\frac{(t'\phi_r)'}{t'}\right)'\right]' = 0 \tag{3.3.33}$$

The solution is given by Eq. (3.3.24).

Backreaction to boundary curve Consider the constant dilaton on the boundary. Under an infinitesimal change in boundary curve, $\tilde{t}(u) \to \tilde{t}(u) + \delta t(u)$ and $\tilde{z}(u) \to \tilde{z}(u) + \delta z(u)$, the change in Schwarzian action in Eq. (3.3.33) is

$$\begin{aligned}\delta \mathrm{Sch}(t,u) &= \left[\frac{1}{t'}\left(\frac{t''}{t'}\right)'\right]' \delta t + \text{total derivatives} \\ &= \frac{\mathrm{Sch}'}{t'}\delta t + \text{total derivatives}\end{aligned} \tag{3.3.34}$$

where the second line can be explicitly checked using $\mathrm{Sch}(t,u) = \frac{t'''}{t'} - \frac{3}{2}\left(\frac{t''}{t'}\right)^2$.

Viewing the change in boundary curve as the large diffeomorphism[6], the variation on the matter is

$$\delta I_M = \int T^M_{\mu\nu}\delta g^{\mu\nu}\mathrm{d}x^2 = \int T^M_{\mu\nu}(\nabla^\mu\xi^\nu + \nabla^\nu\xi^\mu)\mathrm{d}x^2 = \int T^M_{\mu\nu}n^\mu\xi^\nu\sqrt{\gamma}\ \mathrm{d}\Sigma \tag{3.3.35}$$

Plugging the following values and taking the leading order variation

$$n = z\partial_z, \quad \mathrm{d}\Sigma = \sqrt{g_{\mu\nu}\dot{x}^\mu\dot{x}^\nu}\mathrm{d}u \simeq t'\mathrm{d}u, \quad \sqrt{\gamma} = \frac{1}{\epsilon}, \quad \xi^\nu = (\delta t, \epsilon\delta t') \tag{3.3.36}$$

$$\delta I_M = \int T^M_{zt}t'\delta t\ \mathrm{d}u \tag{3.3.37}$$

[6]This looks problematic to me. If it is large diff for the matter, why not for the gravitational part? The large diff variation on the gravitational part results in $8\pi G_N T^\phi_{\mu\nu} = \nabla_\mu\nabla_\nu\phi + g_{\mu\nu}(\nabla^2+2)\phi$, not the derivative of Schwarzian.

Thus, the variation of the total action is

$$\delta I = \int_{bdry} \left[-C \frac{\text{Sch}(t,u)'}{t'} + t' T^M_{tz} \right] \delta t \; \text{d}u \tag{3.3.38}$$

which leads to the equation of motion:

$$C \frac{\text{Sch}(t,u)'}{t'} = t' T^M_{tz} \tag{3.3.39}$$

A more intuitive derivation is using ADM Hamiltonian.

$$M = \frac{1}{8\pi G} \frac{1}{\epsilon} \left[\phi_b - \partial_n \phi \right] = \frac{\bar{\phi}_r}{8\pi G} \text{Sch}(t,u) = C \, \text{Sch}(t,u) \tag{3.3.40}$$

The energy flux is

$$\frac{\text{d}M}{\text{d}u} = t'^2 T^M_{tz} \tag{3.3.41}$$

This equation can be used to find the new boundary curve modified due to the backreaction of the matter.

3.3.4 Boundary graviton propagator

Recall the Schwarzian action for the small fluctuation around the boundary circle

$$t(u) = \tan \frac{\tau(u)}{2}, \quad \tau(u) = \frac{2\pi}{\beta} u + \epsilon\left(\frac{2\pi}{\beta} u \right) \tag{3.3.42}$$

is given by

$$I_{\text{Sch}} = \frac{\pi \bar{\phi}_r}{4 G \beta} \int_0^{2\pi} \text{d}u' \left(\epsilon''^2 - \epsilon'^2 \right) + \mathcal{O}(\epsilon^3) \tag{3.3.43}$$

The boundary graviton's propagator is

$$\langle \epsilon(u) \epsilon(0) \rangle = \frac{4 G \beta}{\pi \bar{\phi}_r} \sum_{|k|>1} \frac{e^{iku}}{k^2(k^2-1)} \tag{3.3.44}$$

The discrete sum can be done by casting it to a contour integral. The result is

$$\langle \epsilon(u) \epsilon(0) \rangle = \frac{1}{2\pi C} \left[-\frac{(|u|-\pi)^2}{2} + (|u|-\pi) \sin|u| + a + b \cos u \right] \tag{3.3.45}$$

where a and b are gauge fixed to zero. We note that the LHS (position space expression) is not analytic because $u < 0$ and $u > 0$ cases have different expressions. There are two ways to see this from the RHS (momentum space expression).

1. Write the sum as the contour integral

$$\sum_{|k|\neq 0,1} \frac{e^{iku}}{k^2(k^2-1)} = \oint_{C_{0,1,sgn(u)}} \frac{\mathrm{d}k}{2\pi} \frac{1}{e^{2\pi ik}-1} \frac{e^{iku}}{k^2(k^2-1)} \tag{3.3.46}$$

where $C_{0,1,sgn(u)}$ is the contour that closes in LHP or UPH depending on the sign of u and avoids $k = 0, 1$ while containing the other poles $k \in \mathbb{Z}\backslash\{0, 1\}$. Because the two contours for $u < 0$ and $u > 0$ are different, the result is different (LHS).

2. More directly, the third derivative of the RHS w.r.t. u is divergent because

$$\sum_{|k|>1} \frac{ke^{iku}}{k^2-1}\bigg|_{u=0} = \infty \tag{3.3.47}$$

This means u is not C^3. Analytic function is by definition C^∞ and hence the RHS, which is convergent, is not analytic. Indeed, the discontinuity in derivatives evaluated at $u = 0$ shows up at third order (continuous in 0th, 1st, 2nd orders).

3.3.5 Scalar bilocal actions and their perturbative expansion

The matter part of the action is

$$\begin{aligned} I_M &= \frac{1}{2}\int_M \sqrt{g}\, \mathrm{d}^2x \left(\partial^\mu\chi\partial_\mu\chi + m^2\chi^2\right) \\ &= \frac{1}{2}\int_{\partial M} \chi\, n^\mu\partial_\mu\chi\, \mathrm{d}\Sigma + \frac{1}{2}\int_M \left[-\chi\partial^\mu(\sqrt{g}\partial_\mu\chi) + \sqrt{g}m^2\chi^2\right] \mathrm{d}^2x \end{aligned} \tag{3.3.48}$$

where again we used $n^\mu\partial_\mu = z\partial_z$ and $\mathrm{d}\Sigma = \frac{t'\mathrm{d}u}{\epsilon}$. The on-shell boundary action is

$$I_M \simeq \frac{1}{2}\int_{\partial M} \chi\partial_z\chi\, t'\mathrm{d}u \tag{3.3.49}$$

We are interested in the case where the $\mathrm{AdS}_2 \times S^2$ is embedded in 4d as the near horizon geometry. The scalar field χ also extends to the full 4d geometry, and so their boundary condition at the cut-off boundary of the near horizon AdS_2 region does not vanish. This requires turning on a non-normalizable source term in the asymptotic AdS_2 boundary. Denoting the source by $\chi_0(u)$, the boundary condition for the scalar at the asymptotic AdS_2

boundary is

$$\lim_{z\to 0}\chi(t,z) = z^{d-\Delta}\chi_0(t) + z^{\Delta}\langle\mathcal{O}\rangle + \cdots \tag{3.3.50}$$

where $\Delta = \frac{1}{2}\left(d + \sqrt{d^2+4m^2}\right)$ is the conformal dimension of deformation $\mathcal{O}$ to the dual quantum mechanics.

Additionally, one imposes the quasi-normal boundary condition at the horizon, $\lim_{z\to\infty}\chi(t,z) =$ positive frequency mode, to restrict to the in-falling modes to the horizon.

The solution to the equation of motion

$$-\chi\partial^{\mu}(\sqrt{g}\partial_{\mu}\chi) + \sqrt{g}m^2\chi^2 = 0 \tag{3.3.51}$$

subjecto the above boundary conditions is given in terms of the bulk-to-boundary propagator

$$\chi(t,z) = \int_{bdry} K_{\Delta}(t,z;t')\chi_0(t')\mathrm{d}t', \quad K_{\Delta}(t,z;t') = \left(\frac{z}{(t-t')^2+z^2}\right)^{\Delta} \tag{3.3.52}$$

which can be checked using the limit of the bulk-to-boundary propagator

$$\begin{aligned}\lim_{z\to 0} z^{\Delta-d}K_{\Delta}\left(z,x;x'\right) &= \delta^{(d)}\left(x-x'\right)\\ \lim_{z\to 0} z^{\Delta-d+1}\partial_z K_{\Delta}\left(z,x;x'\right) &= (d-\Delta)\delta^{(d)}\left(x-x'\right)\end{aligned} \tag{3.3.53}$$

Plugging this solution to the on-shell boundary action

$$\begin{aligned}\lim_{z\to 0}\int_{\partial M}\chi(t,z)\partial_z\chi(t,z)\mathrm{d}t &= \lim_{z\to 0}\int\mathrm{d}t\int\mathrm{d}t_1\frac{Dz^{\Delta}}{\left[(t-t_1)^2+z^2\right]^{\Delta}}\chi_0(t_1)\int\mathrm{d}t_2\frac{D\Delta z^{\Delta-1}\left[(t-t_2)^2+z^2\right]}{\left[(t-t_2)^2+z^2\right]^{\Delta+1}}\chi_0(t_2)\\ &= \int\mathrm{d}t\lim_{z\to 0}\int_{M_1}\mathrm{d}t_1\frac{Dz^{2\Delta-1}}{\left[(t-t_1)^2+z^2\right]^{\Delta}}\chi_0(t_1)\int\mathrm{d}t_2\frac{D\Delta\chi_0(t_2)}{|t-t_2|^{2\Delta}}\end{aligned} \tag{3.3.54}$$

where M_1 is conformally $\mathbb{R}$ with metric $\mathrm{d}s^2 = \frac{\mathrm{d}t^2}{z^2}$. Writing $t_1 = t + zu_1$,

$$\begin{aligned}\lim_{z\to 0}\int_{M_1}\mathrm{d}t_1\frac{Dz^{2\Delta-1}}{\left[(t-t_1)^2+z^2\right]^{\Delta}}\chi_0(t_1) &= \lim_{z\to 0}\int\mathrm{d}u_1\frac{D}{(u^2+1)^{\Delta}}\chi_0(t+zu_1)\\ &= \chi_0(t)\int\mathrm{d}u_1\frac{D}{(u_1^2+1)^{\Delta}}\\ &= \chi_0(t)\\ &= \int_{M_1}\chi_0(t_1)\delta(t-t_1)\ \mathrm{d}t_1\end{aligned} \tag{3.3.55}$$

Plugging this into the boundary action,

$$\begin{aligned}\lim_{z\to 0}\int_{\partial M}\chi(t,z)\partial_z\chi(t,z)\mathrm{d}t &= \int \mathrm{d}t\int \mathrm{d}t_1\ \delta(t-t_1)\chi_0(t_1)\int \mathrm{d}t_2\frac{D\Delta\chi_0(t_2)}{|t-t_2|^{2\Delta}} \\ &= D\Delta\int \mathrm{d}t_1\int \mathrm{d}t_2\frac{\chi_0(t_1)\chi_0(t_2)}{|t_1-t_2|^{2\Delta}}\end{aligned} \tag{3.3.56}$$

In terms of the boundary time $u_{1,2}$, the scalar on-shell action is bi-local, dressed with the boundary graviton $t(u)$.

$$S_{matter} \simeq D\Delta\int \mathrm{d}t_1\mathrm{d}t_2\frac{\chi_0(t_1)\chi_0(t_2)}{|t_1-t_2|^{2\Delta}} \tag{3.3.57}$$

To write this in terms of the boundary time u, we use the boundary condition (3.3.50) to relate the non-normalizable mode $\chi_0(t)$ to the source $\tilde{\chi}(u)$.

$$\begin{aligned}\lim_{z\to 0}\chi(t,z) = z^{d-\Delta}\chi_0(t) = (\epsilon t')^{d-\Delta}\chi_0(t) = \epsilon^{d-\Delta}\left(t'^{d-\Delta}\chi_0(t)\right) \equiv \epsilon^{d-\Delta}\tilde{\chi}_0(u) \\ \chi_0(t)\equiv t'^{\Delta-d}\tilde{\chi}_0(u)\end{aligned} \tag{3.3.58}$$

In terms of the boundary source $\tilde{\chi}_0(u)$, the on-shell action is

$$I_M^{\text{on-shell}} = \frac{D\Delta}{2}\int\left[\frac{t_1't_2'}{(t_1-t_2)^2}\right]^{\Delta}\tilde{\chi}_0(u_1)\tilde{\chi}_0(u_2)\ \mathrm{d}u_1\mathrm{d}u_2 \tag{3.3.59}$$

Consider the small fluctuations of the boundary gravitons that we used earlier.

$$t(u) = \tan\frac{\tau(u)}{2}, \quad \tau(u) = u+\epsilon(u) \tag{3.3.60}$$

where we set $\beta = 2\pi$ for simplicity. Expanding the bilocal action to the first order in the fluctuation $\epsilon(u)$ (for the tree-level 4pt function later),

$$\left[\frac{t'(u_1)\,t'(u_2)}{(t(u_1)-t(u_2))^2}\right]^{\Delta} = \left(\frac{1}{2\sin\frac{u_{12}}{2}}\right)^{2\Delta}\left[1+\Delta\left(\epsilon_1'+\epsilon_2'-\frac{\epsilon_1-\epsilon_2}{\tan\frac{u_{12}}{2}}\right)\right]+\mathcal{O}\left(\epsilon^2\right) \tag{3.3.61}$$

Derivation of boundary limit of bulk-to-boundary propagator In higher dimensions, the normalized bulk-to-boundary propagator is given by

$$K_\Delta(z,\vec{x};\vec{x}') = \frac{\Gamma(\Delta)}{\pi^{d/2}\Gamma(\Delta-d/2)}\left[\frac{z}{(\vec{x}-\vec{x}')^2+z^2}\right]^{\Delta} \tag{3.3.62}$$

We will derive the boundary limit of the bulk-to-boundary propagator in general dimension d.

$$\lim_{z\to 0} z^{\Delta-d} K_\Delta\left(z,x;x'\right) = \delta^{(d)}\left(x-x'\right)$$
$$\lim_{z\to 0} z^{\Delta-d+1}\partial_z K_\Delta\left(z,x;x'\right) = (d-\Delta)\delta^{(d)}\left(x-x'\right) \tag{3.3.63}$$

Let's consider an integral function.

$$I(z,x) = \int_{M_d} \mathrm{d}^d\vec{x}'\; K_\Delta(z,\vec{x};\vec{x}')f(\vec{x}') \tag{3.3.64}$$

where the integral manifold (boundary) is conformally $\mathbb{R}^d$ with the metric

$$M_d, \quad \mathrm{d}s^2 = \frac{\mathrm{d}\vec{x}\cdot\mathrm{d}\vec{x}}{z^2} \tag{3.3.65}$$

Writing $\vec{x}' = \vec{x} + z\vec{u}$ with $\vec{u}\in\mathbb{R}^d$,

$$I(z,\vec{x}) = Dz^{d-\Delta}\int_{\mathbb{R}^d}\mathrm{d}^d\vec{u}\left(\frac{1}{1+u^2}\right)^\Delta f(\vec{x}+z\vec{u}) \tag{3.3.66}$$

Now taking the boundary limit:

$$\begin{aligned}\lim_{z\to 0} I(z,\vec{x}) &= \lim_{z\to 0} Dz^{d-\Delta}\int_{\mathbb{R}^d}\mathrm{d}^d\vec{u}\left(\frac{1}{1+u^2}\right)^\Delta f(\vec{x}+z\vec{u})\\ &= \lim_{z\to 0} Dz^{d-\Delta}f(\vec{x})\int_{\mathbb{R}^d}\mathrm{d}^d\vec{u}\left(\frac{1}{1+u^2}\right)^\Delta\\ &= \lim_{z\to 0} z^{d-\Delta}f(\vec{x})\end{aligned} \tag{3.3.67}$$

Recalling the definition (B.4.15), we can identify (as a distribution)

$$\lim_{z\to 0} z^{\Delta-d}K_\Delta(z,\vec{x};\vec{x}') = \delta^d(\vec{x}-\vec{x}') \tag{3.3.68}$$

Taking derivative with respect to z, we also get

$$\lim_{z\to 0} z^{\Delta-d+1}K_\Delta(z,\vec{x};\vec{x}') = (d-\Delta)\delta^d(\vec{x}-\vec{x}') \tag{3.3.69}$$

3.3.6 Thermal 4pt functions and OTOC

Let's consider two scalar fields ϕ,φ with non-normalisable mode (sources on the boundary; Appendix B.3 explains the basics of this dictionary.) ϕ_0,φ_0 and the dual boundary operators

V, W respectively.

$$\begin{aligned} \phi &\sim \phi_0 z^{\Delta_-} + \langle V \rangle z^{\Delta_+} \\ \varphi &\sim \varphi_0 z^{\Delta_-} + \langle W \rangle z^{\Delta_+} \end{aligned} \tag{3.3.70}$$

There are nontrivial 4 point functions $\langle VWVW \rangle$ at tree level via exchange of the graviton. Since the graviton propagator has two different branches depending on the sign of the time difference, there are two types of Euclidean time-odered 4-point correlators at tree-level[7], namely, $\langle V(t_1)V(t_2)W(t_3)W(t_4)\rangle$ for $t_1 > t_2 > t_3 > t_4$ and $\langle V(t_1)W(t_3)V(t_2)W(t_4)$ for $t_1 > t_3 > t_2 > t_4$. Other diagrams are equivalent to either of these two using the cyclic property of trace and KMS condition. For example, $\langle VWWV \rangle$ is equivalent to $\langle VVWW \rangle$ using

$$\langle V_1 W_3 W_4 V_2 \rangle_\beta = \mathrm{Tr}\left(e^{t_2 H} V e^{-t_2 H} e^{-\beta H} V_1 W_3 W_4\right) = \mathrm{Tr}\left(e^{-\beta H} V_{2+\beta} V_1 W_3 W_4\right) = \langle V_{2+\beta} V_1 W_3 W_4 \rangle_\beta \tag{3.3.71}$$

Let's first consider the time ordering $t_1 > t_2 > t_3 > t_4$. Using the AdS/CFT dictionary (Appendix B.3), the 4pt function can be computed as

$$\begin{aligned} \langle V_1 V_2 W_3 W_4 \rangle &= \left. \frac{\delta Z_{grav}}{\delta\phi_0(u_1)\delta\phi_0(u_2)\delta\varphi_0(u_3)\delta\varphi_0(u_4)} \right|_{\phi_0, \varphi_0 = 0} \\ &= \left(\frac{1}{2\sin\frac{u_{12}}{2} \cdot 2\sin\frac{u_{34}}{2}} \right)^{2\Delta} \\ &\quad \times \left\langle T \left[1 + \Delta\left(\epsilon_1' + \epsilon_2' - \frac{\epsilon_1 - \epsilon_2}{\tan\frac{u_{12}}{2}} \right) \right] \left[1 + \Delta\left(\epsilon_3' + \epsilon_4' - \frac{\epsilon_3 - \epsilon_4}{\tan\frac{u_{34}}{2}} \right) \right] \right\rangle_{conn} \end{aligned} \tag{3.3.72}$$

where in the last line, we single out the connected diagram which has the graviton exchange between two scalars.

$$\frac{\langle V_1 V_2 W_3 W_4 \rangle}{\langle V_1 V_2 \rangle_0 \langle W_1 W_2 \rangle_0} = \Delta^2 \left\langle T \left(\epsilon_1' + \epsilon_2' - \frac{\epsilon_1 - \epsilon_2}{\tan\frac{u_{12}}{2}} \right) \left(\epsilon_3' + \epsilon_4' - \frac{\epsilon_3 - \epsilon_4}{\tan\frac{u_{34}}{2}} \right) \right\rangle \tag{3.3.73}$$

[7] In quantum field theories, one can check that the out-of-Euclidean time ordered correlators are divergent by inserting the complete set of energy eigenstates between time evolution and target operators. On the other hand, in quantum mechanics, the out-of-Euclidean time ordered correlators can be made convergent.

This can be computed using the green's function (B.4.20). Passing through Mathematica, this becomes

$$\frac{\langle V_1 V_2 W_3 W_4 \rangle}{\langle V_1 V_2 \rangle_0 \langle W_1 W_2 \rangle_0} = \frac{\Delta^2}{2\pi C}\left(-2 + \frac{u_{12}}{\tan\frac{u_{12}}{2}}\right)\left(-2 + \frac{u_{34}}{\tan\frac{u_{34}}{2}}\right) \tag{3.3.74}$$

For the other ordering, $t_1 > t_3 > t_2 > t_4$, we flipped from $t_2 > t_3$ to $t_3 > t_2$ and use the time ordered correlator $\langle \epsilon_3 \epsilon_2 \rangle$ in place of $\langle \epsilon_2 \epsilon_3 \rangle$ in the last step of Eq. (3.3.72), which have different expression as they fall into different branches of the 2pt function. The result becomes

$$\begin{aligned}\frac{\langle V_1 W_3 V_2 W_4 \rangle_{\text{grav}}}{\langle V_1 V_2 \rangle \langle W_3 W_4 \rangle} = \frac{\Delta^2}{2\pi C}\Bigg[\left(-2 + \frac{u_{12}}{\tan\frac{u_{12}}{2}}\right)\left(-2 + \frac{u_{34}}{\tan\frac{u_{34}}{2}}\right) + \\ + \frac{2\pi\left[\sin\left(\frac{u_1 - u_2 + u_3 - u_4}{2}\right) - \sin\left(\frac{u_1 + u_2 - u_3 - u_4}{2}\right)\right]}{2\sin\frac{u_{12}}{2}\sin\frac{u_{34}}{2}} + \frac{2\pi u_{23}}{\tan\frac{u_{12}}{2}\tan\frac{u_{34}}{2}}\Bigg]\end{aligned} \tag{3.3.75}$$

We can think of analytically continuing the 4pt function to the Lorenetzian time. Although the graviton 2pt function $\langle \epsilon(u)\epsilon(0)\rangle$ is not analytic, it is separately real-analytic for $\mathrm{Re}(u) > 0$ and $\mathrm{Re}(u) < 0$, and hence at each branch it an be analytically continued to the complex domain. For example, the Euclidean time can be complexified using

$$t_i \to \tau_i = \epsilon_i + it_i, \quad \epsilon_1 > \epsilon_3 > \epsilon_2 > \epsilon_4 \tag{3.3.76}$$

where the Euclidean time ϵ_i must satisfy the ordering while the Lorentzian time t_i don't have any ordering. Thus, we can continue the 4pt function to the out-of-time-ordered correlator.

$$\langle V(a) W_3(b + \hat{u}) V(0) W(\hat{u}) \rangle \sim \frac{\beta\Delta^2}{C} e^{\frac{2\pi\hat{u}}{\beta}}, \quad \frac{\beta}{2\pi} \ll \hat{u} \ll \frac{\beta}{2\pi}\log\frac{C}{\beta} \tag{3.3.77}$$

where the upper bound in $\hat{u}$ is placed to remain in the perturbative regime. The OTOC has exponential growth in separation, which implies the chaos.

3.4 ADM Hamiltonian in Euclidean space and Schwarzian theory

In this section, we derive the Arnowitt-Deser-Misner (ADM) Hamiltonian of the Einstein-Maxwell theory with a massless, charge neutral scalar in 4d asymptotically flat spacetime

$$S=-\frac{1}{4\pi}\int \mathrm{d}^4x\sqrt{-g}\left[\frac{1}{4G}\mathcal{R}+\frac{1}{4}F^2+\frac{1}{2}(\nabla\phi)^2\right] \tag{3.4.1}$$

and in AdS_3

$$S=-\frac{1}{2\pi}\int \mathrm{d}^3x\sqrt{-g}\left[\frac{1}{8G}\left(R+\frac{2}{l^2}\right)+\frac{1}{2}(\nabla\phi)^2\right] \tag{3.4.2}$$

Our starting point is the ADM coordinates

$$\mathrm{d}s^2=-N^2(t,r)\mathrm{d}t^2+L^2(t,r)\left(\mathrm{d}r+N^r(t,r)\mathrm{d}t\right)^2+R^2(t,r)\mathrm{d}\Omega_{d-2}^2 \tag{3.4.3}$$

where $L(t,r)$ and $R(t,r)$ are dynamical while the lapse and shift N, N^r are Lagrange multipliers, as will be clear in the Hamiltonian.

We consider the reduction from the 4d charged near extremal black holes ($d=4$) and from the AdS_3 ($d=3$) in the subsequent subsections. For each case, we first perform the Legendre transformation of the bulk action for gravity, Maxwell and scalar parts in each paragraph. We then consider the on-shell variation to identify the needed boundary action, namely the ADM Hamiltonian.

Once we obtained the ADM Hamiltonian, we move to the Euclidean space and carefully integrate in boundary gravitons and find the identification with the Schwarzian action of the well-known near horizon JT gravity to the leading order in boundary graviton.

3.4.1 ADM Hamiltonian of neutral scalars in 4d

Consider the 4d Einstein-Maxwell theory with a massless, neutral scalar.

$$S=-\frac{1}{4\pi}\int \mathrm{d}^dx\sqrt{-g}\left[\frac{1}{4G}\mathcal{R}+\frac{1}{4}F^2-\frac{1}{2}(\nabla\phi)^2\right] \tag{3.4.4}$$

3.4.1.1 Legendre transformation of bulk action

Gravity part To detange the boundary part of the Einstein-Hilbert action from the bulk part, we use the following Gamma-Gamma formula.

$$\sqrt{-g}\ R = \mathcal{L}_{quad} + \mathcal{L}_{der} \tag{3.4.5}$$

where

$$\mathcal{L}_{quad} = \sqrt{-g}(\delta^c_a g^{bd} - \delta^d_a g^{bc})\Gamma^a_{dk}\Gamma^k_{bc}, \quad \mathcal{L}_{der} = \partial_c\left[\sqrt{-g}(\delta^c_a g^{bd} - \delta^d_a g^{bc})\Gamma^a_{bd}\right] \tag{3.4.6}$$

Plugging the metric into this formula, the gravity part of the action in the s-wave sector (spherically symmetric) is

$$S_G = \frac{1}{4G}\int \mathrm{d}t\mathrm{d}r\frac{\sqrt{-g}\ \mathcal{R}}{\sin\theta} \equiv \int \mathcal{L}_G\ \mathrm{d}t\mathrm{d}r \tag{3.4.7}$$

where

$$\begin{aligned}\mathcal{L}_G =& \frac{N'RR'}{GL} + \frac{NR'^2}{2GL} - \frac{N_r^2RR'L'}{GN} - \frac{LN_rN_r'RR'}{GN} - \frac{LN_r^2R'^2}{2GN}\\ &+ \frac{N_rRR'\dot{L}}{GN} + \frac{N_rL'R\dot{R}}{GN} + \frac{LR\dot{R}N_r'}{GN} + \frac{LR'\dot{R}N_r}{GN}\\ &- \frac{R\dot{R}\dot{L}}{GN} - \frac{L\dot{R}^2}{2GN}\end{aligned} \tag{3.4.8}$$

The conjugate momenta for the metric (L) and dilaton (R) are

$$\pi_L = \frac{R}{GN}\left(N_rR' - \dot{R}\right), \quad \pi_R = \frac{(LN_rR)'}{GN} - \frac{\partial_t(LR)}{GN} \tag{3.4.9}$$

After the Legendre transformation to these Hamiltonian variables, the gravity Lagrangian is

$$\mathcal{L}_G = \pi_L\dot{L} + \pi_R\dot{R} - N_r\mathcal{H}^{grav}_r - N\mathcal{H}^{grav}_t \tag{3.4.10}$$

where the constraints are

$$\mathcal{H}^{grav}_t = \left(\frac{RR'}{GL}\right)' - \frac{R'^2}{2GL} - \frac{G\pi_L\pi_R}{R} + \frac{GL\pi_L^2}{2R}, \quad \mathcal{H}^{grav}_r = R'\pi_R - L\pi_L' \tag{3.4.11}$$

As mentioned earlier, the lapse and shifts N, N^r are non-dynamical Lagrange multipliers and we integrate them out (by solving the constraint equations) even when we consider off-shell.

Maxwell part We consider the s-wave sector with the Coulomb potential.

$$A = A_t(t,r)\mathrm{d}t \tag{3.4.12}$$

$$S_{MW} = \int \mathrm{d}t\mathrm{d}r\ LNR^2\left(-\frac{1}{4}F^2\right) = \int \mathrm{d}t\mathrm{d}r\frac{R^2}{2LN}(A_t')^2 \tag{3.4.13}$$

The equation of motion

$$\frac{\delta S_{MW}}{\delta A_t} = \left(\frac{R^2}{LN}A_t'\right)' = 0 \tag{3.4.14}$$

has the solution

$$A_t' = \frac{LNQ}{R^2} \tag{3.4.15}$$

Plugging this back to the action,

$$S_{MW} = \int \mathrm{d}t\mathrm{d}r\ \frac{LNQ^2}{2R^2} \tag{3.4.16}$$

This action adds the constraint $\mathcal{H}_t^{MW} = -\frac{LQ^2}{2R^2}$.

Massless, neutral scalar part The scalar action in the ADM coordinates is

$$S_\phi = \frac{1}{2}\int \mathrm{d}t\mathrm{d}r\left[\frac{LR^2}{N}\dot{\phi}^2 - \left(\frac{NR^2}{L} - \frac{LR^2N_r^2}{N}\right)\phi'^2 - \frac{2N_rLR^2}{N}\dot{\phi}\phi'\right] \tag{3.4.17}$$

The conjugate momentum is

$$\pi_\phi = \frac{LR^2}{N}\left(\dot{\phi} - N_r\phi'\right) \quad \rightarrow \quad \dot{\phi} = \frac{N}{LR^2}\pi_\phi + N_r\phi' \tag{3.4.18}$$

The Legendre transformation of this Lagrangian is

$$\begin{aligned}\mathcal{L}_\phi =& \pi_\phi\dot{\phi} - \frac{LR^2}{2N}\left(\frac{N}{LR^2}\pi_\phi + N_r\phi'\right)^2 - \frac{1}{2}\left(\frac{NR^2}{L} - \frac{LR^2}{N}N_r^2\right)\phi'^2 \\ =& \pi_\phi\dot{\phi} - \frac{N\pi_\phi^2}{2LR^2} - N_r\phi'\pi_\phi - \frac{NR^2}{2L}\phi'^2\end{aligned} \tag{3.4.19}$$

which contributes to the constraints by

$$\mathcal{H}_t^\phi = \frac{\pi_\phi^2}{2LR^2} + \frac{R^2}{2L}\phi'^2, \quad \mathcal{H}_r^\phi = \phi'\pi_\phi \tag{3.4.20}$$

Gravity, MW and scalar combined Combining all three sectors,

$$S = \int \mathrm{d}t\mathrm{d}r \left(\pi_L \dot{L} + \pi_R \dot{R} + \pi_\phi \dot{\phi} - N_r \mathcal{H}_r - N\mathcal{H}_t \right) \tag{3.4.21}$$

where $\mathcal{H}_t = \mathcal{H}_t^G + \mathcal{H}_t^\phi$, and $\mathcal{H}_r = \mathcal{H}_r^G + \mathcal{H}_r^\phi$ which are given by

$$\begin{gathered} \mathcal{H}_t^G = \left(\frac{RR'}{GL} \right)' - \frac{R'^2}{2GL} - \frac{G\pi_L \pi_R}{R} + \frac{GL\pi_L^2}{2R} + \frac{LQ^2}{2R^2}, \qquad \mathcal{H}_r^G = R'\pi_R - L\pi_L' \\ \mathcal{H}_t^\phi = \frac{\pi_\phi^2}{2LR^2} + \frac{R^2}{2L}\phi'^2, \quad \mathcal{H}_r^\phi = \phi' \pi_\phi \end{gathered} \tag{3.4.22}$$

3.4.1.2 Boundary ADM Hamiltonian

Let's take a variation and identify the boundary terms. These will come from writing $(\cdots)\delta\varphi' = \frac{\mathrm{d}}{\mathrm{d}r}\left[(\cdots)\delta\varphi\right] - (\cdots)'\delta\varphi$. The time derivative will be irrelevant using the periodicity of time. The relevant variations are

$$\begin{aligned} \delta\mathcal{H}_r &= \delta R' \pi_R - L\delta\pi_L' + \pi\phi\delta\phi' + \cdots, \\ \delta\mathcal{H}_t &= \delta\left(\frac{RR'}{GL} \right)' - \frac{R'\delta R'}{GL} + \frac{R^2}{L}\phi'\delta\phi' \end{aligned} \tag{3.4.23}$$

which contributes the following total derivative to the variation.

$$\delta\mathcal{L} \ni -\frac{\mathrm{d}}{\mathrm{d}r}\left[N_r \pi_R \delta R - L\delta\pi_L + \pi_\phi \delta\phi + N\delta\left(\frac{RR'}{GL} \right) - \frac{R'\delta R}{GL} + \frac{R^2\phi'}{L}\delta\phi - \frac{N'R\delta R}{GL} \right] \tag{3.4.24}$$

After gauge fixing and imposing the boundary conditions

$$\pi_L = 0, \quad R = r, \quad \delta\phi\Big|_{bdry} = 0, \quad \delta N\Big|_{bdry} = 0 \tag{3.4.25}$$

the variation on the boundary is

$$\delta S\Big|_{bdry} = -\int \mathrm{d}t\ \delta\left(\frac{Nr}{GL} \right) \tag{3.4.26}$$

To cancel this, it is tempting to identify the following as the ADM Hamiltonian

$$S^0_{ADM} = \int \mathrm{d}t\ \frac{Nr}{GL} \tag{3.4.27}$$

However, on the asymptotically flat 4d boundary, the metric components fall off as $N \sim 1+\frac{N^1}{r}+\cdots$ and $L \sim 1+\frac{L^1}{r}+\cdots$ and hence S^0_{ADM} is divergent. The finite ADM Hamiltonian would be

$$H_{ADM} = \frac{L_1}{G} \tag{3.4.28}$$

As we explain in Appendix B.2, this can be identified with the quasi-local mass of the black hole given by

$$\mathcal{M} = \frac{R}{2G} + \frac{G\pi_L^2}{2R} - \frac{RR'^2}{2GL^2} + \frac{Q^2}{2R} \tag{3.4.29}$$

After gauge fixing, this corresponds to

$$\mathcal{M}(r) = \frac{r}{2G} - \frac{r}{2GL^2} + \frac{Q}{2r} \quad \overset{r\to\infty}{\longrightarrow} \quad \frac{r}{2G}\left(1 - 1 + \frac{2L_1}{r} + \cdots\right) = \frac{L_1}{G} \tag{3.4.30}$$

which agrees with H_{ADM} on the boundary. The quasi-local mass is finite on the boundary, so we take it as the ADM Hamiltonian, i.e.

$$H_{ADM} = \mathcal{M}(\infty) = \frac{r}{2G} - \frac{r}{2GL^2} + \frac{Q}{2r} \tag{3.4.31}$$

Solving constrants and ADM Hamiltonian The ADM Hamiltonian (3.4.31) needs an expression for L, which can be obtained by solving the constarint equation $\mathcal{H}_t = 0$, which after fixing the gauge is

$$\mathcal{H}_t = \left(\frac{r}{GL}\right)' - \frac{1}{2GL} - \frac{L}{2G} + \frac{LQ^2}{2r^2} + \frac{\pi_\phi^2}{2r^2L} + \frac{r^2\phi'^2}{2L} = 0 \tag{3.4.32}$$

Using $\left(\frac{r}{L^2}\right)' = \frac{1}{L^2} - \frac{2rL'}{L^3}$, we see that multiplying by $\frac{2G}{L}$ both hand sides turns the constraint into the form of

$$\left(\frac{r}{L^2}\right)' = 1 - \frac{GQ^2}{r^2} - \frac{r}{L^2}\frac{2Gh(r)}{r}, \qquad h(r) = \frac{1}{2}\left(\frac{\pi_\phi^2}{r^2} + r^2\phi'^2\right) \tag{3.4.33}$$

This differential equation can be written as

$$\frac{\mathrm{d}}{\mathrm{d}r}\left[e^{\int_{r_s}^r \frac{2Gh}{r'}\mathrm{d}r'}\frac{r}{L^2}\right] = e^{\int_{r_s}^r \frac{2Gh}{r'}\mathrm{d}r'}\left(1 - \frac{GQ^2}{r^2}\right) \tag{3.4.34}$$

Integratng both hand sides,

$$\frac{r}{L^2} = \frac{r_s}{L(r_s)^2} e^{-\int_{r_s}^{r} \frac{2Gh}{r'}\mathrm{d}r'} + e^{-\int_{r_s}^{r} \frac{2Gh}{r'}\mathrm{d}r'} \int_{r_s}^{r} e^{\int_{r_s}^{r'} \frac{2Gh}{r''}\mathrm{d}r''}\mathrm{d}r' - e^{-\int_{r_s}^{r} \frac{2Gh}{r'}\mathrm{d}r'} \int_{r_s}^{r} \frac{GQ^2}{r^2} e^{\int_{r_s}^{r'} \frac{2Gh}{r''}\mathrm{d}r''}\mathrm{d}r' \tag{3.4.35}$$

Bringing the exponential in front of the integral to inside,

$$\frac{r}{L^2} = \frac{r_s}{L(r_s)^2} e^{-\int_{r_s}^{r} \frac{2Gh}{r'}\mathrm{d}r'} + \int_{r_s}^{r} e^{-\int_{r'}^{r} \frac{2Gh}{r''}\mathrm{d}r''}\mathrm{d}r' - \int_{r_s}^{r} \frac{GQ^2}{r'^2} e^{-\int_{r'}^{r} \frac{2Gh}{r''}\mathrm{d}r''}\mathrm{d}r' \tag{3.4.36}$$

Following Appendix B in [50], we use integral by part to simplify each term

$$\begin{aligned}\int_{r_s}^{r} e^{-\int_{r'}^{r} \frac{2Gh}{r''}\mathrm{d}r''}\mathrm{d}r' &= \int_{r_s}^{r} \left(\frac{\mathrm{d}}{\mathrm{d}r'}r'\right) e^{-\int_{r'}^{r} \frac{2Gh}{r''}\mathrm{d}r''}\mathrm{d}r' \\ &= -\int_{r_s}^{r} 2Gh(r') e^{-\int_{r'}^{r} \frac{2Gh}{r''}\mathrm{d}r''}\mathrm{d}r' + r - r_s e^{-\int_{r_s}^{r} \frac{2Gh}{r''}\mathrm{d}r''}\mathrm{d}r'\end{aligned} \tag{3.4.37}$$

$$\begin{aligned}-\int_{r_s}^{r} \frac{GQ^2}{r^2} e^{-\int_{r'}^{r} \frac{2Gh}{r''}\mathrm{d}r''}\mathrm{d}r' &= \int_{r_s}^{r} \frac{GQ^2}{r'^2} \frac{\mathrm{d}}{\mathrm{d}r'}\left(\frac{GQ^2}{r'}\right) e^{-\int_{r'}^{r} \frac{2Gh}{r''}\mathrm{d}r''}\mathrm{d}r' \\ &= -\int_{r_s}^{r} \frac{2G^2Q^2}{r'^2} h(r') e^{-\int_{r'}^{r} \frac{2Gh}{r''}\mathrm{d}r''}\mathrm{d}r' + \frac{GQ^2}{r} - \frac{GQ^2}{r_s} e^{-\int_{r_s}^{r} \frac{2Gh(r'')}{r''}\mathrm{d}r''}\end{aligned} \tag{3.4.38}$$

Inside the shell, the metric $L(r_s)^2$ can be matched with the black hole metric:

$$\frac{1}{L^2(r_s)} = 1 - \frac{2GM}{r_s} + \frac{GQ^2}{r_s^2} \tag{3.4.39}$$

and so

$$\frac{r_s}{L(r_s)^2} = r_s - 2GM + \frac{GQ^2}{r_s} \tag{3.4.40}$$

Combining these ingredients,

$$\mathcal{M}(r) = Me^{-\int_{r_s}^{r} \frac{2Gh(r')}{r'}\mathrm{d}r'} + \int_{r_s}^{r} \left(1 + \frac{GQ^2}{r'^2}\right) h(r') e^{-\int_{r'}^{r} \frac{2Gh(r'')}{r''}\mathrm{d}r''}\mathrm{d}r' \tag{3.4.41}$$

The ADM Hamiltonian is the boundary value

$$H_{ADM} = \mathcal{M}(\infty) = Me^{-\int_{r_s}^{\infty} \frac{2Gh(r')}{r'}\mathrm{d}r'} + \int_{r_s}^{\infty} \left(1 + \frac{GQ^2}{r'^2}\right) h(r') e^{-\int_{r'}^{\infty} \frac{2Gh(r'')}{r''}\mathrm{d}r''}\mathrm{d}r' \tag{3.4.42}$$

One can simplify this by writing $1+\frac{GQ^2}{r'^2} = F(r') + \frac{2GM}{r'}$ in the integral, where $F(r) = 1-\frac{2GM}{r}+\frac{GQ^2}{r^2}$. Then this term becomes

$$\begin{aligned}
\mathcal{M}(r) &= Me^{-\int_{r_s}^{r}\frac{2Gh(r')}{r'}\mathrm{d}r'} + \int_{r_s}^{r}\left(F(r')+\frac{2GM}{r'}\right)h(r')e^{-\int_{r'}^{r}\frac{2Gh(r'')}{r''}\mathrm{d}r''}\mathrm{d}r' \\
&= Me^{-\int_{r_s}^{r}\frac{2Gh(r')}{r'}\mathrm{d}r'} + \int_{r_s}^{r}F(r')h(r')e^{-\int_{r'}^{r}\frac{2Gh(r'')}{r''}\mathrm{d}r''}\mathrm{d}r' + M\int_{r_s}^{r}\frac{2Gh(r')}{r'}e^{-\int_{r'}^{r}\frac{2Gh(r'')}{r''}\mathrm{d}r''}\mathrm{d}r' \\
&= Me^{-\int_{r_s}^{r}\frac{2Gh(r')}{r'}\mathrm{d}r'} + \int_{r_s}^{r}F(r')h(r')e^{-\int_{r'}^{r}\frac{2Gh(r'')}{r''}\mathrm{d}r''}\mathrm{d}r' + M\int_{r_s}^{r}\frac{\mathrm{d}}{\mathrm{d}r'}e^{-\int_{r'}^{r}\frac{2Gh(r'')}{r''}\mathrm{d}r''}\mathrm{d}r' \\
&= Me^{-\int_{r_s}^{r}\frac{2Gh(r')}{r'}\mathrm{d}r'} + \int_{r_s}^{r}F(r')h(r')e^{-\int_{r'}^{r}\frac{2Gh(r'')}{r''}\mathrm{d}r''}\mathrm{d}r' + M - Me^{-\int_{r_s}^{r}\frac{2Gh(r'')}{r''}\mathrm{d}r''} \\
&= M + \int_{r_s}^{r}F(r')h(r')e^{-\int_{r'}^{r}\frac{2Gh(r'')}{r''}\mathrm{d}r''}\mathrm{d}r'
\end{aligned} \tag{3.4.43}$$

Using this, the ADM Hamiltonian is

$$H_{ADM} = \mathcal{M}(\infty) = M + \int_{r_s}^{\infty}F(r')h(r')e^{-\int_{r'}^{\infty}\frac{2Gh(r'')}{r''}\mathrm{d}r''}\mathrm{d}r' \tag{3.4.44}$$

To the first order in h,

$$H_{ADM} = M + \int_{r_s}^{\infty}F(r')h(r')\mathrm{d}r' + \mathcal{O}(h^2) \tag{3.4.45}$$

ADM action As we integrated out the graviton L, the dynamic variable we have left is the scalar field. Combining the kinetic terms, the ADM action is an effective action for the scalar field.

$$\begin{aligned}
S_{ADM} &= \int \mathrm{d}t\mathrm{d}r\ \pi_\phi\dot{\phi} - \int \mathrm{d}t\ H_{ADM} \\
&= \int \mathrm{d}t\mathrm{d}r\ \pi_\phi\dot{\phi} - \int \mathrm{d}t\int_{r_s}^{\infty}F(r')h(r')e^{-\int_{r'}^{\infty}\frac{2Gh(r'')}{r''}\mathrm{d}r''}\mathrm{d}r'
\end{aligned} \tag{3.4.46}$$

where we dropped the constant mass term.

Near horizon limit Similarly to JT gravity, the equations of motion in the ADM formulation also restricts the ADM metric to AdS_2 in the near horizon region. As such, we use the following metric ansatz in place of the ADM,

$$\mathrm{d}s^2 = -f(r)\mathrm{d}t^2 + \frac{\mathrm{d}r^2}{f(r)} \tag{3.4.47}$$

where the radial coordinate r is the near-horizon coordinate, not the full 4d r coordinate. On this coordinate, the ADM action is

$$S_{ADM} = \int dtdr\left(\pi_\phi\dot{\phi} - f(r)h(r)e^{-\int_r^\infty dr' 8Gh(r')}\right), \quad h = \frac{1}{2}\left(\frac{\pi_\phi^2}{r} + r\phi'^2\right) \tag{3.4.48}$$

To the leading order in G, the ADM action is

$$S_{ADM} = \int dtdr\left(\pi_\phi\dot{\phi} - f(r)h(r)\right) + 8G\int dt\int_{r_h}^\infty dr\int_r^\infty dr' f(r)h(r)h\left(r'\right) + O\left(G^2h^3\right) \tag{3.4.49}$$

At the zeroth order in G, the solution of the π_ϕ variation is

$$\pi_\phi = \frac{r\dot{\phi}}{f(r)} \tag{3.4.50}$$

Plugging this, we get

$$S = \frac{1}{2}\int dtdrr\left(\frac{1}{f}\dot{\phi}^2 - f\phi'^2\right) + 8G\int dt\int_{r_h}^\infty dr\int_r^\infty dr' f(r)h(r)h\left(r'\right) + O\left(G^2h^3\right) \tag{3.4.51}$$

Writing

$$\begin{aligned} h &= \frac{r}{2f^2}\left(\dot{\phi}^2 + f^2\phi^2\right) \\ &= \frac{r}{2f^2}T_{tt} \end{aligned} \tag{3.4.52}$$

We consider the scalar dynamcis to be concentrated at the near-horizon region, and take $r = r_h$, i.e. $h = \frac{r_h}{2f^2}T_{tt}$, which also corresponds to no-coupling of scalar to the dilaton. The action becomes

$$S_{ADM} = \frac{r_h}{2}\int \mathrm{d}t\mathrm{d}r\left(\frac{1}{f}\dot{\phi}^2 - f\phi'^2\right) + 2r_h^2G\int \mathrm{d}t\int_{r_h}^\infty \mathrm{d}r\int_r^\infty \mathrm{d}r'\frac{T_{tt}(r)}{f(r)}\frac{T_{tt}\left(r'\right)}{f^2\left(r'\right)} + \mathcal{O}\left(G^2h^3\right) \tag{3.4.53}$$

In the following, we will establish the identification between this ADM action and the JT action for zero and finite temperature.

3.4.2 Comparison to Schwarzian action at zero temperature

At zero temperature, the near horizon AdS_2 is described in the Poincare coordinates

$$r = \frac{l^2}{z}, \quad f(r) = \frac{l^4}{z^2} \tag{3.4.54}$$

The metric, energy momentum tensor and the ADM action in these coordinates are

$$\mathrm{d}s^2 = \frac{l^4}{z^2}(-\mathrm{d}t^2 + \mathrm{d}z^2) \tag{3.4.55}$$

$$T_{tt} = \frac{1}{2}(\dot{\phi}^2 + \phi'^2) \tag{3.4.56}$$

and

$$S_{nh} = r_h \int dtdz \frac{1}{2}\left(\dot{\phi}^2 - \phi'^2\right) - 8Gr_h^2 \int dt \int_0^\infty dz' T_{tt}(z') \int_{z'}^0 dz'' \frac{z''^2}{\ell^2} T_{tt}(z'') \tag{3.4.57}$$

Using the conservation of energy momentum tensor $\nabla^\mu T_{\mu\nu} = 0$ in these coordinates

$$\partial_t T_{tt} = \partial_z T_{tz}, \quad \partial_z T_{zz} = \partial_t T_{tz} \tag{3.4.58}$$

we can relate the two components of the energy momentum tensor

$$T_{tt} = \partial_z \frac{1}{\partial_t} T_{tz} \tag{3.4.59}$$

and turn the ADM action (3.4.57), the interaction term (double integral) into a single bulk integral.

$$\begin{aligned} \int dt \int_0^\infty dz' T_{tt}(z') \int_{z'}^0 dz'' \frac{z''^2}{\ell^2} T_{tt}(z'') &= \int dt \int_0^\infty dz' \partial_{z'} \frac{1}{\partial_t} T_{tz}(z') \int_{z'}^0 dz'' \frac{z''^2}{\ell^2} T_{tt}(z'') \\ &= \int dt \int_0^\infty dz' \frac{1}{\partial_t} T_{tz}(z') \frac{z'^2}{\ell^2} T_{tt}(z') \end{aligned} \tag{3.4.60}$$

Now let $F = \frac{1}{\partial_t} T_{tz}$. $T_{tt} = \partial_z F$. Moreover, since $T_{tz} = \phi' \dot{\phi}$, it satisfies the eom, $(\partial_t^2 - \partial_z^2)F = 0$. For the functions that satisfy $(\partial_t^2 - \partial_z^2)F = 0$ and $F(t = \pm\infty) = 0$, the following identity holds.

$$\int_{-\infty}^{\infty} \mathrm{d}t \; 4z^2 F \partial_z F = \int_{-\infty}^{\infty} \mathrm{d}t \; \partial_z \left[z^2 F^2 - \frac{1}{\partial_t}(1 - z\partial_z) F \frac{1}{\partial_t}(1 - z\partial_z) F \right] \tag{3.4.61}$$

Using this,

$$\int dt \int_0^\infty dz' T_{tt}(z') \int_{z'}^0 dz'' \frac{z''^2}{\ell^2} T_{tt}(z'') = \frac{1}{4\ell^2} \int dt \int_0^\infty dz \partial_z \left[z^2 \left(\frac{1}{\partial_t} T_{tz} \right)^2 - \left(\frac{1}{\partial_t^2} (1 - z\partial_z) T_{tz} \right)^2 \right. \tag{3.4.62}$$

Assuming $T_{tz}(z = \infty) = 0$ (horizon), the integral reduces to

$$\int dt \int_0^\infty dz' T_{tt}(z') \int_{z'}^0 dz'' \frac{z''^2}{\ell^2} T_{tt}(z'') = \frac{1}{4\ell^2} \int dt \left(\frac{1}{\partial_t^2} (1 - z\partial_z) T_{tz} \right)^2 \Bigg|_{z=0} \tag{3.4.63}$$

Hence, the on-shell action to $\mathcal{O}(G)$ is

$$S_{nh} = r_h \int dt dz \frac{1}{2} \left(\dot{\phi}^2 - \phi'^2 \right) - \frac{2Gr_h^2}{\ell^2} \int dt \left(\frac{1}{\partial_t^2} (1 - z\partial_z) T_{tz} \right)^2 \Bigg|_{z=0} \tag{3.4.64}$$

Now, we can integrate-in the boundary gravition $\epsilon(t)$ to write the S_{nh} as

$$S_{nh}^\epsilon = r_h \int dt dz \frac{1}{2} \left(\dot{\phi}^2 - \phi^2 \right) - \frac{\alpha^2 \ell^2}{2G} \int dt \epsilon \partial_t^4 \epsilon + \alpha r_h \int dt \epsilon \left[1 - z\partial_z \right] T_{zt} \Bigg|_{z=0} \tag{3.4.65}$$

The kinetic term $\epsilon\partial_t^4\epsilon$ on the boundary corresponds to $\mathrm{Sch}(t(u), u)$ to $\mathcal{O}(\epsilon^2)$, where $t(u) = u + \epsilon(u)$. We will show that the last term $\alpha r_h \int dt \epsilon \left[1 - z\partial_z \right] T_{zt}\big|_{z=0}$ corresponds to the scalar's on-shell bilocal action on the boundary.

The scalar solution with boundary source $\phi_0(t)$ is

$$\phi(t, z) \approx \left[\phi_0(t) + O\left(z^2\right) \right] + \frac{z}{\pi} \int dt' \frac{\phi_0(t')}{(t - t')^2} + O\left(z^2\right) \tag{3.4.66}$$

Plugging this to the last term, we get

Using this and $T_{zt} = \phi'\dot{\phi}$ it's easy to evaluate the (4.34) as

$$\begin{aligned} r_h \int_{z=0} dt \epsilon \left[1 - z\partial_z \right] T_{zt} = \frac{\alpha r_h}{\pi} \int dt_1 dt_2 \frac{\epsilon(t_1) \dot{\phi}_0(t_1) \phi_0(t_2)}{(t_1 - t_2)^2} \\ \frac{\alpha r_h}{2\pi} \int dt_1 dt_2 \frac{\epsilon(t_1) \dot{\phi}_0(t_1) \phi_0(t_2) + \epsilon(t_2) \dot{\phi}_0(t_2) \phi_0(t_1)}{(t_1 - t_2)^2} \\ = -\frac{\alpha r_h}{2\pi} \int dt_1 dt_2 \left[\frac{d}{dt_1} \left(\frac{\epsilon(t_1)}{(t_1 - t_2)^2} \right) + \frac{d}{dt_2} \left(\frac{\epsilon(t_2)}{(t_1 - t_2)^2} \right) \right] \phi_0(t_1) \phi_0(t_2) \\ = -\frac{\alpha r_h}{2\pi} \int \frac{dt_1 dt_2}{(t_1 - t_2)^2} \left[\epsilon'(t_1) + \epsilon'(t_2) - 2\frac{\epsilon(t_1) - \epsilon(t_2)}{t_1 - t_2} \right] \phi_0(t_1) \phi_0(t_2) \end{aligned} \tag{3.4.67}$$

which is the bilocal action

$$-\frac{\alpha r_h}{2\pi}\int \mathrm{d}t_1\mathrm{d}t_2\left[\frac{T'(t_1)T'(t_2)}{(T(t_1)-T(t_2))^2}\right]^{\Delta}\tilde{\phi}_0(t_1)\tilde{\phi}_0(t_2) \tag{3.4.68}$$

with $T(t)=t+\epsilon(t)$, expanded to $\mathcal{O}(\epsilon^2)$.

3.4.3 Comparison to Schwarzian action at finite temperature

At finite temperature, we manipulate the ADM action in a different way. Using the energy momentum conservation $\nabla^{\mu}T_{\mu\nu}=0$.

$$\begin{aligned}\partial_r\left(fT_{tr}\right)&=\frac{1}{f}\partial_t T_{tt}\\ \rightarrow T_{tt}&=f\partial_r\left(f\frac{1}{\partial_t}T_{tr}\right)\end{aligned} \tag{3.4.69}$$

and using integral-by-part for the $\int_{r_h}^{\infty}\mathrm{d}r\ \partial_r(\cdots)$ term in the ADM action (3.4.46), we get

$$\begin{aligned}\int dt\int_{r_h}^{\infty}dr\int_{r}^{\infty}dr'\frac{T_{tt}(r)}{f(r)}\frac{T_{tt}\left(r'\right)}{f^2\left(r'\right)}&=\int dt\int_{r_h}^{\infty}dr\partial_r\left[f(r)\partial_t^{-1}T_{tr}(t)\right]\int_{r}^{\infty}dr'\frac{1}{f\left(r'\right)}\partial_{r'}\left[f\left(r'\right)\partial_t^{-1}T_{tr}\left(r'\right)\right]\\ &=\int dt\int_{r_h}^{\infty}dr\partial_t^{-1}T_{tr}\partial_r\left[f\partial_t^{-1}T_{tr}\right]\end{aligned} \tag{3.4.70}$$

At finite temperature, the near horizon region is described by thermal AdS_2 coordinates.

$$\mathrm{d}r=-f(z)\mathrm{d}z,\quad \frac{1}{f(z)}=\frac{l^2}{r_h^2}\sinh\left(\frac{r_h z}{l^2}\right) \tag{3.4.71}$$

$$r=r_h\coth\left(r_h z\right),\quad z(r=\infty)=0,\quad z\left(r=r_h\right)=\infty \tag{3.4.72}$$

and

$$\tau\cong\tau+\beta,\quad \beta=\frac{2\pi\ell^2}{r_h} \tag{3.4.73}$$

with the metric

$$ds^2=\frac{r_h^2}{\ell^2}\frac{d\tau^2+dz^2}{\sinh^2\left(\frac{r_h z}{\ell^2}\right)^2} \tag{3.4.74}$$

In these coordiantes, the interaction term (3.4.70) becomes

$$\begin{aligned}I_4&=2r_h^2G\int d\tau\int_0^{\infty}dz\frac{1}{f}\partial_\tau^{-1}T_{\tau z}\partial_z\left[\partial_\tau^{-1}T_{\tau z}\right]\\ &=2\ell^2G\int d\tau\int_0^{\infty}dz\sinh^2\left(\frac{r_h z}{\ell}\right)\partial_\tau^{-1}T_{\tau z}\partial_z\left[\partial_\tau^{-1}T_{\tau z}\right]\end{aligned} \tag{3.4.75}$$

In the rescaled coordinates

$$\tau' = \frac{2\pi}{\beta}\tau = \frac{r_h}{\ell^2}\tau, \quad z' = \frac{2\pi}{\beta}z = \frac{r_h}{\ell^2}z \tag{3.4.76}$$

the interaction term becomes

$$I_4 = r_h G \int_0^{2\pi} d\tau' \int_0^{\infty} dz' \sinh^2 z' \partial_{\tau'}^{-1} T_{\tau' z'} \partial_{z'} \left[\partial_{\tau'}^{-1} T_{\tau' z'}\right] \tag{3.4.77}$$

Further doing the integral by part, we finally get

$$\begin{aligned} I_4 &= r_h G \int_0^{2\pi} d\tau' \int_0^{\infty} dz' \sinh^2 z' \partial_{\tau'}^{-1} T_{\tau' z'} \partial_{z'} \left[\partial_{\tau'}^{-1} T_{\tau' z'}\right] \\ &= -\frac{1}{2} r_h G \int_0^{2\pi} d\tau' \int_0^{\infty} dz' \sinh\left(2z'\right) \left[\partial_{\tau'}^{-1} T_{\tau' z'}\right]^2 \end{aligned} \tag{3.4.78}$$

From here on, we drop the primes for the ease of notation.

the energy momentum tensor $T_{\tau z} = \dot{\phi}\phi'$. The solution of the scalar is

$$\phi(\tau, z) = \int \mathrm{d}\tau' K_\Delta(\tau, z; \tau')\phi_0(\tau') \tag{3.4.79}$$

Using the mode expansion of the bulk-to-boundary propagator

$$\begin{aligned} K\left(z, \tau; \tau_i\right) &= \frac{1}{2\pi} \frac{\sinh z}{\cosh z - \cos\left(\tau - \tau_i\right)} \\ &= \frac{1}{2\pi}\left[\frac{1}{1 - e^{-z - i(\tau - \tau_i)}} + \frac{1}{1 - e^{-z + i(\tau - \tau_i)}} - 1\right] \\ &= \frac{1}{2\pi} \sum_n e^{-|n| z - i n(\tau - \tau_i)} \end{aligned} \tag{3.4.80}$$

the energy momentum tensor is

$$\begin{aligned} T_{\tau z} &= \int \mathrm{d}\tau_1 \mathrm{d}\tau_2 \; \partial_\tau^{-1} \left[\partial_\tau K\left(z, \tau - \tau_1\right) \partial_z K\left(z, \tau - \tau_2\right) + \partial_z K\left(z, \tau - \tau_1\right) \partial_\tau K\left(z, \tau - \tau_2\right)\right] \\ &= -\frac{1}{(2\pi)^2} \int \mathrm{d}\tau_1 \mathrm{d}\tau_2 \sum_{n_1, n_2} \left[\frac{n_1 \left|n_2\right| + \left|n_1\right| n_2}{n_1 + n_2}\right] e^{-(|n_1| + |n_2|)z - i(n_1 + n_2)\tau + i(n_1 \tau_1 + n_2 \tau_2)} \end{aligned} \tag{3.4.81}$$

Performing the radial integral of the interaction term,

$$\begin{aligned} &\int_0^\infty dz \sinh(2z) e^{-(|n_1| + |n_2| + |n_3| + |n_4|)z} \\ &= \frac{1}{2}\left[\frac{1}{|n_1| + |n_2| + |n_3| + |n_4| - 2} - \frac{1}{|n_1| + |n_2| + |n_3| + |n_4| + 2}\right] \\ &= \frac{2}{\left(|n_1| + |n_2| + |n_3| + |n_4|\right)^2 - 4} \end{aligned} \tag{3.4.82}$$

Plugging this back to the action, the interaction term is given by

$$
\begin{aligned}
S_{int} =& \frac{1}{(2\pi)^3}\frac{G}{r_h}\int \mathrm{d}\tau_1\mathrm{d}\tau_2\mathrm{d}\tau_3\mathrm{d}\tau_4\,\Big[\\
& \sum_{n_i}\frac{(n_1\,|n_2| + |n_1|\,n_2)}{(n_1+n_2)}\frac{2}{(|n_1|+|n_2|+|n_3|+|n_4|)^2-4}\frac{(n_3\,|n_4|+|n_3|\,n_4)}{(n_3+n_4)} \\
& \times e^{in_1\tau_1+in_2\tau_2+in_3\tau_3+in_4\tau_4}\delta_{n_1+n_2+n_3+n_4}\Big]
\end{aligned}
\tag{3.4.83}
$$

Here, the factor $n_1|n_2| + |n_1|n_2 = 0$ unless n_1 and n_2 have the same sign. Similarly for n_3 and n_4. To satisfy Kronecker-Delta, we can write

$$
n_1 + n_2 = k, \quad n_3 + n_4 = -k, \quad |k| > 1 \tag{3.4.84}
$$

Plugging this into the action,

$$
S_{int} = \frac{1}{4\pi^3}\frac{G}{r_h}\int \mathrm{d}\tau_1\mathrm{d}\tau_2\mathrm{d}\tau_3\mathrm{d}\tau_4 \sum_{k,n_i}{}' \frac{n_1n_2n_3n_4e^{in_1\tau_1+in_2\tau_2+in_3\tau_3+in_4\tau_4}\delta_{n_1+n_2,k}\delta_{n_3+n_4,-k}}{k^2\left(k^2-1\right)} \tag{3.4.85}
$$

where $\sum'$ means sum over n_i with $n_1n_2 > 0$ and $n_3n_4 > 0$. Let's define the current

$$
J_k\left(\tau_1,\tau_2\right) = \sum_{n_1,n_2}{}' n_1n_2e^{in_1\tau_1+in_2\tau_2}\delta_{n_1+n_2,k} \tag{3.4.86}
$$

then the interaction term is written as

$$
S_{int} = \frac{G}{4\pi^3 r_h}\int \mathrm{d}\tau_1\mathrm{d}\tau_2\mathrm{d}\tau_3\mathrm{d}\tau_4 \sum_{|k|>1}\frac{J_k\left(\tau_1,\tau_2\right)J_{-k}\left(\tau_3,\tau_4\right)}{k^2\left(k^2-1\right)}\phi_0(\tau_1)\phi_0(\tau_2)\phi_0(\tau_3)\phi_0(\tau_4) \tag{3.4.87}
$$

We recognize $k^2(k^2-1)$ in the denominator as the propagator of the Schwarzian modes.

$$
\begin{aligned}
I_\epsilon &= \frac{Cr_h}{2G}\int_0^{2\pi} d\tau\,\left[\left(\epsilon''\right)^2 - \left(\epsilon'\right)^2\right] \\
&= \frac{Cr_h}{2G}\sum_{|k|>1}k^2\left(k^2-1\right)\epsilon_k\epsilon_{-k}
\end{aligned}
\tag{3.4.88}
$$

where we mode expanded the boundary graviton $\epsilon(\tau) = \sum_{|k|>1}\epsilon_k e^{-ik\tau}$. Integrating "in" this boundary graviton, the interaction action can be obtained from the Schwarzian + bilocal by integrating "out" the boundary graviton ϵ_k.

$$
I_4\left[\tau_i\right] = \frac{Cr_h}{2G}\sum_{|k|>1}k^2\left(k^2-1\right)\epsilon_k\epsilon_{-k} - i\sqrt{\frac{C}{\pi^3}}\int \mathrm{d}\tau_1\mathrm{d}\tau_2\sum_{|k|>1}J_k\left(\tau_1,\tau_2\right)\epsilon_{-k} \tag{3.4.89}
$$

$$\epsilon_k \sim \int \mathrm{d}\tau_1 \mathrm{d}\tau_2 \sum_{|k|>1} \frac{J_k(\tau_1,\tau_2)}{k^2(k^2-1)} \tag{3.4.90}$$

The first term in the action is apparently the Schwarzian. To see if the second term is the scalar bilocal action, we mode expand the bilocal action.

$$I_{bilocal} = \int \mathrm{d}u_1 \mathrm{d}u_2 \left[\frac{t'(u_1)t'(u_2)}{|t(u_1)-t(u_2)|^2}\right] \phi_0(u_1)\phi_0(u_2) \tag{3.4.91}$$

Writing $t(u) = \tan\left(\frac{\pi}{\beta}u + \frac{1}{2}\epsilon\left(\frac{2\pi u}{\beta}\right)\right)$ and expanding to $\mathcal{O}(\epsilon^2)$,

$$I_{bilocal} = \int_0^{2\pi} du_1 du_2 \phi_1(u_1)\phi_2(u_2) \frac{B(u_1,u_2)}{\left(2\sin\frac{u_{12}}{2}\right)^2} \tag{3.4.92}$$

where

$$B(u_1,u_2) = \varepsilon'(u_1) + \varepsilon'(u_2) - (\varepsilon(u_1) - \varepsilon(u_2))\cot\frac{u_{12}}{2}. \tag{3.4.93}$$

Now mode expanding each piece,

$$\begin{aligned} \phi_1(u_1) &= \sum_{m_1} a_{m_1} e^{-im_1 u_1}, \quad a_m = \frac{1}{2\pi} e^{im_1\tau_1} \\ \phi_2(u_2) &= \sum_{m_2} b_{m_2} e^{-im_2 u_2}, \quad b_m = \frac{1}{2\pi} e^{im_2\tau_2} \\ \epsilon(u) &= \sum_k \epsilon_k e^{-iku} \\ \frac{1}{\left(2\sin\frac{u_{12}-i\delta}{2}\right)^2} &= -\sum_{n=1}^{\infty} n e^{-n\delta} e^{-inu_{12}} \end{aligned} \tag{3.4.94}$$

and taking the $\delta \to 0$ limit at the end, we get the matter second term.

3.5 In-In correlation functions

3.5.1 Euclidean time orderd tree-level 4-point functions

In Section 3.3.6, we computed the Euclidean 4pt functions $\langle V(t_1)V(t_2)W(t_3)W(t_4)\rangle$ and $\langle V(t_1)W(t_3)V(t_2)W(t_4)\rangle$ of two operators V, W dual to two scalars ϕ, ψ within the JT gravity and continued to the real time thermal correlator. The goal of this section is to see if we can recover the same expression using the ADM action.

Indeed, as we identified the ADM action with the Schwarzian + bilocal theory in the previous subsection, the tree-level Euclidean correlators are gauranteed to agree between the two theories. However, we provide an explicit computation and check their identity in the following. Then, we will provide a direct real time calculation using a Schwinger-Keldysh contour, that can be used for states that are not thermal.

We can again write the on-shell scalars as $\int K_\Delta(\tau,z;\tau')\phi_0(\tau')\mathrm{d}\tau'$ and $\int K_\Delta(\tau,z;\tau')\psi_0(\tau')\mathrm{d}\tau'$, the energy momentum tensor is

$$\begin{aligned} T_{\tau z}(\tau,z) &= \dot{\phi}\phi' + \dot{\psi}\psi' \\ &= \int \mathrm{d}\tau_1 \mathrm{d}\tau_2\ \dot{K}_\Delta(\tau,z;\tau_1)K'_\Delta(\tau,z;\tau_2)\left(\phi_0(\tau_1)\phi_0(\tau_2)+\psi_0(\tau_1)\psi_0(\tau_2)\right) \end{aligned} \tag{3.5.1}$$

From the ADM Hamiltonian

$$I_4 = -\frac{1}{2} r_h G \int_0^{2\pi} d\tau' \int_0^\infty dz' \sinh(2z') \left[\partial_{\tau'}^{-1} T_{\tau' z'}\right]^2 \tag{3.5.2}$$

has now a cross-term between $T_{\tau z}^{\phi}$ and $T_{\tau z}^{\psi}$, which connects the same scalars respectively. Taking derivatives with respect to the four sources, the boundary 4pt correlator is

$$\begin{aligned} G_4 &\equiv \langle V(\tau_1)V(\tau_2)W(\tau_3)W(\tau_4)\rangle \\ &= -\frac{1}{2} r_h G \int_0^{2\pi} \mathrm{d}\tau \int_0^\infty \mathrm{d}z \sinh(2z)\, F_\phi(\tau,z;\tau_1,\tau_2) F_\psi(\tau,z;\tau_3,\tau_4) \end{aligned} \tag{3.5.3}$$

where

$$\begin{aligned} F_\phi(\tau,z;\tau_1,\tau_2) &= \partial_\tau^{-1}\left[\partial_\tau K(z,\tau-\tau_1)\,\partial_z K(z,\tau-\tau_2) + \partial_z K(z,\tau-\tau_1)\,\partial_\tau K(z,\tau-\tau_2)\right] \\ F_\psi(\tau,z;\tau_3,\tau_4) &= \partial_\tau^{-1}\left[\partial_\tau K(z,\tau-\tau_3)\,\partial_z K(z,\tau-\tau_4) + \partial_z K(z,\tau-\tau_3)\,\partial_\tau K(z,\tau-\tau_4)\right] \end{aligned} \tag{3.5.4}$$

As before, mode expanding K_Δ

$$\begin{aligned}
F_\phi(\tau,z;\tau_1,\tau_2) &= \partial_\tau^{-1}\left[\partial_\tau K\left(z,\tau-\tau_1\right)\partial_z K\left(z,\tau-\tau_2\right)+\partial_z K\left(z,\tau-\tau_1\right)\partial_\tau K\left(z,\tau-\tau_2\right)\right] \\
&= -\frac{1}{(2\pi)^2}\sum_{n_1,n_2}\left[\frac{n_1\left|n_2\right|+\left|n_1\right|n_2}{n_1+n_2}\right]e^{-(|n_1|+|n_2|)z-i(n_1+n_2)\tau+i(n_1\tau_1+n_2\tau_2)} \\
F_\psi(\tau,z;\tau_3,\tau_4) &= \partial_\tau^{-1}\left[\partial_\tau K\left(z,\tau-\tau_3\right)\partial_z K\left(z,\tau-\tau_4\right)+\partial_z K\left(z,\tau-\tau_3\right)\partial_\tau K\left(z,\tau-\tau_4\right)\right] \\
&= -\frac{1}{(2\pi)^2}\sum_{n_3,n_4}\left[\frac{n_3\left|n_4\right|+\left|n_3\right|n_4}{n_3+n_4}\right]e^{-(|n_3|+|n_4|)z-i(n_3+n_4)\tau+i(n_3\tau_3+n_4\tau_4)}
\end{aligned} \tag{3.5.5}$$

Performing the radial integral and satisfying the Kronecker-delta as we did leading up to Eq. (3.4.87), we get

$$G_4(\tau_i) = \frac{1}{4\pi^3}\frac{G}{r_h}\sum_{k,n_i}{}' n_1 n_2 \frac{1}{k^2\left(k^2-1\right)} n_3 n_4 e^{in_1\tau_1+in_2\tau_2+in_3\tau_3+in_4\tau_4}\delta_{n_1+n_2,k}\delta_{n_3+n_4,-k} \tag{3.5.6}$$

We can replace the factor of $n_1n_2n_3n_4$ with the derivatives w.r.t. τ_i.

$$\frac{4\pi^3 r_h}{G}G_4 = \partial_1\partial_2\partial_3\partial_4\sum_{|k|>1}\frac{1}{k^2(k^2-1)}\sum_{n_1,n_2}{}'\sum_{n_3,n_4}{}' e^{in_1\tau_1+in_2\tau_2+in_3\tau_3+in_4\tau_4}\delta_{n_1+n_2,k}\delta_{n_3+n_4,-k} \tag{3.5.7}$$

We can replace the Kronecker delta by setting $n_2 = k - n_1$ and $n_4 = -k - n_3$ and restricting the sums to

$$\begin{gathered}
n_1 n_2 = n_1(k-n_1) > 0 \quad \text{and} \quad n_3 n_4 = -n_3(k+n_3) > 0 \\
\rightarrow \quad \begin{cases} k>0: \quad 0<n_1<k, \quad -k<n_3<0 \\ k<0: \quad k<n_1<0, \quad 0<n_3<-k \end{cases}
\end{gathered} \tag{3.5.8}$$

which turns the 4pt function into

$$\frac{4\pi^3 r_h}{G}G_4 = -\partial_1\partial_2\partial_3\partial_4\left[\sum_{k>1}\sum_{0<n_1<k}\sum_{-k<n_3<0}+\sum_{k<-1}\sum_{k<n_1<0}\sum_{0<n_3<-k}\right]\frac{e^{in_1\tau_1+in_2\tau_2+in_3\tau_3+in_4\tau_4}}{k^2(k^2-1)} \tag{3.5.9}$$

The sums can be evaluated.

$$\begin{aligned}
k>1: &\quad \sum_{0<n_1<k} e^{in_1\tau_{12}} = \frac{e^{ik\tau_{12}}-e^{i\tau_{12}}}{e^{i\tau_{12}}-1}, \qquad \sum_{-k<n_3<0} e^{in_3\tau_{34}} = -\frac{e^{-i(k-1)\tau_{34}}-1}{e^{i\tau_{34}}-1} \\
k<-1: &\quad \sum_{k<n_1<0} e^{in_1\tau_{12}} = -\frac{e^{i(k+1)\tau_{12}}-1}{e^{i\tau_{12}}-1}, \qquad \sum_{0<n_3<-k} e^{in_3\tau_{34}} = \frac{e^{-ik\tau_{34}}-e^{i\tau_{34}}}{e^{i\tau_{34}}-1}
\end{aligned} \tag{3.5.10}$$

For each case, the product of these sums can be expanded as

$$\begin{aligned}
k>1: &\quad \frac{1}{(e^{i\tau_{12}}-1)(e^{i\tau_{34}}-1)}\left(e^{i\tau_{34}}e^{ik\tau_{13}}-e^{ik\tau_{14}}-e^{i\tau_{12}+i\tau_{34}}e^{ik\tau_{23}}+e^{i\tau_{12}}e^{ik\tau_{24}}\right)\\
k<-1: &\quad \frac{1}{(e^{i\tau_{12}}-1)(e^{i\tau_{34}}-1)}\left(e^{i\tau_{12}}e^{ik\tau_{13}}-e^{i\tau_{12}+i\tau_{34}}e^{ik\tau_{14}}-e^{ik\tau_{23}}+e^{i\tau_{34}}e^{ik\tau_{24}}\right)
\end{aligned} \tag{3.5.11}$$

We note that the sum of these two expressions have the following permutation symmetries (each line corresponds to one such permutation), which can be easily checked.

$$\begin{gathered}
\tau_1 \leftrightarrow \tau_2\\
\tau_3 \leftrightarrow \tau_4\\
\tau_1 \leftrightarrow \tau_3 \quad \& \quad \tau_2 \leftrightarrow \tau_4\\
\tau_1 \leftrightarrow \tau_4 \quad \& \quad \tau_2 \leftrightarrow \tau_3
\end{gathered} \tag{3.5.12}$$

Plugging these expansions into the 4pt function

$$\begin{aligned}
\frac{4\pi^3 r_h}{G}G_4 = &-\sum_{k>1}\frac{1}{k^2(k^2-1)}\partial_1\partial_2\partial_3\partial_4\left[\frac{e^{i\tau_{34}}e^{ik\tau_{13}}-e^{ik\tau_{14}}-e^{i\tau_{12}+i\tau_{34}}e^{ik\tau_{23}}+e^{i\tau_{12}}e^{ik\tau_{24}}}{(e^{i\tau_{12}}-1)(e^{i\tau 34}-1)}\right]\\
&-\sum_{k<-1}\frac{1}{k^2(k^2-1)}\partial_1\partial_2\partial_3\partial_4\left[\frac{e^{i\tau_{12}}e^{ik\tau_{13}}-e^{i\tau_{12}+i\tau_{34}}e^{ik\tau_{14}}-e^{ik\tau_{23}}+e^{i\tau_{34}}e^{ik\tau_{24}}}{(e^{i\tau_{12}}-1)(e^{i\tau 34}-1)}\right]
\end{aligned} \tag{3.5.13}$$

The two summand for $k>1$ and $k<-1$ on the RHS don't seem to be the same, however, after applying the derivatives $\partial_1\partial_2\partial_3\partial_4$, they are actually identified.

$$\begin{aligned}
&\partial_1\partial_2\partial_3\partial_4\left[\frac{1}{(e^{i\tau_{12}}-1)(e^{i\tau 34}-1)}\left(e^{i\tau_{34}}e^{ik\tau_{13}}-e^{ik\tau_{14}}-e^{i\tau_{12}+i\tau_{34}}e^{ik\tau_{23}}+e^{i\tau_{12}}e^{ik\tau_{24}}\right)\right]\\
&=\partial_1\partial_2\partial_3\partial_4\left[\frac{1}{(e^{i\tau_{12}}-1)(e^{i\tau 34}-1)}\left(e^{i\tau_{12}}e^{ik\tau_{13}}-e^{i\tau_{12}+i\tau_{34}}e^{ik\tau_{14}}-e^{ik\tau_{23}}+e^{i\tau_{34}}e^{ik\tau_{24}}\right)\right]
\end{aligned} \tag{3.5.14}$$

Hence we can combine the two sums to write

$$\frac{4\pi^3 r_h}{G}G_4 = -\sum_{|k|>1}\frac{1}{k^2(k^2-1)}\partial_1\partial_2\partial_3\partial_4\left[\frac{e^{i\tau_{34}}e^{ik\tau_{13}}-e^{ik\tau_{14}}-e^{i\tau_{12}+i\tau_{34}}e^{ik\tau_{23}}+e^{i\tau_{12}}e^{ik\tau_{24}}}{(e^{i\tau_{12}}-1)(e^{i\tau 34}-1)}\right] \tag{3.5.15}$$

Now we can distribute the derivatives to match the MSY's result (3.4.87). Using the fact that the k-dependent term is of the form of $e^{ik\tau_{ij}}$, we can take the other two derivatives $\partial_k\partial_l$

$(l, k \notin \{i, j\})$ on its coefficients. The result is

$$
\begin{aligned}
&\partial_1\partial_2\partial_3\partial_4 \left[\frac{1}{(e^{i\tau_{12}}-1)(e^{i\tau 34}-1)}\left(e^{i\tau_{34}}e^{ik\tau_{13}} - e^{ik\tau_{14}} - e^{i\tau_{12}+i\tau_{34}}e^{ik\tau_{23}} + e^{i\tau_{12}}e^{ik\tau_{24}}\right)\right] \\
&= \partial_1\partial_3\left[\partial_2\partial_4\left(\frac{e^{i\tau_{34}}}{(e^{i\tau_{12}}-1)(e^{i\tau_{34}}-1)}\right)e^{ik\tau_{13}}\right] - \partial_1\partial_4\left[\partial_2\partial_3\left(\frac{1}{(e^{i\tau_{12}}-1)(e^{i\tau_{34}}-1)}\right)e^{ik\tau_{14}}\right] \\
&- \partial_2\partial_3\left[\partial_1\partial_4\left(\frac{e^{i(\tau_{12}+\tau_{34})}}{(e^{i\tau_{12}}-1)(e^{i\tau_{34}}-1)}\right)e^{ik\tau_{23}}\right] + \partial_2\partial_4\left[\partial_1\partial_3\left(\frac{e^{i\tau_{12}}}{(e^{i\tau_{12}}-1)(e^{i\tau_{34}}-1)}\right)e^{ik\tau_{24}}\right]
\end{aligned}
\tag{3.5.16}
$$

Plugging into the sum,

$$
\begin{aligned}
&\frac{4\pi^3 r_h}{G}G_4 \\
&= -\sum_{|k|>1}\frac{1}{k^2(k^2-1)}\left\{\partial_1\partial_3\left[\partial_2\partial_4\left(\frac{e^{i\tau_{34}}}{(e^{i\tau_{12}}-1)(e^{i\tau_{34}}-1)}\right)e^{ik\tau_{13}}\right]\right. \\
&\qquad - \partial_1\partial_4\left[\partial_2\partial_3\left(\frac{1}{(e^{i\tau_{12}}-1)(e^{i\tau_{34}}-1)}\right)e^{ik\tau_{14}}\right] - \partial_2\partial_3\left[\partial_1\partial_4\left(\frac{e^{i(\tau_{12}+\tau_{34})}}{(e^{i\tau_{12}}-1)(e^{i\tau_{34}}-1)}\right)e^{ik\tau_{23}}\right] \\
&\qquad \left.+\partial_2\partial_4\left[\partial_1\partial_3\left(\frac{e^{i\tau_{12}}}{(e^{i\tau_{12}}-1)(e^{i\tau_{34}}-1)}\right)e^{ik\tau_{24}}\right]\right\} \\
&= \partial_1\partial_3\left[\partial_2\partial_4\left(\frac{e^{i\tau_{34}}}{(e^{i\tau_{12}}-1)(e^{i\tau_{34}}-1)}\right)\langle\epsilon_1\epsilon_3\rangle\right] - \partial_1\partial_4\left[\partial_2\partial_3\left(\frac{1}{(e^{i\tau_{12}}-1)(e^{i\tau_{34}}-1)}\right)\langle\epsilon_1\epsilon_4\rangle\right] \\
&- \partial_2\partial_3\left[\partial_1\partial_4\left(\frac{e^{i(\tau_{12}+\tau_{34})}}{(e^{i\tau_{12}}-1)(e^{i\tau_{34}}-1)}\right)\langle\epsilon_2\epsilon_3\rangle\right] + \partial_2\partial_4\left[\partial_1\partial_3\left(\frac{e^{i\tau_{12}}}{(e^{i\tau_{12}}-1)(e^{i\tau_{34}}-1)}\right)\langle\epsilon_2\epsilon_4\rangle\right]
\end{aligned}
\tag{3.5.17}
$$

where for the last equality, we used the 2pt function of Schwarzian mode (3.3.44). We can proceed by, for example, $\partial_1\langle\epsilon_1\epsilon_3\rangle$ and $\partial_1\langle\epsilon_1\epsilon_4\rangle$ can be combined because their coefficients are same (up to minus sign):

$$
\partial_3\partial_2\partial_4\left(\frac{e^{i\tau_{34}}}{(e^{i\tau_{12}}-1)(e^{i\tau_{34}}-1)}\right) = \partial_4\partial_2\partial_3\left(\frac{1}{(e^{i\tau_{12}}-1)(e^{i\tau_{34}}-1)}\right) \tag{3.5.18}
$$

which can be checked by subtracting the two which is $\frac{1}{(e^{i\tau_{12}}-1)}$ which do not depend on τ_3 and τ_4 and so will be annihilated by ∂_3 and ∂_4. The result agrees with the computation in the JT theory.

3.5.2 Real time tree-level 4-point functions

As mentioned in Section 3.3.6, the Euclidean 4pt function can be analytically continued to the real time, resulting in thermal correlators.

For the correlators in other states, one has to work in the Lorentzian time. However, the mode expansion of the bulk-to-boundary propagator ($K\left(z,\tau;\tau_i\right)=\frac{1}{2\pi}\sum_n e^{-|n|z-in(\tau-\tau_i)}$ in Euclidean time) is not straightforward because the real time is not periodic unlike the Euclidean time.

Instead, one can compute the real time correlators directly in the position space using the interaction picture and use the Schwinger-Keldysh contour for the out-of-time-ordered correlators. Here, we will compute the simplest, (real) time ordered thermal 4pt function of two dual scalars (or boundary scalars) V and W

$$\text{Tr}\ e^{-\beta H}V(t_1)W(t_2)V(t_3)W(t_4), \quad t_1>t_2>t_3>t_4>0 \tag{3.5.19}$$

Using the interaction picture, this can be expanded as

$$\begin{aligned}\text{Tr}\ e^{-\beta H}V(t_1)W(t_2)V(t_3)W(t_4) =& \text{tr}\ \ \big[e^{-\beta H_0}U_I(\beta)U^\dagger(t_1,0)V_I(t_1)U(t_1,0)\ U^\dagger(t_2,0)W_I(t_2)U(t_2,0)\\ &\quad U^\dagger(t_3,0)V_I(t_3)U(t_3,0)\ U^\dagger(t_4,0)W_I(t_4)U(t_4,0)\big]\\ =& \text{tr}\ \ \big[e^{-\beta H_0}U_I(\beta)U^\dagger(t_1,0)V_I(t_1)U(t_1,t_2)W_I(t_2)U(t_2,t_3)V_I(t_3)\\ &\quad U(t_3,t_4)W_I(t_4)U(t_4,0)\big]\end{aligned} \tag{3.5.20}$$

Using the expressions

$$U(t,0)=T\ e^{-\int_0^t H_I'(t')\mathrm{d}t'}, \quad U_I(\beta)=T_E\ e^{-\int_0^\beta \mathrm{d}H_I'(-i\tau)\tau}=U(-i\beta,0) \tag{3.5.21}$$

where T and T_E are Lorentzian/Euclidean time ordering, we can expand the correlator perturbatively in the interaction Hamiltonian. Using the notation $\langle\cdot\rangle_\beta = \mathrm{tr}\ e^{-\beta H_0}(\cdot)$,

$$
\begin{aligned}
\mathrm{Tr}\ e^{-\beta H} V(t_1)W(t_2)V(t_3)W(t_4) = &- i\int_0^{t_4} \langle V_I(t_1)W_I(t_2)V_I(t_3)W_I(t_4)H_I(t')\rangle_\beta \mathrm{d}t' \\
&- i\int_{t_4}^{t_3} \langle V_I(t_1)W_I(t_2)V_I(t_3)H_I(t')W_I(t_4)\rangle_\beta \mathrm{d}t' \\
&- i\int_{t_3}^{t_2} \langle V_I(t_1)W_I(t_2)H_I(t')V_I(t_3)W_I(t_4)\rangle_\beta \mathrm{d}t' \\
&- i\int_{t_2}^{t_1} \langle V_I(t_1)H_I(t')W_I(t_2)V_I(t_3)W_I(t_4)\rangle_\beta \mathrm{d}t' \\
&+ i\int_0^{t_1} \langle H_I(t')V_I(t_1)W_I(t_2)V_I(t_3)W_I(t_4)\rangle_\beta \mathrm{d}t' \\
&- i\int_0^{-i\beta} \langle H_I(t')V_I(t_1)W_I(t_2)V_I(t_3)W_I(t_4)\rangle_\beta \mathrm{d}t'
\end{aligned}
\tag{3.5.22}
$$

The corresponding SK contour is depicted in Figure 3.1.

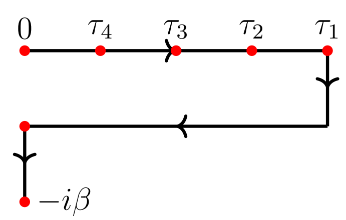

Figure 3.1: Schwinger-Keldysh contour for the thermal 4-point function

The formula can be simplified by using the following two facts.

First, since $H_0 = T_{\tau\tau}$ and H_I is quadratic in $T_{\tau\tau}$, and since $[T_{\tau\tau}(x_1), T_{\tau\tau}(x_2)] = 0$, the two Hamiltonians commute ($[H_0, H_I] = 0$). Hence we have

$$
H_I'(\tau) = e^{iH_0(\tau-\tau_0)} H_I e^{-iH_0(\tau-\tau_0)} = H_I(\tau) \tag{3.5.23}
$$

In our ADM action, this interaction Hamiltonian is

$$
\begin{aligned}
H_I &= -\frac{r_h G}{2}\int \mathrm{d}t \int_0^\infty \mathrm{d}z\ \sinh(2z)\left[\partial_t^{-1} T_{tz}\right]^2 \\
&= -\frac{r_h G}{2}\int \mathrm{d}t \int_0^\infty \mathrm{d}z\ \sinh(2z)\left[\partial_t^{-1}(\dot\phi\phi' + \dot\psi\psi')\right]^2
\end{aligned}
\tag{3.5.24}
$$

We can proceed by plugging this to (3.5.22) on each line. For example, the first line proceeds as

$$
\begin{aligned}
& -i\int_0^{t_4}\langle V_I(t_1)W_I(t_2)V_I(t_3)W_I(t_4)H_I(t')\rangle_\beta \mathrm{d}t' \\
& = -i\int_0^{t_4}\mathrm{d}t\mathrm{d}z\ \sinh(2z)\ \partial_t^{-1}\Big(\langle\phi(t_1)\dot{\phi}(t)\rangle_\beta\langle\phi(t_2)\phi'(t)\rangle_\beta+\langle\phi(t_1)\phi'(t)\rangle_\beta\langle\phi(t_2)\dot{\phi}(t)\rangle_\beta\Big) \\
& \qquad\qquad\qquad\qquad \times\ \partial_t^{-1}\Big(\langle\psi(t_3)\dot{\psi}(t)\rangle_\beta\langle\psi(t_4)\psi'(t)\rangle_\beta+\langle\psi(t_3)\psi'(t)\rangle_\beta\langle\psi(t_4)\dot{\psi}(t)\rangle_\beta\Big)
\end{aligned}
\tag{3.5.25}
$$

where ∂_t^{-1} corresponds to the integral over t, and $\langle\cdot\rangle_\beta=\mathrm{Tr}e^{-\beta H_0}(\cdot)$ is the thermal correlation function computed using the free Hamiltonian. In Appendix B.4, we computed the thermal correlation function

$$
\langle\tilde{\phi}(t,x)\tilde{\phi}(0,0)\rangle_\beta=-\frac{\beta}{4\pi}\log\left\{\sinh\left[\frac{\rho_h}{2}(\tau-z-i\epsilon)\right]\sinh\left[\frac{\rho_h}{2}(\tau+z-i\epsilon)\right]\right\} \tag{3.5.26}
$$

where τ is Lorentzian time.

One can plug in this and evaluate the integral for all 4 segments. This is computationally expensive and we leave the numerical comparison of such a correlator to those obtained above for the later study.

3.5.3 1-loop 2-point functions

The Lorentzian thermal 2pt function of the matter contains spectral information. This is clear if we write the 2pt function of the dual operators $\mathcal{O}$ in the dual quantum mechanics as the spectral sum, which contains the density of states and transition amplitudes.

$$
G_\beta(t)=\frac{1}{Z(\beta)}\int dEdE'\rho(E)\rho\left(E'\right)e^{-\beta E}e^{-i(E'-E)t}\left|\langle E'|\mathcal{O}|E\rangle\right|^2 \tag{3.5.27}
$$

1-loop correction to the thermal 2pt function therefore describes the effects of the boundary time reparameterization modes on the Schwarzian density of states and matrix elements.

It also contains the information of poles of quasi-normal modes. To see this, we recall that the quasi normal modes are nontrivial bulk solution which has two boundary conditions:

1) ingoing at the horizon, 2) no source at the asymptotic AdS_2 boundary. From the leading behaviors of the asymptotic solution of the scalar

$$\phi(t,z) = A(t)z^{1-\Delta} + B(t)z^{\Delta} + \cdots \tag{3.5.28}$$

where $A(t)$ is the boundary source and $B(t)$ is the response, we can read off the Fourier modes of the retarded Green's function as the ratio of the Fourier modes of the response to the source.

$$\tilde{G}_R(\omega) = \frac{\tilde{B}(\omega)}{\tilde{A}(\omega)} \tag{3.5.29}$$

With the time-translation invariance, the time dependence of the solution is $e^{i\omega t}$, and the quasi-normal modes are characterized by quasi-normal frequencies ω_n. As they don't have sources, $A(\omega_n) = 0$, and hence the quasi-normal modes corresponds to the poles of $\tilde{G}_R(\omega)$. In the position space,

$$\begin{aligned} G_R(t) &= \int \frac{\mathrm{d}\omega}{2\pi}\ e^{-i\omega t}\tilde{G}_R(\omega) \\ &= \int \frac{\mathrm{d}\omega}{2\pi}\ e^{-i\omega t}\frac{\tilde{B}(\omega)}{\tilde{A}'(\omega)(\omega-\omega_n) + \mathcal{O}((\omega-\omega_n)^2)} \\ &= i\sum_n e^{i\omega_n t}\tilde{B}(\omega_n) + \cdots \end{aligned} \tag{3.5.30}$$

Due to the ingoing boundary condition at the horizon, the black hole is an open, dissipative system, and hence the kinetic operator is not self-adjoint and the quasi-normal frequencies do not have to be real. This means that the quasi-normal modes decays in general, which is noticeable at late time.

In JT gravity (Schwarzian + bilocal), the 1-loop 2pt function can be computed using the bilocal action

$$I_M^{\text{on-shell}} = \frac{D\Delta}{2}\int \left[\frac{t_1' t_2'}{(t_1-t_2)^2}\right]^{\Delta} \tilde{\chi}_0(u_1)\tilde{\chi}_0(u_2)\ \mathrm{d}u_1\mathrm{d}u_2 \tag{3.5.31}$$

expanded in the small fluctuations of the boundary gravitons

$$t(u) = \tan\frac{\tau(u)}{2}, \quad \tau(u) = u + \epsilon(u) \tag{3.5.32}$$

in

$$\frac{1}{t_{12}^{2\Delta}} \to \frac{\left(1+\varepsilon_1'\right)^{\Delta}\left(1+\varepsilon_2'\right)^{\Delta}}{\left(\sin\frac{u_{12}+\varepsilon_1-\varepsilon_2}{2}\right)^{2\Delta}} \tag{3.5.33}$$

to the second order and contracting using $\langle \epsilon(u_1)\epsilon(u_2)\rangle$.

$$\frac{\langle V_1V_2\rangle_{\text{one loop}}}{\langle V_1V_2\rangle_{\text{tree}}} = \Delta\left\langle \frac{\left(\varepsilon_1-\varepsilon_2\right)^2}{4\sin^2\frac{u}{2}} - \frac{1}{2}\left(\varepsilon_1'^2+\varepsilon_2'^2\right)\right\rangle + \frac{\Delta^2}{2}\left\langle\left(\varepsilon_1'+\varepsilon_2'-\frac{\left(\varepsilon_1-\varepsilon_2\right)}{\tan\frac{u}{2}}\right)^2\right\rangle \tag{3.5.34}$$

There are self contraction and non-self contraction of gravitons, corresponding to the two diagrams below.

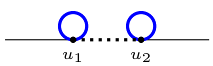

$\propto \langle \epsilon(u_1)^2\rangle \times \langle \epsilon(u_2)^2\rangle \quad +$ 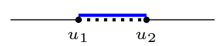

$\propto \langle \epsilon(u_1)\epsilon(u_2)\rangle$

The result is

$$\begin{aligned}\frac{\langle V_1V_2\rangle_{\text{one loop}}}{\langle V_1V_2\rangle_{\text{tree}}} = \frac{1}{2\pi C}\Bigg[&\Delta\frac{(u^2-2\pi u+2-2\cos u+2(\pi-u)\sin u)}{4\sin^2\frac{u}{2}}+\\ &+\frac{\Delta^2}{2}\left(-2+\frac{u}{\tan\frac{u}{2}}\right)\left(-2+\frac{(u-2\pi)}{\tan\frac{u}{2}}\right)\Bigg], \quad u=u_1-u_2>0\end{aligned} \tag{3.5.35}$$

For the later comparison, we can proceed mode expanding Eq. (3.5.34) using

$$\frac{1}{4\sin^2(u/2)} = -\frac{1}{2}\sum_{n\neq 0}|n|e^{-inu} \tag{3.5.36}$$

and

$$\langle \epsilon(u)\epsilon(0)\rangle = \frac{1}{2\pi C}\sum_{|k|>1}\frac{e^{iku}}{k^2\left(k^2-1\right)} \tag{3.5.37}$$

which can be combined to

$$G_2^{\text{self}}(u) + G_2^{\text{non}}(u) = -\frac{1}{2\pi^2 C}\sum_{m=1}^{\infty}\sum_{r=1}^{\infty}\frac{rm^2}{(m+r)^2\left[(m+r)^2-1\right]}\left(e^{imu}+e^{-imu}\right) \tag{3.5.38}$$

Next, we compute the 1-loop 2pt function independently using ADM action, and will see that they match exactly. As we are concerned with 1-loop correlation function, we should not use the traceless-ness of the energy momentum tensor, which acquires trace-anomaly at 1-loop. Hence, we start with the following form of ADM action.

$$I_4 = -g\int d\tau \int_0^{\infty} dz T_{\tau\tau}(\tau,z)\int_0^z dz' \sinh^2 z' T_{\tau\tau}\left(\tau,z'\right) \tag{3.5.39}$$

The 1-loop 2pt function can be obtained by simply Wick-contracting scalars. The bulk scalars can be contracted at the same bulk point or between z and z' through bulk propagator. For example,

Non-self-contraction : 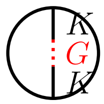

$$\underbrace{\phi_0(\tau_1)\partial_+\phi(\tau,z)}_{\partial_+K(\tau,z;\tau_1)}\overbrace{\partial_-\phi(\tau,z)\partial'_+\phi(\tau,z')}^{\partial_-\partial'_+G(\tau,z;\tau,z')}\underbrace{\partial'_-\phi(\tau,z')\phi_0(\tau_2)}_{K(\tau,z';\tau_2)}$$

Self-contraction : 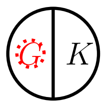

$$\underbrace{\phi_0(\tau_1)\partial_+\phi(\tau,z)}_{\partial_+K(\tau,z;\tau_1)}\underbrace{\partial_-\phi(\tau,z)\overbrace{\partial'_+\phi(\tau,z')\partial'_-\phi(\tau,z')}^{\partial'_+\partial'_-G(\tau,z';\tau,z')}\phi_0(\tau_2)}_{K(\tau,z;\tau_2)} \tag{3.5.40}$$

where K, G are bulk-to-boundary and bulk-bulk propagators. The non-self contraction part is

$$\begin{aligned}\langle T_{\tau\tau}(\tau,z)T_{\tau\tau}\left(\tau,z'\right)\phi\left(\tau_1\right)\phi\left(\tau_2\right)\rangle &= \partial_\tau K_1\partial_{\tau'}K_2\partial_\tau\partial_{\tau'}G\\ &+\partial_z K_1\partial_{z'}K_2\partial_z\partial_{z'}G\\ &-K_\tau K_1\partial_{z'}K_2\partial_\tau\partial_{z'}G\\ &-\partial_z K_1\partial_{\tau'}K_2\partial_z\partial_{\tau'}G\\ &+\tau_1\leftrightarrow\tau_2\end{aligned} \tag{3.5.41}$$

and the self-contraction part vanishes. The non-self contraction part is evaluated to match the JT gravity calculation (3.5.34) exactly, provided $g = \frac{2}{C}$.

CHAPTER 4

Higher Structure of Non-invertible Symmetries from Lagrangian Descriptions

4.1 Introduction and Summary

Global symmetries have proven to be invaluable in the study of quantum field theories, and in the modern perspective, they are viewed as implemented by topological operators [51]. In order to fully specify the symmetry structure of a given theory, one begins by identifying these topological operators and their fusion rules. However, this is not all, and some additional physical information is encoded in the topological junctions and networks that these defects can form, which is referred to as the *higher structure* of the symmetry. This includes, in particular, the set of topological interfaces between pairs of defects, called 1-morphisms, which describe junctions (including fusion junctions) between defects and are also used to encode the associativity structure of the fusion product. This associativity 1-morphism, known as the associator or F-symbol, is an interface obtained by shrinking a certain topological network of defects that captures this associativity (see the next section for more details), and is an important piece of information in specifying the symmetry structure. In two dimensions, the F-symbols are numbers, but in a higher dimension D, they are $D-2$ dimensional topological field theories, and nontrivial interfaces (or 2-morphisms) might also be considered between them. This gives rise to the notion of higher associators, where the F-symbols are considered as 1-associators. Overall, we have $D-1$ higher associators, where the $(D-1)$-associators are numbers. All the associators are part of the mathematical structure describing the symmetry, which is called a fusion $(D-1)$-category, and contain physical information [52]. As an example, let us note that for ordinary symmetries with group-like fusion rules (that is, invertible symmetries), the $(D-1)$-associators are simply the 't Hooft anomalies of the symmetries.

In many occasions, the fusion of the topological defects does not follow a simple group-like law, and the corresponding symmetry is then referred to as non-invertible (see [53,54] for reviews). Our focus in this chapter will be on studying the higher structure of non-invertible symmetries in theories in which an explicit Lagrangian description of the different defects is known. We will use this Lagrangian description to construct explicitly topological junctions between the defects, including fusion junctions in which two defects are fused into a third one, while accounting for the appropriate boundary conditions and boundary terms at the junctions. Then, we will use these junctions as building blocks to construct the topological configurations of defects required for the computation of the F-symbols, and obtain the desired results after carefully shrinking the configuration. We note that even though our focus here will be on the F-symbols, i.e. the 1-associators, the same method can similarly be employed for the computation of the higher associators.

To illustrate our approach, we will analyze in detail two types of theories. The first will be that of the free compact scalar in two dimensions, whose non-invertible symmetries and associated fusion 1-category have been widely studied and are well known (see [55–61] for a partial list of references). This will serve as a good starting point for demonstrating our new method and testing it against known results. Using the Lagrangian descriptions of the shift-symmetry defects and the non-invertible T-duality defects that are present in the theory, we will construct topological junctions and use them to study the networks of defects that capture the different F-symbols. We will compute all the F-symbols this way and find that they indeed match those of the familiar Tambara-Yamagami fusion category $\mathrm{TY}(\mathbb{Z}_N, +1)$.

We will then turn to four dimensions and consider Maxwell theory, which was recently shown to host a variety of interesting non-invertible symmetries [59, 60, 62–68]. In this case, even though the corresponding topological defects and their fusions were studied, the higher-structure data was not computed explicitly (see [69–71] for related work). Focusing on the triality and duality defects found in [64, 59, 62], we will use their Lagrangian descriptions to find the actions describing the topological configurations of defects that capture the F-symbols of the corresponding fusion 3-categories. Then, we will shrink these networks to interfaces and find these F-symbols, which are 2d topological field theories and new results of this chapter (see Table 4.5 and Eq. (D.5.5)). In some cases, we will find that there is more than one possible 2d theory corresponding to a given F-symbol, depending on the choice of boundary conditions used in its computation. In addition to these calculations, as a complementary analysis and to check our results, we will also compute the F-symbols using a different (group theoretical) approach that is not based on the Lagrangian description, and find that the results obtained using the two methods indeed have the same form.[1]

There are a few potential applications of our results, which we leave for future study. First, one can try to relate the F-symbols we compute, which are RG invariant data of the symmetry category, to those of other 4d theories that have duality-preserving deformations to Maxwell theory, and then use it to study other such deformations of these theories, see [72] for a related recent discussion. Note that a simple example for such a flow to Maxwell theory happens on the Coulomb branch of $\mathcal{N} = 4$ SYM, as well as on that of more general $\mathcal{N} = 2$ SCFTs. Second, even though we only compute the F-symbols of the specific duality and triality defects in free Maxwell theory, one should be able to derive all the other consistent F-symbols for defects with the same fusion rules from the ones we computed. For instance, for generic duality-like defects in two dimensions, the SymTFT gives a prescription for how

[1]The triality and duality defects we consider are parameterized by a positive integer N, and in the case of the triality defects the Lagrangian approach will only be used for even N while the group-theoretical one only for certain odd N values. In this case, the two methods will match except for some cases where the final result depends on whether N is even or odd.

to modify certain parts of the known F-symbols in order to get all the inequivalent sets of F-symbols with the same fusion algebra [73]. Generalizing this to 4d duality/triality defects via the SymTFT setup described in [69] will allow us to acquire the full set of consistent F-symbols.

The remainder of the chapter is organized as follows. In section 4.2 we briefly review the higher structure of non-invertible symmetries, focusing on the definition of F-symbols in two and higher dimensions. In section 4.3 we consider the 2d free compact boson theory, and use the Lagrangian description of the symmetry defects to construct topological junctions and networks of them. We then use it to compute the F-symbols of the Tambara-Yamagami fusion category $\mathrm{TY}(\mathbb{Z}_N, +1)$ and recover the known expressions. In section 4.4 we generalize this analysis to the triality defects of 4d Maxwell theory for even values of the integer that parameterizes them, computing the corresponding F-symbols while highlighting some differences compared to the previous section. Then, in section 4.5, we compute the F-symbols for certain odd values of the parameter using a different (group theoretical) approach and find that they take the expected form. A few appendices contain constructions of topological junctions and computations of F-symbols that have been deferred from the main body of the chapter for brevity, and include the case of the duality defect of 4d Maxwell theory.

4.2 Higher structure of symmetry

In this subsection, we briefly review the (higher) fusion category symmetries and their higher structures with a focus on the associators. We begin by reviewing the associators of fusion category symmetry in 2d to set the stage, and then move to explain the associators in higher fusion categories following [52].

4.2.1 Higher structure in fusion categories

Topological defect lines (TDLs) in a 2d QFT are captured by the mathematical structure known as a fusion category. Given two TDLs labeled by $\mathcal{L}_a$ and $\mathcal{L}_b$, we can fuse them by putting them close to each other and generate a new topological line, which then in general decomposes into a finite sum of other topological lines,

$$\mathcal{L}_a \times \mathcal{L}_b = \bigoplus_c N_{ab}^c \mathcal{L}_c \ , \quad N_{ab}^c \in \mathbb{Z}_{\geq 0} \ . \tag{4.2.1}$$

A TDL which cannot be written as a sum of other TDLs is known as a *simple* TDL.

When $N_{ab}^c \neq 0$, the locality of the QFT allows the configurations where $\mathcal{L}_a$ and $\mathcal{L}_b$ join locally and become $\mathcal{L}_c$ at a trivalent junction. Such topological junctions form a complex vector space whose dimension is N_{ab}^c. Similarly, the TDL $\mathcal{L}_c$ can locally split into $\mathcal{L}_a$ and $\mathcal{L}_b$, and the topological junctions also form a vector space with the same dimension. To proceed, we fix the basis for each vector space and denote them as

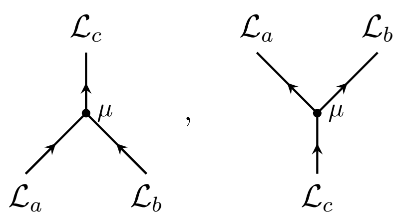

$$, \quad \mu = 1, 2, \cdots, N_{ab}^c \,, \tag{4.2.2}$$

satisfying the following conditions

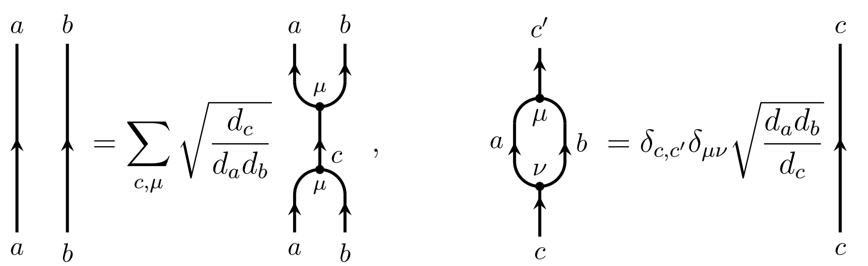

(4.2.3)

where d_a is the quantum dimension of the TDL a defined as

$d_a =$ 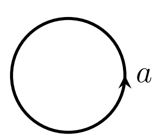

. (4.2.4)

Consider a single TDL splitting into three TDLs, there are two ways in which this process can be done. They are related by the *higher structure* of the fusion category known as the *associativity map*. With the explicit basis (4.2.2), the associativity map is characterized by a set of $\mathbb{C}$-numbers known as the F-symbols

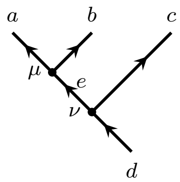

$$= \sum_{f,\rho,\sigma} \left[F^{abc}_{d}\right]_{(e,\mu,\nu),(f,\rho,\sigma)} \tag{4.2.5}$$

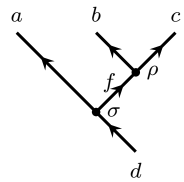

As pointed out in [58, 52], the F-symbols $\left[F^{abc}_{d}\right]_{(e,\mu,\nu),(f,\rho,\sigma)}$ can also be computed by the following relation

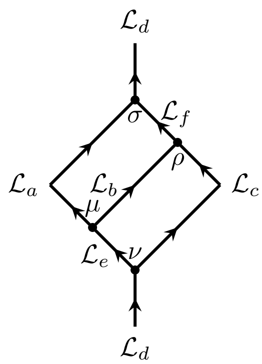

$$= \sqrt{\frac{d_a d_b d_c}{d_d}} \left[F^{abc}_{d}\right]_{(e,\mu,\nu),(f,\rho,\sigma)} \tag{4.2.6}$$

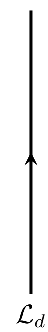

which can be derived first using (4.2.5) and (4.2.3). (4.2.6) is more convenient for extracting F-symbols in the Lagrangian approach in 2d, as well as generalizing to higher dimensions.

To conclude, we consider an example of the Tambara-Yamagami fusion category $\mathrm{TY}(\mathbb{Z}_N, +1)$. This fusion category contains a $\mathbb{Z}_N$ invertible symmetry generated by the line η, as well as a non-invertible duality line T. The fusion rules between η and T are

$$T \times \eta = \eta \times T = T \ , \quad T \times T = \sum_{k=0}^{N-1} \eta^k \ . \tag{4.2.7}$$

The invertible lines η^k have quantum dimension $d_{\eta^k} = 1$, while the duality defect has quantum dimension $d_T = \sqrt{N}$. Most of the F-symbols are equal to 1 for this fusion category, with the non-trivial F-symbols given by

$$F^{T}_{\eta^n,T,\eta^m} = F^{\eta^n}_{T,\eta^m,T} = \exp\left(\frac{2\pi i n m}{N}\right), \qquad \left[F^{T}_{T,T,T}\right]_{\eta^n,\eta^m} = \frac{1}{\sqrt{N}} \exp\left(-\frac{2\pi i n m}{N}\right) \ . \tag{4.2.8}$$

4.2.2 Associator 1-morphisms in 4d QFT

Turning to 4d, we briefly review the higher structure of the fusion 3-category focusing on the associator 1-morphisms. We refer to [52] for more details.

Objects In a 4d QFT, all symmetry operators are captured by a fusion 3-category $\mathfrak{C}^{[3]}$. The objects in $\mathfrak{C}^{[3]}$ are 0-form symmetry operators $\mathcal{D}$ supported on codim-1 surfaces. These objects admit an additive structure from the direct sum of the symmetry operators, as well as a tensor product coming from fusing two symmetry operators. We call an object *simple* if it cannot be written as a direct sum of other objects.

Morphisms Given two codim-1 symmetry operators $\mathcal{D}_1$ and $\mathcal{D}_2$, a topological interfaces (or a junction) between them is a 1-morphism from $\mathcal{D}_1$ to $\mathcal{D}_2$. In particular, the morphisms between identity codim-1 operators are 1-form symmetry operators supported on codim-2 surfaces. All such interfaces between $\mathcal{D}_1$ and $\mathcal{D}_2$ form a 2-category $\mathrm{Hom}_{\mathfrak{C}^{[3]}}(\mathcal{D}_1, \mathcal{D}_2)$; and the fusion 2-category $\mathrm{End}_{\mathfrak{C}^{[3]}}(\mathcal{D}) \equiv \mathrm{Hom}_{\mathfrak{C}^{[3]}}(\mathcal{D}, \mathcal{D})$ describes the symmetry operators living in the world volume of the operator $\mathcal{D}$. Invoking the definition, the fusion 2-category $\mathrm{End}_{\mathfrak{C}^{[3]}}(\mathcal{D})$ contains topological surface operators (as objects in $\mathrm{End}_{\mathfrak{C}^{[3]}}(\mathcal{D})$) and topological line operators (as morphisms between identity surface operators in $\mathrm{End}_{\mathfrak{C}^{[3]}}(\mathcal{D})$) in the 3-dim world-volume of $\mathcal{D}$.

Witt equivalence class Two codim-1 defects are said to be *Witt equivalent* if there is a non-trivial morphism between them[2]. For instance, such junctions can arise by stacking decoupled TQFTs admitting gapped boundaries or gauging a non-anomalous symmetry in $\mathrm{End}_{\mathfrak{C}}(\mathcal{D})$ as shown in Figure 4.1. We use $[\![\mathcal{D}]\!]$ to denote the Witt equivalence class of $\mathcal{D}$.

[2]Notice that unlike the 2d case where any simple line cannot have non-trivial junction to the identity operator $\mathbb{1}$ unless it is $\mathbb{1}$, in 4d, a non-identity simple 0-form symmetry operator can have a non-trivial junction to $\mathbb{1}$.

Generically there is no preferred choice for a representative for each class $[\![\mathcal{D}]\!]$. But for the 0-form symmetry operators considered in this chapter, there is always a canonical choice for the representative, which contains minimal operator content on the world-volume. We denote them by $[\![\mathcal{D}]\!]_0$. A generic operator in $[\![\mathcal{D}]\!]$ can be turned into $[\![\mathcal{D}]\!]_0$ by gauging certain symmetries.

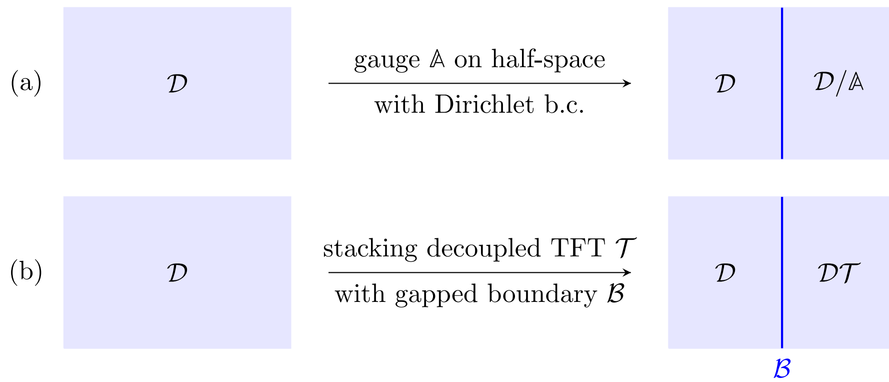

Figure 4.1: (a) Gauging some symmetry $\mathbb{A}$ in $\mathrm{End}_{\mathfrak{C}[3]}(\mathcal{D})$ on half-space with Dirichlet boundary condition creates a non-trivial topological interface between $\mathcal{D}$ and $\mathcal{D}/\mathbb{A}$. (b) Stacking a decoupled 3d TFT $\mathcal{T}$ with the gapped boundary $\mathcal{B}$ creates a non-trivial topological interface between $\mathcal{D}$ and $\mathcal{DT}$. $\mathcal{D}$, $\mathcal{D}/\mathbb{A}$, and $\mathcal{DT}$ are in the same equivalence class, i.e., $[\![\mathcal{D}]\!] = [\![\mathcal{D}/\mathbb{A}]\!] = [\![\mathcal{DT}]\!]$.

Condensation defect An important example is a class of defects known as the condensation defect C [63,71,74]. They are defined as gauging p-form symmetry on an n-dimensional surface $\Sigma^{(n)}$ (where $n \geq p+1$) with a possible discrete torsion. For example, the following condensation defect gauges a 1-form $\mathbb{Z}_N$ symmetry generated by $U(\sigma^{(2)})$ on a 3-surface $\Sigma^{(3)}$.

$$C_k(\Sigma^{(3)}) = \frac{1}{|H^0(\Sigma^{(3)}, \mathbb{Z}_N)|} \sum_{\sigma^{(2)} \in H_2(\Sigma^{(3)}, \mathbb{Z}_N)} e^{\frac{2\pi i}{N} k Q(\Sigma^{(3)}, \sigma^{(2)})} U(\sigma^{(2)}) \ , \tag{4.2.9}$$

where $k \in H^3(B\mathbb{Z}_N, U(1)) \simeq \mathbb{Z}_N$ parameterizes the choice of discrete torsion in the higher gauging. The discrete torsion phase $Q(\Sigma^{(3)}, \sigma^{(2)})$ is defined as

$$Q(\Sigma^{(3)}, \sigma^{(2)}) = \int a^{(1)} \cup \beta(a^{(1)}) \ , \tag{4.2.10}$$

where $a^{(1)} = PD(\sigma^{(2)}, \Sigma^{(3)}) \in H^1(\Sigma^{(3)}, \mathbb{Z}_N)$ is the Poincare dual 1-cocycle of $\sigma^{(2)}$ on $\Sigma^{(3)}$ and $\beta : H^1(\Sigma^{(3)}, \mathbb{Z}_N) \to H^2(\Sigma^{(3)}, \mathbb{Z}_N)$ is the Bockstein homomorphism associated to the short exact sequence $\mathbb{Z}_N \to \mathbb{Z}_{N^2} \to \mathbb{Z}_N$.

Such a condensation defect has higher quantum symmetries generated by $\mathbb{Z}_N$ topological lines living in $\mathrm{End}_{\mathfrak{C}[3]}(C_k)$. The higher quantum symmetries are gaugeable on the world-volume of the condensation defect, and gauging it turns the condensation defect to the identity operator.[3] Hence, a condensation defect is always Witt equivalent to the identity operator and $[\![C_k]\!]_0 = \mathbb{1}$.[4]

Local fusion junctions and associator 1-morphism The fusion of two 0-form symmetry operators $\mathcal{D}_a$ and $\mathcal{D}_b$ can be expanded as a sum of simple operators

$$\mathcal{D}_a \otimes \mathcal{D}_b = \sum_{\mathcal{D}_c : simple} \mathcal{C}_{ab}^c \mathcal{D}_c \ , \tag{4.2.11}$$

where the coefficients $\mathcal{C}_{ab}^c$'s are valued in 3-dimensional topological field theory. In known cases (including the cases considered in this chapter) in $d > 2$, the fusion product of the equivalence class is group-like even if the $\mathcal{D}_a$'s themselves are non-invertible, i.e. there is always a single term appearing on the RHS of (4.2.11).[5] In such cases, we can add a 1-morphism junction to the canonical representative of the Witt equivalence class after the local fusion junction. By combining the fusion and morphism junctions, we can construct a new local fusion junction between the canonical representatives of the equivalence class as demonstrated in Figure 4.2.

[3]Such a junction serves as a topological boundary with Dirichlet boundary conditions are imposed on the quantum symmetry gauge fields of the higher quantum symmetry.

[4]Consequently, fusion with a condensation defect will not change the equivalence class.

[5]This is more explicit after quotienting out the equivalence class in the fusion rule $[\![\mathcal{D}_a]\!] \otimes [\![\mathcal{D}_b]\!] = \sum N_{ab}^c [\![\mathcal{D}_c]\!]$ where the fusion coefficients N_{ab}^c now take non-negative integer values. In known cases, there is always a single term appearing in the RHS. For the remainder of the discussion, we restrict ourselves to this case.

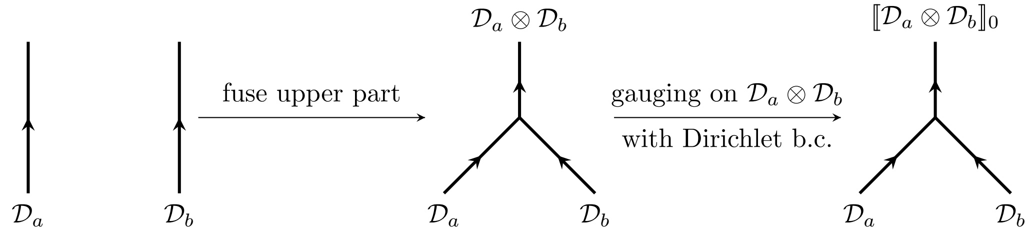

Figure 4.2: Given with two codim-1 defects $\mathcal{D}_a$ and $\mathcal{D}_b$ where $\mathcal{D}_a = [\![\mathcal{D}_a]\!]_0, \mathcal{D}_b = [\![\mathcal{D}_b]\!]_0$, one can always construct a topological local fusion junction into $[\![\mathcal{D}_a \otimes \mathcal{D}_b]\!]_0$ as follows. Starting with two parallel $\mathcal{D}_a$ and $\mathcal{D}_b$, fusing the upper part leads to a topological local fusion junction from $\mathcal{D}_a$ and $\mathcal{D}_b$ to $\mathcal{D}_a \otimes \mathcal{D}_b$. Then, gauging the corresponding symmetry on the world-volume of $\mathcal{D}_a \otimes \mathcal{D}_b$ with Dirichlet boundary condition on the fusion junction leads to a topological local fusion junction with the outgoing line being $[\![\mathcal{D}_a \otimes \mathcal{D}_b]\!]_0$.

We are now ready to define the generalization of the F-symbols in $\mathfrak{C}^{[3]}$. Let's consider the diagram

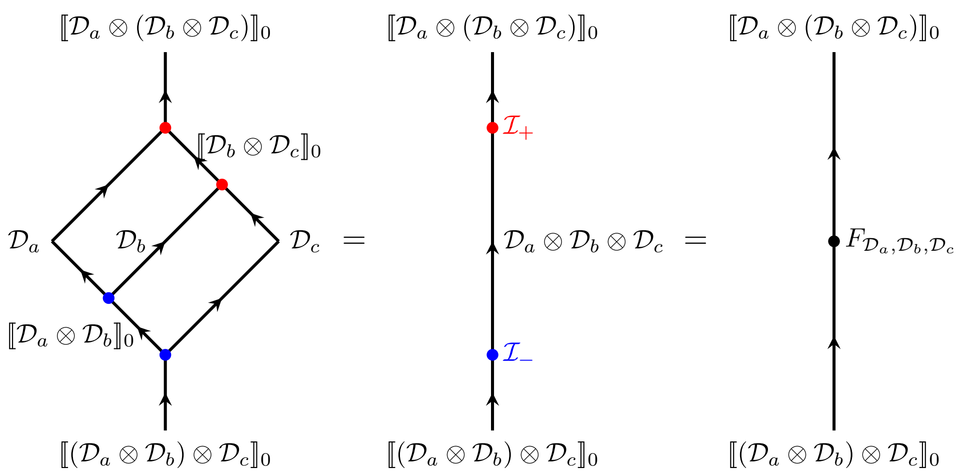

. (4.2.12)

In the first equal sign, we fuse all the defects in the middle and also fuse the fusion (splitting) junctions represented by red (blue) dots into a single interface $\mathcal{I}_+$ and $\mathcal{I}_-$. Then we fuse the interfaces $\mathcal{I}_+$ and $\mathcal{I}_-$ to create an interface from $[\![(\mathcal{D}_a \otimes \mathcal{D}_b) \otimes \mathcal{D}_c]\!]_0$ to $[\![\mathcal{D}_a \otimes (\mathcal{D}_b \otimes \mathcal{D}_c)]\!]_0$; this interface is interpreted as the generalization of the F-symbol 1-morphism in 4d [52], which we denote by $F_{\mathcal{D}_a,\mathcal{D}_b,\mathcal{D}_c} \in \mathrm{Hom}_{\mathfrak{C}^{[3]}}([\![(\mathcal{D}_a \otimes \mathcal{D}_b) \otimes \mathcal{D}_c]\!]_0, [\![\mathcal{D}_a \otimes (\mathcal{D}_b \otimes \mathcal{D}_c)]\!]_0)$.

4.3 Compact boson in 2d

4.3.1 Lagrangians for TY($\mathbb{Z}_N$,+1) symmetry defects

We consider a single 2d compact scalar with periodicity 2π, described by the action

$$S = \frac{R^2}{4\pi}\int_{M_2} \mathrm{d}\phi \wedge \star \mathrm{d}\phi\,, \quad \phi \sim \phi + 2\pi\,. \tag{4.3.1}$$

This theory is completely specified by the choice of radius R, and has the interesting property that it is dual to the theory with radius $1/R$. This duality, called T-duality, maps the operators between the two theories in a nontrivial way, and to see how it arises let us rewrite the action (5.6.5) in terms of an unconstrained 1-form field X (instead of $\mathrm{d}\phi$) and a compact Lagrange multiplier $\widetilde{\phi}$,

$$S = \int_{M_2}\left(\frac{R^2}{4\pi} X\wedge \star X + \frac{i}{2\pi} X \wedge d\widetilde{\phi}\right), \quad \widetilde{\phi} \sim \widetilde{\phi} + 2\pi\,. \tag{4.3.2}$$

The role of the Lagrange multiplier is to restrict X to be closed and with holonomies valued in $2\pi\mathbb{Z}$ (which are the properties of $\mathrm{d}\phi$), and indeed integrating $\widetilde{\phi}$ out sets $X = \mathrm{d}\phi$ and results in the original action (5.6.5). On the other hand, given the action (5.6.4), we can integrate out X using its equation of motion $iR^2 \star X = \mathrm{d}\widetilde{\phi}$ and obtain an action for the Lagrange multiplier field $\widetilde{\phi}$,

$$S = \frac{\widetilde{R}^2}{4\pi}\int_{M_2} \mathrm{d}\widetilde{\phi} \wedge \star \mathrm{d}\widetilde{\phi} \tag{4.3.3}$$

where $\widetilde{R} = 1/R$. We see that we have two dual descriptions, (5.6.5) and (4.3.3), for the same theory, one with radius R and the other with radius $1/R$. Moreover, there is a nontrivial map between the operators of these two descriptions, for example $\mathrm{d}\widetilde{\phi} = iR^2 \star \mathrm{d}\phi$.

Let us next examine some of the symmetries of the theory. First, at any radius R there is a $U(1)_m \times U(1)_w \rtimes \mathbb{Z}_2^C$ symmetry, where $\mathbb{Z}_2^C$ is charge conjugation under which $\phi \to -\phi$ while $U(1)_m$ and $U(1)_w$ are the momentum (or shift) and winding symmetries, respectively, with charges

$$Q_m = iR^2 \oint \frac{\star \mathrm{d}\phi}{2\pi}\,, \quad Q_w = \oint \frac{\mathrm{d}\phi}{2\pi}\,. \tag{4.3.4}$$

Note that using the T-duality map of operators mentioned before, we can immediately see that these two charges map into each other under the duality. Indeed, the winding symmetry $U(1)_w$ of the scalar ϕ turns into the momentum symmetry $U(1)_m$ of the dual scalar $\widetilde{\phi}$ which acts by shifting it, while the momentum symmetry of ϕ turns into the winding symmetry of $\widetilde{\phi}$.

Even though the momentum and winding symmetries have a mixed 't Hooft anomaly, each of them is non-anomalous by itself and can be gauged. Let us consider e.g. the effect of gauging a $\mathbb{Z}_N$ subgroup of the momentum symmetry. Upon such gauging, the periodicity of ϕ changes from 2π to $2\pi/N$, and to have again a compact scalar with periodicity 2π we can define $\phi = \phi'/N$ such that ϕ' has the desired periodicity. This, however, results in the radius of the ϕ' theory being $R' = R/N$ (as can be seen by substituting into (5.6.5)), and we hence see that the effect of gauging a $\mathbb{Z}_N$ subgroup of $U(1)_m$ amounts to changing $R \to R/N$.

At this point, we observe that combining this gauging with T-duality maps the original radius R to N/R, such that the radius $R^2 = N$ is invariant under this combined operation. As a result, gauging $\mathbb{Z}_N \subset U(1)_m$ in half space (with Dirichlet boundary conditions for the corresponding discrete gauge field) followed by T-duality in the same half space results in a nontrivial topological defect as long as $R^2 = N$ (for other values of R we would obtain a topological interface between different theories). Denoting this defect by T and the basic $\mathbb{Z}_N \subset U(1)_m$ defect by η, one can show that they generate together the Tambara-Yamagami fusion category $TY(\mathbb{Z}_N, +1)$ [55]. The corresponding fusion algebra, which was mentioned in subsection 4.2.1 and reproduced here for convenience, is given by

$$\eta^n \times \eta^m = \eta^{n+m}\,, \quad \eta^N = \mathbb{1}\,, \quad T \times \eta = \eta \times T = T\,, \quad T \times T = \sum_{k=0}^{N-1} \eta^k \tag{4.3.5}$$

and the nontrivial F-symbols by

$$F^T_{\eta^n,T,\eta^m} = F^{\eta^n}_{T,\eta^m,T} = \exp\left(\frac{2\pi i n m}{N}\right)\,, \qquad \left[F^T_{T,T,T}\right]_{\eta^n,\eta^m} = \frac{1}{\sqrt{N}} \exp\left(-\frac{2\pi i n m}{N}\right)\,. \tag{4.3.6}$$

As discussed in [59, 64, 60, 75], one can also represent the T and η^k defects using the actions[6]

$$T: \quad S = \frac{N}{4\pi}\int_{x<0} \mathrm{d}\phi_L \wedge \star \mathrm{d}\phi_L + \frac{iN}{2\pi}\int_{x=0} \phi_L \mathrm{d}\phi_R + \frac{N}{4\pi}\int_{x>0} \mathrm{d}\phi_R \wedge \star \mathrm{d}\phi_R \tag{4.3.7}$$

and

$$\eta^k: \quad S = \frac{N}{4\pi}\int_{x<0} \mathrm{d}\phi_L \wedge \star \mathrm{d}\phi_L + \frac{i}{2\pi}\int_{x=0} \mathrm{d}\varphi \left(\phi_L - \phi_R + \frac{2\pi k}{N}\right) + \frac{N}{4\pi}\int_{x>0} \mathrm{d}\phi_R \wedge \star \mathrm{d}\phi_R\,, \tag{4.3.8}$$

where ϕ_L and ϕ_R denote the compact boson on the left and right sides of the defects, which we placed at $x = 0$. Moreover, the field φ in Eq. (4.3.8) is another compact scalar which is supported only on the η^k defect worldvolume, as shown in Figure 4.3.

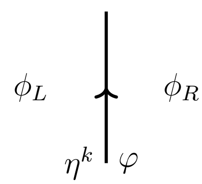

Figure 4.3: Description of an η^k line defect using two fields, ϕ_L and ϕ_R, from the two sides of the defect and a field φ which is supported on the defect.

In general, in order to find what defect actions of the type (4.3.7) or (4.3.8) describe, one should examine the part of the variation of the action which is localized on the defect and deduce from it the way the defect acts on operators. For the T defect, we have

$$\delta S|_{x=0} = \frac{N}{2\pi}\int_{x=0} \left[\delta\phi_L\left(\star \mathrm{d}\phi_L + i\mathrm{d}\phi_R\right) - \delta\phi_R\left(\star \mathrm{d}\phi_R + i\mathrm{d}\phi_L\right)\right] \tag{4.3.9}$$

and therefore $\mathrm{d}\phi_R|_{x=0} = i \star \mathrm{d}\phi_L|_{x=0}$ and $\mathrm{d}\phi_L|_{x=0} = i \star \mathrm{d}\phi_R|_{x=0}$. Using the relation between the compact scalar ϕ and its T-dual $\widetilde{\phi}$, which for the radius $R^2 = N$ we consider is given by $\mathrm{d}\widetilde{\phi} = iN \star \mathrm{d}\phi$ (see the discussion below Eq. (4.3.3)), we have $\mathrm{d}\phi_L|_{x=0} = (1/N)\,\mathrm{d}\widetilde{\phi}_R|_{x=0}$

[6] Let us comment that since the quantum dimension of T is not 1, but instead $\sqrt{N}$ (see subsection 4.2.1), the full insertion in the partition function that describes it is $\sqrt{N}\exp\left(\frac{iN}{2\pi}\int_{x=0}\phi_L \mathrm{d}\phi_R\right)$.

which indeed corresponds to gauging $\mathbb{Z}_N \subset U(1)_m$ in the right half-space followed by T-duality, as expected. For the η^k defect, we notice that integrating out φ in (4.3.8) sets $(\phi_R - \phi_L)|_{x=0} = 2\pi k/N + 2\pi\mathbb{Z}$, as expected.

In the rest of this section, we will use the Lagrangian descriptions (4.3.7) and (4.3.8) of the T and η^k defects to construct topological junctions and networks of defects, paying special attention to the boundary conditions and boundary terms at the junctions. Then, we will use these ingredients to compute the F-symbols, recovering the expressions in (4.3.6).

4.3.2 Local fusion junctions

4.3.2.1 Topological construction of local fusion junctions

For topological defects a, b and c, the local fusion junction $\mathrm{Hom}(a \times b, c)$ can be obtained by taking two parallel defects a and b and fusing the upper parts, as depicted in the figure below.

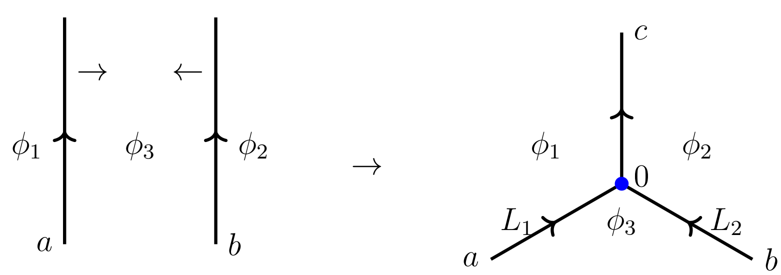

Figure 4.4: Topological construction of the local fusion junction for $\mathrm{Hom}(a \times b, c)$. $L_{1,2}$ in the second diagram are the semi-infinite lines from the bottom that end on the local fusion junction at $t = 0$ (blue dot).

The part of the action which is supported on the defects in this configuration (like the middle terms in Eqs. (4.3.7) and (4.3.8)) is given by

$$S = \int_{L_1} \mathcal{L}_a[\phi_1, \phi_3] + \int_{L_2} \mathcal{L}_b[\phi_3, \phi_2] + \int_{t=0}^{t=\infty} \left(\mathcal{L}_a[\phi_1, \phi_3] + \mathcal{L}_b[\phi_3, \phi_2]\right) \tag{4.3.10}$$

where $L_{1,2}$ denote the two bottom lines that terminate at the local fusion junction, and we use the coordinate $t > 0$ for the upper part of the fused defects. The first two terms describe the defects a and b below the fusion junction, and the last term describes the fusion of the two. One can then manipulate this last term in the upper part into the action of the topological defect(s) expected from the fusion algebra (in this case, the action of the defect c), which in general may result in boundary terms at the junction and a decoupled trivial $\mathbb{Z}_1$ TQFT at the fused segment, i.e.

$$\int_{t=0}^{t=\infty} (\mathcal{L}_a[\phi_1, \phi_3] + \mathcal{L}_b[\phi_3, \phi_2]) = \int_{t=0}^{t=\infty} \mathcal{L}_c[\phi_1, \phi_2, \phi_3] + \frac{i}{2\pi} \int_{t=0}^{t=\infty} \widetilde{\phi}\, \mathrm{d}\widetilde{\varphi} + S_{bdry} \tag{4.3.11}$$

where $\widetilde{\phi}$ and $\widetilde{\varphi}$ in the second term are fields supported only along the defect in the upper part $t > 0$, such as ϕ_3 in Figure 4.4 or the defect field φ in (4.3.8) used in the expression for the η^k defect. Hence, the second term on the RHS describes a trivial decoupled TQFT. We stress that both the boundary terms and the decoupled trivial TQFT are not always present.

Since we are interested in fusion junctions as in Figure 4.4, in which each defect (i.e. a, b and c in the figure) is not accompanied by a decoupled TQFT, when such a TQFT does arise we will need to add a topological boundary for it along the worldvolume of the c defect (i.e. at some $t_0 \in (0, \infty)$) and then push it to the junction at $t = 0$, resulting overall in a topological junction between defects with no decoupled TQFT. The topological boundary condition at the boundary we add along the $t > 0$ segment is that of Dirichlet for both $\widetilde{\phi}$ and $\widetilde{\varphi}$ in (4.3.11), as we explain next in more detail.

Boundary conditions of trivial TQFT Since we consider defects and fusion junctions that lie within a bulk where the periodicity of the compact scalars is maintained, we impose $\phi \sim \phi + 2\pi$ at all the topological boundaries we add when constructing such junctions. For the trivial TQFT in (4.3.11), this implies that the well-defined operators are the vertex operators $e^{in\widetilde{\phi}}$ and $e^{im\widetilde{\varphi}}$, both in its bulk and at the topological boundary we add for it. Now, using the equal-time commutation relation

$$[\widetilde{\phi}(t), \widetilde{\varphi}(t)] = 2\pi i \tag{4.3.12}$$

we see that these vertex operators generate the (gauge) transformations $\widetilde{\varphi} \to \widetilde{\varphi} + 2\pi m$ and $\widetilde{\phi} \to \widetilde{\phi} + 2\pi n$ and commute with each other. As a result, they are identified with the identity operator and the topological boundary condition at the boundary we add along the $t > 0$ segment at some $t = t_0$ is given by[7]

$$\widetilde{\phi}, \widetilde{\varphi}\Big|_{t=t_0} = 0 \mod 2\pi\,. \tag{4.3.13}$$

These boundary conditions are consistent with the variational principle, $\delta S|_{t=t_0} = 0$, and the periodicity (or gauge symmetry) of the compact scalars, $\Delta S = 0 \bmod 2\pi$.

Now that the topological boundary has been added at $t = t_0$, we push it to $t = 0$ and obtain the desired junction. In this junction we have, on top of the other junction data, the boundary condition (4.3.13).

Example: $\boldsymbol{T \times \eta^k = T}$ As an example, let us consider fusing the two defects T and η^k along the segment $t > 0$ as shown in Figure 4.5.

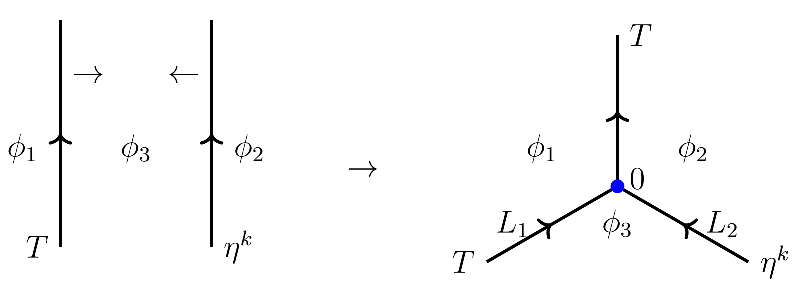

Figure 4.5: Topological construction of the local fusion junction for $\mathrm{Hom}(T \times \eta^k, T)$.

[7]Note also that the path integral over each of the fields $\widetilde{\phi}$ or $\widetilde{\varphi}$ restricts the other one to vanish modulo 2π, such that the boundary condition (4.3.13) is the only one which is compatible with a non-vanishing partition function.

Using (4.3.7) and (4.3.8), the defect part of the action associated with this configuration is

$$\begin{aligned} S =& \frac{iN}{2\pi}\int_{L_1}\phi_1 \mathrm{d}\phi_3 + \frac{i}{2\pi}\int_{L_2}\mathrm{d}\varphi\left(\phi_3-\phi_2+\frac{2\pi k}{N}\right) \\ &+ \frac{iN}{2\pi}\int_{t>0}\phi_1\mathrm{d}\phi_2 + \frac{i}{2\pi}\int_{t>0}\widetilde{\phi}\mathrm{d}\widetilde{\varphi} + S_{bdry}\ , \end{aligned} \tag{4.3.14}$$

where the trivial TQFT fields are

$$\widetilde{\phi} = \phi_3 - \phi_2 + \frac{2\pi k}{N}\,, \quad \widetilde{\varphi} = \varphi - N\phi_1\ , \tag{4.3.15}$$

and the boundary term is

$$S_{bdry} = -\left.\frac{iN}{2\pi}\phi_1\widetilde{\phi}\right|_0\ . \tag{4.3.16}$$

The action on the first line describes the T and η^k defects along the lines L_1 and L_2 below the fusion junction $t=0$, the first term on the second line is the T defect along the fused segment $t>0$, as expected from the fusion algebra $T\times\eta^k = T$, and the last term is the boundary term at the fusion junction $t=0$.

Since, for $t>0$, ϕ_3 and φ are supported only along the fused segment of the defect, the trivial TQFT is decoupled from the bulk; hence, as discussed above, one should impose the Dirichlet boundary conditions

$$\left.\widetilde{\phi}_3\right|_{t=0} = 0 \mod 2\pi\,, \quad \left.\widetilde{\varphi}\right|_{t=0} = 0 \mod 2\pi \tag{4.3.17}$$

(obtained by adding a topological boundary for the TQFT on the $t>0$ segment and pushing it to the $t=0$ junction). Note that we deliberately added the constant $\frac{2\pi k}{N}$ to the expression of $\widetilde{\phi}$ so that the boundary condition is consistent with the relation between the bulk fields set along the η^k line, $\phi_2 = \phi_3 + \frac{2\pi k}{N} \mod 2\pi$. If we did not include this constant in $\widetilde{\phi}$, the boundary term would differ by $\frac{ik}{N}\widetilde{\varphi}(t=0)$, which is not trivial in general. In summary, the boundary conditions and boundary terms at the fusion junction $t=0$ are given by

$$\begin{aligned} \mathrm{Hom}(T\times\eta^k, T):\quad & \left.\phi_3-\phi_2+\frac{2\pi k}{N}\right|_{t=0} = 0\,, \quad \left.\varphi - N\phi_1\right|_{t=0} = 0 \mod 2\pi\,, \\ & S_{bdry} = -\frac{iN}{2\pi}\phi_1\left(\phi_3-\phi_2+\frac{2\pi k}{N}\right)\ . \end{aligned} \tag{4.3.18}$$

Similarly, the junction data at the corresponding splitting junction $\mathrm{Hom}(T, T \times \eta^k)$ is the same except for the boundary term, which has the opposite sign.

4.3.2.2 Extra junction

When the fusion outcome involves the direct sum of more than one simple defect, a specific fusion channel can be obtained by adding an extra junction between the direct sum and the particular simple defect of interest. At the junction, we impose the well-defined variational principle and gauge invariance to get the boundary conditions and required boundary terms. In the following, we illustrate this process using the example of the $T \times T$ fusion.

Example: $\boldsymbol{T \times T = C \to \eta^k}$ Using the method discussed in the previous subsection, a local fusion junction can be constructed for $T \times T = \sum_{n=0}^{N-1} \eta^n \equiv C$, where C denotes the condensation defect[8] for the $\mathbb{Z}_N \subset U(1)_m$ shift symmetry, as shown in Figure 4.6.

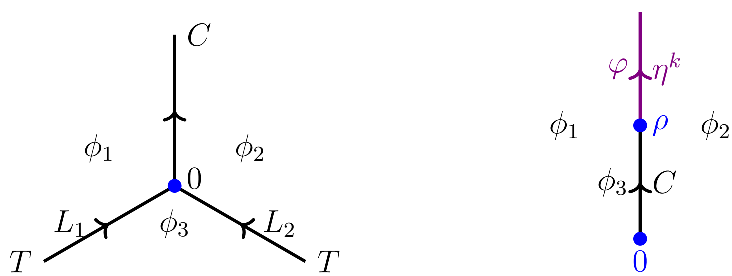

Figure 4.6: The topological fusion junction for $\mathrm{Hom}(T \times T, C)$ at $t = 0$ (left) and the junction $\mathrm{Hom}(C, \eta^k)$ at $t = \rho$ (right).

[8]Notice that this condensation defect is simply the projector for the $\mathbb{Z}_N \subset U(1)_m$ symmetry, and is not simple as a defect.

The defect action in the fused segment is then as follows,

$$\begin{aligned} S &= \frac{iN}{2\pi}\int_{t>0}(\phi_1 \mathrm{d}\phi_3 + \phi_3 \mathrm{d}\phi_2) \\ &= \frac{iN}{2\pi}\int_{t>0}\mathrm{d}\phi_3(\phi_1-\phi_2) - \frac{iN}{2\pi}\phi_3\phi_2\Big|_{t=0} \ , \end{aligned} \tag{4.3.19}$$

where the first term on the second line corresponds to the condensation defect and the second term is a boundary term. To see that the first term indeed describes the condensation defect, let us note that the sum of the $\mathbb{Z}_N \subset U(1)_m$ defects used in the definition of C is given by

$$\sum_{n=0}^{N-1}\exp\left[\frac{i}{2\pi}\int_L \mathrm{d}\varphi\left(\phi_1-\phi_2+\frac{2\pi n}{N}\right)\right] = \exp\left[\frac{i}{2\pi}\int_L \mathrm{d}\varphi\,(\phi_1-\phi_2)\right]\sum_{n=0}^{N-1}\exp\left(\frac{in}{N}\int_L \mathrm{d}\varphi\right) \ , \tag{4.3.20}$$

and the last sum restricts the winding number of φ to be an integer multiple of $2\pi N$. As a result, we can write $\varphi = N\phi$ for some 2π-periodic compact scalar ϕ and have the following equality under the path integral,

$$\sum_{n=0}^{N-1}\exp\left[\frac{i}{2\pi}\int_L \mathrm{d}\varphi\left(\phi_1-\phi_2+\frac{2\pi n}{N}\right)\right] = N\exp\left[\frac{iN}{2\pi}\int_L \mathrm{d}\phi\,(\phi_1-\phi_2)\right], \tag{4.3.21}$$

which results in precisely the first term on the second line of Eq. (5.6.29) with $\phi = \phi_3$.[9]

Selection of a fusion channel A specific fusion channel such as $T \times T \to \eta^k$ can be obtained by adding an additional junction ρ between the condensation defect and η^k as in the right diagram in Figure 4.6. To describe this junction, we start by examining the action

$$S = \frac{iN}{2\pi}\int_{t=0}^{t=\rho}\mathrm{d}\phi_3(\phi_1-\phi_2) + \frac{i}{2\pi}\int_{t>\rho}\mathrm{d}\varphi\left(\phi_1-\phi_2+\frac{2\pi k}{N}\right) . \tag{4.3.22}$$

Under the gauge transformations $\phi_i \to \phi_i + 2\pi n_i$,

$$\Delta S = i(n_1-n_2)(N\phi_3-\varphi)\big|_{t=\rho} \ , \tag{4.3.23}$$

[9] The factor on N on the right hand side of (4.3.21) is expected and corresponds to the two factors of $\sqrt{N}$ that are present in the two T defects which are part of the fusion junction of Figure 4.6 (see footnote 6).

and in order to have gauge invariance, we set

$$(N\phi_3 - \varphi)|_{t=\rho} \in 2\pi\mathbb{Z}\,. \tag{4.3.24}$$

Additionally, we impose

$$\phi_1 - \phi_2 + \frac{2\pi k}{N}\bigg|_{t=\rho} \in 2\pi\mathbb{Z}\ , \tag{4.3.25}$$

since $t = \rho$ is a part of the $\mathbb{Z}_N$ defect η^k on which this relation holds.

Turning to the variational principle, the total variation at the junction $t = \rho$ is given by

$$\delta S|_{t=\rho} = \frac{i}{2\pi}\delta\left(N\phi_3 - \varphi\right)\left(\phi_1 - \phi_2 + \frac{2\pi k}{N}\right)\bigg|_{t=\rho} - ik\delta\phi_3(\rho) = 0\,. \tag{4.3.26}$$

Now, the first term vanishes due to the boundary condition (4.3.24). However, in order to remove the second term we need to add an extra boundary term to (4.3.22) at the junction ρ,

$$S_{bdry} = ik\phi_3(\rho)\,. \tag{4.3.27}$$

In summary, the boundary conditions and the boundary term at the junction $\mathrm{Hom}(C, \eta^k)$ are

$$\begin{aligned} \mathrm{Hom}(C,\eta^k):\quad & (N\phi_3 - \varphi)|_{t=\rho} = 0 \mod 2\pi\,, \quad \left(\phi_1 - \phi_2 + \frac{2\pi k}{N}\right)\bigg|_{t=\rho} = 0 \mod 2\pi\,, \\ & S_{bdry} = ik\phi_3(\rho)\,. \end{aligned} \tag{4.3.28}$$

Now, to obtain the local fusion junction $T \times T \to \eta^k$ we can shrink the condensation defect on the interval $0 < t < \rho$ by taking $\rho \to 0$. Combining the boundary terms from $T \times T \to C$ (5.6.29) and $C \to \eta^k$ (C.3.4), the boundary data at the resulting junction is given by

$$\begin{aligned} \mathrm{Hom}(T\times T,\eta^k):\quad & (N\phi_3 - \varphi)|_{t=0} = 0 \mod 2\pi\,, \quad \left(\phi_1 - \phi_2 + \frac{2\pi k}{N}\right)\bigg|_{t=0} = 0 \mod 2\pi\,, \\ & S_{bdry} = -\frac{iN}{2\pi}\phi_3\left(\phi_2 - \frac{2\pi k}{N}\right)\bigg|_{t=0}\,. \end{aligned} \tag{4.3.29}$$

The analyses above can be generalized to any extra junction between two different topological defects: the gauge invariance and $\delta S = 0$ at the junction fix the boundary conditions and boundary terms.

In Appendix D.1.1, we provided an alternative derivation for the same results (4.3.29) using the previously obtained $T \times \eta^{-k} \to T$ junction data.

Other local fusion junctions In Appendix D.1.1 we provide the junction data for all the other local fusion junctions involving the T and η defects.

4.3.3 *F*-symbols using Lagrangian

4.3.3.1 The method

A specific component of an associator, which is a $\mathbb{C}$-number in 2d, can be computed by collapsing the diamond-shaped region in a corresponding defect network, as described in Figure 4.7 [58].

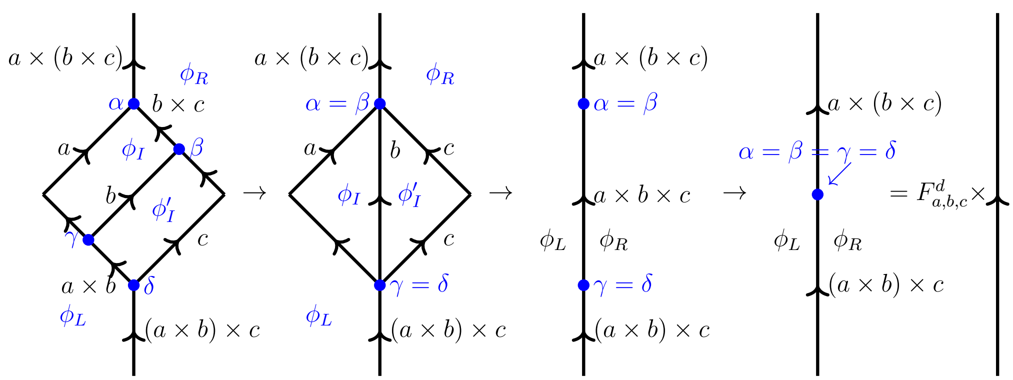

Figure 4.7: The associator $F^d_{a,b,c}$ can be obtained by collapsing the diamond in the middle. First arrow: Merging the two nodes α and β and also the two nodes γ and δ. Second arrow: Parallel fusion of the a, b, c defects in the middle. Third arrow: Reducing the interval between the two nodes $\alpha = \beta$ and $\gamma = \delta$.

We collapse the associator region by taking the following steps:

Step 1: **Junction analysis**: Using the method explained in Section 4.3.2, compute the boundary conditions and boundary terms at each local fusion/splitting junction $\alpha, \beta, \gamma, \delta$ as well as at possible extra junctions.

Step 2: **Merge** the two upper junctions α and β by combining the boundary conditions and boundary terms. Repeat for the lower junctions γ and δ.

Step 3: **Global fusion**: Fuse the three defects a, b, c by adding their actions along the interval between the $\alpha = \beta$ and $\gamma = \delta$ junctions. The result will in general be the sum of the expected defect, some decoupled TQFT (if present) and a boundary term,

$$S = S_{a\times b\times c} + S_{decoupled\ TQFT} + S_{bdry;global}\,. \tag{4.3.30}$$

Step 4: **Interval reduction**: Compute the path integral of the decoupled TQFT as an inner product between the states corresponding to the boundary conditions and some boundary terms.

Step 5: **Associator**: Evaluate all the boundary terms using the boundary conditions in Step 2. The associator is

$$F^{d}_{a,b,c} = (\text{Inner product}) \times e^{-S_{bdry}}\ . \tag{4.3.31}$$

4.3.3.2 Path integral of $\mathbb{Z}_N$ TQFT

The result of the global fusion (4.3.30) may include a 1d decoupled trivial or $\mathbb{Z}_N$ TQFT. After reducing the interval $[\gamma, \beta]$, they are replaced with their path integral subject to the given boundary conditions plus some boundary terms. For the trivial TQFT, the required boundary terms are fixed values. However, for the decoupled $\mathbb{Z}_N$ TQFT

$$S = \frac{iN}{2\pi}\int_{\gamma}^{\beta} \phi \, \mathrm{d}\varphi \tag{4.3.32}$$

the boundary terms might involve unfixed boundary values of the defect fields. However, the unfixed part of the boundary terms will drop out once it is combined with all other boundary terms – those from each junction and those from the global fusion part – and the total boundary term will only involve the fixed boundary values. Therefore, the boundary terms do not affect the path integral over the decoupled defect fields. In this subsection, we illustrate the reduction of the interval when a decoupled $\mathbb{Z}_N$ TQFT shows up after the global fusion.

To perform the path integral, one can add and subtract an appropriate boundary term to write the action as the sum of the part that has a vanishing variation on the boundary with respect to the boundary conditions and the boundary terms. The former part is path integrated to the inner product between the states corresponding to the boundary conditions on the upper and lower junctions.

Example: Distinct boundary conditions As an example, consider the boundary conditions[10]

$$\begin{aligned} \phi(\beta) = \frac{2\pi m}{N}\,, \quad \varphi(\gamma) = \frac{2\pi n}{N} \quad \mod 2\pi \quad (\text{Dirichlet})\,, \\ N\phi(\gamma) = 0\,, \quad N\varphi(\beta) = 0 \quad \mod 2\pi \quad (\text{Neumann})\,. \end{aligned} \tag{4.3.33}$$

Rewriting the action (4.3.32) as

$$S = \left(\frac{iN}{2\pi}\int_\gamma^\beta \phi \mathrm{d}\varphi - \frac{iN}{2\pi}\phi(\beta)\varphi(\beta)\right) + \frac{iN}{2\pi}\phi(\beta)\varphi(\beta)\,, \tag{4.3.34}$$

the terms in the bracket have trivial variation on the boundary with respect to the given boundary conditions. The path integral of this part results in the inner product between the

[10]The Neumann conditions can be written in terms of an unfixed integer $0 \leq k < N$ as $\phi(\gamma) = \frac{2\pi k}{N}$.

states corresponding to Dirichlet boundary conditions at each end. Specifically,[11][12]

$$\int_{DBC} [\mathcal{D}\varphi][\mathcal{D}\phi]\, e^{-S_{PI}} = \langle \phi(\beta) \,|\, \varphi(\gamma) \rangle = \frac{1}{\sqrt{N}} \exp\left(\frac{iN}{2\pi} \phi(\beta)\varphi(\gamma) \right) \,, \tag{4.3.35}$$

where S_{PI} is given by the terms in brackets in Eq. (4.3.34).

The boundary term (last term in (4.3.34)) is carried forward. After combined with other boundary terms from the junction analysis or global fusion, the unfixed part in this term will either be removed or be a part of a fixed boundary value.

To summarize, the contribution to the F-symbol from the decoupled $\mathbb{Z}_N$ theory is the combination of the inner product of the boundary states (4.3.35) and the boundary terms, as stated in Eq. (4.3.31):

$$\frac{1}{\sqrt{N}} \exp\left[\frac{iN}{2\pi} \phi(\beta) \left(\varphi(\gamma) - \varphi(\beta) \right) \right] = \frac{1}{\sqrt{N}} e^{\frac{2\pi i m n}{N}} \exp\left(-\frac{iN}{2\pi} \phi(\beta)\varphi(\beta) \right) . \tag{4.3.36}$$

General cases It is straightforward to generalize the above argument to other boundary conditions. We list the resulting inner products and boundary terms in Table (4.3.37), where the first two columns are the boundary conditions for the fields at the specified boundary, and D, N denote Dirichlet and Neumann boundary conditions, respectively.

$\phi(\gamma,\beta)$	$\varphi(\gamma,\beta)$	S_{bdry}	$\langle DBC_\beta \vert DBC_\gamma \rangle$	Contribution to F
ND	DN	$\frac{iN}{2\pi}\phi(\beta)\varphi(\beta)$	$\frac{1}{\sqrt{N}} \exp\left[\frac{iN}{2\pi}\phi(\beta)\varphi(\gamma)\right]$	$\frac{1}{\sqrt{N}} \exp\left[\frac{iN}{2\pi}\phi(\beta)(\varphi(\gamma)-\varphi(\beta))\right]$
DN	ND	$-\frac{iN}{2\pi}\phi(\gamma)\varphi(\gamma)$	$\frac{1}{\sqrt{N}} \exp\left[-\frac{iN}{2\pi}\varphi(\beta)\phi(\gamma)\right]$	$\frac{1}{\sqrt{N}} \exp\left[\frac{iN}{2\pi}\phi(\gamma)(\varphi(\gamma)-\varphi(\beta))\right]$
DD	NN	$-\frac{iN}{2\pi}\phi\varphi\Big\vert_\gamma^\beta$	$\delta_{\phi(\beta),\phi(\gamma)}$	$\delta_{\phi(\beta),\phi(\gamma)} \exp\left[\frac{iN}{2\pi}\phi\varphi\Big\vert_\gamma^\beta\right]$
NN	DD	0	$\delta_{\varphi(\beta),\varphi(\gamma)}$	$\delta_{\varphi(\beta),\varphi(\gamma)}$

(4.3.37)

[11]The LHS should be understood as the analytic continuation to the Lorentzian spacetime.

[12]The noamalisation constant can be obtained by demanding the orthonormality: $\left\langle \phi = \frac{2\pi i m}{N} \middle\vert\, \phi = \frac{2\pi i n}{N} \right\rangle = \sum_{k=0}^{N-1} \left\langle \phi = \frac{2\pi i m}{N} \middle\vert\, \varphi = \frac{2\pi i k}{N} \right\rangle \left\langle \varphi = \frac{2\pi i k}{N} \middle\vert\, \phi = \frac{2\pi i n}{N} \right\rangle = \delta_{m,n}$.

4.3.3.3 Example: $\left[F^{T}_{T,T,T}\right]_{\eta^m,\eta^n}$

To illustrate the procedure, let us compute $[F^{T}_{T,T,T}]_{\eta^m,\eta^n}$ using the method explained in Sections 4.3.3.1 and 4.3.3.2, namely by collapsing the diamond region in Figure 4.8.

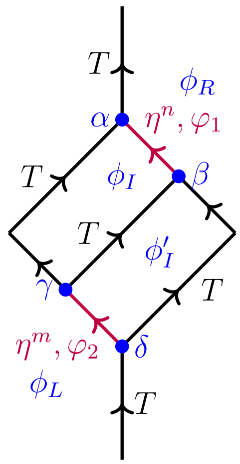

Figure 4.8: The configuration used in computing $[F^{T}_{T,T,T}]_{\eta^m,\eta^n}$.

As a first step, we collect the boundary conditions and boundary terms at each junction $\alpha, \beta, \gamma, \delta$, taken from already computed results. Specifically, the α junction is a fusion junction $T \times \eta^n \to T$ whose data is given in Eq. (4.3.18), the β and γ junctions are fusion and splitting junctions for $T \times T \to \eta^k$ with $k = n$ and $k = m$ respectively, with the data given in Eq. (4.3.29)[13], and δ is the splitting junction $T \to \eta^m \times T$ analyzed in Eq. (D.1.4). Explicitly,

$$\begin{aligned}
\alpha:&\quad \varphi_1 - N\phi_L = 0\,, \quad \phi_I - \phi_R = -\frac{2\pi n}{N}\,, \quad S(\alpha) = -\frac{iN}{2\pi}\phi_L\left(\phi_I - \phi_R + \frac{2\pi n}{N}\right),\\
\beta:&\quad \varphi_1 - N\phi'_I = 0\,, \quad S(\beta) = -\frac{iN}{2\pi}\phi'_I\left(\phi_R - \frac{2\pi n}{N}\right),\\
\gamma:&\quad \varphi_2 - N\phi_I = 0\,, \quad S(\gamma) = \frac{iN}{2\pi}\phi_I\left(\phi'_I - \frac{2\pi m}{N}\right),\\
\delta:&\quad \phi_L - \phi'_I = -\frac{2\pi m}{N}\,, \quad \varphi_2 - N\phi_R = 0\,, \quad S(\delta) = im\phi_R(\delta)\;,
\end{aligned} \tag{4.3.38}$$

[13]For the splitting junction, the boundary term changes the sign.

where all the boundary conditions are written modulo 2π, and $S(\alpha)$ denotes the boundary term at the junction α (and similarly for other junctions). Next, we shrink the interval $[\beta, \alpha]$ to obtain a single upper junction $\beta = \alpha$. As a consequence, we can impose the boundary conditions at the α and β junctions simultaneously. Similarly, we shrink the interval $[\delta, \gamma]$ to get the single lower junction $\gamma = \delta$.

Next, we fuse the three defects $T \times T \times T$ in the middle by adding the corresponding defect actions,

$$\begin{aligned} S &= \frac{iN}{2\pi} \int_\gamma^\beta (\phi_L \mathrm{d}\phi_I + \phi_I \mathrm{d}\phi_I' + \phi_I' \mathrm{d}\phi_R) \\ &= \frac{iN}{2\pi} \int_\gamma^\beta \phi_L \mathrm{d}\phi_R + \frac{iN}{2\pi} \int_\gamma^\beta (\phi_L - \phi_I') \mathrm{d}\,(\phi_I - \phi_R) + \frac{iN}{2\pi}\, \phi_I' \phi_I |_\gamma^\beta \end{aligned} \tag{4.3.39}$$

where the first term is the action for the resulting T defect, the second term is a decoupled $\mathbb{Z}_N$ TQFT and the last term is a boundary term $S_{bdry;global}$. The decoupled TQFT fields have the following boundary conditions,

$$\begin{aligned} N(\phi_L - \phi_I')(\beta) = 0\,, \quad (\phi_I - \phi_R)(\beta) = -\frac{2\pi n}{N} \quad \mathrm{mod}\ 2\pi\,, \\ (\phi_L - \phi_I')(\gamma) = -\frac{2\pi m}{N}\,, \quad N(\phi_I - \phi_R)(\gamma) = 0 \quad \mathrm{mod}\ 2\pi\,, \end{aligned} \tag{4.3.40}$$

namely $\phi_L - \phi_I'$ has a Dirichlet boundary condition at γ and a Neumann one at β, while $\phi_I - \phi_R$ has the opposite boundary conditions. Using the second row in Table (4.3.37), the contribution from this $\mathbb{Z}_N$ theory is hence

$$\frac{1}{\sqrt{N}} e^{-S_{\mathbb{Z}_N}}\,, \qquad S_{\mathbb{Z}_N} = -im(\phi_I - \phi_R)|_\gamma^\beta\,. \tag{4.3.41}$$

As a last step, we combine the boundary terms at the upper and lower junctions, including the phase contribution $S_{\mathbb{Z}_N}$ from the $\mathbb{Z}_N$ TQFT and the boundary term $S_{bdry;global}$ in (4.3.39). At the upper junction,

$$S(\alpha) + S(\beta) + (S_{bdry;global} + S_{\mathbb{Z}_N})_\beta = \frac{iN}{2\pi} \left(-\phi_L + \phi_I' - \frac{2\pi m}{N}\right) \left(\phi_I - \phi_R + \frac{2\pi n}{N}\right) + \frac{2\pi i m n}{N} \tag{4.3.42}$$

and using the boundary conditions at the upper junction (4.3.38), $\frac{N}{2\pi}\left(-\phi_L+\phi_I'-\frac{2\pi m}{N}\right)\in\mathbb{Z}$ and $\left(\phi_I-\phi_R+\frac{2\pi n}{N}\right)\in 2\pi\mathbb{Z}$, we find that the first term in Eq. (4.3.42) is trivial modulo $2\pi i$. Thus, the total phase contribution from the upper junction is given by

$$S(\alpha)+S(\beta)+(S_{bdry;global}+S_{\mathbb{Z}_N})_\beta=\frac{2\pi imn}{N}\,. \tag{4.3.43}$$

Turning to the lower junction, the sum of all the boundary terms vanishes, i.e.

$$S(\gamma)+S(\delta)+(S_{bdry;global}+S_{\mathbb{Z}_N})_\gamma=0\,. \tag{4.3.44}$$

Then, putting everything together we substitute the inner product and the boundary terms (given in Eqs. (4.3.41), (4.3.43)-(4.3.44)) into Eq. (4.3.31) and obtain the F-symbol

$$[F^T_{T,T,T}]_{\eta^m,\eta^n}=\frac{1}{\sqrt{N}}\exp\left(-\frac{2\pi imn}{N}\right)\,, \tag{4.3.45}$$

which agrees with the known value (4.3.6).

Other $\boldsymbol{F}$-symbols All the other F-symbols of the compact boson theory are computed in Appendix D.1.2 and agree with Eq. (4.3.6).

4.4 Maxwell theory in 4d

4.4.1 Non-invertible triality symmetry and defect Lagrangians

We next turn to four dimensions and consider Maxwell theory, which has the Lagrangian

$$\mathcal{L}=\frac{1}{2e^2}F\wedge\star F+\frac{i\theta}{8\pi^2}F\wedge F\,. \tag{4.4.1}$$

Normalizing the 1-from gauge field A so that the corresponding field strength $F=dA$ has fluxes $2\pi\mathbb{Z}$, the theory is specified by the choice of complexified coupling

$$\tau=\frac{\theta}{2\pi}+\frac{2\pi i}{e^2} \tag{4.4.2}$$

and has an $SL(2,\mathbb{Z})$ duality group (on spin manifolds) which is generated by

$$\mathbb{S}: \ \tau \to -1/\tau \quad , \quad \mathbb{T}: \ \tau \to \tau + 1 \tag{4.4.3}$$

with the relations

$$\mathbb{S}^2 = \mathbb{C} \quad , \quad (\mathbb{S}\mathbb{T})^3 = 1 \,, \tag{4.4.4}$$

where $\mathbb{C}$ is the charge-conjugation symmetry under which $A \to -A$. In addition to charge conjugation, the theory also has two 1-form symmetries $U(1)_E^{(1)} \times U(1)_M^{(1)}$ with charges

$$Q_E = \frac{1}{2\pi} \oint \left(-\frac{2\pi i}{e^2} \star F + \frac{\theta}{2\pi} F \right) \quad , \quad Q_M = \frac{1}{2\pi} \oint F \,, \tag{4.4.5}$$

the charged objects being Wilson and 't Hooft lines, respectively. Upon gauging a $\mathbb{Z}_N^{(1)} \subset U(1)_E^{(1)}$ subgroup of the electric 1-form symmetry we cut out all Wilson lines (at least as genuine line operators) whose charges are not integer multiples of N, resulting in the charge quantization $Q_E \in N\mathbb{Z}$ and $Q_M \in \mathbb{Z}/N$. To have the standard quantization $Q_{E,M} \in \mathbb{Z}$ as in the theory before the gauging (i.e. having the same normalization for the gauge field), we rewrite $A = A'/N$ and $\tau = \tau' N^2$ which then results in a theory which is similar to the one before the gauging but with the new coupling $\tau' = \tau/N^2$. We therefore see that gauging $\mathbb{Z}_N^{(1)} \subset U(1)_E^{(1)}$ is equivalent to changing $\tau \to \tau/N^2$. Similarly, gauging a $\mathbb{Z}_N^{(1)} \subset U(1)_M^{(1)}$ subgroup of the magnetic 1-form symmetry would amount to changing $\tau \to \tau N^2$.

In addition to simply gauging a (non-anomalous) $\mathbb{Z}_N^{(1)}$ subgroup of the 1-form symmetry, an operation usually denoted by S, we can also consider combining it with stacking an SPT phase for the corresponding background 2-form gauge field, an operation usually denoted by T (see [51, 76, 64]). Denoting the background field by $B \in H^2(M_4; \mathbb{Z}_N)$ where M_4 is the space in which the theory lives, this SPT phase is given by $\exp(\frac{2\pi i}{2N} \int_{M_4} q(B))$ for even N (where $q : H^2(M_4; \mathbb{Z}_N) \to H^4(M_4; \mathbb{Z}_{2N})$ is the Pontryagin square operation) and by $\exp(\frac{2\pi i}{N} \int_{M_4} \frac{N+1}{2} B^2)$ for odd N. Then, considering e.g. the gauging corresponding to ST, i.e. first stacking the SPT phase and then gauging the $\mathbb{Z}_N^{(1)}$ symmetry, we have $A = A'/N$ and $\theta' = \theta + 2\pi/N$ for even N which amounts to changing $\tau \to \tau/N^2 + 1/N$ in the original theory, and $A = A'/N$ and $\theta' = \theta + 2\pi\left(N+1\right)/N$ for odd N which amounts to the change $\tau \to \tau/N^2 + \left(N+1\right)/N$.

The two ingredients discussed above, i.e. gauging a subgroup of the 1-form symmetry (possibly with stacking an SPT phase) and performing a duality operation, were used recently to construct many new non-invertible defects in the theory [59, 62–64, 60, 65, 66, 68]. For simplicity, we will focus in this section on the triality defects at $\tau = e^{\frac{2\pi i}{3}}N$ found in [64] and on condensation defects [63, 64] associated with electric 1-form gauging, which can be constructed as follows (in appendix D.5 we will also discuss duality defects).

Starting with the triality defect, we consider the coupling $\tau = e^{\frac{2\pi i}{3}}N$ (for any $N \in \mathbb{N}$) and perform an ST gauging of a $\mathbb{Z}_N^{(1)}$ subgroup of the electric 1-form symmetry in half space (with Dirichlet boundary conditions for the corresponding discrete gauge field), resulting in a topological interface between the theory with coupling $\tau = e^{\frac{2\pi i}{3}}N$ and the theory with coupling $\tau/N^2 + 1/N = e^{\pi i/3}/N$ for even N and coupling $\tau/N^2 + \left(N+1\right)/N = e^{\pi i/3}/N + 1$ for odd N. However, since the coupling $e^{\frac{2\pi i}{3}}N$ is obtained by performing an $\mathbb{S}$ transformation to $e^{\pi i/3}/N$ and an $\mathbb{S}\mathbb{T}^{-1}$ transformation to $e^{\pi i/3}/N + 1$, the two sides are in fact equivalent and we get a defect in a single theory, obtained by performing ST $\mathbb{Z}_N^{(1)}$ gauging and $\mathbb{S}$ duality (for even N) or $\mathbb{S}\mathbb{T}^{-1}$ duality (for odd N) in half space. As shown in [64], one can describe this defect, which is denoted by D_3, by the following action,

$$D_3: \quad S = \int_{x<0}\left(\frac{\sqrt{3}N}{8\pi}F_L \wedge \star F_L - \frac{iN}{8\pi}F_L \wedge F_L\right) + \int_{x>0}\left(\frac{\sqrt{3}N}{8\pi}F_R \wedge \star F_R - \frac{iN}{8\pi}\int F_R \wedge F_R\right) \\ + \frac{iN}{2\pi}\int_{x=0}\left(A_L \wedge \mathrm{d}A_R + \frac{1}{2}A_L \wedge \mathrm{d}A_L\right) \tag{4.4.6}$$

where A_L and A_R denote the Maxwell gauge field from the two sides of the defect, which is located at $x = 0$. The equations of motion on the defect that follow from (4.4.6), then, determine the matching conditions between the left and right gauge fields, which in turn results in an action of the defect on operators (whether local or not) which is indeed similar to that of the gauging and duality used in its construction. The corresponding orientation reversal defect, denoted by $\overline{D}_3$, is given by

$$\overline{D}_3 : \quad S = -\frac{iN}{2\pi}\int_{x=0}\left(A_L \wedge dA_R + \frac{1}{2}A_R \wedge dA_R\right) \tag{4.4.7}$$

where we omit the bulk action on both sides of the defect here and below for brevity.

Turning to the condensation defects we are interested in, at any τ we can gauge a $\mathbb{Z}_N^{(1)}$ subgroup of the electric 1-form symmetry with a discrete torsion labeled by $H^3(B\mathbb{Z}_N; U(1)) \cong \mathbb{Z}_N$ over a codimension-1 manifold and obtain a nontrivial defect. As shown in [63, 64], the part of the action describing this defect is given by[14]

$$C_k : \quad S = \int_{M_3}\left[\frac{iN}{2\pi}da \wedge (A_L - A_R) + \frac{ik}{2\pi}(A_L - A_R) \wedge d(A_L - A_R)\right], \tag{4.4.8}$$

where A_L and A_R are as before the Maxwell gauge field from the two sides of the defect, a is a $U(1)$ gauge field living on the worldvolume M_3 and $k \in \mathbb{Z}_N$ is the discrete-torsion label. Integrating the defect field a out sets $A_L - A_R$ to be a flat $\mathbb{Z}_N$ connection,[15] with $e^{i\oint_\gamma (A_L - A_R)}$ generating $\mathbb{Z}_N$ topological line operators which are identified as the higher quantum symmetry on C_k.

Let us also describe what the identity defect looks like in the Lagrangian description in

---

[14]Our defect action for C_k (as well as for the duality defect discussed in appendix D.5) differs from that in [64] by a total derivative term, which we choose this way in order to avoid extra boundary terms when considering junctions between defects.

[15]To see this, let us decompose a as $a = \overline{a} + a'$ where a' has trivial fluxes and $\overline{a}$ is a choice of representative for each flux sector labeled by $H^2(M_3, \mathbb{Z})$. Integrating out a' sets $A_L - A_R$ to be flat, and the sum over the flux sector $\overline{a}$ corresponds to summing over the 1-cycle $\gamma \in H_1(M_3, \mathbb{Z})$ where γ is the Poincaré dual of the first Chern class $c_1 = \frac{d\overline{a}}{2\pi} \in H^2(M_3, \mathbb{Z})$. Decomposing $\gamma = n_i\gamma_i$ where $\{\gamma_i\}$ is the bases of 1-cycles, the remaining path integral becomes

$$\prod_i \sum_{\{n_i\}} e^{iNn_i \oint_{\gamma_i}(A_L - A_R)} \tag{4.4.9}$$

and the sum over n_i implies that the holonomy $e^{i\oint(A_L - A_R)}$ on any γ_i takes values in $\left\{e^{\frac{2\pi i}{N}k}\right\}_{k=0}^{N-1}$.

terms of left and right fields. It is given by the action

$$\mathbb{1}: \quad S = \frac{i}{2\pi}\int_{M_3} \mathrm{d}b \wedge (A_L - A_R) \tag{4.4.10}$$

where b is again a $U(1)$ gauge field living on M_3 which upon integrating it out sets $A_L - A_R$ to be a pure $U(1)$ gauge transformation on M_3.

The descriptions of the defects above can be easily used to find their fusions. For example, one finds [64]

$$D_3 \times D_3 = U(1)_N \overline{D}_3 \ , \ \overline{D}_3 \times \overline{D}_3 = U(1)_{-N} D_3 \ , \ \overline{D}_3 \times D_3 = C_0 \ , \ D_3 \times \overline{D}_3 = C_{\frac{N}{2}} \tag{4.4.11}$$

for even N and

$$D_3 \times D_3 = SU(N)_{-1} \overline{D}_3 \ , \ \overline{D}_3 \times \overline{D}_3 = SU(N)_1 D_3 \ , \ \overline{D}_3 \times D_3 = D_3 \times \overline{D}_3 = C_0 \tag{4.4.12}$$

for odd N.

In the next two subsections, we will show how the Lagrangian descriptions (4.4.6)-(4.4.10) can be used to characterize fusion and morphism junctions between these defects, as well as finding associator theories. We will focus on the triality associator $\left[F^{D_3}_{D_3,D_3,\overline{D}_3}\right]_{\mathbb{1},U(1)_N\overline{D}_3}$ for even values of N and the junctions that appear in its computation, deferring the rest of the associators to appendix D.3. Then, in section 4.5, we will compute the associators using a different (group-theoretical) approach for certain odd values of N and see the agreement with the results of this section, except for certain cases where the final result depends on whether N is even or odd.

In Appendix D.5 we will also discuss the non-invertible duality defects of [59] and compute all the associators using both the Lagrangian (which is valid for all N) and group-theoretical methods and see their agreement.

4.4.2 Local fusion and morphism junctions

In this subsection, we will describe the fusion and morphism junctions of the non-invertible symmetry defects we discussed above using their Lagrangian descriptions, emphasizing the way the boundary conditions and the boundary terms at these junctions arise. Notice that one can also describe the same junctions alternatively by adding additional boundary degrees of freedom as demonstrated in Appendix D.2 (see also [77, 63, 71]). We choose our current approach to simplify the number of fields we need to keep track of.

4.4.2.1 Topological construction of the local fusion junction

As for the 2d case, we obtain the local fusion junction $\mathrm{Hom}(\mathcal{D}_a \times \mathcal{D}_b, \mathcal{D}_c)$ of the topological defects $\mathcal{D}_a, \mathcal{D}_b$ and $\mathcal{D}_c$ by fusion of the upper part of the two parallel defects $\mathcal{D}_a$ and $\mathcal{D}_b$, as depicted in the figure below.

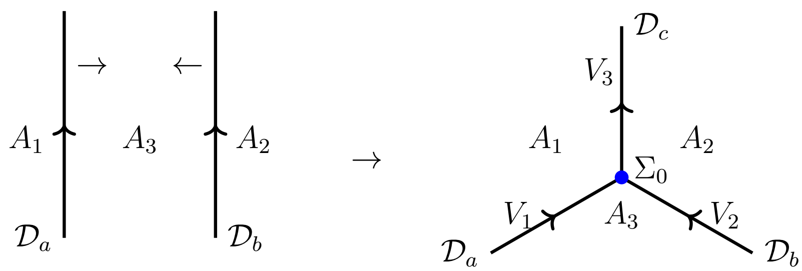

Figure 4.9: Topological construction of the local fusion junction for $\mathrm{Hom}(\mathcal{D}_a \times \mathcal{D}_b, \mathcal{D}_c)$. $V_{1,2,3}$ are the 3-manifolds that end on the 2-dimensional local fusion junction at Σ_0 (blue dot).

The action associated with this configuration is

$$S = \int_{V_1} \mathcal{L}_{\mathcal{D}_a}[A_1, A_3] + \int_{V_2} \mathcal{L}_{\mathcal{D}_b}[A_3, A_2] + \int_{V_3} \left(\mathcal{L}_{\mathcal{D}_a}[A_1, A_3] + \mathcal{L}_{\mathcal{D}_b}[A_3, A_2]\right) \tag{4.4.13}$$

where $V_{1,2}(V_3)$ are 3-manifolds from the bottom (top) that end on the 2-dimensional local fusion junction Σ_0. The first two terms are the actions of the defects $\mathcal{D}_a$ and $\mathcal{D}_b$ below the fusion junction, and the last term describes the fusion of the two. One can then manipulate this last term in the upper part into the action of the topological defect(s) expected from the fusion algebra (in this case, the action of the defect $\mathcal{D}_c$), which in general may result in boundary terms at the junction and a decoupled trivial $\mathbb{Z}_1$ TQFT at the fused segment, i.e.

$$\int_{V_3} \left(\mathcal{L}_{\mathcal{D}_a}[A_1, A_3] + \mathcal{L}_{\mathcal{D}_b}[A_3, A_2]\right) = \int_{V_3} \mathcal{L}_{\mathcal{D}_c}[A_1, A_2, A_3] + \frac{i}{2\pi} \int_{V_3} \widetilde{A} \wedge \mathrm{d}\widetilde{B} + S_{bdry} \tag{4.4.14}$$

where $\widetilde{A}$ and $\widetilde{B}$ are the fields supported only along the defect in the upper half (V_3), such as A_3 in Figure 4.9 or the defect fields of the condensation and identity defects (i.e. a and b in (4.4.8) and (4.4.10)). Hence, the second term on the right-hand side describes a trivial decoupled TQFT. We stress that both the boundary terms and the decoupled trivial TQFT are not always present. As we will see below, however, both do appear e.g. in the construction of the local fusion junctions $\mathbb{1} \times D_3 = D_3$, $D_3 \times \mathbb{1} = D_3$, and their orientation reversals.

Since we are interested in fusion junctions as in Figure 4.9, in which each defect (i.e. $\mathcal{D}_a$, $\mathcal{D}_b$ and $\mathcal{D}_c$ in the figure) is not accompanied with a decoupled TQFT, when such a TQFT does arise we will need to add a topological boundary for it along V_3 and then push it to the junction Σ_0, resulting overall in a topological junction between defects with no decoupled TQFT. The topological boundary condition at the boundary we add along V_3 is that of Dirichlet for both $\widetilde{A}$ and $\widetilde{B}$ in (4.4.14), as we explain next in more detail.

Boundary conditions of decoupled trivial TQFT In the 3d decoupled TQFT in (4.4.14), the gauge-invariant operators are the Wilson lines $e^{i\oint_\gamma \widetilde{A}}$ and $e^{i\oint_{\gamma'} \widetilde{B}}$, which commute with each other as can be seen from the commutation relation between $\widetilde{A}$ and $\widetilde{B}$. As a result, on the topological boundary which we add along V_3, denoted by Σ_0', both of these operators can be fixed. In fact, they have to be fixed to the identity operator (corresponding to trivial holonomies for $\widetilde{A}$ and $\widetilde{B}$) since the path integral over each of the fields restricts the other one to be a pure $U(1)$ gauge (and hence nontrivial boundary holonomies would result in a vanishing partition function). The boundary conditions for $\widetilde{A}$ and $\widetilde{B}$ at Σ_0' are therefore given by

$$\widetilde{A}, \widetilde{B}\Big|_{\Sigma_0'} = \mathrm{d}\widetilde{\phi}_{A,B} \tag{4.4.15}$$

for some compact scalars $\widetilde{\phi}_{A,B}$, and are consistent with the variational principle ($\delta S|_{\Sigma_0'} = 0$) and gauge invariance ($\Delta S = 0$).

Now that the topological boundary has been added at Σ_0', we push it to Σ_0 and obtain the desired junction. In this junction we have, on top of the other junction data, the boundary condition (4.4.15).

Example: $\boldsymbol{D_3} \times \mathbb{1} = \boldsymbol{D_3}$ To illustrate the procedure, let's consider the local fusion junction for $D_3 \times \mathbb{1} = D_3$ shown in the figure below.

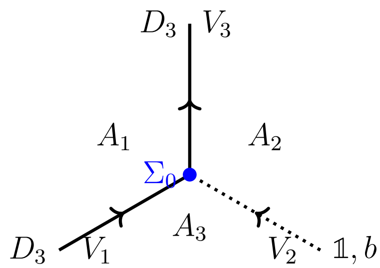

Figure 4.10: $\mathrm{Hom}(D_3 \times \mathbb{1}, D_3)$ junction. b is the defect field on V_2 used in the Lagrangian description of the identity defect.

The part of the action along the V_3 segment obtained by fusing the defects D_3 and $\mathbb{1}$ in the upper part (as in Figure 4.9) is given by[16]

$$\begin{aligned} S &= \frac{i}{2\pi}\int_{V_3}\left[NA_1\mathrm{d}A_3 + \frac{N}{2}A_1\mathrm{d}A_1 + \mathrm{d}b(A_3 - A_2)\right] \\ &= \frac{iN}{2\pi}\int_{V_3}\left(A_1\mathrm{d}A_2 + \frac{1}{2}A_1\mathrm{d}A_1\right) + \frac{i}{2\pi}\int_{V_3}(b + NA_1)\mathrm{d}(A_3 - A_2) - \frac{i}{2\pi}\int_{\Sigma_0} b\wedge(A_3 - A_2)\,, \end{aligned} \tag{4.4.16}$$

where the first term on the last line describes the triality defect D_3 as expected from the fusion algebra, the second term is a trivial $\mathbb{Z}_1$ TQFT and the last term is a boundary term. Since the fields $b + NA_1$ and $A_3 - A_2$ of the trivial TQFT are defect fields living on V_3 (as may become more apparent by shifting b by $-NA_1$ and A_3 by A_2) and do not appear in the first term describing D_3, this TQFT is decoupled from the bulk and from D_3. Thus, as discussed above, we introduce a topological boundary for it along V_3 by imposing Dirichlet

[16]For the brevity of the notation, we leave the wedge product between a 1-form and an external derivative of a 1-form implicit hereafter.

boundary conditions for both of its fields and then push this boundary to the junction Σ_0, effectively setting both $b + NA_1$ and $A_3 - A_2$ to be pure $U(1)$ gauges at the junction.

In summary, the boundary conditions and boundary term at this fusion junction are

$$\begin{aligned} \mathrm{Hom}(D_3 \times \mathbb{1}, D_3): \quad & b + NA_1|_{\Sigma_0}\,,\, A_3 - A_2|_{\Sigma_0} = \text{pure } U(1) \text{ gauge}\,, \\ & S_{bdry} = -\frac{i}{2\pi}\int_{\Sigma_0} b \wedge (A_3 - A_2)\,. \end{aligned} \tag{4.4.17}$$

Other local fusion junctions All other local fusion junctions involving the triality defect are worked out in Appendix D.3.

4.4.2.2 Morphism junctions of condensation defects

As explained in Section 4.2.2, condensation defects and defects containing a decoupled TQFT that admits topological boundary conditions are Witt equivalent to the identity defect. Demanding well-defined variational principle and gauge invariance at the corresponding morphism junctions fixes the boundary conditions and the extra boundary action at these junctions. In this subsection, we illustrate this using the examples of the morphism junctions between the identity defect and the condensation defects C_0 and $C_{\frac{N}{2}}$, and then turn in the next subsection to consider the morphism junction between the defect containing the TQFT $U(1)_N \times U(1)_{-N}$ and the identity defect.

Hom($\boldsymbol{C_0}, \mathbb{1}$) Consider a 2-dimensional morphism junction Σ_0 between the condensation defect C_0 and the identity defect supported at V_{lower} and V_{upper}, respectively, as depicted in Figure 4.11. We denote by a and b the defect fields on C_0 and $\mathbb{1}$, respectively.

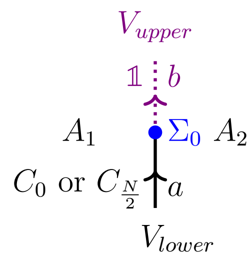

Figure 4.11: $\mathrm{Hom}(C_0, \mathbb{1})$ junction: The lower part V_{lower} supports C_0 (or $C_{\frac{N}{2}}$ later) and the upper part V_{upper} supports $\mathbb{1}$.

The action for this configuration is given by

$$S = \frac{iN}{2\pi}\int_{V_{lower}} \mathrm{d}a\,(A_1 - A_2) + \frac{i}{2\pi}\int_{V_{upper}} \mathrm{d}b\,(A_1 - A_2)\,. \tag{4.4.18}$$

To find the junction data at Σ_0, we demand gauge invariance and a well-defined variational principle at the junction. First, under the gauge transformations $A_{1,2} \to A_{1,2} + \mathrm{d}\lambda_{1,2}$ we have

$$\Delta_\lambda S = \frac{i}{2\pi}\int_{\Sigma_0} (Na - b) \wedge \mathrm{d}(\lambda_1 - \lambda_2)\,. \tag{4.4.19}$$

For small gauge transformations, i.e. $\lambda_{1,2}$ are single-valued such that $\oint \mathrm{d}\lambda_{1,2} = 0$, one can integrate by parts and obtain $\mathrm{d}(Na - b)|_{\Sigma_0} = 0$ for gauge invariance. Then, for the large gauge transformations, i.e $\lambda_{1,2}$ have nontrivial winding modes such that $\oint \mathrm{d}\lambda_{1,2} \neq 0$, one can use the Poincaré dual to demand $\Delta_\lambda S = i\int_{PD(\mathrm{d}(\lambda_1-\lambda_2),\Sigma_0)}(Na - b) \overset{!}{\in} 2\pi i\mathbb{Z}$ for gauge invariance. In other words, $Na - b$ is a pure $U(1)$ gauge at Σ_0. Let us then write $Na - b|_{\Sigma_0} = \mathrm{d}\phi$ for some compact scalar ϕ, and get for the variation at Σ_0 the following

$$\delta S|_{\Sigma_0} = \frac{i}{2\pi}\int_{\Sigma_0} \mathrm{d}\delta\phi \wedge (A_1 - A_2)\,. \tag{4.4.20}$$

Now, since $A_1 - A_2|_{V_2}$ is a pure $U(1)$ gauge on the worldvolume V_2 of the identity defect which includes the junction Σ_0, $\delta S|_{\Sigma_0} = 0$ without needing any extra boundary terms.

In summary, we have the following junction data:

$$\mathrm{Hom}(C_0, \mathbb{1}): \quad b - Na, \quad A_1 - A_2|_{\Sigma_0} = \text{pure } U(1) \text{ gauge}, \quad S_{bdry} = 0\,. \tag{4.4.21}$$

Before moving on, let us describe another approach for arguing (4.4.21). Taking advantage of the topological nature of the configuration in Figure 4.11, we turn the upper part V_{upper} along which the identity defect lies clockwise until it is fused with the condensation defect, resulting in a single defect along V_{lower} that ends topologically at Σ_0. The bulk field A_2 (as well as the defect fields a and b) then becomes a defect field living only on V_{lower}, and the action of this new defect is given by

$$\frac{i}{2\pi}\int_{V_{lower}}(Nda - db)\,(A_1 - A_2) \tag{4.4.22}$$

where the bulk field is now only A_1. To put this action in a more familiar form, we can denote $c = Na - b$ and $\widetilde{A} = A_1 - A_2$ and notice that they are both standard $U(1)$ gauge fields (with fluxes $2\pi\mathbb{Z}$) which live only on V_{lower} (alternatively, we can shift b by Na and A_2 by A_1). That is, we obtain a decoupled trivial $\mathbb{Z}_1$ BF theory on V_{lower} with Lagrangian $(i/2\pi)\widetilde{A}dc$. Now, since this defect ends at Σ_0 topologically, the boundary conditions for the corresponding worldvolume TQFT should be topological, and as discussed in subsection 4.4.2.1 they are given by Dirichlet boundary conditions for both of the fields c and $\widetilde{A}$. This, in turn, yields Eq. (4.4.21).

Example: $\mathbf{Hom}(C_{\frac{N}{2}}, \mathbb{1})$ The discussion above straightforwardly applies to the case with a condensation defect with a nontrivial discrete torsion. For example, for $C_{\frac{N}{2}}$ (for even N)

$$S = \frac{iN}{2\pi}\int_{V_{lower}}\left[(A_1 - A_2)\mathrm{d}a + \frac{1}{2}(A_1 - A_2)\mathrm{d}(A_1 - A_2)\right] + \frac{i}{2\pi}\int_{V_{upper}}(A_1 - A_2)\mathrm{d}b \tag{4.4.23}$$

and the analysis above can be used to find the following boundary conditions without any boundary term:[17]

$$\mathrm{Hom}\left(C_{\frac{N}{2}}, \mathbb{1}\right): \quad Na + \frac{N}{2}(A_1 - A_2) - b\,, \quad A_1 - A_2\Big|_{\Sigma_0} = \text{pure } U(1) \text{ gauge}\,, \quad S_{bdry} = 0\,. \tag{4.4.24}$$

[17]The boundary condition for $\mathcal{C}_k$ is given by the expression below after replacing $\frac{N}{2}$ with k.

4.4.2.3 Morphism junctions of $U(1)_N \times U(1)_{-N}$

When a TQFT has a topological boundary condition, there exists a morphism between a defect on which this TQFT lives and the identity, obtained by imposing the topological boundary condition at the morphism junction.[18] Although a single $U(1)_N$ Chern-Simons theory does not have a topological boundary condition, a $U(1)_N \times U(1)_{-N}$ Chern-Simons theory does. One obvious choice is identifying the $U(1)_N$ and $U(1)_{-N}$ gauge fields, including their gauge transformations and variations, at the junction.[19] However, such a boundary condition is not suitable for the $U(1)_N \times U(1)_{-N}$ theory when the two $U(1)$ fields are made of different bulk gauge fields that are independently gauge invariant. Is there a topological boundary condition that respects both $U(1)$ gauge symmetries? What is the correct action, including the boundary terms, that is compatible with such a boundary condition?

To answer these questions, we note that the $U(1)_N \times U(1)_{-N}$ theory

$$S = \frac{iN}{4\pi} \int_V (a\mathrm{d}a - b\mathrm{d}b) \tag{4.4.25}$$

has two topological boundary conditions for any integer N corresponding to condensing the two Lagrangian algebras[20]

$$\mathcal{A}_\pm = \{l(1, \pm 1) \,|\, l = 0, \cdots, N-1\} \ . \tag{4.4.26}$$

The gauge-invariant way of condensing $\mathcal{A}_\pm$ is to impose

$$a \pm b|_{\partial V} = \text{pure } U(1) \text{ gauge} \tag{4.4.27}$$

[18] Later, we will also refer to the gapped boundary of $U(1)_N \times U(1)_{-N}$ as a junction $U(1)_N \times U(1)_{-N} \to \mathbb{1}$. The $\mathbb{1}$ here denotes the trivial theory and should not be confused with the identity defect (4.4.10) in the Maxwell theory.

[19] This can be thought of as the folding trick—folding the 3-manifold supporting one $U(1)_N$ theory along a 2-dimensional junction and relabeling the $U(1)_N$ field with the opposite parity as a $U(1)_{-N}$ field.

[20] When $N = 2M$ for an odd prime M, the given sets are the only Lagrangian algebras.

which are consistent with the bulk on-shell relations which set a, b to be flat $U(1)$ connections with $\mathbb{Z}_N$ holonomies.

To impose these boundary conditions, one has to couple the two $U(1)$ fields by adding a boundary term[21] to the action as follows,[22]

$$\begin{aligned} S &= \frac{iN}{4\pi}\int_V (a\mathrm{d}a - b\mathrm{d}b) + \frac{iN}{4\pi}\int_{\partial V} a\wedge b \\ &= \frac{iN}{4\pi}\int_V (a+b)\wedge \mathrm{d}(a-b)\,. \end{aligned} \tag{4.4.28}$$

Then, using the invariance under gauge transformations and an infinitesimal variation on the boundary,

$$\begin{aligned} \Delta_\lambda S &= \frac{iN}{4\pi}\int_{\partial V} \mathrm{d}(-\lambda_a+\lambda_b)\wedge(a+b)\,, \\ \delta S|_{\partial V} &= \frac{iN}{4\pi}\int_{\partial V}(a-b)\wedge\delta(a+b) \end{aligned} \tag{4.4.29}$$

and following the analysis around Eq. (4.4.19), the topological boundary conditions that this action can accommodate should satisfy

$$\frac{N}{2}(a+b)\Big|_{\partial V} = k\mathrm{d}\varphi\,, \qquad a-b|_{\partial V} = \text{flat } U(1) \text{ connections} \tag{4.4.30}$$

for some $k|\frac{N}{2}$.[23] We immediately see that this action is not compatible with odd integer N.[24] For even N, these boundary conditions always include a condensation of the Lagrangian

---

[21]One can add the boundary term with the minus sign instead, but that will turn out to be equivalent using the resulting boundary conditions.

[22]On the other hand, the non-gauge invariant condition $a\pm b|_{\partial V}=0$ can be imposed on the bulk action without a boundary term, $S=\frac{iN}{4\pi}\int_V (a\mathrm{d}a-b\mathrm{d}b)$. This can be seen by the gauge transformation and the variation under these boundary conditions, $\Delta S=\frac{iN}{4\pi}\int_{\partial V}\mathrm{d}\lambda\wedge(a\pm b)$ and the variation $\delta S|_{\partial V} = \frac{iN}{4\pi}\int_{\partial V}(a\pm b)\wedge\delta a$, which are trivial.

[23]This is because under the gauge transformation $a\to a+\mathrm{d}\lambda$, $a=\frac{2k}{N}\mathrm{d}\phi\to\frac{2k}{N}\mathrm{d}(\phi+\frac{N}{2k}\lambda)$ and for $\phi+\frac{N}{2k}\lambda$ to be a 2π-periodic boson, $k|\frac{N}{2}$.

[24]We leave finding an action compatible with the gauge invariant topological boundary conditions for odd N to a future work.

algebras $\mathcal{A}_\pm$ for $k = \frac{N}{2}, 1$, given by

$$\text{Hom}(U(1)_N \times U(1)_{-N}, \mathbb{1}): \quad a \pm b\,|_{\partial V} = \text{pure } U(1) \text{ gauge}, \quad S_{bdry} = \frac{iN}{4\pi}\int_{\partial V} a \wedge b\,. \tag{4.4.31}$$

Using the equations of motion $Na, Nb =$ pure $U(1)$ gauge, this is equivalent to[25]

$$\begin{gathered}\text{Hom}(U(1)_N \times U(1)_{-N}, \mathbb{1}): \quad a \pm b, \quad \frac{N}{2}(a \mp b)\bigg|_{\partial V} = \text{pure } U(1) \text{ gauge}, \\ S_{bdry} = \frac{iN}{4\pi}\int_{\partial V} a \wedge b\,. \end{gathered} \tag{4.4.32}$$

Alternatively, one can introduce some scalar fields at the junction that cancel the gauge transformations of the $U(1)$ fields a and b and obtain the same boundary conditions by integrating these scalars out, as explained in Section 6.2.2 of [63]. However, instead of keeping track of these scalars, we will impose Eq. (4.4.32) at the $\text{Hom}(U(1)_N \times U(1)_{-N}, \mathbb{1})$ junctions for simplicity.

Example: $\overline{D}_3 \times (D_3 \times D_3) = D_3\, U(1)_N \times U(1)_{-N} \to D_3$ Consider two consecutive fusions, $\overline{D}_3 \times (D_3 \times D_3)$ as shown in Figure 4.12.

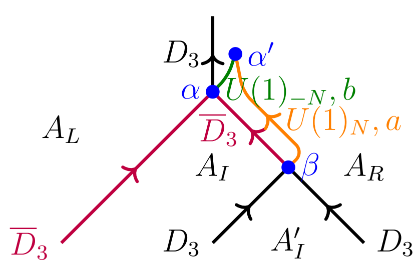

Figure 4.12: The β: $\text{Hom}(D_3 \times D_3, \overline{D}_3 U(1)_N)$, α: $\text{Hom}(\overline{D}_3 \times \overline{D}_3, D_3 U(1)_{-N})$ and α': $\text{Hom}(U(1)_N \times U(1)_{-N}, \mathbb{1})$ junctions.

First, we construct the local fusion junction $D_3 \times D_3$ by fusing the two parallel defects along the upper part above the 2d local fusion junction β. This fused upper part is described

[25] More specifically, $\frac{N}{2}(a \pm b)\big|_{\partial V} = \frac{N}{2}(a \mp b) \pm Nb\,\big|_{\partial V} =$ pure $U(1)$ gauge.

by the action

$$
\begin{aligned}
\mathrm{Hom}(D_3\times D_3,\overline{D}_3U(1)_N): \quad S &= \frac{iN}{2\pi}\int_\beta^\infty \left(A_I\mathrm{d}A_I' + \frac{1}{2}A_I\mathrm{d}A_I + A_I'\mathrm{d}A_R + \frac{1}{2}A_I'\mathrm{d}A_I'\right) \\
&= -\frac{iN}{2\pi}\int_\beta^\infty \left(A_I\mathrm{d}A_R + \frac{1}{2}A_R\mathrm{d}A_R\right) \quad (\leftarrow \overline{D}_3) \\
&\quad + \frac{iN}{4\pi}\int_\beta^\infty (A_I + A_I' + A_R)\mathrm{d}(A_I + A_I' + A_R) \quad (\leftarrow U(1)_N) \\
&\quad + \frac{iN}{4\pi}\int_{\Sigma_\beta} [A_I\wedge A_R + (A_I - A_R)\wedge A_I'] \quad (\leftarrow S_{bdry})
\end{aligned} \tag{4.4.33}
$$

where we denote by the integral from β to ∞ the 3d manifold above the 2d junction β, and by Σ_β the 2d manifold corresponding to the junction β. The fusion outcome has the expected $\overline{D}_3\times U(1)_N$ along with a boundary term at Σ_β. Since A_I' is supported only on the defect above β, the $U(1)_N$ is decoupled from the bulk (this can be seen by shifting $A_I'\to A_I' - A_I - A_R$).

Next, we take another copy of $\overline{D}_3$ and fuse it with the $\overline{D}_3$ we obtained in the previous fusion in the segment above the α junction. The fusion outcome above α is described by the action

$$
\begin{aligned}
\mathrm{Hom}(\overline{D}_3\times\overline{D}_3,U(1)_{-N}D_3): \quad S &= -\frac{iN}{2\pi}\int_\alpha^\infty \left(A_L\mathrm{d}A_I + \frac{1}{2}A_I\mathrm{d}A_I + A_I\mathrm{d}A_R + \frac{1}{2}A_R\mathrm{d}A_R\right) \\
&= \frac{iN}{2\pi}\int_\alpha^\infty \left(A_L\mathrm{d}A_R + \frac{1}{2}A_L\mathrm{d}A_L\right) \quad (\leftarrow D_3) \\
&\quad - \frac{iN}{4\pi}\int_\alpha^\infty (A_L + A_I + A_R)\mathrm{d}(A_L + A_I + A_R) \quad (\leftarrow U(1)_{-N}) \\
&\quad - \frac{iN}{4\pi}\int_{\Sigma_\alpha} [A_L\wedge A_R + (A_L - A_R)\wedge A_I]\ . \quad (\leftarrow S_{bdry})
\end{aligned} \tag{4.4.34}
$$

Since they are decoupled from the bulk, the $U(1)_N\times U(1)_{-N}$ factors above α commute with all other defects, and so it is Witt equivalent to the identity defect on a 3-manifold. Hence, there is a morphism junction between them where the two $U(1)$ theories end at α' in Figure 4.12 with a topological boundary condition. As explained above, this requires coupling the two theories at the morphism junction by adding a boundary term and choosing a boundary condition out of two (or more) options:

$$\mathrm{Hom}\,[U(1)_N \times U(1)_{-N}, \mathbb{1}]: \quad S_{bdry}(\alpha') = \frac{iN}{4\pi}\int_{\Sigma_{\alpha'}} a \wedge b,$$
$$\text{B.c.} \quad \begin{cases} (1) \quad \frac{N}{2}(a+b), \quad a-b\big|_{\Sigma_{\alpha'}} = \text{pure } U(1) \text{ gauge} \\ (2) \quad a+b, \quad \frac{N}{2}(a-b)\big|_{\Sigma_{\alpha'}} = \text{pure } U(1) \text{ gauge} \end{cases} \tag{4.4.35}$$

where a and b denote the $U(1)_N$ and $U(1)_{-N}$ gauge fields which, in our case, are

$$a = A_I + A'_I + A_R\,, \quad b = A_L + A_I + A_R\,. \tag{4.4.36}$$

The coefficients $\frac{N}{2}$ in the boundary conditions can be replaced with N if we further specify $Na, Nb =$ pure $U(1)$ gauge.

4.4.3 Associator 1-morphisms

4.4.3.1 The method

In four dimensions, the associator 1-morphism between three codimension-1 defects (a, b, c) is described by a 2-dimensional TQFT living at the interface between the two different fusions $(a \times b) \times c$ and $a \times (b \times c)$. The first three steps in the method used in Section 4.3.3.1 to compute these associators are still valid in higher-dimensional cases. In particular, the global fusion outcome (Step 3) may contain some decoupled 3d TQFT, either a $\mathbb{Z}_N$ gauge theory or a trivial TQFT. However, since the junctions (points in Figure 4.7) are now 2-manifolds, the last two steps need a slight modification.

Step 4 **Interval reduction**: Using the boundary conditions, obtain the 2d theory from the decoupled TQFT in Step 3 after reducing the 3d interval $[\gamma, \beta]$ to the 2d manifold $\Sigma_{\beta\gamma}$.

Step 5 **Associator**: Evaluate all the boundary actions at the combined junction using the boundary conditions in Step 2 and combine with the 2d theory after the reduction to obtain the associator 1-morphism as

$$F^d_{a,b,c} = (\text{2d theory after reduction}) \otimes (\text{2d theory at the combined junctions})\,. \tag{4.4.37}$$

In Step 4, to get the corresponding 2d theory after reducing the interval, we use a prescription based on the spectrum of the local and line operators on the boundary, as explained in Ref. [78]. The fate of a topological Wilson line $e^{i\oint n_i A_i}$ in 3d after the interval reduction is determined by the boundary conditions of $n_i A_i$ as listed in Table 4.1.

Boundary conditions of $n_i A_i$	Operator from $e^{i\oint n_i A_i}$ after reduction
DBC at both ends	Untwisted local operator
NBC at both ends	Line operator
DBC at one and NBC at the other end	Twisted local operator

Table 4.1: Spectrum of the 2d theory based on the boundary conditions. We say $n_i A_i$ has Dirichlet boundary condition (DBC) if $n_i A_i =$ pure $U(1)$ gauge on the boundary, and $n_i A_i$ has Neumann boundary condition otherwise. Notice that two line operators after reduction arising from $e^{i\oint n_i A_i}$ and $e^{i\oint n'_i A_i}$ are identified if $(n_i - n'_i)A_i$ has DBC on at least one boundary.

For the reduction of an Abelian 3d TQFT, if the 2d theory has untwisted local operators charged under line operators, it is a 2d G-gauge theory (G-SSB phases) where G is the group formed by untwisted local operators. In addition, the theory also contains additional 0-form symmetries (besides G) which act trivially on local operators but may act non-trivially on twisted local operators via the Lasso action. Thus, strictly speaking, the reduced theory is a 2d G-gauge theory enriched by the additional trivially acting symmetry. In the special case where there are no untwisted local operators and G is trivial, this is nothing but an SPT phase of those additional symmetries. In the following, we will restrict ourselves to describe only the untwisted local operators and the line operators, and only keep track of the G-gauge theory part. We will then refer the reduced theory as a trivial theory when there are no untwisted local operators.

4.4.3.2 Interval reduction of $(\mathcal{Z}_N)_N$ (even N)

In some cases, the global fusion (Step 3) of three triality defects contains a $\mathbb{Z}_N$ gauge theory with twist N (denoted as $(\mathcal{Z}_N)_N$),

$$\begin{aligned} S &= \frac{i}{2\pi}\int_V Na'db + \frac{N}{2}a'da' \\ &= \frac{iN}{4\pi}\int_V (a'+b)d(a'+b) - bdb + \frac{iN}{4\pi}\int_{\partial V} b\wedge a' \end{aligned} \tag{4.4.38}$$

which is equivalent to the $U(1)_N \times U(1)_{-N}$ theory together with the required boundary term, upon redefining $a = a' + b$. Thus, the boundary conditions of $U(1)_N \times U(1)_{-N}$ will apply in this case.

Let us briefly describe the interval reduction of this theory when placed on $V = [\gamma, \beta] \times M_2$ for the two boundary conditions $\mathcal{A}_\pm$ discussed in Section 4.4.2.3, with the result summarized in Table 4.2. Apparently, choosing the same boundary conditions on both ends leads to 2d $\mathbb{Z}_N$ gauge theory after reduction. On the other hand, choosing $\mathcal{A}_+$ on one end and $\mathcal{A}_-$ on the other leads to 2d $\mathbb{Z}_2$ gauge theory after reduction. The untwisted local operators have the $\mathbb{Z}_2$ fusion rule and the generator comes from the line $e^{i\oint \frac{N}{2}(a+b)}$. The line operators also have the $\mathbb{Z}_2$ fusion rule and are generated by the reduction of $e^{i\oint a}$, and act non-trivially on the untwisted local operators.

B.C. at γ	B.C. at β	local operators	line operators	2d theory
$\mathcal{A}_+$	$\mathcal{A}_+$	$e^{ik\oint(a+b)}$ $(k\in\mathbb{Z}_N)$	$e^{ik\oint a}$ $(k\in\mathbb{Z}_N)$	$\mathbb{Z}_N$ gauge theory
$\mathcal{A}_-$	$\mathcal{A}_-$	$e^{ik\oint(a-b)}$ $(k\in\mathbb{Z}_N)$	$e^{ik\oint a}$ $(k\in\mathbb{Z}_N)$	
$\mathcal{A}_+$	$\mathcal{A}_-$	$e^{i\frac{Nk}{2}\oint(a+b)}$ $(k\in\mathbb{Z}_2)$	$e^{ik\oint a}$ $(k\in\mathbb{Z}_2)$	$\mathbb{Z}_2$ gauge theory
$\mathcal{A}_-$	$\mathcal{A}_+$			

Table 4.2: The 2d theories obtained after the interval reduction along $[\gamma,\beta]$ for the theory (4.4.38) with different combinations of the boundary conditions $\mathcal{A}_\pm$ at the left boundary α and the right boundary β.

4.4.3.3 Example: Triality defect associator $\left[\boldsymbol{F}^{\boldsymbol{D_3}}_{\boldsymbol{D_3},\boldsymbol{D_3},\overline{\boldsymbol{D}}_3}\right]_{\mathbb{1},\boldsymbol{U(1)_N}\overline{\boldsymbol{D}}_3}$

To illustrate the method discussed above, let us compute a particular triality defect associator, $[F^{D_3}_{D_3,D_3,\overline{D}_3}]_{\mathbb{1},U(1)_N\overline{D}_3}$, by collapsing the diamond region in Figure 4.13 to a 2d interface between the two fusions

$$\begin{aligned}
\text{Upper part}: &\quad D_3\times(D_3\times\overline{D}_3)=D_3\times C_{\frac{N}{2}}\to D_3\times\mathbb{1}=D_3\,,\\
\text{Lower part}: &\quad (D_3\times D_3)\times\overline{D}_3=U(1)_N\ \overline{D}_3\times\overline{D}_3=U(1)_N\times U(1)_{-N}\ D_3\to D_3\,,
\end{aligned}\tag{4.4.39}$$

where we have added the morphism junctions $\beta':C_{\frac{N}{2}}\to\mathbb{1}$ and $\delta':U(1)_N\times U(1)_{-N}\to\mathbb{1}$. For simplicity, we restrict here to $N=2\times$ odd prime.[26]

[26]This is in order to have only two topological boundary conditions for the $U(1)_N\times U(1)_{-N}$ theory compatible with the Lagrangian.

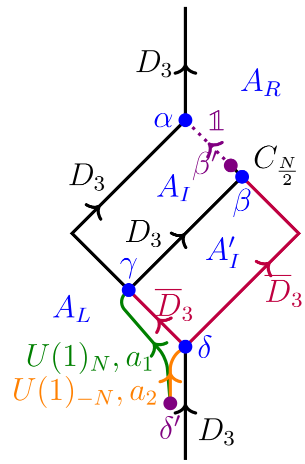

Figure 4.13: The diagram for $\left[F^{D_3}_{D_3,D_3,\overline{D}_3}\right]_{\mathbb{1},U(1)_N\overline{D}_3}$. a_1,a_2 are the gauge fields of the $U(1)_N \times U(1)_{-N}$ theory.

As we did in the 2d case, we first collect the boundary conditions and boundary terms at each junction $\alpha, \beta', \beta, \gamma, \delta, \delta'$ from our junction analyses. Specifically, Eq. (4.4.35) for $\delta' : U(1)_N \times U(1)_{-N} \to \mathbb{1}$, Eq. (4.4.34) for $\delta : D_3\ U(1)_{-N} \to \overline{D}_3 \times \overline{D}_3$, Eq. (4.4.33) for $\gamma : U(1)_N\ \overline{D}_3 \to D_3 \times D_3$, Eq. (D.3.12) for $\beta : D_3 \times \overline{D}_3 \to C_{\frac{N}{2}}$, Eq. (4.4.24) for $\beta' : C_{\frac{N}{2}} \to \mathbb{1}$ and Eq. (4.4.17) for $\alpha : D_3 \times \mathbb{1} \to D_3$. Then, we shrink the interval between the upper junctions α, β' and β and combine the boundary conditions and boundary terms there. We repeat analogously for the lower junctions γ, δ and δ'. Putting them all together,

$$
\begin{aligned}
\alpha, \beta, \beta':\quad & N(A_L + A_I' + A_R), \quad A_I - A_R = \text{pure } U(1) \text{ gauge}\,, \\
& S(\alpha) = \frac{iN}{2\pi}\int_{\Sigma_\alpha} A_L \wedge (A_I - A_R), \quad S(\beta') = \frac{iN}{2\pi}\int_{\Sigma_\alpha}\left(A_R \wedge A_I' - \frac{1}{2}A_I \wedge A_R\right), \\
\gamma, \delta, \delta':\quad & a_1 = A_L + A_I' + A_I, \quad a_2 = A_L + A_I' + A_R, \\
& \begin{cases} (1) \qquad \underbrace{A_I - A_R}_{=a_1 - a_2}, \quad N(A_L + A_I' + A_R) = \text{pure } U(1) \text{ gauge} \\ \text{or } (2) \quad \underbrace{2(A_L + A_I' + A_R) + A_I - A_R}_{=a_1 + a_2}, \quad \frac{N}{2}(A_I - A_R) = \text{pure } U(1) \text{ gauge} \end{cases} \\
& S(\gamma) = -\frac{iN}{4\pi}\int_{\Sigma_\gamma}\left[A_L \wedge A_I' + (A_L - A_I') \wedge A_I\right], \\
& S(\delta) = \frac{iN}{4\pi}\int_{\Sigma_\delta}\left(A_L \wedge A_R + A_L \wedge A_I' + A_I' \wedge A_R\right), \\
& S(\delta') = \frac{iN}{4\pi}\int_{\Sigma_{\delta'}}\left(A_L \wedge A_R + A_I' \wedge A_R + A_I \wedge A_L + A_I \wedge A_I' + A_I \wedge A_R\right)
\end{aligned}
\tag{4.4.40}
$$

where $S(\alpha)$ denotes the boundary term at the junction α (and similarly for the other junctions), a_1 and a_2 are the gauge fields of the $U(1)_N \times U(1)_{-N}$ theory and (1) and (2) are the two possible boundary conditions at the junction δ' : $U(1)_N \times U(1)_{-N} \to \mathbb{1}$.

Next, we fuse the three defects $D_3 \times D_3 \times \overline{D}_3$ in the middle (along the interval $[\gamma, \beta]$) by summing their actions,

$$
\begin{aligned}
S &= \frac{iN}{2\pi}\int_\gamma^\beta \left(A_L \mathrm{d}A_I + \frac{1}{2}A_L \mathrm{d}A_L + A_I \mathrm{d}A_I' + \frac{1}{2}A_I \mathrm{d}A_I - A_I' \mathrm{d}A_R - \frac{1}{2}A_R \mathrm{d}A_R\right) \\
&= \frac{iN}{2\pi}\int_\gamma^\beta \left(A_L \mathrm{d}A_R + \frac{1}{2}A_L \mathrm{d}A_L\right) \qquad (\leftarrow D_3) \\
&\quad + \frac{iN}{2\pi}\int_\gamma^\beta \left[(A_L + A_I' + A_R)\mathrm{d}(A_I - A_R) + \frac{1}{2}(A_I - A_R)\mathrm{d}(A_I - A_R)\right] \qquad (\leftarrow (\mathcal{Z}_N)_N) \\
&\quad + \frac{iN}{2\pi}\int_{\Sigma_\beta - \Sigma_\gamma}\left(A_I' \wedge A_I + \frac{1}{2}A_R \wedge A_I\right) \qquad (\leftarrow S_{bdry;global})
\end{aligned}
\tag{4.4.41}
$$

where the second line is the action for D_3 as expected from the fusion algebra, the third line is a decoupled $\mathbb{Z}_N$ gauge theory with twist N (denoted by $(\mathcal{Z}_N)_N$) and the last line is the boundary term.

At this stage, we are left with the configuration

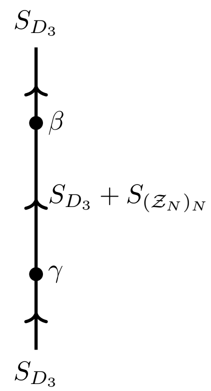

$$. \tag{4.4.42}$$

The total boundary term at the (combined) upper junction β is

$$\begin{aligned} S_{bdy,\beta} &= S(\alpha) + S(\beta') + S_{global}|_{\alpha\beta} \\ &= \frac{iN}{2\pi} \int_{\Sigma_\alpha} (A_L + A'_I + A_R) \wedge (A_I - A_R) \in 2\pi i \mathbb{Z} \end{aligned} \tag{4.4.43}$$

which is trivial by the boundary conditions (4.4.40). Similarly, the total boundary term at the (combined) lower junction γ is

$$\begin{aligned} S_{bdy,\gamma} &= S(\gamma) + S(\delta) + S_{global}|_{\gamma\delta} + S(\delta') \\ &= \frac{iN}{2\pi} \int_{\Sigma_{\gamma\delta}} (A_L + A'_I + A_I) \wedge (A_I - A_R) \in 2\pi i \mathbb{Z}\,, \end{aligned} \tag{4.4.44}$$

which is also trivial by the boundary conditions.

Therefore, we are left with a decoupled $(\mathcal{Z}_N)_N$ theory supported on the interval $[\gamma, \beta]$ in Eq. (4.4.41). By comparing the action given in (4.4.41) with (4.4.38), we identify that the boundary condition at γ corresponds to $\mathcal{A}_-$, while the two boundary conditions (1) and (2) at β correspond to $\mathcal{A}_-$ and $\mathcal{A}_+$, respectively.

More concretely, for the boundary condition (1) the upper and lower junctions have the same boundary conditions for the gauge fields $A_L + A'_I + A_R$ and $A_I - A_R$ in the $(\mathcal{Z}_N)_N$ action in (4.4.41), which are written in Table 4.3. Following the discussion in Section 4.4.3.1, reducing the interval $[\gamma, \beta]$ results in a 2d $\mathbb{Z}_N$ gauge theory.

	$A_L + A_I' + A_R$	$A_I - A_R$
α, β', β	$\mathbb{Z}_N$	pure $U(1)$ gauge
$\gamma, \delta', \delta\,(1)$	$\mathbb{Z}_N$	pure $U(1)$ gauge

Table 4.3: Boundary conditions for the gauge fields in Eq. (4.4.41) for the case (1) of Eq. (4.4.40). Here, by $\mathbb{Z}_N$ we mean that the corresponding gauge field a has the boundary condition $Na =$ pure $U(1)$ gauge and that $e^{i\oint a}$ is a $\mathbb{Z}_N$ line.

Under the boundary condition (2), on the other hand, the gauge fields have different boundary conditions at the upper and lower junctions, as written in Table 4.4. In this case, we only find $\mathbb{Z}_2$ untwisted local operators arising from the Wilson lines $e^{i\frac{Nk}{2}\oint(a_1+a_2)}$ ($k \in \mathbb{Z}_2$). Hence, reducing the interval $[\gamma, \beta]$ results in a $\mathbb{Z}_2$ gauge theory.

	$2(A_L + A_I' + A_R) + (A_I - A_R)$	$A_I - A_R$
α, β', β	$\mathbb{Z}_{\frac{N}{2}}$	pure $U(1)$ gauge
$\gamma, \delta', \delta\,(2)$	pure $U(1)$ gauge	$\mathbb{Z}_{\frac{N}{2}}$

Table 4.4: Boundary conditions for the gauge fields in (4.4.41) for the case (2) of Eq. (4.4.40).

In summary,

$$(\mathcal{Z}_N)_N \quad \xrightarrow{\text{reducing interval}} \quad \begin{cases} (1): & \mathbb{Z}_N \text{ gauge theory} \\ (2): & \mathbb{Z}_2 \text{ gauge theory} \end{cases}. \tag{4.4.45}$$

Overall, we obtained that the boundary terms do not contribute to this associator 1-morphism (see Eqs. (4.4.43) and (4.4.44)), and hence it is given only by the 2d theory obtained by reducing the $(\mathcal{Z}_N)_N$ theory on the interval $[\gamma, \beta]$, which we found in (4.4.45). That is,

$$\left[F^{D_3}_{D_3, D_3, \overline{D}_3}\right]_{\mathbb{1}, U(1)_N \overline{D}_3} = \mathbb{Z}_N \text{ gauge theory} \quad \text{or} \quad \mathbb{Z}_2 \text{ gauge theory} \tag{4.4.46}$$

where the two possibilities correspond to the two options for the boundary conditions at the junction $U(1)_N \times U(1)_{-N} \to \mathbb{1}$.[27]

Other associators We compute all the other associators involving the triality defect D_3 and its orientation reversal $\overline{D}_3$ in Appendix D.3.2. The results are listed in Table 4.5.

	F-symbol associator
$D_3 \times D_3 \times D_3$	$\mathbb{Z}_N$ condensation defect
$D_3 \times \overline{D}_3 \times D_3$	Trivial theory
$D_3 \times D_3 \times \overline{D}_3$ $\overline{D}_3 \times D_3 \times D_3$	$\mathbb{Z}_N$ gauge theory or $\mathbb{Z}_2$ gauge theory

Table 4.5: Associators corresponding to various combinations of the D_3 and $\overline{D}_3$ defects, for $N = 2 \times$ (odd prime) and with trivial Witt elements (i.e. the identity defect) selected at the fusion junctions. The two different possibilities for the associator of the last two combinations correspond to the two types of topological boundary conditions of the $U(1)_N \times U(1)_{-N}$ theory that appears in the fusion process. The other possible four associators are related to those in the table by orientation reversal.

For general even values of N, we expect to have more topological boundary conditions at the morphism junction $U(1)_N \times U(1)_{-N} \to \mathbb{1}$, corresponding to condensing nonanomalous $\mathbb{Z}_{2k}$ lines for $k|\frac{N}{2}$, which results in $\mathbb{Z}_{2k}$ gauge theories for the F-symbol in the last row of Table 4.5.

[27] There are only two possible topological boundary conditions for the $U(1)_N \times U(1)_{-N}$ theory since we have restricted here to $N = 2 \times$ (odd prime).

In the next section, we introduce a group-theoretical construction for the triality defects for certain odd values of N and compute the above associators, which agree with the ones in Table 4.5 except for the $\mathbb{Z}_2$ gauge theory in the last column which becomes the trivial theory.[28]

Lastly, in Appendix D.5, we also provide an example for the computation of a duality defect associator, $[F^{D_2}_{D_2,\overline{D}_2,D_2}]_{\mathbb{1},\mathbb{1}}$, using the Lagrangian method and the group-theoretical approach and list the results for the other duality associators, which agree between the two methods.

4.5 Triality defects in Maxwell theory using group theoretical construction

In this section, we describe a complementary computation of the associativity map for triality defects that admit certain group-theoretical constructions for odd N. Recall that the fusion rules are

$$D_3 \times D_3 = SU(N)_{-1}\overline{D}_3 \ , \ \ \overline{D}_3 \times \overline{D}_3 = SU(N)_1 D_3 \ , \ \ \overline{D}_3 \times D_3 = D_3 \times \overline{D}_3 = C_0 \ . \qquad (4.5.1)$$

Here, CS theory $SU(N)_{\pm 1}$ is a bosonic TQFT containing $\mathbb{Z}_N$ Abelian anyons. Denoting the generating line as a, the topological spin $h(a^k)$ of a^k and the braiding phase $B(a^k, a^{k'})$ are [29]

$$h(a^k) = \pm \frac{k(N-k)}{2N} \mod 1 \ , \quad B(a^k, a^{k'}) = e^{\mp \frac{2\pi i}{N} k k'} \ , \quad \text{for} \quad SU(N)_{\pm 1} \ . \qquad (4.5.2)$$

[28] The $\mathbb{Z}_2$ gauge theory in these associators results from the dimensional reduction of the $\mathbb{Z}_N$ gauge theory with twist N, $(\mathcal{Z}_N)_N$, on the interval. Due to the non-trivial twist N, this theory has an anomaly for even N, and hence the 2d theory obtained after the dimensional reduction cannot be trivial. On the other hand, it is not anomalous for odd N and indeed $(\mathcal{Z}_N)_N \simeq (\mathcal{Z}_N)_0$ for such N, which allows for a trivial TQFT after the dimensional reduction.

[29] This can be directly computed using [79], or use the fact that $SU(N)_1$ is the minimal TQFT $\mathcal{A}^{N,N-1}$ [80, 81] and $\frac{k(N-k)}{2N} = \frac{N-1}{2N} k^2 \mod 1$.

In the case of the spin theory, there is an additional transparent fermion ψ. $SU(N)_{-1} \boxtimes \mathbb{Z}_2^\psi$ now contains $\mathbb{Z}_{2N} = \mathbb{Z}_N^a \times \mathbb{Z}_2^\psi$ Abelian anyons (as N is odd), and is generated by the anyon $b = a\psi$. The topological spin and the braiding phases are

$$h(b^k) = \frac{k^2}{2N} \ , \quad B(b^k, b^{k'}) = e^{\frac{2\pi i}{N} kk'} \ , \tag{4.5.3}$$

which matches the spectrum of the $U(1)_N$ CS theory. This relation is known as the level-rank duality [82]. For the following, we will assume that we work with bosonic theory for simplicity; although the result holds for the spin theory as well since the additional fermion does not have any essential effect due to its transparent nature.

4.5.1 Group-theoretical construction of triality defects

As first pointed out in [62], a non-invertible duality defect in 4d theory can be constructed from gauging a certain 1-form symmetry in a 2-group symmetry with a certain mixed anomaly. In [64], a group-theoretical construction for certain duality and triality defects is provided. Let us first explain in detail the triality defects. Consider a 4d QFT $\mathcal{X}$ with $\mathbb{Z}_N$ (where N is odd) 1-form symmetry, and its partition function is invariant under the following order-3 twisted gauging

$$Z_{\mathcal{X}}[A^{(2)}] = \sum_{a^{(2)} \in H^2(X_4, \mathbb{Z}_N)} Z_{\mathcal{X}}[a^{(2)}] \exp\left(\frac{2\pi i}{N}\frac{N+1}{2}\int a^{(2)} \cup a^{(2)} + \frac{2\pi i}{N}\int a^{(2)} \cup A^{(2)}\right) \ . \tag{4.5.4}$$

One can define a new theory $\widetilde{\mathcal{X}}$ from $\mathcal{X}$ by twisted gauging the 1-form symmetry

$$Z_{\widetilde{\mathcal{X}}}[A^{(2)}] = \sum_{a^{(2)} \in H^2(X_4, \mathbb{Z}_N)} Z_{\mathcal{X}}[a^{(2)}] \exp\left(\frac{2\pi i}{N}p'\int a^{(2)} \cup a^{(2)} + \frac{2\pi i}{N}\int a^{(2)} \cup A^{(2)}\right) \ . \tag{4.5.5}$$

When the odd N is such that the following equation of p' admits solutions

$$(2p')^2 - 2p' + 1 = 0 \mod N \ , \tag{4.5.6}$$

the partition function of $\widetilde{\mathcal{X}}$ satisfies

$$Z_{\widetilde{\mathcal{X}}}[A^{(2)}] = Z_{\widetilde{\mathcal{X}}}[-(2p')^{-1}A^{(2)}] \exp\left(\frac{2\pi i}{N}\left(-\frac{N+1}{2}(2p')^{-1}\right)\int A^{(2)} \cup A^{(2)}\right) \ , \tag{4.5.7}$$

where $(2p')^{-1}$ denotes the mod-N inverse of $(2p')$. By (4.5.6), we can choose $(2p')^{-1} = 1-2p'$ and we will also choose $(2p')$ to be odd such that $(2p')^{-1} = 1 - 2p'$ is even.

Using $(-2p')^3 = 1$ from (4.5.6), one can see that the triality twisted gauging in $\mathcal{X}$ is mapped to an invertible $\mathbb{Z}_3^{(0)}$ automorphism of the dual 1-form symmetry $\mathbb{Z}_N^{(1)}$ in $\widetilde{\mathcal{X}}$. Together, they form a non-Abelian 2-group symmetry $\mathbb{Z}_N^{(1)} \rtimes \mathbb{Z}_3^{(0)}$. The additional phase indicates the mixed anomaly between the $\mathbb{Z}_3^{(0)}$ and $\mathbb{Z}_N^{(1)}$ symmetries. Due to this anomaly, the $\mathbb{Z}_3^{(0)}$-symmetry operator $\mathbb{D}_3$ is not gauge invariant after gauging the dual 1-form symmetry to regain the theory $\mathcal{X}$. To acquire a gauge invariant codim-1 operator, one can stack a TQFT coupled to the gauge field $a^{(2)}$ of the dual symmetry to cancel the anomaly. There is a canonical choice known as the minimal TQFT.

Let us recall some basic properties of the minimal TQFT $\mathcal{A}^{N,p}$ in the special case where N is odd and p is even and coprime with N [80]. The non-spin version of this TQFT contains $\mathbb{Z}_N$ Abelian anyons a^s (where $a^N = 1$) with the topological spin

$$h(a^s) = \frac{ps^2}{2N} \mod 1 \ . \tag{4.5.8}$$

The braiding between any two generic Abelian anyons a_1 and a_2 is

$$B(a_1, a_2) = e^{2\pi i [h(a_1 a_2) - h(a_1) - h(a_2)]} \ . \tag{4.5.9}$$

The minimal TQFT $\mathcal{A}^{N,p}$ can be used to cancel the anomaly of the 1-form symmetry captured by the 4d SPT [80, 81]

$$-\frac{2\pi i}{N}\frac{N+1}{2}p \int B^{(2)} \cup B^{(2)} \ . \tag{4.5.10}$$

Therefore, $D_3 = \mathbb{D}_3 \mathcal{A}^{N,(2p')^{-1}} \left[a^{(2)}\right]$[30] with an even choice of $(2p')^{-1}$ is gauge invariant in $\mathcal{X}$, but becomes non-invertible because of $\mathcal{A}^{N,(2p')^{-1}}[a^{(2)}]$.

[30] Notice that we also use the letter a to denote Abelian anyons. Whenever we use $a^{(n)}$ to refer to gauge fields, we will always add the superscript (n) to denote its degree so the readers can distinguish between n-form gauge fields $a^{(n)}$ and anyons a's.

The orientation reversal of $\overline{D}_3$ is

$$\overline{D}_3 = \mathcal{A}^{N,-(2p')^{-1}}[a^{(2)}]\overline{\mathbb{D}}_3 \ , \tag{4.5.11}$$

where the anomaly of the minimal TQFT is flipped because of the orientation reversal.

It is instructive to check the fusion rule explicitly to highlight two subtleties compared to the simple case in [62]. First, the non-Abelian 2-group here does not commute with the minimal TQFT coupled to $a^{(2)}$:

$$\mathbb{D}_3\mathcal{A}^{N,p}[a^{(2)}] = \mathcal{A}^{N,p}[-(2p')^{-1}a^{(2)}]\mathbb{D}_3 \ . \tag{4.5.12}$$

Notice that here we interpret the action of $\mathbb{D}_3$ as changing how the bulk field $a^{(2)}$ couples to the anyons in the minimal TQFT $\mathcal{A}^{N,p}$, and $\mathbb{D}_3$ itself does not act on the lines in $\mathcal{A}^{N,p}$. Second, for generic minimal TQFTs, it is not easy to manipulate the Lagrangian to prove various relations, and we will demonstrate how to do so by directly analyzing the anyon spectrum.

For instance, let's consider the fusion of $D_3 \times D_3$. We find

$$\begin{aligned} D_3 \times D_3 &= \mathbb{D}_3\mathcal{A}_{a_1}^{N,(2p')^{-1}}[a^{(2)}]\mathbb{D}_3\mathcal{A}_{a_2}^{N,(2p')^{-1}}[a^{(2)}] \\ &= \overline{\mathbb{D}}_3\mathcal{A}_{a_1}^{N,(2p')^{-1}}[-(2p')a^{(2)}]\mathcal{A}_{a_2}^{N,(2p')^{-1}}[a^{(2)}] \\ &= [SU(N)_{-1}]_{a_1 a_2^{2p'}} \ \overline{\mathbb{D}}_3\mathcal{A}^{N,-N+1}_{a_1^{-2p'}a_2}[a^{(2)}] \equiv SU(N)_{-1}\overline{D}_3 \ . \end{aligned} \tag{4.5.13}$$

Here, the subscript under each TQFT denotes its generating line. In the second equal sign, we used

$$\mathbb{D}_3\mathcal{A}^{N,(2p')^{-1}}[a^{(2)}] = \mathcal{A}^{N,(2p')^{-1}}[-(2p')^{-1}a^{(2)}]\mathbb{D}_3 \ , \tag{4.5.14}$$

followed from the action of $\mathbb{Z}_3^{(0)}$ on $\mathbb{Z}_N^{(1)}$. To show the third step, one can consider the anyon spectrum of $\mathcal{A}_{a_1}^{N,(2p')^{-1}}[-(2p')a^{(2)}]\mathcal{A}_{a_2}^{N,(2p')^{-1}}[a^{(2)}]$. We can redefine the generating lines as

$$b_1 = a_1^{-(2p')}a_2 \ , \quad b_2 = a_1 a_2^{(2p')} \ . \tag{4.5.15}$$

Furthermore, because b_1 and b_2 braid trivially with each other, the theory is factorized into two theories generated by b_i, respectively. First, the bulk 2-form gauge field $a^{(2)}$ couples to the $\mathbb{Z}_N$ line b_1 which has topological spin

$$\begin{aligned} h(a_1^{-2p'}a_2) &= \frac{(2p')^{-1}}{2N}\left((-2p')^2+1\right) \mod 1 \\ &= \frac{(2p')^{-1}}{2N}(2p') \mod 1 \\ &= \frac{-N+1}{2N} \mod 1 \end{aligned} \tag{4.5.16}$$

where in the last step we used $(2p')^{-1}(2p') = -N+1 \mod 2N$ (as $(2p')^{-1}(2p')$ is even by our choice). Thus, we see that the theory generated by b_1 is the minimal TQFT $\mathcal{A}_{b_1}^{N,-N+1}[a^{(2)}]$. To see that $\overline{\mathbb{D}}_3\mathcal{A}_{b_1}^{N,-N+1}[a^{(2)}]$ is indeed $\overline{D}_3$ given in (4.5.11), one uses first the commutation relation (4.5.14) and then the certain identity of minimal TQFT

$$\overline{\mathbb{D}}_3\mathcal{A}_{b_1}^{N,-N+1}[a^{(2)}] = \mathcal{A}_{b_1}^{N,-N+1}[-(2p')a^{(2)}]\overline{\mathbb{D}}_3 = \mathcal{A}_{c}^{N,-(2p')^{-1}}[a^{(2)}]\overline{\mathbb{D}}_3 \ , \tag{4.5.17}$$

where $c = b_1^{-2p'}$. The last step can be shown as follows: $a^{(2)}$ couples to the line $b_1^{-2p'}$ with topological spin

$$h(c) = h(b_1^{-2p'}) = \frac{-(2p')^{-1}}{2N} \mod 1 \ , \tag{4.5.18}$$

thus if we consider a change of variable $c = b_1^{-2p'} = a_1^{-(2p')^{-1}}a_2^{-2p'}$, we see that the minimal TQFT can be rewritten as $\mathcal{A}_c^{N,-(2p')^{-1}}[a^{(2)}]$.

On the other hand, the anyons b_2^k form $\mathbb{Z}_N$ and their topological spins are

$$h(b_2^k) = \frac{-N+1}{2N}k^2 \mod 1 = -\frac{k(N-k)}{2N} \mod 1 \ , \tag{4.5.19}$$

thus they give rise to the theory $SU(N)_{-1}$ (4.5.2). Combining the two discussions, we recover the fusion rule (4.5.13).

As another example, let's consider $D_3 \times \overline{D}_3$:

$$D_3 \times \overline{D}_3 = \mathbb{D}_3\mathcal{A}_{a_1}^{N,(2p')^{-1}}[a^{(2)}]\mathcal{A}_{a_2}^{N,-(2p')^{-1}}[a^{(2)}]\overline{\mathbb{D}}_3 = \mathbb{D}_3\mathcal{C}_0\overline{\mathbb{D}}_3 = \mathcal{C}_0 \ . \tag{4.5.20}$$

The key step here is to show that $\mathcal{A}_{a_1}^{N,(2p')^{-1}}[a^{(2)}]\mathcal{A}_{a_2}^{N,-(2p')^{-1}}[a^{(2)}]$ is the condensation defect $\mathcal{C}_0$. We can reparameterize the $\mathbb{Z}_N \times \mathbb{Z}_N$ anyons with the following two generators

$$b_1 = (a_1a_2^{-1})^{-\frac{N+1}{2}p'} \ , \quad b_2 = a_1a_2 \ . \tag{4.5.21}$$

The new generating lines b_i are $\mathbb{Z}_N$ bosons and have mutual braiding

$$B(b_1, b_2) = e^{-\frac{2\pi i}{N}} \ . \tag{4.5.22}$$

This implies that b_i's generate a $\mathbb{Z}_N$ gauge theory with no twist and b_1 and b_2 correspond to the electric line and the magnetic line respectively. Thus, we can write down an action for it

$$S = \frac{2\pi i}{N} \int b^{(1)} \cup \delta \hat{b}^{(1)} + \hat{b}^{(1)} \cup a^{(2)} \ , \tag{4.5.23}$$

where the coupling $\hat{b}^{(1)} \cup a^{(2)}$ comes from the fact that $a^{(2)}$ couples to the line b_2. This is nothing but a condensation defect [62], as

$$\begin{aligned} \int [Db^{(1)}][D\hat{b}^{(1)}] e^{\frac{2\pi i}{N}\int b^{(1)}\cup\delta\hat{b}^{(1)}+\hat{b}^{(1)}\cup a^{(2)}} =& \frac{1}{\sqrt{|H^1(X_3,\mathbb{Z}_N)|}} \sum_{\hat{b}^{(1)}\in H^1(X_3,\mathbb{Z}_N)} e^{\frac{2\pi i}{N}\int b^{(1)}\cup a^{(2)}} \\ =& \frac{1}{\sqrt{|H^1(X_3,\mathbb{Z}_N)|}} \sum_{\sigma\in H_2(X_3,\mathbb{Z}_N)} e^{\frac{2\pi i}{N}\oint_\sigma a^{(2)}} \equiv \mathcal{C}_0 \ , \end{aligned} \tag{4.5.24}$$

where we first integrate out $b^{(1)}$ to set $\hat{b}^{(1)}$ flat and then re-express the sum using the Poincaré dual $\sigma \in H_2(X_3, \mathbb{Z}_N)$ of $\hat{b}^{(1)} \in H^1(X_3, \mathbb{Z}_N)$.

It is interesting to notice that the magnetic line $e^{\frac{2\pi i}{N}\oint_\gamma \hat{b}^{(1)}}$ is topological and corresponds to higher quantum symmetry. The electric line $e^{\frac{2\pi i}{N}\oint_\gamma b^{(1)}}$, however, is no longer a genuine line operator as $b^{(1)}$ due to the modified gauge transformation $b^{(1)} \to b^{(1)} - \lambda_a^{(1)}$ under the gauge transformation of $a^{(2)} \to a^{(2)} + \delta\lambda_a^{(1)}$. This leads to two interesting configurations. First, the bulk 1-form symmetry operator $e^{\frac{2\pi i}{N}\int a^{(2)}}$ can terminate topologically on $\mathcal{C}_0$ (as the 1-form symmetry is gauged on $\mathcal{C}_0$). This is realized by dressing $e^{-\frac{2\pi i}{N}\oint_\gamma b^{(1)}}$ on the intersection of $e^{\frac{2\pi i}{N}\int a^{(2)}}$ with $\mathcal{C}_0$ to ensure the gauge invariance. Second, a non-genuine line operator $L(\partial\sigma)$ bounding the 1-form symmetry operator $e^{\frac{2\pi i}{N}\int_\sigma a^{(2)}}$ (so that the combined $L(\partial\sigma)e^{\frac{2\pi i}{N}\int_\sigma a^{(2)}}$ is gauge invariant) in the bulk will become a genuine line when pushing to $\mathcal{C}_0$ because the 1-form symmetry is gauged. This is described by the gauge invariant line $L(\partial\sigma)e^{-\frac{2\pi i}{N}\oint_{\partial\sigma} b^{(1)}}$. Furthermore, $L(\partial\sigma)e^{-\frac{2\pi i}{N}\oint_{\partial\sigma} b^{(1)}}$ is charged under the higher quantum symmetry generated by the magnetic line. Comparing with the description of the Lagrangian condensation defect in Maxwell theory, we see that the higher quantum symmetry $e^{\frac{2\pi i}{N}\oint_\gamma \hat{b}^{(1)}}$ is matched by $e^{i\oint A_L - A_R}$

there; and the genuine line operator $e^{i\oint a}$ on the condensation defect in the Lagrangian description is an example of the bulk non-genuine line operator which becomes genuine on the condensation defect.

4.5.2 Overview of anyon condensations and fusion of domain walls

Following the general discussion in Section 4.2.2, to compute the associator for the three defects $\mathcal{D}_1, \mathcal{D}_2, \mathcal{D}_3$ (where $\mathcal{D}_i$ are triality defects dressed with corresponding minimal TQFT), we need to evaluate the following diagram

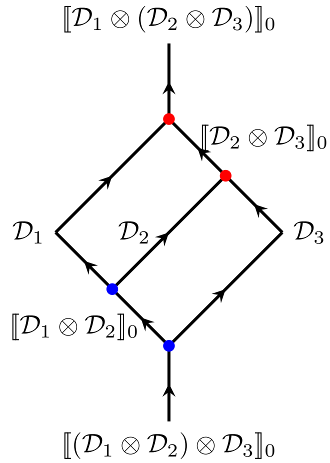

. (4.5.25)

Fusing the defects in the middle, the final result will take the form

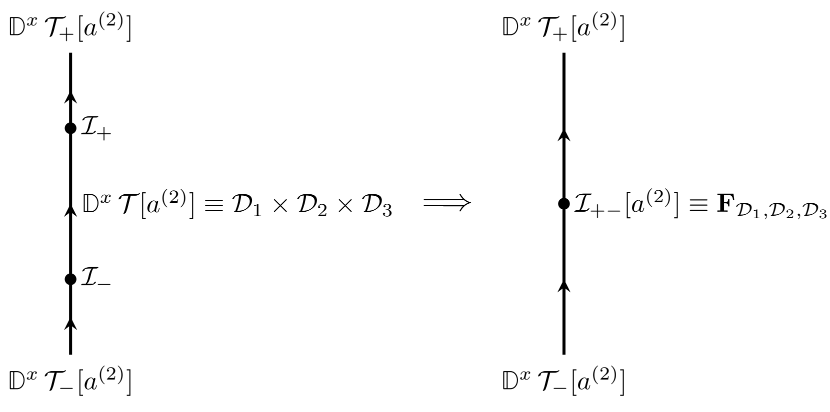

, (4.5.26)

where $x = 0, 1, 2$ depending $\mathcal{D}_i$, $\mathcal{I}_\pm$ are the topological interfaces between $\mathcal{T}$ and $\mathcal{T}_\pm$ respectively. The F-symbol here is then acquired by fusing the two interfaces $\mathcal{I}_+$ and $\mathcal{I}_-$.

The simplification of computing associators in this group-theoretical construction is that everything can be phrased in the language of 3d TQFT, i.e. unitary modular tensor categories (UMTC). Below, we will first include a summary of the results, and will include a detailed description on how to use anyon condensation theory to acquire this in Appendix D.4.

First, the TQFT $\mathcal{T}$ is described by a UMTC and the interfaces $\mathcal{I}_\pm, \mathcal{T}_\pm$ are acquired by anyon condensations. Following [52], we use $\mathbb{A}_\pm$ to denote the group of condensed anyons. Then, we want to describe the topological line operator contents in the following configuration

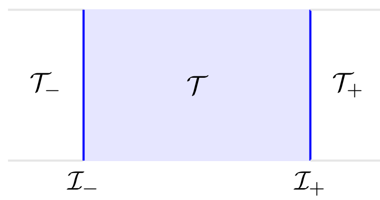

, (4.5.27)

and they are summarized as follows in Table 4.6.

	Line Operators	Fusion rules
$\mathcal{T}_+$	$L_b^+ : b \in \mathcal{T}/\mathbb{A}_+$ and $B(b,a) = 1\ \forall a \in \mathbb{A}_+$	$\mathcal{T}_+ \boxtimes \mathcal{T}_+ \to \mathcal{T}_+ : L_b^+ \times L_{b'}^+ = L_{bb'}^+$
$\mathcal{T}_-$	$L_b^- : b \in \mathcal{T}/\mathbb{A}_-$ and $B(b,a) = 1\ \forall a \in \mathbb{A}_-$	$\mathcal{T}_- \boxtimes \mathcal{T}_- \to \mathcal{T}_- : L_b^- \times L_{b'}^- = L_{bb'}^-$
$\mathcal{I}_+$	$\ell_b^+, \quad b \in \mathcal{T}/\mathbb{A}_+$	$\mathcal{T} \boxtimes \mathcal{I}_+ \to \mathcal{I}_+ : b \otimes \ell_{b'}^+ = \ell_{bb'}^+$
		$\mathcal{I}_+ \boxtimes \mathcal{I}_+ \to \mathcal{I}_+ : \ell_b^+ \otimes \ell_{b'}^+ = \ell_{bb'}^+$
		$\mathcal{I}_+ \boxtimes \mathcal{T}_+ \to \mathcal{I}_+ : \ell_b^+ \otimes L_{b'}^+ = \ell_{bb'}^+$
$\mathcal{I}_-$	$\ell_b^-, \quad b \in \mathcal{T}/\mathbb{A}_-$	$\mathcal{I}_- \boxtimes \mathcal{T} \to \mathcal{I}_- : \ell_b^- \otimes b' = \ell_{bb'}^-$
		$\mathcal{I}_- \boxtimes \mathcal{I}_- \to \mathcal{I}_- : \ell_b^- \otimes \ell_{b'}^- = \ell_{bb'}^-$
		$\mathcal{T}_- \boxtimes \mathcal{I}_- \to \mathcal{I}_- : L_b^- \otimes \ell_{b'}^- = \ell_{bb'}^-$

Table 4.6: The operator contents and fusion rules in (4.5.27). When list the operator contents, by $b \in \mathcal{T}/\mathbb{A}_+$ in $\mathcal{I}_+$ for instance, we mean the line ℓ_b^+ is the same line as $\ell_{b'}^+$ if $b^{-1}b' \in \mathbb{A}_+$. Notice that while we only list the fusion rules, the line operators in $\mathcal{T}_\pm$ actually form a modular tensor category respectively and the braiding structure is inherent from $\mathcal{T}$. The domain walls $\mathcal{I}_\pm$ are fusion categories, but they also carry actions of the theories on both sides, as captured by the additional fusion rules given above.

To acquire the F-symbol, we consider fusing the domain walls $\mathcal{I}_+$ and $\mathcal{I}_-$ which again can be computed using the anyon condensation theory. The outcome is a domain wall $\mathcal{I}_{-+}$ between $\mathcal{T}_-$ and $\mathcal{T}_+$, which we identify as the F-symbol. On the fused domain wall, besides the topological line operators, generically it may also admit local operators, which link non-trivially with the topological line operators on the wall. The result is summarized as follows in Table 4.7 and details can be found in Appendix D.4.

Line operators	$\ell_b^{-+}, \quad b \in \mathbb{A}_- \backslash \mathcal{T} / \mathbb{A}_+$	$\mathcal{I}_{-+} \boxtimes \mathcal{I}_{-+} \to \mathcal{I}_{-+} : \ell_b^{-+} \otimes \ell_{b'}^{-+} = \ell_{bb'}^{-+}$
		$\mathcal{I}_{-+} \boxtimes \mathcal{T}_+ \to \mathcal{I}_{-+} : L_b^- \otimes \ell_{b'}^{-+} = \ell_{bb'}^{-+}$
		$\mathcal{T}_- \boxtimes \mathcal{I}_{-+} \to \mathcal{I}_{-+} : \ell_b^{-+} \otimes L_{b'}^+ = \ell_{bb'}^{-+}$
Local operators	$V_a, \quad a \in \mathbb{A}_+ \cap \mathbb{A}_-$	$B(V_a, \ell_b^{+-}) = B(a, b)$

Table 4.7: The topological operator contents on the fused wall $\mathcal{I}_{-+}$. Generically, there is non-trivial braiding between the local operators and the line operators inherent from the braiding in $\mathcal{T}$.

Finally, one also needs to remember to keep track if the resulting 2d interface $\mathcal{I}_{-+}$ couples to the bulk gauge field $a^{(2)}$. As we will see, this will change the physical meaning of the 2d interface.

4.5.3 Local fusion junctions

In this subsection, we list the local fusion junctions where the defects are given by the simplest representatives in the equivalence classes. We will demonstrate the construction by an example, and list all other results afterwards.

Recall that $D_3 \times \overline{D}_3 = \mathcal{C}_0$, however, because the condensation defect $\mathcal{C}_0$ is in the same equivalence class as the identity operator, we can construct a local fusion junction

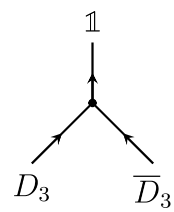

$$, \tag{4.5.28}$$

via anyon condensations. First, recall that we have shown that $\mathbb{Z}_N$-gauge theory coupled to the bulk gauge field $a^{(2)}$ leads to the condensation defect, and in the action,

$$S = \frac{2\pi i}{N} \int \left(b^{(1)} \cup \delta \hat{b}^{(1)} + \hat{b}^{(1)} \cup a^{(2)} \right) \ , \tag{4.5.29}$$

we see that generically only the $\hat{b}^{(1)}$-Wilson line $e^{i \oint_\gamma \hat{b}^{(1)}}$ is topological from the equation of motion, thus is identified as the dual 1-form $\mathbb{Z}_N$ quantum symmetry on the condensation defect. The canonical topological boundary of any condensation defect can be acquired by half-space gauging (condensing) the dual quantum symmetry. Therefore, the following interface $\mathcal{I}$ between $\mathcal{C}_0$ and $\mathbb{1}$

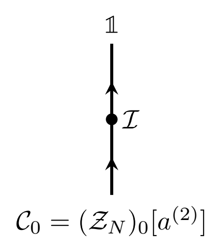

$$, \tag{4.5.30}$$

is acquired by condensing the anyon coupled to the bulk gauge field $a^{(2)}$. Applying this to the local junction (4.5.28), in the global fusion

$$D_3 \times \overline{D}_3 = \mathcal{A}^{N,(2p')^{-1}}_{a_1}[-(2p')a^{(2)}]\mathcal{A}^{N,-(2p')^{-1}}_{a_2}[-(2p')a^{(2)}] = (\mathcal{Z}_7)_0[-(2p')a^{(2)}] \equiv \mathcal{C}_0 \ , \tag{4.5.31}$$

the bulk gauge field $a^{(2)}$ couples to the anyon $b_2 = (a_1 a_2)^{-2p'}$. We thus conclude that the condensed anyon $\mathbb{A} = \langle (a_1 a_2)^{-2p'} \rangle = \langle a_1 a_2 \rangle$.

The other local fusion junctions can be constructed similarly, and we summarize the results in Table 4.8.

Local Junctions	Global Fusion	Condensed Anyons $\mathbb{A}$
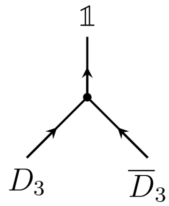	$[D_3]_{a_1} \times [\overline{D}_3]_{a_2}$ $= \mathcal{A}_{a_1}^{N,(2p')^{-1}}[-(2p')a^{(2)}]\mathcal{A}_{a_2}^{N,-(2p')^{-1}}[-(2p')a^{(2)}]$	$\langle a_1 a_2 \rangle$
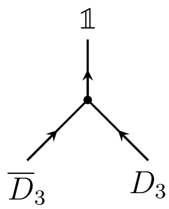	$[\overline{D}_3]_{a_1} \times [D_3]_{a_2} = \mathcal{A}_{a_1}^{N,-(2p')^{-1}}[a^{(2)}]\mathcal{A}_{a_2}^{N,(2p')^{-1}}[a^{(2)}]$	$\langle a_1 a_2 \rangle$
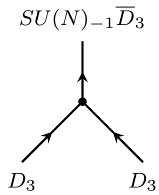	$[D_3]_{a_1} \times [D_3]_{a_2} = [SU(N)_{-1}]_{a_1 a_2^{2p'}}[\overline{D}_3]_{a_1^{-(2p')^{-1}} a_2^{-2p'}}$	$\emptyset$
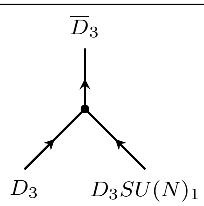	$[D_3]_{a_1} \times [D_3]_{a_2}[SU(N)_1]_{a_3}$ $= [\overline{D}_3]_{a_1^{-(2p')^{-1}} a_2^{-2p'}}[SU(N)_{-1}]_{a_1 a_2^{2p'}}[SU(N)_1]_{a_3}$	$\langle a_1 a_2^{2p'} a_3 \rangle$ or $\langle a_1 a_2^{2p'} a_3^{-1} \rangle$
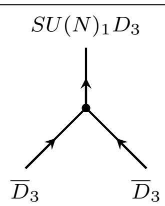	$[\overline{D}_3]_{a_1} \times [\overline{D}_3]_{a_2} = [D_3]_{a_1^{-2p'} a_2^{-(2p')^{-1}}}[SU(N)_1]_{a_1^{2p'} a_2}$	$\emptyset$
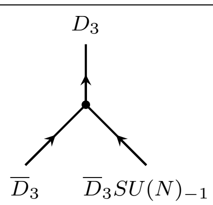	$[\overline{D}_3]_{a_1} \times [\overline{D}_3]_{a_2}[SU(N)_{-1}]_{a_3}$ $= [D_3]_{a_1^{-2p'} a_2^{-(2p')^{-1}}}[SU(N)_1]_{a_1^{2p'} a_2}[SU(N)_{-1}]_{a_3}$	$\langle a_1^{2p'} a_2 a_3 \rangle$ or $\langle a_1^{2p'} a_2 a_3^{-1} \rangle$

Table 4.8: The list of local fusion junctions that requires anyon condensations to construct. We use the subscript a in $[D_3]_a$ and $[\overline{D}_3]_a$ to denote the generating anyons in the stacked minimal TQFT and the presentation of $\overline{D}_3$ in (4.5.11) is used. We also the junctions where no anyon is condensed to make the change of anyon generators explicit. In the 4-th and the last junctions, we use the anyon condensation to remove $[SU(N)_1]_a \times [SU(N)_{-1}]_b$. Since N is odd, it is straightforward to check this is the same as a $\mathbb{Z}_N$-gauge theory with no twist (where ab generates the electric lines and ab^{-1} generates the magnetic lines). Generically there will be more than two choices of condensable anyons we provided depending on N; here, we only list the two which exists for all N.

4.5.4 Associators for triality defects

With the above tools we can now compute the associators of the triality defect admitting the above group-theoretical construction. For simplicity, we will consider the simplest special case where $N = 7$, and it's straightforward to generalize our approach for generic allowed N. We will choose

$$2p' = 3 \ , \quad (2p')^{-1} = 1 - 2p' = -2 \ , \quad -(2p')^{-1} = 2 \ , \tag{4.5.32}$$

and the triality defects are given by

$$D_3 = \mathbb{D}_3 \mathcal{A}^{7,-2}[a^{(2)}] \ , \quad \overline{D}_3 = \mathcal{A}^{7,2}[a^{(2)}]\overline{\mathbb{D}}_3 \ . \tag{4.5.33}$$

In the following, we will demonstrate the computation through the following four examples:

$$D_3 \times D_3 \times D_3 \ , \quad D_3 \times \overline{D}_3 \times D_3 \ , \quad \overline{D}_3 \times D_3 \times D_3 \ , \quad D_3 \times D_3 \times \overline{D}_3 \ , \tag{4.5.34}$$

and the other four are related to the above by orientation reversal.

$\left[\mathbf{F}^{\mathbf{D_3}}_{\mathbf{D_3,D_3,D_3}}\right]_{\mathbf{SU(7)_{-1}\overline{D}_3,SU(7)_{-1}\overline{D}_3}}$

Let's consider the F-symbol for $D_3 \times D_3 \times D_3$. Evaluating the global fusion in two different ways, we find

$$\begin{aligned} &(D_3 \times D_3) \times D_3 = SU(7)_{-1}\overline{D}_3 \times D_3 = SU(7)_{-1}\mathcal{C}_0 \to SU(7)_{-1} \ , \\ &D_3 \times (D_3 \times D_3) = D_3 \times (SU(7)_{-1}\overline{D}_3) = SU(7)_{-1}\mathcal{C}_0 \to SU(7)_{-1} \ . \end{aligned} \tag{4.5.35}$$

Thus, the corresponding diagram is

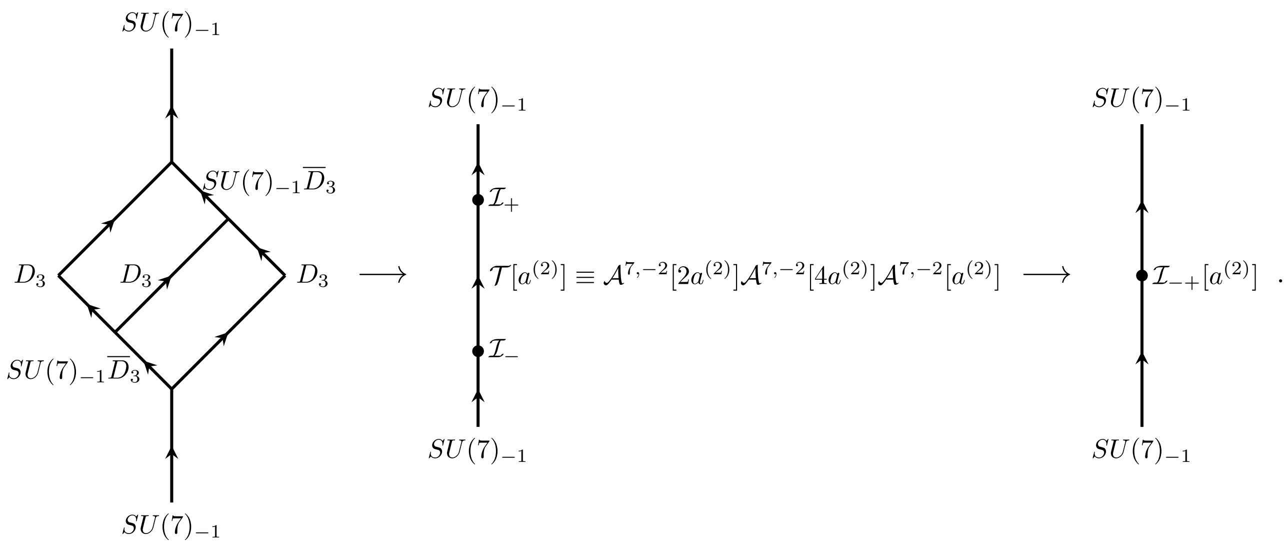

(4.5.36)

Here, the theory $\mathcal{T}$ is extracted using (4.5.14)

$$\begin{aligned} D_3 \times D_3 \times D_3 &= \mathbb{D}_3\mathcal{A}^{7,-2}_{a_1}[a^{(2)}]\mathbb{D}_3\mathcal{A}^{7,-2}_{a_2}[a^{(2)}]\mathbb{D}_3\mathcal{A}^{7,-2}_{a_3}[a^{(2)}] \\ &= \mathbb{D}_3\mathcal{A}^{7,-2}_{a_1}[a^{(2)}]\overline{D}_3\mathcal{A}^{7,-2}_{a_2}[4a^{(2)}]\mathcal{A}^{7,-2}_{a_3}[a^{(2)}] \\ &= \mathcal{A}^{7,-2}_{a_1}[2a^{(2)}]\mathcal{A}^{7,-2}_{a_2}[4a^{(2)}]\mathcal{A}^{7,-2}_{a_3}[a^{(2)}] \ . \end{aligned} \tag{4.5.37}$$

To find that the condensed anyons $\mathbb{A}_+$, let's follow the fusion tree

$$D_3 \times (D_3 \times D_3) = D_3 \times (SU(N)_{-1}\overline{D}_3) = SU(N)_{-1}\mathcal{C}_0 \to SU(N)_{-1} \ . \tag{4.5.38}$$

In the first junction, $(D_3 \times D_3) = U(1)_N\mathcal{A}^{7,2}[a^{(2)}]\overline{\mathbb{D}}_3$, as discussed previously, the minimal TQFT $\mathcal{A}^{7,2}[a^{(2)}]$ is generated by the anyon $a_2^4a_3$ to which the gauge field $a^{(2)}$ couples. No anyon condensation happens here. Next, the second junction is simply the local junction between $D_3 \times \overline{D}_3$ and the $\mathbb{1}$, and as shown previously, the anyon that couples to the gauge field $a^{(2)}$ is condensed on this interface; therefore $\mathbb{A}_+ = \langle a_1^2a_2^4a_3\rangle$. By the similar analysis, one can show that $\mathbb{A}_- = \langle a_1^2a_2^4a_3\rangle$.

Using the result in Table 4.7, we see that both $\mathcal{T}_\pm$ are $SU(7)_{-1}$'s generated by $L^{\pm}_{a_2a_3^3}$ respectively. The fused interface $\mathcal{I}_{-+}$ contains topological line operators factorized into

$\mathbb{Z}_7 \times \mathbb{Z}_7$, where one $\mathbb{Z}_7$ factor corresponds to the unconfined lines in $SU(7)_{-1}$ and the other $\mathbb{Z}_7$ factor corresponds to topological lines confined on the interface. By checking the fusion rule between the $\mathcal{T}_\pm = SU(7)_{-1}$ and the $\mathbb{Z}_7$ unconfined sector, we see that the unconfined $\mathbb{Z}_7$ sector forms the identity interface between $\mathcal{T}_\pm$ theories.

Furthermore, the interface also contains $\mathbb{Z}_7$ topological vertex operators labeled by V_a where $a \in \mathbb{A}_+ \cap \mathbb{A}_- = \langle a_1^2 a_2^4 a_3 \rangle$. From the braiding relation between the vertex operators and the confined lines, we see that they form a 2d $\mathbb{Z}_7$ TQFT on the interface. However, this TQFT actually couples to the bulk gauge field $a^{(2)}$ through the vertex operator, thus an effective action is given by

$$S = \frac{2\pi i}{7} \int \left(b^{(1)} \cup \delta\phi^{(0)} + \phi^{(0)} a^{(2)} \right) \ . \tag{4.5.39}$$

By the similar multiplication where we integrate out $b^{(1)} \in C^1(M_2, \mathbb{Z}_7)$, we see that this is nothing but a 2d condensation defect of the bulk $\mathbb{Z}_7^{(1)}$ symmetry (which is actually just a projector). Hence, we conclude in this case that the F-symbol interface is given by the identity interface of the $SU(7)_{-1}$ TQFT stacked with a 2d condensation defect of the bulk $\mathbb{Z}_7^{(1)}$ symmetry.

Let us briefly comment on the operator spectrum. First, $e^{\frac{2\pi i k}{N}\phi^{(0)}}$ are $\mathbb{Z}_N$ topological local operators (arising from the higher quantum symmetry line $e^{\frac{2\pi i k}{N}\int a^{(1)}}$ stretching between two boundaries) and they can be interpreted as the 1-form higher quantum symmetry on the 2d condensation defect. The gauge field $b^{(1)}$ again has the modified gauge transformation $b^{(1)} \to b^{(1)} - \lambda_a^{(1)}$ under the $a^{(2)}$ gauge transformation $a^{(2)} \to a^{(2)} + \delta\lambda_a^{(1)}$. Therefore, $e^{\frac{2\pi i}{N}\oint b^{(1)}}$ plays the same role as the 3d condensation defect, namely to ensure the non-genuine line bounding the bulk 1-form $\mathbb{Z}_N$ symmetry becomes genuine on the 2d condensation defect. Notice that this matches straightforwardly with the same discussion in the Lagrangian formalism in Appendix 4.5.4.

To summarize, we find

$$\left[\mathbf{F}^{\mathbf{D_3}}_{\mathbf{D_3},\mathbf{D_3},\mathbf{D_3}}\right]_{\mathbf{SU(7)_{-1}\overline{D}_3},\mathbf{SU(7)_{-1}\overline{D}_3}} = \text{2d condensation defect of } \mathbb{Z}_7 \text{ 1-form symmetry}\ . \tag{4.5.40}$$

$\left[\mathbf{F}^{\mathbf{D_3}}_{\mathbf{D_3},\overline{\mathbf{D}}_\mathbf{3},\mathbf{D_3}}\right]_{\mathbb{1},\mathbb{1}}$

As another example, one can consider $D_3 \times \overline{D}_3 \times D_3$. In this case, the diagram can be summarized as

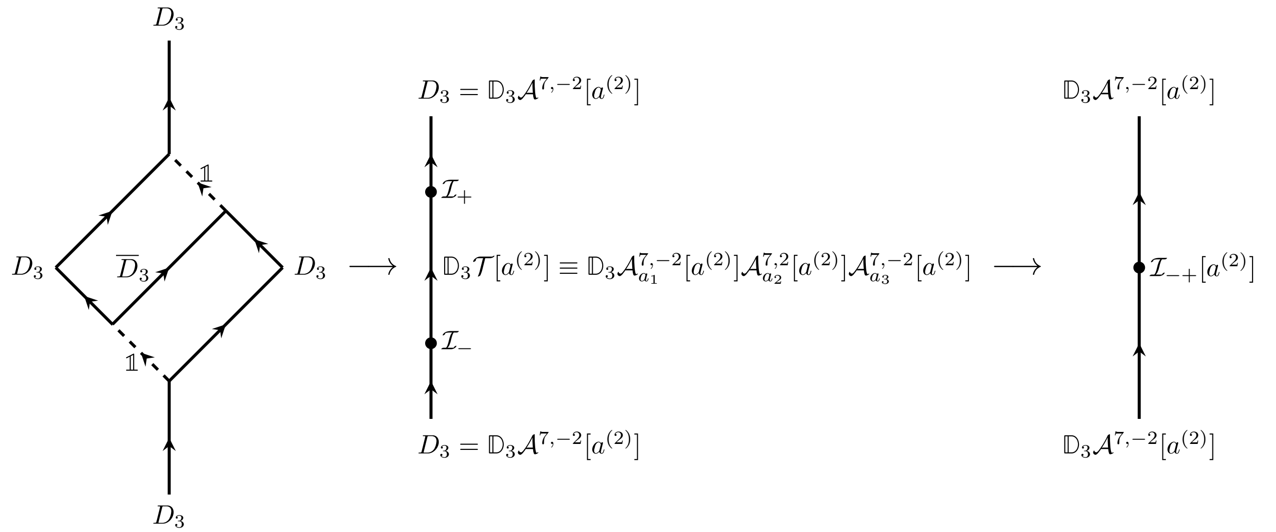

(4.5.41)

The theory $\mathcal{T} = \mathcal{A}^{7,-2}_{a_1}[a^{(2)}]\mathcal{A}^{7,2}_{a_2}[4a^{(2)}]\mathcal{A}^{7,-2}_{a_3}[a^{(2)}]$ is extracted similarly using (4.5.14) with the presentation of $\overline{D}_3 = \mathcal{A}^{7,-2}[a^{(2)}]\overline{\mathbb{D}}_3$. From Table 4.8, we find

$$\mathbb{A}_- = \langle a_1 a_2 \rangle \ , \quad \mathbb{A}_+ = \langle a_2 a_3 \rangle \ . \tag{4.5.42}$$

In this case, the fused domain wall $\mathcal{I}_{-+}$ contains only topological lines labeled by $\mathbb{Z}_7$ and no local operators as $\mathbb{A}_+ \cap \mathbb{A}_-$ is trivial. The theory $\mathcal{T}_+ = \mathcal{A}^{7,-2}[a^{(2)}]$ is generated by the anyon $L^+_{a_1}$ and the theory $\mathcal{T}_- = \mathcal{A}^{7,-2}[a^{(2)}]$ is generated by the anyon $L^-_{a_3}$. Because both $L^+_{a_1}$ and $L^-_{a_3}$ couple to the bulk gauge field $a^{(2)}$ respectively, it is natural to identify the two lines. On the other hand, pushing $L^+_{a_1}$ and $L^-_{a_3}$ to the interface, they become $\ell^{-+}_{a_1}$ and $\ell^{-+}_{a_3}$ respectively. But because $a_1 = a_1(a_1a_2)^{-1}(a_2a_3)$, we see that

$$\ell^{-+}_{a_1} = \ell^{-+}_{a_1(a_1a_2)^{-1}(a_2a_3)} = \ell^{-+}_{a_3} \ , \tag{4.5.43}$$

therefore pushing $L^+_{a_1}$ and $L^-_{a_3}$ leads to the identical line on the interface. Thus, we conclude that the F-symbol interface here is the identity interface between triality defect D_3 and D_3.

$\left[\mathbf{F}^{\mathbf{D_3}}_{\overline{\mathbf{D}}_3,\mathbf{D_3},\mathbf{D_3}}\right]_{\mathbb{1},\mathbf{SU(7)_{-1}\overline{D}_3}}$

This component of the associator relates the following two fusion channels:

$$\begin{aligned} &\overline{D}_3 \times (D_3 \times D_3) = \overline{D}_3 \times (SU(7)_{-1}\,\overline{D}_3) = (SU(7)_1 \times SU(7)_{-1})D_3 \to D_3 \ , \\ &(\overline{D}_3 \times D_3) \times D_3 = C_0 \times D_3 \to D_3 \ , \end{aligned} \tag{4.5.44}$$

and the corresponding diagram can be worked out by referring to Table 4.8:

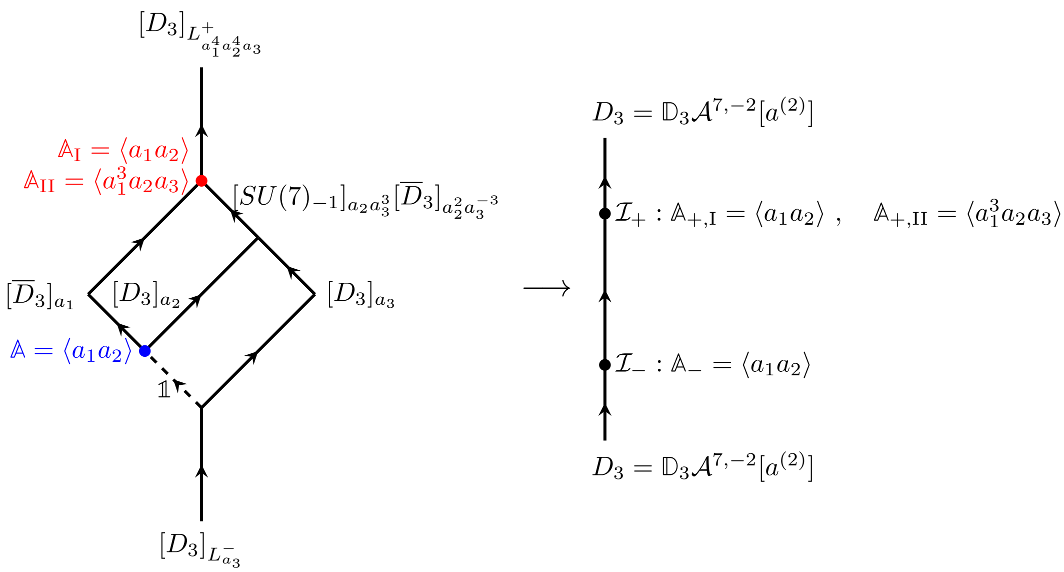

, (4.5.45)

from which we conclude

$$\mathbb{A}_- = \langle a_1 a_2 \rangle \ , \quad \mathbb{A}_{+,\mathrm{I}} = \langle a_1 a_2 \rangle \ , \quad \mathbb{A}_{+,\mathrm{II}} = \langle a_1^3 a_2 a_3 \rangle \ , \tag{4.5.46}$$

where for $\mathbb{A}_+$ we have two choices. For the choice of $\mathbb{A}_{+,\mathrm{I}}$, the interface $\mathcal{I}_{-+}$ contains vertex operators labeled by $\mathbb{A}_{+,\mathrm{I}} \cap \mathbb{A}_- = \langle a_1 a_2 \rangle \simeq \mathbb{Z}_7$ and confined $\mathbb{Z}_7$ topological lines generated by $\ell^{-+}_{a_1 a_2^{-1}}$. Together they form a decoupled 2d $\mathbb{Z}_7$-gauge theory. One can further check from the fusion rules between unconfined lines and the bulk lines that the interface $\mathcal{I}_{-+,\mathrm{I}}$ is the identity interface in the minimal TQFT $\mathcal{A}^{7,-2}[a^{(2)}]$ plus the decoupled 2d $\mathbb{Z}_7$ gauge theory.

For the choice of $\mathbb{A}_{+,\mathrm{II}}$, there are no confined lines and no vertex operators on the interface $\mathcal{I}_{-+}$. And it is straightforward to check that the $\mathcal{I}_{-+,\mathrm{II}}$ is simply the identity interface in the minimal TQFT $\mathcal{A}^{7,-2}[a^{(2)}]$.

In summary,

$$\left[\mathbf{F}^{\mathbf{D_3}}_{\overline{\mathbf{D}}_\mathbf{3},\mathbf{D_3},\mathbf{D_3}}\right]_{\mathbb{1},\mathbf{SU(7)_{-1}}\overline{\mathbf{D}}_\mathbf{3}} = \text{decoupled } \mathbb{Z}_7 \text{ gauge theory} \quad \text{or} \quad \text{trivial TQFT} . \tag{4.5.47}$$

$\left[\mathbf{F}^{\mathbf{D_3}}_{\mathbf{D_3},\mathbf{D_3},\overline{\mathbf{D}}_\mathbf{3}}\right]_{\mathbf{SU(7)_{-1}}\overline{\mathbf{D}}_\mathbf{3},\mathbb{1}}$

This component of the associator relates the two following fusions.

$$\begin{aligned} &D_3 \times (D_3 \times \overline{D}_3) = D_3 \times C_0 \to D_3 \ , \\ &(D_3 \times D_3) \times \overline{D}_3 = SU(7)_{-1}\, \overline{D}_3 \times \overline{D}_3 = SU(7)_{-1} \times SU(7)_1\, D_3 \to D_3 \ , \end{aligned} \tag{4.5.48}$$

and the corresponding diagram can be worked out by referring to Table 4.8:

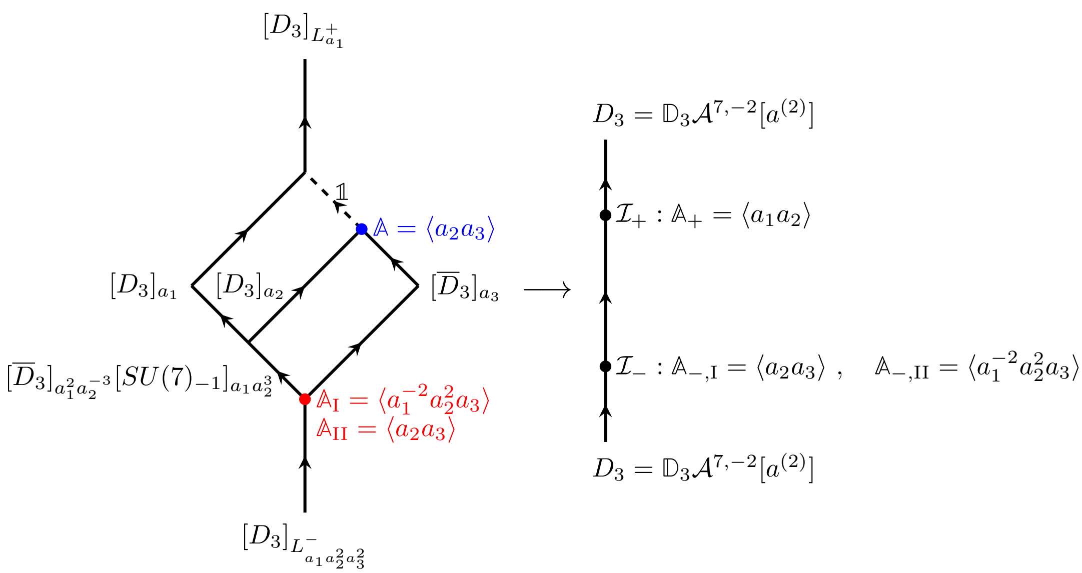

, (4.5.49)

from which we conclude

$$\mathbb{A}_{-,\mathrm{I}} = \langle a_2 a_3 \rangle \ , \quad \mathbb{A}_{-,\mathrm{II}} = \langle a_1^{-2} a_2^2 a_3 \rangle \ , \quad \mathbb{A}_{+,\mathrm{II}} = \langle a_2 a_3 \rangle \ , \tag{4.5.50}$$

where $\mathbb{A}_-$ has two choices. For the choice of $\mathbb{A}_{-,\mathrm{I}}$, the interface $\mathcal{I}_{-+}$ is the identity interface in the minimal TQFT $\mathcal{A}^{7,-2}[a^{(2)}]$ together with a decoupled 2d $\mathbb{Z}_7$ gauge theory. And for the choice of $\mathbb{A}_{-,\mathrm{II}}$, $\mathcal{I}_{-+,\mathrm{II}}$ is simply the identity interface in the minimal TQFT $\mathcal{A}^{7,-2}[a^{(2)}]$. Hence, we find

$$\left[\mathbf{F}^{\mathbf{D_3}}_{\mathbf{D_3},\mathbf{D_3},\overline{\mathbf{D}}_\mathbf{3}}\right]_{\mathbf{SU(7)_{-1}}\overline{\mathbf{D}}_\mathbf{3},\mathbb{1}} = \text{decoupled } \mathbb{Z}_7 \text{ gauge theory} \quad \text{or} \quad \text{trivial TQFT} . \tag{4.5.51}$$

CHAPTER 5

Codimension-1 Non-Conformal Defects in Free Scalar Theories

5.1 Introduction and summary

Defects in quantum field theory arise in a wide variety of physical contexts, and often elucidate features of the ambient theory in which they are embedded. By a "defect" we mean a lower dimensional submanifold that hosts localized interactions and/or degrees of freedom. In this chapter we consider a simple example of such a defect: a codimension-one defect in free scalar field theory. We will be interested mainly in non-conformal defects embedded in a theory that is conformal in the bulk.[1] As we will see, this simple example illustrates a variety of phenomena that are also present in more elaborate contexts.

5.1.1 Two formulations

As we will discuss in detail, there are two distinct formulations of this problem. In the first description, which we refer to as the "perturbative formulation" since it will be based on resumming perturbation theory, we start from a Lagrangian comprising bulk and defect

[1]Non-conformal defects in free field theory were considered in a similar spirit to ours in [83, 84]. The folding trick relates defects to boundaries, and string theory applications arise in the context of boundary string field theory [85,86]. More generally, boundary RG flows have been considered in many works, including [87, 88], along with other references noted below.

contributions,

$$S = \int d^{d-1}y dx \big(\mathcal{L}_{\rm b}(\phi) + \mathcal{L}_{\rm d}(\phi)\delta(x)\big) \tag{5.1.1}$$

where we have taken the defect to lie at $x = 0$. The bulk theory is a free scalar field[2]

$$\mathcal{L}_{\rm b} = \frac{1}{2}\big((\partial\phi)^2 + m^2\phi^2\big) \tag{5.1.2}$$

while the defect Lagrangian contains quadratic terms[3] with any number of derivatives transverse or parallel to the defect, compatible with translation and rotation invariance on the defect, written schematically as

$$\mathcal{L}_{\rm d} = \sum_{m,n,p,q} \alpha_{mnpq}(\partial_y)^m(\partial_x)^n\phi(\partial_y)^p(\partial_x)^q\phi \ . \tag{5.1.3}$$

However, a field redefinition may be used to eliminate all terms with n or q greater than 1; see Appendix C.1 for more details. We may also integrate by parts along the defect to write all terms with derivatives along the defect in the form $\phi(\nabla_y^2)^n\phi$. It will therefore suffice to consider

$$\mathcal{L}_d = c_0^B + \frac{1}{2}c_1^B\phi^2 + c_2^B\phi\phi' + \frac{1}{2}c_3^B(\phi')^2 \tag{5.1.4}$$

where $\phi' = \partial_x\phi$. Here, the dependence on ∇_y^2 has been absorbed into the couplings $c_{1,2,3}^B$; in fact, since we'll work in momentum space along the defect this dependence plays no significant role, and we'll take $c_{1,2,3}^B$ to be constants, noting that the dependence on ∇_y^2 can easily be incorporated by allowing these couplings to depend on the momentum along the defect. The B superscript on the couplings indicates that these are bare couplings; computation of physical quantities in this description will be UV divergent, necessitating a

[2]We mostly work in Euclidean signature and usually set the bulk mass to zero.

[3]The restriction to quadratic terms is made for simplicity but can also be viewed as a starting point for an interacting theory, where the interactions are treated perturbatively in the exactly soluble quadratic theory.

UV cutoff Λ and the introduction of renormalized couplings $c_{1,2,3}$ that are finite as $\Lambda \to \infty$. Choosing a sharp momentum cutoff, $|p| < \Lambda$, we will find

$$
\begin{aligned}
c_1^B &= c_1 + \frac{c_2^2 \hat{\Lambda}}{1 - c_3 \hat{\Lambda}} \\
c_2^B &= \frac{c_2}{1 - c_3 \hat{\Lambda}} \\
c_3^B &= \frac{c_3}{1 - c_3 \hat{\Lambda}}
\end{aligned} \tag{5.1.5}
$$

with $\hat{\Lambda} = \frac{\Lambda}{\pi}$. By the same token, we have included a defect cosmological term c_0^B to cancel divergences arising from vacuum diagrams. This term depends on the defect dimension and the couplings $c_{1,2,3}$. For example, in the case of a line defect embedded in a two-dimensional bulk, and setting $c_2 = c_3 = 0$, we have

$$
c_0^B = -\frac{c_1}{4\pi} \ln\left(\frac{\Lambda}{\mu}\right) \tag{5.1.6}
$$

where μ is an RG scale. Computations in this description, such as correlators involving bulk and boundary fields, are obtained by employing perturbation theory in the couplings c_i and then resumming. The expressions (5.1.5) are obtained by demanding finiteness at each order of perturbation theory.

For general couplings the defect is non-scale invariant and so describes an RG flow, typically between a Neumann boundary condition in the UV and a Dirichlet boundary condition in the IR, as shown in Section 5.3.3.1. For special values of the couplings the defect is conformal or topological, as we discuss in the next section.

In the second description, we use that the theory is quadratic to encode the defect couplings in terms of matching conditions across the defect; this approached was employed in [89] for conformal defects. Using (L, R) to denote values immediately to the left or right of the defect, we impose[4]

$$\begin{pmatrix} \phi_R \\ \phi'_R \end{pmatrix} = \begin{pmatrix} a & b \\ c & d \end{pmatrix} \begin{pmatrix} \phi_L \\ \phi'_L \end{pmatrix} \tag{5.1.7}$$

for some constants (a, b, c, d). As we discuss in the next section, time translation invariance imposes the condition $ad - bc = 1$. The remaining three independent couplings are related to the renormalized couplings defined above as

$$\begin{pmatrix} a & b \\ c & d \end{pmatrix} = \begin{pmatrix} \frac{(2-c_2)^2 - c_1 c_3}{4 - c_2^2 + c_1 c_3} & \frac{-4c_3}{4 - c_2^2 + c_1 c_3} \\ \frac{4c_1}{4 - c_2^2 + c_1 c_3} & \frac{(2+c_2)^2 - c_1 c_3}{4 - c_2^2 + c_1 c_3} \end{pmatrix} . \tag{5.1.8}$$

These relations are fixed by matching observables computed in the two descriptions. Alternatively, we can write down an action in the matching approach involving $(\phi_{L,R}, \phi'_{L,R})$ treated as independent such that the variational principle yields the matching conditions (5.1.8). As we'll see, the couplings in this description may be identified with the renormalized couplings in the perturbative description. Note that the action in the perturbative description involves just (ϕ, ϕ'), and hence would be ambiguous if we attempted to incorporate field discontinuities in the Lagrangian. Physical discontinuities arise in the perturbative approach via the discontinuities of correlators computed after perturbative resummation.

Either of the two descriptions may be more convenient for different purposes. For example, the μ dependence of the c_0^B term in the perturbative description makes it clear that the defect, regarded as an operator, is scale dependent and so acquires an "anomalous dimension", which should be taken into account when considering the modular properties of the torus partition function with a defect insertion. On the other hand, the matching description makes it clear how to understand the fusion of two parallel defects, as it simply involves the multiplication of two matching matrices in (5.1.8), and is also suitable for canonical quantization via mode expansions and computing partition sums. We can pass back and forth between the two descriptions using the dictionary (5.1.8).

[4]Note that this is different than the matching conditions in [89] since we are not imposing conformal invariance.

5.1.2 Computations

In the remainder of the introduction we summarize the computations we have carried out in this theory. The two formulations discussed above are laid out in detail in section 5.2.

In section 5.3 we compute the 2-point function of bulk fields in the presence of the defect using the perturbative description. The computation is carried out by summing up loop diagrams in momentum space; this is possible due to the iterative structure of the loop diagrams. This determines the relation between the bare and renormalized couplings, and we also use the renormalized correlator to read off the effective matching conditions on the field and its normal derivative across the defect. We then discuss various special cases: the UV and IR limits, the conformal defect, and the topological defect, the latter implementing a sign flip of ϕ across the defect.

In section 5.4 we compute the sum of vacuum diagrams, which determines the defect anomalous dimension[5] via the logarithmically divergent part of c_0^B. In particular, the renormalized defect operator $\mathcal{O}_\mathrm{d} = e^{-S_\mathrm{d}}$ obeys the RG equation

$$\mu \frac{d}{d\mu} \mathcal{O}_\mathrm{d} = \gamma_\mathrm{d} \mathcal{O}_\mathrm{d} \tag{5.1.9}$$

A closed form expression for γ_d may be obtained when $c_3 = 0$,

$$\gamma_\mathrm{d} = -\frac{1}{4\pi} \frac{c_1 L_d}{1 + \frac{1}{4} c_2^2} \ , \tag{5.1.10}$$

where L_d is the length of the defect. For c_3 nonzero γ_d is given by a divergent series in the couplings $c_{1,2,3}$.

Section 5.5 considers the fusion of two parallel defects. We verify that perturbative computation of the renormalized two-point function yields a fusion rule result consistent with the multiplication of matching matrices (5.1.8). We also work out the leading dependence

[5] We use the term "anomalous dimension" to characterize the μ dependence, though the defect in general has no well defined scaling dimension since the couplings change under a scale transformation.

of the partition function on the distance L between the two defects, which for $c_2 = c_3 = 0$ can be described in terms of a defect OPE as

$$\mathcal{O}_{\rm d}^{(1)}(L)\mathcal{O}_{\rm d}^{(2)}(0) \approx L^{\frac{c_1^{(1)} c_1^{(2)} L L_d}{4\pi}} \mathcal{O}_{\rm d}^{(12)} \ , \quad L \to 0 \tag{5.1.11}$$

In section 5.6 we canonically quantize the $d = 1+1$ scalar field in the presence of the defect by working out a complete set of mode solutions. Depending on the values of the couplings c_i, these can include bound state solutions, as well as exponentially growing (in real time) solutions that signal an instability. The instabilities, when present, can be stabilized by giving the scalar field a bulk mass term. The bound state solutions are identified with the poles of the two-point function computed in an earlier section.

In section 5.7 we replace the line defect (with $c_2 = c_3 = 0$) with a circular ring defect. The partition function $Z_{\rm ring}$ depends on the dimensionless combination $c_1\beta$, where β is the circumference of the ring. We find

$$\log Z_{\rm ring}(c_1\beta) = \frac{1}{2}\log\frac{\beta c_1}{4\pi} + \log\Gamma\left(\frac{\beta c_1}{4\pi}\right) \ , \tag{5.1.12}$$

up to an additive constant. We can equivalently think of this as the partition function of a ring placed on a cone at a fixed distance from the tip, with the length of the ring β controlled by the opening angle of the cone. We can then compute the "entropy" as

$$\begin{aligned} s &= (1 - \beta\partial_\beta)\log Z_{\rm ring}(c_1\beta) \\ &= \frac{1}{2}\log\frac{\beta c_1}{4\pi} + \log\Gamma\left(\frac{\beta c_1}{4\pi}\right) - \frac{\beta c_1}{4\pi}\Psi\left(\frac{\beta c_1}{4\pi}\right) - \frac{1}{2} \end{aligned} \tag{5.1.13}$$

where $\Psi(x) = \Gamma'(x)/\Gamma(x)$. Using the folding trick to convert this to the partition function of a CFT on a disk with a $c_1\phi^2$ boundary interaction, the entropy s corresponds to the g-function [87,86,88]. The g-function in (5.1.13) is monotonically decreasing in $c_1\beta$, in accord with the g-theorem [88]. Alternatively, the quantity s may be related to the entanglement entropy of a half-space in the presence of two accelerating defects. This interpretation arises from analytic continuation of the Euclidean ring configuration to Lorentzian space time.

In section 5.8 we consider the torus partition function $Z(L_d, L)$ with the c_1 defect wrapped around a cycle of a square torus with length L_d, the length of the other cycle being L. The torus partition function depends on the two dimensionless variables $(c_1 L, c_1 L_d)$ as well as the RG scale μ that is part of the definition of the renormalized defect. The torus partition function may be computed as a sum over states in either of two channels, depending on which direction we view as time. If we take time to run along the defect direction, then the computation involves summing over modes with discontinuities given by the matching conditions. The result in this channel receives a nontrivial contribution from the zero point energy. Alternatively, taking time to run orthogonally to the defect, the computation corresponds to computing matrix elements of the defect operator between excited states of the scalar field. The relation between these two descriptions is a bit subtle due to the fact that the partition function depends on a renormalization scale μ, as in (5.1.9), which must be chosen to agree in the two descriptions.

We can use these results to give a "Cardy formula" for the asymptotic density of states of the defect Hilbert space; i.e. of the Hilbert space of the defect located at a point on a spatial circle of size L. The result depends on relative sizes of the dimensionless combinations of EL and $c_1 L$. For $c_1 L = O(1)$ the asymptotic density of states as a function of energy works out to be

$$\rho(E) \approx \frac{1}{\sqrt{c_1 L}} \left(\frac{6EL}{\pi}\right)^{\frac{1}{8}\sqrt{\frac{c_1^2 L}{6\pi E}}} \left(\frac{L/2\pi}{48E^3}\right)^{1/4} e^{2\pi\sqrt{\frac{EL/2\pi}{3}}} \left(1 + O\left(\frac{1}{\sqrt{EL}}\right)\right) \quad , \quad EL \gg 1 \; . \tag{5.1.14}$$

The divergence as $c_1 \to 0$ corresponds to integration over the scalar field zero mode, which acquires vanishing action in this limit. This same result also applies to the regime $EL \gg (c_1 L)^2 \gg 1$ except the leading correction is $O\left(\frac{c_1 L}{\sqrt{EL}}\right)$. Another regime of interest is $c_1 L \gg EL \gg 1$, for which the partition function becomes that of a Dirichlet defect after carefully taking into account the zero point energy.

In section 5.9 we consider the defect as an operator inserted at a fixed Lorentzian time

$t = 0$. The scalar field is taken to be in the vacuum state for $t < 0$. As in the quench scenario studied in [90], the insertion of the defect creates an excited state at $t > 0$, whose explicit form we work out by computing the Bogoliubov coefficients relating the natural in and out modes. We also compute the expectation value of the stress tensor for $t > 0$, finding it to be UV divergent on account of the sharply localized (in time) nature of the defect. The introduction of a UV regulator Λ yields a result logarithmically divergent in Λ, corresponding to smearing the defect operator over a time window $\Delta t \sim \Lambda^{-1}$.

We conclude by commenting on some natural extensions of these results in section 5.10.

A series of appendices fill in some technical details, and outline how adding bulk interactions can stabilize the defect when the couplings c_i are such that unstable modes are present.

Other references on defects relevant to what follows include [91–121].

5.2 General aspects

In this section we describe our two approaches to the defect problem — the matching approach and the perturbative approach — and their relation. We describe the general space of defect couplings along with special cases that lead to conformal or topological defects.

5.2.1 Matching conditions

We consider a noncompact free massless scalar field ϕ on the Euclidean plane with coordinates (x, t). We place an infinite line defect at $x = 0$, extending in the t direction, and write the action as

$$S = \frac{1}{2}\int_{x<0} d^2x(\partial\phi)^2 + \frac{1}{2}\int_{x>0} d^2x(\partial\phi)^2 + S_{\mathrm{d}} \ , \tag{5.2.1}$$

where S_d is the action associated with the defect. One approach to this system consists of imposing matching conditions across the defect while ignoring direct reference to S_d. We will consider linear matching conditions of the form

$$\begin{pmatrix} \phi_R \\ \phi'_R \end{pmatrix} = \begin{pmatrix} a & b \\ c & d \end{pmatrix} \begin{pmatrix} \phi_L \\ \phi'_L \end{pmatrix} \tag{5.2.2}$$

where $\phi_{L,R}$ are to be evaluated just to the left or right of the defect, and $\phi' = \frac{\partial \phi}{\partial x}$.

Imposing symmetries constrains the values of (a, b, c, d). Consider a correlator in the presence of the defect, $\langle \mathcal{O}_1(x_1, t_1) \ldots \mathcal{O}_n(x_n, t_n) \rangle_d$. Given a current $j^\mu(x, t)$ that is conserved away from the defect, we may attempt to derive a Ward identity in the standard fashion by inserting an integral of j^μ along a contour C that surrounds all the operators, as shown in Figure 5.1.

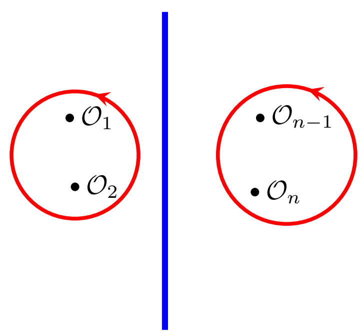

Figure 5.1: A two component contour C (red) surrounding the operators $\mathcal{O}_i$ on each side of the defect (blue). The current j_μ is integrated over the contour.

That is, we insert $\oint_C j_\mu dx^\mu$. On one hand, we can deform the contour into a sum of contours surrounding each operator and then use the $j^\mu \mathcal{O}$ OPE to evaluate the integrals, yielding

$$\begin{aligned} &\langle \oint_C j_\mu(x) dx^\mu \mathcal{O}_1(x_1, t_1) \ldots \mathcal{O}_n(x_n, t_n) \rangle_d \\ &\qquad = \langle \delta\mathcal{O}_1(x_1, t_1) \ldots \mathcal{O}_n(x_n, t_n) + \ldots + \mathcal{O}_1(x_1, t_1) \ldots \delta\mathcal{O}_n(x_n, t_n) \rangle_d \, . \end{aligned} \tag{5.2.3}$$

In the absence of a defect, we alternatively expand the contour to an arbitrarily large circle, which yields zero due to field falloffs at infinity. The Ward identity is then the statement that the right hand side of (5.2.3) vanishes. In the presence of the defect we can instead first expand two contours that surround the operators on either side of the defect into arbitrarily large semi-circles, with the flat sides lying along the defect, as illustrated in Figure 5.2.

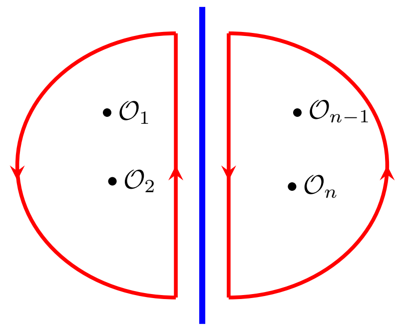

Figure 5.2: Deformation of the contour C into two arbitrarily large semi-circles and flat sides running along the defect.

In order to get zero in the large radius limit, we need that the two segments lying along the defect cancel. That is, the Ward identity (i.e the vanishing of the rhs of (5.2.3)) is only valid provided

$$\int_{-\infty}^{\infty} j_t(\phi_L)dt = \int_{-\infty}^{\infty} j_t(\phi_R)dt \ . \tag{5.2.4}$$

Demanding that the defect preserves a symmetry amounts to the condition that (5.2.4) be obeyed for the Noether current j^μ corresponding to that symmetry.

As a first condition, we require time translation invariance, meaning invariance under a common time shift $t_i \to t_i + \delta t_i$ of all operator insertions. The corresponding current is

$$j_z = \frac{1}{2\pi} T_{zz} \ , \quad j_{\overline{z}} = \frac{1}{2\pi} T_{\overline{z}\overline{z}} \tag{5.2.5}$$

where we use complex coordinates $z = x + it$ and $\overline{z} = x - it$, and the stress tensor has nonzero components

$$T_{zz} = -2\pi(\partial_z\phi)^2 \ , \quad T_{\overline{z}\overline{z}} = -2\pi(\partial_{\overline{z}}\phi)^2 \ . \tag{5.2.6}$$

This gives

$$j_t = \frac{1}{2\pi} T_{xt} = -\phi' \dot{\phi} \ . \tag{5.2.7}$$

Time translation invariance then requires

$$\phi'_R \dot{\phi}_R - \phi'_L \dot{\phi}_L = \frac{dX}{dt} \tag{5.2.8}$$

for some local operator X. Using (5.2.2) it's easy to see that this requires

$$ad - bc = 1 \tag{5.2.9}$$

in which case

$$X = \frac{1}{2}\Big(ac\phi_L^2 + bd{\phi'_L}^2 + bc(\phi_L^2)' \Big) \ . \tag{5.2.10}$$

We will therefore restrict henceforth to matching conditions obeying (5.2.9).

Next we consider the restrictions imposed by demanding invariance of the correlation functions under scale transformations $x_i^\mu \rightarrow \lambda x_i^\mu$. The current is now

$$j_z = \frac{1}{2\pi i} z T_{zz} \ , \quad j_{\overline{z}} = \frac{-1}{2\pi i} \overline{z} T_{\overline{z}\overline{z}} \tag{5.2.11}$$

and the condition (5.2.4) becomes

$$\int_{-\infty}^{\infty} \phi'_L \dot{\phi}_L t dt = \int_{-\infty}^{\infty} \phi'_R \dot{\phi}_R t dt \ . \tag{5.2.12}$$

This now requires equality at the integrand level, $\phi'_L \dot{\phi}_L = \phi'_R \dot{\phi}_R$, which requires that $X = 0$ in (5.2.10). Along with (5.2.9) this imposes $d = 1/a$ with $b = c = 0$ as the condition of scale invariance. Assuming just scale invariance we automatically have conformal invariance since the currents

$$j_z^{(n)} = \frac{1}{2\pi i} z^n T_{zz} \ , \quad j_{\overline{z}}^{(n)} = \frac{(-1)^n}{2\pi i} \overline{z}^n T_{\overline{z}\overline{z}} \ , \quad n = 0, 1, 2, \ldots \tag{5.2.13}$$

automatically obey (5.2.4), corresponding to a single copy of Virasoro currents.

An even more restrictive condition is to allow symmetries under both the holomorphic and anti-holomorphic Virasoro currents. This impose the additional condition $\dot\phi_L^2 - (\phi_L')^2 = \dot\phi_R^2 - (\phi_R')^2$, which requires $a = d = \pm 1$ with $b = c = 0$. This defines a topological (or transparent) interface. In particular, we have the nontrivial case of $a = d = -1$ for which ϕ flips sign across the defect.

Given the matching conditions (5.2.2) it is natural to ask for an action that reproduces these. In this section we look for an action whose variational principle implies the matching conditions. Later we develop a second approach in which the defect action is treated diagrammatically by summing up Feynman diagrams.

In considering the form of a defect action an immediate issue is that the field and its first derivative are discontinuous across the defect, rendering ambiguous the meaning of the "field on the defect". To avoid this issue we work with two fields (ϕ_L, ϕ_R) defined at $(x = 0^-, x = 0^+)$, as already anticipated in (5.2.1). The appropriate form of S_d appearing in (5.2.1) turns out to take the form

$$S_d = \int dt \big[(\phi_R - \phi_L)\, \phi_A' + \frac{1}{2}\tilde c_1 \phi_A^2 + \tilde c_2 \phi_A \phi_A' + \frac{1}{2}\tilde c_3\, (\phi_A')^2 \big] \tag{5.2.14}$$

where we have defined the averaged field

$$\phi_A = \frac{\phi_L + \phi_R}{2}\ . \tag{5.2.15}$$

The tildes on $\tilde c_i$ are there to distinguish these couplings from analogous couplings that will appear in an alternative formulation. To read off the boundary conditions we compute the on-shell variation of the action, which works out to be

$$\delta S = -\int dt \Big([\phi_R' - \phi_L' - \tilde c_1 \phi_A - \tilde c_2 \phi_A']\, \delta\phi_A + [\phi_L - \phi_R - \tilde c_2 \phi_A - \tilde c_3 \phi_A']\, \delta\phi_A' \Big)\ . \tag{5.2.16}$$

A good variational principle is thus achieved by imposing the following conditions at the defect

$$\begin{aligned} &\phi_R' - \phi_L' - \tilde c_1 \phi_A - \tilde c_2 \phi_A' = 0\ , \\ &\phi_L - \phi_R - \tilde c_2 \phi_A - \tilde c_3 \phi_A' = 0\ . \end{aligned} \tag{5.2.17}$$

These conditions may be put in the form (5.2.2) with

$$\begin{pmatrix} a & b \\ c & d \end{pmatrix} = \begin{pmatrix} \frac{(2-\tilde{c}_2)^2-\tilde{c}_1\tilde{c}_3}{4-\tilde{c}_2^2+\tilde{c}_1\tilde{c}_3} & \frac{-4\tilde{c}_3}{4-\tilde{c}_2^2+\tilde{c}_1\tilde{c}_3} \\ \frac{4\tilde{c}_1}{4-\tilde{c}_2^2+\tilde{c}_1\tilde{c}_3} & \frac{(2+\tilde{c}_2)^2-\tilde{c}_1\tilde{c}_3}{4-\tilde{c}_2^2+\tilde{c}_1\tilde{c}_3} \end{pmatrix} . \tag{5.2.18}$$

This obeys $ad - bc = 1$ as expected. Inverting gives

$$\tilde{c}_1 = \frac{4ac}{(a+1)^2+bc} , \quad \tilde{c}_2 = \frac{2a(d-a)}{(a+1)^2+bc} , \quad \tilde{c}_3 = \frac{-4ab}{(a+1)^2+bc} . \tag{5.2.19}$$

The condition of conformal invariance, $a = 1/d$ and $b = c = 0$ translates to $\tilde{c}_1 = \tilde{c}_3 = 0$, giving $a = \frac{2-\tilde{c}_2}{2+\tilde{c}_2}$. Further taking $\tilde{c}_2 \rightarrow \pm\infty$ yields the nontrivial topological defect with $b = c = 0$ and $a = d = -1$.

Although we will not consider it further in this chapter, in order to make contact with previous work [89] we now comment on how to incorporate matching conditions of the form

$$\begin{pmatrix} \dot{\phi}_R \\ \phi'_R \end{pmatrix} = \begin{pmatrix} a & b \\ c & d \end{pmatrix} \begin{pmatrix} \dot{\phi}_L \\ \phi'_L \end{pmatrix} \tag{5.2.20}$$

in this framework. For example, the case $a = d = 0$, $b = 1/c$ yields a conformal defect not included in our analysis above. To incorporate this example we consider the action (5.2.1) and now choose

$$S_d = c \int dt \dot{\phi}_L \phi_R \tag{5.2.21}$$

so that

$$\delta S = \int dt \big[(\phi'_L - c\dot{\phi}_R)\delta\phi_L - (\phi'_R - c\dot{\phi}_L)\delta\phi_R \big], \tag{5.2.22}$$

which implies the stated matching conditions.

5.2.2 Perturbative action approach

Another approach is to consider the action

$$S = \int d^2x (\partial\phi)^2 + S_d \tag{5.2.23}$$

with

$$S_d = \int dt \left(c_0^B + \frac{1}{2} c_1^B \phi^2 + c_2^B \phi\phi' + \frac{1}{2} c_3^B \phi'^2 \right) \tag{5.2.24}$$

and to compute correlators and other quantities via perturbative expansion in the couplings c_i^B, as in [83,84]. To regulate the ultraviolet divergences that appear in perturbation theory we introduce a cutoff on the momentum transverse to the defect, $|p| < \Lambda$, and express the bare couplings c_i^B in terms of renormalized couplings c_i as in (5.1.5). This will be illustrated in the next section when we compute the scalar 2-point function in the presence of the defect by summing up the perturbative expansion.

In this approach ϕ and ϕ' are treated as being continuous across the defect at each order in perturbation theory.[6] Indeed, the defect action (5.2.24) would be ambiguous if discontinuities were allowed. Nonetheless the resummed two-point correlation exhibits discontinuities that satisfy the matching conditions (5.2.2). So we recover the same correlators as in the (ϕ_L, ϕ_R) approach, and the dictionary equating the two turns out to be extremely simple, $\tilde{c}_i = c_i$.

We now explain the sense in which the action (5.2.24) represents what is effectively the most general local action quadratic in fields. First consider the inclusion of terms with time derivatives, $\frac{1}{2}\dot{\phi}^2$ etc. In momentum space this becomes $\frac{1}{2}\omega^2\tilde{\phi}^2$, where ω represents the momentum along the time direction. Since the action is quadratic and ω is conserved by time translation invariance, there is no mixing among different values of ω. Hence the effect of a $\frac{1}{2}\dot{\phi}^2$ term is equivalent to redefining $c_1^B \to c_1^B + \omega^2$. More generally, all terms involving time derivatives can be included by allowing $c_{1,2,3}^B$ to be arbitrary functions of ω. Computing momentum space correlation functions in the presence of ω dependent couplings is the same as for constant couplings since the value of ω is conserved in any connected correlator. For this reason we will not explicitly consider terms with time derivatives, noting that they are simple to include if desired.

[6] Since we impose a momentum cutoff Λ the defect is effectively smeared out, and the fields are continuous within this smeared region, which shrinks to zero as the cutoff is removed.

We can also add terms in the defect action involving ϕ'' and higher transverse derivatives. However, by using the field equations — equivalently, the equations of motion — such terms can always be traded for terms involving only ϕ and ϕ' and time derivatives thereof,[7] and we already discussed the incorporation of such time derivative terms in the previous paragraph.

Finally, it is worth commenting that while we focus on $d = 1 + 1$ examples with a line defect, what really matters as far as most of our computations go is the defect codimension. A codimension-1 planar defect in d dimension can be treated uniformly for any d, as follows from the fact that the $d - 1$ momenta parallel to the defect are conserved in any connected diagram contributing to a momentum space correlator. On the other hand, extending our computations to codimension-q defects is nontrivial, since the 1-dimensional loop integrals we encounter turn into q-dimensional loop integrals, which of course changes the divergence structure among other things. Other codimensions were considered in [83, 84]

5.3 Scalar two-point function in presence of defect

In this section we use the perturbative approach described in section 5.2.2 to compute the scalar two-point function in the presence of a defect. The defect is placed at $x = 0$ and the Euclidean action is

$$\begin{aligned} S &= \frac{1}{2}\int d^2x(\dot{\phi}^2 + \phi'^2) + \int dt\big(\frac{1}{2}c_1^B\phi^2 + c_2^B\phi\phi' + \frac{1}{2}c_3^B\phi'^2\big) \\ &= \frac{1}{2}\int \frac{d\omega dp}{(2\pi)^2}\tilde{\phi}(-\omega,-p)(\omega^2+p^2)\tilde{\phi}(\omega,p) \\ &\quad + \frac{1}{2}\int \frac{d\omega dp_1 dp_2}{(2\pi)^3}\tilde{\phi}(-\omega,p_2)\big(c_1^B + ic_2^B(p_1+p_2) - c_3^B p_1 p_2\big)\tilde{\phi}(\omega,p_1) \end{aligned} \tag{5.3.1}$$

where we Fourier transformed as

$$\phi(x,t) = \int \frac{d\omega dp}{(2\pi)^2}\tilde{\phi}(\omega,p)e^{i\omega t + ipx} \ . \tag{5.3.2}$$

[7] We illustrate this with an example in appendix C.1.

The c_i^B denote bare couplings that depend on a UV cutoff Λ to be introduced below. These will eventually be re-expressed in terms of renormalized couplings c_i that are finite as $\Lambda \to \infty$. In the above we have omitted the defect cosmological constant term $\int dt c_0^B$ since it doesn't affect the connected diagrams contributing to the 2-point function. The full correlator is the product of the connected part and vacuum diagram contribution; the latter will be included in section 5.4, while in this section we consider only the connected part.

5.3.1 Computation

Our strategy in this section is to treat the defect action as a perturbation and then sum up contributions to all orders. We will compute the sum of connected diagrams in momentum space (thus omitting the defect self-energy vacuum diagrams, which will be discussed in section 5.4). This is shown in Figure 5.3.

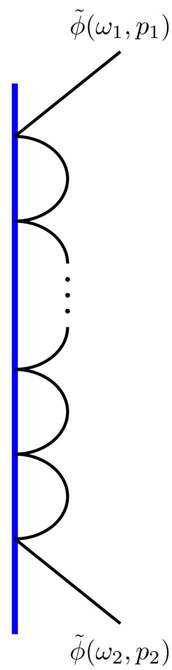

Figure 5.3: The defect (blue) contributes the quadratic interaction vertices to the connected two point correlation function (shown in momentum space). We sum up these contributions.

The two-point function takes the form

$$\langle\tilde{\phi}(\omega_1,p_1)\tilde{\phi}(\omega_2,p_2)\rangle = \langle\tilde{\phi}(\omega_1,p_1)\tilde{\phi}(\omega_2,p_2)\rangle_0 + \langle\tilde{\phi}(\omega_1,p_1)\tilde{\phi}(\omega_2,p_2)\rangle_d \tag{5.3.3}$$

where the correlator in the absence of the defect is

$$\langle\tilde{\phi}(\omega_1,p_1)\tilde{\phi}(\omega_2,p_2)\rangle_0 = \frac{1}{\omega_1^2+p_2^2}(2\pi)^2\delta(\omega_1+\omega_2)\delta(p_1+p_2) \tag{5.3.4}$$

while the contribution from the defect takes the form

$$\langle\tilde{\phi}(\omega_1,p_1)\tilde{\phi}(\omega_2,p_2)\rangle_d = \frac{2\pi\delta(\omega_1+\omega_2)}{(\omega_1^2+p_1^2)(\omega_2^2+p_2^2)}X(\omega_1,p_1,p_2)\ . \tag{5.3.5}$$

where the to-be-computed object X may be expanded in powers of the bare couplings,

$$X(\omega_1,p_1,p_2) = \sum_{n=0}^{\infty} I_n(\omega_1,p_1,-p_2)\ , \quad I_n \sim (c_i^B)^{n+1}\ . \tag{5.3.6}$$

An elementary computation yields

$$I_0(\omega_1,p_1,p_2) = -c_1^B + ic_2^B(p_1-p_2) - c_3^B p_1 p_2\ . \tag{5.3.7}$$

The $I_{n>0}$ are then determined recursively via

$$\begin{aligned} I_{n+1}(\omega_1,p_1,p_2) &= \int_{-\Lambda}^{\Lambda}\frac{dq_1}{2\pi}\cdots\frac{dq_{n+1}}{2\pi}\frac{I_0(\omega_1,p_1,q_1)I_0(\omega_1,q_1,q_2)\ldots I_0(\omega_1,q_{n+1},p_2)}{(\omega_1^2+q_1^2)\ldots(\omega_1^2+q_{n+1}^2)} \\ &= \int_{-\Lambda}^{\Lambda}\frac{dq_{n+1}}{2\pi}\frac{I_n(\omega_1,p_1,q_{n+1})I_0(\omega_1,q_{n+1},p_2)}{\omega_1^2+q_{n+1}^2} \end{aligned} \tag{5.3.8}$$

where we have introduced the UV cutoff Λ. Evaluating for $n=0$ gives a linearly divergent part and a finite part,

$$\begin{aligned} I_1(\omega_1,p_1,p_2) &= \hat{\Lambda}(c_2^B - ic_3^B p_1)(c_2^B + ic_3^B p_2) \\ &\quad - \left[(c_1^B - ic_2^B p_1)(c_1^B + ic_2^B p_2) - \omega_1^2(c_2^B - ic_3^B p_1)(c_2^B + ic_3^B p_2)\right] f_\Lambda(\omega_1) \end{aligned} \tag{5.3.9}$$

where

$$\hat{\Lambda} \equiv \frac{\Lambda}{\pi} \tag{5.3.10}$$

and

$$f_\Lambda(\omega_1) = \frac{1}{2\pi}\int_{-\Lambda}^{\Lambda}\frac{dq}{q^2+\omega_1^2} = \frac{1}{\pi\omega_1}\tan^{-1}\frac{\Lambda}{\omega_1}\ . \tag{5.3.11}$$

To solve the recursion relation it's useful write out the p_2 dependence of $I_n(\omega_1, p_1, p_2)$ as

$$I_n(\omega_1, p_1, p_2) = a_n + b_n p_2\ . \tag{5.3.12}$$

From (5.3.7) we have

$$\begin{aligned} a_0 &= -c_1^B + ic_2^B p_1\ , \\ b_0 &= -ic_2^B - c_3^B p_1\ . \end{aligned} \tag{5.3.13}$$

Then the recursion relation (5.3.8) becomes

$$\begin{pmatrix} a_{n+1} \\ b_{n+1} \end{pmatrix} = \begin{pmatrix} M_{11} & M_{12} \\ M_{21} & M_{22} \end{pmatrix}\begin{pmatrix} a_n \\ b_n \end{pmatrix} \tag{5.3.14}$$

with

$$\begin{aligned} M_{11} &= -c_1^B f_\Lambda(\omega_1) \qquad M_{12} = ic_2^B\left(\hat{\Lambda} - \omega_1^2 f_\Lambda(\omega_1)\right) \\ M_{21} &= -ic_2^B f_\Lambda(\omega_1) \qquad M_{22} = -c_3^B\left(\hat{\Lambda} - \omega_1^2 f_\Lambda(\omega_1)\right)\ . \end{aligned} \tag{5.3.15}$$

This allows us to compute X as

$$\begin{aligned} X(\omega_1, p_1, p_2) &= \sum_{n=0}^{\infty} I_n(\omega_1, p_1, -p_2) \\ &= \sum_{n=0}^{\infty}(a_n - b_n p_2) \\ &= \sum_{n=0}^{\infty}\begin{pmatrix} 1 & -p_2 \end{pmatrix}\begin{pmatrix} a_n \\ b_n \end{pmatrix} \\ &= \sum_{n=0}^{\infty}\begin{pmatrix} 1 & -p_2 \end{pmatrix} M^n \begin{pmatrix} a_0 \\ b_0 \end{pmatrix} \\ &= \begin{pmatrix} 1 & -p_2 \end{pmatrix}(I - M)^{-1}\begin{pmatrix} a_0 \\ b_0 \end{pmatrix}\ . \end{aligned} \tag{5.3.16}$$

Evaluating gives

$$X(\omega_1, p_1, p_2) = \\ \frac{-c_1^B + (c_1^B c_3^B - (c_2^B)^2)\left[\hat{\Lambda} - \omega_1^2 f_\Lambda(\omega_1)\right] + ic_2^B(p_1+p_2) + \left[(c_1^B c_3^B - (c_2^B)^2) f_\Lambda(\omega_1) + c_3^B\right] p_1 p_2}{\det(I-M)} \tag{5.3.17}$$

with

$$\det(I-M) = 1 + c_1^B f_\Lambda(\omega_1) + \left[(c_1^B c_3^B - (c_2^B)^2) f_\Lambda(\omega_1) + c_3^B\right]\left[\hat{\Lambda} - \omega_1^2 f_\Lambda(\omega_1)\right] . \tag{5.3.18}$$

Now we wish to remove the cutoff Λ. To do so, we expand order by order in the c_i^B, and then rewrite them in terms of Λ and renormalized couplings c_i such that $\Lambda \to \infty$ limit at fixed c_i is well defined. This procedure results in

$$\begin{aligned} c_1^B &= c_1 + \frac{c_2^2 \hat{\Lambda}}{1 - c_3 \hat{\Lambda}} , \\ c_2^B &= \frac{c_2}{1 - c_3 \hat{\Lambda}} , \\ c_3^B &= \frac{c_3}{1 - c_3 \hat{\Lambda}} . \end{aligned} \tag{5.3.19}$$

Taking the large Λ limit, using $\lim_{\Lambda \to \infty} f_\Lambda(\omega_1) = \frac{1}{2|\omega_1|}$, then yields our final result for the renormalized correlator

$$X(\omega_1, p_1, p_2) = \frac{-c_1 + \frac{|\omega_1|}{2}(c_1 c_3 - c_2^2) + ic_2(p_1+p_2) + \left(\frac{1}{2|\omega_1|}(c_1 c_3 - c_2^2) + c_3\right) p_1 p_2}{1 + \frac{1}{2|\omega_1|}(c_1 - c_3 \omega_1^2) - \frac{1}{4}(c_1 c_3 - c_2^2)} . \tag{5.3.20}$$

5.3.2 Matching conditions from the correlator

The result (5.3.20) can be used to infer matching conditions (5.2.2) across the defect. We first Fourier transform to position space in the direction transverse to the defect by defining

$$\begin{aligned} G(x_1, x_2) &= \int \frac{dp_1}{2\pi}\frac{dp_2}{2\pi} \langle \tilde{\phi}(\omega_1, p_1) \tilde{\phi}(\omega_2, p_2) \rangle e^{ip_1 x_1 + ip_2 x_2} \\ &= \hat{G}(x_1, x_2) 2\pi \delta(\omega_1 + \omega_2) \end{aligned} \tag{5.3.21}$$

with

$$\hat{G}(x_1,x_2)=\int\frac{dp_1}{2\pi}\frac{e^{ip_1(x_1-x_2)}}{p_1^2+\omega_1^2}+\int\frac{dp_1}{2\pi}\frac{dp_2}{2\pi}\frac{X(\omega_1,p_1,p_2)}{(\omega_1^2+p_1^2)(\omega_2^2+p_2^2)}e^{ip_1x_1+ip_2x_2}\ . \tag{5.3.22}$$

Note that in G and $\hat{G}$ we have suppressed the dependence on the frequencies $\omega_{1,2}$. Now suppose a function takes the form

$$f(x)=\int_{-\infty}^{\infty}\frac{dp}{2\pi}\frac{\alpha+\beta p}{\omega^2+p^2}e^{ipx}\ . \tag{5.3.23}$$

Using elementary contour integration, the values of the function on either side of the origin are

$$f(\pm\epsilon)=\frac{\alpha}{2|\omega|}\pm\frac{i\beta}{2}\ ,\quad f'(\pm\epsilon)=\mp\frac{\alpha}{2}-\frac{i\beta|\omega|}{2}\ . \tag{5.3.24}$$

If we apply these formulas to (5.3.21) and (5.3.20) for $x_1=\pm\epsilon$ we find

$$\begin{pmatrix}\hat{G}(\epsilon,x_2)\\ \hat{G}'(\epsilon,x_2)\end{pmatrix}=\begin{pmatrix}a&b\\ c&d\end{pmatrix}\begin{pmatrix}\hat{G}(-\epsilon,x_2)\\ \hat{G}'(-\epsilon,x_2)\end{pmatrix} \tag{5.3.25}$$

with

$$\begin{pmatrix}a&b\\ c&d\end{pmatrix}=\begin{pmatrix}\frac{(2-c_2)^2-c_1c_3}{4-c_2^2+c_1c_3}&\frac{-4c_3}{4-c_2^2+c_1c_3}\\ \frac{4c_1}{4-c_2^2+c_1c_3}&\frac{(2+c_2)^2-c_1c_3}{4-c_2^2+c_1c_3}\end{pmatrix}\ . \tag{5.3.26}$$

We recognize the matrix as being the same as appeared in (5.2.18), except that the couplings are now the renormalized couplings that appear in the perturbative formulation. Hence we identify $\tilde{c}_i=c_i$. The equality between these two sets of couplings is not obvious a priori.

5.3.3 Special cases

We now consider several special cases of interest.

5.3.3.1 IR/UV limit

To extract the IR/UV limits we rescale the momenta as $(\omega, p) \to (\lambda\omega, \lambda p)$. From (5.3.20) we find

$$X(\omega, p_1, p_2) \to \begin{cases} -2|\omega| & (\omega, k) \to 0 \\ -\frac{2p_1 p_2}{|\omega|} & (\omega, k) \to \infty \end{cases} . \tag{5.3.27}$$

This implies (after a bit of rewriting) the following result for the IR/UV limit of the correlator

$$\langle \phi(t_1, x_1)\phi(t_2, x_2)\rangle = \int_{-\infty}^{\infty} \frac{d\omega}{2\pi} \frac{e^{i\omega(t_1-t_2)}}{2|\omega|} \left[e^{-|\omega||x_1-x_2|} \pm e^{-|\omega|(x_1+x_2)}\right] \tag{5.3.28}$$

where we have taken $x_{1,2} > 0$, and the relative sign is $+$ in the UV and $-$ in the IR. The first term on the right hand side is the correlator in the absence of the defect, and the second term represents the image charge contribution appropriate for a Neumann ($+$ sign) or Dirichlet ($-$ sign) boundary condition. This aligns with the fact that the $c_3(\phi')^2$ term in the defect action dominates in the UV, setting $\phi' = 0$ on the defect; while $c_1\phi^2$ dominates in the IR, setting $\phi = 0$ on the defect.

5.3.3.2 Conformal defect

Here we set the dimensionful couplings to zero: $c_1 = c_3 = 0$. We take $x_1 > 0$ but allow either sign for x_2, yielding the defect contribution

$$\langle \phi(t_1, x_1)\phi(t_2, x_2)\rangle_d = \int_{-\infty}^{\infty} \frac{d\omega}{2\pi} \frac{e^{i\omega(t_1-t_2)}}{2|\omega|} \left\{ \begin{array}{ll} -\frac{2c_2^2}{4+c_2^2} e^{-|\omega|(x_1-x_2)} & x_2 < 0 \\ -\frac{4c_2}{4+c_2^2} e^{-|\omega|(x_1+x_2)} & x_2 > 0 \end{array} \right\} . \tag{5.3.29}$$

5.3.3.3 Topological defect

For this we take the $c_2 \to \infty$ limit of the conformal case. The total correlator in this limit, including the free part, is

$$\langle \phi(t_1, x_1)\phi(t_2, x_2)\rangle = \int_{-\infty}^{\infty} \frac{d\omega}{2\pi} \frac{e^{i\omega(t_1-t_2)}}{2|\omega|} \left\{ \begin{array}{cc} -e^{-|\omega|(x_1-x_2)} & x_2 < 0 \\ e^{-|\omega||x_1-x_2|} & x_2 > 0 \end{array} \right\} \tag{5.3.30}$$

where we have again taken $x_1 > 0$ but allow either sign of x_2. This exhibits a sign flip of the correlator as x_2 crosses the origin, as characterizes the topological defect.

5.3.4 Poles

The correlator exhibits poles in ω_1 when the denominator of $X(\omega_1, p_1, p_2)$ in (5.3.20) vanishes. Rewriting this vanishing condition in terms of (a, b, c, d) given in (5.3.26) yields

$$\text{poles}: \quad b\omega_1^2 + (a+d)|\omega_1| + c = 0 \ . \tag{5.3.31}$$

For $b \neq 0$ the roots are

$$\omega_{\pm} = \frac{-(a+d) \pm \sqrt{(a-d)^2 + 4}}{2b} \tag{5.3.32}$$

These roots are related to the existence of normalizable bound state modes in the presence of the defect, as we discuss in section 5.6.2. The existence of solutions with positive $\omega_{\pm}$ correspond to instabilities, i.e. modes that grow exponentially in real time. Coupling space can thus be divided into stable and unstable regions, as will be discussed in section 5.6.

5.4 Vacuum diagrams

We now consider the sum of vacuum diagrams in the presence of the defect as illustrated in Figure 5.4.

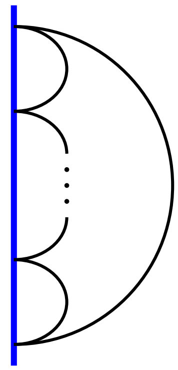

Figure 5.4: Defect contributions to the connected vacuum diagram for $\langle e^{-S_d}\rangle$

This can equivalently be thought of as computing the vacuum expectation value of the defect operator,

$$Z_{\text{vac}} = e^W = \langle e^{-S_d}\rangle \ , \tag{5.4.1}$$

where W represents the connected contributions. We can evaluate W by summing diagrams, similarly to how we computed the correlator, and arrive at

$$W = -c_0^B L_d + L_d \sum_{n=0}^{\infty} \frac{1}{2(n+1)} \int_{-\infty}^{\infty} \frac{d\omega dp}{(2\pi)^2} \frac{I_n(p,p)}{\omega^2+p^2} \tag{5.4.2}$$

where $I_n(p_1,p_2)$ is the same integral defined in (5.3.8)-(5.3.9) that appeared in the correlator computation. To get a finite result we have given the defect a large but finite length L_d. We have also included the defect counterterm c_0^B.

To evaluate the sum it is useful to use the identity

$$\sum_{n=0}^{\infty} \frac{M^n}{n+1} = \int_0^1 \frac{dz}{I - zM} \tag{5.4.3}$$

involving the matrix M. We introduce a UV cutoff Λ and relate the bare couplings in S_d in terms of renormalized couplings as in (5.3.19). After some algebra we obtain

$$\begin{aligned} W &= -c_0^B L_d - L_d \int_0^1 dz \int_0^{\Lambda} \frac{d\omega}{2\pi} \frac{1}{\omega} \frac{\big(-2c_1 + \omega z(c_1c_3 - c_2^2)\big)\omega - \big(c_2^2 z - (2\omega + zc_1)c_3\big)\omega^2}{c_1c_3\omega z^2 - z^2c_2^2\omega + 2z\omega^2 c_3 - 2zc_1 - 4\omega} \\ &= -c_0^B L_d - L_d \int_0^{\Lambda} \frac{d\omega}{2\pi} \ln\left[\frac{-2c_3\omega^2 - (c_1c_3 - c_2^2 - 4)\omega + 2c_1}{4\omega}\right] \ . \end{aligned} \tag{5.4.4}$$

The divergence structure depends on whether the irrelevant c_3 and marginal c_2 couplings are turned on. In the simplest case with $c_2 = c_3 = 0$ we have

$$W = -c_0^B L_d - \frac{c_1 L_d}{4\pi} \ln \frac{2\Lambda}{c_1} - \frac{c_1 L_d}{4\pi} \ . \tag{5.4.5}$$

We therefore take $c_0^B = -\frac{c_1}{4\pi} \ln \frac{\Lambda}{\mu}$ where μ is an RG scale, yielding

$$W = -\frac{c_1 L_d}{4\pi} \left[1 - \ln\left(\frac{c_1}{2\mu}\right)\right] \tag{5.4.6}$$

The imaginary part for $c_1 < 0$ reflects the presence of unstable modes. The renormalized defect operator thus depends on the arbitrary RG scale μ as $\langle e^{-S_d}\rangle \propto \mu^{-\frac{c_1 L_d}{4\pi}}$. The fact that the log divergence is linear in c_1 implies that the defect anomalous dimension γ_d defined in (5.1.9) is one-loop exact when $c_2 = c_3 = 0$. However, for more general couplings γ_d gets contributions at all loop orders. For example, setting $c_3 = 0$ is easily found to imply a log divergent term that is canceled by taking

$$c_0^B = -\frac{1}{1 + \frac{1}{4}c_2^2} \frac{c_1}{4\pi} \ln(\Lambda/\mu) + [\text{linear divergence}] \tag{5.4.7}$$

yielding γ_d in (5.1.10). With all couplings $c_{1,2,3}$ nonzero one instead finds a divergent series.

5.5 Multiple defects

We now consider two parallel defects separated by a distance L. The partition function, which can be interpreted as computing the inter-defect potential, may be computed in the same manner as for the single defect.

5.5.1 Two defect partition function

Writing the defect action as

$$S_d = \sum_{a=1}^{2} \int dt \left(c_0^{(a),B} + \frac{1}{2} c_1^{(a),B} \phi^2(x_a, t) + c_2^{(a),B} \phi(x_a, t)\phi'(x_a, t) + \frac{1}{2} c_3^{(a),B} \phi'^2(x_a, t)\right) \tag{5.5.1}$$

with $x_2 - x_1 = L$ we compute $Z(L) = e^{W(L)} = \langle e^{-S_d} \rangle$ by summing vacuum diagrams. For simplicity we will just give the result for $c_2^{(a),B} = c_3^{(a),B} = 0$, which is

$$W(L) = L_d \left[\int_0^\Lambda \frac{d\omega}{2\pi} \ln \left(\left(1 + \frac{c_1^{(1)}}{2\omega}\right)\left(1 + \frac{c_1^{(2)}}{2\omega}\right) - \frac{c_1^{(1)} c_1^{(2)}}{4\omega^2} e^{-2\omega L} \right) - \frac{c_1^{(1)} + c_1^{(2)}}{4\pi} \ln \frac{\Lambda}{\mu} \right] \tag{5.5.2}$$

where we have rewritten the bare couplings in terms of renormalized couplings using the same expressions as before. The integral is log divergent, but the divergence is canceled by the c_0^B counterterms yielding a finite result as $\Lambda \to \infty$. For small separation we have

$$W(L) = \frac{(c_1^{(1)} + c_1^{(2)}) L_d}{4\pi} \left[1 - \ln \left(\frac{c_1^{(1)} + c_1^{(2)}}{2\mu} \right) \right] + \frac{c_1^{(1)} c_1^{(2)} L_d}{4\pi} L \ln L + \ldots \tag{5.5.3}$$

so that

$$Z(L) \approx Z(0) L^{c_1^{(1)} c_1^{(2)} L L_d / 4\pi} \, . \tag{5.5.4}$$

For $L = 0$ we recover the partition function of a single defect with $c_1 = c_1^{(1)} + c_1^{(2)}$, but the expansion in small L is neither analytic nor a power law.

5.5.2 Fusion of two defects

We now consider the fusion of two parallel defects. On general grounds, the fusion of two defects with some quadratic couplings $c_i^{(1,2)}$ should result a defect with new quadratic couplings c_i. The expectation is that the couplings c_i are determined by the composition of the matching conditions associated to two fused defects,

$$\begin{pmatrix} a & b \\ c & d \end{pmatrix} = \begin{pmatrix} a^{(2)} & b^{(2)} \\ c^{(2)} & d^{(2)} \end{pmatrix} \begin{pmatrix} a^{(1)} & b^{(1)} \\ c^{(1)} & d^{(1)} \end{pmatrix} \tag{5.5.5}$$

where we have taken defect 2 to be to the right of defect 1. According to this, the couplings c_i are then extracted from the map between (a, b, c, d) and c_i provided by (5.3.26). This yields a rather complicated relation between the c_i and the $c_i^{(1,2)}$.

To verify this, we can compute the scalar two-point function in the presence of the two defects separated by a distance L, then take $L \to 0$ and compare to our result for the single defect correlator. The contribution of the vacuum diagrams is summarized by (5.5.3). To define the fused defect via an OPE type procedure, we should strip off the factor of $L^{c_1^{(1)} c_1^{(2)} L L_d / 4\pi}$. The connected diagrams contributing to the correlator may be summed up using the same steps as for the single defect. The result for general L is complicated and unenlightening. In appendix C.2 we write the result for $L \to 0$. The result is as expected: the fused couplings c_i are in accord with the rule (5.5.4).

5.6 Mode expansion

Consider a free massive or massless ($m = 0$) non-compact scalar theory in $d = 1 + 1$ Minkowski spacetime

$$S = \int \mathrm{d}^2 x \, \frac{1}{2} \left[- \left(\partial_t \phi\right)^2 + \left(\partial_x \phi\right)^2 + m^2 \phi^2 \right] \; . \tag{5.6.1}$$

We are interested in a timelike defect described by the matching conditions at $x = 0$ that preserve the time translation symmetry

$$\begin{pmatrix} \phi_R \\ \phi_R' \end{pmatrix} = \begin{pmatrix} a & b \\ c & d \end{pmatrix} \begin{pmatrix} \phi_L \\ \phi_L' \end{pmatrix} , \quad ad - bc = 1 \tag{5.6.2}$$

where $\phi_{L,R} = \lim_{x \to 0^{\mp}} \phi(t, x)$. Assuming this matching condition, the Klein-Gordon (KG) inner product of two solutions,

$$(f, g) \equiv -i \int_{-\infty}^{\infty} \left(f \dot{g}^* - \dot{f} g^* \right) \mathrm{d}x \; . \tag{5.6.3}$$

is time independent if and only if $ad - bc = 1$, as indicated.

5.6.1 Massless scattering modes

There are two sets of scattering solutions to the field equation $\partial_\mu \partial^\mu \phi = 0$ subject to the matching condition (5.6.2), corresponding to waves incident from the left or right,

$$\varphi^v_\omega = \begin{cases} x < 0 : & \frac{1}{\sqrt{2\omega}} t_\omega e^{-i\omega v} \\ x > 0 : & \frac{1}{\sqrt{2\omega}} \left(e^{-i\omega v} + r^v_\omega e^{-i\omega u}\right) \end{cases}, \qquad \varphi^u_\omega = \begin{cases} x < 0 : & \frac{1}{\sqrt{2\omega}} \left(e^{-i\omega u} + r^u_\omega e^{-i\omega v}\right) \\ x > 0 : & \frac{1}{\sqrt{2\omega}} t_\omega e^{-i\omega u} \end{cases} \tag{5.6.4}$$

where $u = t - x$, $v = t + x$, and the transmission and reflection coefficients are

$$t_\omega = \frac{2i\omega}{b\omega^2 + i(a+d)\omega - c}, \quad r^v_\omega = \frac{b\omega^2 + i(a-d)\omega + c}{b\omega^2 + i(a+d)\omega - c}, \quad r^u_\omega = \frac{b\omega^2 - i(a-d)\omega + c}{b\omega^2 + i(a+d)\omega - c} . \tag{5.6.5}$$

We normalised the modes with respect to the KG inner product such that

$$(\varphi^v_\omega, \varphi^v_{\omega'}) = 2\pi\delta(\omega - \omega'), \quad (\varphi^u_\omega, \varphi^u_{\omega'}) = 2\pi\delta(\omega - \omega'), \quad (\varphi^u_\omega, \varphi^v_{\omega'}) = 0 \tag{5.6.6}$$

If there are no bound states, the scalar field can be quantised using the scattering solutions as

$$\phi(t, x) = \int_0^\infty \frac{\mathrm{d}\omega}{2\pi} \left(a^v_\omega \varphi^v_\omega + a^u_\omega \varphi^u_\omega + \text{h.c.}\right), \quad \pi(t, x) = \dot{\phi}(t, x) . \tag{5.6.7}$$

Writing

$$\begin{aligned} a^{v,u}_\omega &= (\phi, \varphi^{v,u}_\omega) = -i \int_{-\infty}^{\infty} \left(\phi(x) \dot{\varphi}^{v,u*}_\omega(x) - \pi(x) \varphi^{v,u*}_\omega(x)\right) \mathrm{d}x \\ a^{v,u\dagger}_\omega &= -\left(\phi, \varphi^{v,u*}_\omega\right) = i \int_{-\infty}^{\infty} \left(\phi(x) \dot{\varphi}^{v,u}_\omega(x) - \pi(x) \varphi^{v,u}_\omega(x)\right) \mathrm{d}x \end{aligned} \tag{5.6.8}$$

and using $[\phi(x), \pi(y)] = i\delta(x - y)$ at equal time, one can derive the canonical quantization conditions

$$[a_\omega, a^\dagger_{\omega'}] = 2\pi\delta(\omega - \omega') . \tag{5.6.9}$$

For this to be consistent, the classical solutions should satisfy the completeness condition derived from the the equal-time commutator

$$\begin{aligned} [\phi(x), \pi(y)] &= \int_0^\infty \frac{\mathrm{d}\omega}{2\pi} \left(\varphi^v_\omega(x) \dot{\varphi}^{v*}_\omega(y) - \varphi^{v*}_\omega(x) \dot{\varphi}^v_\omega(y)\right) + (v \leftrightarrow u) \\ &= i\delta(x - y) . \end{aligned} \tag{5.6.10}$$

Evaluated on the scattering solutions (5.6.4) and (5.6.5) we find,

$$[\phi(x), \pi(y)] = \begin{cases} i\delta(x-y) + i\int_0^\infty \frac{\mathrm{d}\omega}{2\pi} r_\omega e^{i\omega|x+y|} \ , & xy > 0 \\ i\int_0^\infty \frac{\mathrm{d}\omega}{2\pi} t_\omega \, e^{i\omega|x-y|} \ , & xy < 0 \end{cases} . \tag{5.6.11}$$

We see that completeness is satisfied provided r_ω and t_ω are analytic in the upper half ω-plane, since then the integrals can be converted into closed contour integrals that vanish by Cauchy's theorem. On the other hand, the existence of poles in the upper-half plane implies that the scattering solutions should be accompanied by bound states for completeness.

5.6.2 Bound state modes

The potential incompleteness of scattering modes leads us to examine the existence of normalizable bound state modes. These are solutions that decay exponentially as $|x| \to \infty$, and either grow or decay exponentially in t (the two cases being related by time reversal.) Plugging the following ansatz for modes that grow in t,

$$\phi = \begin{cases} x < 0 : & Ae^{\kappa v} \\ x > 0 : & Be^{\kappa u} \end{cases} , \qquad Re(\kappa) > 0 \tag{5.6.12}$$

where $Re(\kappa) > 0$ for normalizability, into the gluing condition (5.6.2), a normalizable mode is seen to exist if at least one solution to

$$b\kappa^2 + (a+d)\kappa + c = 0 \tag{5.6.13}$$

has a positive real part. Upon writing $\kappa = -i\omega$ we recognize (5.6.13) as giving the locations of the poles in the transmission/reflection coefficients (5.6.5). For $b \neq 0$ normalizable solutions exist if

$$\kappa_+ > 0 \ \text{ or } \ \kappa_- > 0, \quad \kappa_\pm = -\frac{a+d \pm \sqrt{(a-d)^2+4}}{2b} . \tag{5.6.14}$$

For $b = 0$ we have $\kappa = -\frac{ac}{1+a^2}$ (using $d = 1/a$) so that normalizable modes exist for $ac < 0$. In the previous section, we saw that the scattering modes alone are not complete when

$\mathrm{Im}(\omega_+) > 0$ or $\mathrm{Im}(\omega_-) > 0$. This is precisely the condition for the existence of the bound states, $\mathrm{Re}(\kappa_+) > 0$ or $\mathrm{Re}(\kappa_-) > 0$, illustrated in Figure 5.5.

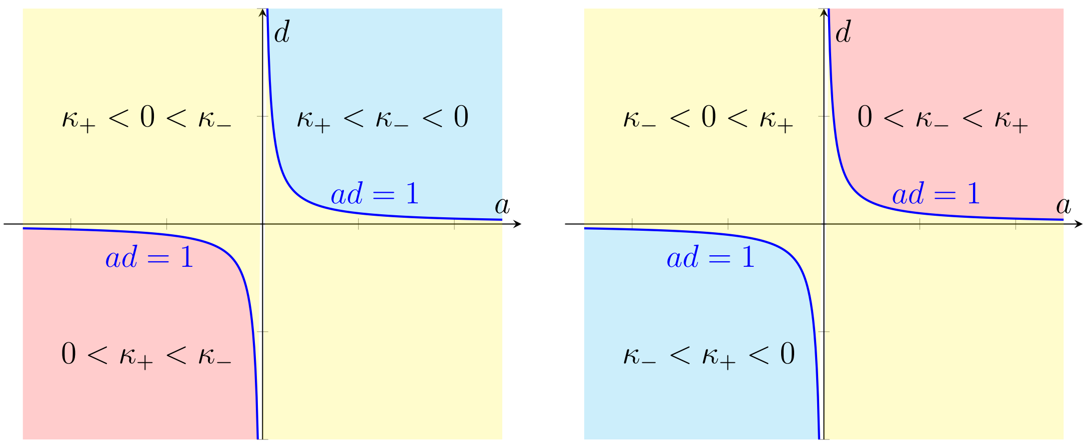

(a) $b > 0$ (b) $b < 0$

Figure 5.5: Regions of (a, b, d) space where $\kappa_\pm$ have various signs. One of the signs flips across the blue curves. There are two normalisable decaying modes in the red region, one in yellow region and none in the blue region respectively.

For such a case, the solutions come in a pair $(\phi_\pm, \bar{\phi}_\pm)$ related by time reversal,

$$\phi_\pm = \begin{cases} x < 0 : & N_\pm^{-1} e^{\kappa_\pm v} \\ x > 0 : & N_\pm^{-1} \left(a + b\kappa_\pm\right) e^{\kappa_\pm u} \end{cases}, \qquad \bar{\phi}_\pm = \begin{cases} x < 0 : & \bar{N}_\pm^{-1} e^{-\kappa_\pm u} \\ x > 0 : & \bar{N}_\pm^{-1} \left(a + b\kappa_\pm\right) e^{-\kappa_\pm v} \end{cases} \tag{5.6.15}$$

where the normalization

$$N_\pm^{-1} = \bar{N}_\pm^{-1} = \frac{1}{\sqrt{1 + \left(a + b\kappa_\pm\right)^2}} \tag{5.6.16}$$

is chosen such that the solutions are real-valued and satisfy $(\phi_\pm, \bar{\phi}_\pm) = i$.

The $\phi_\pm$ modes grow exponentially in time, hence the theory is unstable when such modes exist. Nonetheless, we can formally quantize the scalar field as

$$\phi(t, x) = \int_0^\infty \frac{\mathrm{d}\omega}{2\pi} \left(a_\omega \varphi_\omega^L + b_\omega \varphi_\omega^R + \text{ h.c. }\right) + c_+\phi_+ + \bar{c}_+\bar{\phi}_+ + c_-\phi_- + \bar{c}_-\bar{\phi}_- \tag{5.6.17}$$

where $c_\pm$ are hermitian, for $\omega_\pm > 0$ and similarly for other cases. The same process used to derive (5.6.9) can be recycled to derive the commutation of the modes for the bound states

$$[c_\pm, \bar{c}_\pm] = (\phi_\pm, \bar{\phi}_\pm) = i \ . \tag{5.6.18}$$

Using this, the contribution from the decaying modes to the equal-time commutator $[\phi(x), \pi(y)]$ exactly cancels the incomplete contribution (5.6.11) from the scattering modes and hence restores the completeness

$$[\phi(x), \pi(y)] = i\delta(x - y) \ . \tag{5.6.19}$$

5.6.3 Spectrum

The classical normalizable modes grow exponentially in time, and when such modes exist the Hamiltonian suffers from a spectrum unbounded from below. To see this, first note that the bulk Hamiltonian $H = \frac{1}{2}\int_{-\infty}^{\infty}\left(\dot{\phi}^2 + (\phi')^2\right) \mathrm{d}x$ has a time dependence

$$\frac{\mathrm{d}H}{\mathrm{d}t} = \frac{\mathrm{d}}{\mathrm{d}t}\left(bc\phi_L'\phi_L + \frac{ac}{2}\phi_L^2 + \frac{bd}{2}\left(\phi_L'\right)^2\right) \ . \tag{5.6.20}$$

The Hamiltonian can be made time-independent by subtracting the total derivative above

$$H_{tot} = H - \left(bc\phi_L'\phi_L + \frac{ac}{2}\phi_L^2 + \frac{bd}{2}\left(\phi_L'\right)^2\right) \tag{5.6.21}$$

corresponding to the defect Hamiltonian. The total Hamiltonian restricted to the normalizable modes is

$$H_{tot} = -\frac{\kappa_+}{2}\left(c_+\bar{c}_+ + \bar{c}_+c_+\right) - \frac{\kappa_-}{2}\left(c_-\bar{c}_- + \bar{c}_-c_-\right) \ . \tag{5.6.22}$$

Renaming $c_+ = \frac{1}{\sqrt{2}}(p + x), \bar{c}_+ = \frac{1}{\sqrt{2}}(p - x)$, H_{tot} is that of the inverted harmonic oscillator, which is known to have continuous spectrum unbounded from below and above, assuming a boundary condition that requires the wave function to vanish at spatial infinity [122]. The unbounded spectrum implies that whenever there is a bound state, the massless theory with matching condition (5.6.2) is ill-defined. However, the instability of the classical solutions and the unbounded spectrum can by cured by adding a mass, as we describe in the next subsection, or by adding bulk interactions, as discussed in Appendix C.3. Alternatively, we can restrict attention to the stable regime shown in Figure 5.5 (blue region).

5.6.4 Massive scalar mode expansion

The massive scalar theory with matching condition (5.6.2) has scattering modes given by

$$\varphi_k^L = \begin{cases} x < 0 : & \frac{1}{\sqrt{2\omega}} t_k e^{-i\omega t - ikx} \\ x > 0 : & \frac{1}{\sqrt{2\omega}} \left(e^{-i\omega t - ikx} + r_k e^{-i\omega t + ikx} \right) \end{cases} \tag{5.6.23}$$

$$\varphi_k^R = \begin{cases} x < 0 : & \frac{1}{\sqrt{2\omega}} \left(e^{-i\omega t + ikx} + r_k e^{-i\omega t - ikx} \right) \\ x > 0 : & \frac{1}{\sqrt{2\omega}} t_k e^{-i\omega t + ikx} \end{cases} \tag{5.6.24}$$

where $\omega = \sqrt{k^2 + m^2}$ and t_k and r_k are the same as t_ω and r_ω (5.6.5) with $\omega \to k$.

As in the massless case, bound state modes exist if at least one of $\kappa_\pm$ given in Eq. (5.6.14) has positive real part. When they exist, those with $\kappa_+^2 > m^2$ or $\kappa_-^2 > m^2$ are unstable, while those with $\kappa_+^2 < m^2$ or $\kappa_- < m^2$ are oscillatory. We focus on the oscillatory modes, which are given by

$$\phi_\pm = \begin{cases} x < 0 : & N_\pm^{-1} e^{-i\bar{\omega}_\pm t + \kappa_\pm x} \\ x > 0 : & N_\pm^{-1} \left(a + b\kappa_\pm \right) e^{-i\bar{\omega}_\pm t - \kappa_\pm x} \end{cases} \tag{5.6.25}$$

where

$$\kappa_\pm = -\frac{a + d \pm \sqrt{(a-d)^2 + 4}}{2b} > 0, \quad \bar{\omega}_\pm = \sqrt{m^2 - \kappa_\pm^2} \in \mathbb{R} \tag{5.6.26}$$

and

$$N_+^{-1} = \sqrt{\frac{\kappa_+}{\bar{\omega}_+}} \sqrt{\frac{1}{1 + \left(a + b\kappa_+\right)^2}} \in \mathbb{R}^+ \tag{5.6.27}$$

The scalar field is quantized as

$$\phi(t,x) = \int_0^\infty \frac{\mathrm{d}\kappa}{2\pi} \left(a_\kappa \varphi_\kappa^L + b_\kappa \varphi_\kappa^R + h.c. \right) + \left(c_+ \phi_+ + c_- \phi_- + h.c. \right) \tag{5.6.28}$$

where

$$\left[c_\pm, c_\pm^\dagger \right] = \left(\phi_\pm, \phi_\pm \right) = 1 \tag{5.6.29}$$

when both $\kappa_\pm > 0$ and similarly for other cases by dropping some bound state modes. The Hamiltonian restricted to the bound states is

$$H = \frac{\bar{\omega}_+}{2}\left(c_+^\dagger c_+ + c_+ c_+^\dagger\right) + \frac{\bar{\omega}_+}{2}\left(c_-^\dagger c_- + c_- c_-^\dagger\right) \;\; = \bar{\omega}_+\left(\bar{c}_+ c_+ + \frac{1}{2}\right) + \bar{\omega}_-\left(\bar{c}_- c_- + \frac{1}{2}\right) \;. \tag{5.6.30}$$

Defining the vacuum state as $c_\pm|0\rangle = 0$, one can see that the spectrum is positive.

5.7 Ring partition function, g-function, and entanglement entropy of accelerating defects

5.7.1 Ring partition function

In this section we compute the partition function of a ring shaped defect. In order to apply this result to the applications that follows, we consider placing the ring on a cone. Namely, we consider

$$ds^2 = dr^2 + r^2 d\theta^2 \;, \quad \theta \cong \theta + \beta \tag{5.7.1}$$

with the ring placed at $r = 1$.[8] The ring partition function may be written as

$$Z(\beta) = \langle 0|e^{-S_d}|0\rangle \tag{5.7.2}$$

where we interpret the states in terms of radial quantization and think of e^{-S_d} as an operator on this Hilbert space. We will consider the simplest case of $c_2 = c_3 = 0$; in this case e^{-S_d} is diagonalized in the field eigenstate basis, since the "conjugate momentum" ϕ' does not appear in the defect action. Letting $\overline{\phi}(\theta) = \phi(r = 1, \theta)$ we then have

$$Z(\beta) = \int \mathcal{D}\overline{\phi}\langle 0|\overline{\phi}\rangle e^{-S_d[\overline{\phi}]}\langle\overline{\phi}|0\rangle \;. \tag{5.7.3}$$

We compute $\langle\overline{\phi}|0\rangle$ by computing the free scalar path integral in the region $r \leq 1$ with boundary condition $\phi(r = 1, \theta) = \overline{\phi}(\theta)$. We will only be interested in the c_1 dependence of

[8] Choosing $r = 1$ implies no loss of generality since we can always rescale r along with the couplings.

$\log Z(\beta)$, in which case we only need the saddle point approximation to the path integral since the fluctuation determinant does not depend on c_1.

Writing

$$\overline{\phi}(\theta) = \overline{\phi}_0 + \sum_{n\neq 0} \overline{\phi}_n e^{\frac{2\pi i n\theta}{\beta}} \ , \quad \overline{\phi}_{-n} = \overline{\phi}_n^* \tag{5.7.4}$$

the scalar field solution is

$$\phi(r,\theta) = \overline{\phi}_0 + \sum_{n=1}^{\infty} \left(\overline{\phi}_{-n} e^{\frac{2\pi i n\theta}{\beta}} + \overline{\phi}_n e^{-\frac{2\pi i n\theta}{\beta}}\right) r^{2\pi n/\beta} \tag{5.7.5}$$

The action interior to the ring is

$$S_{r<1} = \int_{r<1} d^2x \frac{1}{2}(\partial\phi)^2 = 2\pi \sum_{n=1}^{\infty} n\overline{\phi}_n\overline{\phi}_{-n} \ . \tag{5.7.6}$$

The contribution of the exterior region $S_{r>1}$ takes the same form, as follows from symmetry under $r{\to}1/r$. The defect action, including the c_0^B counterterm, is

$$S_d = \int d\theta \left(c_0^B + \frac{1}{2}c_1\overline{\phi}^2\right) = \beta c_1 \left[\sum_{n=1}^{\infty} \overline{\phi}_n\overline{\phi}_{-n} + \frac{1}{2}\overline{\phi}_0^2\right] + \beta c_0^B \ . \tag{5.7.7}$$

The ring partition function is then

$$\begin{aligned}
Z(\beta) &= \mathcal{N}\left[\prod_n \int d\overline{\phi}_n\right] e^{-S_{r<1}-S_{r>1}-S_d} \\
&= \mathcal{N}e^{-\beta c_0^B}\int_{-\infty}^{\infty} d\overline{\phi}_0 e^{-\frac{1}{2}\beta c_1\overline{\phi}_0^2} \prod_{n\geq 1}\int d\overline{\phi}_n d\overline{\phi}_{-n} e^{-(4\pi n+\beta c_1)\overline{\phi}_n\overline{\phi}_{-n}} \\
&= \mathcal{N}\frac{e^{-\beta c_0^B}}{\sqrt{\beta c_1}} \prod_{n\geq 1}(4\pi n+\beta c_1)^{-1} \\
&= \mathcal{N}\frac{e^{-\beta c_0^B}}{\sqrt{\beta c_1}} \prod_{n\geq 1}\left(1+\frac{\beta c_1}{4\pi n}\right)^{-1} \ .
\end{aligned} \tag{5.7.8}$$

where in the final equality we have absorbed a constant factor into $\mathcal{N}$. We thus find

$$\log Z(\beta) = \log\mathcal{N} - \frac{1}{2}\log\frac{\beta c_1}{4\pi} - \sum_{n=1}^{N}\log\left(1+\frac{\beta c_1}{4\pi n}\right) - \beta c_0^B \ , \tag{5.7.9}$$

where we imposed a UV cutoff on the mode sum. To cancel the log divergence we take

$$c_0^B = -\frac{c_1}{4\pi} \log N \ . \tag{5.7.10}$$

We then take $N\to\infty$ using the formula[9]

$$\lim_{N\to\infty} \left[\sum_{n=1}^{N} \log\left(1+\frac{z}{n}\right) - z\log N \right] = -\log\Gamma(1+z) \ . \tag{5.7.11}$$

We finally arrive at

$$\log Z(\beta) = \log\mathcal{N} + \frac{1}{2}\log\frac{\beta c_1}{4\pi} + \log\Gamma\left(\frac{\beta c_1}{4\pi}\right) \ , \tag{5.7.12}$$

where we recall that $\mathcal{N}$ does not depend on c_1.

5.7.2 Defect g-function

Thinking of $Z(\beta)$ as a thermal partition function we can define the associated thermodynamic entropy,[10]

$$s = (1-\beta\partial_\beta)\log Z(\beta) \ . \tag{5.7.13}$$

Keeping just the c_1 dependent part, this evaluates to

$$s = \frac{1}{2}\log\frac{\beta c_1}{4\pi} + \log\Gamma\left(\frac{\beta c_1}{4\pi}\right) - \frac{\beta c_1}{4\pi}\Psi\left(\frac{\beta c_1}{4\pi}\right) - \frac{1}{2} \tag{5.7.14}$$

where $\Psi(x) = \Gamma'(x)/\Gamma(x)$.

We now comment on the relation of this result to the g-theorem [87, 86, 88]. We first observe that s is a monotonically decreasing function of c_1, which is in accord with the g-theorem. The connection to the g-theorem, which is usually phrased in terms of a theory

[9]This follows from the Weierstrass formula for the Gamma function, $-\ln\Gamma(z+1) = \sum_{m=1}^{\infty}\left[\log(1+\frac{z}{m}) - \frac{z}{m}\right] + \gamma z$ where γ is the Euler-Mascheroni constant, $\gamma = \lim_{N\to\infty}\left[\sum_{m=1}^{N}\frac{1}{m} - \log N\right]$.

[10]We use s to avoid confusion with the action S.

defined on a space with boundary, is made via the folding trick under which our ring partition function is related to the scalar field partition function on a disk with a $c_1\phi^2$ interaction on the boundary. Such partition functions were considered in the context of boundary string field theory [85, 86, 123, 124]. It would be natural to extend our computation to allow for general $c_{1,2,3}$ couplings but we were unable to obtain a closed form expression. The result should decrease along the RG flow according to the argument in [88]. We also note that the g-theorem, defects, and relations to ring partition functions have been considered in more general contexts in [95, 96].

5.7.3 Entanglement entropy of accelerating defects

This section involves the following problem. We consider two defects under going constant proper acceleration a in opposite directions. At time $t = 0$ they are mutually at rest and located at positions $x = \pm a^{-1}$. The field ϕ is assumed to be in the Lorentz invariant quantum state compatible with the Lorentz invariance of the defect trajectories. Given this setup, we wish to compute the entanglement entropy at $t = 0$ between the two half-spaces $x < 0$ and $x > 0$. The motivation for posing this precise question is that the answer is easily obtained from the partition function (5.7.12).

The Lorentzian trajectories of the defects are

$$x(\tau) = \pm\frac{1}{a}\cosh(a\tau)\ , \quad t(\tau) = \frac{1}{a}\sinh(a\tau) \tag{5.7.15}$$

where τ is proper time. Rotating to Euclidean time via $t\to it$ and $\tau\to i\tau$ the trajectory turns into a circle of radius $R = 1/a$,

$$x(\tau) = \frac{1}{a}\cos(a\tau)\ , \quad t(\tau) = \frac{1}{a}\sin(a\tau) \tag{5.7.16}$$

where τ is now periodic, $\tau \cong \tau + 2\pi/a$. This is illustrated in Figure 5.6.

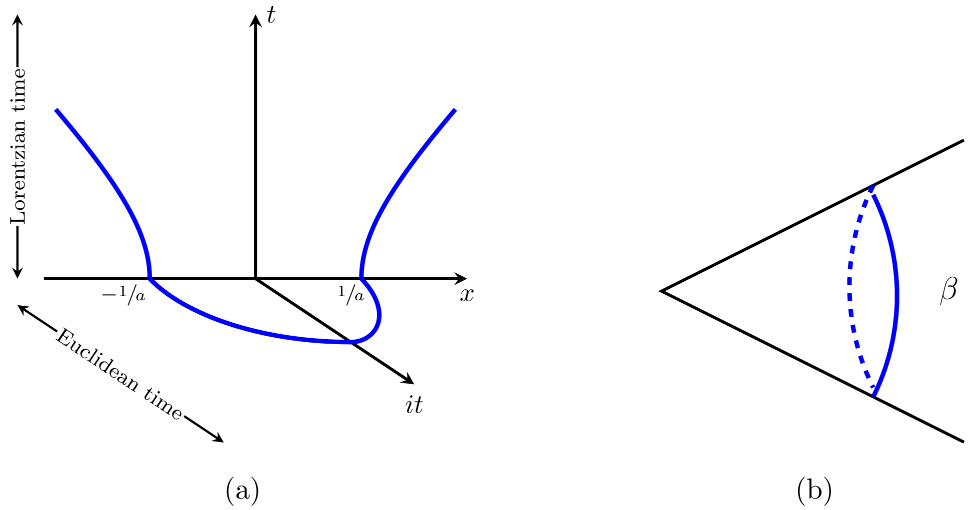

Figure 5.6: Figure 5.6a: The blue curve depicts the Lorentzian trajectory of the accelerating defect and its Euclidean counter part. Figure 5.6b: The ring defect in Euclidean space that corresponds to the accelerating defect in the Lorentzian spacetime. Here $\beta = 2\pi/a$, and we have included a cone to indicate that we will be varying β to compute the entanglement entropy.

The density matrix $\rho_R[\phi_+, \phi_-]$ describing the $x > 0$ half-space has a standard path integral representation, obtained (up to normalization) by doing the path integral on the Euclidean plane with boundary conditions $\phi_+(\phi_-)$ imposed just above (below) the positive real axis, as shown in figure 5.7.

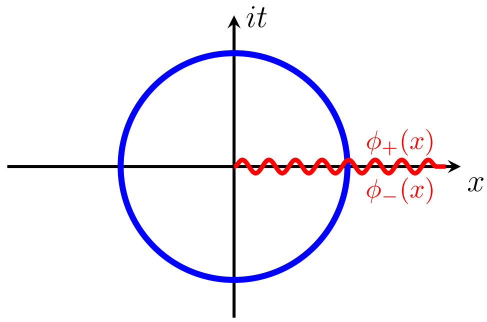

Figure 5.7: Pair of accelerating defects continued to imaginary time where they describe a ring. The density matrix describing the $x > 0$ half-space is obtained by performing the path integral in the presence of the defect with prescribed boundary conditions above and below the cut along the positive real axis.

The entanglement entropy is obtained as

$$s = -\,\mathrm{Tr}(\rho \ln \rho)\ . \tag{5.7.17}$$

As in the absence of the defect, it's convenient to think of the usual angular direction θ on the plane as a time direction generated by a Rindler Hamiltonian $H_{\mathrm{Rin}} \sim \partial_\theta$. In particular the density matrix becomes

$$\rho[\phi_+, \phi_-] = N \langle \phi_- | e^{-2\pi H_{\mathrm{Rin}}} | \phi_+ \rangle \tag{5.7.18}$$

where N is the normalization factor needed to set $\mathrm{Tr}\,\rho = 1$. If we define

$$Z(\beta) = \mathrm{Tr}\, e^{-\beta H_{\mathrm{Rin}}} \tag{5.7.19}$$

then the entanglement entropy can be obtained as the entropy associated to the partition function $Z(\beta)$ using the standard thermodynamic expression

$$s = (1 - \beta\partial_\beta) \log Z(\beta)\Big|_{\beta=2\pi}\ . \tag{5.7.20}$$

Finally, $Z(\beta)$ also has a simple path formulation: it is given by the path integral on the cone, since the periodicity $\theta \cong \theta + 2\pi$ has been replaced by the periodicity $\theta \cong \theta + \beta$ according to (5.7.18).

For simplicity we will only consider the defect with the $c_1\phi^2$ coupling. The entanglement entropy will be a function of the dimensionless combination c_1/a. This being the case we will henceforth set $a = 1$, as it can always be restored by taking $c_1 \to c_1/a$. The entanglement entropy is then obtained by setting $\beta = 2\pi$ in (5.7.14), which gives

$$s = \frac{1}{2}\log\frac{c_1}{2} + \log\Gamma\left(\frac{c_1}{2}\right) - \frac{c_1}{2}\Psi\left(\frac{c_1}{2}\right) - \frac{1}{2}\,. \tag{5.7.21}$$

It follows that this entanglement entropy monotonically decreases with increasing c_1, yielding an entanglement interpretation of the g-theorem in this example.

5.8 Defect on torus

In this section we consider the torus partition function with a defect wrapped around one of the cycles. One motivation is to understand how to relate the computation of the partition via a trace in either of two channels on the torus; this is a bit more subtle than usual due to the μ dependence of the defect. The partition function will also allow us to obtain a Cardy type formula for the asymptotic density of states of the defect Hilbert space. We restrict out attention to the c_1 defect, with $c_2 = c_3 = 0$.

5.8.1 Defect Hilbert space calculation

We first compute the torus partition function in the channel where the c_1-defect is placed along the Euclidean time direction as shown in Figure 5.8. We denote the result as $Z_d(L_d, L, \mu)$ where μ is the RG scale, as will be discussed shortly. Here, the subscript d denotes that the partition function is a trace over c_1-defect Hilbert space.

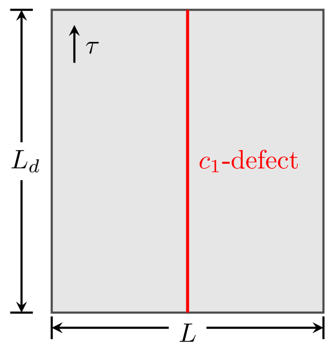

Figure 5.8: We choose the Euclidean time along c_1-defect direction, and the result computed in this channel is denoted as $Z_d(L_d, L, \mu)$.

In this channel, the partition function is computing the trace of $e^{-\beta(H-1/12)}$ over the defect Hilbert space. We will parameterize the spatial direction $x \in [0, L)$ and place the defect at $x = 0$. From (5.2.18), we learn that a c_1-defect will impose the following twisted boundary condition at $x = 0$

$$\begin{pmatrix} \phi(L) \\ \phi'(L) \end{pmatrix} = \begin{pmatrix} 1 & 0 \\ -c_1 & 1 \end{pmatrix} \begin{pmatrix} \phi(0) \\ \phi'(0) \end{pmatrix} . \tag{5.8.1}$$

For $c_1 > 0$, the eigenfunctions satisfying the above boundary conditions fall into two classes. The first class is

$$\psi_n^I(x) = \sqrt{2} \sin\left(\frac{2\pi n}{L} x\right) , \quad n \in \mathbb{Z}_{>0} . \tag{5.8.2}$$

Notice that these eigenfunctions satisfy the boundary condition (5.8.1) as $\psi_n^I(0) = \psi_n^I(L) = 0$ and $\psi_n^{I\prime}(0) = \psi_n^{I\prime}(L)$, and are independent of the coupling c_1.

The second class is

$$\psi_\omega^{II}(x) = A(\omega)(\cos(\omega x) + \cos(\omega(L_2 - x))) , \tag{5.8.3}$$

where the normalization factor $A(\omega) = \sqrt{\frac{\omega L}{2(\omega L + \sin(\omega L))}}$ and $\omega > 0$ satisfies

$$2\omega \tan\left(\frac{\omega L}{2}\right) = c_1 . \tag{5.8.4}$$

As one can see, the second class depends continuously on the coupling c_1, and the modes can be viewed as the flows of the periodic eigenfunctions $\sqrt{2}\cos(\frac{2\pi n x}{L})$ $(n \in \mathbb{Z}_{\geq 0})$ for $c_1 = 0$. Therefore, we can naturally use ω_n $(n \geq 0)$ to denote solutions at positive c_1.

It is notable that the zero mode $\psi = const.$ at $c_1 = 0$ is lifted upon turning on the coupling, which we take to be positive. Furthermore, at small c_1, the leading behavior of ω_0 as a function of c_1 is distinct from the other ω_n's, as one can see in Figure 5.9. It is

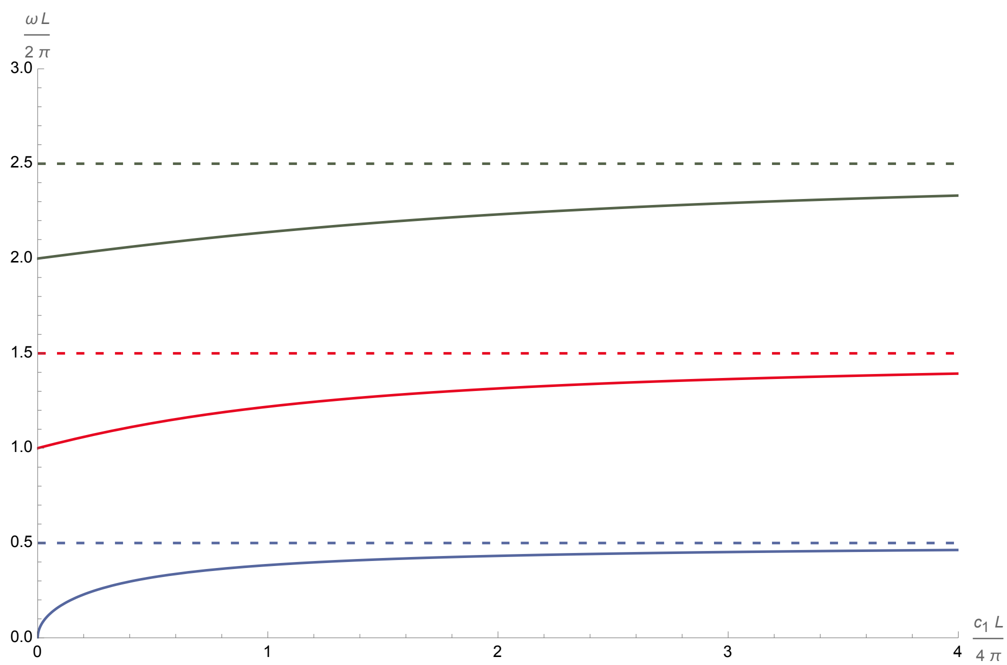

Figure 5.9: Here, we plot the first three solutions to the equation (5.8.4) as a function of the coupling c_1. Notice that we have rescaled ω and c_1 with $\frac{1}{L}$ so that they are dimensionless.

straightforward to check that at small c_1 the solutions ω_n admit an expansion in c_1:

$$\omega_0 = \sqrt{\frac{c_1}{L}}\left(1 - \frac{c_1 L}{24} + O(c_1^2)\right) \ , \quad \omega_n = \frac{2\pi n}{L} + \frac{c_1}{2n\pi} + O(c_1^2) \ , \quad n > 0 \ . \tag{5.8.5}$$

In the limit where $c_1 \to \infty$, all the solutions ω_n have the same behavior:

$$\omega_n \to \frac{2\pi}{L}\left(n + \frac{1}{2}\right)\left(1 - \frac{4\pi}{c_1 L} + O\left(\frac{1}{c_1^2}\right)\right) \ , \quad c_1 \to \infty \ . \tag{5.8.6}$$

For finite c_1 one can see in Figure 5.9 that as n gets larger ω_n slowly approaches $\left(n+\frac{1}{2}\right)\frac{2\pi}{L}$. We can also write down an expansion for large n at fixed c_1:

$$\omega_n = \frac{2\pi n}{L} + \frac{c_1}{2n\pi} + O\left(\frac{1}{n^2}\right) . \tag{5.8.7}$$

On the other hand, if $c_1 < 0$, the system is pathological because one eigenfunction will have imaginary ω. It's not hard to see this as the perturbative expansion (5.8.5) holds for negative c_1 as well, and ω_0 becomes imaginary when turning on small negative c_1. For finite negative c_1, the function $2ix\tan\left(\frac{ixL}{2}\right) = -2x\tanh\left(\frac{\omega L}{2}\right)$ remains negative and monotonically decreasing for $x > 0$, thus (5.8.4) always has a purely imaginary solution when $c_1 < 0$. Quantization of this mode either leads to non-unitarity or an energy spectrum unbounded from below. Thus, we will only consider the case where $c_1 > 0$.

Once we understand the eigenfunctions, it is straightforward to construct the defect Hilbert space, as the states are formed from the harmonic oscillators with frequencies given by the ω_n's from the eigenfunctions. Naively assembling the partition functions of each oscillator together, we find

$$Z_d(L_d, L) = \left(\prod_{n=1}^{\infty} \frac{q^{\frac{n}{2}}}{1-q^n}\right)\left(\prod_{n=0}^{\infty} \frac{q^{\frac{\omega_n L}{4\pi}}}{1-q^{\frac{\omega_n L}{2\pi}}}\right) , \tag{5.8.8}$$

where $q = e^{-2\pi\frac{L_d}{L}}$. Notice that the factor arising from the vacuum energy of the oscillators:

$$q^{\sum_{n=1}\frac{n}{2}+\sum_{n=0}\frac{\omega_n L}{4\pi}} , \tag{5.8.9}$$

is divergent and therefore requires regularization. We split it into three parts as

$$\frac{1}{2}\sum_{n=1}^{\infty} n + \frac{1}{2}\sum_{n=0}^{\infty}\frac{\omega_n L}{2\pi} = \sum_{n=1}^{\infty} n + \frac{c_1 L}{8\pi^2}\sum_{n=1}^{\infty}\frac{1}{n} + \frac{L}{4\pi}\left(\omega_0 + \sum_{n=1}^{\infty}\left(\omega_n - \frac{2\pi n}{L} - \frac{c_1}{2n\pi}\right)\right) . \tag{5.8.10}$$

The first piece is regularized using familiar ζ-function regularization, and leads to $-\frac{1}{12}$. The second piece diverges logarithmically, and we regulate it by considering an energy cut-off at

Λ; since the momentum is measured in the unit of $\frac{1}{L}$, this will cut the infinite sum at ΛL. Then we add a counter term along the defect

$$\frac{c_1}{4\pi}\int dt \log\left(\frac{\Lambda}{\mu}\right) \ , \tag{5.8.11}$$

where μ is the RG scale. Taking the limit $\Lambda \to \infty$, we find

$$\lim_{\Lambda\to\infty}\left[-\frac{c_1 L}{8\pi^2}\log\left(\frac{\Lambda}{\mu}\right)+\frac{c_1 L}{8\pi^2}\sum_{n=1}^{\Lambda L}\frac{1}{n}\right]=\frac{c_1 L}{8\pi^2}[\gamma+\log(\mu L)] \ , \tag{5.8.12}$$

where γ is the Euler–Mascheroni constant. The remaining part of (5.8.10) is finite as one can see from (5.8.7) and numerically verify. To summarize, the partition function computed in this channel is

$$\begin{aligned} Z_d(L_d,L,\mu) &= e^{-\frac{c_1 L_d}{4\pi}(\gamma+\log(\mu L))} q^{-\frac{1}{12}+\frac{L}{2\pi}E_0(c_1)}\prod_{n=0}^{\infty}\left(1-q^{\frac{\omega_n L}{2\pi}}\right)^{-1}\prod_{m>0}(1-q^m)^{-1} \\ &= e^{-\frac{c_1 L_d}{4\pi}(\gamma+\log(\mu L))}\frac{q^{-\frac{1}{24}+\frac{L}{2\pi}E_0(c_1)}}{\eta(q)}\prod_{n=0}^{\infty}\frac{1}{1-q^{\frac{\omega_n L}{2\pi}}} \ , \end{aligned} \tag{5.8.13}$$

where the constant $E_0(c_1)$ represents the shifted ground state energy

$$E_0(c_1)=\frac{\omega_0}{2}+\frac{1}{2}\sum_{n=1}^{\infty}\left(\omega_n-\frac{2\pi n}{L}-\frac{c_1}{2n\pi}\right) \ . \tag{5.8.14}$$

As a consistency check, one can also compute the partition function from the path integral by expanding the scale field $\phi(t,x)$ using the eigenfunctions described above. The path integral then reduces to a infinite product of Gaussian integrals, which can then be regulated following the same approach taken for a free scalar field [79]. This reproduces the result (5.8.13), and after a further regularization leads to the same final result (5.8.13).

To conclude, we want to quickly point it out that the coefficient $-\frac{c_1 L}{4\pi}$ in front of the $-\frac{c_1 L}{4\pi}\log(\mu L)$ term can be viewed as the anomalous dimension of the c_1-defect. This way of computing anomalous dimension can be generalized to the case where both c_1 and c_2 are activated. In this case, the twisted boundary condition is given by

$$\begin{pmatrix}\phi(L)\\ \phi'(L)\end{pmatrix}=\begin{pmatrix}\frac{(2-c_2)^2}{4-c_2^2} & 0\\ -\frac{c_1}{4-c_2^2} & \frac{(2+c_2)^2}{4-c_2^2}\end{pmatrix}\begin{pmatrix}\phi(0)\\ \phi'(0)\end{pmatrix} \ , \tag{5.8.15}$$

and the equation for the eigenvalues become

$$2\omega\tan\left(\frac{\omega L}{2}\right)=c_1+\frac{c_2^2}{2}\omega\cot\left(\frac{\omega L}{2}\right)\ . \tag{5.8.16}$$

Notice that the equations can be solved exactly when $c_1=0$, and for large ω they admit a similar expansion as (5.8.5) (where for simplicity we assume $c_2>0$)

$$\begin{aligned}
\omega_n &= +\frac{2}{L}\left(\arctan\left(\frac{c_2}{2}\right)\right)+\frac{2\pi n}{L}+\frac{c_1}{4+c_2^2}\frac{1}{n\pi+\arctan(c_2/2)}+O(c_1^2)\ , \quad n\geq 0\ ,\\
\omega_n' &= -\frac{2}{L}\left(\arctan\left(\frac{c_2}{2}\right)\right)+\frac{2\pi n}{L}+\frac{c_1}{4+c_2^2}\frac{1}{n\pi+\arctan(c_2/2)}+O(c_1^2)\ , \quad n>0\ .
\end{aligned} \tag{5.8.17}$$

Then the logarithmic divergence in the zero point energy sum contributes to the partition function as

$$\begin{aligned}
&\exp\left(-\frac{L_d}{2}\left(\sum_{n=0}^{\infty}\omega_n+\sum_{n=1}^{\infty}\omega_n'\right)\right)\\
&\supset\exp\left(-\frac{L_d}{2}\left(\sum_{n=0}^{\Lambda}\frac{c_1}{4+c_2^2}\frac{1}{n\pi+\arctan(c_2/2)}+\sum_{n=1}^{\Lambda}\frac{c_1}{4+c_2^2}\frac{1}{n\pi+\arctan(c_2/2)}\right)\right)\\
&\simeq\exp\left(-\frac{c_1L_d}{4\pi}\frac{1}{1+c_2^2/4}\log(\Lambda)\right)\ .
\end{aligned} \tag{5.8.18}$$

Thus, we see that the anomalous dimension for a c_1,c_2-defect is given by $-\frac{c_1L_d}{4\pi}\frac{1}{1+c_2^2/4}$, matching the calculation in (5.4.7).

5.8.2 Torus partition function with the space-like defect

Next, we compute the same torus partition function but now as a trace in the dual channel where Euclidean time is taken run transverse to the defect, as shown in figure 5.10. We emphasize that this is precisely the same setup as in Figure 5.8, and we are simply identifying Euclidean time differently than before. Naturally, we expect to get the same answer as (5.8.13); nevertheless, for the moment we will use Z_o to denote the corresponding result. The calculation can be computed using either the Hamiltonian approach or the path-integral approach; below we demonstrate explicitly the Hamiltonian approach and briefly sketch on the path integral computation.

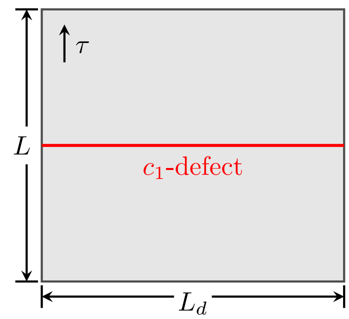

Figure 5.10: In the dual channel, we choose the Euclidean time to run transversely to the c_1-defect, and the result computed in this channel is denoted as $Z_d(L_d, L, \mu)$.

Because the defect is placed along the spatial direction, it should be treated as an operator insertion that does not change the Hilbert space but rather acts on it. Because of this, we take the familiar expansion of the free scalar field, $\phi(x,t) = \sum_n \varphi_n(t) e^{\frac{2\pi i n x}{L_d}}$, to get the free Hamiltonian (and use the ζ-function to regularize the vacuum energy)

$$H_{free} = -\frac{\pi}{6L_d} + \frac{1}{2L_d}\hat{\pi}_0^2 + \frac{2\pi}{L_d}\sum_{n>0} n(\hat{b}_n^\dagger \hat{b}_n + \hat{d}_n^\dagger d_n) \ , \tag{5.8.19}$$

as well as the defect operator

$$e^{-S_d} = \exp\left(-\frac{c_1 L_d}{2}\hat{\varphi}_0^2 - \frac{c_1 L_d}{4\pi}\sum_{n>0}\frac{1}{n}(\hat{b}_n^\dagger - \hat{d}_n)(\hat{b}_n - \hat{d}_n^\dagger)\right) \ . \tag{5.8.20}$$

Here, the $\hat{b}_n, \hat{b}_n^\dagger$'s and $\hat{d}_n, \hat{d}_n^\dagger$'s represent creation and annihilation operators of harmonic oscillators with normalization $[\hat{b}_n, \hat{b}_n^\dagger] = [\hat{d}_n, \hat{d}_n^\dagger] = 1$, and $\hat{\pi}_0$ and $\hat{\varphi}_0$ represent the momentum and the coordinate of the zero mode. Note that the defect operator effectively introduces a mass term for the zero mode.

The torus partition function in this channel may be computed by inserting a complete basis of states (formed by the eigenstates of the free Hamiltonian H_{free}) in the trace

$$Z_o(L_d, L, \mu) = \mathrm{Tr}(e^{-S_d} e^{-LH_{free}}) = \sum_{\psi,\phi}\langle\psi|e^{S_d}|\phi\rangle\langle\phi|e^{-LH_{free}}|\psi\rangle \ , \tag{5.8.21}$$

where again the RG scale μ will be introduced shortly. It is useful to note that the defect operator e^{-S_d} only mixes the two oscillators labeled by the same n, thus the partition function factorizes. The contribution for a given n can be computed by expanding $e^{-\frac{c_1}{4\pi n}(\hat{b}_n^\dagger-\hat{d}_n)(\hat{b}_n-\hat{d}_n^\dagger)}$ and use $[\hat{b}_n^\dagger-\hat{d}_n,\hat{b}_n-\hat{d}_n^\dagger]=0$. We find

$$\sum_{\ell,\tilde{\ell}=0}^{\infty}\langle\ell,\tilde{\ell}|e^{-\frac{c_1L_d}{4\pi n}(b_n^\dagger-d_n)(b_n-d_n^\dagger)}|\ell,\tilde{\ell}\rangle\tilde{q}^{n\ell+n\tilde{\ell}}=\left[(1-\tilde{q}^n)\left(1+\frac{c_1L_d}{4\pi n}-\tilde{q}^n\left(1-\frac{c_1L_d}{4\pi n}\right)\right)\right]^{-1}\ , \tag{5.8.22}$$

where $\tilde{q}=e^{-2\pi\frac{L}{L_d}}$. And the contribution from the zero mode is

$$\sqrt{\frac{1}{2\pi}}\int d\pi_0\langle\pi_0|e^{-\frac{c_1L_d}{2}\hat{\varphi}_0^2}|\pi_0\rangle e^{-\frac{\pi_0^2L}{2L_d}}=\frac{1}{2\pi}\int d\pi_0d\varphi_0\langle\pi_0|e^{-\frac{c_1L_d}{2}\varphi_0^2}|\varphi_0\rangle\langle\varphi_0|\pi_0\rangle e^{-\frac{\pi_0^2L}{2L_d}}=\frac{1}{\sqrt{c_1L}}\ . \tag{5.8.23}$$

Combining everything together, we find the partition function is given by

$$\frac{1}{\sqrt{c_1L}}\tilde{q}^{-\frac{1}{12}}\prod_{n=1}^{\infty}\frac{1}{(1-\tilde{q}^n)(1+\frac{c_1L_d}{4\pi n}-\tilde{q}^n(1-\frac{c_1L_d}{4\pi n}))}\ , \tag{5.8.24}$$

where the factor $\tilde{q}^{-\frac{1}{12}}$ comes from the vacuum energy term in H_{free}. The above expression contains a similar divergent term, which can be seen by writing

$$\begin{aligned}\prod_{n=1}^{\infty}\frac{1}{1+\frac{c_1L_d}{4\pi n}-\tilde{q}^n(1-\frac{c_1L_d}{4\pi n})}&=\exp\left[-\sum_{n>0}\log\left(1+\frac{c_1L_d}{4\pi n}-\tilde{q}^n\left(1-\frac{c_1L_d}{4\pi n}\right)\right)\right]\\&=\exp\left[-\sum_{n>0}\frac{c_1L_d}{4\pi n}\left(1+O\left(\frac{1}{n}\right)\right)\right]\ ,\end{aligned} \tag{5.8.25}$$

and we will regularize it in the same way as in the previous calculation. Namely, we first introduce the same UV cut-off at energy Λ. But because the energy is measured in unit of $\frac{1}{L_d}$, this would instead cut the infinite sum at ΛL_d. Next, we introduce the same counter term

$$\frac{c_1}{4\pi}\int dt\ \log\left(\frac{\Lambda}{\mu}\right)\ , \tag{5.8.26}$$

and taking the limit $\Lambda\to\infty$ then leads to

$$\lim_{\Lambda\to\infty}\left[\frac{c_1L_d}{4\pi}\log\left(\frac{\Lambda}{\mu}\right)-\frac{c_1L_d}{4\pi}\sum_{n=1}^{\Lambda L_d}\frac{1}{n}\right]=-\frac{c_1L_d}{4\pi}[\gamma+\log(\mu L_d)]\ . \tag{5.8.27}$$

The partition function is then given by

$$Z_o(L_d,L,\mu)=e^{-\frac{c_1L_d}{4\pi}(\gamma+\log(\mu L_d))}\frac{1}{\sqrt{c_1L}}\frac{\tilde{q}^{-\frac{1}{24}}}{\eta(\tilde{q})}\prod_{n=1}^{\infty}\frac{e^{\frac{c_1L_d}{4\pi n}}}{1+\frac{c_1L_d}{4\pi n}-\tilde{q}^n(1-\frac{c_1L_d}{4\pi n})}\ ,\quad\tilde{q}=e^{-2\pi\frac{L}{L_d}}\ . \tag{5.8.28}$$

As a consistency check, let's consider the vacuum expectation value from (5.8.28), which can be obtained from the coefficient of the leading term in the $\tilde{q}$-expansion:

$$\langle e^{-S_d}\rangle = e^{-\frac{c_1 L_d}{4\pi}(\gamma+\log(\mu L_d))}\frac{1}{\sqrt{c_1 L}}\prod_{n=1}^{\infty}\frac{e^{\frac{c_1 L_d}{4\pi n}}}{1+\frac{c_1 L_d}{4\pi n}} = \frac{e^{-\frac{c_1 L_d}{4\pi}\log(\mu L_d)}}{\sqrt{c_1 L}}\Gamma\left(1+\frac{c_1 L_d}{4\pi}\right) \ , \tag{5.8.29}$$

The path integral calculation can be done by expanding the scalar field $\phi(x,t)$ using periodic functions and treat the defect operator e^{-S_d} as an operator insertion in the Gaussian integral. It is straightforward to check that it reproduces the same unregularized result (5.8.24).

5.8.3 Matching the two calculations

As pointed out, since we are computing the same configuration with the same counter terms, we expect the result $Z_d(L_d, L, \mu)$ and $Z_o(L_d, L, \mu)$ to match exactly:

$$Z_d(L_d, L, \mu) = Z_o(L_d, L, \mu) \ . \tag{5.8.30}$$

This equality amounts to the claim

$$\begin{aligned} & e^{-\frac{c_1 L_d}{4\pi}(\gamma+\log(\mu L))}\frac{q^{-\frac{1}{24}+\frac{L}{2\pi}E_0(c_1)}}{\eta(q)}\prod_{n=0}^{\infty}\frac{1}{1-q^{\frac{\omega_n L}{2\pi}}} \\ =& e^{-\frac{c_1 L_d}{4\pi}(\gamma+\log(\mu L_d))}\frac{1}{\sqrt{c_1 L}}\frac{\tilde{q}^{-\frac{1}{24}}}{\eta(\tilde{q})}\prod_{n=1}^{\infty}\frac{e^{\frac{c_1 L_d}{4\pi n}}}{1+\frac{c_1 L_d}{4\pi n}-\tilde{q}^n(1-\frac{c_1 L_d}{4\pi n})} \ . \end{aligned} \tag{5.8.31}$$

The RG scale μ automatically cancels out from both sides, and leads to

$$\frac{q^{-\frac{1}{24}+\frac{L}{2\pi}E_0(c_1)}}{\eta(q)}\prod_{n=0}^{\infty}\frac{1}{1-q^{\frac{\omega_n L}{2\pi}}} = \left(\frac{L}{L_d}\right)^{\frac{c_1 L_d}{4\pi}}\frac{\tilde{q}^{-\frac{1}{24}}}{\eta(\tilde{q})}\prod_{n=1}^{\infty}\frac{e^{\frac{c_1 L_d}{4\pi n}}}{1+\frac{c_1 L_d}{4\pi n}-\tilde{q}^n(1-\frac{c_1 L_d}{4\pi n})} \ . \tag{5.8.32}$$

Let's first check (5.8.32) at the leading order of c_1. Keeping the leading term on both sides, we find

$$\begin{aligned} LHS &= \sqrt{\frac{L}{c_1}}\frac{1}{L_d}\frac{1}{|\eta(q)|^2}\left(1+O(c_1)\right) \ , \quad q = e^{-2\pi\frac{L_d}{L}} \ , \\ RHS &= \frac{1}{\sqrt{c_1 L}}\frac{1}{\eta(\tilde{q})^2}\left(1+O(c_1)\right) \ , \quad \tilde{q} = e^{-2\pi\frac{L}{L_d}} \ . \end{aligned} \tag{5.8.33}$$

The modular property of $\eta(q)$ (that is, $\eta(\tilde{q}) = \sqrt{L_d/L}\eta(q)$) implies the two sides agree at the leading order. This agreement has a simple interpretation, that is, at the leading order, the c_1-defect provides a mass-like regulator of the zero mode. This regulator is only modular covariant as it soaks up the modular transformation of the partition function of the oscillator modes to ensure the full partition function is modular invariant at this order.

To see the effect of the anomalous dimension $\left(\frac{L}{L_d}\right)^{\frac{c_1 L_d}{4\pi}}$, we have to consider the next order correction. Using

$$\frac{e^{\frac{c_1 L_d}{4\pi n}}}{1+\frac{c_1 L_d}{4\pi n} - \tilde{q}^n(1-\frac{c_1 L_d}{4\pi n})} = \frac{1}{1-\tilde{q}^n}\left(1 - \frac{c_1 L_d}{2\pi n}\frac{\tilde{q}^n}{1-\tilde{q}^n} + O(c_1^2)\right) , \tag{5.8.34}$$

we find

$$\begin{aligned} RHS =& \frac{1}{\sqrt{c_1 L}}\frac{1}{|\eta(\tilde{q})|^2}\left[1 - \frac{c_1 L_d}{2\pi}\left(\frac{1}{2}\log\left(\frac{L_2}{L}\right) + \sum_{n=1}^{\infty}\frac{1}{n}\frac{\tilde{q}^n}{1-\tilde{q}^n}\right) + O(c_1^2)\right] \\ =& \frac{1}{\sqrt{c_1 L}}\frac{1}{|\eta(\tilde{q})|^2}\left[1 - \frac{c_1 L_d}{2\pi}\left(-\frac{\pi}{12}\frac{L}{L_d} + \frac{1}{2}\log\left(\frac{L_d}{L}\right) - \log(\eta(\tilde{q}))\right) + O(c_1^2)\right] , \end{aligned} \tag{5.8.35}$$

where we have used

$$\sum_{n=1}^{\infty}\frac{1}{n}\frac{\tilde{q}^n}{1-\tilde{q}^n} = \sum_{n,m=1}^{\infty}\frac{1}{n}\tilde{q}^{nm} = -\sum_{m=1}^{\infty}\log(1-\tilde{q}^m) = -\frac{\pi}{12}\frac{L}{L_d} - \log(\eta(\tilde{q})) . \tag{5.8.36}$$

To derive the first order correction in c_1 on the LHS of (5.8.32), first notice that from (5.8.5) we have

$$\frac{q^{\frac{\omega_0 L}{4\pi}}}{1-q^{\frac{\omega_0 L}{2\pi}}} = \frac{1}{L_d}\sqrt{\frac{L}{c_1}}\left(1 + \frac{c_1 L_d}{2\pi}\frac{\pi}{12}\left(\frac{L}{L_d} - \frac{L_d}{L}\right) + O(c_1^2)\right) , \tag{5.8.37}$$

and

$$\frac{1}{1-q^{\frac{\omega_n L}{2\pi}}} = \frac{1}{1-\tilde{q}^n}\left(1 - \frac{c_1 L_d}{2n\pi}\frac{q^n}{1-q^n} + O(c_1^2)\right) , \quad n > 0 , \tag{5.8.38}$$

where $q = e^{-2\pi\frac{L_d}{L}}$. Combining these contributions, we find

$$\begin{aligned} LHS =& \frac{1}{L_d}\sqrt{\frac{L}{c_1}}\frac{1}{|\eta(q)|^2}\left[1 - \frac{c_1 L_d}{2\pi}\left(-\frac{\pi}{12}\frac{L}{L_d} - \log(\eta(q))\right) + O(c_1^2)\right] \\ =& \frac{1}{\sqrt{c_1 L}}\frac{1}{|\eta(\tilde{q})|^2}\left[1 - \frac{c_1 L_d}{2\pi}\left(-\frac{\pi}{12}\frac{L}{L_d} + \frac{1}{2}\log\left(\frac{L_d}{L}\right) - \log(\eta(\tilde{q}))\right) + O(c_1^2)\right] , \end{aligned} \tag{5.8.39}$$

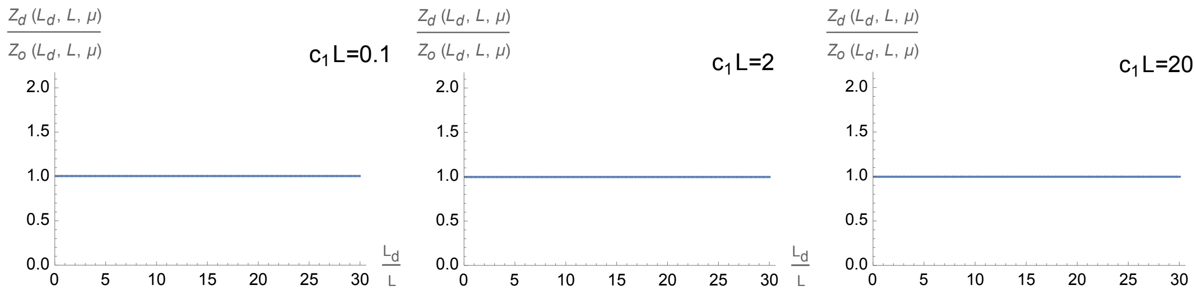

(a) $c_1 L = 0.1$ (b) $c_1 L = 2$ (c) $c_1 L = 20$

Figure 5.11: Numerical verification of (5.8.32), where we fix $c_1 L = 0.1, 2, 20$ and plot $\frac{Z_d(L_d,L,\mu)}{Z_o(L_d,L,\mu)}$ as a function $\frac{L_d}{L}$ (recall that the ratio does not depends on the RG scale μ).

where we find agreement with (5.8.35) after using the modular property of the Dedekind η-function $\eta(q) = \sqrt{L/L_d}\eta(\tilde{q})$.

To conclude, we consider numerical verification of (5.8.32). To do so, we fix the value of $c_1 L$ and plot the ratio (recall that the ratio does not depend on μ)

$$\frac{Z_o(L_d, L, \mu)}{Z_d(L_d, L, \mu)} \tag{5.8.40}$$

as a function of $\frac{L_d}{L}$. We find a nice numerical match of (5.8.32) as shown in Figure 5.11.

5.8.4 Cardy formulas

The modular invariance of a CFT with compact spectrum relates the high and low temperature limits, allowing one to estimate the asymptotic growth of the density of states, yielding a Cardy formula [125]. Though we consider a non-conformal defect, we can apply the same reasoning by computing the partition function in the two different channels.

5.8.4.1 Review of the standard Cardy formula

Let us first recall the derivation in the case of a generic compact CFT with finite central charge c. Its partition function on a square torus is defined as

$$Z(L_d, L) = \int_0^\infty dE\, \rho(E) e^{-L_d(E - \frac{\pi c}{6L})} \tag{5.8.41}$$

where $\rho(E)$ is the density of states, and we use L_d to denote the length of the Euclidean time cycle, and L denotes the length of the spatial circle, even though no defect is inserted. Modular invariance implies that $Z(L_d, L) = Z(L, L_d)$, and in the limit $\frac{L_d}{L} \to 0$, $Z(L, L_d) \simeq e^{\frac{\pi L}{6 L_d}}$ and we find

$$\int_0^\infty dE\, \rho(E) e^{-L_d E} \simeq e^{-\frac{\pi c L_d}{6L}} e^{\frac{\pi c L}{6 L_d}} \ . \tag{5.8.42}$$

The inverse Laplace transformation $\rho_0(E)$ of the RHS then describes the asymptotic growth of $\rho(E)$ in the sense that

$$\frac{\int_0^{E_{max}} dE\, \rho(E)}{\int_0^{E_{max}} dE\, \rho_0(E)} \to 1 \ , \quad E_{max} \to \infty \ . \tag{5.8.43}$$

The inverse Laplace transformation

$$\rho_0(E) = \frac{1}{2\pi i} \int_{-i\infty}^{i\infty} dL_d\, e^{E L_d + \frac{\pi c L}{6 L_d} - \frac{\pi c L_d}{6L}} \tag{5.8.44}$$

can be evaluated using the saddle point approximation. Upon changing variable $L_d = \frac{iz}{\sqrt{E}}$, the integral becomes

$$\rho_0(E) = \frac{1}{2\pi\sqrt{E}} \int_{-\infty}^{\infty} dz\, e^{\sqrt{E}(iz - \frac{i\pi c L}{6z}) + \frac{i\pi c}{6\sqrt{E} L} z} \ , \tag{5.8.45}$$

and the large E saddle point can be seen from

$$iz - \frac{i\pi c L}{6z} = \sqrt{\frac{2\pi c L}{3}} - \sqrt{\frac{6}{\pi c L}} (z - z_0)^2 + \dots \tag{5.8.46}$$

where $z_0 = -i\sqrt{\frac{\pi c L}{6}}$. Evaluating the integral around z_0 leads to

$$\rho_0(E) = \left(\frac{cL/2\pi}{48 E^3}\right)^{1/4} e^{2\pi\sqrt{\frac{cEL/2\pi}{3}}} \left(1 + O\left(\frac{1}{\sqrt{cEL}}\right)\right) \ . \tag{5.8.47}$$

Notice that we have neglected the term $e^{\frac{i\pi c}{6\sqrt{EL}}z}$ in the integral for the following reasons. First, while it modifies the location of the saddle point, the leading error is of order $\frac{c^{5/2}}{(EL)^{3/2}}$ which is negligible compared to the leading error of the saddle point approximation. Second, the leading order contribution of $e^{\frac{i\pi c}{6\sqrt{EL}}z}$ at the saddle point is of order $\frac{c^{\frac{3}{2}}}{\sqrt{EL}}$ which is again negligible as it belongs to $O\left(\frac{1}{\sqrt{cEL}}\right)$ (recall that we have assume that c is finite therefore of order $O(1)$).

5.8.4.2 Defect Cardy formula

We can similarly derive a Cardy formula for the spectrum of the Hamiltonian acting on the Hilbert space of the c_1 defect. In this case, the relation (5.8.32) relates the density of states $\rho_{c_1}(E)$ of the defect Hilbert space to the high temperature limit of the partition function in the following way. First, expanding $\eta(q)$ on the LHS of (5.8.32) leads to

$$q^{-\frac{1}{12}+\frac{L}{2\pi}E_0(c_1)}\left[\prod_{n=1}^{\infty}(1-q^n)^{-1}\prod_{n=0}^{\infty}(1-q^{\frac{\omega_n L}{2\pi}})^{-1}\right]=\left(\frac{L}{L_d}\right)^{\frac{c_1L_d}{4\pi}}\frac{\tilde{q}^{-\frac{1}{24}}}{\eta(\tilde{q})}\prod_{n=1}^{\infty}\frac{e^{\frac{c_1L_d}{4\pi n}}}{1+\frac{c_1L_d}{4\pi n}-\tilde{q}^n(1-\frac{c_1L_d}{4\pi n})}\,, \tag{5.8.48}$$

and the two infinite products on the LHS can be expressed using the density of states $\rho_{c_1}(E)$

$$\left[\prod_{n=1}^{\infty}(1-q^n)^{-1}\prod_{n=0}^{\infty}(1-q^{\frac{\omega_n L}{2\pi}})^{-1}\right]=\int_0^{\infty}\rho_{c_1}(E)e^{-EL_d}dE\,, \tag{5.8.49}$$

where we have chosen the ground state energy to be $E=0$. This implies that

$$\int_0^{\infty}\rho_{c_1}(E)e^{-EL_d}dE=q^{\frac{1}{12}-\frac{L}{2\pi}E_0(c_1)}\left(\frac{L}{L_d}\right)^{\frac{c_1L_d}{4\pi}}\frac{\tilde{q}^{-\frac{1}{24}}}{\eta(\tilde{q})}\prod_{n=1}^{\infty}\frac{e^{\frac{c_1L_d}{4\pi n}}}{1+\frac{c_1L_d}{4\pi n}-\tilde{q}^n(1-\frac{c_1L_d}{4\pi n})}\,, \tag{5.8.50}$$

and in the high temperature limit $\frac{L_d}{L}\to 0$, the RHS is dominated by the contribution from the vacuum state, and we find

$$\int_0^{\infty}\rho_{c_1}(E)e^{-L_dE}\approx\frac{1}{\sqrt{c_1L}}e^{L_d\left(E_0(c_1)-\frac{\pi}{6L}\right)}e^{-\frac{c_1L_d}{4\pi}\log\left(\frac{L_d}{L}\right)}e^{\frac{\pi L}{6L_d}}e^{\frac{c_1L_d\gamma}{4\pi}}\Gamma\left(1+\frac{c_1L_d}{4\pi}\right)\,,\quad\frac{L_d}{L}\to 0\,. \tag{5.8.51}$$

Inverse Laplace transformation of the RHS of (5.8.51) then leads to an approximate density of state $\rho_{c_1,0}(E)$ capturing the asymptotic behavior of ρ_{c_1}. However, since now we have two dimensionless parameters EL and c_1L, the result of the saddle point approximation will then depends on the relation between E and c_1.

$c_1L = O(1)$

Let us first consider the simplest case where $c_1L = O(1)$, which is to say that c_1L is held fixed at a nonzero value of order 1 while we take $EL \gg 1$. To evaluate the saddle point approximation only requires $EL \gg 1$, and it is straightforward to check that the saddle point remains the same as the usual Cardy case, and we find

$$\rho_{c_1,0}(E) = \frac{1}{\sqrt{c_1L}}\left(\frac{L/2\pi}{48E^3}\right)^{1/4} e^{\sqrt{\frac{\pi}{6EL}}\frac{c_1L}{8\pi}\log\left(\frac{6EL}{\pi}\right)} e^{2\pi\sqrt{\frac{EL/2\pi}{3}}}\left(1+O\left(\frac{1}{\sqrt{EL}}\right)\right) \ , \quad EL \gg 1 \ . \tag{5.8.52}$$

Notice that the factor $e^{\sqrt{\frac{\pi}{6EL}}\frac{c_1L}{8\pi}\log\left(\frac{6EL}{\pi}\right)}$ is kept as the next leading term in its expansion is of order $\frac{\log E}{\sqrt{E}}$.

On the other hand, when $c_1L \gg 1$, we must carefully discuss the relation between c_1L and EL. As we will demonstrate, there are three regimes as shown in Figure 5.12.

$EL \gg (c_1L)^2 \gg 1$

Let us first consider the first regime $EL \gg (c_1L)^2 \gg 1$. In the case, we can still take the saddle point to be the same as the previous conventional Cardy case, and the saddle point approximation leads to a similar result as (5.8.52)

$$\rho_{c_1,0}(E) = \frac{1}{\sqrt{c_1L}}\left(\frac{L/2\pi}{48E^3}\right)^{1/4} e^{\sqrt{\frac{\pi}{6EL}}\frac{c_1L}{8\pi}\log\left(\frac{6EL}{\pi}\right)} e^{2\pi\sqrt{\frac{EL/2\pi}{3}}}\left(1+O\left(\frac{c_1L}{\sqrt{EL}}\right)\right) \ , \quad EL \gg (c_1L)^2 \gg 1 \ , \tag{5.8.53}$$

except now the leading error is of the order $O\left(\frac{c_1L}{\sqrt{EL}}\right)$.

$c_1L \gg EL \gg 1$ and comparison to Dirichlet defect

Another interesting regime that can be computed is where $c_1L \gg EL \gg 1$, which can be analyzed by expanding the RHS of (5.8.51) for large c_1L, and inverse Laplace transforming

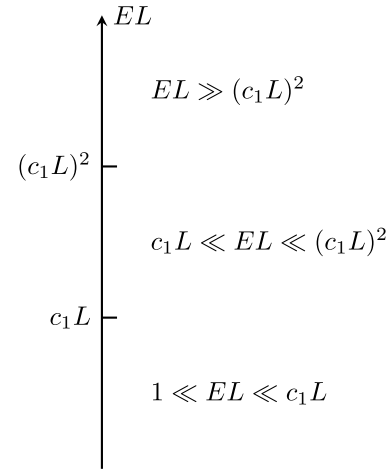

Figure 5.12: There are three regimes when $c_1L \gg 1$. When $EL \gg (c_1L)^2$, the asymptotic density of states take a similar form (5.8.53) as in the case $c_1L = O(1)$. When $1 \ll EL \ll c_1L$, the asymptotic density of states can be approximated by the asymptotic density of states of a Dirichlet defect as in (5.8.57). Finally, the regime where $c_1L \ll EL \ll (c_1L)^2$ is hard to compute analytically.

the leading term. The leading order contribution of expanding (5.8.51) can be computed by taking $c_1L \to +\infty$; alternatively, it can be computed using the fact that $c_1 = +\infty$ corresponds to Dirichlet defect.

To be more concrete, let's consider the massless scalar with boundary conditions $\phi(x = 0) = \phi(x = L) = 0$. The allowed mode solutions are then given by

$$\phi_n(x) = \sin\left(\frac{\pi n}{L}x\right) \ , \quad n = 1, 2, \cdots \ , \tag{5.8.54}$$

with allowed frequency $\omega_n = \frac{\pi n}{2}$. Notice this can also be derived from taking $c_1 \to \infty$ limit for the two classes of modes discussed in Section 5.8.1. The torus partition function computing the trace over defect Hilbert space can then be straightforwardly computed as

$$Z_{Dir}(L_d, L) = \prod_{n=1}^{\infty} \frac{q^{\frac{1}{4}n}}{1 - q^{\frac{1}{2}}} = q^{-\frac{1}{48}} \prod_{n=1}^{\infty}(1 - q^{\frac{n}{2}}) = \eta(q^{\frac{1}{2}}) \ , \quad q = e^{-2\pi\frac{L_d}{L}} \ , \tag{5.8.55}$$

where we have regularized the zero point energy using $\sum_{n=1}^{\infty} n = -\dfrac{1}{12}$. The high temperature limit of the dual channel can then be established using the modular property of the Dedekind eta function, and we find

$$\int_0^\infty \rho_{c_1=\infty}(E) e^{-EL_d} dE \approx \sqrt{\frac{L_d}{2L}} e^{\frac{\pi L}{6L_d}} e^{-\frac{\pi L_d}{24L}} \ , \quad \frac{L_d}{L} \to 0 \ . \tag{5.8.56}$$

From this, we conclude that the asymptotic density of states in the regime $c_1 L \gg EL \gg 1$ can be approximated by the inverse Laplace transformation of the RHS of (5.8.56)

$$\rho_{c_1,0}(E) = \frac{1}{4\sqrt{3}E} e^{2\pi\sqrt{\frac{EL/2\pi}{3}}} \left(1 + O\left(\frac{EL}{c_1 L}\right) + O\left(\frac{1}{\sqrt{EL}}\right)\right) \ , \quad c_1 L \gg EL \gg 1 \ . \tag{5.8.57}$$

To conclude, we want to point out that this analysis implies that the leading order term in the large c_1 expansion of the RHS of (5.8.51) must agree with the (5.8.56). In the following, we will show that this is indeed the case up to $O(1)$ number in the $c_1 L \to \infty$ limit as a consistency check. Using the Stirling approximation, it is straightforward to write the RHS of (5.8.51) as

$$\begin{aligned} &\frac{1}{\sqrt{c_1 L}} e^{L_d\left(E_0(c_1) - \frac{\pi}{6L}\right)} e^{-\frac{c_1 L_d}{4\pi}\log\left(\frac{L_d}{L}\right)} e^{\frac{\pi L}{6L_d}} e^{\frac{c_1 L_d \gamma}{4\pi}} \Gamma\left(1 + \frac{c_1 L_d}{4\pi}\right) \\ =&\sqrt{\frac{L_d}{2L}} e^{\frac{\pi L}{6L_d}} \exp\left[L_d\left(E_0(c_1) - \frac{\pi}{6L} + \frac{c_1}{4\pi}\log\left(\frac{c_1 L}{4\pi}\right) - \frac{c_1}{4\pi}(1-\gamma)\right)\right]\left(1 + O\left(\frac{1}{c_1 L_d}\right)\right) \ . \end{aligned} \tag{5.8.58}$$

To match with the calculation from the Dirichlet defect (5.8.56), we must have

$$E_0(c_1) = -\frac{c_1}{4\pi}\log\left(\frac{c_1 L}{4\pi}\right) + \frac{c_1}{4\pi}(1-\gamma) + \frac{\pi}{8L} + O\left(\frac{1}{c_1 L^2}\right) \ , \quad c_1 L \to \infty \ . \tag{5.8.59}$$

To study this, let's recall that

$$E_0(c_1) = \frac{\omega_0}{2} + \frac{1}{2}\sum_{n=1}^\infty \left(\omega_n - \frac{2\pi n}{L} - \frac{c_1}{2\pi n}\right) \ . \tag{5.8.60}$$

To estimate its large c_1 behavior, we notice that the expansion (5.8.5) is valid when $n \gg \sqrt{c_1 L}$ while the expansion (5.8.6) is valid when $n \ll c_1 L$. In the region $\sqrt{c_1 L} \ll n \ll c_1 L$, both expansions are simultaneously valid.

Thus, we consider split the infinite sum at $N = \epsilon c_1 L$ into two pieces

$$E_0(c_1) = \frac{\omega_0}{2} + \frac{1}{2}\sum_{n=1}^N \left(\omega_n - \frac{2\pi n}{L} - \frac{c_1}{2\pi n}\right) + \frac{1}{2}\sum_{n=N+1}^\infty \left(\omega_n - \frac{2\pi n}{L} - \frac{c_1}{2\pi n}\right) \tag{5.8.61}$$

where ϵ is chosen such that $\sqrt{c_1 L} \ll \epsilon c_1 L \ll c_1 L$. Notice that even though this implies that $\frac{1}{\sqrt{c_1 L}} \ll \epsilon \ll 1$, we still consider ϵ as being independent of $c_1 L$.

The first two terms in (5.8.61) we estimate using the expansion (5.8.6), which leads to

$$\begin{aligned}
&\frac{\omega_0}{2} + \frac{1}{2}\sum_{n=1}^{\epsilon c_1 L}\left(\omega_n - \frac{2\pi n}{L} - \frac{c_1}{2\pi n}\right) \\
=&\frac{\pi}{2L} + \frac{1}{2}\sum_{n=1}^{\epsilon c_1 L}\left(-\frac{8\pi^2}{c_1 L^2}n + \frac{\pi}{L}\left(1 - \frac{4\pi}{c_1 L}\right) - \frac{c_1}{2n\pi}\right) + O\left(\frac{1}{c_1 L^2}\right) \\
=&-\frac{c_1}{4\pi}\log(c_1 L) + c_1\left(-\frac{1}{4\pi}\log\epsilon - \frac{\gamma}{4\pi} + O(\epsilon)\right) + \left(\frac{\pi}{2L} + O(\epsilon)\right) + O\left(\frac{1}{c_1 L^2}\right)\ .
\end{aligned} \tag{5.8.62}$$

To estimate the last term, we use the expansion (5.8.5), and to compute the $O(c_1)$ and $O(1)$ contribution, one must use a more detailed version of (5.8.5)

$$\begin{aligned}
\omega_n - \frac{2\pi n}{L} - \frac{c_1}{2n\pi} =& -\frac{L}{8\pi^3 n^3}c_1^2 \\
&+ \left(-\frac{L^2}{96\pi^3 n^3} + \frac{L^2}{16n^5\pi^5}\right)c_1^3 \\
&+ \left(+\frac{L^3}{96n^5\pi^5} - \frac{5L^3}{128n^7\pi^7}\right)c_1^4 \\
&+ \left(+\frac{L^4}{2560n^5\pi^5} + O\left(\frac{1}{n^7}\right)\right)c_1^5 \\
&+ \left(-\frac{23}{30720n^7\pi^7} + O\left(\frac{1}{n^9}\right)\right)c_1^6 \\
&+ \cdots \\
&+ \left(\alpha_{2m}\frac{L^{2m-1}}{n^{2m+1}} + O\left(\frac{1}{n^{2m+3}}\right)\right)(c_1)^{2m} \\
&+ \left(\frac{2(-1)^m}{(2m+1)(4\pi)^m}\frac{L^{2m}}{n^{2m+1}} + O\left(\frac{1}{n^{2m+3}}\right)\right)(c_1)^{2m+1} \\
&+ \cdots\ .
\end{aligned} \tag{5.8.63}$$

As we will see shortly, the order $O(c_1)$ contribution arises from the term of the form $\sum_{n=\epsilon c_1 L_1+1}^{\infty}\frac{(c_1)^{2m+1}}{n^{2m+1}}$ while the order $O(1)$ contribution arises from the term of the form $\sum_{n=\epsilon c_1 L_1+1}^{\infty}\frac{(c_1)^{2m}}{n^{2m+1}}$. But because we do not have a generic expression for the coefficients α_{2m} of the latter term, we only managed to compute explicitly the order $O(c_1)$ contribution.

To see this, we notice that

$$\sum_{n=\epsilon c_1 L_1+1}^{\infty} \frac{1}{n^p} = \frac{(-1)^p}{(p-1)!}\psi^{(p-1)}(\epsilon c_1 L_1+1) = \frac{1}{p-1}\frac{1}{(\epsilon c_1 L)^{p-1}}\left(1+O\left(\frac{1}{\epsilon c_1 L}\right)\right) \ , \tag{5.8.64}$$

thus the order $O(c_1)$ contribution of the second sum is given by

$$\begin{aligned}
&\frac{1}{2}\sum_{n=\epsilon c_1 L+1}^{\infty} \omega_n - \frac{2\pi n}{L} - \frac{c_1}{2n\pi} \\
=&\frac{c_1}{4\pi}\sum_{m=1}^{\infty}\frac{(-1)^m}{2m(2m+1)}\left(\frac{1}{4\pi\epsilon}\right)^{2m} + O(1) \\
=&\frac{c_1}{4\pi}\left(1+\log\left(4\pi\epsilon\right)+O(\epsilon)\right)+O(1) \ ,
\end{aligned} \tag{5.8.65}$$

where the last result is acquired by explicitly summing over m (which we omit for simplicity) and then expand near small ϵ.

Combining the two results, we find that the result correctly matches the expected behavior (5.8.59) up to an order 1 number:

$$E_0(c_1) = -\frac{c_1}{4\pi}\log\left(\frac{c_1 L}{4\pi}\right) + \frac{c_1}{4\pi}\left(1-\gamma\right) + O(1) \ . \tag{5.8.66}$$

5.9 Spacelike c_1 defect and quench

In this section we consider time evolution on the Lorentzian plane in the presence of a spacelike defect. For $t < 0$ the scalar field is in its standard (no defect) vacuum state. A spacelike defect is then inserted at $t = 0$, leading to an excited state at $t > 0$. We compute this excited state, along with the two-point scalar correlator and stress tensor expectation value therein. This is a particular example of a quench, described by an instantaneous change in the Hamiltonian.

5.9.1 In and out vacuum states for the general defect

In the presence of a spacelike defect inserted at $t = 0$, there are two types of *in* modes which are either left or right moving purely positive frequency waves for $t < 0$. To find them, we can plug the ansatz

$$\phi^{\omega}_{in,L} = \begin{cases} t<0: & N\, e^{-i\omega v} \\ t>0: & N\left(Ae^{-i\omega v} + Be^{i\omega u}\right) \end{cases}, \qquad \phi^{\omega}_{in,R} = \begin{cases} t<0: & N'\, e^{-i\omega u} \\ t>0: & N'\left(A'e^{-i\omega u} + B'e^{i\omega v}\right) \end{cases} \tag{5.9.1}$$

where $u = t - x, v = t + x$, into the matching condition

$$\begin{pmatrix} \phi(t=0^+,x) \\ \dot\phi(t=0^+,x) \end{pmatrix} = \begin{pmatrix} a & b \\ c & d \end{pmatrix} \begin{pmatrix} \phi(t=0^-,x) \\ \dot\phi(t=0^-,x) \end{pmatrix}, \qquad ad - bc = 1 \tag{5.9.2}$$

and normalise them so their KG inner products (5.6.3) are,

$$(\phi^{\omega}_{L,in}, \phi^{\omega'}_{L,in}) = 2\pi\delta(\omega-\omega') = (\phi^{\omega}_{R,in}, \phi^{\omega'}_{R,in}), \quad \text{all other inner products} = 0\ . \tag{5.9.3}$$

Note that the condition $ab - bc = 1$ is necessary (and sufficient) for conservation of the KG inner product across the defect. The resulting *in* modes are

$$\phi^{\omega}_{in,L} = \begin{cases} t<0: & \frac{1}{\sqrt{2\omega}}\, e^{-i\omega v} \\ t>0: & \frac{1}{\sqrt{2\omega}}\left(A_\omega e^{-i\omega v} + B_\omega e^{i\omega u}\right) \end{cases} \tag{5.9.4}$$

$$\phi^{\omega}_{in,R} = \begin{cases} t<0: & \frac{1}{\sqrt{2\omega}} e^{-i\omega u} \\ t>0: & \frac{1}{\sqrt{2\omega}}\left(A_\omega e^{-i\omega u} + B_\omega e^{i\omega v}\right) \end{cases} \tag{5.9.5}$$

where

$$\begin{aligned} A_\omega &= \frac{1}{2}\left(-\frac{c}{i\omega} + a + d - i\omega b\right) = t_\omega^{-1} \\ B_\omega &= \frac{1}{2}\left(\frac{c}{i\omega} + a - d - i\omega b\right) = \frac{r^v_\omega}{t_\omega} \end{aligned} \tag{5.9.6}$$

where r_ω and t_ω are the reflection and transmission coefficients given in Eq. (5.6.5). While A_ω doesn't vanish for the real-valued frequency ω and (a, b, c, d) satisfying $ad - bc = 1$, B_ω vanishes for the trivial $(a = d = 1, b = c = 0)$ and $\mathbb{Z}_2$ $(a = d = -1, b = c = 0)$ defects, as it is analogous to the reflection coefficients in the presence of the time-like defect.

To quantise the theory we define the *in* vacuum as

$$a_\omega|0; in\rangle = 0, \quad b_\omega|0; in\rangle = 0, \quad \forall\omega \tag{5.9.7}$$

where the only non-trivial commutators between the oscillators are

$$[a_\omega, a^\dagger_{\omega'}] = 2\pi\delta(\omega-\omega') = [b_\omega, b^\dagger_{\omega'}] \ . \tag{5.9.8}$$

Then, one can quantise the scalar field using the in modes (5.9.5) as

$$\phi(t,x) = \int_0^\infty \frac{\mathrm{d}\omega}{2\pi}\left(a_\omega\phi^\omega_{in,L} + b_\omega\phi^\omega_{in,R} + h.c.\right) \ . \tag{5.9.9}$$

For $t>0$, which is the time after the defect insertion, one can single out the positive frequency modes in the mode expansion

$$\begin{aligned}\phi(t>0,x) &= \int_0^\infty \frac{\mathrm{d}\omega}{2\pi}\left[\frac{e^{-i\omega v}}{\sqrt{2\omega}}\left(A_\omega a_\omega + B^*_\omega b^\dagger_\omega\right) + \frac{e^{-i\omega u}}{\sqrt{2\omega}}\left(B^*_\omega a^\dagger_\omega + A_\omega b_\omega\right) + h.c.\right] \\ &\equiv \int_0^\infty \frac{\mathrm{d}\omega}{2\pi}\left(c_\omega\frac{e^{-i\omega v}}{\sqrt{2\omega}} + d_\omega\frac{e^{-i\omega u}}{\sqrt{2\omega}} + h.c.\right)\end{aligned} \tag{5.9.10}$$

where we defined the new oscillators

$$c_\omega = A_\omega a_\omega + B^*_\omega b^\dagger_\omega \ , \qquad d_\omega = B^*_\omega a^\dagger_\omega + A_\omega b_\omega \ . \tag{5.9.11}$$

From the commutators of old oscillators (5.9.8), it follows that the new oscillators are canonically quantised, i.e.

$$[c_\omega, c^\dagger_{\omega'}] = 2\pi\delta(\omega-\omega') = [d_\omega, d^\dagger_{\omega'}] \ . \tag{5.9.12}$$

These oscillators define the *out* vacuum state such that

$$c_\omega|0;out\rangle = 0 \ , \quad d_\omega|0;out\rangle = 0, \quad \forall\omega \ . \tag{5.9.13}$$

Due to the appearance of the old creation operators in the new annihilation operators, the *in* vacuum state is not annihilated by c_ω and d_ω and hence differs from the *out* vacuum state for $t>0$. Said differently, to an observer at $t>0$, the *in* vacuum state corresponds to an excited state. To write the *in* vacuum state in the Fock space basis of the *out* vacuum w.r.t. the new oscillators we use an ansatz

$$|0;in\rangle = \bigotimes_\omega\left(\sum_{n_\omega,m_\omega} C^\omega_{n_\omega,m_\omega}|n_\omega,m_\omega;out\rangle\right) \ , \tag{5.9.14}$$

For ease of notation, let's consider a fixed frequency ω and drop the subscript ω. The two defining equations of the *in* vacuum state, i.e. $a_\omega|0;in\rangle = b_\omega|0;in\rangle = 0$, provide two relations of the coefficients

$$\begin{aligned} A^*_\omega\sqrt{m+1}C_{m+1,n} &= B^*_\omega\sqrt{n}C_{m,n-1} \ , \\ A^*_\omega\sqrt{n}C_{m+1,n} &= B^*_\omega\sqrt{m+1}C_{m,n-1} \ . \end{aligned} \tag{5.9.15}$$

which are solved as

$$C_{n,m} = \delta_{n,m}\left(\frac{B^*_\omega}{A^*_\omega}\right)^n C_{0,0} = \delta_{n,m}\left(\frac{b\omega^2 - i(a-d)\omega + c}{b\omega^2 - i(a+d)\omega - c}\right)^n C_{0,0} \ . \tag{5.9.16}$$

Hence the *in* vacuum state is

$$|0;in\rangle = \prod_\omega \exp\left(\frac{1}{2\pi}\frac{b\omega^2 - i(a-d)\omega + c}{b\omega^2 - i(a+d)\omega - c}c^\dagger_\omega d^\dagger_\omega\right) C^\omega_{0,0}|0;out\rangle \ . \tag{5.9.17}$$

where $C^\omega_{0,0}$ are normalisation constants which should be fixed so that $\langle 0;in|0;in\rangle = 1$. For example, for the c_1 defect $(a = d = 1, b = 0, c = c_1)$

$$|0;in\rangle = \prod_\omega \exp\left(-\frac{1}{2\pi}\frac{c_1}{2i\omega + c_1}c^\dagger_\omega d^\dagger_\omega\right) C^\omega_{0,0}|0;out\rangle \ . \tag{5.9.18}$$

5.9.2 Correlation functions

The scalar two-point correlation function is a solution of the field equation subject to the matching condition. When both points are below the defect, i.e. $t_{1,2} < 0$, the correlation function in the in vacuum state is the standard free theory correlation function

$$\langle in|\phi(t_1,x_1)\phi(t_2,x_2)|in\rangle = -\frac{1}{4\pi}\log\left[m^2\left((x_1-x_2)^2 - (t_1-t_2-i\epsilon)^2\right)\right] \ , \tag{5.9.19}$$

where the $i\epsilon$ prescription is chosen so that the correlator is analytic in the lower half $t_1 - t_2$ plane, as appropriate for this operator ordering. We will be working in the massless theory but have introduced m^2 in the above as an IR regulator. Due to the discontinuity across the defect, the two-point function behaves differently depending on whether one or both points is (are) placed above or below the defect. There are six different cases:

$$\begin{aligned} &\mathrm{I}: \quad t_1 > t_2 > 0 \ , \qquad &&\mathrm{I}': \qquad t_2 > t_1 > 0 \ , \\ &\mathrm{II}: \quad t_1 > 0 > t_2 \ , \qquad &&\mathrm{II}': \qquad t_2 > 0 > t_1 \ , \\ &\mathrm{III}: \quad 0 > t_1 > t_2 \ , \qquad &&\mathrm{III}': \qquad 0 > t_2 > t_1 \ . \end{aligned} \tag{5.9.20}$$

Let's denote the two-point function at Region $X = \mathrm{I}, \cdots, \mathrm{III}'$ by

$$f^X(t_1, x_1; t_2, x_2) \equiv \langle 0; in|\phi(t_1, x_1)\phi(t_2, x_2)|0; in\rangle \ . \tag{5.9.21}$$

When at least one point is above the defect, one can use f^{III} or $f^{\mathrm{III}'}$ and the matching conditions to fix the "initial data" to the immediate future of the defect and use that to solve the field equation. Namely, we look for solutions of the initial value problem

$$\begin{aligned} \varphi(x, 0) =& \varphi_0(x) \ , \quad \dot{\varphi}(x, 0) = v_0(x) \ , \\ &\left(\partial_t^2 - \partial_x^2\right)\varphi = 0 \end{aligned} \tag{5.9.22}$$

where the initial data $\varphi_0(x)$ and $v_0(x)$ are obtained by f^{III} or $f^{\mathrm{III}'}$ (5.9.19) and the matching condition. The solution of d'Alembert [126] is

$$\varphi(t, x) = \frac{\varphi_0(x+t) + \varphi_0(x-t)}{2} + \frac{1}{2}\int_{x-t}^{x+t} v_0(s)\mathrm{d}s \ . \tag{5.9.23}$$

In Region II ($t_1 > 0 > t_2$), the initial data are

$$\begin{aligned} \varphi_0(x_1) &= f^{\mathrm{III}}(0, x_1; t_2, x_2) = -\frac{1}{4\pi}\log[m^2(x_{12} - t_2 - i\epsilon)(x_{12} + t_2 + i\epsilon)] \ , \\ v_0(x_1) &= \partial_{t_1} f^{\mathrm{III}}(0, x_1; t_2, x_2) + c_1 f^{\mathrm{III}}(0, x_1; t_2, x_2) \ , \end{aligned} \tag{5.9.24}$$

where $x_{12} \equiv x_1 - x_2$.

Plugging into d'Alembert's solution (5.9.23), the correlation function is

$$\begin{aligned} f^{\mathrm{II}}&(t_1, x_1; t_2, x_2) \\ &= -\frac{1}{4\pi}\log\left[m^2(u_2 - u_1 + i\epsilon)(v_1 - v_2 - i\epsilon)\right] + \frac{c_1}{4\pi}(u_1 + v_1) \\ &\quad - \frac{c_1}{8\pi}\Big[(v_1 - v_2)\log\left[m(v_1 - v_2 - i\epsilon)\right] + (u_1 + v_2)\log\left[m(-u_1 - v_2 - i\epsilon)\right] \\ &\qquad\qquad + (v_1 + u_2)\log\left[m(v_1 + u_2 + i\epsilon)\right] - (u_2 - u_1)\log\left[m(u_2 - u_1 + i\epsilon)\right]\Big] \ . \end{aligned} \tag{5.9.25}$$

Following the same procedure at Region I using f^{II} obtained above, the correlation function is

$$
\begin{aligned}
&f^{\mathrm{I}}\left(t_1, x_1; t_2, x_2\right) \\
&\quad = -\frac{1}{4\pi}\log\left[m^2\left(u_2-u_1+i\epsilon\right)\left(v_1-v_2-i\epsilon\right)\right]+\frac{c_1}{4\pi}\left(u_1+v_1+u_2+v_2\right) \\
&\qquad -\frac{c_1}{8\pi}\left[\left(v_1+u_2\right)\log\left[m^2(v_1+u_2)^2+\epsilon^2\right]+\left(u_1+v_2\right)\log\left[m^2(u_1+v_2)^2+\epsilon^2\right]\right] \\
&\qquad +\frac{3c_1^2}{16\pi}\left(u_1+v_1\right)\left(u_2+v_2\right) \\
&\qquad +\frac{c_1^2}{32\pi}\Bigg[\left(v_1-v_2\right)^2\log\left[m^2(v_1-v_2)^2+\epsilon^2\right]+\left(u_1-u_2\right)^2\log\left[m^2(u_1-u_2)^2+\epsilon^2\right] \\
&\qquad\qquad -\left(v_1+u_2\right)^2\log\left[m^2(v_1+u_2)^2+\epsilon^2\right]-\left(u_1+v_2\right)^2\log\left[m^2(u_1+v_2)^2+\epsilon^2\right]\Bigg] \, .
\end{aligned}
\tag{5.9.26}
$$

One can also compute these correlation functions in momentum space, starting from Region III and consecutively applying the matching condition and Fourier transforming back to the position space.

Using the correlation function, one can compute the energy momentum tensor in the *in*-vacuum state. After subtracting off the value in the absence of the defect we have

$$
\begin{aligned}
\langle 0; in|T_{uu}(u)|0; in\rangle - \langle 0; in|T_{uu}(u)|0; in\rangle\big|_{c_1=0} &= \lim_{u_1,u_2\to u}\partial_{u_1}\partial_{u_2} f^{\mathrm{I}}(t_1, x_1; t_2, x_2) \\
&= \frac{c_1^2}{16\pi}\log\frac{\Lambda}{m} \ , \\
\langle 0; in|T_{vv}(v)|0; in\rangle - \langle 0; in|T_{vv}(v)|0; in\rangle\big|_{c_1=0} &= \lim_{v_1,v_2\to v}\partial_{v_1}\partial_{v_2} f^{\mathrm{I}}(t_1, x_1; t_2, x_2) \\
&= \frac{c_1^2}{16\pi}\log\frac{\Lambda}{m} \ .
\end{aligned}
\tag{5.9.27}
$$

where we regulated the UV divergence through the point splitting, $|u_1-u_2| = \Lambda^{-1} = |v_1-v_2|$.

Using these, the energy density and the flux are

$$\begin{aligned}
\langle 0;in|T_{tt}(u,v)|0;in\rangle - \langle \mathrm{in}|T_{tt}(u,v)|0;in\rangle|_{c_1=0} &= [\langle 0;in|T_{uu}(u)|0;in\rangle + \langle 0;in|T_{vv}(v)|0;in\rangle]^{c_1}_{c_1=0} \\
&= \frac{c_1^2}{8\pi}\log\frac{\Lambda}{m} \ , \\
\langle 0;in|T_{tx}(u,v)|0;in\rangle &= [-\langle 0;in|T_{uu}(u)|0;in\rangle + \langle 0;in|T_{vv}(v)|0;in\rangle] \\
&= 0 \ .
\end{aligned} \tag{5.9.28}$$

T_{uu} and T_{vv} for $t > 0$ (5.9.27) have no $O(c_1)$ term, because such a term comes from a single interaction vertex on the defect given by $c_1\phi(p)\phi(-p)$ which contains both left and right moving particles while T_{uu} (T_{vv}) contain only right(left) moving particles. On the other hand, the $O(c_1^2)$ term comes from two interaction vertices on the defect, allowing two like-moving fields to contract against each other, leaving two like-moving fields to contribute to T_{uu} and T_{vv}. All higher order vertices are suppressed in the limit $\Lambda \to \infty$.

It is also worth pointing out that for the defect in Euclidean signature we have $\langle T_{\mu\nu}\rangle = 0$ at any point not on the defect, as can be easily shown as follows. Conservation implies that $\langle T_{zz}\rangle$ can only depend on $z = x + it$. Taking the defect to extend along t, we must have that $\langle T_{zz}\rangle$ is independent of t by time translation invariance. This implies that $\langle T_{zz}\rangle$ is a constant. But since it must also vanish at infinity, it must vanish at all points off of the defect. The same holds for $\langle T_{\bar{z}\bar{z}}\rangle$. Note that it is the last condition of vanishing at infinity that does not hold for the spacelike quench defect, as this defect creates an excited state that does not disperse at late times.

5.10 Comments

In this chapter we studied various aspects of codimension-one defects in free scalar field theory. Even in this simplified setting there are many possible extensions that could be pursued. For example: non-parallel defects; defects with cusps and their associated anomalous dimensions; moving and dynamical defects, and so forth. Going beyond free field theory there are a large number of directions, many of which have been studied in the existing literature in one form or another. For example, one could add dynamical degrees of freedom on the defect; replace the bulk theory with an interacting CFT such as Liouville theory; couple the defect to gravity, etc. For many of these cases, our simplified free field theory treatment should serve as a useful starting point for perturbation theory, where applicable.

APPENDIX A

Systematics of Boundary Action

A.1 Forms Conventions

For convenience we collect some conventions and useful expressions involving forms which are used elsewhere in this work. For a general p-form,

$$\omega = \frac{1}{p!}\omega_{\mu_1\cdots\mu_p}\mathrm{d}x^{\mu_1}\wedge\cdots\wedge\mathrm{d}x^{\mu_p}, \qquad \mathrm{d}\omega = \frac{1}{p!}\partial_\nu\omega_{\mu_1\cdots\mu_p}\mathrm{d}x^{\nu}\wedge\mathrm{d}x^{\mu_1}\wedge\cdots\wedge\mathrm{d}x^{\mu_p}$$
$$= \frac{1}{p!}\nabla_\nu\omega_{\mu_1\cdots\mu_p}\mathrm{d}x^{\nu}\wedge\mathrm{d}x^{\mu_1}\wedge\cdots\mathrm{d}x^{\mu_p} \tag{A.1.1}$$

so long as the connection ∇ is torsionless. This also implies

$$\frac{1}{p!}\partial_{[\nu}\omega_{\mu_1\cdots\mu_p]} = \frac{1}{(p+1)!}(\mathrm{d}\omega)_{\nu\mu_1\cdots\mu_p} \tag{A.1.2}$$

where the antisymmetrization is defined to include a division by the order of the symmetric group[1]. The contraction is defined by

$$i_\xi\omega = \frac{1}{(p-1)!}\xi^\nu\omega_{\nu\mu_2\cdots\mu_p}\mathrm{d}x^{\mu_2}\wedge\cdots\wedge\mathrm{d}x^{\mu_p}, \qquad (i_\xi\omega)_{\mu_2\cdots\mu_p} = \xi^\nu\omega_{\nu\mu_2\cdots\mu_p}. \tag{A.1.3}$$

We often find it useful to define

$$(\mathrm{d}^{D-p}x)_{\mu_1\cdots\mu_p} = \frac{1}{(D-p)!}\epsilon_{\mu_1\cdots\mu_p\nu_1\cdots\nu_{D-p}}\mathrm{d}x^{\nu_1}\wedge\cdots\wedge\mathrm{d}x^{\nu_{D-p}} \tag{A.1.4}$$

and it is useful to note

$$i_\xi(\mathrm{d}^{D-p}x)_{\mu_1\cdots\mu_p} = \xi^\nu(\mathrm{d}^{D-(p+1)}x)_{\mu_1\cdots\mu_p\nu}. \tag{A.1.5}$$

[1] For example these conventions imply $(\mathrm{d}\omega)_{\alpha\beta} = \partial_\alpha\omega_\beta - \partial_\beta\omega_\alpha$.

With these notations the Hodge star is defined by

$$\star\omega = \frac{\sqrt{|g|}}{p!(D-p)!}\omega^{\mu_1\cdots\mu_p}\epsilon_{\mu_1\cdots\mu_p\nu_{p+1}\cdots\nu_D}\mathrm{d}x^{\nu_{p+1}}\wedge\cdots\wedge\mathrm{d}x^{\nu_D} = \frac{\sqrt{|g|}}{p!}\omega_{\mu_1\cdots\mu_p}(\mathrm{d}^{D-p}x)^{\mu_1\cdots\mu_p} \tag{A.1.6}$$

where $\epsilon_{\mu_1\cdots\mu_D}$ is the totally antisymmetric numeric array with entries ± 1. With this definition $\star^2 = (g)(-1)^{p(D-p)}$. It is sometimes also convenient to define $\varepsilon_{\mu_1\cdots\mu_D} = \sqrt{|g|}\epsilon_{\mu_1\cdots\mu_D}$.

One may also show, assuming torsionless connection, that for $p+1 \neq D$

$$\nabla_\nu X^{\mu_1\cdots\mu_{D-(p+1)}\nu}(\mathrm{d}^{p+1}x)_{\mu_1\cdots\mu_{D-(p+1)}} = \mathrm{d}\left(\frac{1}{D-(p+1)}X^{\mu_1\cdots\mu_{D-(p+1)}\nu}(\mathrm{d}^p x)_{\mu_1\cdots\mu_{D-(p+1)}\nu}\right). \tag{A.1.7}$$

Note there is no factorial in the coefficient. A useful special case of this is $p = D-2$ (so $\mathrm{d}\omega$ is a $(D-1)$-form current) is

$$\nabla_\nu X^{\mu\nu}(\mathrm{d}^{D-1}x)_\nu = \mathrm{d}\left(\frac{1}{2}X^{\mu\nu}(\mathrm{d}^{D-2}x)_{\mu\nu}\right). \tag{A.1.8}$$

For the special case $p = D$, if $\omega = \nabla_\mu j^\mu\sqrt{|g|}\mathrm{d}^D x$, then $\omega = \mathrm{d}J$ with $J = \star j = \sqrt{|g|}j^\mu(\mathrm{d}^{D-1}x)_\mu$.

Finally, suppose Σ is a codimension-1 (non-null) surface in M and let ϕ^* be the pullback to Σ, as would appear in an integral over Σ. Then

$$\phi^*\left[\sqrt{|g|}(\mathrm{d}^{D-1}x)_\mu\right] = \sigma\hat{n}_\mu(\Sigma) \tag{A.1.9}$$

where $\hat{n}_\mu$ is the unit normal to Σ and $\sigma = \hat{n}^\mu\hat{n}_\mu$ depends on whether Σ is timelike or lightlike. The orientation choice here is $(M) = \hat{n}\wedge(\Sigma)$.

A.2 Identically Closed Forms

The Poincaré lemma ensures that if J is any closed form on spacetime then, at least locally, there exists a potential Q satisfying $J = \mathrm{d}Q$. Though such conserved currents are common in physics due to Noether's theorem, the Poincaré lemma is not typically useful because it carries no guarantee that Q can be constructed locally from the fields in our theory. Indeed, for a general current J, Q will indeed be non-local. The exception to this, of course, are the Noether currents associated to gauge symmetries. These are currents J_ξ which are closed for every possible set of free functions ξ parametrizing the gauge transformation. This additional ingredient, closure despite depending on an arbitrary function, is what we need to ensure the potential Q_ξ can be constructed as a local functional of ξ and the other fields in the theory, assuming J_ξ was local to begin with.

This result has appeared in the physics literature in [127] and [128, 129], the latter referring to the older mathematical literature on the bivariational complex[2] where this result is established by finding a homotopy operator. While [127] is clear on the recursive algorithm for constructing the potential Q_ξ, insights from the more mathematical literature on the utility of higher Euler operators allow us solve the recursion explicitly in a natural way[3].

As most of this work only relies on the existence of an algorithm to compute a local Q_ξ and not on its details, we state the result as a theorem here[4]:

Theorem 1 *As elsewhere, suppose M is a D-dimensional spacetime, ϕ is some collection of fields over M, and ξ are some functions over M. Let J be a p-form over M ($p < D$) and a local functional of ϕ and ξ, meaning at each point $x \in M$ it depends on only ϕ and ξ, and finitely many of their derivatives, at x. Suppose further that* $\mathrm{d}J = 0$ *for all free functions ξ and that $J = J_0$ when $\xi = 0$. Then there exists a local functional Q of ϕ and ξ such that $J = J_0 + \mathrm{d}Q$.*

[2] See [130, 131] for textbook treatments on this perspective.

[3] This is essentially deriving the homotopy operator, though we will only show that it constructs local potentials and not that it obeys the stronger property of defining a homotopy operator.

[4] The original statement in [127] is slightly more general as the ξ are allowed to be sections of an arbitrary bundle rather than functions, but this is all we will require and allows us to include the statement about $\xi = 0$.

For the interested reader, we have included a short but pedagogical review of how the algorithm can be derived, by way of a simple example, in section A.2.1. The statement of the algorithmic procedure can be found in section A.2.2, along with a small notational dictionary to some other locations in the literature.

A.2.1 Motivation

The idea underlying this algorithm, in this presentation, relies on a simple observation which can be demonstrated by considering the special case where J is a 2-form which depends only linearly on the functions ξ up to the first derivative. It is also conceptually simpler to start with a potential for J, say $\tilde{Q}$, rather than J itself[5]. Writing $\tilde{Q}$ as an expansion in the derivative order of ξ we have

$$\begin{aligned}\tilde{Q} &= \left[\tilde{Q}_{k\alpha}\xi^k + \tilde{Q}^{\mu}_{k\alpha}\partial_\mu\xi^k\right]\mathrm{d}x^\alpha \\ &= \left[\xi^k E_k(\tilde{Q}_\alpha) + \partial_\mu[\xi^k E^\mu_k(\tilde{Q}_\alpha)]\right]\mathrm{d}x^\alpha \end{aligned} \tag{A.2.1}$$

where in the second line we have integrated by parts until no derivatives act directly on the ξ^k. We will refer to the coefficients $E^{\mu_1\cdots\mu_r}_k(\tilde{Q}_\alpha)$ as the Euler coefficients[6]. Here we would have

$$E_k(\tilde{Q}_\alpha) = \tilde{Q}_{k\alpha} - \partial_\mu\tilde{Q}^\mu_{k\alpha}, \qquad E^\mu_k(\tilde{Q}_\alpha) = \tilde{Q}^\mu_{k\alpha}. \tag{A.2.2}$$

Since the ξ^k are free functions, the coefficients in the derivative expansion are unique. Since there are only finitely many derivatives present we can always convert between the derivative

---

[5]This $\tilde{Q}$ will be related to the potential Q we construct in the end, but in general will be different. The actual algorithm makes no reference to this $\tilde{Q}$, so it's only purpose here is as a useful intermediary to motivate the key ideas.

[6]This language is inherited from the mathematical literature where the $E^{\mu_1\cdots\mu_r}_k$ would be called the higher Euler operators as they are generalizations of the Euler-Lagrange operator which produces the equations of motion from a Lagrangian.

and Euler expansions by integration by parts identities, so the Euler expansion must also be unique[7].

Of course, this is merely a rewriting of $\tilde{Q}$, but it's a rewriting with the advantage that when we take the differential of $\tilde{Q}$ we find

$$\begin{aligned} \mathrm{d}\tilde{Q} &= \frac{1}{1!}\Big[\quad 0 \quad + \quad \partial_\rho[\xi^k E_k(\tilde{Q}_\alpha)] \quad + \quad \partial_\rho\partial_\mu[\xi^k E_k^\mu(\tilde{Q}_\alpha)]\Big]\mathrm{d}x^\rho\wedge\mathrm{d}x^\alpha \\ &= \frac{1}{2!}\Big[\quad \xi^k E_k(\mathrm{d}\tilde{Q}_{\rho\alpha}) \quad + \quad \partial_\mu[\xi^k E_k^\mu(\mathrm{d}\tilde{Q}_{\rho\alpha})] \quad + \quad \partial_\mu\partial_\nu[\xi^k E_k^{\mu\nu}(\mathrm{d}\tilde{Q}_{\rho\alpha})]\Big]\mathrm{d}x^\rho\wedge\mathrm{d}x^\alpha \end{aligned} \tag{A.2.3}$$

where in the second line we have written the generic Euler expansion for $\mathrm{d}\tilde{Q} = J$. But because the Euler expansion is unique, the aligned terms must match so

$$\frac{1}{2!}E_k(J_{\rho\alpha}) = 0, \qquad \frac{1}{2!}E_k^\mu(J_{\rho\alpha}) = \delta^\mu_{[\rho}E_k(\tilde{Q}_{\alpha]}), \qquad \frac{1}{2!}E_k^{\mu\nu}(J_{\rho\alpha}) = \delta^{(\mu}_{[\rho}E_k^{\nu)}(\tilde{Q}_{\alpha]}). \tag{A.2.4}$$

Throughout this section, antisymmetrization will not include the k index as it's generically of a different type. If we were able to invert these equations for the Euler coefficients of $\tilde{Q}$, we would have determined $\tilde{Q}$ in terms of J.

Unfortunately, we cannot invert these equations, but we don't need to because J doesn't have a unique potential. So really since our goal is to construct a potential for J, we only need to reconstruct $\tilde{Q}$ up to a closed form. To do this we want to eliminate the Kronecker deltas, and we may do so by taking a trace between μ and ρ in (A.2.4). We find

$$\begin{aligned} \frac{1}{2!}E_k^\mu(J_{\mu\alpha}) &= \frac{1}{2!}\Big(DE_k(\tilde{Q}_\alpha) - E_k(\tilde{Q}_\alpha)\Big), \\ \frac{1}{2!}E_k^{\mu\nu}(J_{\mu\alpha}) &= \frac{1}{2!2!}\Big(DE_k^\nu(\tilde{Q}_\alpha) - E_k^\nu(\tilde{Q}_\alpha) + E_k^\nu(\tilde{Q}_\alpha) - \delta^\nu_\alpha E_k^\mu(\tilde{Q}_\mu)\Big). \end{aligned} \tag{A.2.5}$$

The overall factors come from the (anti-)symmetrization and we see that we can classify the types of terms which appear. If either μ or ρ (or both) appear on the delta, we obtain a term proportional to an Euler coefficient of $\tilde{Q}$. If both indices do not appear on the delta, then we obtain a term which still contains a delta. In the case both μ and ρ appear on the

[7] This is the step which requires the "finite derivative order" part of locality. In [127] it was that the recursion started with the highest derivative order.

delta we find the coefficient to be the dimension. If only μ is on the delta we obtain a minus sign[8], if only ρ is on the delta then we obtain a plus sign.

We may rewrite (A.2.5) in the form

$$\begin{aligned} E_k(\tilde{Q}_\alpha) &= \frac{1}{D-1} E_k^\mu(J_{\mu\alpha}). \\ E_k^\nu(\tilde{Q}_\alpha) &= \frac{2}{D} E_k^{\mu\nu}(J_{\mu\alpha}) + \frac{1}{D}\delta_\alpha^\nu E_k^\mu(\tilde{Q}_\mu). \end{aligned} \tag{A.2.6}$$

The second equation does not specify the Euler coefficient[9] of $\tilde{Q}$ in terms of only J, but observe that if we try to build $\tilde{Q}$ back from these expressions we find

$$\tilde{Q} = \left[\frac{1}{D-1}\xi^k E^\mu(J_{\mu\alpha}) + \partial_\nu\left(\xi^k\left[\frac{2}{D}E_k^{\mu\nu}(J_{\mu\alpha}) + 2\delta_\alpha^\nu E_k^\mu(\tilde{Q}_\mu)\right]\right)\right]\mathrm{d}x^\alpha. \tag{A.2.7}$$

So the term preventing us from completely determining the Euler coefficients of $\tilde{Q}$ in terms of those of J has collected itself into an exact form! Furthermore, we can see that this will be a generic conclusion because all of the upper spacetime indices (besides μ which is already contracted) have to contract on derivatives when we construct the form from the Euler coefficients. In the "delta type" terms, at least one of these derivatives will therefore contract on the delta and hence on a form index, making the term a total differential.

This means we can always write $\tilde{Q} = Q + \mathrm{d}\alpha$ where α is constructed from all of the "delta type" terms. Since Q, which is thus constructed entirely from the Euler coefficients of J, is related to $\tilde{Q}$ by an exact form, both are equally good potentials for J and so there is no loss in taking Q over $\tilde{Q}$.

---

[8]That this observation generalizes to higher forms and more derivatives of ξ is not completely obvious, but is nonetheless true. The proof is essentially an exercise in combinatorics.

[9]In fact, the inability to invert these equations is related to the fact that we are really defining a homotopy operator. If the homotopy operator is denoted h, then $\tilde{Q} = h\mathrm{d}\tilde{Q} + \mathrm{d}h\tilde{Q} = hJ + \mathrm{d}h\tilde{Q}$. The "delta terms" in our organization of the contraction collects into the second term here as we argue shortly. See e.g. [130] for a proof that these terms organize into the particular form $\mathrm{d}h\tilde{Q}$. These extra terms are not important to our particular application.

The generalization to higher form degrees and arbitrary derivative orders in ξ is now mostly a matter of making sure we get the coefficients on the various terms in the contraction correct. This is not completely trivial, but a straightforward combinatorics problem, the main difficulty resting with the result mentioned in Footnote 8.

A.2.2 General algorithm

Suppose that J is an identically closed p-form ($p < D$) depending on a set of free functions ξ^k and finitely many derivatives thereof. We give the algorithm in three steps. First we state it for the special case where J depends only linearly on ξ and its derivatives. We then point out the simple generalization to other derivative operators. Finally, we state how the algorithm for the linear case also gives the solution to the non-linear case.

Since J is linear in ξ and its derivatives, it can always be written in the form

$$\begin{aligned} J &= \left[J_{k\alpha_1\cdots\alpha_p}\xi^k + J^{\mu}_{k\alpha_1\cdots\alpha_p}\partial_\mu\xi^k + \cdots\right] \mathrm{d}x^{\alpha_1}\wedge\cdots\wedge\mathrm{d}x^{\alpha_p} \\ &= \left[\xi^k E_k(J_{\alpha_1\cdots\alpha_p}) + \partial_\mu[\xi^k E^{\mu}_k(J_{\alpha_1\cdots\alpha_p})] + \cdots\right] \mathrm{d}x^{\alpha_1}\wedge\cdots\wedge\mathrm{d}x^{\alpha_p} \end{aligned} \tag{A.2.8}$$

where in the second line we have integrated by parts to remove all derivatives from ξ. The Euler coefficients, $E^{\mu_1\cdots\mu_r}_k(J_{\alpha_1\cdots\mu_p})$, are all the data we need to construct a local potential for J. Note that the upper indices of the Euler coefficients are assumed to be symmetrized.

With this, the potential is given by

$$Q = \frac{1}{(p-1)!}\sum_{r=0}\frac{r+1}{D-p+r+1}\partial_{\mu_1}\cdots\partial_{\mu_r}[\xi^k E^{\nu\mu_1\cdots\mu_r}_k(J_{\nu\alpha_2\cdots\alpha_p})]\mathrm{d}x^{\alpha_2}\wedge\cdots\mathrm{d}x^{\alpha_p} \tag{A.2.9}$$

where the upper bound on the sum over r depends on the derivative order J as it's a sum over all of J's Euler coefficients. We also take the convention where $r=0$ indicates no derivatives should be taken. The factor of $(p-1)!$ can be absorbed into a contraction against the vector ∂_ν to write

$$Q = \sum_{r=0}\frac{r+1}{D-p+r+1}\partial_{\mu_1}\cdots\partial_{\mu_r}[\xi^k E^{\nu\mu_1\cdots\mu_r}_k(i_{\partial_\nu}J)]. \tag{A.2.10}$$

This formula appears elsewhere in the literature using slightly different notation. In [129, 132] a multi-index notation is used (multi-index notation is also employed in [130, 131], but the conventions are slightly different which makes coefficients look different) wherein (μ) is a tuple of indices, $|\mu|$ is its length, and $((\mu)\nu)$ is the concatenation of the tuple (μ) with the additional index ν. If we further denote $E_k^{\mu_1\cdots\mu_r} = \frac{\delta}{\delta\xi^k_{(\mu)}}$ and $i_{\partial_\nu} J = \frac{\partial J}{\partial \mathrm{d}x^\nu}$ then (A.2.10) may be written compactly as

$$Q = \frac{|\mu|+1}{D-p+|\mu|+1}\partial_{(\mu)}\left[\xi^k \frac{\delta}{\delta\xi^k_{(\nu(\mu))}}\frac{\partial J}{\partial \mathrm{d}x^\nu}\right] \tag{A.2.11}$$

where a summation over the length of the tuple (μ) is to be understood. For example, this is equation (A36) in [132].

The generalization from partial derivatives to covariant derivatives of arbitrary type is described in [127]. In the proof of (A.2.9) the only property of the derivatives used is that they obey the product rule and that the upper indices of the Euler coefficients are completely symmetric. Symmetry of the indices follows trivially for partial derivatives, but for covariant derivatives we can always work with the symmetrized derivatives at the cost of introducing field strengths. So if we assume that all derivatives have first been symmetrized, we can write[10]

$$J = \left[\xi^k E_k(J_{\alpha_1\cdots\alpha_p}) + \nabla_\mu[\xi^k E_k^\mu(J_{\alpha_1\cdots\alpha_p})] + \cdots\right] \mathrm{d}x^{\alpha_1}\wedge\cdots\wedge \mathrm{d}x^{\alpha_p} \tag{A.2.12}$$

with potential

$$Q = \frac{1}{(p-1)!}\sum_{r=0}\frac{r+1}{D-p+r+1}\nabla_{\mu_1}\cdots\nabla_{\mu_r}[\xi^k E_k^{(\nu\mu_1\cdots\mu_r)}(J_{\nu\alpha_2\cdots\alpha_p})]\mathrm{d}x^{\alpha_2}\wedge\cdots\wedge \mathrm{d}x^{\alpha_p}. \tag{A.2.13}$$

For the generalization to non-linear dependence of J on ξ we consider an arbitrary 1-parameter path $\xi(\lambda)$ through ξ-space. Denote by J_λ the evaluation of J on $\xi(\lambda)$. This J_λ is

[10] Though we use the same symbol for the Euler coefficient, the Euler coefficients computed using symmetrized covariant derivatives and using partial derivatives will, of course, not generally be the same.

still identically closed and so it's λ derivative is as well:

$$\mathrm{d}\dot{J}_\lambda = 0 \tag{A.2.14}$$

where we have denoted the λ derivative by a dot.

Now $\dot{J}_\lambda$ is an identically closed form which depends only linearly on $\dot{\xi}$, which is arbitrary and independent of $\xi(\lambda)$. Hence we may apply the (A.2.13) for the linear case to $\dot{J}$ using $\dot{\xi}$ as our free function to find

$$Q_\lambda = \sum_{r=0} \frac{r+1}{D-p+r+1} \nabla_{\mu_1} \cdots \nabla_{\mu_r} [\dot{\xi}^k E_k^{(\nu\mu_1\cdots\mu_r)}(i_{\partial_\nu} J)] \tag{A.2.15}$$

which satisfies $\dot{J}_\lambda = \mathrm{d}Q_\lambda$. The Euler coefficients now, of course, must be understood to have been computed from integrating by parts on $\dot{\xi}^k$.

Taking the λ integral we find

$$J_1 = J_0 + \mathrm{d}\int_0^1 Q_\lambda \mathrm{d}\lambda. \tag{A.2.16}$$

If we choose the flow $\xi(\lambda)$ such that $\xi(0) = 0$ and $\xi = \xi(1)$, then theorem 1 is an immediate consequence.

A useful choice of path is the contracting flow[11] $\xi(\lambda) = \lambda\xi$. In this case the potential for J is

$$Q = \int_0^1 \mathrm{d}\lambda \sum_{r=0} \frac{r+1}{D-p+r+1} \nabla_{\mu_1} \cdots \nabla_{\mu_r} [\xi^k E_k^{(\nu\mu_1\cdots\mu_r)}(i_{\partial_\nu} J(\lambda\xi))] \tag{A.2.17}$$

where it should be understood that the Euler coefficients used here should be those of $\dot{J}_\lambda$. Making the notational changes described above (A.2.11), we see that this expression is (A.9) in [129].

[11] Much like the Poincaré contracting homotopy, this choice is not invariant under redefinitions of the ξ. Furthermore, there may be cases where this path is not suitable. We refer the reader to the discussion in [127] for some considerations in this direction. The contracting flow is always possible when the ξ are functions on spacetime.

A.2.3 Examples

As a simple first example we may derive the Komar term (2.3.61). Using (2.3.41) and (2.3.42) we find

$$J_\xi = \frac{\sqrt{-g}}{16\pi G}\left(\nabla_\nu(\nabla^\mu\xi^\nu + \nabla^\nu\xi^\mu) - 2\nabla^\mu\nabla_\nu\xi^\nu\right)(\mathrm{d}^d x)_\mu - i_\xi L. \tag{A.2.18}$$

The potential is simple to compute in this case without using the heavy machinery introduced above. We need only write

$$\nabla^\mu\nabla_\nu\xi^\nu = -R^\mu_\nu\xi^\nu + \nabla_\nu\nabla^\mu\xi^\nu \tag{A.2.19}$$

so

$$J_\xi = \left(\frac{\sqrt{-g}}{8\pi G}R^\mu_\nu\xi^\nu(\mathrm{d}^d x)_\mu - i_\xi L\right) + \frac{\sqrt{-g}}{16\pi G}\nabla_\nu(\nabla^\nu\xi^\mu - \nabla^\mu\xi^\nu)(\mathrm{d}^d x)_\mu. \tag{A.2.20}$$

The first pair of terms, linear in ξ with no derivatives thereof, vanish on the equations of motion. The latter pair of terms can be identified as yielding the Komar term via (A.1.8).

To demonstrate the heavy machinery, note first that we only need the linear case (A.2.10) and that only Euler derivatives with at least one upper index (meaning at least one derivative in the Euler expansion of J_ξ) contribute. So any terms linear in ξ with no derivatives, after putting J_ξ in Euler form, will not contribute. Indeed, we can see in the example (A.2.4) that these terms must vanish when J_ξ is closed[12]. In particular, this means the $i_\xi L$ term will not contribute to Q_ξ, which we also found in (2.3.67).

Since only the $i_{V_\xi}\theta$ terms in J_ξ will contribute. In the remaining terms we need to symmetrize the covariant derivatives so the Euler coefficients will have symmetrized upper derivatives. Here the derivatives are all 2nd order, so the anti-symmetrization will produce Riemann curvatures with no additional derivatives on ξ. These terms will again not

[12]This is actually a familiar statement. Note that the zeroth Euler coefficient is precisely the Euler-Lagrange operator acting on J_ξ. This is then the standard statement that the Euler-Lagrange equations annihilate total derivatives.

contribute. The result is now

$$J_\xi = \frac{\sqrt{-g}}{16\pi G}\nabla_{(\alpha}\nabla_{\beta)}\left[\left(g^{\beta\mu}\delta_k^\alpha + g^{\alpha\beta}\delta_k^\mu - 2g^{\alpha\mu}\delta_k^\beta\right)\xi^k\right](\mathrm{d}^d x)_\mu + (\cdots)_k\xi^k. \tag{A.2.21}$$

The relevant Euler coefficients are then

$$E_k^\alpha(J_\xi) = 0, \qquad E_k^{\alpha\beta}(J_\xi) = \frac{1}{2}\left(2g^{\alpha\beta}\delta_k^\mu - g^{\alpha\mu}\delta_k^\beta - g^{\beta\mu}\delta_k^\alpha\right)(\mathrm{d}^d x)_\mu. \tag{A.2.22}$$

The reconstruction (A.2.10) now produces

$$\begin{aligned} Q_\xi &= \frac{\sqrt{-g}}{16\pi G}\left\{0 + \frac{1+1}{D-(D-1)+1+1}\nabla_\alpha\left[\xi^k E_k^{\alpha\beta}(i_{\partial_\beta}J_\xi)\right]\right\} \\ &= \frac{\sqrt{-g}}{16\pi G}\frac{2}{3}\frac{1}{2}\nabla_\alpha\left[\xi^k\left(g^{\alpha\beta}\delta_k^\mu - g^{\alpha\mu}\delta_k^\beta - g^{\beta\mu}\delta_k^\alpha\right)(\mathrm{d}^{d-1}x)_{\mu\beta}\right] \end{aligned} \tag{A.2.23}$$

which is again the Komar term, though this algorithm is obviously not unnecessary for this example.

Another example, this time non-linear in ξ, would be the calculation (2.3.62). This example is again simple enough that we can simply obtain the result (2.3.63) without applying the general algorithm. To do this we need only (2.3.14) to find

$$16\pi G\delta k_\xi = \frac{4\Lambda}{D-2}\sqrt{-g}\left[\xi^\nu\wedge\nabla_\nu\xi^\mu + \nabla_\nu\xi^\nu\wedge\xi^\mu\right](\mathrm{d}^d x)_\mu \tag{A.2.24}$$

which is (2.3.63) upon collecting the total derivative and using (A.1.8).

To find this result using the general algorithm, we first take a derivative of δk_ξ to obtain

$$\begin{aligned} 16\pi G\delta\dot{k}_\xi &= \frac{4\Lambda}{D-2}\sqrt{-g}\nabla_\nu\left(\dot{\xi}^\nu\wedge\xi^\mu + \xi^\nu\wedge\dot{\xi}^\mu\right)(\mathrm{d}^d x)_\mu \\ &= \frac{4\Lambda}{D-2}\sqrt{-g}\nabla_\nu\left[\dot{\xi}^k\wedge(\delta_k^\nu\xi^\mu - \delta_k^\mu\xi^\nu)\right](\mathrm{d}^d x)_\mu. \end{aligned} \tag{A.2.25}$$

From this we extract the Euler coefficient

$$E_k^\nu(\delta\dot{k}_\xi) = \frac{1}{16\pi G}\frac{4\Lambda}{D-2}\sqrt{-g}\wedge(\delta_k^\nu\xi^\mu - \delta_k^\mu\xi^\nu)(\mathrm{d}^d x)_\mu \tag{A.2.26}$$

where we have included a dangling wedge to remind ourselves that when we perform the potential reconstruction the $\dot{\xi}$ appears to the left of this coefficient.

Since $\delta k_\xi = 0$ when $\xi = 0$, we have (A.2.16) with $J_0 = 0$ if we use the contracting flow (A.2.17). The reconstruction (A.2.17) then yields

$$
\begin{aligned}
16\pi G\tilde{k}_\xi &= \int_0^1 \mathrm{d}\lambda \frac{0+1}{D-(D-1)+0+1}\frac{4\Lambda}{D-2}\sqrt{-g}\xi^k \wedge \lambda(\delta_k^\nu \xi^\mu - \delta_k^\mu \xi^\nu)(\mathrm{d}^{d-1}x)_{\mu\nu} \\
&= -\frac{2\Lambda}{D-2}\sqrt{-g}\xi^\mu \wedge \xi^\nu (\mathrm{d}^{d-1}x)_{\mu\nu},
\end{aligned} \tag{A.2.27}
$$

as we have already shown should be the case.

A.3 Diffeomorphism Charges for Generally non-Covariant Lagrangians

In section 2.2.2.2, we reviewed a general procedure for computing the Noether charge associated to an arbitrary gauge symmetry. In the special case where the gauge transformation is a diffeomorphism, additional simplifications are possible [14].

The transformation of the Lagrangian under a diffeomorphism ξ can generally be separated into covariant and non-covariant pieces as

$$k_\xi = i_\xi L + Y_\xi. \tag{A.3.1}$$

We may do the same for the action of the diffeomorphism on θ:

$$\mathcal{L}_{V_\xi}\theta = \mathcal{L}_\xi \theta + \tilde{\Pi}_\xi. \tag{A.3.2}$$

With these separations together, (2.2.24) becomes

$$\mathrm{d}\Pi_\xi = \mathrm{d}i_\xi\theta + (\tilde{\Pi}_\xi - \delta Y_\xi). \tag{A.3.3}$$

That is, the covariant part of the transformations collect automatically into a total derivative, so the task of computing Π_ξ is reduced to just finding a potential Σ_ξ satisfying

$$\mathrm{d}\Sigma_\xi = \tilde{\Pi}_\xi - \delta Y_\xi. \tag{A.3.4}$$

The computation of C_ξ in (2.2.26) is now

$$\delta C_\xi = i_\xi\theta + \Sigma_\xi - i_{V_\xi}\delta B. \tag{A.3.5}$$

These considerations only alter the computations we need to find C_ξ and do not change the identification of the charge in (2.2.27) as (2.2.28).

A.4 Non-Abelian CS

Here we consider a non-Abelian CS theory in $D = 3$. This is an important example and stress test of our techniques because of the CS/WZW correspondence which, at first glance, might seem to be in tension with our methods. In particular, recall the well known fact that one must supply an explicit parametrization in order to reduce a WZW model to an explicit boundary theory, and in particular the theory cannot be reduced explicitly to the boundary in terms of the gauge element g.

On the other hand, the charges for CS theory can be explicitly constructed on the boundary from g and its derivatives. The construction (2.3.25) would then seem to suggest that Ω can also be constructed explicitly from g, and we will see that this is indeed the case. In order for our construction (2.2.29) of the boundary action to be consistent with this known property of WZW models, it must be the case that while Ω can be explicitly constructed from g, the canonical 1-form Θ cannot. This is a non-trivial requirement and we will see that it is indeed the case.

So then to define the theory we take the background manifold to be $M = \mathbb{R} \times D$ where the spatial slices are disks. The Lagrangian and some useful quantities are

$$L = \mathrm{tr}\left(A \wedge \mathrm{d}A + \frac{2}{3}A^3\right), \qquad E = 2F, \qquad \theta = -\,\mathrm{tr}(A \wedge \delta A), \qquad k_\lambda = \mathrm{tr}(\lambda \mathrm{d}A). \qquad \text{(A.4.1)}$$

We choose the chiral boundary conditions $A_t = A_\phi$ so there is no need for a boundary contribution to the action, $B = \ell = 0$, in light of (2.2.15).

The Noether current associated to gauge transformations is

$$J_\lambda = \mathrm{tr}\left[\mathrm{d}(\lambda A) - 2\lambda F\right] = \mathrm{d}\,\mathrm{tr}(\lambda A) \qquad \text{(A.4.2)}$$

so $Q_\lambda = tr(\lambda A)$. Thus one may check that the full Noether charges are

$$H[\lambda] = 2\int_0^{2\pi} \mathrm{d}\phi \, tr(\lambda A), \qquad H_t = \int_0^{2\pi} \mathrm{d}\phi \, tr(A_\phi^2). \tag{A.4.3}$$

Before attempting to apply our techniques to this theory, we should use the WZW correspondence to see that the boundary action produced by standard techniques should be. Since we will need an explicit parametrization, and hence gauge group, we wil choose for simplicity $SU(2)$ with the parametrization

$$g = e^{i\alpha_1\sigma_1} e^{i\alpha_2\sigma_2} e^{i\alpha_3\sigma_3}, \qquad z = 2\sin(2\alpha_2) \tag{A.4.4}$$

where σ_k are the Pauli matrices and z turns out to be a convenient definition.

By solving the Lagrange multiplier constraint, the action produced by the Lagrangian (A.4.1) becomes the WZW model

$$S = -\frac{1}{3}\int_M tr\left[\left(g^{-1}\mathrm{d}g\right)^3\right] - \int tr\left[g^{-1}\partial_t g g^{-1}\partial_\phi g\right] \mathrm{d}t \wedge \mathrm{d}\phi + \int_{\partial M} tr\left[A_\phi^2\right] \mathrm{d}t \wedge \mathrm{d}\phi. \tag{A.4.5}$$

Using $-\frac{1}{3}\, tr(g^{-1}\mathrm{d}g)^3 = \mathrm{d}(z\mathrm{d}\alpha_1 \wedge \mathrm{d}\alpha_3)$ the boundary action may be written

$$S = -2\int_{\partial M} \mathrm{d}t\mathrm{d}\phi \left[\alpha_1'(\dot\alpha_1 - \alpha_1') + \alpha_2'(\dot\alpha_2 - \alpha_2') + (\alpha_3' - z\alpha_1')(\dot\alpha_3 - \alpha_3')\right] \tag{A.4.6}$$

where the minus sign comes from identifying the boundary orientation to be $\mathrm{d}\phi \wedge \mathrm{d}t$, as commented on in footnote 17.

With this result in mind, since we already have the full Noether charges in hand, the simplest approach is to compute the symplectic form via (2.3.25). This produces

$$\Omega = \int_0^{2\pi} tr\left[\delta A_\phi \wedge g^{-1}\delta g\right] \mathrm{d}\phi = \int_0^{2\pi} tr\left[\delta(g^{-1}\partial_\phi g) \wedge g^{-1}\delta g\right] \mathrm{d}\phi. \tag{A.4.7}$$

As promised at the beginning of this section, due to the g^{-1} factor, this cannot be written as δ of something directly in terms of g. Instead we must go to the explicit parametrization (A.4.4) in order to find the canonical 1-form.

But this is a straightforward calculation to perform, the result being

$$\Omega = -2\delta \int_0^{2\pi} [\alpha_1' \delta\alpha_1 + \alpha_2' \delta\alpha_2 + (\alpha_3' - z\alpha_1')\delta\alpha_3] \, \mathrm{d}\phi. \tag{A.4.8}$$

Together with

$$H_t = -2 \int_0^{2\pi} \left[\alpha_1'^2 + \alpha_2'^2 + (\alpha_3' - z\alpha_1')\alpha_3'\right] \mathrm{d}\phi \tag{A.4.9}$$

we find the phase space action

$$S = -2 \int \mathrm{d}t \int_{\partial\Sigma} \mathrm{d}\phi \, [\alpha_1'(\dot{\alpha}_1 - \alpha_1') + \alpha_2'(\dot{\alpha}_2 - \alpha_2') + (\alpha_3' - z\alpha_1')(\dot{\alpha}_3 - \alpha_3')] \, . \tag{A.4.10}$$

We could also find this result by the methods in section 2.3.3. Since we already have Q_λ from (A.4.2), we only need to compute the potential for δk_w with $w = g^{-1}\delta g$. In the case of diffeomorphisms it's simple to use (2.3.12) as our free function with respect to which the potential $\tilde{k}_w$ can be constructed. Here, however, $w = g^{-1}\delta g$ is not a completely free function and we must use $\delta\alpha$ as our free function instead. This unfortunately means that we cannot write down a potential $\tilde{k}_w$ without specifying the gauge group.

Using the parametrization (A.4.4) we find

$$\tilde{k}_w = \delta z \wedge \delta\alpha_3 \mathrm{d}\alpha_1 + \delta\alpha_3 \wedge \delta\alpha_1 \mathrm{d}z + \delta\alpha_1 \wedge \delta z \mathrm{d}\alpha_3. \tag{A.4.11}$$

Furthermore we may compute

$$\begin{aligned} \delta Q_w = \; & \delta z \wedge (\mathrm{d}\alpha_3 \delta\alpha_1 + \mathrm{d}\alpha_1 \delta\alpha_3) + z(\mathrm{d}\delta\alpha_3 \wedge \delta\alpha_1 + \mathrm{d}\delta\alpha_1 \wedge \delta\alpha_3) \\ & + 2(\delta\alpha_1 \wedge \mathrm{d}\delta\alpha_1 + \delta\alpha_2 \wedge \mathrm{d}\delta\alpha_2 + \delta\alpha_3 \wedge \mathrm{d}\delta\alpha_3). \end{aligned} \tag{A.4.12}$$

Adding these forms we find

$$\delta Q_w + \tilde{k}_w = -2\delta \, [\mathrm{d}\alpha_1 \delta\alpha_1 + \mathrm{d}\alpha_2 \delta\alpha_2 + (\mathrm{d}\alpha_3 - z\mathrm{d}\alpha_2)\delta\alpha_1] + \mathrm{d}(z\delta\alpha_3 \wedge \delta\alpha_1). \tag{A.4.13}$$

Integrating this over the ϕ circle the total derivative term does not contribute and we evidently reproduce (A.4.8), from which the phase space action (A.4.10) follows.

A.5 Relation to Schwarzian Action for JT gravity

From the perspective of the current paper, it is most illuminating to view JT gravity and its Schwarzian action description [48] as a special case of our approach to 3D gravity. The 3D origin of the JT/Schwarzian is discussed in [133].

In 3D we have the Euclidean action

$$S_3 = -\frac{1}{16\pi G}\int \mathrm{d}^3x\sqrt{g_3}(R_3+2) - \frac{1}{8\pi G}\int_{\partial M}\mathrm{d}^2x\sqrt{h_3}(K_3-1) \tag{A.5.1}$$

The 3D class of metrics we consider are

$$ds_3^2 = \frac{\mathrm{d}z^2}{z^2} + \left(\frac{1}{z^2}+\frac{z^2}{4}L\overline{L}\right)\mathrm{d}w\mathrm{d}\overline{w} - \frac{1}{2}L\mathrm{d}w^2 - \frac{1}{2}\overline{L}\mathrm{d}\overline{w}^2 \tag{A.5.2}$$

with $w=\phi+it$, $\overline{w}=\phi-it$, $(L,\overline{L})$ are functions of (ϕ,t) that take the form

$$\begin{aligned} L &= \{F(\phi,t),\phi\} + \frac{\kappa}{2}F'^2 \\ \overline{L} &= \{\overline{F}(\phi,t),\phi\} + \frac{\overline{\kappa}}{2}\overline{F}'^2 \end{aligned} \tag{A.5.3}$$

where $(\kappa,\overline{\kappa})$ are constants and $'=\partial_\phi$. At fixed t, the functions $(F,\overline{F})$ are elements of diff(S^1). In general, the metrics (A.5.2) are off-shell; to be on-shell the functions $(F,\overline{F})$ must be, respectively, holomorphic and anti-holomorphic in w.

It is rather tricky to obtain the off-shell action governing (A.5.2) by direct substitution into (A.5.1), in part because the coordinates are not globally smooth. Instead, we apply phase space methods, viewing $(F,\overline{F})$ at fixed time as points on phase space and building an action out of the gravitational symplectic form and Hamiltonian on this phase space. This procedure [134] leads to the Alekseev-Shatashvili action [19],

$$S_{AS} = -\frac{1}{16\pi G}\int \mathrm{d}^2x\left[\kappa F'\partial_{\bar{w}}F - \left(\frac{1}{F'}\right)''\partial_{\bar{w}}F + \bar{\kappa}\bar{F}'\partial_w\bar{F} - \left(\frac{1}{\bar{F}'}\right)''\partial_w\bar{F}\right]\ . \tag{A.5.4}$$

We now turn to the 2D story. One approach is to KK reduce the 3D action by considering metrics

$$\mathrm{d}s_3^2 = \mathrm{d}s_2^2 + \Phi^2\mathrm{d}t^2\ ,\quad t\cong t+2\pi \tag{A.5.5}$$

taking the metric components to be t independent. Using

$$\int_{M_3} \mathrm{d}^3x\sqrt{g_3}(R_3-\Lambda) = \int_{M_2} \mathrm{d}^2x\sqrt{g_2}\Phi(R_2-\Lambda) - 2\int_{\partial M_2} \mathrm{d}x\sqrt{h}n^\mu\partial_\mu\Phi \tag{A.5.6}$$

where the metric on the $2d$ boundary is h and n^μ is the outward pointing unit normal to the boundary, along with

$$\sqrt{g_3}K_3 = \sqrt{h}\Phi K_2 + \sqrt{h}n^\nu\partial_\mu\Phi \tag{A.5.7}$$

we find that the 3D action (A.5.2) reduces to the JT action

$$S_3 = -\frac{1}{16\pi G_2}\int \mathrm{d}^2x\sqrt{h}\Phi(R_2+2) - \frac{1}{8\pi G_2}\int \mathrm{d}\phi\sqrt{h}\Phi(K_2-1) \tag{A.5.8}$$

with $G_2 = G/2\pi$.

Coming back to our 3D picture, to be in accordance with (A.5.5) we should take $F = F(\phi)$ and $\overline{F} = F(\phi)$, along with $\kappa = \overline{\kappa}$. We are thus considering 3D metrics (generically off-shell) of the form

$$\mathrm{d}s_3^2 = \frac{\mathrm{d}z^2}{z^2} + \frac{1}{z^2}\left(1-\frac{Lz^2}{2}\right)^2\mathrm{d}\phi^2 + \frac{1}{z^2}\left(1+\frac{Lz^2}{2}\right)^2\mathrm{d}t^2 \tag{A.5.9}$$

with $L(\phi) = \{F(\phi),\phi\}+\frac{\kappa}{2}F'^2$. For this restricted class of off-shell metrics it is straightforward to evaluate the 3D action S_3 on the form (A.5.9). In particular, we have $R_2 = -2$ so only the boundary term survives. Cutting off the space at $z = z_c$ and taking $\Phi|_{z=z_c} = z_c^{-1}$, we find the action as $z_c \to 0$,

$$S_3 = -\frac{1}{8\pi G_2}\int L(\phi)\mathrm{d}\phi + \text{constant} \tag{A.5.10}$$

which is the Schwarzian action (supplemented with the κ term).[13] Alternatively, we can apply the reduction to the AS action (A.5.4). After integrating over t and doing some integration by parts, we find that (A.5.4) is equal to (A.5.10).

[13]The original approach to obtaining this action involved considering cutouts of AdS_2 with wiggly boundary. Here the boundary is at fixed coordinate location $z = z_c$, and wiggles are instead encoded in fluctuations of the metric via the function $L(\phi)$.

APPENDIX B

Hamiltonian formulation of near-extremal charged black holes

B.1 ADM Hamiltonian of neutral scalars from AdS$_3$

Consider the Einstein-Hilbert gravity with a charge neutral scalar in asymptotically AdS$_3$.

$$S = -\frac{1}{2\pi}\int \mathrm{d}^3x\sqrt{-g}\left[\frac{1}{8G}\left(R+\frac{2}{l^2}\right)+\frac{1}{2}(\nabla\phi)^2\right] \tag{B.1.1}$$

Using the Gamma-Gamma formula,

$$\begin{aligned}\sqrt{-g}R = &\frac{2N'R'}{L} - \frac{2N_r^2L'R'}{N} + \frac{2N_rR'\dot{L}}{N} - \frac{2\dot{R}}{N}(\dot{L}-N_rL') - \frac{2LN_rN_r'R'}{N} + \frac{2L\dot{R}N_r'}{N}\\ &-\frac{\mathrm{d}}{\mathrm{d}t}\left(\frac{RLN_r'}{N}\right)+\left(\frac{RL\dot{N}_r}{N}\right)'\end{aligned} \tag{B.1.2}$$

The Legendre transformation to the Hamiltonian variables is

$$S = \int dtdr\left[\pi_L\dot{L}+\pi_R\dot{R}+\pi_\phi\dot{\phi}-N\mathcal{H}_t-N^r\mathcal{H}_r\right]-\int dt\alpha\mathcal{M}(\infty) \tag{B.1.3}$$

where $\mathcal{M}$ is the quasi-local mass of the BTZ black hole, which appears in the Schwarzschild coordinates of BTZ black holes as

$$\begin{aligned}\mathrm{d}s^2 = -f(R)\mathrm{d}T^2+\frac{\mathrm{d}R^2}{f(R)}+R^2\mathrm{d}\Omega^2, \quad f(R)=\frac{R^2-R_h^2}{l^2}\\ M=\frac{R_h^2}{l^2}\end{aligned} \tag{B.1.4}$$

As for the 4d black holes, the quasi-local mass can be written in terms of the ADM metric and their canonical conjugates by first relating the metric in ADM and Schwarzschild coordinates.

$$\begin{aligned}
\mathrm{d}s^2 &= -f(R)\mathrm{d}T^2 + \frac{\mathrm{d}R^2}{f(R)} + R^2\mathrm{d}\psi^2 \\
&= -f(R)(\dot{T}\mathrm{d}t + T'\mathrm{d}r)^2 + \frac{(\dot{R}\mathrm{d}t + R'\mathrm{d}r)^2}{f(R)} + R^2\mathrm{d}\psi^2 \\
&= -N(t,r)^2\mathrm{d}t^2 + L(t,r)^2\left(\mathrm{d}r + N^r(t,r)\mathrm{d}t\right)^2 + R(t,r)^2\mathrm{d}\psi^2
\end{aligned} \tag{B.1.5}$$

Comparing the g_{tt}, g_{tr}, g_{rr} components, we get three equations.

$$\begin{aligned}
f\dot{T}^2 - \frac{\dot{R}^2}{f} &= N^2 - L^2N_r^2 \\
-f\dot{T}T' + \frac{\dot{R}r'}{f} &= L^2N_r \\
-fT'^2 + \frac{R'^2}{f} &= L^2
\end{aligned} \tag{B.1.6}$$

The first two equations relate N_r, L^2 to f, T, R. At the end, we get

$$\pi_L = -\frac{1}{4GN}\left(N_rR' - \dot{R}\right) = \frac{fT'}{4GL} \quad \rightarrow \quad T' = \frac{4GL\pi_L}{f} \tag{B.1.7}$$

Plugging this into the last equation, we get

$$-16G^2\pi_L^2 + \frac{R'^2}{L^2} = f(R) = \frac{R^2}{l^2} - M \tag{B.1.8}$$

and hence the quasi-local mass is

$$H_{ADM} = \mathcal{M} = \frac{M}{8G} = 2G\pi_L^2 - \frac{R'^2}{8GL^2} + \frac{R^2}{8Gl^2} \tag{B.1.9}$$

The factor of $\frac{1}{8G}$ is there in the Brown-York/ADM charge $Q[\partial_t]$ and also to cancel the boundary term in the variation of the bulk pieces. The boundary term is

$$S_{ADM} = -\int \mathrm{d}t\ \mathcal{M}(\infty) \tag{B.1.10}$$

After gauge fixing

$$\pi_L = 0, \quad R = r \tag{B.1.11}$$

$$\mathcal{M}(r) = -\frac{1}{8GL(t,r)^2} + \frac{r^2}{8Gl^2} \tag{B.1.12}$$

$$S_{ADM} = -\int \mathrm{d}t \ \left(-\frac{1}{8GL(\infty)^2} + \frac{r^2}{8Gl^2}\right) \tag{B.1.13}$$

The solution of $\mathcal{H}_t = 0$ constraint equation

$$\left(\frac{1}{L^2}\right)' = \frac{2r}{\ell^2} - \frac{8G}{L^2}h \tag{B.1.14}$$

where

$$h = \frac{1}{2}\left(\frac{\pi_\phi^2}{r} + r\phi'^2\right) \tag{B.1.15}$$

fixes the $\frac{1}{L^2(r)}$. The solution is

$$\begin{aligned}
\frac{1}{L^2(r)} &= \int_{r_h}^{r} dr' \frac{2r'}{\ell^2} e^{-\int_{r'}^{r} dr'' 8Gh(r'')} \\
&= \int_{r_h}^{r} dr' \frac{d}{dr'}\left(\frac{r'^2}{\ell^2}\right) e^{-\int_{r'}^{r} dr'' 8Gh(r'')} \\
&= \frac{r^2}{\ell^2} - \frac{r_h^2}{\ell^2} e^{-\int_{r_h}^{r} dr'' 8Gh(r'')} - \int_{r_h}^{r} dr' \frac{r^2}{\ell^2} 8Gh\left(r'\right) e^{-\int_{r'}^{r} dr'' 8Gh(r'')} \\
&= f(r) - \int_{r_h}^{r} dr' f\left(r'\right) 8Gh\left(r'\right) e^{-\int_{r'}^{r} dr'' 8Gh(r'')}
\end{aligned} \tag{B.1.16}$$

where

$$f(r) = \frac{r^2 - r_h^2}{\ell^2} \tag{B.1.17}$$

Plugging this, the quasi-local mass at the boundary is

$$\mathcal{M}(\infty) = \frac{r_h^2}{8G\ell^2} + \int_{r_h}^{\infty} dr f(r) h(r) e^{-\int_{r}^{\infty} dr' 8Gh(r')} \tag{B.1.18}$$

and action including this boundary action is

$$S = \int dt dr \left(\pi_\phi \dot{\phi} - f(r) h(r) e^{-\int_{r}^{\infty} dr' 8Gh(r')}\right) - \int dt M_0 \tag{B.1.19}$$

where $M_0 = \frac{r_h^2}{8Gl^2}$ is the quasi-local mass without a matter. Let's call this ADM action.

Schwarzschild coordinates We can change the coordinates to the Schwarzschild coordinates

$$\mathrm{d}s^2 = -f(R)\mathrm{d}T^2 + \frac{\mathrm{d}R^2}{f(R)} + R^2\mathrm{d}\psi^2 \tag{B.1.20}$$

First, the gauge fixing already related $R(t,r) = r$. Using the g_{tt}, the T and t are related by

$$\mathrm{d}t = \frac{f(r)}{N^2}\mathrm{d}T \tag{B.1.21}$$

On the boundary,

$$\mathrm{d}t|_{r=\infty} = \mathrm{d}T \tag{B.1.22}$$

The kinetic term in the ADM action

$$\int \mathrm{d}t\ \pi_\phi \dot{\phi} = \int \mathrm{d}T\ \pi_\phi \frac{\mathrm{d}\phi}{\mathrm{d}T} \tag{B.1.23}$$

and the ADM Hamiltonian

$$\int \mathrm{d}t\ \mathcal{M}(\infty) = \int \mathrm{d}T\ \mathcal{M}(\infty) \tag{B.1.24}$$

Combining these, the ADM action in the Schwarzschild coordinates is

$$S = \int \mathrm{d}T\mathrm{d}r \left(\pi_\phi\dot{\phi} - f(r)h(r)e^{-\int_r^\infty \mathrm{d}r' 8Gh(r')}\right) - \int \mathrm{d}T\ M_0 \tag{B.1.25}$$

Now for convenience, we relabel

$$T \to t \tag{B.1.26}$$

$$\mathrm{d}s^2 = -f(r)\mathrm{d}t^2 + \frac{\mathrm{d}r^2}{f(r)} + r^2\mathrm{d}\psi^2 \tag{B.1.27}$$

and the ADM action is

$$S = \int \mathrm{d}t\mathrm{d}r \left(\pi_\phi\dot{\phi} - f(r)h(r)e^{-\int_r^\infty \mathrm{d}r' 8Gh(r')}\right) - \int \mathrm{d}t\ M_0 \tag{B.1.28}$$

$\mathbf{AdS_2}$? We comment that the constraint equations along with π_L, π_R variations don't gaurantee the AdS_2 geometry. AdS_2 arises by solving the equations of motion. This contrasts to JT gravity where the geometry is locally AdS_2 off-shell.

B.2 Derivation of Quasi local mass

In this subsection, we derive the quasi-local mass, following the calculations in Section 4.1 of [135] for the charged black holes in 4d. Let $T(t,r)$ and $R(t,r)$ be the coordinates of the RN black holes with the metric

$$\mathrm{d}s^2 = F(R)\mathrm{d}T^2 + \frac{\mathrm{d}R^2}{F(R)} + R^2\mathrm{d}\Omega^2, \quad F(R) = 1 - \frac{2GM}{R} + \frac{GQ^2}{R^2} \tag{B.2.1}$$

We will first find the ADM metric components N, N^r, L in terms of this metric and use that to write the black hole's mass M in terms of the canonical variables, $L, \pi_L, N, N_r, \cdots$. First,

$$\begin{aligned}
\mathrm{d}s^2 &= -F(\dot{T}\mathrm{d}t + T'\mathrm{d}r)^2 + \frac{1}{F}\left(\dot{R}\mathrm{d}t + R'\mathrm{d}r\right)^2\mathrm{d} + R^2\mathrm{d}\Omega^2 \\
\mathrm{d}s_2^2 &= \left(-F\dot{T}^2 + \frac{\dot{R}^2}{F}\right)\mathrm{d}t^2 + 2\left(-F\dot{T}T' + \frac{1}{F}\dot{R}R'\right)\mathrm{d}t\mathrm{d}r + \left(-FT'^2 + \frac{R'^2}{F}\right)\mathrm{d}r^2 \\
&= -(N^2 - L^2N_r^2)\mathrm{d}t^2 + 2L^2N_r\mathrm{d}t\mathrm{d}r + L^2\mathrm{d}r^2
\end{aligned} \tag{B.2.2}$$

Identifying the metric by components,

$$\begin{aligned}
F\dot{T}^2 - \frac{\dot{R}^2}{F} &= N^2 - L^2N_r^2 \\
-F\dot{T}T; + \frac{\dot{R}r'}{F} &= L^2N_r \\
-FT'^2 + \frac{R'^2}{F} &= L^2
\end{aligned} \tag{B.2.3}$$

The last two equations can be solved for N^r and L as

$$\begin{aligned}
N_r &= \frac{F\dot{T}T' - F^{-1}\dot{R}R'}{FT'^2 - F^{-1}R'^2} \\
L^2 &= -FT'^2 + \frac{R'^2}{F}
\end{aligned} \tag{B.2.4}$$

Substituting these two into the first equation, we get N given by

$$N = \frac{\dot{T}R' - T'\dot{R}}{L} \tag{B.2.5}$$

Plugging these expressions into the expression of π_L in terms of the Lagrangian variables,

$$\pi_L = \frac{R}{GN}(N_rR' - \dot{R}) = -\frac{RFT'}{GL} \quad \rightarrow \quad T' = -R^{-1}F^{-1}GL\pi_L \tag{B.2.6}$$

Plugging this T' into the last equation, we get the F in terms of the canonical variables:

$$F = -\frac{G^2\pi_L^2}{R^2} + \frac{R'^2}{L^2} = 1 - \frac{2GM}{R} + \frac{GQ^2}{R^2} \tag{B.2.7}$$

Hence, we get the mass of the black hole (quasi-local mass)

$$M = \frac{R}{2G} + \frac{G\pi_L^2}{2R} - \frac{RR'^2}{2GL^2} + \frac{Q^2}{2R} \tag{B.2.8}$$

B.3 AdS/CFT dictionary for the matter

Inclusion of the matter corresponds to the deformation of the CFT with the dual operator

$$S_{matter} \quad \leftrightarrow \quad \Delta S = \int \mathrm{d}^d x \; \phi_0(x) O(x) \tag{B.3.1}$$

whose conformal dimension is $\Delta = \sqrt{\frac{d^2}{4} + m^2 \ell_{AdS}^2}$. Then we have the dictionary

$$\begin{aligned} S_{matter} \quad &\leftrightarrow \quad \int \mathrm{d}^d x \; \phi_0(x) O(x) \\ \text{Non-normalisable mode, } \phi_0 \quad &\leftrightarrow \quad \text{Source} \\ \text{Normalisable mode} \quad &\leftrightarrow \quad \text{response, } \langle O \rangle \\ Z_{grav} &= Z_{CFT} \end{aligned} \tag{B.3.2}$$

In the boundary theory, the correlation function for the dual operator O can be obtained by taking derivatives of Z_{CFT} w.r.t. the sources, ϕ_0. Through the last equality and ϕ_0 as the non-normalisable mode, such a boundary correlation function can also be computed by taking derivative of Z_{grav} w.r.t. the boundary value of the field.

$$\langle TO(x_1)O(x_2)\cdots\rangle = \left.\frac{\delta \log Z_{grav}}{\delta\phi_0(u_1)\delta\phi_0(u_2)\cdots}\right|_{\phi_0=0} \tag{B.3.3}$$

Time ordering Even though the derivatives $\frac{\delta}{\delta\phi_0}\cdots$ commute, it results in the time-ordered correlation function and hence changing the ordering say, from $u_1 > u_2$ to $u_2 > u_1$

which uses the same expression $\frac{\delta \log Z_{grav}}{\delta\phi_0(u_1)\delta\phi_0(u_2)}$ that results in the different answers,

$$\langle TO(u_1)O(u_2)\rangle = \begin{cases} u_1 > u_2 : & \langle O(u_1)O(u_2)\rangle \\ u_2 > u_1 : & \langle O(u_2)O(u_1)\rangle \end{cases} \tag{B.3.4}$$

For example, the 2pt correlation function in the dual quantum mechanics of the scalars in AdS_2 at the tree-level (no graviton in the loop) is given by

$$\begin{aligned} \langle V_1 V_2\rangle_0 &= \frac{\delta Z_{grav}}{\delta\phi_0(u_1)\delta\phi_0(u_2)}\bigg|_{\phi_0,\varphi_0=0} \\ &= \left\langle \left(\frac{1}{2\sin\frac{u_{12}}{2}}\right)^{2\Delta}\left[1+\Delta\left(\epsilon_1'+\epsilon_2'-\frac{\epsilon_1-\epsilon_2}{\tan\frac{u_{12}}{2}}\right)\right]\right\rangle \\ &= \left(\frac{1}{2\sin\frac{u_{12}}{2}}\right)^{2\Delta} \end{aligned} \tag{B.3.5}$$

B.4 Thermal 2pt function in 4d s-wave sector in the near-horizon region

For a charged black hole in 4d formed by collapse of a shell, the geometry of the region outside the shell is Reissener-Nordstrom black hole with the metric given by

$$\mathrm{d}s^2 = -f(r)\mathrm{d}u\mathrm{d}v + r^2\mathrm{d}\Omega^2, \quad u = t - r_*, \quad v = t + r_* \tag{B.4.1}$$

where the tortoise coordinate r_* is

$$r_* = r + \frac{r_+^2}{r_+ - r_-}\log(r - r_+) - \frac{r_-^2}{r_+ - r_-}\log(r - r_-) \tag{B.4.2}$$

such that the horizon $r = r_+$ is at $r_* = -\infty$.

Writing

$$\phi = \frac{\tilde{\phi}}{r} \tag{B.4.3}$$

the eom in terms of the field outside the shell is

$$\left(-\partial_t + \partial_{r_*}^2 + V(r_*)\right)\tilde{\phi}(t, r_*) = 0 \tag{B.4.4}$$

Using the fact that $V(r_*) \simeq 0$ near horizon, the eom reduces to the free KG equation, and we can mode expand using the plane waves.

$$\tilde{\phi}(t,x) = \int \frac{\mathrm{d}k}{2\pi}\frac{1}{\sqrt{2\omega_k}}\left(a_k e^{-i\omega_k t+ikx} + a_k^\dagger e^{i\omega_k t-ikx}\right), \qquad \omega_k = |k| \tag{B.4.5}$$

Using the thermal occupation number

$$\langle a_k^\dagger a_{k'}\rangle_\beta = 2\pi\delta(k-k')\frac{1}{e^{\beta\omega_k}-1} \tag{B.4.6}$$

the thermal 2 point function is

$$\begin{aligned}
\langle\tilde{\phi}(t,x)\tilde{\phi}(0,0)\rangle_\beta &= \int_{-\infty}^{\infty}\frac{\mathrm{d}k}{2\pi}\frac{\mathrm{d}k'}{2\pi}\frac{1}{2\sqrt{\omega_k\omega_{k'}}}\left(\langle a_k a_{k'}^\dagger\rangle_\beta e^{-i\omega_k t+ikx} + \langle a_k^\dagger a_{k'}\rangle_\beta e^{i\omega_k t-ikx}\right)\\
&= \int_{-\infty}^{\infty}\frac{\mathrm{d}k}{2\pi}\frac{1}{2\omega_k}\left(\frac{e^{-i\omega_k t+ikx}}{e^{\beta\omega_k}-1} + \frac{e^{\beta\omega_k}e^{i\omega_k t-ikx}}{e^{\beta\omega_k}-1}\right)\\
&= \int_0^{\infty}\frac{\mathrm{d}k}{2\pi}\frac{1}{k}\left(\frac{e^{-ikt}\cos kx}{e^{\beta k}-1} + \frac{e^{(\beta+it)k}\cos kx}{e^{\beta k}-1}\right)\\
&= \int_0^{\infty}\frac{\mathrm{d}k}{2\pi}\frac{1}{k}\frac{\cos kx}{e^{\beta k}-1}\left(e^{-ikt} + e^{k(\beta+it)}\right)
\end{aligned} \tag{B.4.7}$$

where I use $x = r_*$ and the invariance under simultaneous translation. Now using $it = \tau$ and

$$\frac{1}{e^{\beta k}-1} = \sum_{n=1}^{\infty} e^{-n\beta k} \tag{B.4.8}$$

we get

$$\begin{aligned}
\langle\tilde{\phi}(t,x)\tilde{\phi}(0,0)\rangle_\beta &= \sum_{n=1}^{\infty}\int_0^{\infty}\frac{\mathrm{d}k}{2\pi}\frac{1}{k}\frac{\cos kx}{e^{\beta k}-1}\left(e^{-(it+n\beta)k} + e^{-[(n-1)\beta-\tau]k}\right)\\
&= \sum_{n=1}^{\infty}\int_0^{\infty}\frac{\mathrm{d}k}{2\pi}\frac{1}{k}\frac{\cos kx}{e^{\beta k}-1}\left(e^{-(n\beta+\tau)k} + e^{-(n\beta-\tau)k}\right) + \int_0^{\infty}\frac{\mathrm{d}k}{2\pi}\frac{1}{k}\frac{\cos kx}{e^{\beta k}-1}e^{\tau k}
\end{aligned} \tag{B.4.9}$$

Using

$$\begin{aligned}
\int_0^{\infty}\mathrm{d}k\;\frac{2}{k}\cos kx\; e^{-ak} &= \int_a^{\infty}\mathrm{d}a'\int_0^{\infty}\mathrm{d}k\left(e^{(ix-a')k} + e^{-(ix+a')k}\right)\\
&= \int_a^{\infty}\mathrm{d}a'\left(-\frac{1}{ix-a'} + \frac{1}{ix+a'}\right)\\
&= \log(a'^2+x^2)\Big|_a^{\infty}\\
&= -\log(a^2+x^2) + \log(\Lambda^2+x^2)
\end{aligned} \tag{B.4.10}$$

where Λ is an IR regulator, and

$$\begin{aligned}\int_0^\infty \mathrm{d}k \frac{2}{k} \cos kx \; e^{k\tau} &= \int_{-\infty}^{\tau} \mathrm{d}\tau' \int_0^\infty \mathrm{d}k \left(e^{k(\tau'+ix)} + e^{k(\tau'-ix)} \right) \\ &= -\int_{-\infty}^{\tau} \mathrm{d}\tau' \left(\frac{1}{\tau'+ix} + \frac{1}{\tau'-ix} \right) \\ &= -\log(\tau^2+x^2) + \log(\Lambda^2+x^2)\end{aligned} \tag{B.4.11}$$

the two point function becomes

$$\begin{aligned}\langle\tilde{\phi}(t,x)\tilde{\phi}(0,0)\rangle_\beta &= -\frac{1}{4\pi}\sum_{n=1}^\infty \log\left[(n\beta+\tau)^2+x^2\right]\left[(n\beta-\tau)^2+x^2\right] - \frac{1}{4\pi}\log(x^2+\tau^2) \\ &= -\frac{1}{4\pi}\sum_{n=1}^\infty \log(n\beta+\tau+ix)(n\beta+\tau-ix)(n\beta-\tau+ix)(n\beta-\tau-ix) \\ &\quad - \frac{1}{4\pi}\log(x^2+\tau^2) \\ &= -\frac{1}{4\pi}\sum_{n=1}^\infty \log\left[(n\beta)^2+(x-i\tau)^2\right]\left[(n\beta)^2+(x+i\tau)^2\right] - \frac{1}{4\pi}\log(x^2+\tau^2) \\ &= -\frac{1}{4\pi}\log\prod_{n=1}^\infty\left[1+\left(\frac{x-i\tau}{n\beta}\right)^2\right] - \frac{1}{4\pi}\log\prod_{n=1}^\infty\left[1+\left(\frac{x+i\tau}{n\beta}\right)^2\right] \\ &\quad + \frac{1}{2\pi}\sum_{n=1}^\infty \log(n\beta)^2 - \frac{1}{4\pi}\log(x^2+\tau^2)\end{aligned} \tag{B.4.12}$$

Using the product formula

$$\frac{\sinh \pi z}{\pi z} = \prod_{n=1}^\infty\left(1+\frac{z^2}{n^2}\right) \tag{B.4.13}$$

$$\begin{aligned}\langle\tilde{\phi}(t,x)\tilde{\phi}(0,0)\rangle_\beta =& -\frac{1}{4\pi}\log\left\{\frac{\beta}{\pi(x-i\tau)}\sinh\left[\frac{\pi}{\beta}(x-i\tau)\right]\right\} - \frac{1}{4\pi}\log\left\{\frac{\beta}{\pi(x+i\tau)}\sinh\left[\frac{\pi}{\beta}(x+i\tau)\right]\right\} \\ & + \frac{1}{2\pi}\sum_{n=1}^\infty\log(n\beta)^2 - \frac{1}{4\pi}\log(x^2+\tau^2) \\ =& -\frac{1}{4\pi}\log\left\{\frac{\beta^2}{\pi^2}\sinh\left[\frac{\pi}{\beta}(x-i\tau)\right]\sinh\left[\frac{\pi}{\beta}(x+i\tau)\right]\right\} + \frac{1}{2\pi}\sum_{n=1}^\infty\log(n\beta)^2\end{aligned} \tag{B.4.14}$$

where the last term is a spacetime independent constant that we can ignore. Now Wick rotating back to the Lorentzian time,

$$\langle\tilde{\phi}(t,x)\tilde{\phi}(0,0)\rangle_\beta = -\frac{1}{4\pi}\log\left\{\frac{\beta^2}{\pi^2}\sinh\left[\frac{\pi}{\beta}(x-t)\right]\sinh\left[\frac{\pi}{\beta}(x+t)\right]\right\} \tag{B.4.15}$$

where we used $x = r_*$ and since it is invariant under the simultaneous translation, the arguments can be shifted to u_{12} and v_{12}.

The near horizon limit is

$$t = \frac{r_0^2}{\lambda}\tau = \frac{r_0^2\rho_h}{\delta}\tau, \quad r = r_0 + \lambda\rho, \quad \frac{\delta}{\lambda} = \rho_h, \quad T_H \approx \frac{\delta}{2\pi r_0^2} \tag{B.4.16}$$

The tortoise coordinate is

$$r_* \approx r_0 + \frac{r_0^2}{2\delta}\log\left(\frac{\rho-\rho_h}{\rho+\rho_h}\right) + \frac{2\rho}{\rho_h}\log\left[\lambda^2(\rho^2-\rho_h^2)\right] + \mathcal{O}(\lambda,\delta) \tag{B.4.17}$$

and so

$$\begin{aligned}\pi T_H\ u &= \frac{1}{2}\left(\rho_h\tau - \log\sqrt{\frac{\rho-\rho_h}{\rho+\rho_h}}\right) - \frac{\delta}{2r_0^2}\left(r_0 + \log\left[\lambda^2(\rho^2-\rho_h^2)\right]\right)\\ \pi T_H\ v &= \frac{1}{2}\left(\rho_h\tau + \log\sqrt{\frac{\rho-\rho_h}{\rho+\rho_h}}\right) + \frac{\delta}{2r_0^2}\left(r_0 + \log\left[\lambda^2(\rho^2-\rho_h^2)\right]\right)\end{aligned} \tag{B.4.18}$$

Taking the near-horizon limit, $\delta \to 0$, let's leave only the first term:

$$\begin{aligned}\pi T_H\ u &\approx \frac{1}{2}\left(\rho_h\tau - \log\sqrt{\frac{\rho-\rho_h}{\rho+\rho_h}}\right)\\ \pi T_H\ v &\approx \frac{1}{2}\left(\rho_h\tau + \log\sqrt{\frac{\rho-\rho_h}{\rho+\rho_h}}\right)\end{aligned} \tag{B.4.19}$$

Using these,

$$\begin{aligned}\sinh\left(\frac{\pi}{\beta}u_{12}\right)\sinh\left(\frac{\pi}{\beta}v_{12}\right) = &\left[e^{-\frac{1}{2}\rho_h\tau_{12}}\left(\frac{\rho_1+\rho_h}{\rho_1-\rho_h}\frac{\rho_2-\rho_h}{\rho_2+\rho_h}\right)^{\frac{1}{4}} - e^{\frac{1}{2}\rho_h\tau_{12}}\left(\frac{\rho_1-\rho_h}{\rho_1+\rho_h}\frac{\rho_2+\rho_h}{\rho_2-\rho_h}\right)^{\frac{1}{4}}\right]\\ &\times\left[e^{-\frac{1}{2}\rho_h\tau_{12}}\left(\frac{\rho_1-\rho_h}{\rho_1+\rho_h}\frac{\rho_2+\rho_h}{\rho_2-\rho_h}\right)^{\frac{1}{4}} - e^{\frac{1}{2}\rho_h\tau_{12}}\left(\frac{\rho_1+\rho_h}{\rho_1-\rho_h}\frac{\rho_2-\rho_h}{\rho_2+\rho_h}\right)^{\frac{1}{4}}\right]\\ &= \left(e^{-\rho_h\tau_{12}} + e^{\rho_h\tau_{12}}\right) - \left(\sqrt{\frac{\rho_1+\rho_h}{\rho_1-\rho_h}\frac{\rho_2-\rho_h}{\rho_2+\rho_h}} + \sqrt{\frac{\rho_1-\rho_h}{\rho_1+\rho_h}\frac{\rho_2+\rho_h}{\rho_2-\rho_h}}\right)\\ &= 2\cosh\rho_h\tau_{12} - \left(\sqrt{\frac{\rho_1+\rho_h}{\rho_1-\rho_h}\frac{\rho_2-\rho_h}{\rho_2+\rho_h}} + \sqrt{\frac{\rho_1-\rho_h}{\rho_1+\rho_h}\frac{\rho_2+\rho_h}{\rho_2-\rho_h}}\right)\end{aligned} \tag{B.4.20}$$

The AdS_2 Schwarzchild coordinates (τ, ρ) has the metric

$$\mathrm{d}s^2 = -f(\rho)\mathrm{d}\tau^2 + \frac{\mathrm{d}\rho^2}{f(\rho)}, \quad f(\rho) = \rho^2 - \rho_h^2 \tag{B.4.21}$$

Performing the coordinate transformation

$$\rho = \rho_h \coth(\rho_h z) \tag{B.4.22}$$

we can move to the thermal AdS_2 coordinates (τ, z) with the metric

$$\mathrm{d}s^2 = \rho_h^2 \frac{-\mathrm{d}\tau^2 + \mathrm{d}z^2}{\sinh^2 \rho_h z} \tag{B.4.23}$$

In particular,

$$\frac{\rho + \rho_h}{\rho - \rho_h} = e^{2\rho_h z}, \quad \frac{\rho - \rho_h}{\rho + \rho_h} = e^{-2\rho_h z} \tag{B.4.24}$$

Hence, Eq. (B.4.20) becomes

$$\sinh\left(\frac{\pi}{\beta} u_{12}\right) \sinh\left(\frac{\pi}{\beta} v_{12}\right) = 2\cosh \rho_h \tau_{12} - 2\cosh \rho_h z_{12} \tag{B.4.25}$$

and hence the 2pt function is

$$\langle \phi(t,x)\phi(0,0)\rangle_\beta = -\frac{1}{4\pi r_+^2} \log\left[\frac{2\beta^2}{\pi^2}\left(-\cosh \rho_h \tau_{12} + \cosh \rho_h z_{12}\right)\right] \tag{B.4.26}$$

where we used $\phi = \frac{\tilde{\phi}}{r_+}$ near the horizon.

Using the coordinate transformations between the Schwarzschild AdS_2 and thermal AdS_2 given by $\rho = \rho_h \coth \rho_h z$, we can write the lightcone coordinates as

$$\begin{aligned} \pi T_H\, u &\approx \frac{1}{2}\left(\rho_h \tau - \log\sqrt{\frac{\rho - \rho_h}{\rho + \rho_h}}\right) = \frac{\rho_h}{2}(\tau + z) \\ \pi T_H\, v &\approx \frac{1}{2}\left(\rho_h \tau + \log\sqrt{\frac{\rho - \rho_h}{\rho + \rho_h}}\right) = \frac{\rho_h}{2}(\tau - z) \end{aligned} \tag{B.4.27}$$

Using this, the 2pt function in the thermal AdS_2 coordinates takes the same form as in the coordinates outside the collapsing shell:

$$\langle \tilde{\phi}(t,x)\tilde{\phi}(0,0)\rangle_\beta = -\frac{1}{4\pi} \log\left\{\frac{\beta^2}{\pi^2} \sinh\left[\frac{\rho_h}{2}(\tau - z)\right] \sinh\left[\frac{\rho_h}{2}(\tau + z)\right]\right\} \tag{B.4.28}$$

APPENDIX C

Non-conformal Defects

C.1 Higher transverse derivative terms

In this appendix we illustrate how defect terms with higher transverse derivatives can be traded away for terms with at most first transverse derivatives. As a concrete example consider

$$S = \frac{1}{2}\int d^2x(\partial\phi)^2 + \int dt\big(\frac{1}{2}c_1^B\phi^2 + c_2^B\phi\phi' + \frac{1}{2}c_3^B\phi'^2 + c_4^B\phi\phi''\big) \ . \tag{C.1.1}$$

The expectation is that we can use the equations of motion to replace $\phi'' \to -\ddot{\phi}$, which in momentum space will correspond to a shift of c_1^B proportional to ω^2. This quick argument does not take into account the renormalization of couplings, so it is worthwhile to flesh this out explicitly.

The two-point function is computed in the same manner as before. The expression (5.3.7) for $I_0(\omega_1, p_1, p_2)$ is now

$$I_0(\omega_1, p_1, p_2) = -c_1^B + ic_2^B(p_1 - p_2) - c_3^B p_1 p_2 + c_4^B(p_1^2 + p_2^2) \ . \tag{C.1.2}$$

The relationship between the bare and renormalized couplings is now found to be

$$\begin{aligned}
c_1^B &= \frac{\left(\frac{\pi^2}{3}\hat{\Lambda}^3 - \omega_1^2\hat{\Lambda}\right)c_4^2}{(1+\hat{\Lambda}c_4)^2} + \frac{c_1}{(1+\hat{\Lambda}c_4)^2} + \frac{\hat{\Lambda}c_2^2}{(1+\hat{\Lambda}c_4)^2(1-c_3\hat{\Lambda})} \\
c_2^B &= \frac{c_2}{(1+\hat{\Lambda}c_4)(1-c_3\hat{\Lambda})} \\
c_3^B &= \frac{c_3}{1-c_3\hat{\Lambda}} \\
c_4^B &= \frac{c_4}{1+c_4\hat{\Lambda}}
\end{aligned} \tag{C.1.3}$$

We then work out the function $X(\omega_1, p_1, p_2)$ appearing in (5.3.5) as

$$\begin{aligned}
X_{num} = &-c_1 + \frac{1}{2}|\omega_1|(c_1c_3 - c_2^2) + \frac{1}{2}|\omega_1|^3c_4^2 - \frac{1}{4}\omega_1^4c_3c_4^2 \\
&+ ic_2(1 + \frac{1}{2}|\omega_1|c_4)(p_1+p_2) \\
&+ c_4(1+\frac{1}{2}|\omega_1|c_4)(1-\frac{1}{2}|\omega_1|c_3)(p_1^2+p_2^2) \\
&+ \left(c_3 + \frac{1}{2|\omega_1|}(c_1c_3 - c_2^2 + 2c_3c_4\omega_1^2)\right)p_1p_2 \\
&+ \frac{i}{2|\omega_1|}c_2c_4(p_1+p_2)p_1p_2 \\
&+ \frac{1}{2|\omega_1|}c_4^2(1-\frac{1}{2}|\omega_1|c_3)p_1^2p_2^2
\end{aligned} \tag{C.1.4}$$

and

$$X_{den} = 1 + \frac{1}{2|\omega_1|}\left(c_1 + 2c_4\omega_1^2 - c_3\omega_1^2\right) - \frac{1}{4}\left((c_1 + 2c_4\omega_1^2)c_3 - c_2^2\right) . \tag{C.1.5}$$

We are interested in correlation functions of fields inserted away from the defect. Such correlators are unaffected by the shift

$$X(\omega_1, p_1, p_2) \rightarrow X(\omega_1, p_1, p_2) + \sum_{m,n\geq 0}{}' a_{mn}(p_1^2+\omega_1^2)^m(p_2^2+\omega_1^2)^n \tag{C.1.6}$$

where $\sum'$ instructs to omit the $m = n = 0$ term, since this just adds to the position space correlator terms which are delta function localized on the defect. Therefore, in (C.1.4) we are free to make the replacements $p_1^2 \rightarrow -\omega_1^2$ and $p_2^2 \rightarrow -\omega_1^2$, since this just changes X by terms of the form in (C.1.6). Doing so gives

$$X_{num} = -\tilde{c}_1 + \frac{|\omega_1|}{2}(\tilde{c}_1 c_3 - c_2^2) + ic_2(p_1+p_2) + \big(\frac{1}{2|\omega_1|}(\tilde{c}_1 c_3 - c_2^2) + c_3\big)p_1 p_2 \tag{C.1.7}$$

with

$$\tilde{c}_1 = c_1 + 2c_4\omega_1^2\ . \tag{C.1.8}$$

Examining (C.1.5) and (C.1.7) we see that all c_4 dependence has been absorbed into the definition of $\tilde{c}_1$. This confirms our expectation that the c_4 coupling can be traded for an ω_1 dependent shift of c_1. The same mechanism holds for all higher transverse derivative defect terms.

C.2 Fusion of two defects

We write the two-defect correlator in the form (5.3.5), and write

$$X(\omega_1, p_1, p_2) = \frac{X_{\rm num}}{X_{\rm den}}\ . \tag{C.2.1}$$

We find, in the coincident limit $L = 0$,

$$\begin{aligned}
X_{\rm num} = &\frac{1}{2}|\omega_1|\Big[(c_1^{(1)}+c_1^{(2)})(c_3^{(1)}+c_3^{(2)}) - (c_2^{(1)}+c_2^{(2)})^2\Big]\\
&-\frac{1}{4}\Big[c_1^{(1)}(c_2^{(2)}+2)^2 + c_1^{(2)}(c_2^{(1)}-2)^2 - c_1^{(1)}c_1^{(2)}(c_3^{(1)}+c_3^{(2)})\Big]\\
&+i\Big[c_2^{(1)}+c_2^{(2)}+\frac{1}{2}(c_1^{(1)}c_3^{(2)} - c_1^{(2)}c_3^{(1)}) - \frac{1}{4}(c_1^{(2)}c_2^{(1)}c_3^{(2)} + c_1^{(1)}c_2^{(2)}c_3^{(1)})\\
&\quad+\frac{1}{4}c_2^{(1)}c_2^{(2)}(c_2^{(1)}+c_2^{(2)})\Big](p_1+p_2)\\
&+\frac{1}{2|\omega_1|}\left[(c_1^{(1)}+c_1^{(2)})(c_3^{(1)}+c_3^{(2)}) - (c_2^{(1)}+c_2^{(2)})^2\right]p_1p_2\\
&+\frac{1}{4}\Big[c_3^{(1)}(c_2^{(2)}-2)^2 + c_3^{(2)}(c_2^{(1)}+2)^2 - c_3^{(1)}c_3^{(2)}(c_1^{(1)}+c_1^{(2)})\Big]p_1p_2
\end{aligned} \tag{C.2.2}$$

and

$$
\begin{aligned}
X_{\text{den}} &= \frac{1}{8|\omega_1|}\left(-c_1^{(1)}c_1^{(2)}\left(c_3^{(1)}+c_3^{(2)}\right)+c_1^{(1)}\left(c_2^{(2)}+2\right)^2+c_1^{(2)}\left(c_2^{(1)}-2\right)^2\right)\\
&+\frac{1}{16}\left((c_1^{(2)}c_3^{(1)}c_3^{(2)}-c_2^{(2)2}c_3^{(1)}-4c_3^{(1)}-8c_3^{(2)})c_1^{(1)}-(c_2^{(1)2}c_3^{(2)}+8c_3^{(1)}+4c_3^{(2)})c_1^{(2)}\right)\\
&+\left(1+\frac{c_2^{(1)}c_2^{(2)}}{4}\right)^2+\frac{(c_2^{(1)}+c_2^{(2)})^2}{4}+\frac{|\omega_1|}{8}\left(c_3^{(1)}c_3^{(2)}(c_1^{(1)}+c_1^{(2)})-c_3^{(1)}(c_2^{(2)}-2)^2-c_3^{(2)}(c_2^{(1)}+2)^2\right)\ .
\end{aligned}
\tag{C.2.3}
$$

In the above the couplings are the renormalized versions, defined in terms of the bare couplings by the relations (5.3.19). The couplings of the fused defect are then read off by equating the expression for X above with that of a single defect

$$
X(\omega_1,p_1,p_2)=\frac{-c_1+\frac{1}{2}(c_1c_3-c_2^2)|\omega_1|+ic_2(p_1+p_2)+\left(\frac{1}{2|\omega_1|}(c_1c_3-c_2^2)+c_3\right)p_1p_2}{1+\frac{1}{2|\omega_1|}(c_1-c_3\omega_1^2)-\frac{1}{4}(c_1c_3-c_2^2)}\ . \tag{C.2.4}
$$

As noted in the main text, this results in expressions for the fused couplings c_i that agree with those computed by composing the matching relations.

C.3 Stabilization by interactions

The unstable modes bound to the defect are analogous to the small k modes of a tachyonic $m^2<0$ free scalar, with $\omega=\sqrt{k^2+m^2}$. In that case, the scalar potential is unbounded from below but can be stabilized by adding an interaction term such as $\frac{\lambda}{4}\phi^4$. In this subsection, we add a $\frac{\lambda}{4}\phi^4$ term to the free massless scalars in the presence of a defect described by the matching conditions, and discuss the solutions and fluctuations around them.

With the interaction term added, the field equation implies

$$
\phi''=V'(\phi)=\lambda\phi^3,\quad\rightarrow\quad\phi'=\pm\sqrt{\frac{\lambda}{2}}\phi^2 \tag{C.3.1}
$$

where the sign can be fixed in terms of the boundary values

$$
\phi(x=\pm\infty)=0,\quad\phi(x=0^-)=\phi_L,\quad\phi(x=0^+)=\phi_R \tag{C.3.2}
$$

where $\phi_{L,R}$ are determined by the matching conditions (5.6.2). The solution is

$$\phi = \begin{cases} x < 0 : & \frac{1}{\phi_L^{-1} - \mathrm{sgn}(\phi_L)\sqrt{\frac{\lambda}{2}}x} \\ x > 0 : & \frac{1}{\phi_R^{-1} + \mathrm{sgn}(\phi_R)\sqrt{\frac{\lambda}{2}}x} \end{cases} . \tag{C.3.3}$$

Plugging them into the matching condition (5.6.2), one gets

$$\begin{aligned} \phi_R &= a\phi_L + b \cdot \mathrm{sign}\left(\phi_L\right)\sqrt{\frac{\lambda}{2}}\phi_L^2 \ , \\ \phi_L &= d\phi_R + b \cdot \mathrm{sign}\left(\phi_R\right)\sqrt{\frac{\lambda}{2}}\phi_R^2 \ . \end{aligned} \tag{C.3.4}$$

The existence of solutions, which we refer to as solitons, depend on the matching matrix. For $b > 0$,

- $0 < \frac{1}{d} < a$: No soliton (also no non-oscillatory bound states around $\phi = 0$)
- $0 < a < \frac{1}{d}$ or $\frac{1}{d} < a < 0$: One pair of $\phi_L\phi_R > 0$ solitons
- $a < \frac{1}{d} < 0$: One $\phi_L\phi_R > 0$ solition *and* one $\phi_L\phi_R < 0$ soliton

This is illustrated in Figure C.1a. The number of solitonic solutions matches the number of bound state modes around $\phi = 0$ as can be seen from Figure C.1b. Thus, in the interacting theory, whenever there is a decaying mode around $\phi = 0$, the solitonic solution is also available.

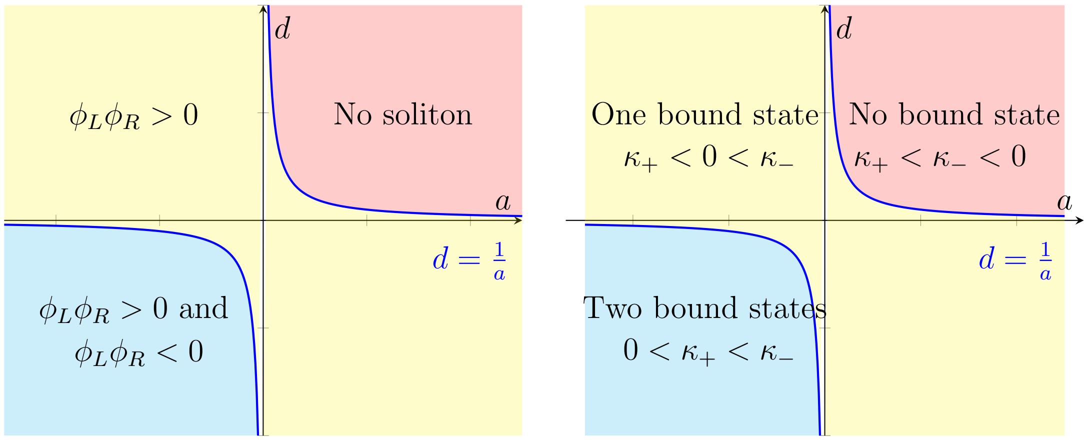

(a) Soliton solutions for $b > 0$ (b) Non-oscillatory decaying modes for $b > 0$

Figure C.1: The parameter space of unstable bound state modes and solitons in the (a, d) domain.

To see which solution is energetically preferred, we use that the Hamiltonian in the solitonic background is

$$H_{\text{tot}} = H + Y \tag{C.3.5}$$

where

$$\begin{aligned} H &= \int_{-\infty}^{\infty} \left(\frac{1}{2}\phi'^2 + \frac{\lambda}{4}\phi^4 \right) \mathrm{d}x \\ &= \int_{-\infty}^{\infty} \frac{\lambda}{2}\phi^4 \, \mathrm{d}x \\ &= \frac{1}{3}\sqrt{\frac{\lambda}{2}} \left(|\phi_L|^3 + |\phi_R|^3 \right) \end{aligned} \tag{C.3.6}$$

and Y is

$$\begin{aligned} Y &= bc\phi_L'\phi_L + \frac{ac}{2}\phi_L^2 + \frac{bd}{2}\left(\phi_L'\right)^2 \\ &= \phi_L^2 \left(\frac{ac}{2} + bc\sqrt{\frac{\lambda}{2}}\,|\phi_L| + \frac{\lambda}{4} bd\phi_L^2 \right) \ . \end{aligned} \tag{C.3.7}$$

Plugging the solutions $\phi_{L,R}$ of the matching equations (C.3.4), we find that the maximum energy is negative in all regions on the (a, d) plane where there is a soliton. Hence, we conclude that the solitonic solutions are energetically preferred to the trivial $\phi = 0$ solution.

In principle, we should also consider fluctuations around the solitons and check for stability, but we have not done so.

APPENDIX D

Higher Structure of Non-invertible Symmetries

D.1 Fusion junctions and associators in the 2d compact boson theory

D.1.1 Local fusion junctions

In this subsection, we analyze the $T \times T \to \eta^k$ junction using the junction data for the fusion $T \times \eta^{-k} \to T$, and then complete our analysis of the local fusion junctions by analyzing the $\eta^k \times T = T$ and $\eta^m \times \eta^n = \eta^{m+n}$ junctions.

$\boldsymbol{T \times T \to \eta^k}$ using $\boldsymbol{T \times \eta^{-k} \to T}$ One can begin with the local fusion junction for $T \times \eta^{-k} \to T$ and flip the direction of the η^k defect along L_2 and similarly also that of the T defect along $t > 0$, as described in Figure D.1.

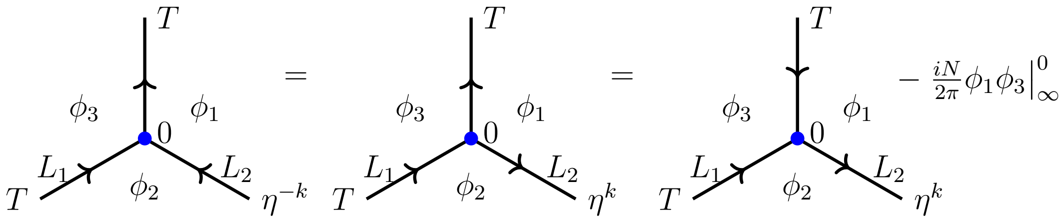

Figure D.1: The local fusion junction $\mathrm{Hom}(T \times T, \eta^k)$, obtained by flipping the directions of η^{-k} on L_2 and T on $t > 0$.

Flipping the direction of η^k corresponds to taking its inverse, i.e. $S_{\eta^{-k}}(L_2) = S_{\eta^k}(-L_2)$, because

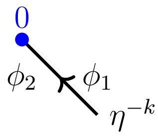

$$= \frac{i}{2\pi}\int_{L_2} \mathrm{d}\varphi \left(\phi_2 - \phi_1 + \frac{2\pi\eta}{N}\right) = \frac{i}{2\pi}\int_{-L_2} \mathrm{d}\varphi \left(\phi_1 - \phi_2 - \frac{2\pi\eta}{N}\right) =$$

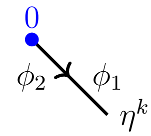

(D.1.1)

However, flipping the direction of the T-defect requires a boundary term since

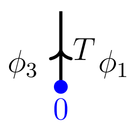

$$= \frac{iN}{2\pi}\int_0^\infty \phi_3 \mathrm{d}\phi_1 = \frac{iN}{2\pi}\int_\infty^0 \phi_1 \mathrm{d}\phi_3 - \frac{iN}{2\pi}\phi_1\phi_3\Big|_\infty^0 =$$

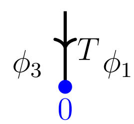

$$- \frac{iN}{2\pi}\phi_1\phi_3\Big|_\infty^0 .$$

(D.1.2)

Combining the results from $T \times \eta^{-k} = T$ (4.3.18) with a suitable relabeling of the fields and the extra boundary term (D.1.2) needed for flipping the direction of T, one reproduces the boundary data (4.3.29).

$\boldsymbol{\eta^k \times T = T}$ Consider fusing the upper part of the two defects η^k and T to obtain the local fusion junction in Figure D.2 (left).

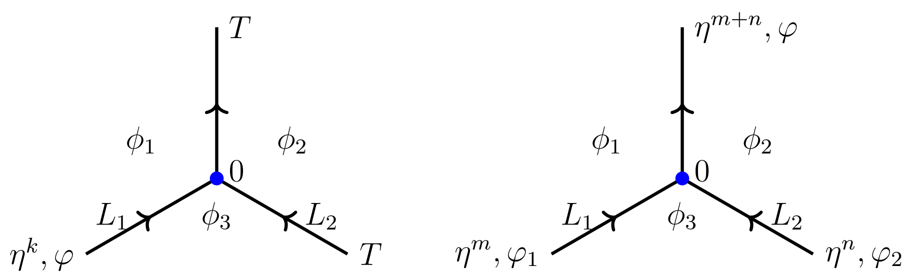

Figure D.2: The local fusion junctions $\mathrm{Hom}(\eta^k \times T, T)$ (left) and $\mathrm{Hom}(\eta^m \times \eta^n, \eta^{m+n})$ (right).

The defect action in the fused part at $t > 0$ is given by

$$\begin{aligned} S =& \frac{i}{2\pi}\int_{L_1} \mathrm{d}\varphi \left(\phi_1 - \phi_3 + \frac{2\pi k}{N}\right) + \frac{iN}{2\pi}\int_{L_2} \phi_3 \mathrm{d}\phi_2 \\ &+ \frac{i}{2\pi}\int_{t>0} \left[N\phi_1 \mathrm{d}\phi_2 + \left(\phi_1 - \phi_3 + \frac{2\pi k}{N}\right)\mathrm{d}\left(\varphi - N\phi_2\right)\right] + ik\phi_2|_0^\infty \end{aligned} \tag{D.1.3}$$

where the first term on the second line corresponds to the T-duality defect as expected from the fusion outcome, the second term is a trivial decoupled TQFT and the last term is a boundary term. The trivial TQFT in the current form is such that its Dirichlet boundary conditions are consistent with the relation between the bulk fields across the η^k defect, $\phi_1 - \phi_3 + \frac{2\pi k}{N}\big|_{L_1} = 0 \bmod 2\pi$. The Dirichlet boundary conditions and the boundary term at this junction can be summarized as

$$\begin{aligned}\mathrm{Hom}(\eta^k \times T, T): \quad \phi_1 - \phi_3 + \frac{2\pi k}{N}\bigg|_{t=0} = 0\,, \quad \varphi - N\phi_2|_{t=0} = 0 \quad \bmod 2\pi \\ S_{bdry} = -ik\phi_2(0)\,.\end{aligned} \tag{D.1.4}$$

$\boldsymbol{\eta^m \times \eta^n = \eta^{m+n}}$ Following the same steps for the local fusion junction $\eta^m \times \eta^n = \eta^{m+n}$ in Figure D.2 (right), the action along the fused segment takes the form

$$\begin{aligned} S =& \frac{i}{2\pi}\int_{t>0}\left[\mathrm{d}\varphi_1\left(\phi_1 - \phi_3 + \frac{2\pi m}{N}\right) + \mathrm{d}\varphi_2\left(\phi_3 - \phi_2 + \frac{2\pi n}{N}\right)\right] \\ =& \frac{i}{2\pi}\int_{t>0}\left[\mathrm{d}\varphi_1\left(\phi_1 - \phi_2 + \frac{2\pi(m+n)}{N}\right) + \left(\phi_3 - \phi_2 + \frac{2\pi n}{N}\right)\mathrm{d}(\varphi_2 - \varphi_1)\right]\,. \end{aligned} \tag{D.1.5}$$

The first term on the second line is the action for the expected η^{m+n} defect and the second term is a trivial decoupled TQFT, whose Dirichlet boundary condition is consistent with the relation between the bulk fields on the defect. Hence, there is no boundary term but the boundary condition is given by

$$\begin{aligned}\mathrm{Hom}(\eta^m \times \eta^n, \eta^{m+n}): \quad \phi_3 - \phi_2 + \frac{2\pi n}{N}\bigg|_{t=0} = 0\,, \quad \varphi|_{t=0} = \varphi_2|_{t=0} = \varphi_1|_{t=0} \quad \bmod 2\pi \\ S_{bdry} = 0\,.\end{aligned} \tag{D.1.6}$$

D.1.2 $\boldsymbol{F}$-symbols

In this subsection, we compute all the F-symbols in the 2d compact boson theory except for $F^T_{T,T,T}$. In Figure D.3, we collected the diagrams for the first three F-symbols.

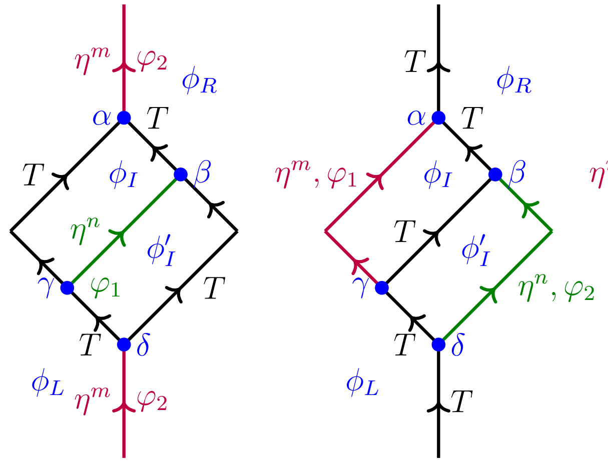

Figure D.3: The diagrams for $F^{\eta^m}_{T,\eta^n,T}$, $F^{T}_{\eta^m,T,\eta^n}$, and $F^{T}_{\eta^m,\eta^n,T}$.

$\boldsymbol{F^{\eta^m}_{T,\eta^n,T}}$ Using the results from the previous subsection, the boundary conditions and boundary terms at each junction are

$$\begin{aligned}
\alpha: &\quad \varphi_2 - N\phi_I = 0\,, \quad \phi_L - \phi_R + \frac{2\pi m}{N} = 0\,, \quad S(\alpha) = -\frac{iN}{2\pi}\phi_I\left(\phi_R - \frac{2\pi m}{N}\right), \\
\beta: &\quad \phi_I - \phi'_I + \frac{2\pi n}{N} = 0\,, \quad \varphi_1 - N\phi_R = 0\,, \quad S(\beta) = -in\phi_R(\beta), \\
\gamma: &\quad \phi_I - \phi'_I + \frac{2\pi n}{N} = 0\,, \quad \varphi_1 - N\phi_L = 0\,, \quad S(\gamma) = \frac{iN}{2\pi}\phi_L\left(\phi_I - \phi'_I + \frac{2\pi n}{N}\right), \\
\delta: &\quad \varphi_2 - N\phi'_I = 0\,, \quad \phi_L - \phi_R + \frac{2\pi m}{N} = 0\,, \quad S(\delta) = \frac{iN}{2\pi}\phi'_I\left(\phi_R + \frac{2\pi\eta_2}{N}\right).
\end{aligned} \tag{D.1.7}$$

The result of the global fusion of the three defects, T, η^n, T in the middle is

$$\begin{aligned}
S =& \frac{iN}{2\pi}\int_\gamma^\beta \mathrm{d}\phi_I\left(\phi_L - \phi_R + \frac{2\pi m}{N}\right) + \frac{i}{2\pi}\int_\gamma^\beta \left(\phi_I - \phi'_I + \frac{2\pi n}{N}\right)\mathrm{d}\left(\varphi_1 - N\phi_R\right) \\
&+ \underbrace{\left[-im\phi_I + \frac{iN}{2\pi}\phi_R\phi_I + in\phi_R\right]_\gamma^\beta}_{S_{bdry;global}}
\end{aligned} \tag{D.1.8}$$

where the first term is the expected η^m defect, the second term is a trivial decoupled TQFT, and the last term is a collection of boundary terms. Both decoupled TQFT fields $\varphi_1 - N\phi_R$ and $\phi_I - \phi'_I + \frac{2\pi n}{N}$ have trivial Dirichlet boundary conditions from the boundary conditions (D.1.7), and hence the decoupled TQFT does not contribute to the F-symbol after reducing the interval. Adding the boundary terms at the upper junction,

$$S(\alpha) + S(\beta) + S_{bdry;global}|_\beta = 0 \tag{D.1.9}$$

and at the lower junction,

$$\begin{aligned} S(\gamma) + S(\delta) + S_{bdry;global}|_\delta &= \frac{iN}{2\pi}\left(\phi_L - \phi_R + \frac{2\pi m}{N}\right)\left(\phi_I - \phi_I' + \frac{2\pi n}{N}\right) - \frac{2\pi imn}{N} \\ &= -\frac{2\pi imn}{N} \mod 2\pi\,. \end{aligned} \tag{D.1.10}$$

Hence, the F-symbol is

$$F^{\eta^m}_{T,\eta^n,T} = \exp\left(\frac{2\pi imn}{N}\right)\,. \tag{D.1.11}$$

$\boldsymbol{F^{T}_{\eta^m,T,\eta^n}}$ Using the results from the previous subsection, the boundary conditions (modulo 2π) and the boundary terms at each junction are

$$\begin{aligned} \alpha: &\quad \phi_L - \phi_I + \frac{2\pi m}{N} = 0, \quad \varphi_1 - N\phi_R = 0, \quad S(\alpha) = -im\phi_R(\alpha), \\ \beta: &\quad \varphi_2 - N\phi_I = 0, \quad \phi_I' - \phi_R + \frac{2\pi n}{N} = 0, \quad S(\beta) = -\frac{iN}{2\pi}\phi_I\left(\phi_I' - \phi_R + \frac{2\pi n}{N}\right), \\ \gamma: &\quad \phi_L - \phi_I + \frac{2\pi m}{N} = 0, \quad \varphi_1 - N\phi_I' = 0, \quad S(\gamma) = im\phi_I'(\gamma), \\ \delta: &\quad \varphi_2 - N\phi_I = 0, \quad \phi_I' - \phi_R + \frac{2\pi n}{N} = 0, \quad S(\delta) = \frac{iN}{2\pi}\phi_L\left(\phi_I' - \phi_R + \frac{2\pi n}{N}\right) \end{aligned} \tag{D.1.12}$$

and the result of the global fusion of η^m, T, η^n in the middle is

$$\begin{aligned} S =& \frac{iN}{2\pi}\int_\gamma^\beta \phi_L \mathrm{d}\phi_R + \left[\frac{i}{2\pi}\left(\phi_I' - \phi_R + \frac{2\pi n}{N}\right)\varphi_2 + im\phi_I'\right]_\gamma^\beta \\ &+ \frac{i}{2\pi}\int_\gamma^\beta \left(\phi_L - \phi_I + \frac{2\pi m}{N}\right)\mathrm{d}(\varphi_1 - N\phi_I') - \frac{i}{2\pi}\int_\gamma^\beta (\varphi_2 - N\phi_L)\,\mathrm{d}\left(\phi_I' - \phi_R + \frac{2\pi n}{N}\right). \end{aligned} \tag{D.1.13}$$

The trivial TQFT fields have trivial Dirichlet boundary conditions and do not contribute to the F-symbol. Adding the boundary terms at the upper junction,

$$\begin{aligned} S(\alpha) + S(\beta) + S_{bdry;global}|_\beta &= \frac{i}{2\pi}(\varphi_2 - N\phi_I)\left(\phi_I' - \phi_R + \frac{2\pi n}{N}\right) + im\left(\phi_I' - \phi_R\right) \\ &= -\frac{2\pi imn}{N} \end{aligned} \tag{D.1.14}$$

and at the lower junction

$$S(\gamma) + S(\delta) + S_{bdry;global}\big|_\delta = \frac{i}{2\pi}\left(\phi_I' - \phi_R + \frac{2\pi n}{N}\right)(N\phi_L - \varphi_2) = 0\,. \tag{D.1.15}$$

Hence,

$$F^T_{\eta^m,T,\eta^n} = \exp\left(\frac{2\pi imn}{N}\right)\ . \tag{D.1.16}$$

$\boldsymbol{F^T_{\eta^m,\eta^n,T}}$ The boundary conditions and boundary terms at each junction are

$$\begin{aligned}
\alpha:&\quad \phi_L - \phi_I + \frac{2\pi m}{N} = 0,\quad \varphi_1 - N\phi_R = 0,\quad S(\alpha) = -im\phi_R(\alpha)\ ,\\
\beta:&\quad \phi_I - \phi_I' + \frac{2\pi n}{N} = 0,\quad \varphi_2 - N\phi_R = 0,\quad S(\beta) = -in\phi_R(\beta)\ ,\\
\delta:&\quad \phi_L - \phi_I' + \frac{2\pi(m+n)}{N} = 0,\quad \varphi - N\phi_R = 0,\quad S(\delta) = i(m+n)\phi_R(\delta)\ ,\\
\gamma:&\quad \varphi = \varphi_1 = \varphi_2,\quad \phi_I - \phi_I' + \frac{2\pi n}{N} = 0,\quad S(\gamma) = 0\ .
\end{aligned} \tag{D.1.17}$$

The global fusion of η^m, η^n, T in the middle is

$$\begin{aligned}
S =& \frac{iN}{2\pi}\int_\gamma^\beta \phi_L \mathrm{d}\phi_R + i(m+n)\phi_R\big|_\gamma^\beta\\
&+ \frac{i}{2\pi}\int_\gamma^\beta \left(\phi_L - \phi_I + \frac{2\pi m}{N}\right)\mathrm{d}(\varphi_1 - \varphi_2) + \left(\phi_L - \phi_I' + \frac{2\pi(m+n)}{N}\right)\mathrm{d}(\varphi_2 - N\phi_R)\ ,
\end{aligned} \tag{D.1.18}$$

and the trivial decoupled TQFT fields have the trivial Dirichlet boundary conditions. The sums of the boundary terms at the upper and lower junctions vanish, and thus the F-symbol is trivial,

$$F^T_{\eta^m,\eta^n,T} = 1\,. \tag{D.1.19}$$

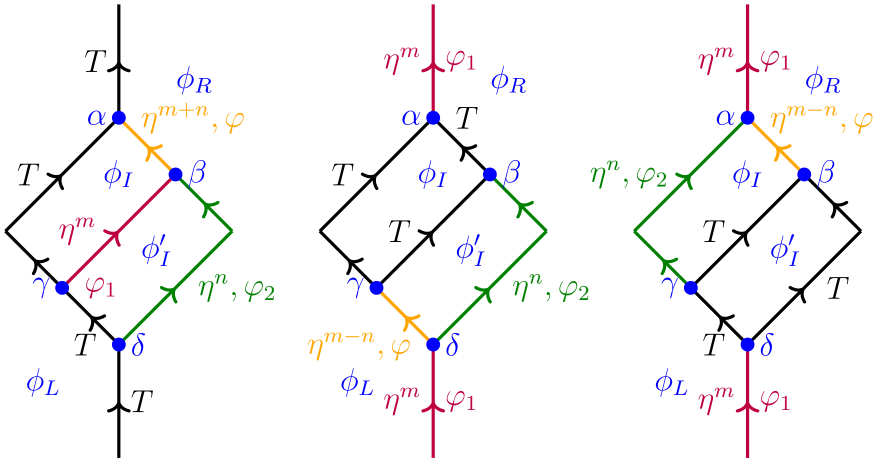

Figure D.4: The diagrams for F^{T}_{T,η^m,η^n}, $F^{\eta^m}_{T,T,\eta^n}$ and $F^{\eta^m}_{\eta^n,T,T}$.

$\boldsymbol{F^{T}_{T,\eta^m,\eta^n}}$ The boundary conditions (mod 2π) and boundary terms at each junction are

$$
\begin{aligned}
&\alpha: \quad \phi_I - \phi_R + \frac{2\pi(m+n)}{N} = 0, \quad \varphi - N\phi_L = 0, \quad S(\alpha) = -\frac{iN}{2\pi}\phi_L\left(\phi_I - \phi_R + \frac{2\pi(m+n)}{N}\right) \ , \\
&\beta: \quad \varphi = \varphi_1 = \varphi_2, \quad \phi_I' - \phi_R + \frac{2\pi n}{N} = 0, \quad S(\beta) = 0 \ , \\
&\gamma: \quad \phi_I - \phi_I' + \frac{2\pi m}{N} = 0, \quad \varphi_1 - N\phi_L = 0, \quad S(\gamma) = \frac{iN}{2\pi}\phi_L\left(\phi_I - \phi_I' + \frac{2\pi m}{N}\right) \ , \\
&\delta: \quad \phi_I' - \phi_R + \frac{2\pi n}{N} = 0, \quad \varphi_2 - N\phi_L = 0, \quad S(\delta) = \frac{iN}{2\pi}\phi_L\left(\phi_I' - \phi_R + \frac{2\pi n}{N}\right) \ ,
\end{aligned}
\tag{D.1.20}
$$

and the global fusion of the three defects η^m, η^n, T is

$$
\begin{aligned}
S =& \frac{iN}{2\pi}\int_\gamma^\beta \phi_L \mathrm{d}\phi_R + \left[\frac{i}{2\pi}\varphi_1\left(\phi_I - \phi_R + \frac{2\pi(m+n)}{N}\right)\right]_\gamma^\beta \\
&+ \frac{i}{2\pi}\int_\gamma^\beta \left[(N\phi_L - \varphi_1)\mathrm{d}(\phi_I - \phi_R + \frac{2\pi(m+n)}{N}) + \left(\phi_I' - \phi_R - \frac{2\pi\eta_2}{N}\right)\mathrm{d}(\varphi_2 - \varphi_1)\right] .
\end{aligned}
\tag{D.1.21}
$$

All trivial decoupled TQFT fields have the trivial Dirichlet boundary conditions and so the two decoupled TQFTs do not contribute to the F-symbol. The sum of the boundary terms at the upper junction is given by

$$S(\alpha)+S(\beta)+S_{bdry;global}|_{\beta}=\frac{i}{2\pi}(\varphi_1-N\phi_L)\left(\phi_I-\phi_R+\frac{2\pi(m+n)}{N}\right)=0\mod 2\pi \tag{D.1.22}$$

and at the lower junction by

$$S(\gamma)+S(\delta)+S_{bdry;global}|_{\gamma}=\frac{i}{2\pi}(N\phi_L-\varphi_1)\left(\phi_I-\phi_R+\frac{2\pi(m+n)}{N}\right)=0\mod 2\pi\,. \tag{D.1.23}$$

Hence, the F-symbol is trivial,

$$F^{T}_{T,\eta^m,\eta^n}=1\,. \tag{D.1.24}$$

$\boldsymbol{F^{\eta^m}_{T,T,\eta^n}}$ The boundary conditions (mod 2π) and boundary terms at each junction are

$$\begin{aligned}
&\alpha: \quad \varphi_1-N\phi_I=0,\quad \phi_L-\phi_R+\frac{2\pi m}{N}=0,\quad S(\alpha)=-\frac{iN}{2\pi}\phi_I\left(\phi_R-\frac{2\pi m}{N}\right),\\
&\beta: \quad \varphi_2-N\phi_I=0,\quad \phi_I'-\phi_R+\frac{2\pi n}{N}=0,\quad S(\beta)=-\frac{iN}{2\pi}\phi_I\left(\phi_I'-\phi_R+\frac{2\pi n}{N}\right),\\
&\gamma: \quad \varphi-N\phi_I=0,\quad \phi_L-\phi_I'+\frac{2\pi(m-n)}{N}=0,\quad S(\gamma)=\frac{iN}{2\pi}\phi_I\left(\phi_I'-\frac{2\pi(m-n)}{N}\right),\\
&\delta: \quad \varphi=\varphi_1=\varphi_2,\quad \phi_I'-\phi_R+\frac{2\pi n}{N}=0,\quad \phi_L-\phi_R+\frac{2\pi m}{N}=0,\quad S(\delta)=0\ ,
\end{aligned} \tag{D.1.25}$$

and the global fusion of the three defects T,T,η^n in the middle is

$$\begin{aligned}
S=&\frac{iN}{2\pi}\int_\gamma^\beta\left(\phi_L-\phi_R+\frac{2\pi m}{N}\right)\mathrm{d}\phi_I+\frac{i}{2\pi}\int_\gamma^\beta(\phi_I'-\phi_R+\frac{2\pi n}{N})\mathrm{d}(\varphi_2-N\phi_I)\\
&+\frac{iN}{2\pi}\left[\phi_I\left(\phi_I'-\frac{2\pi(m-n)}{N}\right)\right]_\gamma^\beta.
\end{aligned} \tag{D.1.26}$$

The trivial decoupled TQFT fields have trivial Dirichlet boundary conditions. The sum of the boundary terms at the upper junction vanishes,

$$S(\alpha)+S(\beta)+S_{bdry;global}|_{\beta}=0\ , \tag{D.1.27}$$

and the sum at the lower junction vanishes as well,

$$S(\gamma)+S(\delta)+S_{bdry;global}|_{\gamma}=0\,. \tag{D.1.28}$$

Hence, the F-symbol is trivial:

$$F^{\eta^m}_{T,T,\eta^n} = 1\,. \tag{D.1.29}$$

$\boldsymbol{F^{\eta^m}_{\eta^n,T,T}}$ The boundary conditions (mod 2π) and boundary terms at each junction are

$$\begin{aligned}
\alpha:&\quad \varphi_1 = \varphi_2 = \varphi, \quad \phi_L - \phi_R + \frac{2\pi m}{N} = 0, \quad \phi_L - \phi_I + \frac{2\pi n}{N} = 0, \quad S(\alpha) = 0,\\
\beta:&\quad \varphi - N\phi_I' = 0, \quad \phi_I - \phi_R + \frac{2\pi(m-n)}{N} = 0, \quad S(\beta) = -\frac{iN}{2\pi}\phi_I'\left(\phi_R - \frac{2\pi(m-n)}{N}\right),\\
\gamma:&\quad \phi_L - \phi_I + \frac{2\pi n}{N} = 0, \quad \varphi_2 - N\phi_I' = 0, \quad S(\gamma) = in\phi_I'(\gamma),\\
\delta:&\quad \varphi_1 - N\phi_I' = 0, \quad \phi_L - \phi_R + \frac{2\pi m}{N} = 0, \quad S(\delta) = \frac{iN}{2\pi}\phi_I'\left(\phi_R - \frac{2\pi m}{N}\right)
\end{aligned} \tag{D.1.30}$$

and the global fusion of the three defects η^n, T, T in the middle is

$$\begin{aligned}
S =& \frac{i}{2\pi}\int_\gamma^\beta \mathrm{d}\varphi_1\left(\phi_L - \phi_R + \frac{2\pi m}{N}\right) + \left[\frac{iN}{2\pi}\phi_I'\left(\phi_R - \frac{2\pi(m-n)}{N}\right)\right]_\gamma^\beta\\
&+ \frac{i}{2\pi}\int_\gamma^\beta\left(\phi_L - \phi_R + \frac{2\pi m}{N}\right)\mathrm{d}(N\phi_I' - \varphi_1) + \frac{i}{2\pi}\int_\gamma^\beta\left(\phi_L - \phi_I + \frac{2\pi n}{N}\right)\mathrm{d}(\varphi_2 - N\phi_I')\,.
\end{aligned} \tag{D.1.31}$$

All decoupled trivial TQFT fields have trivial Dirichlet boundary conditions, and the sum of the boundary terms at both the upper and lower junctions vanishes,

$$S(\alpha) + S(\beta) + S_{bdry;global}|_\beta = 0\,, \quad S(\gamma) + S(\delta) + S_{bdry;global}|_\gamma = 0\,. \tag{D.1.32}$$

Hence, the F-symbol is trivial,

$$F^{\eta^m}_{\eta^n,T,T} = 1\,. \tag{D.1.33}$$

D.2 Comments on alternative formalisms on the local junctions

The topological boundary/interface of a topological defect (or a TFT) can be described either in terms of boundary conditions or by introducing boundary degrees of freedom. In Section 4.4, we take the first approach, and in this Appendix, we want to present the alternative description commonly used in the literature [63,71] and discuss their relations in the concrete example of the 3d $\mathbb{Z}_N$ gauge theory written in terms of the CS action. Notice that there are no new results here, and we simply hope to clarify a few subtleties in various formalisms.

Let's first recall the topological boundary condition for $\mathbb{Z}_N$ gauge theory given by the CS action

$$S = \frac{iN}{2\pi} \int_V a \wedge db \ . \tag{D.2.1}$$

For generic $N > 1$, there always exist two boundary conditions

$$\begin{aligned} &(\mathrm{I}): \quad a|_{\partial V} = d\phi_a \ , \quad Nb|_{\partial V} = d\phi_b \ , \\ &(\mathrm{II}): Na|_{\partial V} = d\phi_a \ , \qquad b|_{\partial V} = d\phi_b \ , \end{aligned} \tag{D.2.2}$$

and we will restrict our discussion to these two for simplicity.

In the boundary condition (I), the gauge transformations are given by

$$a \to a + d\lambda_a \ , \quad b \to b + d\lambda_b \ , \quad \phi_a \to \phi_a + \lambda_a \ , \quad \phi_b \to \phi_b + N\lambda_b \ . \tag{D.2.3}$$

It is straightforward to check that the action is gauge invariant and is consistent with the variation principle. In this boundary condition, the a-Wilson line is allowed to terminate on the boundary, described by the gauge-invariant operator

$$\exp\left(-i\phi_a(p) + i\int_\gamma a\right) \ , \quad \gamma \cap \partial V = \{p\} \ , \tag{D.2.4}$$

where γ is some path in the bulk V that terminates at the boundary point $p \in \partial V$. On the boundary, the charge N b-Wilson line is identified with the identity line as there exists a local junction between the two. In other words, the line $e^{iN\int b}$ can terminate on the vertex operator $e^{-i\phi_b}$ in a gauge-invariant way[1]. Hence, $e^{i\oint_\gamma b}$ generates $\mathbb{Z}_N$ symmetry on the boundary for the boundary condition (I). Combined, we see the boundary condition (I) yields the correct operator spectrum for the $e^{i\oint a}$-condensed boundary. It is straightforward to repeat the same

[1] Notice that similar story happens in the bulk, except the role of $e^{i\phi_b}$ is played by the monopole operator of a [136].

analysis for the boundary condition (II) and see it describes the $e^{i\oint b}$-condensed boundary correctly.

The same boundary conditions can also be described by introducing boundary scalars and coupling them to the bulk field, while leaving the bulk fields completely free in the action on the boundary. The boundary coupling as well as the gauge transformations are given by

$$\begin{aligned}
(\mathrm{I}) : S_{\partial V} &= \frac{iN}{2\pi}\int_{\partial V} \phi db \ , \\
& \quad a \to a + d\lambda_a \ , \quad b \to b + d\lambda_b \ , \quad \phi \to \phi - \lambda_a \ , \\
(\mathrm{II}) : S_{\partial V} &= \frac{iN}{2\pi}\int_{\partial V} \phi da + a \wedge b \ , \\
& \quad a \to a + d\lambda_a \ , \quad b \to b + d\lambda_b \ , \quad \phi \to \phi - \lambda_b \ .
\end{aligned} \tag{D.2.5}$$

It is straightforward to check that both boundary conditions are well-defined and yield the correct operator spectrum. In the boundary condition (I), $e^{i\int a}$ can terminate on the $e^{-i\phi}$ in a gauge-invariant way on the boundary. At the same time, the equation of motion of ϕ implies that $e^{iN\oint b} = \mathbb{1}$ thus $e^{i\oint b}$ generates $\mathbb{Z}_N$ symmetry on the boundary[2]. Similarly, in the boundary condition (II), $e^{i\int b}$ can terminate on the boundary while $e^{i\oint a}$ generates $\mathbb{Z}_N$-symmetry instead.

The advantage of this formalism is that one can manifestly produce an action in terms of continuous fields in the interval reduction. For instance, let's consider placing the theory on $[0,1]_t \times M_2$. Let us first consider choosing boundary condition (I) for both $t=0$ and $t=1$ boundaries. In this case, the full action is given by

$$\frac{iN}{2\pi}\int_{[0,1]_t\times M_2} a \wedge db - \frac{iN}{2\pi}\int_{M_2|_{t=0}} \phi\, db + \frac{iN}{2\pi}\int_{M_2|_{t=1}} \widetilde{\phi}\, db \ , \tag{D.2.6}$$

[2]To see that $e^{iN\int b}$ can terminate on the boundary, we notice that there exists a boundary operator $\mathcal{O}(x)$, defined by removing the point x from ∂V and require the compact scalar ϕ to have unit winding around x when inserting in the path integral. $e^{iN\int b}$ can terminate gauge-invariantly on $\mathcal{O}(x)$.

with the gauge transformation

$$a \to a + d\lambda_a \ , \quad b \to b + d\lambda_b \ , \quad \phi \to \phi - \lambda_a \ , \quad \widetilde{\phi} \to \phi - \lambda_a \ . \tag{D.2.7}$$

Reducing along the interval by fusing two boundaries leads to the 2d action

$$\frac{iN}{2\pi} \int_{M_2} (\widetilde{\phi} - \phi) \, db \equiv \frac{iN}{2\pi} \int_{M_2} \Phi \, db \ , \tag{D.2.8}$$

which becomes the standard 2d $\mathbb{Z}_N$ gauge theory upon introducing the gauge invariant compact scalar $\Phi = \widetilde{\phi} - \phi$, thus reproduces the well-known result.

On the other hand, one can also consider choosing boundary condition (I) for the $t = 0$ boundary and boundary condition (II) for the $t = 1$ boundary. In this case, the full action is given by

$$\frac{iN}{2\pi} \int_{[0,1]_t \times M_2} a \wedge db - \frac{iN}{2\pi} \int_{M_2|_{t=0}} (\phi \, da + a \wedge b) + \frac{iN}{2\pi} \int_{M_2|_{t=1}} \widetilde{\phi} \, db \ , \tag{D.2.9}$$

with the gauge transformation

$$a \to a + d\lambda_a \ , \quad b \to b + d\lambda_b \ , \quad \phi \to \phi - \lambda_b \ , \quad \widetilde{\phi} \to \phi - \lambda_a \ . \tag{D.2.10}$$

Upon the reduction, we find the 2d action

$$\frac{iN}{2\pi} \int_{M_2} -a \wedge b - \phi \, da + \widetilde{\phi} \, db \ , \tag{D.2.11}$$

with the gauge transformation (D.2.10). Despite having a seemingly non-trivial action, the 2d theory is actually trivial as there are no gauge-invariant operators which do not commute upon canonical quantization, also matching the well-known result.

D.3 Triality fusion junctions and associators in 4d Maxwell theory

D.3.1 Triality fusion junctions

The triality and the condensation defects form a closed non-invertible fusion algebra. In this section, we focus on the associator for the fusion of three triality defects (not of a condensation defect) for even N and analyze the following relevant local fusion and morphism junctions,

$$
\begin{gathered}
C_0 \to \mathbb{1}\ (4.4.21), \quad C_{\frac{N}{2}} \to \mathbb{1}\ (4.4.24), \quad U(1)_N \times U(1)_{-N} \to \mathbb{1}\ (4.4.35), \\
D_3 \times \mathbb{1} = D_3\ (4.4.17), \quad \mathbb{1} \times D_3 = D_3\ (\text{D.3.3}), \quad \mathbb{1} \times \overline{D}_3 = \overline{D}_3\ (\text{D.3.5}), \quad \overline{D}_3 \times \mathbb{1} = \overline{D}_3\ (\text{D.3.7}) \\
D_3 \times D_3 = U(1)_N \overline{D}_3\ (4.4.33), \quad \overline{D}_3 \times \overline{D}_3 = U(1)_{-N} D_3\ (4.4.34), \\
\overline{D}_3 \times D_3 = C_0\ (\text{D.3.9}), \quad D_3 \times \overline{D}_3 = C_{\frac{N}{2}}\ (\text{D.3.12})\,.
\end{gathered}
\tag{D.3.1}
$$

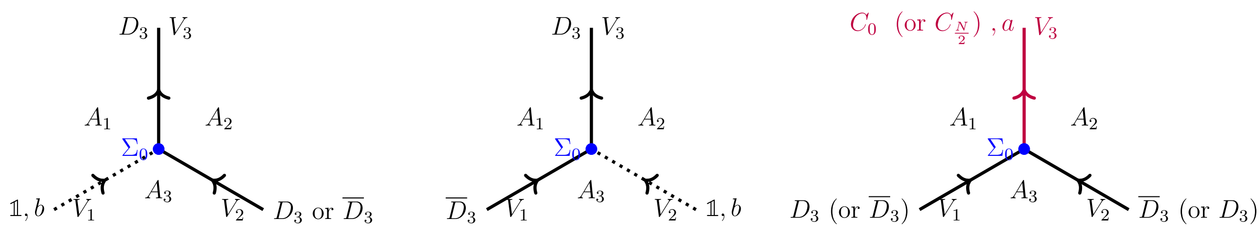

Figure D.5: Fusion junctions on the second line of Eq. (D.3.1); b is the defect field on V_2 for the identity defect.

$\mathbb{1} \times \boldsymbol{D_3} = \boldsymbol{D_3}$ Consider the local fusion junction for $\mathbb{1} \times D_3 \to D_3$, the first diagram of Figure D.5. The action along the fused upper part V_3 is

$$
\begin{aligned}
S &= \frac{i}{2\pi}\int_{V_3}\left[\mathrm{d}b(A_1 - A_3) + NA_3\mathrm{d}A_2 + \frac{N}{2}A_3\mathrm{d}A_3\right] \\
&= \frac{iN}{2\pi}\int_{V_3}\left(A_1\mathrm{d}A_2 + \frac{1}{2}A_1\mathrm{d}A_1\right) + \frac{iN}{4\pi}\int_{\Sigma_0} A_1 \wedge A_3 \\
&\quad + \frac{i}{2\pi}\int_{V_3}(A_1 - A_3)\,\mathrm{d}\left(b - \frac{N}{2}A_3 - \frac{N}{2}A_1 - NA_2\right)
\end{aligned}
\tag{D.3.2}
$$

where the first term on the last line describes the triality defect D_3 as expected from the fusion algebra, second term is the boundary term and the last term is a trivial TQFT. Since the fields A_3 and b above Σ_0 are supported only along the D_3 defect, (by shifting $A_3 \to A_3 + A_1$ and $b \to b + \frac{N}{2}A_3 + \frac{N}{2}A_1 + NA_2$, the TQFT is decoupled from the bulk. Thus, we impose the boundary conditions (4.4.15). In summary,

$$\begin{aligned} \mathrm{Hom}(\mathbb{1}\times D_3, D_3): \quad & A_1 - A_3\ , \quad b - \frac{N}{2}A_3 - \frac{N}{2}A_1 - NA_2\Big|_{\Sigma_0} = \text{pure } U(1) \text{ gauge}\ , \\ & S_{bdry} = \frac{iN}{4\pi}\int_{\Sigma_0} A_1\wedge A_3\ . \end{aligned} \tag{D.3.3}$$

$\mathbb{1}\times \overline{\boldsymbol{D}}_{\boldsymbol{3}} = \overline{\boldsymbol{D}}_{\boldsymbol{3}}$ We again use the first diagram in Figure D.5 with the action along the V_3 segment,

$$\begin{aligned} S &= \frac{i}{2\pi}\int_{V_3}\left[\mathrm{d}b(A_1 - A_3) - NA_3\mathrm{d}A_2 - \frac{N}{2}A_2\mathrm{d}A_2\right] \\ &= \underbrace{-\frac{iN}{2\pi}\int_{V_3}\left(A_1\mathrm{d}A_2 + \frac{1}{2}A_2\mathrm{d}A_2\right)}_{\overline{D}_3} + \underbrace{\frac{i}{2\pi}\int_{V_3}(A_1 - A_3)\mathrm{d}(b + NA_2)}_{\text{Decoupled trivial TQFT}}\ . \end{aligned} \tag{D.3.4}$$

$$\mathrm{Hom}(\mathbb{1}\times \overline{D}_3, \overline{D}_3): \quad A_1 - A_3, \quad b + NA_2|_{\Sigma_0} = \text{pure } U(1) \text{ gauge}, \quad S_{bdry} = 0\ . \tag{D.3.5}$$

$\overline{\boldsymbol{D}}_{\boldsymbol{3}}\times\mathbb{1} = \overline{\boldsymbol{D}}_{\boldsymbol{3}}$ This corresponds to the second diagram in Figure D.5 with the action along the V_3 segment given by

$$\begin{aligned} S &= \frac{i}{2\pi}\int_{V_3}\left[-NA_1\mathrm{d}A_3 - \frac{N}{2}A_3\mathrm{d}A_3 + \mathrm{d}b\wedge(A_3 - A_2)\right] \\ &= \underbrace{-\frac{iN}{2\pi}\int_{V_3}\left(A_1\mathrm{d}A_2 + \frac{1}{2}A_2\mathrm{d}A_2\right)}_{\overline{D}_3} + \underbrace{\frac{i}{2\pi}\int_{V_3}(A_3 - A_2)d\left[b - NA_1 - \frac{N}{2}(A_2 + A_3)\right]}_{\text{Decoupled trivial TQFT}} \\ &\quad \underbrace{-\frac{i}{2\pi}\int_{\Sigma_0} NA_1\wedge(A_3 - A_2) + \frac{N}{2}A_2\wedge A_3}_{S_{bdry}}\ . \end{aligned} \tag{D.3.6}$$

Imposing the boundary conditions (4.4.15) for the decoupled TQFT, we have

$$\begin{aligned} \mathrm{Hom}(\overline{D}_3\times\mathbb{1}, \overline{D}_3): \quad & b - NA_1 - \frac{N}{2}(A_2 + A_3), \quad A_2 - A_3\Big|_{\Sigma_0} = \text{pure } U(1) \text{ gauge}\ , \\ & S_{bdry} = -\frac{i}{2\pi}\int_{\Sigma_0} NA_1\wedge(A_3 - A_2) + \frac{N}{2}A_2\wedge A_3\ . \end{aligned} \tag{D.3.7}$$

$\boldsymbol{\overline{D}_3 \times D_3 = C_0}$ This junction corresponds to the third diagram of Figure D.5. The action along the fused part V_3 is

$$\begin{aligned} S &= \frac{iN}{2\pi}\int_{V_3}\left(-A_1 \mathrm{d}A_3 - \frac{1}{2}A_3\mathrm{d}A_3 + A_3\mathrm{d}A_2 + \frac{1}{2}A_3\mathrm{d}A_3\right) \\ &= \underbrace{-\frac{iN}{2\pi}\int_{V_3}\mathrm{d}A_3\,(A_1 - A_2)}_{C_0} \underbrace{- \frac{iN}{2\pi}\int_{\Sigma_0} A_2 \wedge A_3}_{S_{bdry}} \ . \end{aligned} \tag{D.3.8}$$

No particular boundary condition is imposed, hence

$$\mathrm{Hom}(\overline{D}_3 \times D_3, C_0) : \text{no b.c.}, \quad S_{bdry} = -\frac{iN}{2\pi}\int_{\Sigma_0} A_2 \wedge A_3 \ . \tag{D.3.9}$$

Attaching a morphism junction between C_0 and the identity (with the identity defect field being b) using Eq. (4.4.21), we get

$$\mathrm{Hom}(\overline{D}_3 \times D_3, \mathbb{1}) : b + NA_3, \quad A_1 - A_2| = \text{pure } U(1) \text{ gauge}, \quad S_{bdry} = -\frac{iN}{2\pi}\int_{\Sigma_0} A_2 \wedge A_3 \ . \tag{D.3.10}$$

$\boldsymbol{D_3 \times \overline{D}_3 = C_{\frac{N}{2}}}$ This junction corresponds to the third diagram of Figure D.5, with the action along the fused segment V_3 given by

$$\begin{aligned} S &= \frac{iN}{2\pi}\int_{V_3}\left(A_1\mathrm{d}A_3 + \frac{1}{2}A_1\mathrm{d}A_1 - A_3\mathrm{d}A_2 - \frac{1}{2}A_2\mathrm{d}A_2\right) \\ &= \underbrace{\frac{iN}{2\pi}\int_{V_3}\left[(A_1 - A_2)\mathrm{d}(A_3 + A_2) + \frac{1}{2}(A_1 - A_2)\mathrm{d}(A_1 - A_2)\right]}_{C_{\frac{N}{2}}} + \underbrace{\frac{iN}{2\pi}\int_{\Sigma_0}\left(A_2 \wedge A_3 - \frac{1}{2}A_1 \wedge A_2\right)}_{S_{bdry}} . \end{aligned} \tag{D.3.11}$$

There is no particular boundary condition imposed here, hence

$$\mathrm{Hom}(D_3 \times \overline{D}_3, C_{\frac{N}{2}}) : \quad \text{No b.c.}, \quad S_{bdry} = \frac{iN}{2\pi}\int_{\Sigma_0}\left(A_2 \wedge A_3 - \frac{1}{2}A_1 \wedge A_2\right) . \tag{D.3.12}$$

Attaching a morphism junction between C_0 and the identity (with the identity defect field being b) using Eq. (4.4.24), we have

$$\begin{aligned} \mathrm{Hom}(D_3 \times \overline{D}_3, \mathbb{1}) : \quad & N(A_2 + A_3) - b, \quad A_1 - A_2 = \text{pure } U(1) \text{ gauge}, \\ & S_{bdry} = \frac{iN}{2\pi}\int_{\Sigma_0}\left(A_2 \wedge A_3 - \frac{1}{2}A_1 \wedge A_2\right) \ . \end{aligned} \tag{D.3.13}$$

D.3.2 Triality defect associator

In this subsection, we focus on the first three associators among the following defect trios, with morphism junctions to the identity added whenever it is possible:

$$D_3 \times D_3 \times D_3\,, \quad D_3 \times \overline{D}_3 \times D_3\,, \quad D_3 \times D_3 \times \overline{D}_3\,, \quad \overline{D}_3 \times D_3 \times D_3\,. \tag{D.3.14}$$

These are drawn in Figure D.6.

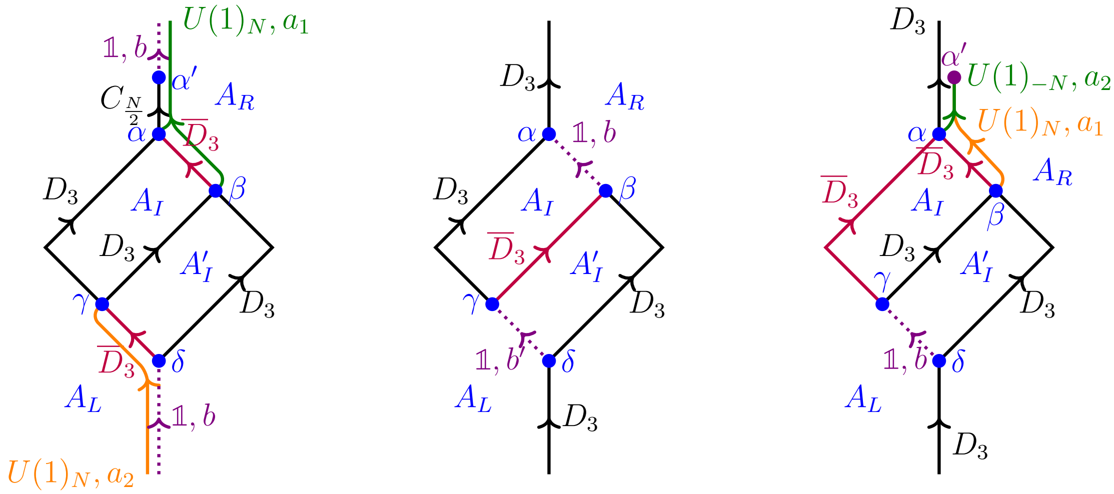

Figure D.6: The triality defect associators. Morphism junctions appear in purple and are adjacent to a local fusion junction. From left to right: $[F^{U(1)_N}_{D_3,D_3,D_3}]_{U(1)_N\overline{D}_3,U(1)_N\overline{D}_3}$, $[F^{D_3}_{D_3,\overline{D}_3,D_3}]_{\mathbb{1},\mathbb{1}}$ and $[F^{D_3}_{\overline{D}_3,D_3,D_3}]_{\mathbb{1},U(1)_N\overline{D}_3}$.

D.3.2.1 $\left[F^{U(1)_N}_{D_3,D_3,D_3}\right]_{U(1)_N\overline{D}_3,U(1)_N\overline{D}_3}$

This associator (first diagram of Figure D.6) relates the following two different fusions:

$$\begin{aligned} (D_3 \times D_3) \times D_3 &= U(1)_N\,\overline{D}_3 \times D_3 = U(1)_N\,C_0 \to U(1)_N\,, \\ D_3 \times (D_3 \times D_3) &= U(1)_N\,D_3 \times \overline{D}_3 = U(1)_N\,C_{\frac{N}{2}} \to U(1)_N\,. \end{aligned} \tag{D.3.15}$$

Using the junction analyses in the previous subsection, the boundary data at each junction is

$$\begin{aligned}
&\alpha\beta: \quad A_L - A_R, \quad N(A_I + A_R) + \frac{N}{2}(A_L - A_R) - b = \text{pure } U(1) \text{ gauge} \\
&\qquad S(\alpha) + S(\beta) = \frac{iN}{4\pi}\int_{\Sigma_{\alpha\beta}} [A_R \wedge A_I - A_L \wedge A_R + (A_I - A_R)\wedge A_I'] \ , \\
&\gamma\delta: \quad A_L - A_R, \quad b + NA_I' = \text{pure } U(1) \text{ gauge} \ , \\
&\qquad S(\gamma) + S(\delta) = -\frac{iN}{4\pi}\int_{\Sigma_{\gamma\delta}} [A_L \wedge A_I + A_L \wedge A_I' + A_I \wedge A_I' - 2A_R \wedge A_I'] \ .
\end{aligned} \tag{D.3.16}$$

After the parallel fuison of three D_3 defects in the middle,

$$\begin{aligned}
S &= \frac{iN}{2\pi}\int_\gamma^\beta \left(A_L \mathrm{d}A_I + \frac{1}{2}A_L \mathrm{d}A_L + A_I \mathrm{d}A_I' + \frac{1}{2}A_I \mathrm{d}A_I + A_I' \mathrm{d}A_R + \frac{1}{2}A_I' \mathrm{d}A_I' \right) \\
&= \frac{iN}{4\pi}\int_\gamma^\beta (A_L + A_I + A_I')\mathrm{d}(A_L + A_I + A_I') \quad \leftarrow U(1)_N \\
&\quad - \frac{iN}{2\pi}\int_\gamma^\beta \mathrm{d}A_I' \, (A_L - A_R) \quad \leftarrow \text{ Condensation defect } C_0 \\
&\quad + \frac{iN}{2\pi}\int_{\Sigma_\beta - \Sigma_\gamma} \left[-A_I' \wedge A_R + \frac{1}{2}(A_I \wedge A_L + A_I' \wedge A_L + A_I' \wedge A_I) \right] \quad \leftarrow S_{bdry;global}
\end{aligned} \tag{D.3.17}$$

the interval hosts a $U(1)_N$ Chern-Simons theory, a condensation defect and some boundary terms. Summing the boundary terms from the upper junctions along with $S_{bdry;global}$ we get

$$S(\alpha) + S(\beta) + S_{bdry;global}|_{\alpha\beta} = -\frac{iN}{4\pi}\int_\Sigma (A_I + A_I' + A_L) \wedge (A_R + A_I + A_I') \ , \tag{D.3.18}$$

while the sum of boundary terms at the lower junctions vanishes,

$$S(\gamma) + S(\delta) + S_{bdry;global}|_{\gamma\delta} = 0 \ . \tag{D.3.19}$$

The total boundary term (D.3.18) at the upper junction connects the $U(1)_N$ theories at the junction β. To see this, we notice that the $U(1)_N$ theories above β, below γ and between them are

$$\begin{aligned}
\text{Above } \beta \quad & \frac{iN}{4\pi}\int_\beta^\infty (A_R + A_I + A_I')\mathrm{d}(A_R + A_I + A_I') \ , \\
[\gamma, \beta] \text{ and Below } \gamma \quad & \frac{iN}{4\pi}\int_{-\infty}^\beta (A_L + A_I + A_I')\mathrm{d}(A_L + A_I + A_I') \ .
\end{aligned} \tag{D.3.20}$$

Following a similar discussion as in Section 4.4.2.3 (or applying the folding trick here), we see that the boundary term (D.3.18) ensures the gauge invariance from both sides, and the gluing condition, $(A_L + A_I + A'_I) - (A_I + A'_I + A_R) =$ pure $U(1)$ gauge, indicates that this is a trivial interface of the $U(1)_N$ theory.

Thus, we are left with a 3d condensation defect on the interval. Reducing it along the interval leads to a 2d condensation defect of the bulk 1-form symmetry (which is simply a projector). Notice that this is consistent with the operator spectrum analysis. First, as follows from the boundary conditions, the $\mathbb{Z}_N$ higher quantum symmetry line $e^{i\int(A_L - A_R)}$ on the 3d condensation defect can stretch between the two boundaries. After reduction, it becomes a topological local operator and can be interpreted as the higher quantum 1-form symmetry on the 2d condensation defect. Second, in the 4d bulk, an open $\mathbb{Z}_N$ 1-form symmetry operator can be viewed as a non-genuine line operator bounding the symmetry operator; but on the condensation defect, $\mathbb{Z}_N$ is gauged and this line operator should become genuine. This is guaranteed by the e.o.m. of A_L (or A_R), which allows us to rewrite such an open $\mathbb{Z}_N$ 1-form symmetry operator as the A'_I-Wilson line $e^{i\oint A'_I}$. After reduction, $e^{i\oint A'_I}$ remains a line operator by the boundary conditions, encoding the fact that an open $\mathbb{Z}_N$ 1-form symmetry operator becomes genuine in the 2d condensation defect.

We also want to highlight that the existence of local junctions $C_k \to \mathbb{1}$ in the initial diamond diagrams we considered does not necessarily imply there will be a reduction of the condensation defect in the end. This is because we will need to perform the global fusion to collapse the diagram, during which the condensation defect can become a decoupled $\mathbb{Z}_N$-gauge theory. Only when the condensation defect appears in the global fusion, will we have the interval reduction of the 3d condensation defect which leads to the 2d condensation defect.

Overall, we see that the 2d theory corresponding to the associator 1-morphism results solely from the 3d condensation defect in the interval, which reduces to a 2d condensation defect. As a result,

$$\left[F^{U(1)_N}_{D_3,D_3,D_3}\right]_{U(1)_N\overline{D}_3,U(1)_N\overline{D}_3} = \text{2d } \mathbb{Z}_N \text{ condensation defect}\,. \tag{D.3.21}$$

D.3.2.2 $\left[\boldsymbol{F}^{\boldsymbol{D_3}}_{\boldsymbol{D_3,\overline{D}_3,D_3}}\right]_{\mathbb{1},\mathbb{1}}$

This associator relates the following fusions above and below as depicted in the second diagram of Figure D.6:

$$\begin{aligned} &D_3\times(\overline{D}_3\times D_3) = D_3\times C_0 \to D_3\times\mathbb{1} = D_3\ ,\\ &(D_3\times\overline{D}_3)\times D_3 = C_{\frac{N}{2}}\times D_3 \to \mathbb{1}\times D_3 = D_3\ . \end{aligned} \tag{D.3.22}$$

The boundary data at each junction can be collected to

$$\begin{aligned} \alpha,\beta,\beta' :\quad & b+NA_L,\quad b+NA_I',\quad A_I-A_R = \text{pure } U(1) \text{ gauge}\ ,\\ & S(\alpha) = -\frac{i}{2\pi}\int_{\Sigma_\alpha} b\wedge(A_I-A_R),\quad S(\beta) = -\frac{iN}{2\pi}\int_{\Sigma_\beta} A_R\wedge A_I'\ ,\\ \gamma,\gamma',\delta :\quad & N(A_I+A_I')-b',\quad A_L-A_I',\quad b-NA_L-NA_R = \text{pure } U(1) \text{ gauge}\ ,\\ & S(\gamma) = -\frac{iN}{2\pi}\int_{\Sigma_\gamma}\left(A_I'\wedge A_I - \frac{1}{2}A_L\wedge A_I'\right),\quad S(\delta) = -\frac{iN}{4\pi}\int_{\Sigma_\delta} A_L\wedge A_I'\ . \end{aligned} \tag{D.3.23}$$

Fusing the three defects in the middle by summing their actions result in the following actions:

$$\begin{aligned} S &= \frac{iN}{2\pi}\int_\gamma^\beta\left(A_L\mathrm{d}A_I + \frac{1}{2}A_L\mathrm{d}A_L - A_I\mathrm{d}A_I' - \frac{1}{2}A_I'\mathrm{d}A_I' + A_I'\mathrm{d}A_R + \frac{1}{2}A_I'\mathrm{d}A_I'\right)\\ &= \underbrace{\frac{iN}{2\pi}\int_\gamma^\beta\left(A_L\mathrm{d}A_R + \frac{1}{2}A_L\mathrm{d}A_L\right)}_{D_3} + \underbrace{\frac{iN}{2\pi}\int_\gamma^\beta(A_L-A_I')\mathrm{d}(A_I-A_R)}_{\text{decoupled } \mathbb{Z}_N \text{ gauge theory}}\\ &\quad+\underbrace{\frac{iN}{2\pi}\int_{\Sigma_\beta-\Sigma_\gamma} A_I\wedge A_I'}_{S_{bdry;global}}\ . \end{aligned} \tag{D.3.24}$$

Collecting the boundary terms, at the upper junctions

$$S(\alpha)+S(\beta)+S_{bdry;global}\big|_{\alpha\beta} = -\frac{i}{2\pi}\int_{\Sigma_{\alpha\beta}}(b+NA_I')\wedge(A_I-A_R)\in 2\pi i\mathbb{Z} \tag{D.3.25}$$

where we used the boundary conditions, and at the lower junctions,

$$S(\gamma) + S(\delta) + S_{bdry;global}|_{\gamma\delta} = 0 \ . \tag{D.3.26}$$

Hence, we find a decoupled 3d $\mathbb{Z}_N$ on the interval. Since $A_L - A'_I$ has (ND) and $A_I - A_R$ has (DN) boundary conditions on $\alpha\beta$ and $\gamma\delta$ respectively, there is no untwisted local operators after reduction and the decoupled $\mathbb{Z}_N$ gauge theory becomes the trivial theory after reducing the interval $[\gamma, \beta]$. Hence,

$$\left[F^{D_3}_{D_3,\overline{D}_3,D_3}\right]_{\mathbb{1},\mathbb{1}} = \text{Trivial theory}\,. \tag{D.3.27}$$

D.3.2.3 $[\boldsymbol{F^{D_3}_{\overline{D}_3,D_3,D_3}}]_{\mathbb{1},\boldsymbol{U(1)_N\overline{D}_3}}$

Lastly, let's compute the associator in the last diagram of D.6 which relates

$$\begin{aligned} &\text{Upper part}: \quad \overline{D}_3\times(D_3\times D_3) = \overline{D}_3\times\overline{D}_3\ U(1)_N = D_3\ U(1)_{-N}\times U(1)_N \to D_3\ , \\ &\text{Lower part}: \quad (\overline{D}_3\times D_3)\times D_3 = C_0\times D_3 \to \mathbb{1}\times D_3 = D_3\ . \end{aligned} \tag{D.3.28}$$

The boundary data at each junction is

$$\begin{aligned}
\alpha',\alpha,\beta: \quad & a_1 = A_I + A'_I + A_R\ , \quad a_2 = a_L + A_I + A_R\ , \\
& \begin{cases} (1) \qquad N(A'_I + A_I + A_R), \quad A_L - A'_I = \text{pure } U(1) \text{ gauge}\ , \\ \text{or } (2) \quad A_L - A'_I + 2(A'_I + A_I + A_R), \quad \frac{N}{2}(A_L - A'_I) = \text{pure } U(1) \text{ gauge}\ , \end{cases} \\
& S(\alpha) = -\frac{iN}{4\pi}\int_{\Sigma_\alpha} A_L\wedge A_R + (A_L - A_R)\wedge A_I\ , S(\beta) = \frac{iN}{4\pi}\int_{\Sigma_\beta} A_I\wedge A_R + (A_I - A_R)\wedge A'_I\ , \\
& S(\alpha') = -\frac{iN}{4\pi}\int_{\Sigma_{\alpha'}} (A_I + A'_I + A_R)\wedge(A_L + A_I + A_R)\ , \\
\gamma,\gamma',\delta: \quad & A_L - A'_I, \quad N(A_L + A_I + A_R) = \text{pure } U(1) \text{ gauge}\ , \\
& S(\gamma) = \frac{iN}{2\pi}\int A'_I\wedge A_I\ , \quad S(\delta) = -\frac{iN}{2\pi}A_L\wedge A'_I\ .
\end{aligned} \tag{D.3.29}$$

Next, we fuse the three defects $\overline{D}_3 \times D_3 \times D_3$ in the middle by summing their actions,

$$
\begin{aligned}
S =& \frac{iN}{2\pi}\int_\gamma^\beta (-A_L dA_I - \frac{1}{2}A_I dA_I + A_I dA_I' + \frac{1}{2}A_I dA_I + A_I' dA_R + \frac{1}{2}A_I' dA_I')\\
=& \frac{iN}{2\pi}\int_\gamma^\beta \left(A_L \mathrm{d}A_R + \frac{1}{2}A_L \mathrm{d}A_L\right) \quad (\leftarrow D_3)\\
&+ \frac{iN}{2\pi}\int_\gamma^\beta \left[\frac{1}{2}(A_I' - A_L)\mathrm{d}(A_I' - A_L) + (A_I' - A_L)\wedge \mathrm{d}(A_I + A_L + A_R)\right] \quad (\leftarrow (\mathcal{Z}_N)_N)\\
&+ \frac{iN}{2\pi}\int_{\Sigma_\beta - \Sigma_\gamma} \left[A_I' \wedge (A_I + \frac{1}{2}A_L)\right] \quad (\leftarrow S_{bdry;global})\ ,
\end{aligned}
\tag{D.3.30}
$$

where the first line is the action for D_3 as expected from the fusion algebra, the second line is a decoupled $\mathbb{Z}_N$ gauge theory with the twist N (denoted by $(\mathcal{Z}_N)_N$ and the last term is the boundary term.

The total boundary term at the upper junction is

$$
S(\alpha) + S(\beta) + S(\alpha') + S_{bdry;global}|_\beta = 0\ , \tag{D.3.31}
$$

and the total boundary term at the lower junction is

$$
S(\gamma) + S(\delta) + S_{bdry;global}|_\gamma = 0\ . \tag{D.3.32}
$$

Therefore, we indeed find a decoupled $(\mathcal{Z}_N)_N$ theory on the interval.

On the upper junction, we have two boundary conditions (1) and (2) from condensing $U(1)_N \times U(1)_{-N}$. Under the boundary condition (1), the upper and lower junctions have the same boundary conditions on gauge fields $A_I + A_L + A_R$ and $A_L - A_I'$ as written in Table D.1. Following the discussion in Section 4.4.3.1, reducing the interval results in a 2d $\mathbb{Z}_N$ gauge theory.

	$A_I + A_L + A_R$	$A_L - A_I'$
$\alpha\beta\,(1)$	$\mathbb{Z}_N$	pure $U(1)$ gauge
$\gamma\gamma'$	$\mathbb{Z}_N$	pure $U(1)$ gauge

Table D.1: Boundary conditions for the case (1) of Eq. (D.3.29)

Under the boundary condition (2), on the other hand, the gauge fields have different boundary conditions at the upper and lower junctions, as written in Table D.2. In this case, we only find $\mathbb{Z}_2$ untwisted local operators arising from the Wilson lines $e^{i\frac{Nk}{2}\oint a_1+a_2}$ ($k \in \mathbb{Z}_2$). Hence, reducing the interval $[\gamma, \beta]$ results in a $\mathbb{Z}_2$ gauge theory.

	$(A_L - A_I') + 2(A_I + A_L + A_R)$	$A_L - A_I'$
$\alpha\beta\,(2)$	pure gauge	$\mathbb{Z}_{\frac{N}{2}}$
$\gamma\gamma'$	$\mathbb{Z}_{\frac{N}{2}}$	pure gauge

Table D.2: Boundary conditions for the case (2) of Eq. (D.3.29)

In summary,

$$(\mathcal{Z}_N)_N \quad \xrightarrow{\text{reducing interval}} \quad \begin{cases} (1): & \mathbb{Z}_N \text{ gauge theory} \ , \\ (2): & \mathbb{Z}_2 \text{ gauge theory} \ . \end{cases} \tag{D.3.33}$$

Combining the reduction of the $\mathbb{Z}_N$ theory on the interval and the boundary actions, there are two choices for the associator 1-morphism,

$$\left[F^{D_3}_{\overline{D}_3,D_3,D_3}\right]_{U(1)_N\overline{D}_3,\mathbb{1}} = \mathbb{Z}_N \text{ gauge theory} \quad \text{or} \quad \mathbb{Z}_2 \text{ gauge theory} \ . \tag{D.3.34}$$

D.4 Details on anyon condensation and domain wall fusion

In this appendix, we give some details on the anyon condensation computations and the fusion of the domain walls used in Section 4.5.

Recall that we want to describe the topological operator spectrum for the following two diagrams

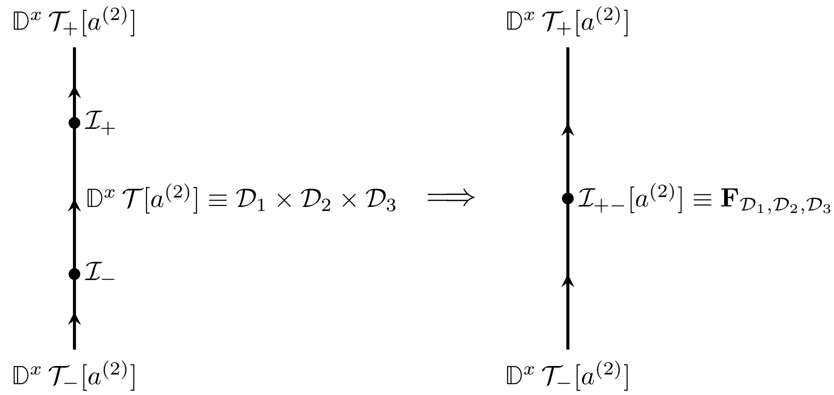

(D.4.1)

First, let us explain the line operator spectrum in the following configuration summarized by Table 4.6.

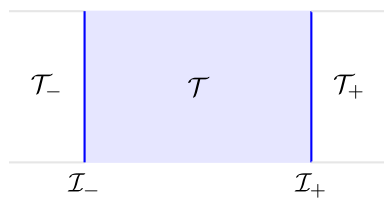

, (D.4.2)

From the math literature of anyon condensation [74, 137], the interface $\mathcal{I}_\pm$ is given the fusion category of $\mathbb{A}_\pm$-modules in $\mathcal{T}$[3], and the theory $\mathcal{T}_\pm$ on the other side of the interface is described by the category of local $\mathbb{A}_\pm$-modules (which is a modular tensor category). The interfaces $\mathcal{I}_\pm$ carry the structure as bimodule categories of $\mathcal{T}$ and $\mathcal{T}_\pm$. Physically, condensing $\mathbb{A}_\pm$ means gauging the 1-form symmetry $\mathbb{A}_\pm$. The 1-form symmetry $\mathbb{A}_\pm$ can act on the line operators by fusion and by braiding, and after gauging we keep only the operators invariant under $\mathbb{A}_\pm$ action. On the interface $\mathcal{I}_\pm$, $\mathbb{A}_\pm$ can only act by fusion as $\mathcal{I}_\pm$ is 2-dimension. The simple invariant line operators on $\mathcal{I}_\pm$ must be invariant under fusion with any lines in $\mathbb{A}_\pm$, therefore must take the form

$$\ell_b^\pm \equiv \sum_{a\in\mathbb{A}_\pm} b \times a \tag{D.4.3}$$

for any simple line operator b in $\mathcal{T}$. Clearly, $\ell_b^\pm$ and $\ell_{b'}^\pm$ parameterize the same invariant lines if $b^{-1}b' \in \mathbb{A}_\pm$. The $\ell_b^\pm$ constructed above is a $\mathbb{A}_\pm$-module, and all the $\ell_b^\pm$'s form the category

[3] Here we view $\mathbb{A}_\pm$ as an algebra object in $\mathcal{T}$.

$\mathcal{T}_{\mathbb{A}_\pm}$ of $\mathbb{A}_\pm$-modules describing the topological line operators on the interface $\mathcal{I}_\pm$. The fusion rules for those invariant lines are simply given by[4]

$$\ell_b^\pm \times \ell_{b'}^\pm = \ell_{bb'}^\pm \ . \tag{D.4.4}$$

It is also possible to fuse the bulk line in $\mathcal{T}$ with the interface lines with the fusion rules

$$\ell_b^+ \otimes b' = \ell_{bb'}^+ \ , \quad b' \otimes \ell_b^- = \ell_{b'b}^- \ , \quad \forall b' \in \mathcal{T} \ . \tag{D.4.5}$$

On the other hand, in the theory $\mathcal{T}_\pm$ acquired by gauging $\mathbb{A}_\pm$, where the 1-form symmetry $\mathbb{A}_\pm$ also acts via braiding. Hence, only the ℓ_b's that braid trivially with $\mathbb{A}_\pm$ are invariant under the $\mathbb{A}_\pm$ action[5]. Those ℓ_b's are known as local $\mathbb{A}_\pm$-modules, and together they form a modular tensor category (often denoted as $\mathcal{T}_{\mathbb{A}_\pm}^{loc}$) describing the 3d TQFT $\mathcal{T}_\pm$.

Next, we explain the domain wall fusion step between $\mathcal{I}_+$ and $\mathcal{I}_-$ in (D.4.1). The outcome is a domain wall $\mathcal{I}_{-+}$ between $\mathcal{T}_-$ and $\mathcal{T}_+$, which we identify as the F-symbol. The result has been summarized in Table 4.7, and the result is derived from the math tools known as balanced Deligne tensor product which captures the domain wall fusion as shown in [137]

$$\mathcal{I}_{+-} = \mathcal{I}_+ \boxtimes_{\mathcal{T}} \mathcal{I}_- \ . \tag{D.4.6}$$

In the special case where $\mathcal{T}$ contains only Abelian anyons, the computation can be done as follows[6]. First, one takes $\mathcal{I}_+ \boxtimes \mathcal{I}_-$ corresponding to naively stacking two interfaces on top of

[4]Notice that the tensor product of $\mathbb{A}_\pm$-modules is the balanced tensor product $\otimes_{\mathbb{A}_\pm}$ over the algebra object $\mathbb{A}_\pm$ which gives rise to the correct multiplicity below.

[5]For that, we only need to check any one of the line in the sum braids trivially with all the lines in $\mathbb{A}_\pm$. This is because in order to condense $\mathbb{A}_\pm$, every anyon in $\mathbb{A}_\pm$ must be boson and braids trivially with each other.

[6]For experts, here we are simply using the result that, for a fusion category $\mathcal{C}$, the balanced tensor product $\mathcal{M} \boxtimes_{\mathcal{C}} \mathcal{N}$ between a right $\mathcal{C}$-module category $\mathcal{M}$ and a left $\mathcal{C}$-module category $\mathcal{N}$ can be computed by first viewing $\mathcal{M} \boxtimes \mathcal{N}$ as a module category over $\mathcal{C} \boxtimes \mathcal{C}^{rev}$ and taking the category of modules over the algebra $\mathcal{A} = \oplus_{X \in Irr(\mathcal{C})} X \boxtimes X^*$ in $\mathcal{M} \boxtimes \mathcal{N}$. For more details, see Remark 3.9 in [138].

each other. Using our previous notation, simple line operators on $\mathcal{I}_+ \boxtimes \mathcal{I}_-$ can be labeled as

$$\ell_{b,b'} \equiv \ell^+_b \boxtimes \ell^-_b \ . \tag{D.4.7}$$

To get the spectrum of line operators in $\mathcal{I}_{+-} = \mathcal{I}_+ \boxtimes_{\mathcal{T}} \mathcal{I}_-$, one can simply make the identification

$$\ell_{b,b'} \simeq \ell_{ba,a^{-1}b'} \quad \forall a \in \mathcal{T} \ . \tag{D.4.8}$$

Notice that one can also fuse the lines in $\mathcal{T}_\pm$ to lines on the interface $\mathcal{I}_{+-}$, with the fusion rules

$$\ell^+_{b_1} \otimes \ell_{b_2,b_3} = \ell_{b_1 b_2, b_3} \ , \quad \ell_{b_2,b_3} \otimes \ell^-_{b_1} = \ell_{b_2, b_3 b_1} \ . \tag{D.4.9}$$

Finally, the interface $\mathcal{I}_{+-}$ will be a multi-fusion category, namely it contains local operators (corresponding to the multiple junctions between the identity lines), if $\mathbb{A}_+ \cap \mathbb{A}_-$ is non-trivial. And the local operators are exactly labeled by $\mathbb{A}_+ \cap \mathbb{A}_-$, corresponding to the lines stretching between two interfaces. When this happens, it usually means the 2d interface contains a sub-sector described by a decoupled 2d TQFT.

Finally, one also needs to remember to keep track of whether the resulting 2d interface $\mathcal{I}_{-+}$ couples to the bulk gauge field $a^{(2)}$. When it does, this will turn the decoupled 2d TQFT to a 2d condensation defect of the 1-form symmetry.

D.5 Duality defect associators

In this section, we briefly explain the non-invertible duality symmetry in 4d Maxwell theory at $\tau = iN$ found in Ref. [59,62] and compute one particular associator of the duality defects using the Lagrangian method and group-theoretical approach. Other associators can be computed using the same methods and the results are listed. We find an agreement and comment on the efficiency and validity of the two approaches.

D.5.1 Non-invertible duality symmetry and defect Lagrangians

At couplings $\tau = iN$, there is a duality symmetry constructed as follows. We first gauge a $\mathbb{Z}_N^{(1)}$ subgroup of the electric 1-form symmetry in half space (with Dirichlet boundary conditions for the corresponding discrete gauge field), resulting in a topological interface between the theory with coupling $\tau = iN$ and the theory with coupling i/N. However, since under $\mathbb{S}$-duality the coupling i/N maps to iN, the two sides are in fact equivalent and we get a defect in a single theory, obtained by performing $\mathbb{Z}_N^{(1)}$ gauging and $\mathbb{S}$-duality in half space. As shown in [59], one can describe this defect, which is denoted by D_2, by the following action,

$$D_2: \quad S = \frac{N}{4\pi}\int_{x<0} dA_L \wedge \star dA_L + \frac{N}{4\pi}\int_{x>0} dA_R \wedge \star dA_R + \frac{iN}{2\pi}\int_{x=0} A_L \wedge dA_R \tag{D.5.1}$$

where A_L and A_R denote the Maxwell gauge field from the two sides of the defect, which is located at $x = 0$.

The corresponding orientation reversal defect, denoted by $\overline{D}_2$, is given by

$$\overline{D}_2: \quad S = \frac{N}{4\pi}\int_{x<0} dA_L \wedge \star dA_L + \frac{N}{4\pi}\int_{x>0} dA_R \wedge \star dA_R - \frac{iN}{2\pi}\int_{x=0} A_R \wedge dA_L\ . \tag{D.5.2}$$

Together and with the condensation defect C_0, they satisfy the non-invertible fusion algebra

$$\begin{gathered} D_2 \times \overline{D}_2 = C_0 = \overline{D}_2 \times D_2, \quad D_2 \times D_2 = U \times C_0 = \overline{D}_2 \times \overline{D}_2, \\ D_2 \times C_0 = C_0 \times D_2 = D_2, \quad \overline{D}_2 \times C_0 = C_0 \times \overline{D}_2 = \overline{D}_2 \end{gathered} \tag{D.5.3}$$

where U is the charge conjugation defect given by

$$U: \quad \frac{N}{4\pi}\int_{x<0} dA_L \wedge \star dA_L + \frac{N}{4\pi}\int_{x>0} dA_R \wedge \star dA_R + \frac{i}{2\pi}\int db \wedge (A_L + A_R)\ . \tag{D.5.4}$$

Let us first analyze the structure of the F-symbol by the number of incoming invertible charge conjugation defects U. First, when there are two incoming U defects, then the global fusion in the middle contains no decoupled TQFT or condensation defect supported on the interval; hence the F-symbol must be the trivial theory. Second, when there is one incoming

U defect and two non-invertible defects, then the global fusion in the middle always contains a condensation defect supported on the interval; under the interval reduction, this always leads to a 2d condensation of the $\mathbb{Z}_N$ 1-form symmetry. Thus, we can now focus on the cases where all three incoming twist defects are non-invertible symmetries. We find

$$\left[F^{\overline{D}_2}_{D_2,D_2,D_2}\right]_{U,U}, \quad \left[F^{D_2}_{\overline{D}_2,D_2,D_2}\right]_{\mathbb{1},U}, \quad \left[F^{D_2}_{D_2,\overline{D}_2,D_2}\right]_{\mathbb{1},\mathbb{1}}, \quad \left[F^{D_2}_{D_2,D_2,\overline{D}_2}\right]_{U,\mathbb{1}} = \text{Trivial TQFT}, \tag{D.5.5}$$

and the remaining ones are related to the above ones via orientation reversal. Below, we will only demonstrate explicitly the computation for $\left[F^{D_2}_{D_2,\overline{D}_2,D_2}\right]_{\mathbb{1},\mathbb{1}}$ using the Lagrangian method since the other ones can be computed similarly. Notice that unlike the triality case, here the approach holds for all N.

D.5.2 Lagrangian method for $\left[\boldsymbol{F}^{\boldsymbol{D_2}}_{\boldsymbol{D_2},\overline{\boldsymbol{D}}_{\boldsymbol{2}},\boldsymbol{D_2}}\right]_{\mathbb{1},\mathbb{1}}$

In this subsection, we compute the associator 1-morphism $\left[F^{D_2}_{D_2,\overline{D}_2,D_2}\right]_{\mathbb{1},\mathbb{1}}$ for any N using the Lagrangian method in Section 4.4.3.1. To obtain $\left[F^{D_2}_{D_2,\overline{D}_2,D_2}\right]_{\mathbb{1},\mathbb{1}}$, we collapse the diamond-shaped region in Figure D.7 to a 2d associator manifold. We begin by analysing each fusion/splitting and morphism junctions.

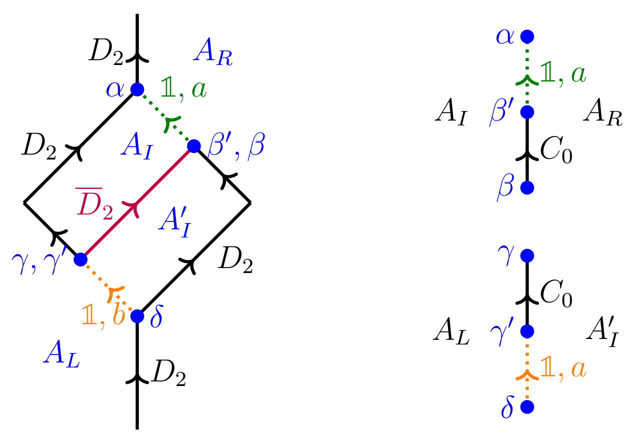

Figure D.7: Left: Diagram for $\left[F^{D_2}_{D_2,\overline{D}_2,D_2}\right]_{\mathbb{1},\mathbb{1}}$. Right: Resolution of the morphism junctions β' and γ'.

β: $D_2 \times \overline{D}_2 = C_0$ The action along the fused part is

$$\begin{aligned} S &= \frac{iN}{2\pi} \int_{\beta}^{\infty} (-A'_I \mathrm{d}A_I + A'_I \mathrm{d}A_R) \\ &= \frac{iN}{2\pi} \int_{\beta}^{\infty} \mathrm{d}(-A'_I) \wedge (A_I - A_R) + \frac{iN}{2\pi} \int_{\Sigma_\beta} A'_I \wedge (A_R - A_I) \end{aligned} \tag{D.5.6}$$

where $\int_{\beta}^{\infty}$ is the 3d integral above the β junction and Σ_β is the 2d manifold supporting the β junction. Therefore, at this junction, the boundary term is

$$\beta: \quad \text{No boundary condition,} \quad S(\beta) = \frac{iN}{2\pi} \int_{\Sigma_\beta} A'_I \wedge (A_R - A_I) \ . \tag{D.5.7}$$

β' : $C_0 \to \mathbb{1}$ junction Since we are interested in the trivial element of the Witt class, we add another junction β' between $C_0 \to \mathbb{1}$. The corresponding action is

$$S = \frac{iN}{2\pi} \int_{\beta}^{\beta'} \mathrm{d}(-A'_I) \wedge (A_I - A_R) + \frac{i}{2\pi} \int_{\beta}^{\infty} \mathrm{d}a \wedge (A_I - A_R) \ . \tag{D.5.8}$$

Using the analysis in Section 4.4.2.2, especially Eq. (4.4.21), we impose the boundary condition and add the boundary term

$$\beta': \quad a + NA'_I|_{\beta'} \ , \quad A_I - A_R|_{\beta'} = \text{pure } U(1) \text{ gauge}, \quad S(\beta') = 0 \ . \tag{D.5.9}$$

α: $D_2 \times \mathbb{1} \to D_2$

$$\begin{aligned} S &= \frac{i}{2\pi} \int_{\alpha}^{\infty} NA_L \mathrm{d}A_I + \mathrm{d}a(A_I - A_R) \\ &= \underbrace{\frac{i}{2\pi} \int_{\alpha}^{\infty} (a + NA_L) \mathrm{d}(A_I - A_R)}_{\text{decoupled trivial TQFT}} + \underbrace{\frac{iN}{2\pi} \int_{\alpha}^{\infty} A_L \mathrm{d}A_R}_{D_2} \underbrace{- \frac{i}{2\pi} \int_{\Sigma_\alpha} a \wedge (A_I - A_R)}_{S(\alpha)} \ . \end{aligned} \tag{D.5.10}$$

Following the discussion in Section 4.4.2.1, the decoupled trivial TQFT fields are condensed on the boundary. Hence,

$$\alpha: \quad a + NA_L|_{\alpha} \, , \quad A_I - A_R|_{\alpha} = \text{pure } U(1) \text{ gauge}, \quad S(\alpha) = -\frac{i}{2\pi} \int_{\Sigma_\alpha} a \wedge (A_I - A_R) \ . \tag{D.5.11}$$

γ: $C_0 \to D_2 \times \overline{D}_2$ The fusion outcome is C_0 without other terms.

$$S = \frac{iN}{2\pi}\int_{-\infty}^{\gamma}(A_L - A_I')\mathrm{d}A_I \ . \tag{D.5.12}$$

γ': $\mathbb{1} \to C_0$

$$S_d = \frac{i}{2\pi}\int_{\gamma'}^{\gamma} N\mathrm{d}A_I(A_L - A_I') + \frac{i}{2\pi}\int_{-\infty}^{\gamma'}\mathrm{d}b(A_L - A_I') \ . \tag{D.5.13}$$

Again, using Eq. (4.4.21),

$$\gamma' : \quad A_L - A_I', \quad b - NA_I|_{\gamma'} = \text{pure } U(1) \text{ gauge}, \quad S(\gamma') = 0 \ . \tag{D.5.14}$$

δ: $D_2 \to \mathbb{1} \times D_2$

$$\begin{aligned} S &= \frac{i}{2\pi}\int_{-\infty}^{\delta}[\mathrm{d}b(A_L - A_I') + NA_I'\mathrm{d}A_R] \\ &= \underbrace{\frac{i}{2\pi}\int_{-\infty}^{\delta}(A_L - A_I')\mathrm{d}(b - NA_R)}_{\text{decoupled trivial TQFT}} + \underbrace{\frac{iN}{2\pi}\int_{-\infty}^{\delta}A_L\mathrm{d}A_R}_{D_2} \ . \end{aligned} \tag{D.5.15}$$

The boundary conditions are

$$\delta : \quad A_L - A_I' \quad b - NA_R|_{\delta} = \text{pure } U(1) \text{ gauge}, \quad S(\delta) = 0 \ . \tag{D.5.16}$$

Merging the upper and lower junctions As the next step, we collapse all the upper junctions into one and combine the boundary data, and similarly for the lower junctions. We get

$$\begin{aligned} &\alpha, \beta, \beta' : \quad a + NA_L, \quad a + NA_I', \quad A_I - A_R = \text{pure } U(1) \text{ gauge} \\ &\qquad S_\alpha = -\frac{i}{2\pi}\int_{\Sigma_\alpha} a \wedge (A_I - A_R), \quad S_\beta = \frac{iN}{2\pi}\int_{\Sigma_\beta} A_I' \wedge (A_R - A_I) \\ &\gamma, \gamma', \delta : \quad b = NA_I, \quad A_L - A_I', \quad b - NA_R = \text{pure } U(1) \text{ gauge} \\ &\qquad S_\gamma = S_{\gamma'} = S_\delta = 0 \ . \end{aligned} \tag{D.5.17}$$

Global fusion Next, we fuse the three defects $D_2, \overline{D}_2, D_2$ in the middle (Figure D.8).

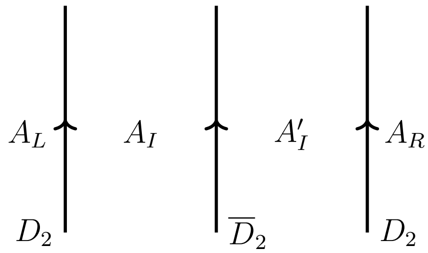

Figure D.8: Fusing $D_2, \overline{D}_2, D_2$ at $[\gamma, \beta]$.

The corresponding action is the sum of these defect actions, which can be rewritten as

$$\begin{aligned} S &= \frac{iN}{2\pi}\int_\gamma^\beta (A_L - A'_I)\mathrm{d}A_I + A'_I \mathrm{d}A_R \\ &= \underbrace{\frac{iN}{2\pi}\int_\gamma^\beta (A_L - A'_I)\mathrm{d}(A_I - A_R)}_{\mathbb{Z}_N \text{ gauge theory}} + \underbrace{\frac{iN}{2\pi}\int_\gamma^\beta A_L \mathrm{d}A_R}_{D_2} \ . \end{aligned} \tag{D.5.18}$$

The first term corresponds to the $\mathbb{Z}_N$ gauge theory. Collecting the boundary terms at the upper junctions,

$$S(\alpha) + S(\beta) = \frac{i}{2\pi}\int_{\Sigma_{\alpha\beta}} (a + NA'_I) \wedge (A_R - A_I) \in 2\pi i \mathbb{Z} \ , \tag{D.5.19}$$

where we used the boundary conditions $a + NA'_I$ and $A_R - A_I$ being pure $U(1)$ gauge at the upper junction. And the total boundary term at the lower junction simply vanishes. The boundary conditions of each conjugate are

$$\begin{aligned} &\alpha\beta: \quad N(A_L - A'_I) = \text{pure } U(1) \text{ gauge} \quad (N), \qquad A_I - A_R = \text{pure } U(1) \text{ gauge}\,(D) \ , \\ &\gamma\delta: \quad A_L - A'_I = \text{pure } U(1) \text{ gauge} \qquad (D), \qquad N(A_I - A_R) = \text{pure } U(1) \text{ gauge}\,(N) \ . \end{aligned} \tag{D.5.20}$$

Following the discussion in Sections 4.4.3.1, there is no untwisted local operator, and hence the 2d effective theory for the 3d $\mathbb{Z}_N$ gauge theory on the interval with the above boundary conditions is a trivial theory. Thus we find

$$\left[F^{D_2}_{D_2,\overline{D}_2,D_2}\right]_{\mathbb{1},\mathbb{1}} = \text{Trivial TQFT} \ . \tag{D.5.21}$$

D.5.3 Group-theoretical approach

D.5.3.1 Group theoretical construction

For some special values of N, the non-invertible duality can be constructed group-theoretically [139, 62,64]. In particular, if N is odd *and* if $\exists\, p$ such that $p^2 = -1 \bmod N$[7], the non-invertible duality defect in a QFT $\mathcal{X}$ becomes invertible after the ST gauging with the following discrete torsion.

$$Z_{\widetilde{\mathcal{X}}}[C^{(2)}] = \sum_{c^{(2)} \in H^2(M_4, \mathbb{Z}_N)} Z_{\mathcal{X}}[c^{(2)}]\; e^{\frac{2\pi i}{N} \int_{M_4} \left(\frac{N+1}{2} p\; c^{(2)} \cup c^{(2)} + c^{(2)} \cup C^{(2)}\right)} \tag{D.5.22}$$

where $\widetilde{\mathcal{X}}$ is the QFT obtained by the above ST gauging in QFT $\mathcal{X}$ and $C^{(2)}$ is the 2-form background field of $\mathbb{Z}_N$ 1-form symmetry. Utilising the duality

$$Z_{\widetilde{\mathcal{X}}}[C^{(2)}] = \sum_{c^{(2)} \in H^2(M_4, \mathbb{Z}_N)} Z_{\mathcal{X}}[c^{(2)}]\; e^{\frac{2\pi i}{N} \int_{M_4} c^{(2)} \cup C^{(2)}}\;, \tag{D.5.23}$$

it follows that

$$Z_{\widetilde{\mathcal{X}}}[C^{(2)}] = Z_{\widetilde{\mathcal{X}}}[pC^{(2)}]\; e^{\frac{2\pi i}{N} \frac{N+1}{2} p \int_{M_4} C^{(2)} \cup C^{(2)}}\;. \tag{D.5.24}$$

This implies that the non-invertible duality defect in $\mathcal{X}$ is mapped to a $\mathbb{Z}_4^{(0)}$ invertible 0-form symmetry in the theory $\widetilde{\mathcal{X}}$, which is an automorphism of the dual 1-form symmetry sending $C^{(2)} \mapsto pC^{(2)}$. The additional phase in (D.5.24) represents the mixed anomaly between the 0-form symmetry and the 1-form symmetry. Let $\mathbb{D}$ be the generator of the $\mathbb{Z}_4^{(0)}$ symmetry. As for the triality case, we dress the minimal TQFT to make $\mathbb{D}$ a gauge invariant operator, consistent of gauging the dual 1-form symmetry in $\widetilde{\mathcal{X}}$,

$$D_2 = \mathbb{D}_2 \mathcal{A}^{N,p}[c^{(2)}] \tag{D.5.25}$$

where c is the gauge field for the bulk 1-form symmetry. Applying the relation (D.5.25) twice

$$Z_{\widetilde{\mathcal{X}}}[C^{(2)}] = Z_{\widetilde{\mathcal{X}}}[-C^{(2)}]\;, \tag{D.5.26}$$

[7] Notice that when N is odd and such p exists, we can always and will choose p to be even.

we see that $\mathbb{D}^2$ acts as charge conjugation of the dual 1-form symmetry without a mixed anomaly in $\widetilde{\mathcal{X}}$. Finally, the orientation reversal of D_2 is given by

$$\overline{D}_2 = \mathcal{A}^{N,-p}[c^{(2)}]\mathbb{D}^{-1} \ . \tag{D.5.27}$$

It is straightforward to check the above defects do reproduce the generic fusion rules (D.5.3) following a similar approach in the triality case.

We can then proceed to work out the local fusion junctions and compute the F-symbols, and we find the results agree with the Lagrangian method. We will skip the details here, and only briefly list the results. For simplicity, we will choose $N = 5$ (and take $p = 2$), but it is completely straightforward to acquire the result for the generic cases. With this choice,

$$D_2 = \mathbb{D}\mathcal{A}^{5,2}[c^{(2)}], \quad \overline{D}_2 = \mathcal{A}^{5,-2}[c^{(2)}]\mathbb{D}^{-1} \tag{D.5.28}$$

and the invertible 0-form symmetry $\mathbb{D}$ acts on the 1-form symmetry operators as the $\mathbb{Z}_4$ automorphism

$$\mathbb{D}\mathcal{A}^{5,\pm 2}[c^{(2)}]\mathbb{D}^{-1} = \mathcal{A}^{5,\pm 2}[-2c^{(2)}] \ , \quad \mathbb{D}^{-1}\mathcal{A}^{5,\pm 2}[c^{(2)}]\mathbb{D} = \mathcal{A}^{5,\pm 2}[2c^{(2)}] \ . \tag{D.5.29}$$

D.5.3.2 Fusion and condensation

The 3d $\mathbb{Z}_5$ gauge theory with 0-twist coupled to the external dynamical 1-form $\mathbb{Z}_5$ gauge field $c \in H^2(M_4, \mathbb{Z}_5)$ with the following Lagrangian

$$\mathcal{L}_{(\mathcal{Z}_5)_0}[c^{(2)}] = \frac{2\pi i}{5} a^{(1)} \cup \delta b^{(1)} + \frac{2\pi i}{5} a^{(1)} \wedge c^{(2)} \tag{D.5.30}$$

represents the condensation defect C_0 in the path integral. To see this, we integrate $b^{(1)}$ out to limit $a \in H^1(M_3, \mathbb{Z}_5)$ and replace $a^{(1)}$ with its Poincaré dual $\int_{M_3} a^{(1)} \cup \cdots = \int_{\Sigma_2} \cdots$ in the integral. The path integral is then

$$\sum_{a \in H^1(M_3,\mathbb{Z}_5)} e^{\frac{2\pi i}{5}\int_{M_3} a^{(1)} \cup c^{(2)}} = \sum_{\Sigma_2 \in H_2(M_3,\mathbb{Z}_5)} e^{\frac{2\pi i}{5}\oint_{\Sigma_2} c^{(2)}} = \sum_{i,\{m_i \in \mathbb{Z}_5\}} e^{\frac{2\pi i}{5} m_i \oint_{\Sigma_{2,i}} c^{(2)}} \tag{D.5.31}$$

where $\{\Sigma_{2,i}\}$ are basis of the non-contractible 2-cycles on M_3, and we normalised c in the integral so that the 1-form charge is integer quantised. In this form, the path integral is manifestly the 1-form symmetry condensation defect.

If one condenses a by restricting to a trivial cohomology element in the path integral, we see that the constrained path integral is trivial, i.e. it is the identity defect. Using this, the morphism $C_0 \to \mathbb{1}$ is implemented by condensing a at the morphism junction (and along $\mathbb{1}$).

With all necessary ingredients at hand, we discuss the anyon condensation at the local fusion and morphism junctions.

$\boldsymbol{D_2 \times \overline{D}_2 = C_0 \to \mathbb{1}}$ Consider a fusion

$$D_2 \times \overline{D}_2 = \mathcal{A}^{5,2}_{a_1}[-2c^{(2)}] \otimes \mathcal{A}^{5,-2}_{a_2}[-2c^{(2)}] \tag{D.5.32}$$

where we used the $\mathbb{D}$ action on the minimal TQFTs (D.5.28), and $a_{1,2}$ denotes the generating anyons of the minimal TQFT in each theory. To see if the theory on the RHS is the condensation defect $\mathbb{Z}_N$ gauge theory (D.5.30), we first note that $a = (a_1)^2(a_2)^2$ is coupled to the external field $c^{(2)}$ as in (D.5.30) and has the topological spin $h[a] = 0$. This means that it is enough to find b such that a and b have the correct topological spin and braiding to be the pure electric line and the pure magnetic line in $(\mathcal{Z}_N)_0$. Let $b = (a_1)^m(a_2)^n$. Then $h[b] = 0$ and $B[a,b] = \exp\left(\frac{2\pi i}{5}\right)$ for $b = (a_1)^{-2}(a_2)^2$. Hence the fusion outcome is C_0 as expected. Then the morphism junction $C_0 \to \mathbb{1}$ is obtained by condensing the Wilson lines in $\langle (a_1)^{-2}(a_2)^{-2}\rangle = \langle a_1 a_2\rangle$, i.e.

$$D_2 \times \overline{D}_2 = C_0 \to \mathbb{1} \quad \text{by condensing } \langle a_1 a_2\rangle\ . \tag{D.5.33}$$

$\boldsymbol{\overline{D}_2 \times D_2 = C_0 \to \mathbb{1}}$ Following the same discussion, we can confirm the fusion algebra $\overline{D}_2 \times D_2 = C_0$ with $a = a_1 a_2$ and $b = a_1(a_2)^{-1}$. Hence, at the morphism junction,

$$\overline{D}_2 \times D_2 = C_0 \to \mathbb{1} \quad \text{by condensing } \langle a_1 a_2\rangle\ . \tag{D.5.34}$$

$\boldsymbol{D_2 \times D_2 = U \times C_0 \to U}$ This time, consider the fusion

$$D_2 \times \overline{D}_2 = \mathbb{D}^2 \mathcal{A}^{5,2}_{a_1}[2c^{(2)}] \otimes \mathcal{A}^{5,2}_{a_2}[c^{(2)}] \ . \tag{D.5.35}$$

We note that $\mathbb{D}^2 = U$ is the charge conjugation. Following the same argument, the minimal TQFT part corresponds to C_0 with $a = (a_1)^2 a_2$ and $b = (a_1)^2 (a_2)^{-1}$. Again, $C_0 \to \mathbb{1}$ is done by condensing $\langle (a_1)^2 a_2 \rangle$.

$$D_2 \times D_2 = U \times C_0 \to U \quad \text{by condensing } \langle (a_1)^2 a_2 \rangle \ . \tag{D.5.36}$$

$\boldsymbol{\overline{D}_2 \times \overline{D}_2 = U \times C_0 \to U}$ The above discussion straightforwardly applies to this fusion and morphism junctions, with $a = a_1 (a_2)^2$ and $b = (a_1)^{-2} a_2$.

$$\overline{D}_2 \times \overline{D}_2 = U \times C_0 \to U \quad \text{by condensing } \langle a_1 (a_2)^2 \rangle \ . \tag{D.5.37}$$

D.5.3.3 Associator

In this subsection, we compute the associator 1-morphism for the three defects, say $1, 2, 3$, by first collapsing the upper junctions (23) and $1(23)$ into $\mathcal{I}_+$ and similarly for the lower junctions (first arrow in Figure D.9), and finally reducing the interval to merge $\mathcal{I}_\pm \to \mathcal{I}$. At this final step, we identify the resulting 2d theory on the associator 1-morphism using the spectrum of the local and line operators.

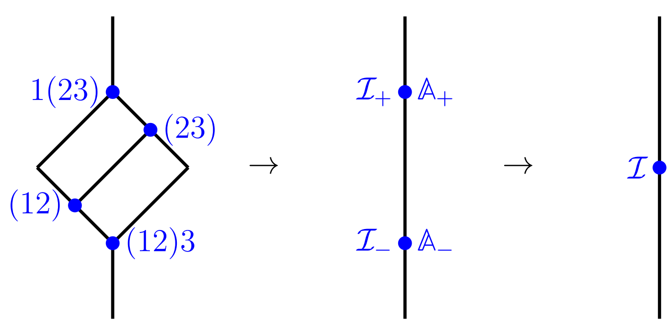

Figure D.9: Anyon condensation in the associator 1-morphism of defects $1, 2, 3$

To be specific, let's first denote by $\mathbb{A}_{ij}$ the condensed anyons at the local fusion $i \times j$ junction. For example, anyons in $\mathbb{A}_{23}$ are condensed at the junction (23) and above, and anyons in $\mathbb{A}_{12}$ are condensed at the junction (12) and below. After merging the two upper junctions 1(23) and (23) into $\mathcal{I}_+$, the anyons in $\mathbb{A}_+ = \mathbb{A}_{1(23)} \times \mathbb{A}_{23}$ are condensed and similarly at the lower junctions with $\mathbb{A}_- = \mathbb{A}_{12} \times \mathbb{A}_{(12)3}$.

The lines that are condensed at both $\mathcal{I}_\pm$ (i.e. $\mathbb{A}_+ \cap \mathbb{A}_-$) stretch between the two junctions. Hence, after merging $\mathcal{I}_\pm \to \mathcal{I}$, they become a vertex operator.

The line operators on $\mathcal{I}$ are the lines on three defects after quotient out $\mathbb{A}_+$ and $\mathbb{A}_-$. The remaining lines can be in the 3d minimal TQFT coupling to the bulk fields $c^{(2)}$, which are neutral under $\mathbb{A}_+ \times \mathbb{A}_-$. Quotient out those lines, we then acquire the lines in the decoupled 2d theory.

In summary, the spectrum of the decoupled 2d theory on $\mathcal{I}$ after the reduction is

$$\begin{aligned} \text{Vertex operators}: &\quad \mathbb{A}_+ \cap \mathbb{A}_- \\ \text{Line operators}: &\quad (\text{neutral lines under } \mathbb{A}_+ \times \mathbb{A}_-)\backslash \mathbb{Z}_5 \times \mathbb{Z}_5 \times \mathbb{Z}_5/(\mathbb{A}_+ \times \mathbb{A}_-) \end{aligned} \tag{D.5.38}$$

Example: $\left[\boldsymbol{F}^{\boldsymbol{D_2}}_{\boldsymbol{D_2},\overline{\boldsymbol{D}}_{\boldsymbol{2}},\boldsymbol{D_2}}\right]_{\mathbb{1},\mathbb{1}}$ Using Eqs. (D.5.33) and (D.5.34), we identify

$$\mathbb{A}_{23} = \langle a_2 a_3 \rangle, \quad \mathbb{A}_{1(23)} = 0, \quad \mathbb{A}_{12} = \langle a_1 a_2 \rangle, \quad \mathbb{A}_{(12)3} = 0 \tag{D.5.39}$$

and hence

$$\mathbb{A}_+ = \langle a_2 a_3 \rangle, \quad \mathbb{A}_- = \langle a_1 a_2 \rangle \ . \tag{D.5.40}$$

Since $\mathbb{A}_+ \cap \mathbb{A}_- = 0$, there is no vertex operator on $\mathcal{I}$. The lines that are neutral under $\mathbb{A}_+ \times \mathbb{A}_-$ are those in $\langle a_1 a_2 a_3 \rangle$ which has no overlap with $\mathbb{A}_+ \times \mathbb{A}_-$, the lines condensed on $\mathcal{I}$. Therefore, there is no line left on the 2d theory in the double coset (D.5.38). In other words,

$$\left[F^{D_2}_{D_2,\overline{D}_2,D_2}\right]_{\mathbb{1},\mathbb{1}} = \text{Trivial TQFT} \ . \tag{D.5.41}$$

This is consistent with the result using the Lagrangian method (D.5.21) with $N = 5$.

Other associators Using the same procedures, one can compute the other associators, which are all trivial TQFT, matching the results of the Lagrangian method,

$$\left[F^{\overline{D}_2}_{D_2,D_2,D_2}\right]_{U,U}, \quad \left[F^{D_2}_{\overline{D}_2,D_2,D_2}\right]_{\mathbb{1},U}, \quad \left[F^{D_2}_{D_2,\overline{D}_2,D_2}\right]_{\mathbb{1},\mathbb{1}}, \quad \left[F^{D_2}_{D_2,D_2,\overline{D}_2}\right]_{U,\mathbb{1}} = \text{Trivial TQFT} . \tag{D.5.42}$$

Lagrangian vs group-theoretical methods While the group-theoretical approach is simpler than the Lagrangian method, it is not available for some N (of $\mathbb{Z}_N$ 1-form symmetry) while the Lagrangian method applies to all N.

[1] S. Kim and E. D. Stewart, *Constraining Affleck-Dine Leptogenesis after Thermal Inflation*, JCAP 09 (2020) 045, arXiv:1904.13158 [hep-ph].

[2] S. Kim, P. Kraus, and R. M. Myers, *Systematics of boundary actions in gauge theory and gravity*, JHEP 04 (2023) 121, arXiv:2301.02964 [hep-th].

[3] S. Kim, P. Kraus, R. Monten, and R. M. Myers, *S-matrix path integral approach to symmetries and soft theorems*, JHEP 10 (2023) 036, arXiv:2307.12368 [hep-th].

[4] S. Kim, P. Kraus, and Z. Sun, *Codimension one defects in free scalar field theory*, JHEP 06 (2025) 065, arXiv:2502.19547 [hep-th].

[5] S. Kim, O. Sela, and Z. Sun, *Higher structure of non-invertible symmetries from Lagrangian descriptions*, arXiv:2509.20540 [hep-th].

[6] S. Bintanja, S. Kim, and P. Kraus, *Enhanced correlations in hawking radiation from near-extremal collapse*, arXiv:2607.12989 [hep-th]. https://arxiv.org/abs/2607.12989.

[7] S. Elitzur, G. W. Moore, A. Schwimmer, and N. Seiberg, *Remarks on the Canonical Quantization of the Chern-Simons-Witten Theory*, Nucl. Phys. B 326 (1989) 108–134.

[8] C. Crnkovic and E. Witten, *Covariant description of canonical formalism in geometrical theories*, in Three Hundred Years of Gravitation, pp. 676–684. Cambridge University Press, 1987.

[9] R. M. Wald and A. Zoupas, *A General definition of 'conserved quantities' in general relativity and other theories of gravity*, Phys. Rev. D 61 (2000) 084027, arXiv:gr-qc/9911095.

[10] G. Compère and A. Fiorucci, *Advanced Lectures on General Relativity*, arXiv:1801.07064 [hep-th].

[11] D. Harlow and J.-Q. Wu, *Covariant phase space with boundaries*, JHEP 10 (2020) 146, arXiv:1906.08616 [hep-th].

[12] J. Lee and R. M. Wald, *Local symmetries and constraints*, J. Math. Phys. 31 (1990) 725–743.

[13] R. M. Wald, *Black hole entropy is the Noether charge*, Phys. Rev. D 48 no. 8, (1993) R3427–R3431, arXiv:gr-qc/9307038.

[14] Y. Tachikawa, *Black hole entropy in the presence of Chern-Simons terms*, Class. Quant. Grav. 24 (2007) 737–744, arXiv:hep-th/0611141.

[15] S. Ebert, E. Hijano, P. Kraus, R. Monten, and R. M. Myers, *Field Theory of Interacting Boundary Gravitons*, SciPost Phys. 13 no. 2, (2022) 038, arXiv:2201.01780 [hep-th].

[16] S. R. Coleman, J. Wess, and B. Zumino, *Structure of phenomenological Lagrangians. 1.*, Phys. Rev. 177 (1969) 2239–2247.

[17] C. G. Callan, Jr., S. R. Coleman, J. Wess, and B. Zumino, *Structure of phenomenological Lagrangians. 2.*, Phys. Rev. 177 (1969) 2247–2250.

[18] G. Compère, W. Song, and A. Strominger, *New Boundary Conditions for AdS3*, JHEP 05 (2013) 152, arXiv:1303.2662 [hep-th].

[19] A. Alekseev and S. L. Shatashvili, *Path Integral Quantization of the Coadjoint Orbits of the Virasoro Group and 2D Gravity*, Nucl. Phys. B 323 (1989) 719–733.

[20] M. Bañados, *Three-dimensional quantum geometry and black holes*, AIP Conf. Proc. 484 no. 1, (1999) 147–169, arXiv:hep-th/9901148.

[21] V. Iyer and R. M. Wald, *Some properties of Noether charge and a proposal for dynamical black hole entropy*, Phys. Rev. D 50 (1994) 846–864, arXiv:gr-qc/9403028.

[22] S. Deser, R. Jackiw, and S. Templeton, *Topologically Massive Gauge Theories*, Annals Phys. 140 (1982) 372–411. [Erratum: Annals Phys. 185, 406 (1988)].

[23] D. Anninos, W. Li, M. Padi, W. Song, and A. Strominger, *Warped AdS(3) Black Holes*, JHEP 03 (2009) 130, arXiv:0807.3040 [hep-th].

[24] C. Nazaroglu, Y. Nutku, and B. Tekin, *Covariant Symplectic Structure and Conserved Charges of Topologically Massive Gravity*, Phys. Rev. D 83 (2011) 124039, arXiv:1104.3404 [hep-th].

[25] A. Bouchareb and G. Clement, *Black hole mass and angular momentum in topologically massive gravity*, Class. Quant. Grav. 24 (2007) 5581–5594, arXiv:0706.0263 [gr-qc].

[26] G. Compere and S. Detournay, *Semi-classical central charge in topologically massive gravity*, Class. Quant. Grav. 26 (2009) 012001, arXiv:0808.1911 [hep-th]. [Erratum: Class.Quant.Grav. 26, 139801 (2009)].

[27] G. Compere and S. Detournay, *Boundary conditions for spacelike and timelike warped AdS_3 spaces in topologically massive gravity*, JHEP 08 (2009) 092, arXiv:0906.1243 [hep-th].

[28] M. Blagojevic and B. Cvetkovic, *Asymptotic structure of topologically massive gravity in spacelike stretched AdS sector*, JHEP 09 (2009) 006, arXiv:0907.0950 [gr-qc].

[29] D. M. Hofman and B. Rollier, *Warped Conformal Field Theory as Lower Spin Gravity*, Nucl. Phys. B 897 (2015) 1–38, arXiv:1411.0672 [hep-th].

[30] T. Azeyanagi, S. Detournay, and M. Riegler, *Warped Black Holes in Lower-Spin Gravity*, Phys. Rev. D 99 no. 2, (2019) 026013, arXiv:1801.07263 [hep-th].

[31] S. Detournay, T. Hartman, and D. M. Hofman, *Warped Conformal Field Theory*, Phys. Rev. D 86 (2012) 124018, arXiv:1210.0539 [hep-th].

[32] E. D'Hoker and P. Kraus, *Magnetic Brane Solutions in AdS*, JHEP 10 (2009) 088, arXiv:0908.3875 [hep-th].

[33] E. D'Hoker, P. Kraus, and A. Shah, *RG Flow of Magnetic Brane Correlators*, JHEP 04 (2011) 039, arXiv:1012.5072 [hep-th].

[34] T. Adawi, M. Cederwall, U. Gran, B. E. W. Nilsson, and B. Razaznejad, *Goldstone tensor modes*, JHEP 02 (1999) 001, arXiv:hep-th/9811145.

[35] M. Cederwall, U. Gran, M. Holm, and B. E. W. Nilsson, *Finite tensor deformations of supergravity solitons*, JHEP 02 (1999) 003, arXiv:hep-th/9812144.

[36] J. D. Bekenstein, *Black holes and entropy*, Phys. Rev. D 7 (Apr, 1973) 2333–2346. https://link.aps.org/doi/10.1103/PhysRevD.7.2333.

[37] J. M. Bardeen, B. Carter, and S. W. Hawking, *The four laws of black hole mechanics*, Communications in Mathematical Physics 31 no. 2, (June, 1973) 161–170.

[38] N. Banerjee and M. Saha, *Revisiting leading quantum corrections to near extremal black hole thermodynamics*, JHEP 07 (2023) 010, arXiv:2303.12415 [hep-th].

[39] R. Jackiw, *Lower Dimensional Gravity*, Nucl. Phys. B 252 (1985) 343–356.

[40] C. Teitelboim, *Gravitation and Hamiltonian Structure in Two Space-Time Dimensions*, Phys. Lett. B 126 (1983) 41–45.

[41] S. W. Hawking, *Particle creation by black holes*, Communications in Mathematical Physics 43 no. 3, (1975) 199 – 220.

[42] J. Preskill, P. Schwarz, A. D. Shapere, S. Trivedi, and F. Wilczek, *Limitations on the statistical description of black holes*, Mod. Phys. Lett. A 6 (1991) 2353–2362.

[43] L. V. Iliesiu and G. J. Turiaci, *The statistical mechanics of near-extremal black holes*, JHEP 05 (2021) 145, arXiv:2003.02860 [hep-th].

[44] C. G. Callan and J. M. Maldacena, *D-brane approach to black hole quantum mechanics*, Nucl. Phys. B 472 (1996) 591–610, arXiv:hep-th/9602043.

[45] J. M. Maldacena and L. Susskind, *D-branes and fat black holes*, Nucl. Phys. B 475 (1996) 679–690, arXiv:hep-th/9604042.

[46] J. Maldacena and A. Strominger, *Universal low-energy dynamics for rotating black holes*, Phys. Rev. D 56 (Oct, 1997) 4975–4983. https://link.aps.org/doi/10.1103/PhysRevD.56.4975.

[47] A. Almheiri and J. Polchinski, *Models of AdS_2 backreaction and holography*, JHEP 11 (2015) 014, arXiv:1402.6334 [hep-th].

[48] J. Maldacena, D. Stanford, and Z. Yang, *Conformal symmetry and its breaking in two dimensional Nearly Anti-de-Sitter space*, PTEP 2016 no. 12, (2016) 12C104, arXiv:1606.01857 [hep-th].

[49] G. Sárosi, *AdS_2 holography and the SYK model*, PoS Modave2017 (2018) 001, arXiv:1711.08482 [hep-th].

[50] P. Kraus, *Hamiltonian approach to near-extremal black hole evaporation and backreaction*, arXiv:2509.04293 [hep-th].

[51] D. Gaiotto, A. Kapustin, N. Seiberg, and B. Willett, *Generalized Global Symmetries*, JHEP 02 (2015) 172, arXiv:1412.5148 [hep-th].

[52] C. Copetti, M. Del Zotto, K. Ohmori, and Y. Wang, *Higher Structure of Chiral Symmetry*, Commun. Math. Phys. 406 no. 4, (2025) 73, arXiv:2305.18282 [hep-th].

[53] S. Schafer-Nameki, *ICTP Lectures on (Non-)Invertible Generalized Symmetries*, arXiv:2305.18296 [hep-th].

[54] S.-H. Shao, *What's Done Cannot Be Undone: TASI Lectures on Non-Invertible Symmetry*, arXiv:2308.00747 [hep-th].

[55] R. Thorngren and Y. Wang, *Fusion category symmetry. Part II. Categoriosities at c = 1 and beyond*, JHEP 07 (2024) 051, arXiv:2106.12577 [hep-th].

[56] J. Fuchs, M. R. Gaberdiel, I. Runkel, and C. Schweigert, *Topological defects for the free boson CFT*, J. Phys. A 40 (2007) 11403, arXiv:0705.3129 [hep-th].

[57] A. Kapustin and M. Tikhonov, *Abelian duality, walls and boundary conditions in diverse dimensions*, JHEP 11 (2009) 006, arXiv:0904.0840 [hep-th].

[58] L. Bhardwaj and Y. Tachikawa, *On finite symmetries and their gauging in two dimensions*, JHEP 03 (2018) 189, arXiv:1704.02330 [hep-th].

[59] Y. Choi, C. Cordova, P.-S. Hsin, H. T. Lam, and S.-H. Shao, *Noninvertible duality defects in 3+1 dimensions*, Phys. Rev. D 105 no. 12, (2022) 125016, arXiv:2111.01139 [hep-th].

[60] P. Niro, K. Roumpedakis, and O. Sela, *Exploring non-invertible symmetries in free theories*, JHEP 03 (2023) 005, arXiv:2209.11166 [hep-th].

[61] R. Argurio, A. Collinucci, G. Galati, O. Hulik, and E. Paznokas, *Non-Invertible T-duality at Any Radius via Non-Compact SymTFT*, SciPost Phys. 18 (2025) 089, arXiv:2409.11822 [hep-th].

[62] J. Kaidi, K. Ohmori, and Y. Zheng, *Kramers-Wannier-like Duality Defects in (3+1)D Gauge Theories*, Phys. Rev. Lett. 128 no. 11, (2022) 111601, arXiv:2111.01141 [hep-th].

[63] K. Roumpedakis, S. Seifnashri, and S.-H. Shao, *Higher Gauging and Non-invertible Condensation Defects*, Commun. Math. Phys. 401 no. 3, (2023) 3043–3107, arXiv:2204.02407 [hep-th].

[64] Y. Choi, C. Cordova, P.-S. Hsin, H. T. Lam, and S.-H. Shao, *Non-invertible Condensation, Duality, and Triality Defects in 3+1 Dimensions*, Commun. Math. Phys. 402 no. 1, (2023) 489–542, arXiv:2204.09025 [hep-th].

[65] A. Hasan, S. Meynet, and D. Migliorati, *$SL_2(\mathbb{R})$ symmetries of SymTFT and non-invertible U(1) symmetries of Maxwell theory*, JHEP 12 (2024) 131, arXiv:2405.19218 [hep-th].

[66] E. Paznokas, *Non-invertible SO(2) symmetry of 4d Maxwell from continuous gaugings*, JHEP 06 (2025) 014, arXiv:2501.14419 [hep-th].

[67] O. Sela, *Emergent Noninvertible Symmetries in N=4 Supersymmetric Yang-Mills Theory*, Phys. Rev. Lett. 132 no. 20, (2024) 201601, arXiv:2401.05032 [hep-th].

[68] S.-H. Shao and S. Zhong, *Where Non-Invertible Symmetries End: Twist Defects for Electromagnetic Duality*, arXiv:2509.21279 [hep-th].

[69] L. Bhardwaj, T. Décoppet, S. Schafer-Nameki, and M. Yu, *Fusion 3-Categories for Duality Defects*, Commun. Math. Phys. 406 no. 9, (2025) 208, arXiv:2408.13302 [math.CT].

[70] M. Del Zotto, M. Dell'Acqua, and E. Riedel Gårding, *The Higher Structure of Symmetries of Axion-Maxwell Theory*, arXiv:2411.09685 [hep-th].

[71] I. Bah, E. Leung, and T. Waddleton, *On the Physics of Higher Condensation Defects*, arXiv:2506.04346 [hep-th].

[72] J. A. Damia, R. Argurio, F. Benini, S. Benvenuti, C. Copetti, and L. Tizzano, *Non-invertible symmetries along 4d RG flows*, JHEP 02 (2024) 084, arXiv:2305.17084 [hep-th].

[73] D.-C. Lu, Z. Sun, and Z. Zhang, *SymSETs and self-dualities under gauging non-invertible symmetries*, arXiv:2501.07787 [hep-th].

[74] L. Kong, *Anyon condensation and tensor categories*, Nucl. Phys. B 886 (2014) 436–482, arXiv:1307.8244 [cond-mat.str-el].

[75] G. Arias-Tamargo, C. Hull, and M. L. Velásquez Cotini Hutt, *Non-invertible symmetries of two-dimensional Non-Linear Sigma Models*, arXiv:2503.20865 [hep-th].

[76] L. Bhardwaj, Y. Lee, and Y. Tachikawa, *$SL(2,\mathbb{Z})$ action on QFTs with $\mathbb{Z}_2$ symmetry and the Brown-Kervaire invariants*, JHEP 11 (2020) 141, arXiv:2009.10099 [hep-th].

[77] A. Kapustin and N. Seiberg, *Coupling a QFT to a TQFT and Duality*, JHEP 04 (2014) 001, arXiv:1401.0740 [hep-th].

[78] L. Bhardwaj, L. E. Bottini, D. Pajer, and S. Schäfer-Nameki, *Gapped phases with non-invertible symmetries: (1+1)d*, SciPost Phys. 18 no. 1, (2025) 032, arXiv:2310.03784 [hep-th].

[79] P. Di Francesco, P. Mathieu, and D. Senechal, *Conformal Field Theory*, . Graduate Texts in Contemporary Physics. Springer-Verlag, New York, 1997.

[80] P.-S. Hsin, H. T. Lam, and N. Seiberg, *Comments on One-Form Global Symmetries and Their Gauging in 3d and 4d*, SciPost Phys. 6 no. 3, (2019) 039, arXiv:1812.04716 [hep-th].

[81] Y. Choi, H. T. Lam, and S.-H. Shao, *Noninvertible Global Symmetries in the Standard Model*, Phys. Rev. Lett. 129 no. 16, (2022) 161601, arXiv:2205.05086 [hep-th].

[82] P.-S. Hsin and N. Seiberg, *Level/rank Duality and Chern-Simons-Matter Theories*, JHEP 09 (2016) 095, arXiv:1607.07457 [hep-th].

[83] W. D. Goldberger and M. B. Wise, *Renormalization group flows for brane couplings*, Phys. Rev. D 65 (2002) 025011, arXiv:hep-th/0104170.

[84] B. Michel, E. Mintun, J. Polchinski, A. Puhm, and P. Saad, *Remarks on brane and antibrane dynamics*, JHEP 09 (2015) 021, arXiv:1412.5702 [hep-th].

[85] E. Witten, *Some computations in background independent off-shell string theory*, Phys. Rev. D 47 (1993) 3405–3410, arXiv:hep-th/9210065.

[86] D. Kutasov, M. Marino, and G. W. Moore, *Some exact results on tachyon condensation in string field theory*, JHEP 10 (2000) 045, arXiv:hep-th/0009148.

[87] I. Affleck and A. W. W. Ludwig, *Universal noninteger 'ground state degeneracy' in critical quantum systems*, Phys. Rev. Lett. 67 (1991) 161–164.

[88] D. Friedan and A. Konechny, *On the boundary entropy of one-dimensional quantum systems at low temperature*, Phys. Rev. Lett. 93 (2004) 030402, arXiv:hep-th/0312197.

[89] C. Bachas, J. de Boer, R. Dijkgraaf, and H. Ooguri, *Permeable conformal walls and holography*, JHEP 06 (2002) 027, arXiv:hep-th/0111210.

[90] P. Calabrese and J. L. Cardy, *Time-dependence of correlation functions following a quantum quench*, Phys. Rev. Lett. 96 (2006) 136801, arXiv:cond-mat/0601225.

[91] A. Raviv-Moshe and S. Zhong, *Phases of surface defects in Scalar Field Theories*, JHEP 08 (2023) 143, arXiv:2305.11370 [hep-th].

[92] S. Giombi and B. Liu, *Notes on a surface defect in the O(N) model*, JHEP 12 (2023) 004, arXiv:2305.11402 [hep-th].

[93] M. Trépanier, *Surface defects in the O(N) model*, JHEP 09 (2023) 074, arXiv:2305.10486 [hep-th].

[94] V. Bashmakov and J. Sisti, *Exploring Defects with Degrees of Freedom in Free Scalar CFTs*, arXiv:2410.01716 [hep-th].

[95] H. Casini, I. Salazar Landea, and G. Torroba, *Entropic g Theorem in General Spacetime Dimensions*, Phys. Rev. Lett. 130 no. 11, (2023) 111603, arXiv:2212.10575 [hep-th].

[96] G. Cuomo, Z. Komargodski, and A. Raviv-Moshe, *Renormalization Group Flows on Line Defects*, Phys. Rev. Lett. 128 no. 2, (2022) 021603, arXiv:2108.01117 [hep-th].

[97] O. Diatlyk, H. Khanchandani, F. K. Popov, and Y. Wang, *Defect fusion and Casimir energy in higher dimensions*, JHEP 09 (2024) 006, arXiv:2404.05815 [hep-th].

[98] P. Kravchuk, A. Radcliffe, and R. Sinha, *Effective theory for fusion of conformal defects*, arXiv:2406.04561 [hep-th].

[99] O. Diatlyk, H. Khanchandani, F. K. Popov, and Y. Wang, *Effective Field Theory of Conformal Boundaries*, Phys. Rev. Lett. 133 no. 26, (2024) 261601, arXiv:2406.01550 [hep-th].

[100] T. Shachar, R. Sinha, and M. Smolkin, *The defect b-theorem under bulk RG flows*, JHEP 09 (2024) 057, arXiv:2404.18403 [hep-th].

[101] G. Cuomo, Y.-C. He, and Z. Komargodski, *Impurities with a cusp: general theory and 3d Ising*, JHEP 11 (2024) 061, arXiv:2406.10186 [hep-th].

[102] T. Shachar, *On Intersecting Conformal Defects*, arXiv:2411.14543 [hep-th].

[103] S. Fredenhagen, M. R. Gaberdiel, and C. A. Keller, *Bulk induced boundary perturbations*, J. Phys. A 40 (2007) F17, arXiv:hep-th/0609034.

[104] W. H. Pannell and A. Stergiou, *Line defect RG flows in the ε expansion*, JHEP 06 (2023) 186, arXiv:2302.14069 [hep-th].

[105] I. Brunner and D. Roggenkamp, *Defects and bulk perturbations of boundary Landau-Ginzburg orbifolds*, JHEP 04 (2008) 001, arXiv:0712.0188 [hep-th].

[106] D. Gaiotto, *Domain Walls for Two-Dimensional Renormalization Group Flows*, JHEP 12 (2012) 103, arXiv:1201.0767 [hep-th].

[107] I. Brunner and C. Schmidt-Colinet, *Reflection and transmission of conformal perturbation defects*, J. Phys. A 49 no. 19, (2016) 195401, arXiv:1508.04350 [hep-th].

[108] S. Shimamori, *Conformal field theory with composite defect*, JHEP 08 (2024) 131, arXiv:2404.08411 [hep-th].

[109] D. Ge, T. Nishioka, and S. Shimamori, *Localized RG flows on composite defects and $\mathcal{C}$-theorem*, JHEP 02 (2025) 012, arXiv:2408.04428 [hep-th].

[110] S. Giombi, E. Helfenberger, and H. Khanchandani, *Line defects in fermionic CFTs*, JHEP 08 (2023) 224, arXiv:2211.11073 [hep-th].

[111] J. Barrat, P. Liendo, and P. van Vliet, *Line defect correlators in fermionic CFTs*, arXiv:2304.13588 [hep-th].

[112] A. Konechny, *Fusion of conformal interfaces and bulk induced boundary RG flows*, JHEP 12 (2015) 114, arXiv:1509.07787 [hep-th].

[113] E. Lauria, P. Liendo, B. C. Van Rees, and X. Zhao, *Line and surface defects for the free scalar field*, JHEP 01 (2021) 060, arXiv:2005.02413 [hep-th].

[114] L. Di Pietro, E. Lauria, and P. Niro, *3d large N vector models at the boundary*, SciPost Phys. 11 no. 3, (2021) 050, arXiv:2012.07733 [hep-th].

[115] C. Behan, L. Di Pietro, E. Lauria, and B. C. Van Rees, *Bootstrapping boundary-localized interactions*, JHEP 12 (2020) 182, arXiv:2009.03336 [hep-th].

[116] C. Behan, L. Di Pietro, E. Lauria, and B. C. van Rees, *Bootstrapping boundary-localized interactions II. Minimal models at the boundary*, JHEP 03 (2022) 146, arXiv:2111.04747 [hep-th].

[117] L. Castiglioni, S. Penati, M. Tenser, and D. Trancanelli, *Interpolating Wilson loops and enriched RG flows*, JHEP 08 (2023) 106, arXiv:2211.16501 [hep-th].

[118] L. Castiglioni, S. Penati, M. Tenser, and D. Trancanelli, *Wilson loops and defect RG flows in ABJM*, JHEP 06 (2023) 157, arXiv:2305.01647 [hep-th].

[119] L. Di Pietro, E. Lauria, and P. Niro, *Conformal boundary conditions for a 4d scalar field*, SciPost Phys. 16 no. 4, (2024) 090, arXiv:2312.11633 [hep-th].

[120] I. Nagar, A. Sever, and D.-l. Zhong, *Planar RG flows on line defects*, JHEP 06 (2024) 110, arXiv:2404.07290 [hep-th].

[121] X. Sun and S.-K. Jian, *Boundary operator expansion and extraordinary phase transition in the tricritical O(N) model*, arXiv:2501.06287 [cond-mat.str-el].

[122] G. Barton, *Quantum mechanics of the inverted oscillator potential*, Annals of Physics 166 no. 2, (1986) 322–363. https://www.sciencedirect.com/science/article/pii/0003491686901429.

[123] P. Kraus and F. Larsen, *Boundary string field theory of the D anti-D system*, Phys. Rev. D 63 (2001) 106004, arXiv:hep-th/0012198.

[124] T. Takayanagi, S. Terashima, and T. Uesugi, *Brane - anti-brane action from boundary string field theory*, JHEP 03 (2001) 019, arXiv:hep-th/0012210.

[125] J. L. Cardy, *Operator Content of Two-Dimensional Conformally Invariant Theories*, Nucl. Phys. B 270 (1986) 186–204.

[126] M. Stone and P. Goldbart, *Mathematics for physics: A guided tour for graduate students*, . Cambridge University Press, 2009.

[127] R. M. Wald, *On identically closed forms locally constructed from a field*, Journal of Mathematical Physics 31 no. 10, (1990) 2378–2384, https://doi.org/10.1063/1.528839. https://doi.org/10.1063/1.528839.

[128] G. Barnich, F. Brandt, and M. Henneaux, *Local BRST cohomology in gauge theories*, Phys. Rept. 338 (2000) 439–569, arXiv:hep-th/0002245.

[129] G. Barnich and F. Brandt, *Covariant theory of asymptotic symmetries, conservation laws and central charges*, Nucl. Phys. B 633 (2002) 3–82, arXiv:hep-th/0111246.

[130] P. J. Olver, *Applications of Lie Groups to Differential Equations*, . Graduate Texts in Mathematics. Springer New York, NY, 1986.

[131] I. M. Anderson, *The Variational Bicomplex*, . Utah State University, 1989.

[132] G. Compere, *Symmetries and conservation laws in Lagrangian gauge theories with applications to the mechanics of black holes and to gravity in three dimensions*, . PhD thesis, Brussels U., 2007. arXiv:0708.3153 [hep-th].

[133] T. G. Mertens, *The Schwarzian theory — origins*, JHEP 05 (2018) 036, arXiv:1801.09605 [hep-th].

[134] P. Kraus, R. Monten, and R. M. Myers, *3D Gravity in a Box*, SciPost Phys. 11 (2021) 070, arXiv:2103.13398 [hep-th].

[135] K. V. Kuchar, *Geometrodynamics of Schwarzschild black holes*, Phys. Rev. D 50 (1994) 3961–3981, arXiv:gr-qc/9403003.

[136] A. Kapustin and N. Saulina, *Topological boundary conditions in abelian Chern-Simons theory*, Nucl. Phys. B 845 (2011) 393–435, arXiv:1008.0654 [hep-th].

[137] A. Kitaev and L. Kong, *Models for Gapped Boundaries and Domain Walls*, Commun. Math. Phys. 313 no. 2, (2012) 351–373, arXiv:1104.5047 [cond-mat.str-el].

[138] P. Etingof, D. Nikshych, V. Ostrik, and w. a. a. b. E. Meir, *Fusion categories and homotopy theory*, arXiv:0909.3140 [math.QA].

[139] Z. Sun and Y. Zheng, *When are Duality Defects Group-Theoretical?*, arXiv:2307.14428 [hep-th].